A. Sharp

U.S. Army
Coastal Engineering
Research Center

SHORE PROTECTION MANUAL

Volume II
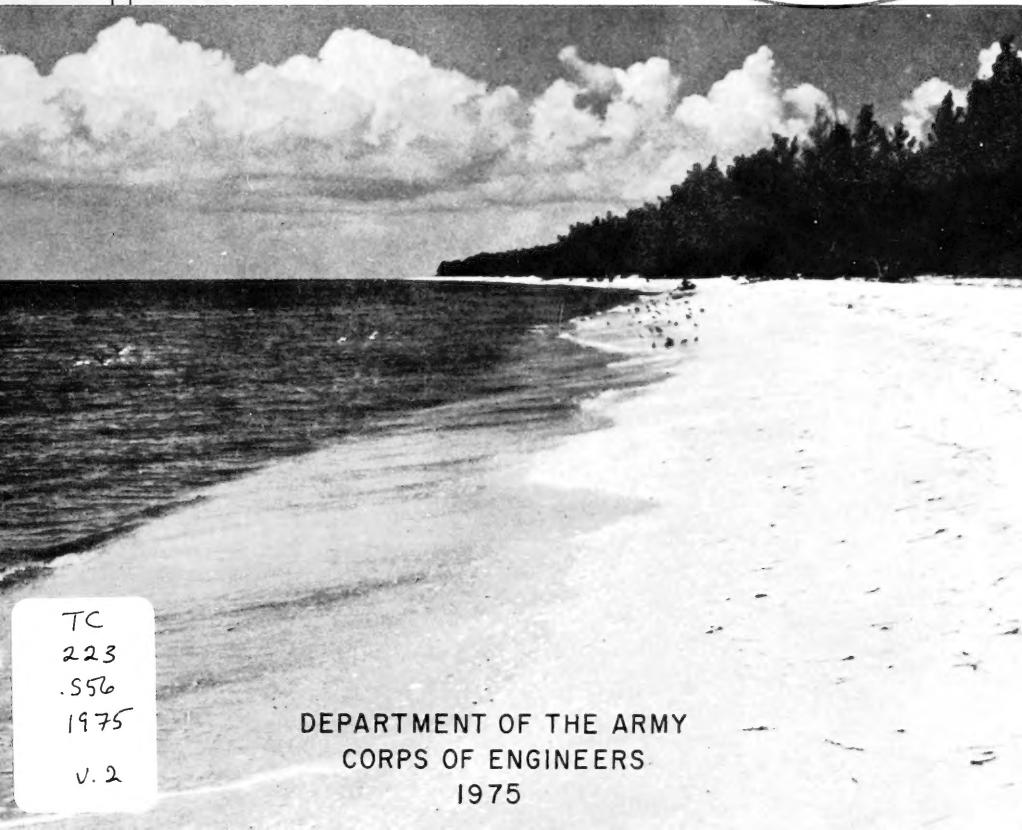
DEPARTMENT OF THE ARMY
CORPS OF ENGINEERS
1975

SHORE PROTECTION MANUAL

VOLUME II

(Chapters 5 Through 8)

U.S. ARMY COASTAL ENGINEERING RESEARCH CENTER

1975

Second Edition

TABLE OF CONTENTS

VOLUME I

VOLUME III

TABLE OF CONTENTS

VOLUME II

CHAPTER 5 - PLANNING ANALYSIS

CHAPTER 6 - STRUCTURAL FEATURES

CHAPTER 8 - ENGINEERING ANALYSIS - CASE STUDY

LIST OF FIGURES

FIGURE

LIST OF TABLES

CHAPTER 5

PLANNING

ANALYSIS

DANA POINT, CALIFORNIA —

PLANNING ANALYSIS

5.1 GENERAL

Coastal engineering problems may be classified into four general categories: shoreline stabilization, backshore protection (from waves and surge), inlet stabilization, and harbor protection. (See Figure 5-1.) A coastal problem may fall into more than one category. Once classified, there are various solutions available to the coastal engineer. Some of these are structural; however, other techniques may be employed, such as zoning and land use management. This Manual deals primarily with structural solutions, but basic design factors may also apply to other types of solutions.

Figure 5-1 indicates structures or protective works that fit into the four general problem classifications and factors that must be considered in analyzing the problem. Hydraulic considerations include wind, waves, currents, tides, storm surge or wind setup and the basic bathymetry of the area. Sedimentation considerations include the littoral material and processes (i.e., direction of movement; rate of transport, net and gross; and sediment classification and characteristics) and changes in shore alignment. Navigation considerations include the design craft or vessel data, traffic lanes, channel depth, width, length and alignment. Control structure considerations include selection of the protective works evaluating type, use, effectiveness, economics, and environmental impact. In selecting the shape, size, and location of shore-protection works, the objective should be not only to design an engineering work which will accomplish the desired results most economically, but also to consider effects on adjacent areas. Economic evaluation includes the maintenance costs and interest on and amortization of first cost. If any plan considered would result in enlarging the problem by extending its effects to a larger coastal stretch or prevent such enlargement, the economic effect of each such consequence should be evaluated. A convenient yardstick for comparing various plans on an economic basis is the total cost per year per foot of shore protected.

Effects on adjacent lands are considered to the extent of providing the required protection with the least amount of disturbance to current and future land use, environmental factors, and aesthetics of the area. The form, texture, and color of material selected for the design should be considered as well as how the material is used. Proper planning analysis also requires consideration of legal and social consequences where shore protection measures may be expected to result in significant effects on physical or ecological aspects of the environment.

The following sections describe the most common structural solutions now used to meet functional requirements, and provide guidelines for the application of these solutions. This manual treats only the structural solutions to problems. The environmental effects of all such solutions must, by law as well as normal engineering concerns, be studied.

Figure 5-1. General Classification of Coastal Engineering Problems

5.2   SEAWALLS, BULKHEADS, AND REVETMENTS

5.21 FUNCTIONS

Seawalls, bulkheads, and revetments are structures placed parallel, or nearly parallel, to the shoreline, to separate a land area from a water area. The primary purpose of a bulkhead is to retain or prevent sliding of the land, with the secondary purpose of affording protection to the upland against damage by wave action. The primary purpose of a seawall or revetment is to protect the land and upland property from damage by waves, with incidental functions as a retaining wall or bulkhead. There are no precise distinctions between the three structures, and often the same type of structure in different localities bears a different name. Thus, it is difficult to say whether a stone or concrete facing designed to protect a vertical scarp is a seawall or a revetment, and often just as difficult to determine whether a retaining wall subject to wave action should be termed a seawall or bulkhead. All these structures, however, have one feature in common, in that they separate land and water areas. These structures are generally used where it is necessary to maintain the shore in an advanced position relative to that of adjacent shores, where there is a scant supply of littoral material and little or no protective beach, as along an eroding bluff, or where it is desired to maintain a depth of water along the shoreline, as for a wharf.

5.22   LIMITATIONS

These structures afford protection only to the land immediately behind them, and none to adjacent areas up- or downcoast. When built on a receding shoreline, the recession will continue and may be accelerated on adjacent shores. Any tendency toward loss of beach material in front of such a structure may well be intensified. Where it is desired to maintain a beach in the immediate vicinity of such structures, companion works may be necessary.

5.23   FUNCTIONAL PLANNING OF THE STRUCTURE

The planning of seawalls, bulkheads, and revetments is an elementary process, since their functions are restricted to the maintenance of fixed boundaries. Factors in designing such a structure are: use and overall shape of the structure, location with respect to the shoreline, length, height, and often stability of the soil and ground and water level seaward and landward of the wall.

5.24   USE AND SHAPE OF THE STRUCTURE

The use of the structure dictitates the selection of the shape. Face profile shapes may be classed roughly as vertical or nearly vertical, sloping, convex curved, concave curved, reentrant, or stepped. Each cross section has certain functional applications. If unusual functional criteria are required, a combination of cross sections may be used.

A vertical or nearly vertical face structure lends itself to use as a quay wall, docking or mooring place. Where a light structure is required, a vertical face (of sheet piling, for example) may often be constructed more quickly and more cheaply than other types. This ease or speed of construction is important where emergency protection is needed. A vertical face is less effective against wave attack, and specifically against overtopping, than the concave curved and reentrant face. The use of vertical or nearly vertical face walls can result in severe scouring when the toe or base of the wall is in shallow water. Waves breaking against a wall deflect energy both upward and downward. The downward component causes scouring erosion of the material at the base of the wall. To prevent scouring, toe protection should be provided in the form of a toe or armor stone of adequate size to prevent displacement, and of such gradation as to prevent the loss of the foundation material through the voids of the stone and consequent settlement of the stone.

Convex curved face and smooth slopes are least effective in reducing wave runup and overtopping. The rubble sloping seawall and revetment is effective in dissipating and absorbing wave energy, and reduces wave runup and overtopping. Sloping face structures, generally reduce scouring, and may have an advantage over vertical face structures.

Concave curved or reentrant faced structures are the most effective for reducing wave overtopping when onshore winds are light. Where the structure crest is to be used for a road, promenade, or other purpose, this design may be the best shape for protecting the crest and reducing spray. This is especially true if the fronting beach is narrow or non-existant, or if the water level is above the structure base. If onshore winds occur at the same time as high waves, a rubble slope should also be considered.

A stepped-face wall provides the easiest access to beach areas from protected areas, and reduces the scouring of wave backwash.

5.25 LOCATION OF STRUCTURE WITH RESPECT TO SHORELINE

A seawall, bulkhead, or revetment is usually constructed along that line landward of which further recession of the shoreline must be stopped. Where an area is to be reclaimed, a wall may be constructed along the seaward edge of the reclaimed area.

5.26 LENGTH OF STRUCTURE

A seawall, bulkhead, or revetment protects only the land and improvements immediately behind it. These structures provide no protection to either up- or downcoast areas as do beach fills. Usually, where erosion may be expected at both ends of a structure, wing walls or tie-ins to adjacent land features must be provided to prevent flanking and possible progressive failure of the structure at the ends. Short-term beach changes due to storms, as well as seasonal and annual changes, are design considerations. Erosion updrift from such a structure will continue unabated after the wall is built, and downdrift erosion will probably be intensified.

5.27 HEIGHT OF STRUCTURE

Seawalls, bulkheads, and revetments can be built so high that no water would overtop the crest of the structure, regardless of severity of wave attack and storm-surge levels, though it is sometimes not economically feasible to do so. Wave runup and overtopping criteria on which the height of a structure should be based can be estimated from data presented in Section 7.2 "WAVE RUNUP, OVERTOPPING, AND TRANSMISSION." Specific model tests for the design case can be carried out if greater detail or accuracy is warranted.

5.28 DETERMINATION OF GROUND ELEVATION IN FRONT OF A STRUCTURE

Seawalls and revetments are usually built to protect a shore from the effects of continuing erosion and to protect shore improvements from damage by wave attack. The exact effect of such a structure on erosion processes cannot be fully determined, but can be estimated by the method given in this section. For safety, even though erosion processes seem to have been halted or reversed, the designer must assume that they will continue. A determination of the beach profile that will exist after construction of the structure can be estimated through experience, observations, and general guides.

Scour may be anticipated at the toe of the structure as an initial short-term effect. Scour will form a trough with dimensions governed by the type of structure face, the nature of wave attack, and the resistance of the bed material. At a rubble-mound seawall, scour may undermine the toe stone, causing it to sink to an ultimately lower stable position. The resultant settlement of stone on the seaward face may be offset by overbuilding the cross-section to allow for settlement. Another method is to provide excess stone at the toe to fill the anticipated scour trough. The face of a vertical structure may be protected similarly against scour by the use of stone. A gravity wall must be protected from undermining by scour by providing impermeable cutoff walls at the base. *As a general guide, maximum depth of a scour trough below the natural bed is about equal to the height of the maximum unbroken wave that can be supported by the original depth of water at the toe of the structure.* For example, if the controlling depth of water seaward of the face of the structure is 10 feet, the offshore bottom slope is 1 on 30, and a design wave period of 8 seconds is assumed, the maximum unbroken wave height that can be supported is 10.4 feet. (See Section 7.1.) Therefore, the maximum depth of scour at the toe of the structure would be 10.4 feet below the original bottom, or a total of 20.4 feet below the design water level. The placement of a rock blanket with an adequate bedding material seaward from the toe of the structure will prevent erosion at the toe, and will result in a more stable structure. (See Section 7.3 for design methods.)

For long-term effects, it is preferable to assume that the structure would have no effect on reducing the erosion of the beach seaward of the wall. Such erosion would continue as if the wall were not there. Since the determination of scour can only be approximate, general guides are usually adopted.

Consider the beach shown in Figure 5-2 where the solid line represents an average existing profile. It is desired to place a seawall at point A as shown. From prior records, either the loss of beach width per year or the annual volume loss of material over an area which includes the profile, is known. In the latter case, *the annual volume loss may be converted to an annual loss of beach width by the general rule: loss of 1 cubic yard of beach material is equivalent to loss of 1 square foot of beach area on the berm.* This rule is applicable primarily at the ocean front. In shallow, protected bays, the ratio of volume to area is usually much less.
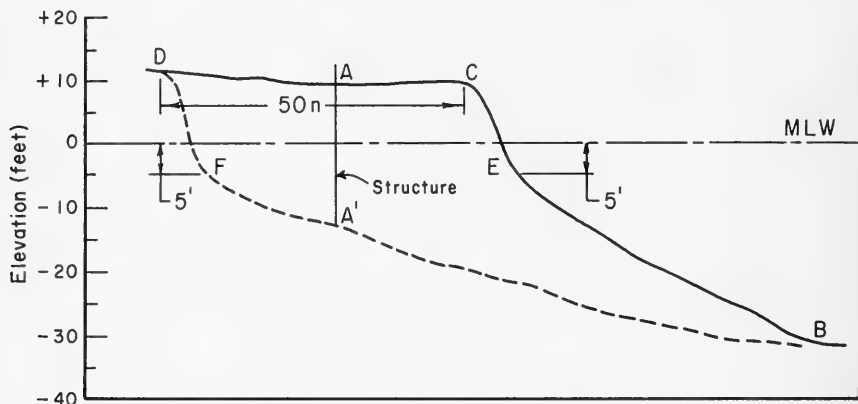
Figure 5-2. Effects of Erosion.

Nearshore slopes are usually gentle seaward of the bar. Slopes are steeper inshore of the bar, and may be as steep as 1 on 5 at the waterline with coarse sand. Analyses of profiles at eroding beaches indicate that it may be assumed that the slope seaward of a depth of 30 feet will remain nearly unchanged, that the point of slope break E will remain at about the same elevation, and that the profile shoreward of the point of break in slope will remain nearly unchanged. Thus, the ultimate depth at the wall may be estimated as follows:

(a) In Figure 5-2, let B represent a water depth of 30 feet, E the point of slope break at the depth of about 5 feet, and C the present position of the berm crest. If it is desired to build a structure at A whose economic life is estimated at 50 years, and it is found that n is the annual loss of beach width at the berm, then in 50 years without the wall this berm will retreat a distance $50n$ to point D.

(b) From D to the elevation of point E, draw a profile $D F$ parallel to $C E$, and connect points B and F. This dashed line, $D F B$, will represent the approximate profile of beach after 50 years without the presence of the wall. The receded beach elevation at the wall's location will be approximated by point A'. Similar calculations may be made for

anticipated short-time beach losses caused by storms. Erosion caused by storms generally results in a greater loss of beach material above the mean low water level, because the superelevation of the water level (storm surge) allows storm waves to act on the upper part of the beach.

Other factors in planning and design are the depth of wall penetration to prevent undermining, tie backs or end walls to prevent flanking, stability against saturated soil pressures, and the possibility of soil slumping under the wall.

5.3 PROTECTIVE BEACHES

5.31 FUNCTIONS

Beaches of suitable dimensions are effective in dissipating wave energy, and, when they can be maintained to proper dimensions, afford protection for the adjacent upland, and are classed as shore-protection structures. Such beaches dissipate wave energy without causing adverse effects. When studying an erosion problem, it is advisable to investigate the feasibility of mechanically or hydraulically placing borrow material on the shore to restore or form, and subsequently maintain, an adequate protective beach, and to consider other remedial measures as auxiliary to this solution. The method of placing beach fill to ensure sand supply at the required replenishment rate is important. Suitable beach material may be stockpiled at the updrift section of the problem area where stabilization of an eroding beach is the problem. The establishment and periodic replenishment of such a stockpile is termed *artificial beach nourishment*. If the solution of a problem requires restoration of the eroded beach and its stabilization at the restored position, fill is placed directly on the eroded beach. Then artificial nourishment is accomplished by stockpiling. When conditions are suitable for artificial nourishment, long reaches of shore may be protected at a cost relatively low compared to costs of other adequate protective structures. An equally important advantage is that artificial nourishment directly remedies the basic cause of most erosion problems - a deficiency in natural sand supply - and benefits rather than damages the shore beyond the immediate problem area. An added consideration is that the widened beach may have value as a recreation feature.

Under certain conditions, a properly designed groin system may improve a protective beach. This method must be used with caution, for if a beach is restored or widened by impounding the natural supply of littoral material, a corresponding decrease in supply may occur in downdrift areas with resultant expansion or transfer of the problem area. Detrimental effects of groins may usually be prevented by placing artificial fill in suitable quantity concurrently with groin construction; such stockpiling is called *filling the groins*. Groins may be included in a beach restoration project to reduce the rate of loss and thus the nourishment requirements. When groins are considered for use with artificial fill, their benefits should be carefully evaluated to determine their justification. Such justification could be that groins would reduce annual nourishment costs in excess of the groin annual charges. (See Section 5.610 Economic Determination for Groin Construction.)

5-7

5.32 LIMITATIONS

Whether to provide a protective beach, with or without groins, depends on the availability of suitable sand for the purpose. Artificial nourishment is usually quite costly on a unit length basis when applied to short segments of shore, because the widened beach protuding seaward of its adjacent shores erodes rapidly. This results in high nourishment costs, but is not necessarily a limitation if artificial nourishment over a short length of beach prevents the enlargement of that problem area to downdrift shores. However, difficulties could be encountered in financing a shore protection method which provides protection beyond the immediate problem area.

5.33 PLANNING CRITERIA

Planning of a protective beach by artificial nourishment requires:

(a) Determination of the predominant direction of longshore transport and deficiency of material supply to the problem area;

(b) Determination of the composite average characteristics of the existing beach material or native sand in the zone between the 30-foot depth and the dune or cliff line (the zone of active littoral movement);

(c) Evaluation and selection of borrow material for initial beach fill and periodic nourishment, including the determination of any extra amount of borrow material required for placement based on the comparison of the native beach sand and borrow material;

(d) Determination of beach berm elevation and width;

(e) Determination of wave-adjusted foreshore slopes;

(f) Determination of feeder-beach (stockpile) location.

5.331 Direction of Longshore Transport and Deficiency of Supply. The methods of determining the predominant direction of longshore transport are outlined in Section 4.5. The deficiency of material supply is the rate of loss of beach material; it is the rate at which the material supply must be increased to balance the transport by littoral forces to prevent net loss. If no natural supply is available, as on shores downdrift from a major barrier to longshore transport, the net rate of longshore transport will approximate the deficiency in supply. Comparison of surveys of impoundment or eroding areas over a long period of time is the best method of estimating the rate of nourishment required to maintain stability of the shore. Since surveys suitable for volume measurement are rarely available, approximations computed from changes in the shore position, as determined from aerial photographs or other suitable records, are often necessary. *For such computations, the relationship in which 1 square foot of change in beach surface area equals 1 cubic yard of beach material appears to provide acceptable values on exposed seacoasts.* For less exposed shores, this ratio would probably result in volume estimates in excess of the actual value.

5.332 Selection of Borrow Material. After the characteristics of the native sand and the longshore-transport processes in the area are determined, the next step is to select borrow material for beach fill and for periodic nourishment. When sand is mechanically deposited on the beach, waves immediately start a sorting and winnowing action on the surface layer of the fill, moving finer particles seaward, and leaving coarser material at or shoreward of the plunge point. This sorting continues until a layer of coarser particles compatible with the wave climate armors the beach and makes the slope temporarily stable for normal wave conditions. However, if this armor is disturbed by a storm, the underlying material is again subjected to the sorting process.

Because of these processes, beach fill with organic material or large amounts of the finer sand fractions may be used since natural processes will clean the fill material. This has been confirmed with fills containing foreign matter at Anaheim Bay, California, and Palm Beach, Florida. Material finer than that exposed on the natural beach face, if exposed on the surface during a storm, will move to a depth compatible with its size to form nearshore slopes flatter than normal slopes before placement. Fill coarser than the sand on the natural beach will remain on the foreshore, and may be expected to produce a steeper beach. The relationship between grain size and slope is discussed in Section 4.526. If borrow sand is very coarse, it will probably be stable under normal conditions, but it may make the beach less desirable for recreation. If the borrow material is much finer than the native beach material, a large amount will move offshore and be lost.

The distribution of grain sizes naturally present on a stable beach represents a state of dynamic equilibrium between the supply and loss of material of each size. Coarser particles generally have a lower supply rate and a lower loss rate; fine particles are usually more abundant, but are rapidly moved alongshore and offshore. Where fill is to be placed on a natural beach that has been stable or only slowly receding, the size characteristics of the native material can be used to evaluate the suitability of potential borrow material. A borrow material with the same grain size distribution as the native material, or one slightly coarser, will usually be suitable for fill. If such borrow material is available, the volume required for fill can be determined directly from the project dimensions, assuming that only insignificant amounts will be lost through sorting and selective transport.

Unfortunately it is often difficult to find economic sources of borrow material with the desired properties. When the potential borrow material is finer than the native material, large losses of the borrow material often take place immediately following its emplacement. Currently there is no proven method for computing the amount of overfill required to satisfy project dimensions once the fill material has undergone this initial sorting action and attained a stable configuration. Studies by Krumbein (1957) provide a quantitative basis for comparison on the material characteristics considered to have the greatest effect on this relationship. His subsequent work with James (Krumbein & James,

1965) developed a technique that may be used to indicate probable behavior of the borrow material on the beach.

The procedure requires enough core borings in the borrow zone and samples from the beach and nearshore zones to adequately describe the size distribution of borrow and beach material. Mechanical size analyses of the borings and samples are used to compute composite size distributions for the two types of material. These composite distributions are compared to determine the suitability of the borrow material. Almost any borrow source near the shore will include some material of suitable size. Since the source will control cost to a major degree, evaluation of the proportional volume of material of the desired characteristics in the borrow areas is important in economic design. Krumbein and James (1965) provide the design engineer with criteria for estimating an additional amount of borrow material required to meet project dimensions when the borrow material does not match the characteristics of native sand or those required for a stable beach. These techniques have not been fully tested in the field, and should be used only as a general indication of possible fill behavior. The techniques have been evaluated in one field situation with favorable results (Section 6.3 PROTECTIVE BEACHES), but further investigations are required before the quantitative reliability of these techniques can be assessed.

The mathematical basis of the technique is straightforward. Given a borrow material with a size distribution different from the native or stable material size distribution, the method determines the proportion of material which must be removed from each size class of the borrow material to produce a modified borrow material size distribution with the same shape as that of the native material. If size distributions of native and borrow material are known, and if there is some borrow material in each size class that comprises the native material, the computation could be made directly by finding the phi size class with the maximum ratio of native to borrow weight proportions. This ratio, called the *critical ratio* ($R_{\phi\ crit}$), represents the estimated cubic yards of fill material required to produce one cubic yard of material having the desired particle size distribution (i.e., similar to native or stable material).

In practice this procedure is usually not reliable. Several factors lead to errors in the estimates of weight proportions of both size distributions. These errors can be due to sampling inadequacy, estimation of composite properties from individual samples, and laboratory error in mechanical analysis. Computation of the critical ratio is usually subject to less error if the first two graphic moments of each size distribution are computed, and these values substituted into the following equation:

$$R_{\phi\ crit} = \frac{\sigma_{\phi b}}{\sigma_{\phi n}}\ e^{-\left[\frac{\left(M_{\phi n} - M_{\phi b}\right)^2}{2\left(\sigma_{\phi n}^2 - \sigma_{\phi b}^2\right)}\right]} \tag{5-1}$$

where

$R_{\phi\ crit}$ = ratio of proportions of native material to the borrow material at the critical phi value (when phi value is that ϕ size with greatest ratio of the proportions of native sand to borrow material),

σ_ϕ = $(\phi_{84} - \phi_{16})/2$ Standard deviation is a measure of sorting. (See Section 4.2) $\qquad$ (5-2)

M_ϕ = $\phi_{84} + \phi_{16})/2$ phi mean diameter of grain size distribution. (See Section 4.2) $\qquad$ (5-3)

$-_b$ = subscript b refers to borrow material

$-_n$ = subscript n refers to natural sand on beach

ϕ_{84} = 84th percentile in phi units

ϕ_{16} = 16th percentile in phi units

e = (base of natural logarithms, 2.718)

This formula assumes that both composite native and borrow material distributions are nearly lognormal. This assumption can be expected to be satisfied for the composite grain size distribution of most natural beaches and for naturally deposited borrow material that is almost homogeneous. Pronounced skewness or bimodality might be encountered with borrow sources that contain alternating horizons of coarse and fine material, such as clay-sand depositional sequences, or in borrow zones that cross cut flood plain deposits associated with ancient river channels.

The formula for $R_\phi\ crit$ is not applicable to all possible combinations of grain size moments for borrow and native material. The possible combinations can be subdivided into the four basic cases given in Table 5-1, and indicated as quadrants in Figure 5-3. Table 5-1 shows that, $R_\phi\ crit$ is assumed to have direct application in only one of the four cases.

In Case 1, the borrow material has an average grain size finer than that of the native material, but the borrow material is more poorly sorted. The basic prerequisite is satisfied that there is some borrow material present for each of the size classes which contain native material. There will be some coarser size classes beyond which this supply will be more than adequate. However, a large part of the borrow material is finer than that expected to remain in the active littoral zone. The best estimate of the overfill ratio is the critical ratio calculated by Equation 5-1. This should be a conservative estimate since overage quantities in all size classes other than that for $R_\phi\ crit$ would not all be expected to be completely lost from the active area.

Table 5–1. Applicability of $R_{\phi\,crit}$ Calculations for Various Combinations of the Graphic Phi Moments of Borrow and Native Material Grain Size Distributions.

| Category | | Relationship of Phi Means | Relationship of Phi Standard Deviations | Response to Sorting Action |
Case	Quadrant in Fig. 5-3			
I	1	$M_{\phi b} > M_{\phi n}$ Borrow material is finer than native material	$\sigma_{\phi b} > \sigma_{\phi n}$ Borrow material is more poorly sorted than native material	Best estimate of required overfill ratio is given by $R_{\phi\,crit}$
II	2	$M_{\phi b} < M_{\phi n}$ Borrow material is coarser than native material		Required overfill ratio is probably less than that computed for $R_{\phi\,crit}$
III	3	$M_{\phi b} < M_{\phi n}$ Borrow material is coarser than native material	$\sigma_{\phi b} < \sigma_{\phi n}$ Borrow material is better sorted than native material	The distributions cannot be matched but the fill material should all be stable; may induce added scour of native material fronting toe of fill.
IV	4	$M_{\phi b} > M_{\phi n}$ Borrow material is finer than native material		The distributions cannot be matched. Fill loss cannot be predicted but will probably be large
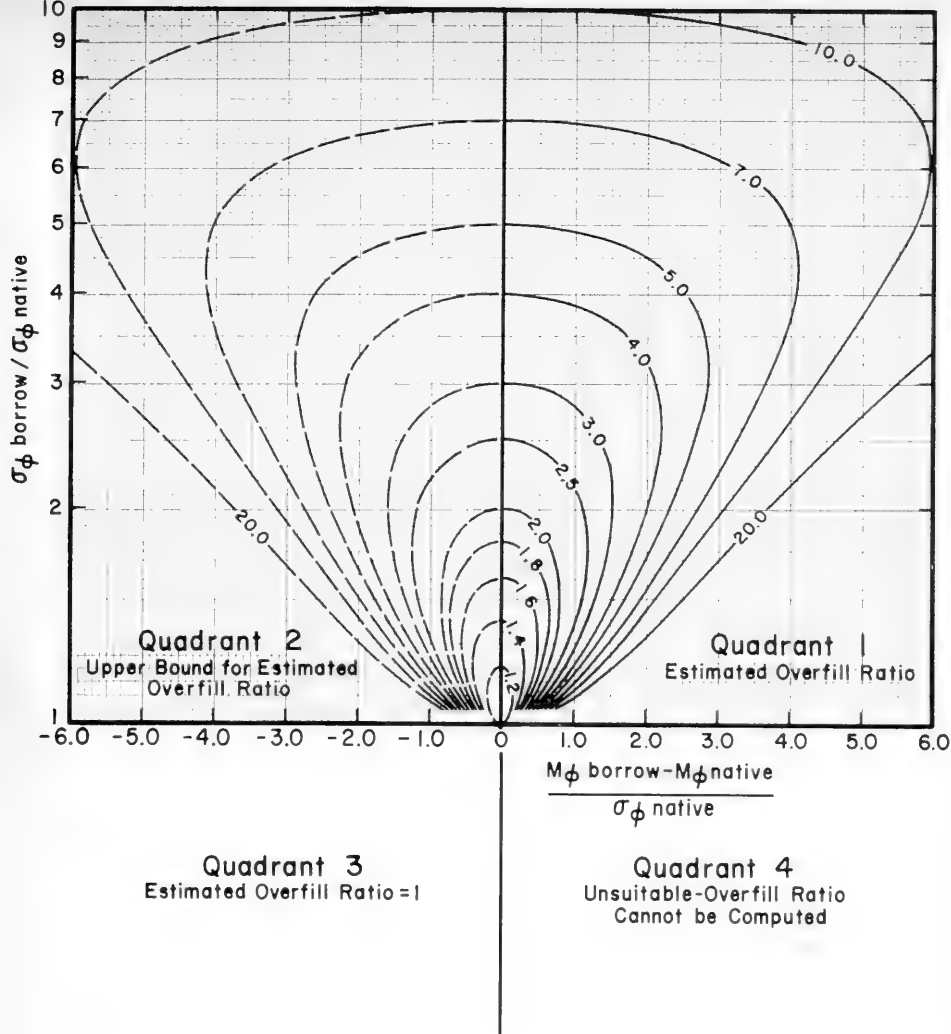
Figure 5-3. Equal Value Contours R_ϕ *critical* Versus Relative Differences Between Borrow and Native Textural Parameters

In Case II (Table 5-1), the borrow material is also more poorly sorted than the native material, but the larger part of borrow material is coarser than the average grain size of the native material. Since the sorting processes that modify the grain size distribution of the fill material are most active on the finer size classes, much of the excess coarse material included in the initial fill will remain in the stabilized beach profile. In this case, the grain size distribution of the stabilized fill is not expected to completely match that of the original native sand. It is expected that part of borrow material lost from the fill will be less than that calculated from $R_{\phi\ crit}$. The computed value of the critical ratio can be assumed to represent an upper bound.

In Case IV (Table 5-1), the borrow material is finer and better sorted than the native material. The equation for $R_{\phi\ crit}$ does not apply in Case IV, because the equation denotes a minimum rather than a maximum in the ratio of native to borrow weight proportion at the critical phi value. This indicates that borrow material of this type is unsuitable as fill material. The native and borrow size distributions cannot be matched through selective sorting processes. The mathematics imply that none of the original fill material will remain as stable fill after the initial sorting. This implication is not totally realistic, and the instability of borrow material of this type in a fill depends on the degree of difference between the average grain size of the stable and borrow materials. If borrow material of this type is selected, large initial losses should be expected, but no method in current use provides even a crude estimate of loss.

In Case III, borrow material is coarser and better sorted than the native material. The equation for $R_{\phi\ crit}$ does not apply for the same reason it does not apply to borrow material in Case IV. Practical implications in Case III are the opposite of those for IV. In III, there is a marked deficiency of material in the finer size classes which are more responsive to the sorting processes. Hence the borrow material is stable from the outset, and no significant losses are to be expected. The overfill ratio may be assumed to be unity. If the material has a large coarse fraction, foreshore slopes may be steepened enough to alter wave runup and reflection and induce scour and loss of existing native material fronting the toe of the coarse fill. It may also result in a beach fill having profile slopes and textural properties not well suited for recreation.

The engineering application of the techniques discussed above require that basic sediment size data be collected in both the potential borrow zones and in the project area. Estimation of the composite grain size characteristics of native material should follow the guidelines set forth by Krumbein (1957). The estimation of composite distribution of properties of material in the borrow zone depends upon the heterogeneity of the textural properties in the zone. If material in the borrow zone exhibits large vertical or horizontal gradients in textural properties, extensive coring may be required to obtain reliable estimates of the composite properties of the borrow material. Practical guidelines for reliable

estimation of borrow material properties have not been established when the borrow zone is heterogeneous. Hence special attention must be given when suitable borrow material from homogeneous deposits cannot be found.

The relationship between the critical ratio and the relative divergence between the phi moments of native and borrow materials is shown in Figure 5-3. The horizontal axis is a dimensionless measure of the relative difference between borrow and native phi means. It is computed as the borrow phi mean minus the native phi mean divided by the native phi standard deviation. The vertical axis (plotted on a logarithmic scale) is the ratio of borrow phi standard deviation to native phi standard deviation. Any value plotting to the right of the origin indicates a borrow material finer than the native material $(M_{\phi b} > M_{\phi n})$. Any point plotting above the horizontal axis indicates a borrow material more poorly sorted than the native material $(\sigma_{\phi b} > \sigma_{\phi n})$. Hence the four categories discussed above are separated into the four quadrants on this plot.

The curves in Figure 5-3 indicate equal-value contours of the critical ratio. Contours are dashed lines in quadrant 2, because here the critical ratio is assumed to be an upper bound to the true loss ratio. In quadrant 1, the critical ratio is assumed to be a conservative estimate of the true loss ratio and the curves are solid lines. No curves are plotted in quadrants 3 and 4, because the computed value of critical ratio has no meaning when the borrow material is well sorted in comparison to the native material.

This plot shows the general behavior of the critical ratio as functions of the differences in textural characteristics between borrow and native materials. The following relationships are noteworthy:

(a) For any fixed ratio between the sorting of borrow and native material, the critical ratio changes only slowly with small differences in phi means, then more rapidly as this difference becomes larger.

(b) For larger ratios of the sorting parameter σ_ϕ, the stability of the computed critical ratio is greater, i.e., if the ratio of borrow to native sorting is large the computed critical ratio is nearly insensitive to the difference in phi means.

(c) For any fixed finite difference in phi means, there will be some ratio of borrow to native sorting for which the critical ratio will be a minimum. For sorting ratios less than this value, the critical ratio rises rapidly and approaches infinity as the sorting ratio approaches unity. For sorting ratios larger than this optimal value, the critical ratio increases slowly.

These relations indicate that the computed value for critical ratio is generally more sensitive to the phi sorting ratio than to differences in phi means. If the borrow material is poorly sorted in comparison to the native material, errors in determination of the difference in phi means will not cause significant errors in the computation of the critical ratio.

Conversely, if the borrow and native materials have nearly equal phi sorting values, small errors in determining the difference in phi means can cause enormous errors in computation of the critical ratio. As an example, where the ratio of borrow phi sorting to native phi sorting is 1.25, the normalized difference in phi means is 0.5 unit so that the true difference is 1.0 unit. The true critical ratio is about 3.0 which means twice as much borrow material is required than that estimated with the erroneous value. On the other hand, where the sorting ratio is 3, the same "erroneous" and "true" values apply to the normalized difference in phi means. Here the two critical ratios are approximately 3.05 and 3.20, a difference of only 5 percent. This example indicates that selecting a poorly sorted borrow material may be safer when the borrow material must be finer than the native material.

Application of the above techniques is demonstrated below with two example problems.

* * * * * * * * * * * * * * EXAMPLE PROBLEM * * * * * * * * * * * * * * * *

GIVEN: Composite native beach material phi parameters

$$\phi_{84} = 2.47 \ \phi \ (0.180 \ \text{mm}),$$

$$\phi_{16} = 1.41 \ \phi \ (0.376 \ \text{mm}).$$

composite borrow material parameters

$$\phi_{84} = 3.41 \ \phi \ (0.094 \ \text{mm}),$$

$$\phi_{16} = 1.67 \ \phi \ (0.314 \ \text{mm}).$$

FIND:

(a) $R_\phi \ crit$

(b) Applicable case for computing overfill ratio

(c) Interpreted overfill ratio (cy fill/cy project requirements)

SOLUTION:

(a) Using Equation 5-3

$$M_\phi = \frac{\phi_{84} + \phi_{16}}{2} ,$$

$$M_{\phi n} = \frac{2.47 + 1.41}{2} = 1.94 \ (0.261 \ \text{mm}) ,$$

and

$$M_{\phi b} = \frac{3.41 + 1.67}{2} = 2.54 \ (0.172 \ \text{mm}) .$$

5-16

Using Equation 5-2

$$\sigma_\phi = \frac{\phi_{84} - \phi_{16}}{2} \ ,$$

$$\sigma_{\phi n} = \frac{2.47 - 1.41}{2} = 0.53 \ ,$$

and

$$\sigma_{\phi b} = \frac{3.41 - 1.67}{2} = 0.87 \ .$$

Using Equation 5-1

$$R_{\phi \ crit} = \frac{\sigma_{\phi b}}{\sigma_{\phi n}} \ e^{\left[-\frac{(M_{\phi n} - M_{\phi b})^2}{2(\sigma_{\phi n}^2 - \sigma_{\phi b}^2)} \right]}$$

$$R_{\phi \ crit} = \frac{0.87}{0.53} \ e^{\left[-\frac{(1.94 - 2.54)^2}{2((0.53)^2 - (0.87)^2)} \right]} \ ,$$

$$R_{\phi \ crit} = (1.64)(1.46) = 2.40 \ .$$

(b) $M_{\phi b} > M_{\phi n}$ (2.54 > 1.94) and $\sigma_{\phi b} > \sigma_{\phi n}$ (0.87 > 0.53).
Hence from Table 5-1 this is Case I.

(c) $R_{\phi \ crit}$ is the best estimate of the overfill ratio.
This project requires 2.40 cubic yards of fill of this
borrow material to satisfy each cubic yard demanded by
the project dimensions.

* *

* * * * * * * * * * * * * * EXAMPLE PROBLEM * * * * * * * * * * * * * * *

GIVEN: Composite native beach material phi parameters

$$\phi_{84} = 3.10 \ ,$$

$$\phi_{16} = 1.86 \ .$$

Composite borrow material phi parameters

$$\phi_{84} = 3.25 \ ,$$

$$\phi_{16} = 0.17 \ .$$

FIND:

(a) R_ϕ *crit*

(b) Applicable case for computing overfill ratio

(c) Interpreted overfill ratio

SOLUTION:

(a) Using Equation 5-3

$$M_\phi = \frac{\phi_{84} + \phi_{16}}{2},$$

$$M_{\phi n} = \frac{3.10 + 1.86}{2} = 2.48 \ (0.179 \text{ mm}),$$

and

$$M_{\phi b} = \frac{3.25 + 0.17}{2} = 1.71 \ (0.306 \text{ mm}).$$

Using Equation 5-2

$$\sigma_\phi = \frac{\phi_{84} - \phi_{16}}{2},$$

$$\sigma_{\phi n} = \frac{3.10 - 1.86}{2} = 0.62,$$

and

$$\sigma_{\phi b} = \frac{3.25 - 0.17}{2} = 1.54.$$

Using Equation 5-1

$$R_{\phi \ crit} = \frac{\sigma_{\phi b}}{\sigma_{\phi n}} e^{-\left[\frac{\left(M_{\phi n} - M_{\phi b}\right)^2}{2\left(\sigma_{\phi n}^2 - \sigma_{\phi b}^2\right)}\right]},$$

$$R_{\phi \ crit} = \frac{1.54}{0.62} e^{-\left[\frac{(2.48 - 1.71)^2}{2\left[(0.62)^2 - (1.54)^2\right]}\right]},$$

$$R_{\phi \ crit} = (2.48) \ (1.16) = 2.88.$$

(b) $M_{\phi b} < M_{\phi n}$ and $\sigma_b > \sigma_n$ Using Table 5-1, this is Case II.

5-18

(c) Overfill ratio is less than 2.88. It is expected that project
     demands will be met with *less than* 2.88 cubic yards of borrow
     for each cubic yard of fill needed.

* *

As indicated previously, this procedure involves the procurement of
core borings in the borrow area and samples from the beach and nearshore
zones, and size analyses of all borings and samples. Readily available
sources of borrow material have frequently been in bays and lagoons where
the material is finer than the native beach material. In such cases, a
required volume of borrow material several times the needed in-place
volume on the beach would not be uncommon. Because of less availability
of bay and lagoon material, and ecological considerations in its use,
future planning is looking toward the use of offshore sources of fill
material. Since the source of borrow material will control the cost of
a beach fill to a major degree, evaluation of the required volume of
material from available areas is an important factor in economic design.
Ecological considerations in the borrow area are also important.

5.333 Berm Elevation and Width. Beach berms are formed by the deposit
of material by wave action. The height of a berm is related to the cyclic
change in water level, normal foreshore and nearshore slopes, and the wave
regime. Some beaches have no berms; others have one or several. Figure
A-1 of Appendix A illustrates a beach zone with two berms. The lower berm,
the natural or normal berm, is formed by the uprush of normal wave action
during the ordinary range of water-level fluctuations. The higher berm,
or storm berm, is formed by wave action during storm conditions. During
most storms the water level will be higher than normal on the beach.
Wave overtopping may completely obliterate the normal beach berm, if over-
topping lasts long enough. The degree of protection to the backshore
depends greatly on the effectiveness of the storm berm. Beach berms must
be given careful consideration in the planning of a beach fill. If a beach
fill is placed to a height lower than the natural berm crest, a ridge will
form along the crest, and high water and high waves may overtop the berm
crest causing ponding and temporary flooding of the backshore. Such flood-
ing, if undesirable, may be avoided by filling the berm to a height slightly
above the natural berm crest. Several alternative techniques may be em-
ployed to estimate the height of the berm for design purposes. (See
Section 7.2 WAVE RUNUP, OVERTOPPING AND TRANSMISSION.) If a beach exists
at the site, the natural berm crest height can be measured, and an estimate
of future berm elevations can be made. An estimate also may be made by
comparison with other sites with similar exposure characteristics (waves
and tides) and beach material. If enough wave data (either developed from
synoptic surface weather charts or actual records) are available and appli-
cable to the project site, these data may be applied to the relationships
of wave runup, given by Savage (1959) which are discussed in Section 7.2,
to establish an estimated design berm crest height.

Criteria for specifying berm width depend upon several factors. If
the purpose of the fill is to restore an eroded beach to protect backshore

improvements from damage by major storms, the width may be determined as the protective width which has been lost during storms of record plus the minimum required to prevent wave action from reaching improvements. Where the beach is used for recreation, justification for the increased width of the beach may be governed by the area required for recreational use. The current (1972) U.S. Government standard is 75 square feet of dry beach per bather. Where the beach fill serves as a stockpile to be periodically replenished, the berm should be wide enough to provide for expected recession during the intervals between replenishment operations.

5.334 Slopes. The toe of a stockpile of beach material should not extend so deep that material on the surface of the stockpile would not be moved alongshore in sufficient quantities by wave action. There is no firm specification for this maximum depth, but depths of about 30 feet below low-water datum on seacoasts and about 20 feet on the Great Lakes are appropriate. The initial slope of any beach fill will naturally be steeper than that of the natural profile over which it is placed. Subsequent behavior of the slope depends upon the characteristics of the fill material and the nature of the wave climate. In practice, the initial fill slope is designed parallel to the local or comparable natural beach slope above low-water datum. The design of the slope should be determined after careful investigation of all pertinent data from low-water datum to about the 30-foot depth. The design slope is derived through synthesis and averaging of existing data within and adjacent to the problem area, and is usually significantly flatter than the foreshore slope. Design slopes based on such data are usually in the range of 1:20 to 1:30 from low-water datum to the intersection with the existing bottom. However, they are used for computation of quantities only. It is unnecessary and usually impracticable to grade beach slopes artificially below the berm crest since they will be shaped naturally by wave action. Fills placed to a desired berm width but with steep initial slopes will quickly adjust to a natural slope, narrowing the berm and leaving the impression that much of the fill has been lost, although it has only moved to establish the natural slope.

5.335 Feeder Beach Location. Dimensions of a stockpile or feeder beach are generally governed primarily by economic consideration involving comparisons of costs for different replenishment intervals. Therefore, planning a stockpile location must generally be considered in conjunction with stockpile dimensions. If the problem area is part of a continuous and unobstructed beach, the stockpile is located at the updrift end of the problem area. Until the stockpile material is transported by littoral forces to the beach zone downdrift of the stockpile location, that beach zone may be expected to recede at the same rate as determined from historical survey data. If economically justified, stockpiles may be placed at points along the problem area. Such placement decreases the time interval between stockpile placement and complete nourishment of the area. Stockpile lengths from a few hundred feet to a mile have been employed successfully. If the plan involves a feeder beach just downdrift from a coastal inlet, wave refraction and inlet currents must be considered to locate the feeder beach so that a minimum of material is

lost into the inlet. A supplementary structure (as a groin) may be needed
to reduce material movement into the inlet caused by either tidal currents
or change in longshore transport.

The nearly continuous interception of littoral materials on the up-
drift side of an inlet and mechanical transportation of the materials to
a point on the downdrift shore (sand bypassing) constitutes a form of
stockpiling for artificial nourishment to the downdrift shore. In this
type of operation, the stockpile or feeder beach will generally be small
in size as the stockpile material will be transported downdrift by nat-
ural forces at a rate about equal to or greater than the rate of deposi-
tion. For the location of the stockpile or feeder beach for this type
of operation, see Section 6.5, SAND BYPASSING. The need for a jetty or
groin between the stockpile or feeder beach and the inlet to prevent
return of the material to the inlet must be evaluated where such struc-
tures do not already exist.

5.4   SAND DUNES

5.41   FUNCTIONS

Sand dunes are an important protective formation. The dune ridges
along the coast bar the movement of storm tides and waves into the area
behind the beach. Dunes prevent storm waters from flooding the low in-
terior areas. Dune ridges farther inland also protect, but to a lesser
degree than foredunes. Well-stabilized inland ridges are a second line
of defense against water erosion should the foredunes be destroyed by
storms. Use of native vegetation may be desirable to stabilize dune sand
that might migrate over adjacent areas and damage property. (See Figure
5-4.) Stabilizing dunes also prevents the loss of their protection. At
locations with an adequate natural supply of sand, and which are subject
to inundation by storms, a belt of dunes can provide protection more
effectively at a lower cost than a seawall. (See Section 6.4, SAND DUNES.)

Sand dunes near the beach not only protect against high water and
waves, but also serve as stockpiles to feed the beach. Sand accumulating
on the seaward slope of a dune will extend or build the dune toward the
shoreline. This sand, once in the dune, may be returned to the beach by
a severe storm and thus nourish the beach. Figure 5-5 is a schematic
diagram of storm wave attack on the beach and dune. As shown, the initial
attack of storm waves is on the beach berm fronting the dune. When the berm
is eroded waves attack the dune. If the wave attack lasts long enough, the
dune can be overtopped by waves with resultant lowering of the dune crest.
Much of the sand eroded from the berm and dune is transported directly
offshore and deposited in a bar formation. This process not only helps
to dissipate incident wave energy during a storm, but offshore deposits
will normally be transported back to the beach by swells after the storm.
Onshore winds transport the sand from the beach toward the foredune area
and the dune building proceeds on another natural cycle. This dune build-
ing, however, is generally at a very slow rate unless supplemented by
fences or vegetation.

5-21

High, well-stabilized barrier dune

Migration of unstabilized dune across a road

Figure 5-4. Stabilized and Migrating Dunes
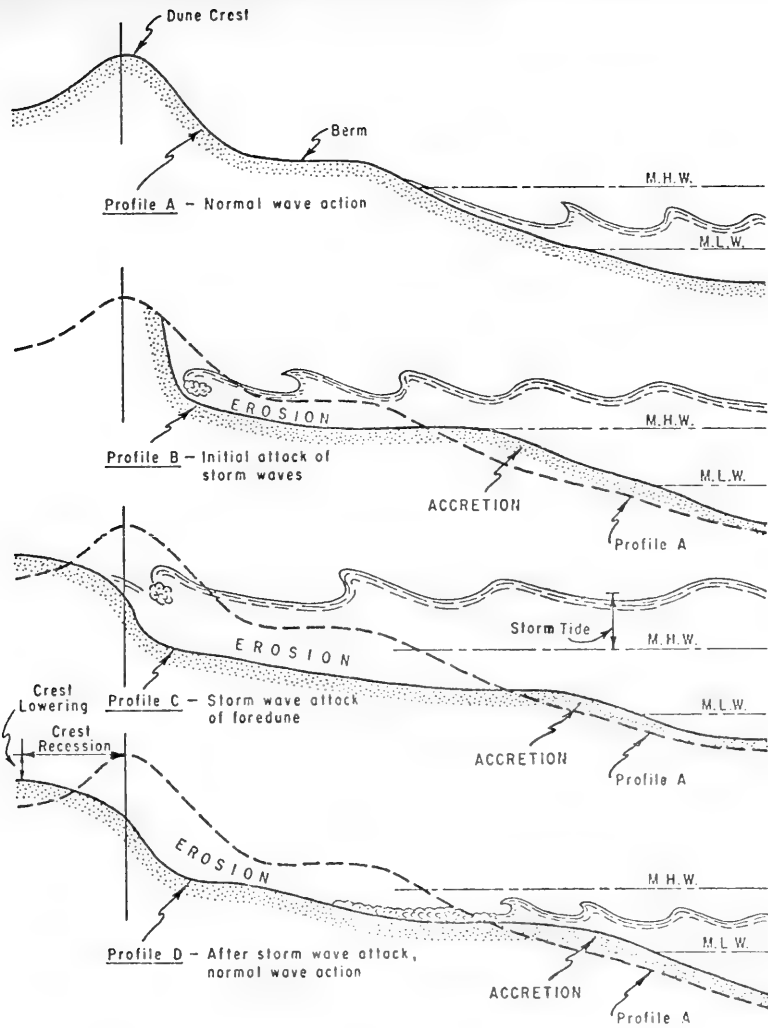
Figure 5-5. Schematic Diagram of Storm Wave Attack on Beach and Dune

5.5   SAND BYPASSING

5.51   GENERAL

An inlet is a short narrow waterway connecting the sea or major lake with interior waters.   Inlets, either natural or improved to meet navigation requirements, interrupt sediment transport along the shore. Natural inlets have a well-defined bar formation on the seaward side of the inlet.   A part of the sand transported alongshore ordinarily moves across the inlet by way of this outer bar - natural sand bypassing.   However, the supply reaching the downdrift shore is usually intermittent rather than regular, and the downdrift shore is usually unstable for a considerable distance.   If the tidal flow through the inlet into the interior body of water is strong, part of the material moving alongshore is carried into and permanently stored in the interior body of water as a middleground shoal, reducing the supply available to nourish downdrift shores.   The outer bar normally migrates with a migrating inlet, but the middleground shoal does not.   Thus the middleground shoal increases in length as the inlet migrates, and the volume of material stored in the inlet increases.

When an inlet is deepened by dredging, through the outer or inner bars or through the channel, additional storage capacity is created to trap available littoral drift, and the quantity which would naturally pass the inlet is reduced.   If the dredged material is deposited in deep water or beyond the limits of littoral currents, the supply to the downdrift shore may be nearly eliminated.   The resulting erosion is proportional to the reduction in rate of supply.

An often-used method of inlet improvement has been to flank the inlet channel with jetties or breakwaters.   These structures form a barrier to longshore transport of littoral drift.   Jetties have one or more of the following functions: to block the entry of littoral drift into the channel, to serve as training walls for inlet tidal currents, to stabilize the position of the navigation channel, to increase the velocity of tidal currents and flush sediments from the channel, and to serve as breakwaters to reduce wave action in the channel.   Where there is no predominant direction of longshore transport, jetties may stabilize nearby shores, but only to the extent that sand is impounded at the jetties.   The amount of sand available to downdrift shores is reduced, at least until a new equilibrium shore is formed at the jetties.   Usually, where longshore transport predominates in one direction, jetties cause accretion of the updrift shore and erosion of the downdrift shore.

Stability of the shore downdrift from inlets, with or without jetties, may be improved by artificial nourishment to make up the deficiency in supply due to storage in the inlet.   When such nourishment is done mechanically by using the available littoral drift from updrift sources, the process is called sand bypassing.

Types of littoral barriers (jetties and breakwaters) which have been generally employed in connection with inlet and harbor improvement are

shown on Figure 5-6. Where littoral transport predominates in one direction, any of these types would cause accretion to the updrift shore and erosion of the downdrift shore, unless provision is made for sand bypassing.

At a jettied inlet, Figure 5-6 (Type I), bypassing can normally be performed best by a land-based dredging plant or land vehicles. A floating plant can be used only where the impounding zone is subject to periods of light wave action, or by breaking into the landward part of the impoundment and dredging behind the beach berm thus leaving a protective barrier for the dredge. Such an operation was performed at Port Hueneme, California, in 1953 (See Section 6.5 SAND BYPASSING.) In any of the types of operations at such a jettied inlet, it is unlikely that bypassing of all of the littoral drift can be attained, and some material will pass around the updrift jetty into the channel, especially after the impounding capacity of the jetty has been reached.

To ensure more complete bypassing of the littoral drift, the combination of the jettied inlet and offshore breakwater, Figure 5-6 (Type II), was developed. In this design, a floating plant works effectively, completely protected by the breakwater and nearly all of the sand moving inshore of the offshore breakwater is bypassed. Practically no shoaling of the channel by sand would be expected. Although this type is considered the most effective type of improvement for both navigation and sand bypassing, it is also normally the most costly.

The shore-connected breakwater with impoundment at its seaward end, Figure 5-6 (Type III), has been used effectively. Bypassing is performed by a floating plant, although heavy wave action could cause delays when the outer portion of the impoundment is being removed. Nearly all of the sand transported alongshore would be bypassed, either naturally or mechanically, but some shoaling of the navigation channel is likely between dredging operations.

The shore-connected breakwater or jetty with a low sill or weir and impounding zone or deposition basin behind the breakwater, Figure 5-6 (Type IV), was designed in an effort to provide for bypassing of the littoral drift moving inshore of the seaward end of the weir by a floating plant, thus not permitting any of that part of the littoral drift to shoal the navigation channel. Although weir jetties have been constructed at three inlets and partly installed at another inlet, none of them has been in operation long enough to provide complete assurances concerning their performance. A successful bypassing operation at Hillsboro Inlet, Florida, (Hodges, 1955), where a basin behind a natural rock ledge is dredged periodically, formed the basis of this design.

5.52 METHODS

Several techniques have been employed for mechanically bypassing sand at inlets. Sometimes a combination of techniques has proved to be most practicable and economical. The basic methods are: land-based dredging plants, floating dredges, and land-based vehicles.

TYPE I. JETTIED INLET

TYPE II. JETTIED INLET AND OFFSHORE BREAKWATER

TYPE III. SHORE CONNECTED BREAKWATER
(Impounding Zone at Seaward End of Breakwater)

TYPE IV. SHORE CONNECTED BREAKWATER
(Impounding Zone at Shoreward End of Breakwater)
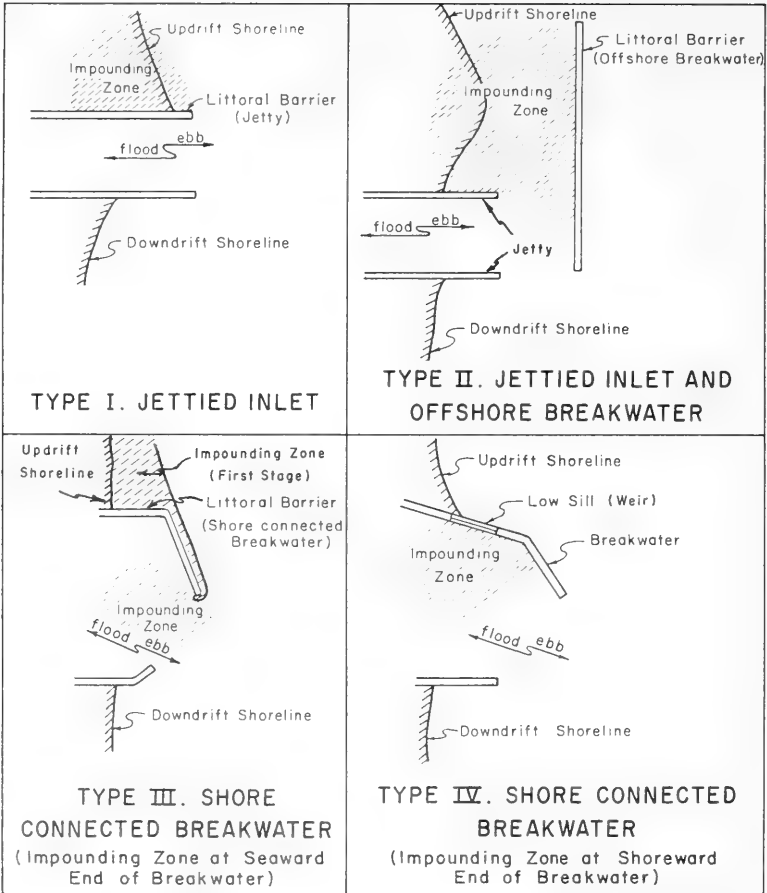
(Watts, 1965)

Figure 5-6.   Types of Littoral Barriers where Sand-Transfer Systems have been Employed

5.521 Land-based Dredging Plants.

a. Plant Considerations. This type of operation usually employs a dredging plant at a fixed position near the beach from which the sand transported alongshore is intercepted as it moves within reach of the plant. Presently, plants are of the pump type and operate basically as an ordinary suction dredge. Plants are positioned on an existing structure; however some are on an independent foundation. Moveable plants located on a pier with capability of dredging along the length and on both sides of the pier have been proposed, but none has been built to date. Such a plant would have a much larger littoral reservoir or deposition basin to accumulate the littoral drift during storm periods when the rate of transport exceeds the pumping capacity of the plant. A plan, using an eductor and pumps located in an impoundment area updrift of an inlet and capable of being moved within that area, is a possible method of bypassing for large-scale operations. Although not used for that purpose, an operation of this nature was used at Los Angeles (El Segundo), California, to level ancient dunes well behind the shoreline and transport the sand to the beach.

Shore processes at a littoral barrier must be studied critically to design and position a fixed bypassing plant. The average annual rate of longshore transport moving to the barrier must be known. This annual rate will normally be the controlling criterion for determining the capacity of the pumping plant. The average annual impoundment of littoral materials by the littoral barrier is equal to the minimum quantity that must be supplied to the downdrift shores to achieve stability. Short-term fluctuations of the actual rate of littoral material movement to the barrier as on an hourly, daily, or weekly basis may be many times greater or less than the estimated annual rate reduced arithmetically to an hourly, daily, or weekly basis. Therefore, even though a bypassing plant may be designed to handle the total amount of drift reaching a barrier on an annual basis, there will be occasions during the year when the quantity of sand reaching the barrier will greatly exceed the pumping capacity of the plant and occasions when the plant may operate well below capacity due to an insufficiency of material reaching the barrier.

To establish design criteria, a detailed study must be made of the beach profile updrift of the littoral barrier to determine the best location for the plant along the profile. A comparison of foreshore profiles over a period of time will aid in predicting the future position of the foreshore and allow a determination of the best position of the plant. Location of the plant too far landward may result in a *land-locked* plant when the rate of transport reaching the barrier in a short interval of time exceeds the plant's pumping capacity. Such a location may also result in large losses of material around the barrier. A location too far seaward may result in ineffective operation until sufficient materials have been impounded by the barrier and are within reach of the intake mechanism. The disadvantage of the fixed position plant has led to consideration of a movable dredging unit on a trestle with the capability of dredging a long deposition reservoir on both sides. This would increase the capacity

of the littoral reservoir and reduce the possibility of land-locking the plant. Mobility of a land-based dredging plant may overcome some deficiencies of a fixed plant, but this has not been demonstrated in field installations. It seems unlikely that such a mobile plant would be able to bypass all material when the rate of arrival at the site is high. Therefore, some material would be lost around the barrier.

b. Discharge Line Considerations. The best alignment of the discharge line from the fixed plant to the downdrift side of the littoral barrier or inlet is controlled by local conditions. The discharge line must traverse a channel maintained for vessel traffic, and a floating discharge line is impracticable. If the line is positioned on the channel bottom, allowance must be made for protection of the line against damage by pitching ships and by maintenance dredging of the channel. Also, a submerged line may need a special flushing system designed to keep the line from clogging when the pumps are shut down.

The point of discharge on the downdrift side of the littoral barrier may be of critical importance. The discharge point is not critical in an area with unidirectional longshore transport. However, in areas with transport reversals, some of the material at the point of discharge is transported back toward the littoral barrier or into the inlet during periods of transport reversal. This should be kept to a minimum to reduce channel maintenance, and, where transport reversals occur, a detailed study must be made of the distribution of littoral forces downdrift of the barrier. Tidal currents toward the inlet may frequently predominate over other forces and produce a strong movement of material toward the downdrift jetty, or into the inlet particularly if no downdrift jetty is included in the plan. In this case, the best discharge point will be a point on the shore just beyond the influence of the downdrift jetty and littoral forces tending to move material in an updrift direction. Establishment of this point requires the use of statistical wave data, wave refraction and diffraction diagrams, and data on nearshore tidal currents. If such currents are present, they may sometimes dominate the littoral processes immediately downdrift of the littoral barrier. Alternative points of discharge nearer the barrier may also be considered, using groins to impede updrift movement of material at the discharge point. Such alternative considerations are of value in determining the most economical discharge point.

5.522 Floating Dredges. The operation of floating dredges may be classified in two general categories, hydraulic and mechanical. Hydraulic dredges include the suction pipeline dredge with plain suction or with cutter-head for digging in hard material, and the self-propelled hopper dredge. Mechanical types include the dipper and bucket dredges.

The pipeline dredges employ a discharge pipeline to transport dredged material to the point or area of placement. Booster pumps may be used in this line if required by distance to discharge point. The standard hopper dredge, although its bins are filled hydraulically, usually discharges by dumping the dredged material out of the bottom of the bins. This type of

dredge requires disposal areas with enough depth to allow dumping. The hopper dredge is not suitable for bypassing operations unless it discharges in an area where the material may be rehandled by another type of dredge or is equipped to pump the material ashore. Since about 1960, a number of hopper dredges have been equipped to pump the material from their bins; thus the hopper dredge has greatly increased in importance in bypassing operations.

Mechanical dredges require auxiliary equipment (such as dump scows, conveyors and eductors) to transport material to the point of placement. Equipment and techniques are continually being improved in the transportation of sand; therefore, incorporating a mechanical-type dredge to bypass material may be most favorable in some cases. In considering a floating dredge for a bypassing operation, each type of dredge plant must be evaluated. This evaluation should include: first, the feasibility of using various types of floating dredges; second, the operational details; and finally, the economics to determine which floating plant will transfer the material at the least unit cost. Local site conditions will vary, and factors to be considered for each type of floating plant cannot be standardized. Some of the more important factors to evaluate follow:

a. Exposure of Plant to Wave Action. Wave action limits the effective operation of a floating dredge; the exact limitation depends on plant type and size, and intensity of wave action. This factor is particularly critical if the dredge will be exposed to open waters where high waves may be expected. No standard criteria are available for the maximum permissible wave action for operation of various types of dredges. Such data must be obtained from dredge operators who are familiar with the dredge plant and the area in question. However, as mentioned in Section 6.3 PROTECTIVE BEACHES, a specially designed pipeline dredge has been used successfully at Malaga Cove (Redondo Beach), California, for pumping sand to the beach from offshore in an exposed location. Hopper dredges may be operated in higher waves than the other types of floating dredge plants. Pipeline dredges exposed to hazardous wave action are subject to damage of the ladder carrying the suction line, breakage of spuds, and damage of the pontoon-supported discharge pipe. Thus, estimates must be made of the probable operational time with and without manmade structures or natural ground features to protect the dredge and auxiliary equipment. Determination of the time of year when least wave action will prevail will allow estimates to be made for plant operation under the most favorable conditions. Also, protection of the plant during severe storms in the area of the project must be considered.

b. Plant Capacity. Use of a floating dredge of a specific capacity is generally controlled by economic consideration. If the impounding zone of a littoral barrier is large, a periodic bypassing operation may be considered in which a large plant is scheduled and utilized for short periods of time. An alternative would be the use of a small-capacity plant for longer periods of time. If long pumping distances to the discharge point necessitate too many booster pumps, a larger plant may provide most economical operation. The choice sometimes depends on availability of plant equipment.

c. Discharge Line. See Section 5.521-b.

5.523 Land-Based Vehicles. Local site conditions may favor the use of wheeled vehicles for bypassing operations. Typical factors to be considered and evaluated would be the existence or provision of adequate roadways and bridges, accessibility to the impounding zone by land-based equipment, the volume of material to be bypassed and the time required to transport the material. Factors involved in locating deposition areas are also the same as discussed in Section 5.521-b.

5.53 LEGAL ASPECTS

The legal consequences stemming from any considered plan of improvement are many and complex. Legal problems will vary dependent upon the physical solution employed as well as the jurisdiction in which construction is to occur. The complexities of the legal problems are due not so much to the fact that legal precedent will differ from jurisdiction to jurisdiction, but rather from the application of any given factual setting to a particular body of law. It should also be noted that insofar as the Federal Government is concerned, liability for personal or property damage will be determined by reference to the Federal Tort Claims Act.

Where there is an accumulation at an inlet, whether due to an existing jetty system or as a result of natural action, and where it is desirable to transfer some of that material to the downdrift beach by whatever method is most feasible, it does not follow that any agency - Federal, State or local - has the right to make the transfer. The accreted land is not necessarily in the public domain. In at least one case in the State of New Jersey, for example, it was decided that an accumulation (although clearly due to an existing inlet jetty system) was owned by the holder of the title to the adjacent upland. The court stated that "gradual and imperceptible accretions belong to the upland owners though they may have been induced by artificial structures."

The phrase "gradual and imperceptible accretions" is open to legal determination since it would be unusual for one to stand on a beach and clearly see an accretion taking place. Accretion might be detected by surveys at intervals of a month or more. Thus, any agency contemplating bypassing must consult the local legal precedent.

At an inlet employing a weir jetty and a deposition basin, updrift accretion may be uncertain. If the weir so interferes with littoral transport that it causes the beach initially to fill to the elevation of the top of the weir, it is conceivable that there will be a gradual advance of beach elevations well above the elevation of the weir. This will cause movement of material over the weir to decrease, and there will be accretion for some distance updrift of the jetty with consequent legal questions concerning ownership. As impairment of movement over the weir reduces effectiveness of bypassing, it will be desirable to take steps to restore the efficiency of the weir. Such action will inevitably result in loss of updrift accretions, and again legal considerations may arise.

If the deposition basin in the lee of an offshore breakwater is not cleared of accumulations regularly, it is possible that continuing accretion may ultimately produce land from the former shoreline out to the breakwater. Resumption of bypassing operations may then require ownership determination.

Legal considerations may even arise on the downdrift beach receiving bypassed sand despite the obvious advantages to most property owners. Another case involved a pier used for fishing, located on a beach that had been artificially nourished. Before this work was commenced, water of adequate depth existed for fishing, but after beach nourishment was commenced, depths decreased along the pier to such an extent that fishing was greatly impaired. The owner then brought suit seeking payment for the loss of value to his pier.

It is not the purpose here to set forth a comprehensive discussion of the legal problems encountered in connection with sand bypassing. The above discussion is merely to alert the planner that such problems do arise, and it is therefore prudent to seek legal counsel at the earliest stages of project formulation.

5.6   GROINS

5.61   INTRODUCTION

The groin is probably the type of structure most widely used for shore protection purposes; yet the detailed operation of the groin is poorly understood. Groins or groin systems in many locations have achieved the intended purpose. In other locations, only negligible benefits have resulted, or damaging recession of the downdrift shoreline has been caused, even when groins were apparently successful in accomplishing the design objective. Failures can be traced to a lack of understanding of the functional design of groins and the littoral processes to which the structures are subjected.

5.62   DEFINITION

A groin is a shore protection structure designed to build a protective beach or to retard erosion of an existing or restored beach by trapping littoral drift. Groins are usually perpendicular to the shore and extend from a point landward of predicted shoreline recession into the water far enough to accomplish their purpose. Groins are narrow, and vary in length from less than 100 feet to several hundred feet. Since most of the littoral drift moves in the zone landward of the normal breaker zone (for example about the 6-foot contour on the Atlantic coast), extending a groin seaward of that depth is generally uneconomical. The normal breaker zone for the Gulf coast and less exposed shores of the Great Lakes ranges from 3- to 4-foot depths; more exposed shores of the Great Lakes approach the 6-foot depth. The Pacific coast ranges from 7- to 10-foot depths depending on exposure.

Groins may be classified as permeable or impermeable, high or low, long or short, and fixed or adjustable. They are constructed of timber, steel, stone, concrete, or other materials. Impermeable groins have a solid or nearly solid structure which prevents littoral drift from passing through the structure. Permeable groins have openings through the structure big enough to permit passage of significant quantities of littoral drift. Some permeable stone groins are made impermeable by heavy marine growth. A series of groins acting together to protect a long section of shoreline is called a groin system or groin field.

Groins differ from jetties structurally and functionally. Jetties are larger with more massive components, and are used primarily to direct and confine the stream or tidal flow at the mouth of a river or inlet, and to prevent littoral drift from shoaling the channel.

5.63 PURPOSE

The purpose of groins is to provide or maintain a protective or recreational beach. Groins may be used to:

(a) Build or widen a beach by trapping littoral drift;

(b) Stabilize a beach, subject to excessive storms or seasonal periods of advance and recession, by reducing the rate of loss;

(c) Reduce the rate of longshore transport out of an area by re-orienting a section of the shoreline to an alignment more nearly perpendicular to the predominant wave direction;

(d) Reduce losses of material out of an area by compartmenting the beach, usually a relatively short section of beach artificially filled seaward of adjacent shores; and

(e) Prevent accretion in a downdrift area by acting as a littoral barrier.

These ends are attained by reducing the longshore transport rate which decreases the quantity of drift reaching downdrift shores. This can lead to the need for downdrift extension of the system or for artificially nourishing the downdrift shore, unless the system is artificially filled initially and suitably renourished.

5.64 TYPES OF GROINS

5.641 Permeable Groins. Permeability helps avoid the abrupt offset in shore alignment found at impermeable groins. Part of the littoral forces and materials pass through the groin, and induce sand deposition on both sides of the groin. Many types of permeable groins have been employed. The degree of permeability above the ground line affects the pattern and amount of deposition within the limits of the groin's influence. Insufficient empirical data have been compiled to establish quantitative relationships between littoral forces, permeability, and resulting shore behavior.

Until such data are available to develop a functional design of permeable groins similar to that in Sections 5.65 through 5.68 for impermeable groins, evaluation and design of permeable groins will be inexact. In general, the desired degree of sand passing the groin can be achieved as effectively and economically by appropriate design of groin height and length, or by notching or lowering the groin on the shore end. Permeable groins are not normally used to retain fill placed to restore or widen a beach. Permeable groins are used in rich-drift areas to widen or prevent recession of specific beach areas and to reduce scalloping (saw-tooth shape) of the shoreline.

5.642 High and Low Groins. The amount of sand passing a groin partly depends on the height of the groin. Groins based where it is unnecessary or undesirable to maintain a sand supply downdrift of the groin, may be built high enough to completely block sand moving in the zone influenced by the groin. Such groins are called *terminal groins*. Where it is necessary to maintain a sand supply downdrift, the groin may be built low enough to allow overtopping by storm waves, or by waves at high tide. Such low groins serve a purpose similar to that of permeable groins.

5.643 Adjustable Groins. Nearly all groins are permanent, fixed structures. However, in England and Florida, adjustable groins have been used. These groins consist of removable panels between piles. These panels can be added or removed to maintain the groin at a specific height (usually 1 to 2 feet) above the beach level, thus allowing a part of the sand to pass over the groin and maintain the downdrift beach. However, if these structures undergo even slight movement and distortion, removal or addition of panels becomes difficult or even impossible.

5.65 GROIN OPERATION

A groin is a barrier to sand moving in the zone between its seaward end and the limit of uprush. Height, length, and permeability of the groin determine its effect on longshore transport. The way a groin modifies the littoral transport rate is about the same whether the groin operates singly or as one of a system, provided spacing between adjacent groins is adequate. However a single groin or the updrift groin of a system, may impound less than the other individual groins of a system.

The typical groin, illustrated in Figure 5-7, extends from a point landward of the top of the berm to the normal breaker zone (for instance, the 6-foot depth contour on the Atlantic coast). The predominant direction of wave attack shown by the orthogonals will cause a predominant movement of littoral drift.

The groin acts as a partial dam that intercepts a part of the normal longshore transport. As material accumulates on the updrift side, supply to the downdrift shore is reduced, and the downdrift shore recedes. This results in a progressively steepening slope on the updrift side and a flattening slope on the downdrift side, since both slopes reach a common elevation near the end of the groin. Since the grain size of the beach

material normally increases to establish a steeper than normal slope, the residual accreted material is probably, by selective processes, the coarser fraction of the material that was in transport.

When the accreted slope reaches ultimate steepness for the coarser fraction of available material, impoundment stops, and all littoral drift passes the groin. If the groin is so high that no material passes over it, all transport must be in depths beyond the end of the groin. Because of the nature of transporting currents, the material in transit does not move directly shoreward after passing the groin, and transport characteristics do not become normal for some distance on the downdrift side of the groin. Thus, a system of groins too closely spaced would divert sediment offshore rather than create a widened beach.

The accretion fillet on the updrift side of the groin creates a departure from normal shore alignment, tending toward a stable alignment perpendicular to the resultant of wave attack. The impounding capacity of the groin thus depends on the stability slope and stability alignment of the accretion fillet. These in turn depend upon characteristics of the littoral material and the direction of wave attack.

Figure 5-8 shows the general configuration of the shoreline expected for a system of two or more groins. It assumes a well-established net longshore transport in one direction.

5.66   DIMENSIONS OF GROINS

Groin dimensions depend on wave forces to be withstood, the type of groin, and the construction materials used. The length, profile, spacing of groins in a system, direction of wave approach, and rate of longshore transport are important functional considerations.

The length of a groin is determined by the distance to depths offshore where normal storm waves break, and by how much sand is to be trapped. The groin should be long enough to interrupt enough material to create the desired stabilization of the shoreline or accretion of new beach areas. Damage to downdrift shores must be considered in determining the groin length. For functional design purposes, a groin may be considered in three sections: (a) horizontal shore section, (b) intermediate sloped section, and (c) outer section.

5.661 Horizontal Shore Section. This section extends far enough landward from the desired location of the crest of berm to anchor the groin and prevent flanking. The height of the shore section depends on the degree to which it is desirable for sand to overtop the groin and replenish the downdrift beach. The minimum height for a groin is the height of the desired berm, which is usually the height of maximum high water, plus the height of normal wave uprush. Economic justification for building a groin higher than this is doubtful except for terminal groins. With stone groins, a height about 1 foot above the minimum is sometimes used to reduce passage of sand between large cap stones. The maximum height of a
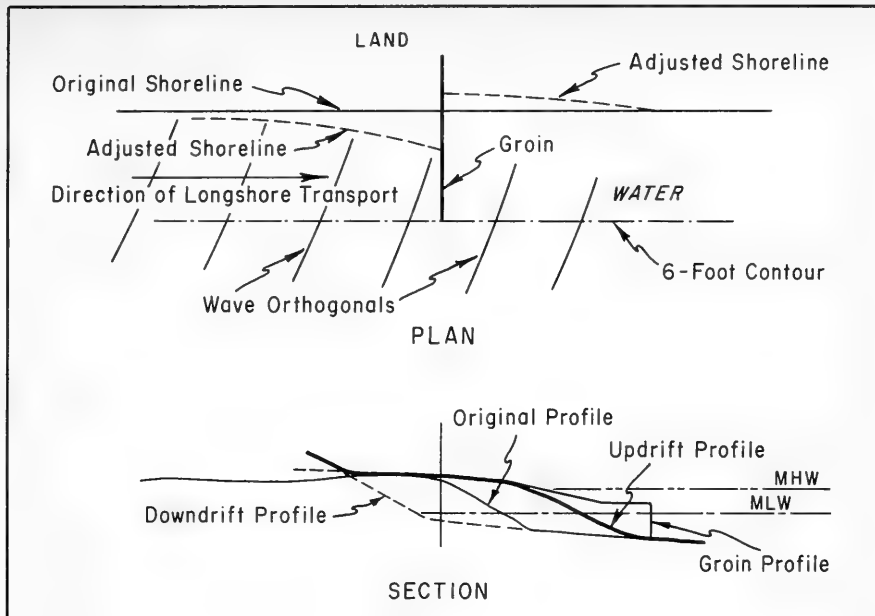
Figure 5-7. Illustration of a Typical Groin
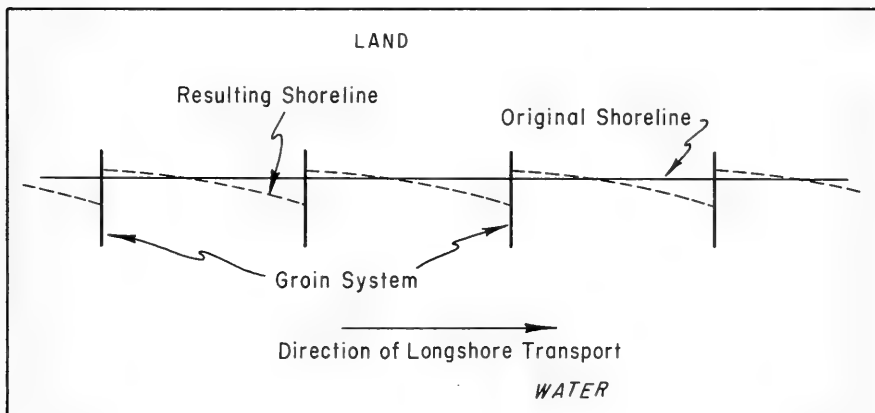
Figure 5-8. General Shoreline Configuration for Two or More Groins

groin to retain all sand reaching the area (a high groin) is the height
of maximum high water and maximum wave uprush during all but the most
severe storms. This section is horizontal or sloped slightly seaward,
paralleling the existing beach profile or the desired slope if a wider
beach is desired or a new beach is to be built.

5.662 Intermediate Sloped Section. The intermediate section extends be-
tween the shore section and the level outer section. This part should
approximately parallel the slope of the foreshore the groin is expected
to maintain. The elevation at the lower end of the slope will usually be
determined by the construction methods used, the degree to which it is
desirable to obstruct the movement of the material, or the requirements
of swimmers or boaters.

5.663 Outer Section. The outer section includes all of the groin extend-
ing seaward of the intermediate sloped section. With most types of groins,
this section is horizontal at as low an elevation as is consistent with
economy of construction and safety, since it will be higher than the de-
sign updrift bottom slope in any case. The length of the outer section
will depend on the design slope of the updrift beach.

5.664 Spacing of Groins. The spacing of groins in a continuous system
is a function of the length of the groin and the expected alignment of
the accretion fillet. The length and spacing must be so correlated that
when the groin is filled to capacity, the fillet of material on the up-
drift side of each groin will reach to the base of the adjacent updrift
groin with a sufficient margin of safety to maintain the minimum beach
width desired or to prevent flanking of the updrift groin. Figure 5-9
shows the desirable resultant shoreline if groins are properly spaced.
The solid line shows the shoreline as it may develop when erosion is at
a maximum at the updrift groin. The erosion shown occurs while the up-
drift groin is filling. At the time of maximum recession, the solid
line is nearly normal to the direction of the resultant of wave approach
and the triangle of recession, a, is approximately equal to the triangle
of accretion, b. The dashed line $m\,n$ shows the stabilized shoreline
that will obtain after material passes the updrift groin to fill the
area between groins and, in turn, commences to pass the downdrift groin.
The fillet of sand between groins tends to become and remain perpendicu-
lar to the predominant direction of wave attack. This alignment may be
quite stable after equilibrium is reached. However, if there is a marked
variation in the direction and intensity of wave attack, either season-
ally or as a result of prolonged storms, there will be a corresponding
variation in the alignment and slope of the shore between groins. Where
there is a periodic reversal in the direction of longshore transport, an
area of accretion may form on both sides of a groin as shown in Figure
5-10. Between groins, the fillet may actually oscillate from one groin
to the other as shown by the dashed lines, or may form a U-shaped beach
somewhere in between, depending on the rate of supply of littoral mate-
rial. With regular reversals in the direction of longshore transport,
the maximum line of recession would probably be somewhat as shown by the
solid line, with the triangular area a plus triangular area c about
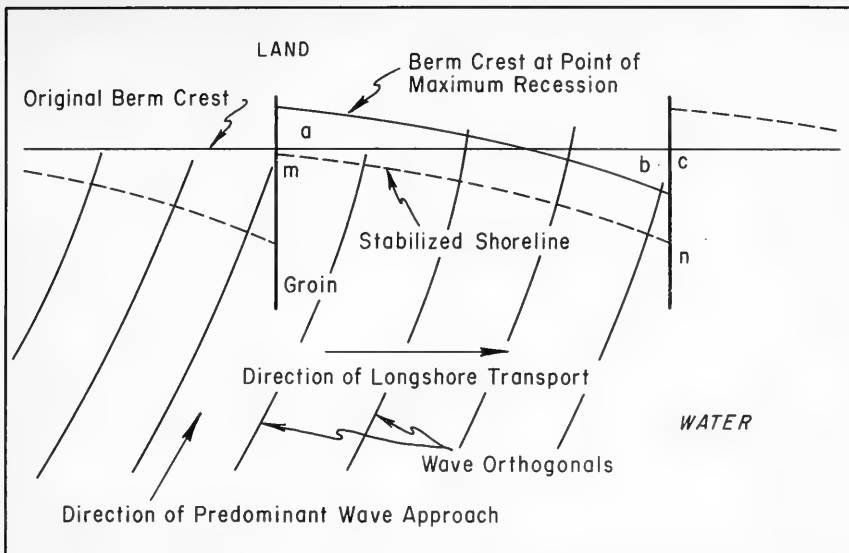
Figure 5-9. Factors in Determining Beach Width Updrift of a Groin
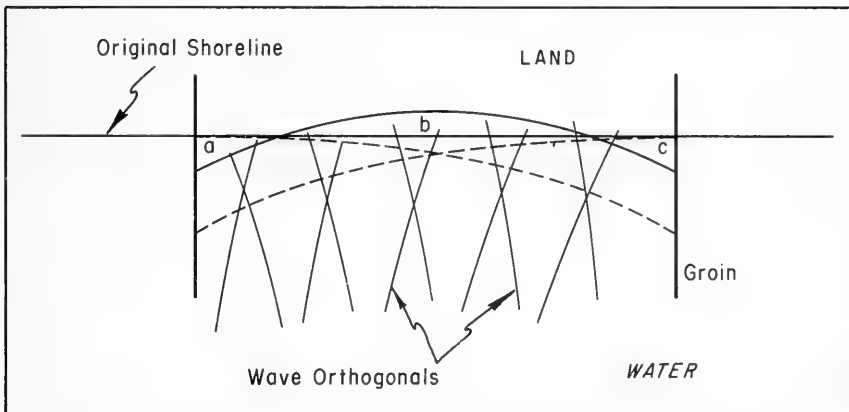
Figure 5-10. Groin System Operation with Reversal of Transport

equal to the circular segment b. The extent of probable beach recession must be taken into account in establishing the length of the horizontal shore section of groin and in estimating the minimum width of beach that may be built by the groin system. *As a guide to the spacing of groins, the following general rule is suggested: The spacing between groins should equal two to three times the groin length from the berm crest to the seaward end.*

5.665 Length of Groin. To determine the horizontal shore and intermediate sloped section shoreline position adjacent to a groin, it is necessary to predict the ultimate stabilized beach profile on each side of the groin. Total length, including the horizontal outer (seaward) section, is based on projected position of the breaking zone for normal waves. The steps involved for a typical groin are:

(a) Determine the original beach profile in the vicinity of the groin.

(b) Determine the direction of longshore transport. (See Section 4.5, Littoral Transport.)

(c) Determine the shape of the accretion fillet by the shape of the average impounded fillet over a sufficient period of time at an existing structure where the shore has similar orientation and exposure. If no such structure is available, an estimate may be made by plotting a refraction diagram for the mean wave condition, i.e., the wave condition which would produce the greatest rate of longshore transport, and drawing the shoreline or berm crest normal to the orthogonals.

(d) Determine the minimum beach width desired updrift of the groin. This may be a width desired to provide adequate recreational area; adequate protection of the backshore area; or with a groin system, adequate width of beach at the next groin updrift to prevent flanking of this groin by wave action. The last condition is shown at point m on Figure 5-9, if line $m\,n$ represents the berm crest of the beach.

(e) The position and alignment of the desired beach relative to the groin under study is indicated by the line $m\,n$, Figure 5-9, the line being constructed approximately to the orthogonals based on mean wave conditions from m to n.

(f) Apply the distance $c\,n$ from Figure 5-9 to Figure 5-11; this distance plus enough length landward of c to prevent flanking, will represent the length of the horizontal shore section.

(g) The slope of the ground line from the crest of the berm seaward to about the mean low water line will depend on the gradation of the beach material and the character of the wave action. This section of groin, the intermediate sloped section, Figure 5-11, is usually designed parallel to the original beach profile. The ground line will assume the slope of the groin section $n\,p$ or a steeper slope if the material trapped is

coarser than the original beach material. The length of the outer section $p\ r$ depends on the amount of littoral drift it is desired to intercept. It should extend deep enough for the new profile $p\ s$ to intercept the old profile $c\ d\ s$ within the toe of the groin.

(h) The final beach profile on the updrift side of the typical groin shown in Figure 5-11 is indicated by the line $c\ n\ p\ s$.

Until the groins are filled, the shoreline on the downdrift side of a groin will be different for an intermediate groin in a system than it will for a single groin or for the farthest downdrift groin in a system. If the system is properly planned and constructed, the shorelines would be about the same for the single and downdrift groins.

Considering first an intermediate groin in a groin system, the maximum shore recession on the downdrift side of the groin would occur before the updrift groins fill. During this time the maximum recession would occur when the shoreline between the intermediate groin and the next downdrift groin has reoriented to a position normal to the predominant wave orthogonals such that area $\underline{a}$ = area $\underline{b}$ in Figure 5-12.

To determine the profile of maximum recession of the downdrift side of the groin, draw the proposed groin on the original beach profile as in Figure 5-12. From the crest of berm at d, lay off distance $f\ d$ taken from Figure 5-12. Draw the foreshore from crest of berm f to datum plane (MLW) parallel to the original beach slope, and connect that point of intersection with the original profile at the seaward end of the groin.

After the line of maximum recession has been reached, as shown by $f\ g$ on Figure 5-12, the shoreline will begin to advance seaward, maintaining its alignment perpendicular to the net wave orthogonals until enough material flows around or over the downdrift groin to produce a stabilized shoreline as shown by the line $m\ n$ in Figure 5-12.

To determine the stabilized downdrift line, see Figure 5-13. From the crest of berm at d, lay off the distance $d\ m$ taken from Figure 5-12. Draw the foreshore slope from the crest of berm f to datum plane (MLW) parallel to the original beach line, then connect that point of intersection with the original profile at the seaward end of the groin.

Considering a single groin or the downdrift groin of a system, the maximum recession that could occur may be determined by assuming that the downdrift area loses an amount equal to the full rate of longshore transport for the period required for the groin to fill to capacity. It is known that a percentage of the total littoral drift moves seaward of the seaward ends of the groins. It is also known that an additional percentage of the material moving shoreward of the seaward ends of the groins will bypass the groin before it is completely filled. Accordingly, to approximate the position of the downdrift ground line, it is believed safe to reduce the net longshore transport by some amount depending on
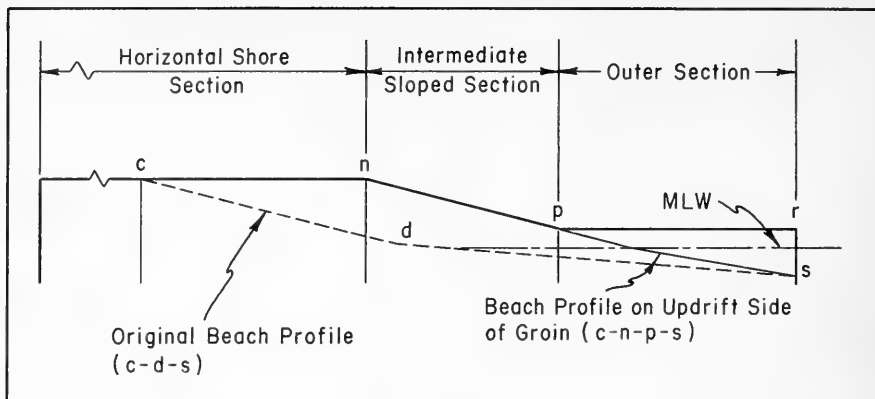
Figure 5-11. Representation of Intermediate Sloped Groin Section
Designed Perpendicular to the Beach
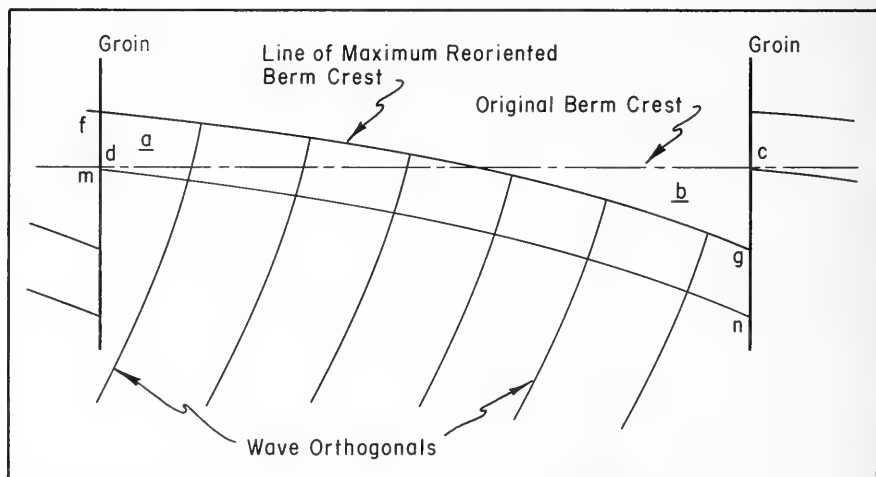
Figure 5-12. Stabilized Shoreline Produced by Material Flowing Over or
Around Downdrift Groin

the type of groin constructed. Percentage of net longshore transport considered conservative for computing downdrift losses due to certain groin types based on the normal breaker zone occurring at the 6-foot depth contour (Atlantic coast) is given as follows:

(a) For high groins extending to a depth of water 10 feet or more, use 100 percent of the total longshore transport.

(b) For high groins extending to a depth of 4 to 10 feet below mean low water (or mean lower low water), or for low groins extending to a depth greater than 10 feet, use 75 percent of the total longshore transport.

(c) For high groins extending from mean low water to 4 feet below mean low water (or mean lower low water), or for low groins extending to a depth less than 10 feet below mean low water, use 50 percent of the total annual rate of longshore transport.

The following steps can now be used to determine the position of the downdrift shoreline or berm crest line:

(a) Estimate the time required for the updrift side of the groin to fill.

(b) Draw receded shoreline, $d\ e$ (Figure 5-14) with an alignment determined for the updrift fillet such that area $d\ e\ c$ in square feet is equal to the volume of littoral material in cubic yards (reduced according to groin type) determined by the time for the groin to fill.

(c) Plot the original bottom profile, and show the groin on this profile as in Figure 5-13. Plot $c\ d$ as the maximum recession to be expected.

This method assumes an erodible bottom and backshore. Wherever a nonerodible substance is encountered, recession would halt at that point. This would also be true where the groins are tied to a seawall or bulkhead. In this case the expected profile seaward of the seawall would be determined as if the seawall were not there or in a similar manner as for scour at a seawall. The position of the bottom where it intersects the seawall would determine the approximate scour to be expected in front of the wall. The deficiency in material would tend to be made up by recession of the shoreline beyond the downdrift end of the seawall.

5.67 ALIGNMENT OF GROINS

Examples may be found of almost every conceivable groin alignment, and advantages are claimed by proponents of each type. Based on the theory of groin operation, which establishes the depth to which the groin extends as the critical factor affecting its impounding capacity, maximum economy in cost is achieved with a straight groin perpendicular to the shoreline. Various modifications such as a *T-* or *L-head* are usually designed with
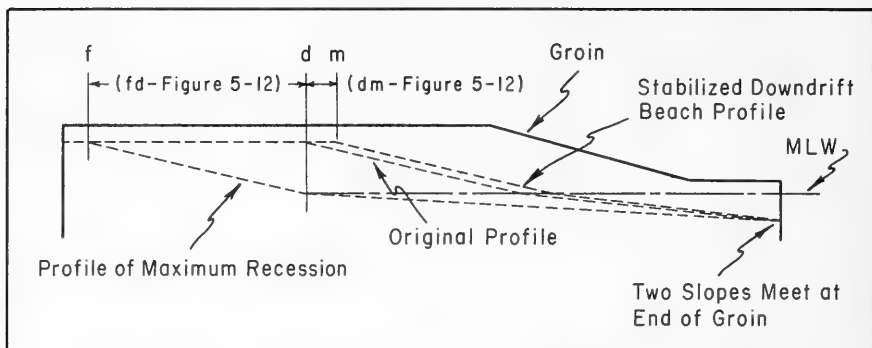
Figure 5-13. Determining Stabilized Downdrift Beach Profile
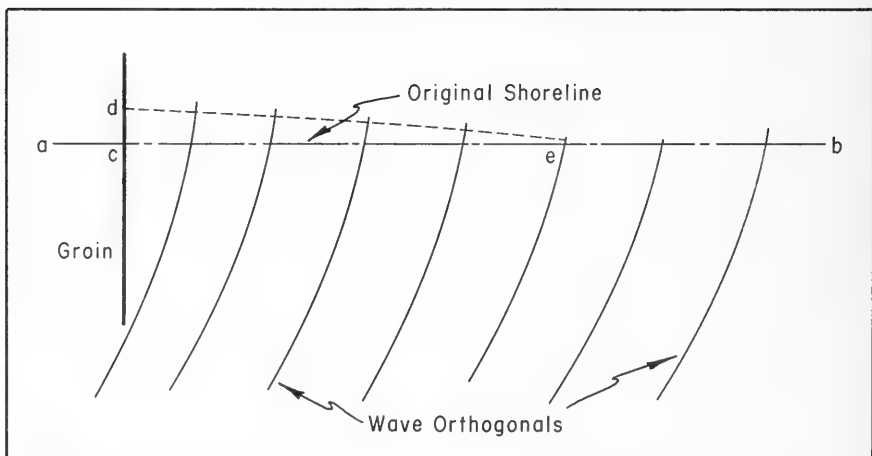
Figure 5-14. Receded Shoreline Assuming an Erodible Bottom and Backshore

the primary purpose of limiting recession on the downdrift side of a groin. While these may achieve the intended purpose, the zone of maximum recession is often simply shifted downdrift from the groin, and benefits are thus limited. Storm waves will normally produce greater scour at the seaward extremities of the *T-* or *L-head* structures than at the end of a straight groin perpendicular to the shore, delaying the return to normal profile after storm conditions have abated.

Curved, hooked, or angle groins have been employed for the same purposes as the *T-* or *L-head* head types. They also invite excessive scour, and are more costly to build and maintain than the straight, perpendicular groin. Where the adjusted shore alignment expected to result from a groin system will differ greatly from the alignment at the time of construction, it may be desirable to align the groins normal to the adjusted shore alignment to avoid angular wave attack on the structures after the shore has stabilized. This condition is most likely to be encountered in the vicinity of inlets and along the sides of bays.

5.68   ORDER OF GROIN CONSTRUCTION

At sites where a groin system is under consideration, two conditions arise:

(a)   The groin system will be filled artificially, and it is desired to stabilize the new beach in its advanced position; and

(b)   Littoral transport is depended upon to make the fill, and it is desired to stabilize the existing beach or build additional beach with a minimum of detrimental effect on downdrift areas.

With artificial fill, the only interruption of longshore transport will be between the time the groin system is constructed and the time the artificial fill is made. For economy, the fill is normally placed in one continuous operation, especially if it is being accomplished by hydraulic dredge. Accordingly, to reduce the time between groin construction and deposition of fill, all groins should preferably be constructed concurrently. Deposition of fill should commence as soon as the stage of groin construction will permit.

When depending on littoral transport no groin can fill until all of the preceding updrift groins have been filled. Any natural filling will reduce the supply to downdrift beaches. The time required for the entire system to fill and the material to resume its unrestricted movement downdrift may be so long that severe damage will result Accordingly, to reduce downdrift damage, only the groin or group of groins at the downdrift end should be constructed initially. The second groin, or group should not be started until the first has filled and material passing around or over the groins has again stabilized the downdrift beach. Although this method may increase costs, it will not only aid in reducing damage, but will also provide a practicable guide to spacing of groins to verify the design spacing.

Because of its limitations, a groin should be used as a major protective feature only after careful consideration of the many factors involved. Principal factors to be considered are:

(a)   The adequacy of natural sand supply to ensure that groins will function as desired.

(b)   Where the supply of littoral drift is insufficient to permit the withdrawal from the littoral stream of enough material to fill the groin or groin system without damage to downdrift areas, artificial placement of fill may be required to fill the groin or groin system and thus minimize the reduction of the natural littoral drift to downdrift shores. As previously mentioned, any groin system will reduce the rate of longshore transport to some degree.

(c)   The adequacy of shore anchorage of the groins to prevent flanking as a result of downdrift erosion.

(d)   The extent to which the downdrift beach will be damaged by a reduction of material supply if groins are used.

(e)   The economic justification for groins in comparison with stabilization by nourishment alone.

Groins are usually considered in areas where the supply of littoral drift is less than the capacity of the littoral transport forces.   In these areas, a shoreline adjustment resulting from the installation of a groin or groin system may not reduce the actual transport rate but result only in a reduction of the expected additional losses from the beach fill within the groin system. However, for this to occur, the groins must extend to the surf zone thereby diverting some of the littoral material to the offshore zone resulting in adverse affects to downdrift beaches.

Where littoral drift supply satisfies the capacity of transporting forces, the adjustment in the shore alinement resulting from a groin system may result in a reduction in capacity of longshore transport forces at the groined site. Thus, less material is transported alongshore than was the case prior to the construction of the groins, and a permanent adverse effect to the downdrift shore would result. Adverse effects on adjacent shores described above are not necessarily a measure of the effectiveness of the groin or groin system since these groins might well have diverted some of the longshore transport to deep water which in turn has deprived the downdrift beach from receiving a full amount of longshore transport and produced the adverse effect (erosion).

5.610   ECONOMIC DETERMINATION OF GROIN CONSTRUCTION   Beaches exposed to wave action constantly change due to variation in wave direction and wave characteristics. In spite of the constant movement of beach materials, a beach will be stable if the rate of loss from an area does not exceed the

rate of supply to that area. If the rate of supply is less than the rate of loss, erosion and recession of the beach will occur. An eroding beach can be restored by artificially placing a protective beach and subsequently stabilized by artificial nourishment, that is artificial placement of sand to make up the deficiency in rate of supply, or by artificial nourishment supplemented by structures (groins) to reduce the rate of loss. Justification of groins must be based on the relative costs of the two methods of shore stabilization.

On long straight beaches, making up the deficiency of supply presumably affects and stabilizes much of the entire reach of shore. A groin system for such a long reach is obviously expensive, but requires less artificial nourishment, especially where nourishment of the shore downdrift of the reach is not required. A method sometimes used for economic determination of such a groin system is to estimate the annual cost of the system, including the annual cost of artificially nourishing the reach with groins and the downdrift shore, to find if this annual cost is less than the estimated annual cost of stabilizing by artificial nourishment alone. No firm guide is available on the reduction in nourishment requirements where a complete groin system is built.

Where the littoral transport rate is high, a groin system will not require artificial nourishment while the groins and offshore area are filling. After filling, no nourishment will be required if the littoral transport rate has not been reduced. The volume required to fill the groin system is easily estimated; the volume required to fill the offshore area, which is equally important, is difficult to estimate. Therefore, the time needed for complete filling is difficult to estimate, but it may take several years for long groins: During this long time, the downdrift shore will erode unless it is artificially nourished. This nourishment volume will be equal to the volume impounded by the groin system and its offshore area plus any deficiency suffered before groin construction. After complete filling and shore realignment at the groin system, the littoral transport rate will probably be reduced from that required during the filling period and the downdrift shores may require more nourishment.

Another approach for economic determination of a groin system for a long reach of shore is to estimate the annual cost as before, and convert this cost to the equivalent quantity of sand that could be placed annually at the estimated cost of sand over the life of the project. This will indicate how much the groins must reduce annual nourishment requirements to be at the *break-even* point. A judgment is then made as to whether the groin system will actually reduce annual nourishment requirements below the *break-even* point. The groin system would be justified only if its costs (including reduced nourishment costs) are less than the costs of artificial nourishment alone.

Where it is necessary to widen a short beach, perhaps 1 mile or less, it becomes impracticable to maintain the increased width by artificial nourishment of that beach alone. The nourishment material would rapidly

spread to adjacent shores, and the desired widening of the beach would not be maintained. Here groins are necessary to stabilize the widened beach within the limited reach. This justification by comparison of the estimated annual costs with and without the groin system is therefore impracticable.

At the downdrift end of a beach, where it is desired to reduce losses of material into an inlet and stabilize the lip of the inlet, a terminal groin is used. Such a groin must often be justified by benefits from the stabilized shore, as no other method of stabilization would be as suitable and available for a comparative cost. Terminal groins should not be long enough to perform the functions of jetties, but should impound only enough littoral drift to stabilize the lip or edge of the inlet.

5.611 LEGAL ASPECTS   The legal considerations discussed previously under Section 5.53 are applicable as well to the construction of groins. Legal problems which arise are varied and often complex, due to the diversity of legal precedent in different jurisdictions and the application of the factual setting to a particular body of law.

Previous sections covering the functional design of groins emphasize the fact that adverse downdrift shore erosion can be expected if the updrift side of the groin is not artificially filled to its impounding capacity at the time of groin construction. Liability for property damage insofar as the Federal Government is concerned will be determined with reference to the Federal Tort Claims Act.

It is therefore incumbent on the owner of groin-type structures to recognize the legal implications of this coastal structure, and to plan, design, construct and maintain the structure accordingly. It is thus prudent to seek legal counsel at the earliest stages of formulation.

5.7   JETTIES

5.71   DEFINITION

A jetty is a structure extending into the water to direct and confine river or tidal flow into a channel, and to prevent or reduce the shoaling of the channel by littoral material. Jetties located at the entrance to a bay or river also serve to protect the entrance channel from wave action and cross currents. When located at inlets through barrier beaches, they also stabilize the inlet location.

5.72   TYPES

In the United States, jetties built on the open coast are generally of rubble-mound construction. In the Great Lakes, jetties have also been built of steel sheet-pile cells, caissons, and cribs using timber, steel, or concrete. In sheltered areas, a single row of braced and tied Wakefield timber piling and steel sheet piling have been used.

5.73 SITING

The proper siting and spacing of jetties for the improvement of a coastal inlet are important. Careful study, including model studies in some cases, must be given to the following hydraulic, navigation, control structure, sedimentation, and maintenance considerations:

a. **Hydraulic Factors of Existing Inlet**.

(1) The tidal prism and cross-section of the gorge in the natural state;

(2) Historical changes in inlet position and dimensions (i.e., length, width, and cross-section area of the inlet throat);

(3) Range and time relationship (lag) of tide inside and outside the inlet;

(4) Influence of storm surge or wind setup on the inlet;

(5) Influences of the inlet on tidal prism of the estuary and effects of fresh water inflow on estuary;

(6) Influence of other inlets on the estuary; and

(7) Tidal and wind-induced currents in the inlet.

b. **Hydraulic Factors of Proposed Improved Inlet**.

(1) Dimensions of inlet (length, width and cross-section area);

(2) Effects of inlet improvements on currents in the inlet, and on the tidal prism, salinity in the estuary, and on other inlets into the estuary;

(3) Effects of waves passing through the inlet; and

(4) Interaction of the Hydraulic Factors (item b.) on Navigation and Control Structure Factors, (item c. and d.).

c. **Navigation Factors of the Proposed Improved Inlet**.

(1) Effects of wind, waves, tides and currents on navigation channel;

(2) Alignment of channel with respect to predominant wave direction and natural channel of unimproved inlet;

(3) Effects of channel on tide, tidal prism and storm surge of the estuary;

(4) Determination of channel dimensions based on design vessel data and number of traffic lanes; and

(5) Other navigation factors such as:

    (a) Relocation of navigation channel to alternative site;

    (b) Provision for future expansion of channel dimensions; and

    (c) Effects of harbor facilities and layout on channel alignment.

d. Control Structure Factors.

(1) Determination of jetty length and spacing by considering the navigation, hydraulic, and sedimentation factors;

(2) Determination of the design wave for structural stability and wave runup and overtopping considering structural damage and maintenance; and

(3) Effects of crest elevation and structure permeability on waves in channel.

e. Sedimentation Factors.

(1) Effects of both net and gross longshore transport on method of sand bypassing, size of impoundment area, and channel maintenance; and

(2) Legal aspects of impoundment area and sand bypassing process. (See Section 5.53.)

f. Maintenance Factor. Dredging will be required, especially if the cross-section area required between the jetties is too large to be maintained by the currents associated with the tidal prism.

5.74 EFFECTS ON THE SHORELINE

Effects of entrance jetties on the shoreline are illustrated by Figure 5-15. A jetty (other than the weir type) interposes a total littoral barrier in that part of the littoral zone between the seaward end of the structure and the limit of wave uprush on the beach. Jetties are sometimes extended seaward to the position of the contour equivalent to project depth of the channel. Accretion takes place updrift from the structures at a rate proportional to the longshore transport rate, and erosion downdrift at about the same rate. The quantity of the accumulation depends on the length of the structure and the angle at which the resultant of the natural forces strikes the shore. If the angle that the shoreline of the impounded area makes with the structure is acute, the

5-48

impounding capacity is less than it would be if the angle were obtuse. Structures perpendicular to the shore have greater impounding capacity for a given length, and thus are usually more economical than those at an angle, because perpendicular jetties can be shorter and still reach the same depth. If the angle is acute, channel maintenance will be required sooner due to littoral drift passing around the end of the structure. Planning for jetties at an entrance should include some method of bypassing the littoral drift to eliminate or reduce channel shoaling and erosion of the downdrift shore. (See Section 5.5 - SAND BYPASSING.)
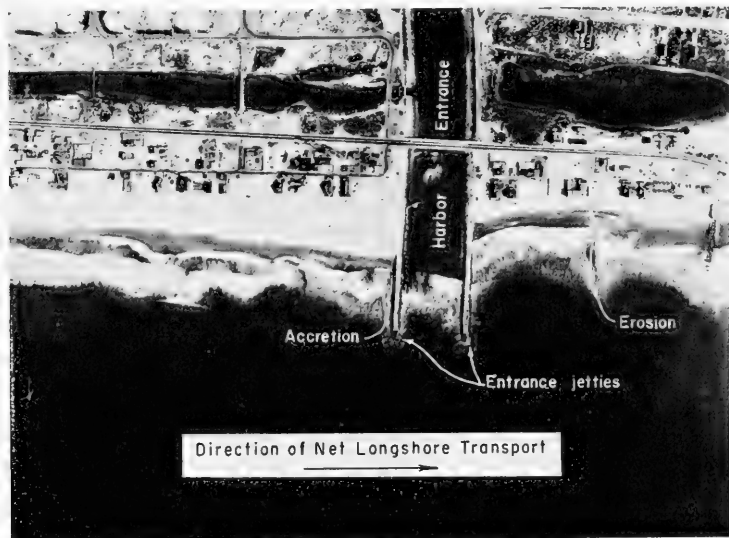
Ballona Creek, California–Jan. 1946

Figure 5-15. Effects of Entrance Jetties on Shoreline.

5.8   BREAKWATERS - SHORE-CONNECTED

5.81   DEFINITION

A breakwater is a structure protecting a shore area, harbor, anchorage, or basin from waves. Breakwaters for navigation purposes are constructed to create calm water in a harbor area, and provide protection for safe mooring, operating and handling of ships, and protection for harbor facilities.

5.82   TYPES

Breakwaters may be rubble mound, composite, concrete-caisson, sheet-piling cell, crib, or mobile. In the United States, breakwaters built on the open coast are generally of rubble-mound construction. Occasionally,

5-49

they are modified into a composite structure by using a concrete cap for stability. Precast concrete shapes, such as tetrapods or tribars, are also used for armor stone when rock of sufficient size is not obtainable. In the Great Lakes area, timber, steel, or concrete caissons or cribs have been used. In relatively sheltered areas breakwaters are occasionally built of a single row of braced and tied Wakefield (triple lap) timber piling or steel sheet piling. Several types of floating breawaters have been designed and tested, but few are in use at this time (1972).

5.83   SITING

Shore connected breakwaters provide a protected harbor for vessels. The most important factor of siting a breakwater is to determine the best location that will produce a harbor area with minimum wave and surge action over the greatest period of time in the year. This determination is made through the use of refraction and diffraction analyses. Other siting factors are the direction and magnitude of longshore transport, the harbor area required, the character and depth of the bottom material in the proposed harbor, and available construction equipment and operating capability. Shore-connected structures are usually built with shore-based equipment. (See Section 5.73 - JETTIES - SITING.)

5.84   EFFECT ON THE SHORELINE

The effect of a shore-connected breakwater on the shoreline is illustrated by Figure 5-16. As does a jetty, the shore arm of the breakwater interposes a total littoral barrier in the zone between the seaward end of the shore arm and the limit of wave uprush until the impounding capacity of the structure is reached and natural bypassing of the littoral material is resumed. The same accretion and erosion patterns result from the installation of this type of breakwater. The accretion, however, is not limited to the shore arm, but eventually extends along the seaward face of the sea arm, building a berm over which littoral material is transported to form a large accretion area at the end of the structure in the less turbulent waters of the harbor. This type of shoal creates an ideal condition for sand bypassing. A pipeline dredge can lie in the relatively quiet waters behind the shoal, and transfer accumulated material to nourish the downdrift shore. (See Section 5.5, SAND BYPASSING.)

5.9   BREAKWATERS - OFFSHORE

5.91   DEFINITION

An offshore breakwater is a structure designed to protect an area from wave action. Offshore breakwaters may serve as an aid to navigation, a shore-protection structure, a trap for littoral drift, or may serve a combined purpose.

5.92   TYPE

Almost without exception, offshore breakwaters in the United States are of rubble-mound construction.
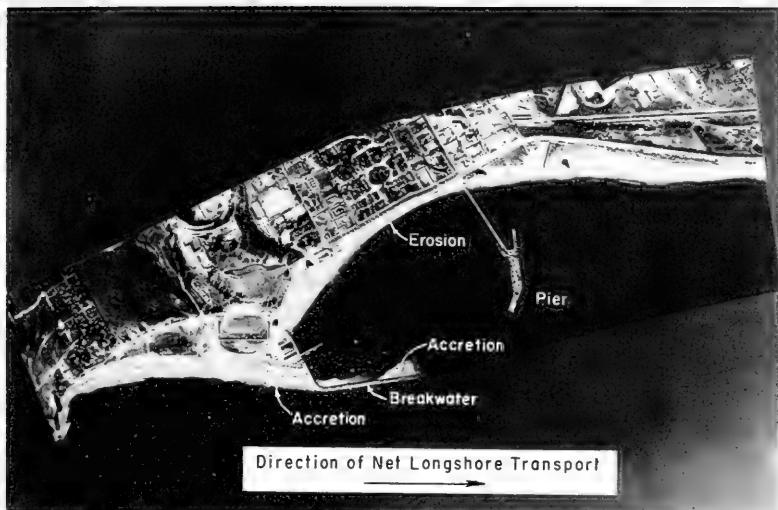
Figure 5-16.   Effects of Shore-Connected Breakwater on Shoreline

5.93   SITING

Offshore breakwaters are sited to provide shelter to a harbor
entrance, or to create a littoral reservoir. They may also provide a
calm area where small craft may seek refuge or where a pipeline dredge
can operate to pump sand to downdrift shores (see Section 5.5, SAND BY-
PASSING). An example of this type of siting or use is illustrated in
Figure 5-17, which shows Channel Island Harbor entrance at Ventura,
California. Offshore breakwaters have also been sited seaward of massive
seawalls to provide a first line of defense as illustrated in Figure 5-18.

5.94   EFFECTS ON THE SHORELINE

The effects of an offshore breakwater on a shoreline are illustrated
by Figure 5-19. Offshore breakwaters are probably the most effective means
of completely intercepting movement of littoral material. They are usually
positioned in water significantly deeper than the seaward ends of jetties or
groins. This makes it possible for them to control a wider part of the
littoral zone than structures tied to the shore. Because longshore trans-
port is the direct result of wave action, the extent to which the breakwater
intercepts the movement of littoral drift is directly proportional to the
extent of wave attenuation by the breakwater.

5.95   OPERATION OF AN OFFSHORE BREAKWATER

An offshore breakwater initially causes littoral drift to deposit
on the shore in its lee by dissipating the wave forces that cause littoral
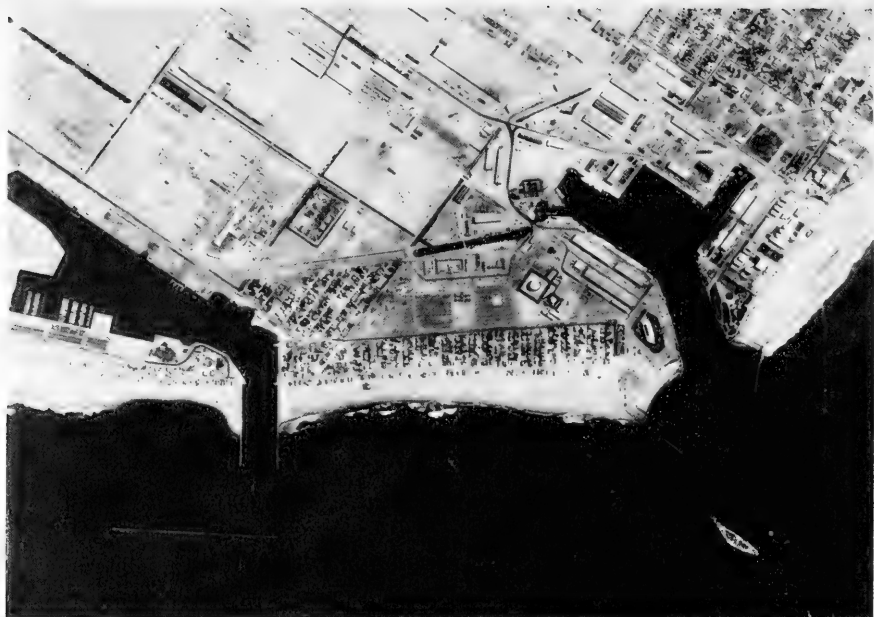
Channel Islands Harbor – Port Hueneme, California – Sept. 1965
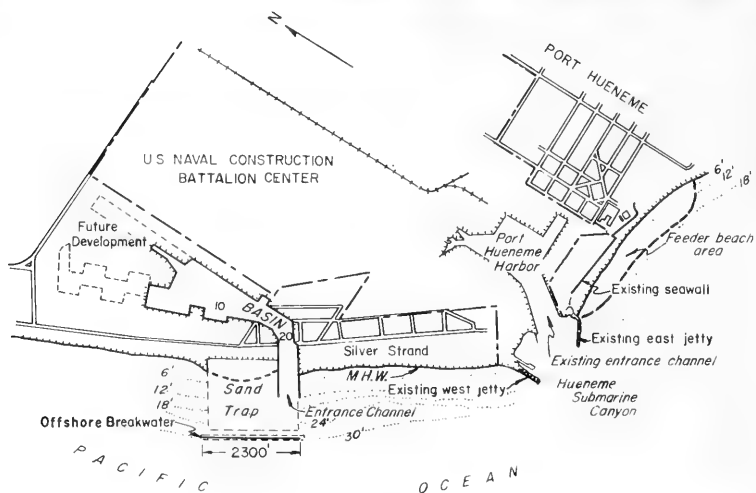
Figure 5-17. Siting of Offshore Breakwaters for Sheltering Harbor Entrance

Offshore Breakwaters

Seawall

Direction of Net
Longshore Transport
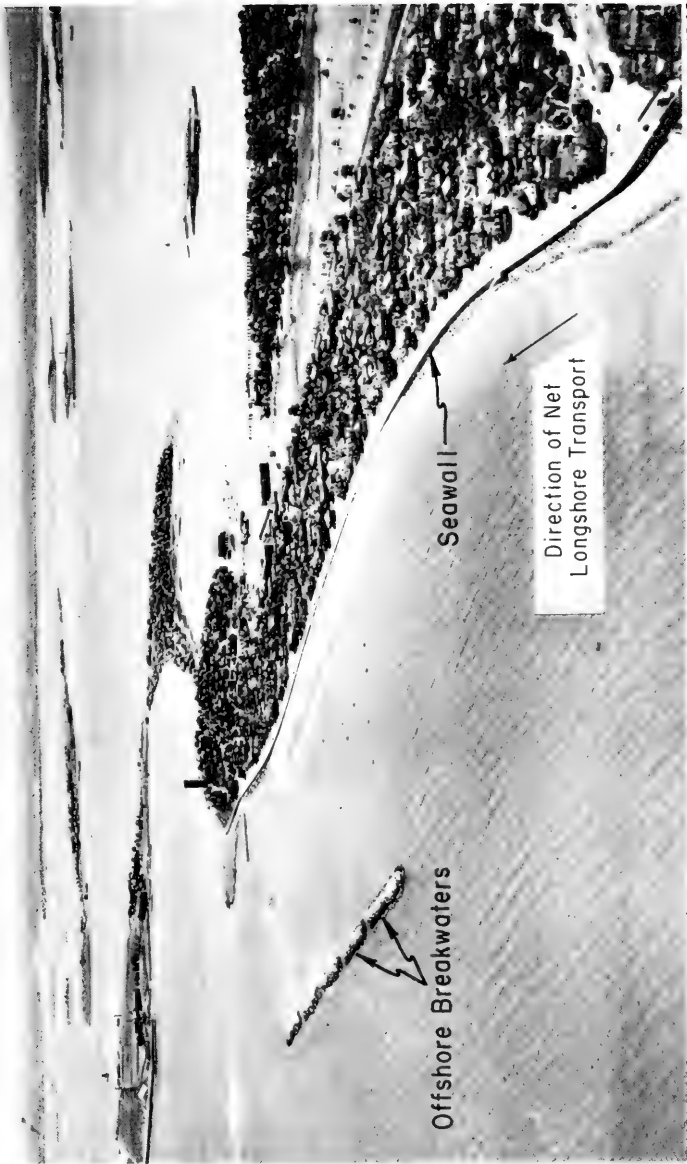
Winthrop Beach, Massachusetts - 1949

Figure 5-18. Siting Offshore Breakwaters Seaward of Seawalls for Protection

5-53

Figure 5-19. Operation of Breakwater in Diffraction of Wave Forces

Within the figure:

Depth in fathoms

Direction of wave approach

Contours shown represent the shoreline at the end of 11 years

Santa Monica, Calif.
Beta (1948)

Diffraction diagram

Wave period 9 secs.

transport. The typical diffraction diagram drawn on Figure 5-19 shows
that wave heights within the breakwater geometric shadow are less than
one-half the wave heights outside the breakwater. As sand is deposited,
a seaward projection of the shore is formed in the still water behind
the breakwater. This projecting shore alignment in turn acts as a groin,
which causes the updrift shoreline to advance. As the projection enlarges
and the zone of longshore transport moves closer to the breakwater, the
salient becomes increasingly efficient as a littoral barrier. If the
breakwater is long enough relative to its distance from the shore to act
as a complete littoral barrier, the sand depositing action may continue
until a tombolo is formed with the breakwater at its apex. (See Figure
5-20.)

The precise shape of the salient deposit is difficult to predict.
In general, there is accretion updrift from the breakwater and erosion
downdrift. The area immediately behind the breakwater assumes a form
convex seaward. At complete barriers, a large percentage of the total
accumulation collects in the breakwater lee during the first year, and
the ratio of material in the lee of the structure t cotal material
trapped decreases steadily until the trap is fille. and littoral material
begins moving seaward around the structure.

5.96   OFFSHORE BREAKWATERS IN SERIES

It is not necessary to build offshore breakwaters as a single unit.
A series of short structures will have the same general effect as one long
structure, but the efficiency of the series as a sand trap will be decreased,
a condition which is sometimes desirable. The tendency for a tombolo to
form will be decreased. Figure 5-18 is an aerial photograph taken in 1949
of the breakwater series off Winthrop Beach, Massachusetts, constructed in
1931-33. The characteristic convex accretion in the lee of the breakwater
is evident, as is also the erosion zone downdrift. (See Figure 5-19.)
The shoals extending landward from the breakwater in Figure 5-18 indicate
that this breakwater series is in the littoral transport zone.

5.97   HEIGHT OF AN OFFSHORE BREAKWATER

One of the factors determining the effectiveness of an offshore
breakwater as a sand trap and in providing a protected area is the height
in relation to the wave action and variation in water levels at the site.
A structure which can completely eliminate wave action in its lee will
provide a protected harbor and function as a complete littoral barrier.
The most efficient type of breakwater then is one whose crest permits no
significant overtopping by waves. Model studies (Hudson, 1959) indicate
that the required crest elevation of a rubble type of breakwater depends
on wave height, wave period, wave length, face slope of the structure,
and the permeability of the structure. Data given in Figure 7-20 indicate
values for wave runup on rubble-mound structures. Until further verifica-
tion can be made, runup values at least as great as those indicated by
these curves should be accepted as design criteria. It might be desirable
to build an offshore breakwater that is not completely effective as a
littoral barrier. This may be accomplished by constructing the breakwater

5-55

Venice, California (before 1948)

Figure 5-20. Breakwater Acting as Complete Littoral Barrier Causing a Tombolo
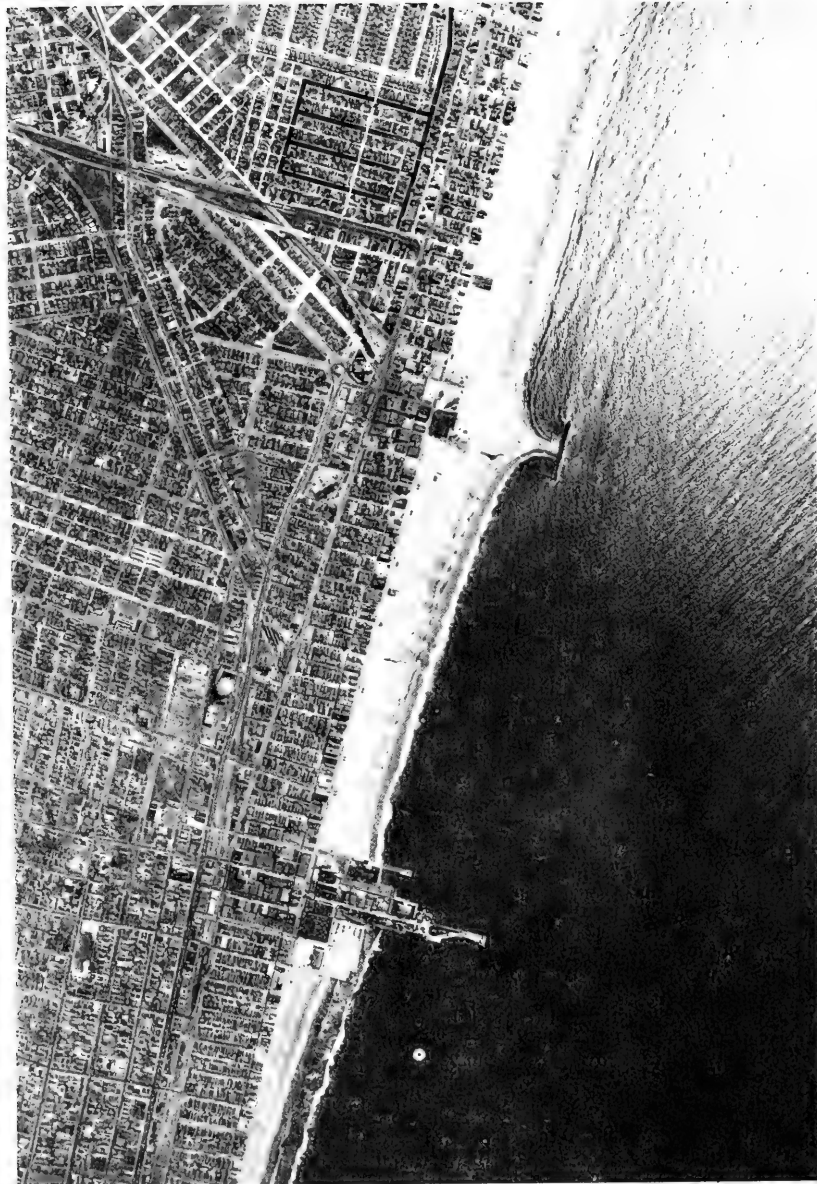
to a height less than that sufficient to prevent overtopping. Such partial barriers need not even extend above low water. Since construction and maintenance requirements for a submerged breakwater are economically less than those for a high breakwater, such structures should be seriously considered when a partial barrier is adequate. Provisions should be made to indicate the location of the submerged structure so that it is not a hazard to navigation.

5.10   ENVIRONMENTAL CONSIDERATIONS

Shore protection measures by their very nature are planned to result in some modification of the physical environment. However, thorough planning and design require that the full impact of that modification on the ecological and aesthetic aspects of the environment be fully considered and understood. If there is potential for significant adverse effect to any environmental feature, design analysis of a shore improvement project should include alternatives for avoiding or mitigating that adverse effect. Therefore, design analysis should include a multidiscipline appraisal of the total impact of the project, to include environmental quality as well as economic benefits. The necessity for this appraisal at the planning and design stage is apparent and required by law. If there is a probability for conflict between planned construction and environmental quality, a final decision by appropriate authority based upon social, technical, and economic analysis will be required.

In recent years the question of total environmental quality reached top levels of public concern. Published technical information on this question is scattered through many disciplines, and the lack of quantifiable base-line data precludes reliable quantitative forecasting of most environmental and ecological changes resulting from manmade structures. Two recent works addressed specifically to this question are Rounsefell (1972) on the ecological effects of offshore construction and Thompson (1973) on ecological effects of offshore dredging and beach nourishment. Both papers include state-of-the-art evaluations from the ecologist's perspective, and extensive bibliographies, with some entries annotated. Both describe and discuss direct and indirect effects of several categories of coastal protective works, and discuss procedures for evaluating those effects. Both agree that it is of utmost importance to obtain necessary data on probable environmental impact of proposed construction at an early stage of the project planning. Accurate assessment of preproject environment is essential, not only for initial planning and design, but also for later design modification or alternatives that could bear on either mitigation of environmental change or enhancement of other aspects of the environment. The works of Rounsefell and Thompson suggest that the methods of shore protection discussed in this manual would generally not result in long-term undesirable ecological changes for individual projects. However, this opinion is qualified to the extent that cumulative effects of numerous works of certain types could conceivably result in some deterimental long-term changes. A further requirement is recognized for additional base-line data and knowledge of the quantitative ecological-physical relationships. This information can be developed by monitoring before-, during-, and after-construction effects on coastal projects.

5-57

BERG, D.W., "Factors Affecting Beach Nourishment Requirements at Presque Isle Peninsula, Erie, Pennsylvania," Great Lakes Research Division, University of Michigan, Pub. No. 13, 1965, pp. 214-221.

BERG, D.W. and WATTS, G.M., "Variations in Groin Design," *Journal of the Waterways and Harbors Division*, ASCE, Vol. 93, Proceedings Paper WW2, No. 5241, May 1967, pp. 79-100.

DAVIS, J.H., "Dune Formation and Stabilization by Vegetation and Plantings," U.S. Army, Corps of Engineers, Beach Erosion Board, TM-101. 1957.

GAGE, B.O., "Experimental Dunes of the Texas Coast," U.S. Army, Corps of Engineers, Coastal Engineering Research Center, MP-1-70, 1970.

HALL, J.V., JR., "Artificially Nourished Constructed Beaches," U.S. Army, Corps of Engineers, Beach Erosion Board, TM-29, 1952.

HERRON, W.J., "Beach Erosion Control and Small Craft Harbor Development at Port Hueneme," *Shore and Beach*, Vol. 28, No. 2, 1960, pp. 11-15.

HODGES, T.K., "Sand Bypassing at Hillsboro Inlet, Florida," U.S. Army, Corps of Engineers, Beach Erosion Board, Bulletin, Vol. 9, No. 2, 1955.

HUDSON, R.Y., "Laboratory Investigation of Rubble-Mound Breakwaters," *Journal of the Waterways and Harbors Division*, ASCE, Proceedings Paper Vol. 85, WW3, No. 2171, September 1959.

KRUMBEIN, W.C., "A Method for Specification of Sand for Beach Fills," U.S. Army, Corps of Engineers, Beach Erosion Board, TM-102, 1957.

KRUMBEIN, W.C. and JAMES, W.R., "A Lognormal Size Distribution Model for Estimating Stability of Beach Fill Material," U.S. Army, Corps of Engineers, Coastal Engineering Research Center, TM-16, 1965.

LILLEVANG, O.J, "Groins and Effects - Minimizing Liabilities," *Coastal Engineering, Santa Barbara Specialty Conference*, Oct. 1965; ASCE, Ch. 31, 1966, pp. 749-754.

MAGNUSON, N.C., "Planning and Design of a Low-weir Section Jetty at Masonboro Inlet, North Carolina," *Coastal Engineering, Santa Barbara Specialty Conference*, Oct. 1965; ASCE, Ch. 36, 1966, pp. 807-820.

MAURIELLO, L.J., "Experimental Use of a Self-Unloading Hopper Dredge for Rehabilitation of an Ocean Beach," *Proceedings of the World Dredging Conference*, 1967, pp. 367-396.

RAYNER, A.C. and MAGNUSON, N.C., "Stabilization of Masonboro Inlet, North Carolina," *Shore and Beach*, Vol. 34, No. 2, 1966, pp. 36-41.

ROUNSEFELL, G.A., "Ecological Effects of Offshore Construction," *Marine Science*, Marine Science Institute, Bayon LaBatre, Alabama, Vol. 2, No. 1, 1972.

SAVAGE, R.P., "Notes on the Formation of Beach Ridges," U.S. Army, Corps of Engineers, Beach Erosion Board, Bulletin, Vol. 13, Jul. 1959.

SAVAGE, R.P. and WOODHOUSE, W.W., JR., "Creation and Stabilization of Coastal Barrier Dunes," *Proceedings of 11th Conference on Coastal Engineering*, Sep. 1968, ASCE, Ch. 43, 1969, pp. 671-700.

THOMPSON, J.R., "Ecological Effects of Offshore Dredging and Beach Nourishment," MP 1-73, U.S. Army, Corps of Engineers Coastal Engineering Research Center, Jan. 1973.

U.S. Army, Corps of Engineers, "Shore of New Jersey from Sandy Hook to Barnegat Inlet, Beach Erosion Control Study," House Document No. 361, 84th Congress, 2d Session, U.S. Government Printing Office, Washington, D.C., 1957.

U.S. Army Engineer District, Philadelphia, "Study on Use of Hopper Dredges for Beach Nourishment," Hopper Dredge Improvement Program, No. 10, 1967.

WATTS, G.M., "Trends in Sand Transfer Systems," *Coastal Engineering, Santa Barbara Specialty Conference*, Oct. 1965, ASCE, Ch. 34, 1966, pp. 799-804.

ZELLER, R.P., "A General Reconnaissance of Coastal Dunes of California," U.S. Army, Corps of Engineers, Beach Erosion Board, MP-1-62, 1962.

CHAPTER 6

STRUCTURAL

FEATURES

PALM BEACH, FLORIDA — 3 October 1964

CHAPTER 6

STRUCTURAL FEATURES

6.1 INTRODUCTION

This chapter provides illustrations of various structural features and detailed discussions of selected coastal engineering projects. This chapter complements discussions in Chapter 5, Planning Analysis.

Sections 6.2 through 6.9 provide details of typical seawalls, bulkheads, revetments, protective beaches, sand dunes, groins, jetties, and breakwaters. These details form a basis for comparing one type of structure with another. They are not intended as recommended dimensions for application to other structures or sites. Section 6.10, Construction Materials, discusses materials for shore structures. Section 6.11, Miscellaneous Design Practices, lists recommendations concerning prevention or reduction of deterioration of concrete, steel and timber waterfront structures.

6.2 SEAWALLS, BULKHEADS, AND REVETMENTS

6.21 TYPES

The distinction between seawalls, bulkheads and revetments is mainly a matter of purpose. Design features are determined at the functional planning stage, and the structure is named to suit its intended purpose. In general, seawalls are the most massive of the three, because they resist the full force of the waves. Bulkheads are next in size; their function is to retain fill, and they are generally not exposed to severe wave action. Revetments are the lightest, because they are designed to protect shorelines against erosion by currents or light wave action.

A curved-face seawall and a combination stepped and curved-face seawall are illustrated in Figures 6-1 and 6-2. These massive structures are built to resist high wave action and reduce scour. Both seawalls have sheet-pile cutoff walls to prevent loss of foundation material by wave scour and leaching from overtopping water or storm drainage beneath the wall. The curved-face seawall also has an armoring of large rocks at the toe to reduce scouring by wave action.

The stepped seawall (Figure 6-3) was designed for stability against moderate waves. The tongue groove provides a space between piles that may be grouted to form a sandtight cutoff wall. Instead of grouting this space, a plastic filter cloth can be used to line the landward side of the sheet piling. The filter-cloth liner provides a sand-tight barrier, and eliminates the buildup of hydrostatic pressure which is relieved through the cloth and the joints between the sheet piles.

The rubble-mound seawall (Figure 6-4) was built to withstand severe wave action. Although scour of the fronting beach may occur, rock

6-1

Galveston, Texas (1965)
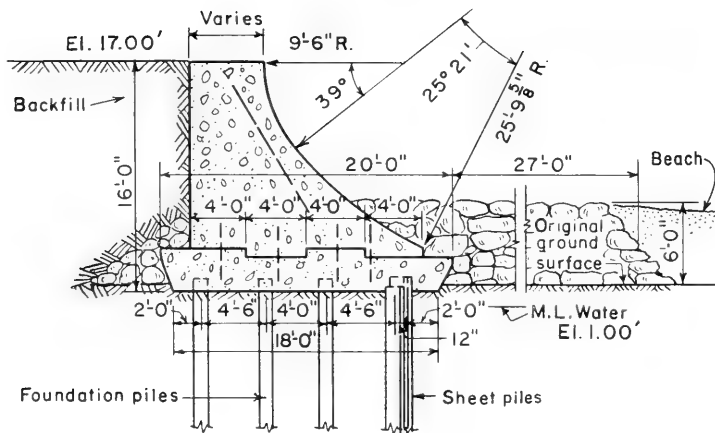
Figure 6-1. Concrete Curved-Face Seawall

San Francisco, California (1930)
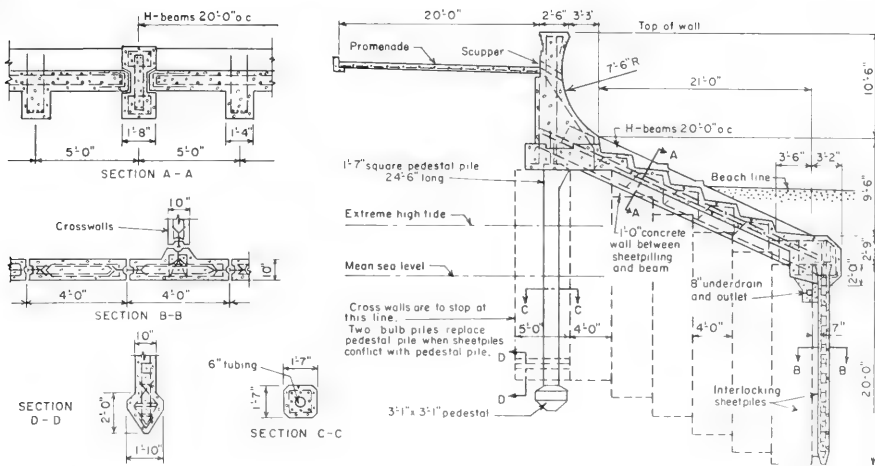
Figure 6-2.   Concrete Combination Stepped and Curved-Face Seawall

Harrison County, Mississippi (1953)
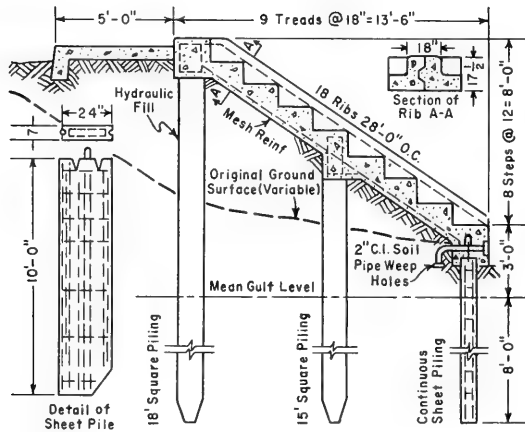
Figure 6-3.   Concrete Stepped-Face Seawall

Fernandina Beach, Florida (December 1964)
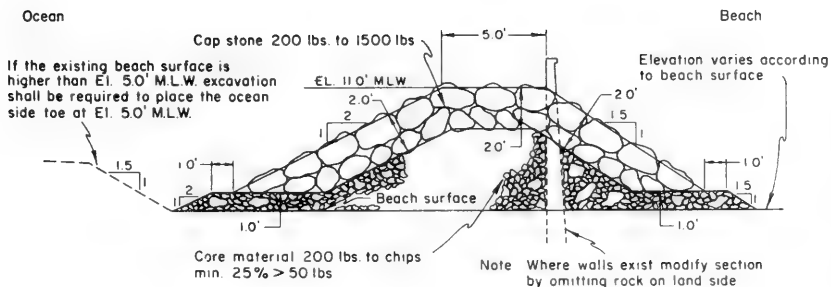
Figure 6-4.   Rubble-Mound Seawall

comprising the seawall can readjust and settle without causing structural
failure. Figure 6-5 shows an adaptation of the rubble-mound seawall shown
in Figure 6-4; the stage placement of A and B stone utilizes the bank
material to reduce the stone required in the structure.
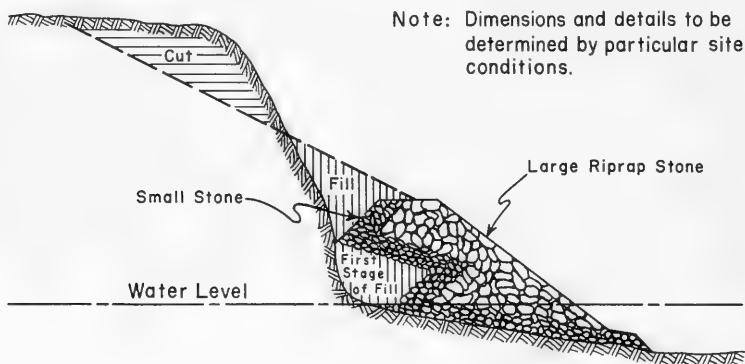
Figure 6-5. Rubble-Mound Seawall (Typical-Stage Placed)

Three structural types of bulkheads (concrete, steel and timber) are
shown in Figures 6-6 through 6-8. Cellular steel sheet-pile bulkheads are
used where rock is near the surface, and adequate penetration is impossible
for the anchored sheet-pile bulkhead illustrated in Figure 6-7. When verti-
cal or nearly vertical bulkheads are constructed and the water depth at the
wall is less than twice the anticipated maximum wave height, the design
should provide for riprap armoring at the base to prevent scouring. Exces-
sive scouring may endanger the stability of the wall.

Structural types of revetments used for coastal protection in exposed
and sheltered areas are illustrated in Figures 6-9 through 6-13. There
are two types of revetments: the rigid, cast-in-place concrete type illus-
trated in Figure 6-9, and the flexible or articulated armor unit type illus-
trated in Figures 6-10 through 6-13. A rigid concrete revetment provides
excellent bank protection, but the site must be dewatered during construc-
tion to pour the concrete. A flexible structure also provides excellent
bank protection, and can tolerate minor consolidation or settlement with-
out structural failure. This is true for the riprap revetment and to a
lesser extent for the interlocking concrete block revetment. Both the
articulated block structure and the riprap structure allow for the relief
of hydrostatic uplift pressure generated by wave action. The underlying
plastic filter cloth and gravel or a crushed-stone filter and bedding
layer provide for relief of pressure over the entire foundation area
rather than through specially constructed weep holes.

Interlocking concrete blocks have been used extensively for shore
protection in the Netherlands and England, and have recently become popular

Virginia Beach, Virginia (March 1953)
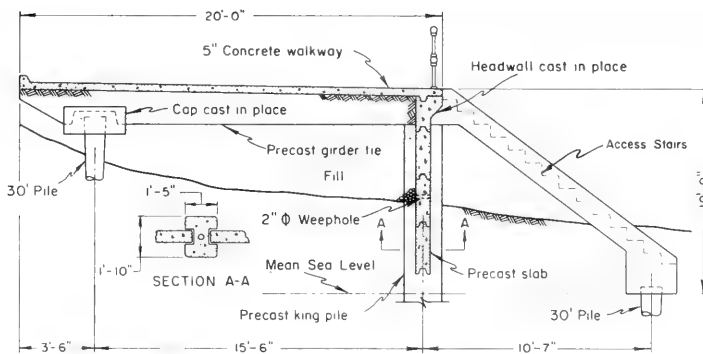
Figure 6-6.   Concrete Slab and King-Pile Bulkhead

Nantucket Island, Massachusetts (1972)
Photograph, Courtesy of U.S. Steel
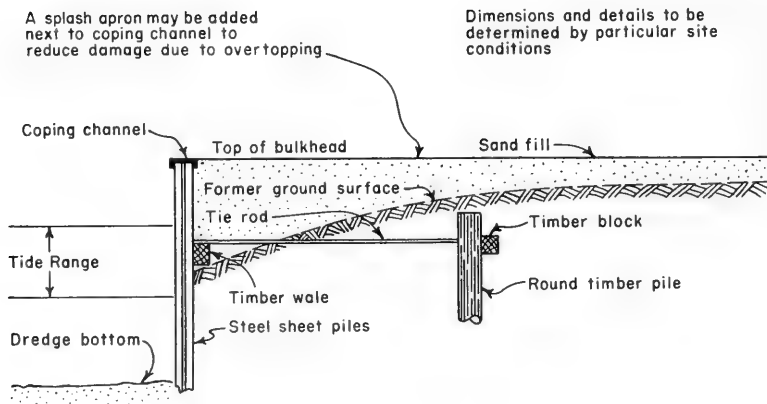
Figure 6-7. Steel Sheet-Pile Bulkhead

Avalon, New Jersey (Sept. 1962)
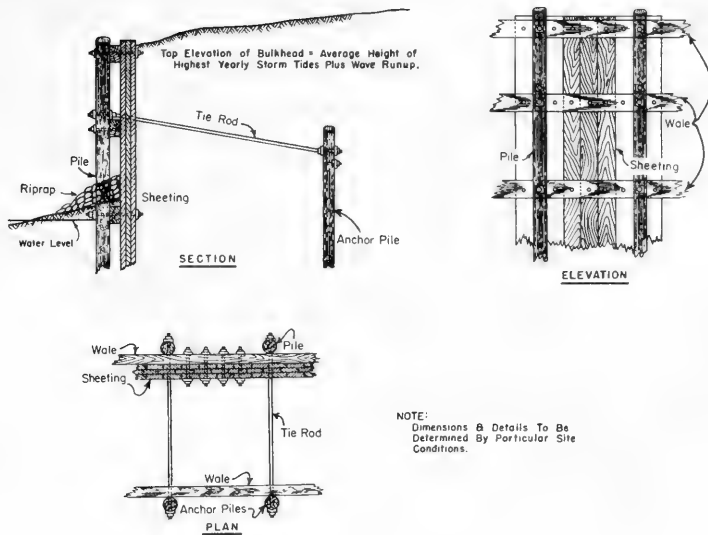
Figure 6-8. Timber Sheet-Pile Bulkhead

Pioneer Point, Cambridge, Maryland (before 1966)
Courtesy of Portland Cement Association
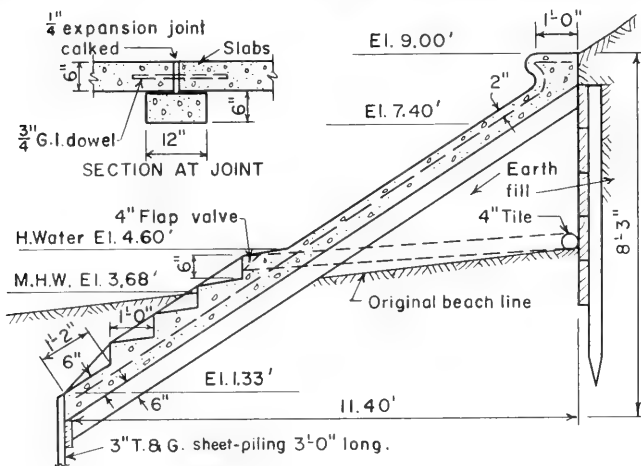
Figure 6-9.   Concrete Revetment

Chesapeake Bay, Maryland (1972)
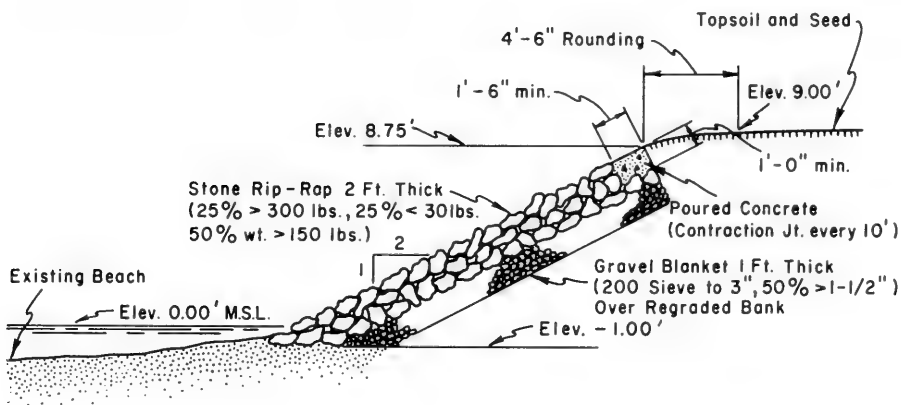
Figure 6-10. Riprap Revetment

Jupiter Island, Florida (1965)
Courtesy of Carthage Mills Inc.
Erosion Control Division
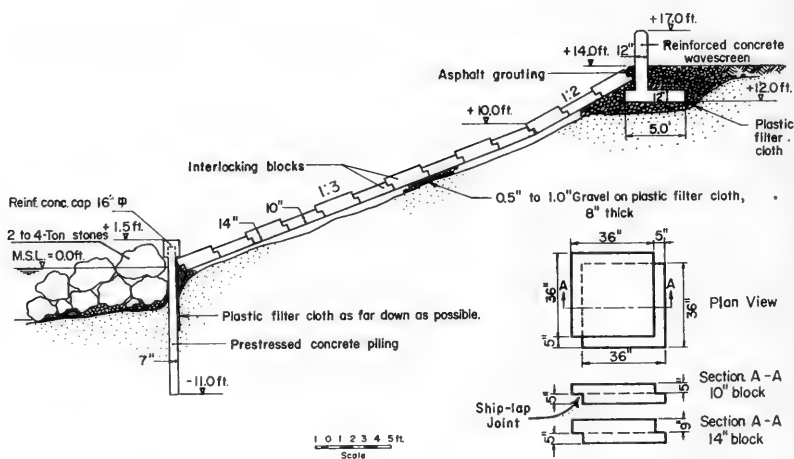
Figure 6-11.   Interlocking Concrete-Block Revetment

Benedict, Maryland (October 1964)
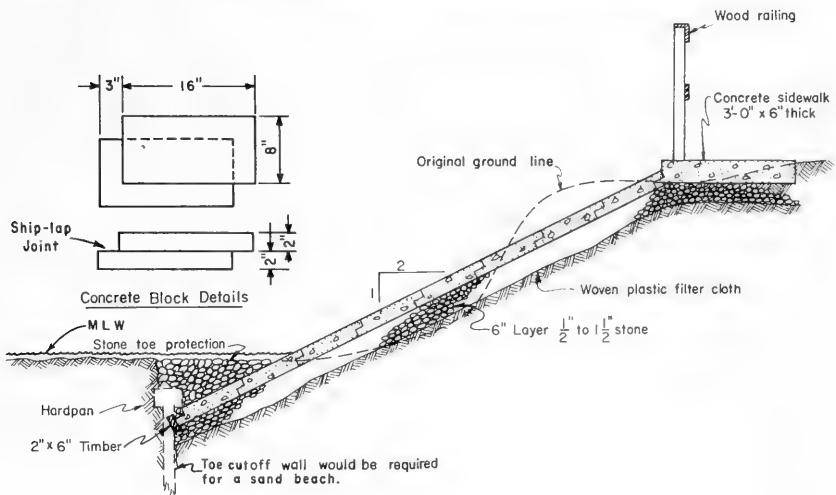
Figure 6-12. Interlocking Concrete-Block Revetment

6-13

Cedarhurst, Maryland (1970)
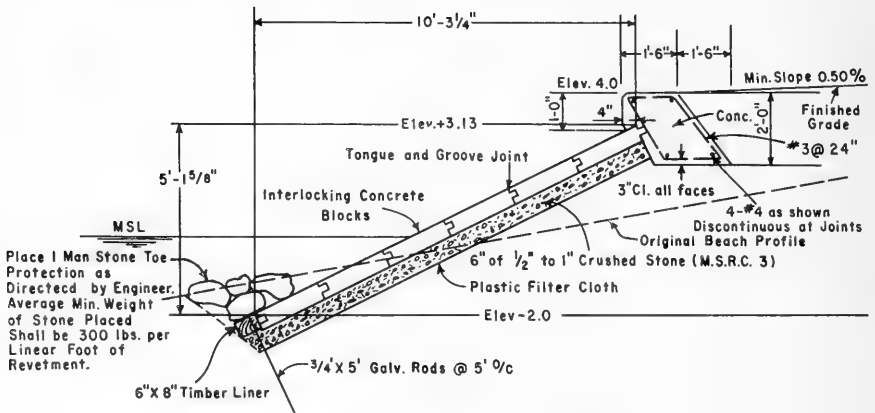
Figure 6-13.   Interlocking Concrete-Block Revetment

in the United States. Typical blocks are generally square slabs with ship-lap type interlocking joints as shown in Figures 6-11 and 6-12. The joint of the ship-lap type provides a mechanical interlock with adjacent blocks.

Stability of an interlocking concrete block depends largely on the type of mechanical interlock. It is impossible to analyze block stability under specified wave action based on the weight alone. However, prototype tests at CERC on blocks having ship-lap joints and tongue-and-groove joints indicate that stability of tongue-and-groove blocks is much greater than the ship-lap blocks. (Hall, 1967.) An installation of the tongue-and-groove interlock block is shown in Figure 6-13.

6.22 SELECTION OF STRUCTURAL TYPE

Major considerations for selection of a structural type are: foundation conditions, exposure to wave action, availability of materials and costs. The following paragraphs illustrate a procedure for reviewing these factors.

6.221 Foundation Conditions. Foundation conditions may have a significant influence on the selection of type of structure, and can be considered from two general aspects. First, foundation material must be compatible with the type of structure. A structure that depends on penetration for stability is not suitable for a rock bottom. Random stone or some type of flexible structure using a stone mat or plastic filter cloth could be used on a soft bottom, although a cellular steel sheet-pile structure might be used under these conditions. Second, the presence of a seawall, bulkhead or revetment may induce bottom scour and cause failure. Thus, a masonry or mass concrete wall must be protected from the effects of settlement due to bottom scour induced by the wall itself.

6.222 Exposure to Wave Action. Wave exposure may control the selection of both structural type and details of design geometry. In areas of severe wave action, light structures such as timber crib or light riprap revetment should not be used. Where waves are high, a curved, reentrant face wall or possibly a combination of a stepped-face wall with a recurved upper face might be considered over a stepped-face wall.

6.223 Availability of Materials. This factor is related to construction and maintenance costs as well as to structural type. If materials are not available near the construction site, or are in short supply, a particular type of seawall or bulkhead may not be economically feasible. A cost compromise may have to be made or a lesser degree of protection provided. Cost analysis includes the first costs of design and construction and annual costs over the economic life of the structure. Annual costs include interest and amortization on the investment, plus average maintenanc costs. The best structure is one that will provide the desired protection at the lowest annual or total cost. Because of wide variations in first cost and maintenance costs, comparison is usually made by reducing all costs to an annual basis for the estimated economic life of the structure.

6.3 PROTECTIVE BEACHES

6.31 GENERAL

Planning analysis for a protective beach is described in Section 5.3. Protective beaches may be built with land-hauled sand fill or by pumping sand with a floating dredge through a pipeline to the beach. The dredge picks up the material at the borrow area and pumps it directly to the fill area. The direct pumping method is better suited where the borrow area is not exposed to wave action, although a specially equipped dredge was used successfully in an exposed location in Redondo Beach, Malaga Cove, California. (See Section 6.323.) This dredge was held in position by cables and anchors rather than spuds, and used a flexible suction line with jet agitation rather than the conventional rigid ladder and cutterhead. Dredges with a rigid ladder and cutterhead were used on beach fills at Pompano Beach and Fort Pierce, Florida, where the borrow area was off-shore and exposed to the open ocean.

Some hopper dredges are now available with pump-out capability. Hopper dredges load at the borrow site, (normally offshore), move close to the fill site, and then pump from the hoppers through a submerged pipe-line to the beach. (See Section 6.322.)

The choice of method depends on the location of the borrow source and availability of suitable equipment. Borrow sources in bays and lagoons may become depleted, or unexploitable because of injurious ecological effects. It is now necessary to place increased reliance on offshore sources. CERC is studying the geomorphology, sediments, and structure of the Inner Continental Shelf with the primary purpose of finding sand deposits suitable for beach fill. Results are published as they become available. (Duane and Meisburger, 1969, Meisburger and Duane, 1971, Meisburger, 1972.) Sand from offshore sources is frequently of better quality for beach fill, because it contains less fine grain size materials. However, equipment suitable for dredging and transporting sand to the beach is not yet readily available. As equipment becomes available, offshore borrow areas will become more important sources of beach fill material.

6.32 EXISTING PROTECTIVE BEACHES

Restoration and widening of beaches have come into increasing use in recent years. Examples are Ocean City, New Jersey (Watts, 1956), Virginia Beach, Virginia (Watts, 1959), (Wrightsville Beach and Carolina Beach, North Carolina (Vallianos, 1970), and Harrison County, Mississippi (Escoffier and Dolive, 1954 and Watts, 1958.) Figures 6-14 through 6-23 illustrate details of these projects with before-and-after photographs. A test of beach widening and nourishment from an offshore source by hopper dredge, in 1966, at Sea Girt, New Jersey is described in Section 6.322. In 1968, beach widening and nourishment from an offshore source was accomplished by a pipeline dredge at Redondo Beach, California. (See Section 6.323.) Of the projects mentioned, Carolina Beach, Sea Girt and Redondo Beach are discussed.

6.321 Carolina Beach, North Carolina. A protective beach was part of the project at Carolina Beach, and is used to illustrate the planning of such a beach. (See Figures 6-20 and 6-21.) The project included hurricane protection, but the illustration of protective beach planning will include only the feature which would have been provided for beach erosion control alone. The report on which the project is based was completed in 1961 (U.S. Army Engineer District, Wilmington, 1961), and the project was partly constructed in 1965.

The predominant direction of longshore transport is from north to south. This conclusion was based on southerly growth of an offshore bar at Carolina Beach Inlet, and shoaling at Cape Fear, 12 miles south of Carolina Beach. Subsequent erosion south of Carolina Beach Inlet and accretion north of a jetty at Masonboro Inlet, about 9 miles north of Carolina Beach, have confirmed the direction. The long-term average annual deficiency in material supply for the area was estimated in the basic report at about 4 cubic yards per linear foot of beach. This estimate was based on the rate of loss from 1938 to 1957, from the dune line to the 24-foot depth contour. Carolina Beach Inlet, opened in 1952, apparently had little effect on the shore of Carolina Beach before 1957; therefore, that deficiency in supply was considered the normal deficiency without regard to the new inlet.

For planning, it was estimated that 60 percent of the material in the proposed borrow area in Myrtle Sound (behind Carolina Beach) would be compatible with the native material on the beach and nearshore bottom, and would be suitable for beach fill. This estimate assumed that 40 percent of the borrow material was finer in size characteristics than the existing beach material and therefore would be winnowed due to its incompatibility with the wave climate. The method of Krumbein and James (1965), was considered for determining the amount of fill to be placed. However, insufficient samples were taken from the foreshore and nearshore slopes to develop characteristics of grain-size distribution for the native beach sand.

Although samples taken from the beach after construction may not be entirely indicative of the characteristics of the native sand, they do represent to some extent the borrow material after it has been subjected to wave action, presumably typical of the wave climate associated with sorting on the natural beach. Samples taken from the original borrow material and from the active beach profile in May 1967 were therefore used to estimate the amount of material lost from the original fill as a result of sorting action.

The estimate was made by computing the *critical ratio* ($R_{\phi crit}$), defined as the ratio of the volume required to be placed to the volume retained on the beach in equilibrium with shore processes assuming the specific gravities of the borrow and native materials are the same.

$$R_{\phi crit} = \frac{\sigma_{\phi b}}{\sigma_{\phi n}} \; e^{\; -\frac{\left(M_{\phi n} - M_{\phi b}\right)^2}{2\left(\sigma_{\phi n}^2 - \sigma_{\phi b}^2\right)}} \qquad (6-1)$$

6-17
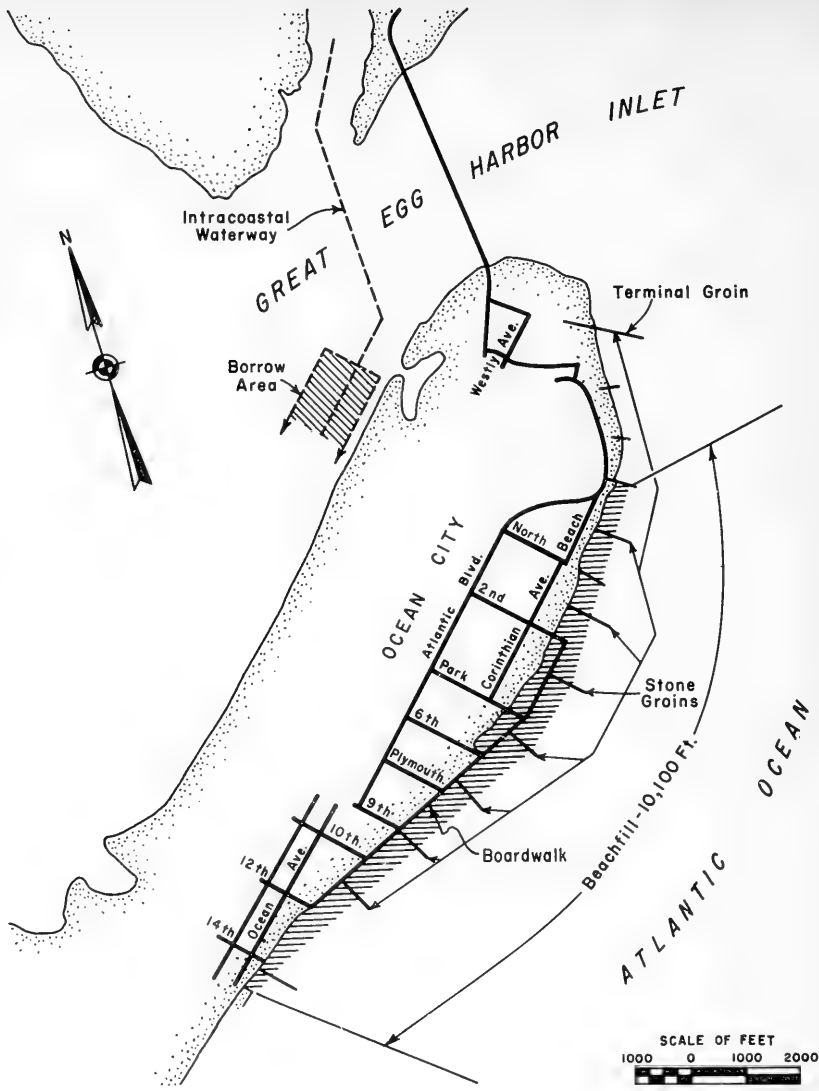
Figure 6-14. Protective Beach (Ocean City, New Jersey)

Before Restoration   (1951)

After Restoration   (1952)

Figure 6-15.   Protective Beach (Ocean City, New Jersey)
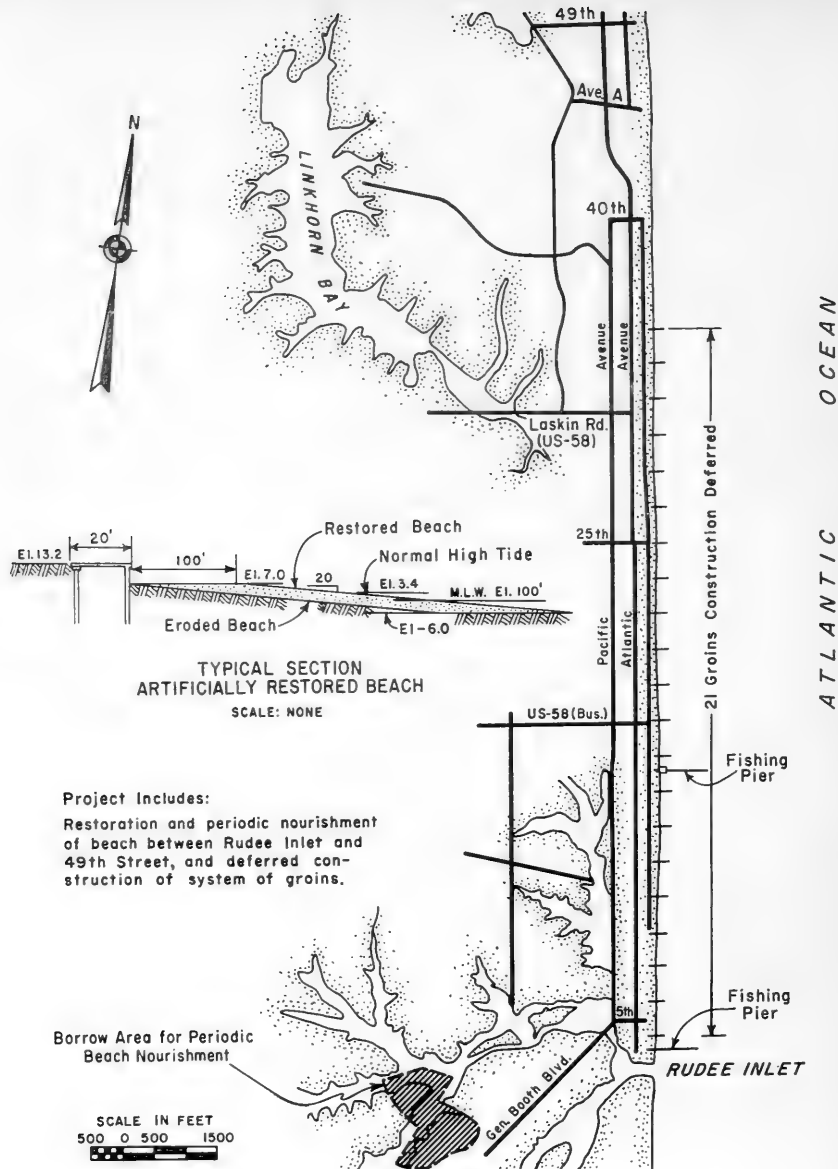
Figure 6-16. Protective Beach (Virginia Beach, Virginia)

Before Restoration   (1951)

After Restoration   (1960)

Figure 6-17. Protective Beach (Virginia Beach, Virginia)
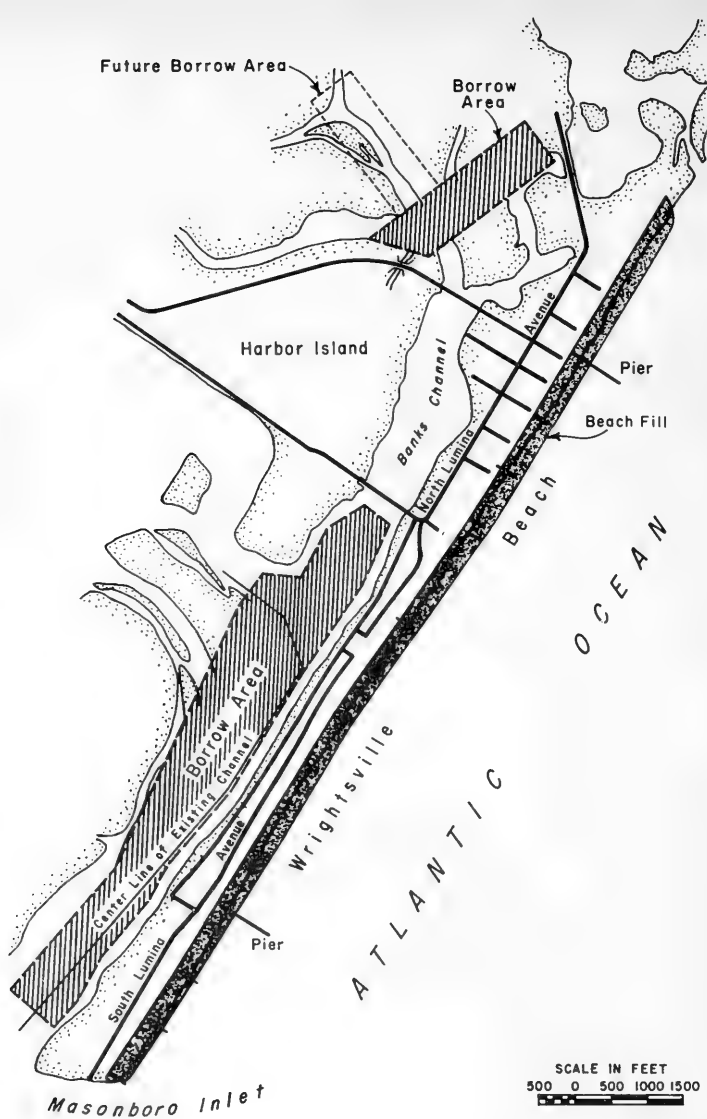
Figure 6-18.   Protective Beach (Wrightsville Beach, North Carolina)

Before Restoration   (February 1965)

After Restoration   (June 1965)

Figure 6-19.   Protective Beach (Wrightsville Beach, North Carolina)
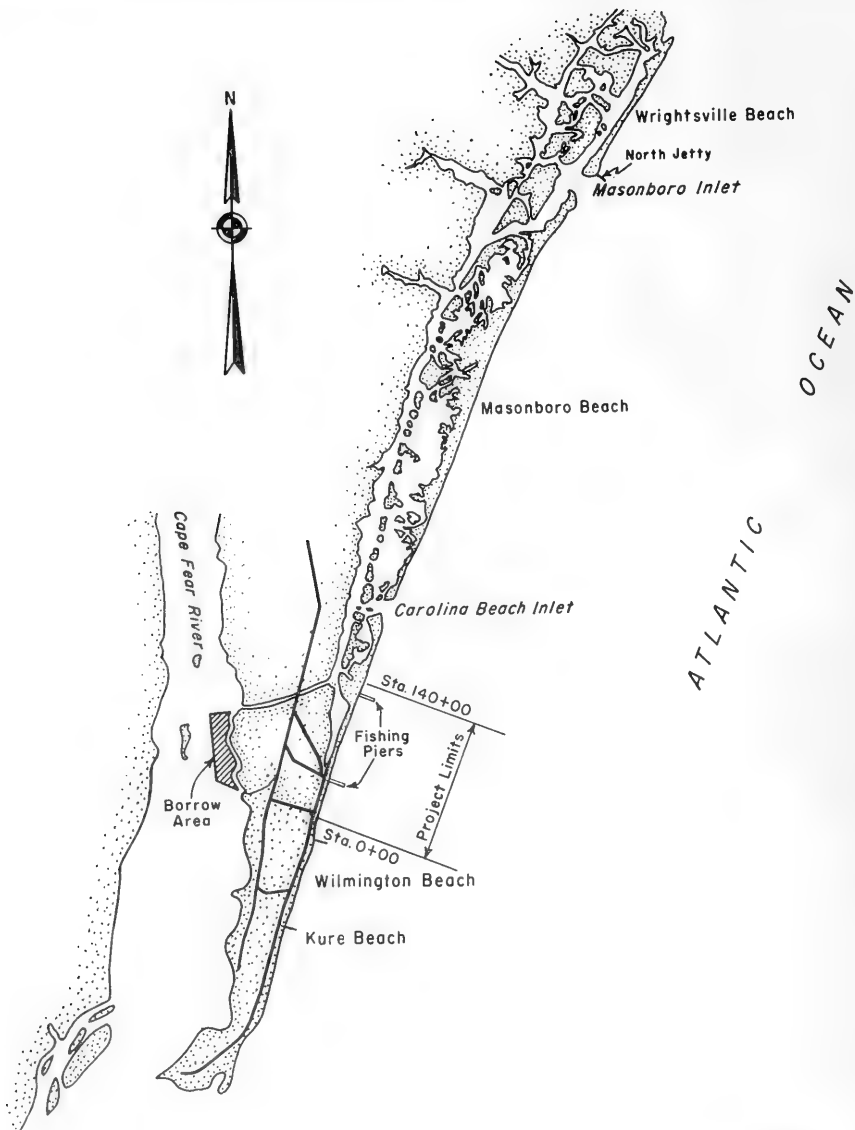
Figure 6-20. Protective Beach (Carolina Beach, North Carolina)

Before Restoration   (1964)

After Restoration   (1965)

Figure 6-21. Protective Beach (Carolina Beach, North Carolina)

Profile of Beach
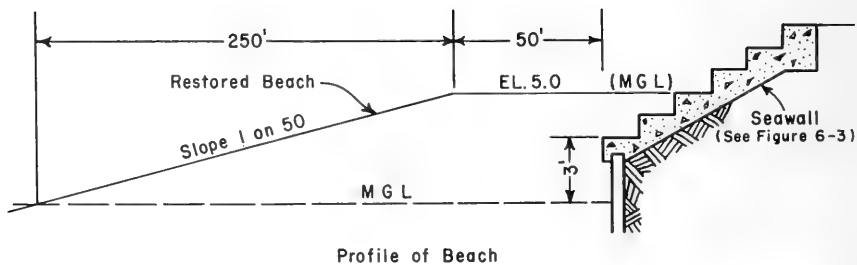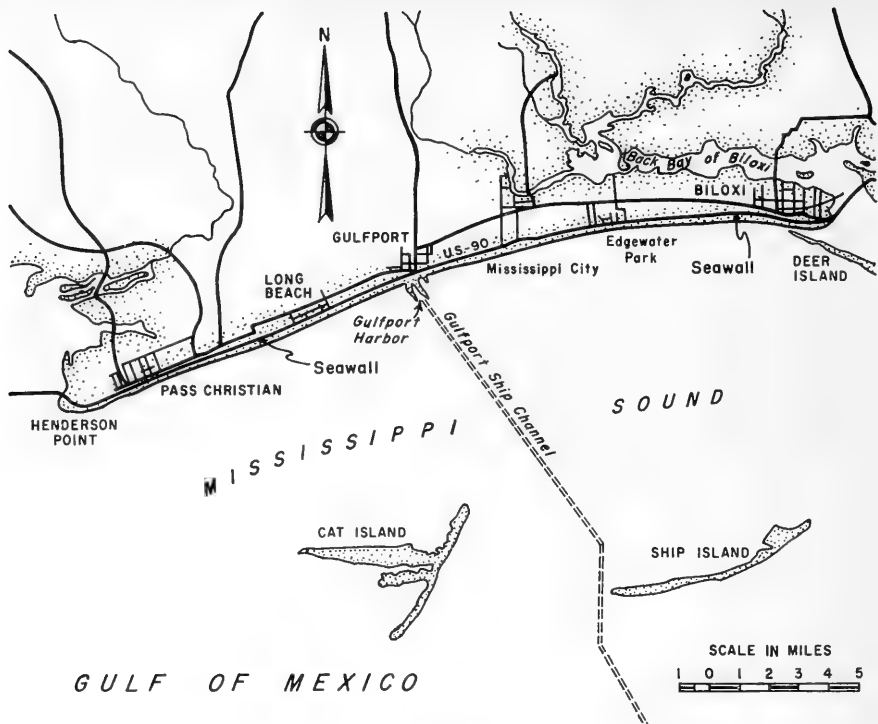
Figure 6-22. Protective Beach (Harrison County, Mississippi)

Before Restoration   (1950)

After Restoration   (1952)

Figure 6-23.   Protective Beach (Harrison County, Mississippi)

in which $\sigma_{\phi b}$ and $\sigma_{\phi n}$ are the standard deviation in ϕ units of the borrow and native materials (in this case 1.28 and 0.91, respectively) and $M_{\phi b}$ and $M_{\phi n}$ are the ϕ means of the borrow and native materials (in this case 0.88 and 1.69 respectively). The critical ratio was computed to be 2.1, indicating that for every cubic yard of material on the active profile in 1967, 2.1 cubic yards of borrow material should have been placed.

In April 1965, approximately 2,632,000 cubic yards of borrow material were placed along the 14,000 linear feet of shore fronting Carolina Beach. (Vallianos, 1970.) Figure 6-21 shows the before-and-after conditions of the beach. The fill consisted of a dune having a width of 25 feet at an elevation of 15 feet above mean low water, fronted by a 50-foot wide berm at an elevation of 12 feet above mean low water. Along the northern-most 3,700 feet of the project, (Figure 6-20), the berm was widened to 70 feet to provide a beach-nourishment stockpile.

Following construction, rapid erosion occurred along the entire length of the beach fill. Initial adjustments were expected based on the use of $R_{\phi crit}$ = 2.1 which resulted in an excess of 1,350,000 cubic yards of fill being placed on the beach to account for the unsuitability of part of the borrow material. However, the actual rates of change, particularly those evidenced along the onshore section of the project, were much greater than originally anticipated considering that all of the fill had not been sub-jected to winnowing by wave action.

In the first 2 years, erosion persisted along the entire length of fill. The erosion along the southern 10,000 feet of the project was less than that along the northern 4,000 feet.

During these years (1965-1967), approximately 712,000 cubic yards, of the 1,652,000 cubic yards initially placed, were moved from the southern 10,000-foot section to depths seaward of the 22-foot contour. This loss was about 43 percent of the total fill placed. Therefore, in terms of fill, protection was reduced by 43 percent. Beach changes resulted in an 82-foot recession of the high water line, and the loss of the horizontal berm of the design profile. By the end of the second year, the southern 10,000 linear feet of project was stabilized, and remained in about the same condition as of 1972.

In the first 2 years after the placement of 980,000 cubic yards of fill, erosion along the 4,000-foot northern section was greater than that in the 10,000-foot southern section. About 550,000 cubic yards of fill were lost from the active profile, amounting to a 56 percent reduction in the total in-place fill. By March 1967, the high water line along this section receded 140 feet, resulting in the complete loss of 1,500 linear feet of original fill, and the severe loss of an additional 1,200 feet of fill. This erosion progressed rapidly in a southward direction and threat-ened the more stable southern section of the project.

In March 1967, emergency measures were taken. The north end was restored by placing about 360,000 cubic yards of fill, and by building a 405-foot groin near the north end. The groin was necessary, because there was a reversal in the predominant direction of longshore transport at the north end. In the next year, approximately 203,000 cubic yards of emergency fill eroded, and most of the shoreline returned to about where it was before the emergency work. The shoreline immediately south of the groin, for a distance of about 400 feet, has remained nearly stable, and the loss of emergency fill along this small segment was about 42 percent less than the loss along the remaining emergency section.

Survey records from 1938 to 1957 (reported in the original project report), show that the average annual recession rate was about 1 foot per year, with a short-term maximum rate of 2.8 feet from 1952 to 1957, when the area had been exposed to four major hurricanes. The annual loss of material for the entire active profile was estimated to be about 4 cubic yards per linear foot.

During the 2 years following the fill, the effects of shore processes were radically different from processes determined from historical records, During April 1965--April 1966 and April 1966--April 1967, the shoreline receded 67 and 15 feet, respectively, with corresponding losses of 370,000 and 342,000 cubic yards. In the third year, April 1967--April 1968, a marked change occurred in the response of the fill. The rate of shoreline recession dropped to 5 feet per year, and the volume change of material amounted to a slight accretion of about 17,000 cubic yards. Surveys in 1969 indicated that the project was in nearly the same condition as in 1968. Full verification of the project performance will depend on future surveys. However, it can be assumed that the project required 2 years of exposure to reach a state of equilibrium with the prevailing enviornment.

Rapid recession of the shoreline during the first 2 years was a result of profile adjustment along the active profile which terminates at depths of profile adjustment along the active profile which terminates at depths between -22 and -30 feet mean low water, as well as net losses in volume resulting from natural sorting action which displaced fine material to depths seaward of the active profile. The foreshore and nearshore design profile slope of 1 on 20 was terminated at a depth of 4 feet below mean low water. The adjusted project profile of April 1968 shows the actual profile closing at a depth of about 22 feet below mean low water, with a characteristic bar and trough system. Thus, displacement of the initial fill with the accompanying reduction of the beach design section was the result of normal sorting action and the reestablishment of the normal profile configuration.

6.322 Sea Girt, New Jersey. The feasibility of pumping sand to a beach from an offshore source by hopper dredge was tested from 28 March to 20 May 1966. (U.S. Army Engineer District, Philadelphia, 1967, and Mauriello, 1967). The beach site at Sea Girt, (Figure 6-24) was selected because it was State owned, required nourishment, and a typical ocean environment would be encountered. Other factors which influenced selection of the
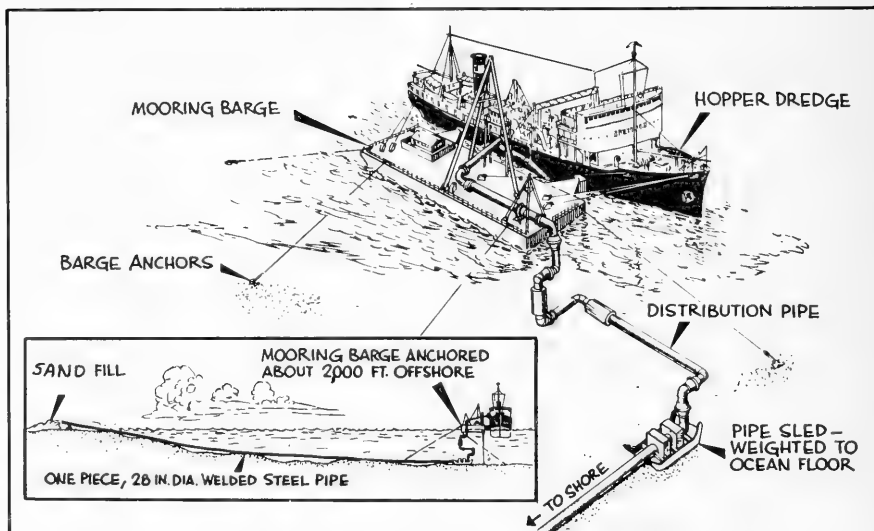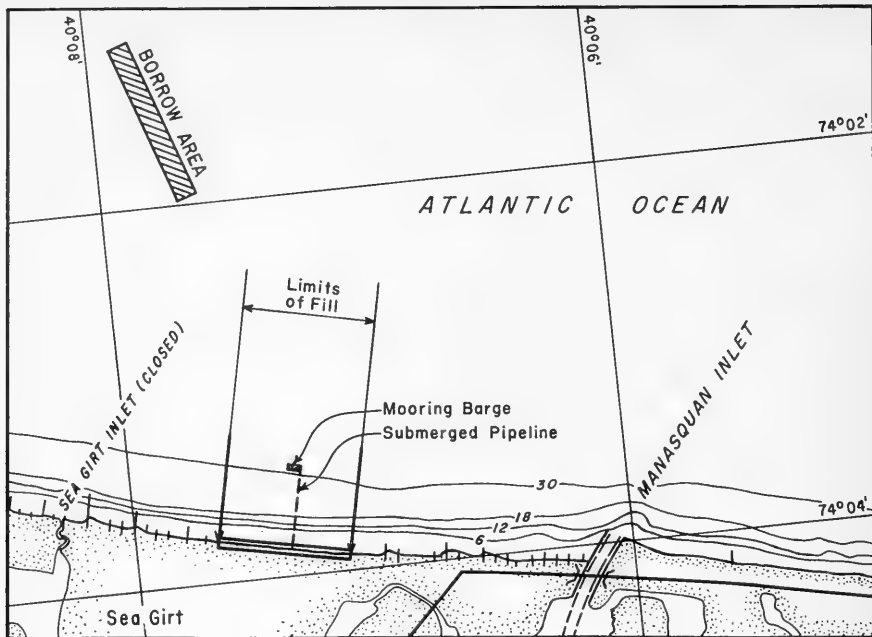
Figure 6-24. Protective Beach at Sea Girt, New Jersey

Before Restoration   (March 1966)

After Restoration   (June 1966)

Figure 6-25. Protective Beach at Sea Girt, New Jersey

6-31

site were an adequate area for assembly of pipeline, the nearness of off-shore sand deposits to the beach, and enough depth (about 30 feet) close to shore to float the dredge and reduce the length of the submerged pipe-line.

The hopper dredge, *Goethals* (bin capacity, 5,623 cubic yards), dredged sand from the ocean bottom and transported it to an anchored barge where sand in the bins was pumped out through a submerged 28-inch pipeline onto the beach. (See Figure 6-24.) About 250,000 cubic yards were deposited on 3,800 linear feet of beach. Operations were interrupted by sea conditions and failure of the pipeline connection system. However, total accomplishment of the project was successful, providing information required for improvement of the equipment, and verifying the feasibility of replensihment of beaches by hopper dredges. Figure 6-25 illustrates, with before-and-after photographs, the beach restoration.

6.323 Redondo Beach (Malaga Cove), California (Fisher, 1969, and U.S. Army Engineer District, Los Angeles, 1970). An authorized beach restora-tion project at Redondo Beach, California, provided another opportunity to use an offshore sand source. (See Figure 6-26.) The availability of sand below the 30-foot contour immediately seaward of the project was in-vestigated in two stages. The first stage, a geophysical survey with an acoustic profiler, indicated that enough sand was available for the pro-ject. In the second stage, core samples were obtained from the ocean bottom using a vibrating core-extraction device. Analysis of the core samples verified an underwater sand source of acceptable quantity and quality. This source covered an area 1.4 miles long by 0.5 miles wide about 1,100 feet offshore (shoreward limit). It would produce 2,500,000 cubic yards of sand if it could be worked to a depth 52 feet below MLLW between the 30- to 60-foot isobaths. An additional 2,500,000 cubic yards of sand could be recovered by extending the depth of excavation to 60 feet below MLLW. The median diameter of the beach sand was 0.5 millimeter; the median diameter of the offshore sand ranged from 0.4 to 0.7 millimeter. The offshore sand was considered an excellent source of material for beach replenishment. Several land sources were also investigated, and found suitable in quantity and quality.

Bids, received in August 1967 for land hauling or ocean-bottom re-covery, ranged from $1.07 per cubic yard to more than $2.00 per cubic yard. A contract was awarded to remove the sand from the ocean source. The con-tractor used a modified 16-inch hydraulic dredge, with a water-jet head on the end of a 90-foot ladder. Although the water-jet technique had been used in excavating channels, filling and emptying coffer dams, and pros-pecting for minerals in rivers, its application to dredging in the ocean appears to be unique. Actual dredging began in early December 1967. On 17 December, ocean swells rose to a height of 7 feet. With the dredge heading into the swells, the 90-foot ladder and dredge vessel as a unit could not respond to the short-period waves. Water came into the hold shorting out electrical equipment. Air in the fuel and ballast tanks kept the dredge afloat, and it was towed into Redondo Harbor for extensive modi-fications to make it watertight and seaworthy. Ultimately the dredge

operated in seas up to 5 feet; at 6-foot seas it proceeded to Redondo Harbor for shelter.

The dredge was held in position with its beam to the sea by an arrangement on the stern and bow lines. On the end of the dredge ladder was a combination head that provided both cutting action and suction action. The force to lift the suspended material was provided by a suction pump in the well of the dredge, assisted by water jets powered by a separate 250 horsepower pump. Sand was removed by working the head down to the bottom of the cut and keeping it in that position until the sandy material stopped running to the head. The head was then raised and the dredge would pivot about 40 feet to the next position in the cutting row, where the process would be repeated. The dredge could cut a row 250 feet wide. At the completion of a row, the dredge was moved ahead on its lines about 40 feet for the next row cut.

For most of the project, it was possible to excavate to -55 to -65 feet, with a cut bank of 20 to 30 feet. This is desirable for high production because it reduces moving and swinging of the dredge.

The sand slurry was transported ashore through a combination pontoon and submerged line. The pontoon line was a 16-inch diameter pipe supported in 60-foot lengths by steel pontoons; each section was joined with a ball-joint coupling. At every third coupling, a 15-foot-long rubber hose was inserted to provide greater flexibility. The pontoon line was connected to the dredge by a quick-release couple that allowed the dredge to be moved swiftly to shelter if a storm arose. The submerged line was steel pipe (with a wall thickness of 3/8 inch) joined to the floating line by a flexible rubber hose. As the beach fill progressed, the submerged line was moved by capping the shore end of the discharge, and then pumping water out of the line. This created a floating pipeline that was towed to the next discharge position. As pumping resumed, the pipeline filled and sank to the bottom.

The submerged line was connected to the beach fill pipe on shore with a bolted connection. The fill was accomplished by a double-pipe system. The system consisted of a yoke attached to the discharge line, and by use of a double-valve arrangement, the discharge slurry was selectively distributed to one pipe or the other or to both pipes simultaneously.

The beach was built by placing the first discharge pipe at the desired final elevation of the fill, in this case at +12 MLLW (Figure 6-26) and pumping until the desired elevation was reached. During this pumping period, the second line was built parallel to the first. The valve controlling the first line was closed and the valve to the second line was opened. The first pipe was then advanced to the next discharge point. By alternating between these two discharge lines, the beach width of 200 feet was built to the full cross section as they advanced. (See Figure 6-27.) The final placement totaled 1.4 million cubic yards at a cost of $1.5 million. Between 4,000 and 15,000 cubic yards per day were placed on the beach, averaging 8,000 cubic yards per day. Recent measurements indicated only minor beach changes, and the beach has been relatively stable.
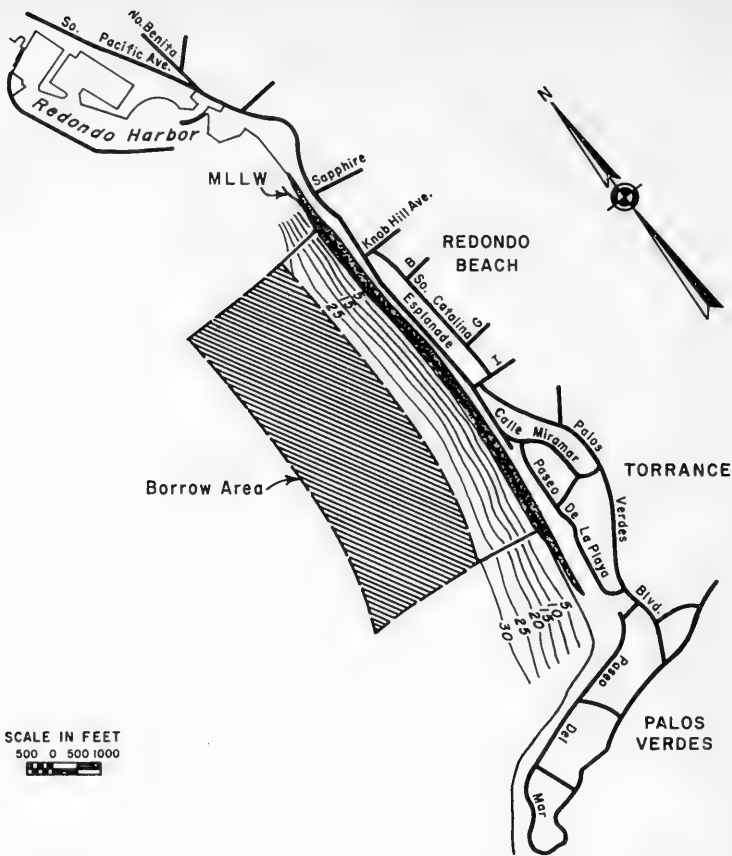
6-33
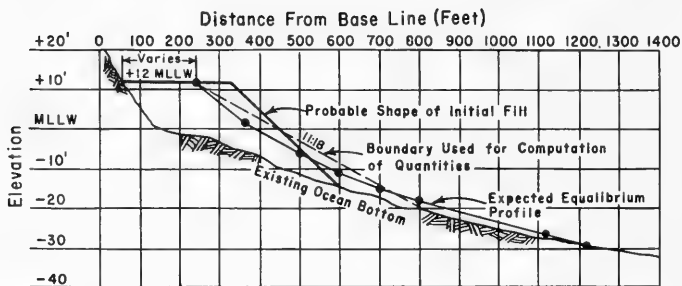
Figure 6-26. Protective Beach (Redondo Beach, California)

Before Restoration   (April 1962)

SUBMERGED PIPELINE   OFFSHORE DREDGE

After Restoration   (September 1968)

Photographs Courtesy of Shellmaker Corporation

Figure 6-27.   Protective Beach (Redondo Beach, California)

6-35

This project was the first in the United States in which an unprotected hydraulic pipeline dredge was operated successfully in the open sea. Although highly successful in this project, this procedure has a critical limitation--the necessity for a nearby harbor. Experience gained on this project and the hopper-dredge operation at Sea Girt, (Section 6.322) provides the techniques for further recovery of valuable beach sand from offshore sources.

6.4 SAND DUNES

Foredunes (Fig. 6-28) form just behind the beach and perform an important role in littoral processes. (See Sections 5.4 and 4.6.) Foredunes function as a reservoir of sand to nourish eroding beaches during high water, and as a levee to prevent waves from damaging backshore areas. As such, they are valuable nonrigid shore protection structures. Foredunes are created naturally by the combined action of sand, wind, and biota. Behind sandy beaches, foredunes often form a continuous line to resist overtopping by high water and wave action.

Figure 6-28. Foredune System

6.41 SAND MOVEMENT

Winds with sufficient velocity to move sand particles deflate the exposed beach, and transport sand in three ways:

(a) <u>Suspension</u>. Small or light grains are lifted into the air stream and carried appreciable distances;

(b) <u>Saltation</u>. Individual particles are carried by the wind in a series of short jumps along the beach surface; and

(c) <u>Surface Creep</u>. Particles are rolled or bounced along the ground as a result of wind forces or impact of descending saltating particles.

These three ways of transportation effectively sort the original beach material. Smaller particles are removed from the beach and dune area. Larger particles remain on the beach. Medium-sized particles form the foredunes. Although most sand particles move by saltation, surface creep may account for 20 to 25 percent of the sand moved. (Bagnold, 1942.)

6.42 DUNE FORMATION

Dune building begins when an obstruction causes deposition of sand grains. As the dune builds, the seaward slope may become so steep that saltating or creeping particles come to rest there. With higher wind velocities, particles move up the face of the dune, settle in the lee of the dune, and cause the dune to migrate in the direction the wind is blowing. Foredunes are often created and maintained by the action of the beachgrasses in trapping and stabilizing sand blown off the beach.

Foredunes may be destroyed by the waves and tides of severe storms, by drought or disease destroying the beachgrasses, or by overgrazing that reduces the vegetative cover permitting local "blowouts." Foredune management has two divisions--stabilization and maintenance of naturally occurring dunes, and creation and stabilization of protective dunes where they do not exist. Although dunes can be constructed by mechanical structures, a preferred procedure is to create a stabilized dune through the use of vegetation.

6.43 DUNE CONSTRUCTION--SAND FENCE

Various mechanical methods, such as fencing made of brush or by driving individual pickets into the sand, have been used to construct a foredune. (Blumenthal, 1965, Jagschitz and Bell, 1966a, McLaughlin and Brown, 1942, Gage, 1970.) Relatively inexpensive, readily available slat-type snow fencing (Figure 6-29) is used almost exclusively in artificial dune construction. Plastic fabrics have been investigated for use as sand fences. (Savage and Woodhouse, 1969.) Although some preliminary results were encouraging, these fabrics have not been tested sufficiently to provide an adequate evaluation. Satisfactory, but short-term results have been obtained with jute-mesh fabric. (Barr, 1966.)

Studies to develop techniques for constructing dunes of a desired size and profile through use of sand fences have been conducted at Cape Cod,

Figure 6-29. Erecting Snow-type Sand Fencing

(Savage, 1962)

Figure 6-30. Snow-type Sand Fencing Filled to Capacity

Massachusetts; Core Banks, North Carolina; and Padre Island, Texas. Conclusions and recommendations based upon these studies are:

(a) Fencing with a porosity (ratio of area of open space to total projected area) of about 50 percent should be used. (Savage and Woodhouse, 1969.) Open and closed areas should be smaller than 2 inches in width.

(b) Only straight fence alignment is recommended. (See Figure 6-30.) Fence configurations with side spurs or a zigzag alignment do not increase the trapping effectiveness enough to be economical. (Savage, 1962.)

(c) Placement of the fence at the proper distance shoreward of the berm crest may be critical. The fence must be far enough back from the berm crest to be away from frequent wave attack. Efforts have been most successful when the selected fence line coincided with the natural vegetation line or foredune line prevalent in the area. This distance is usually greater than 200 feet shoreward of the berm crest.

(d) The fence should parallel the shoreline. It need not be perpendicular to the prevailing wind direction. The fence will fill if constructed with some angularity to sand-transporting winds.

(e) If sand moves on the beach, sand fencing with 50 percent porosity will usually fill to capacity within 1 year. (Savage and Woodhouse, 1969.) The dune will be about as high as the fence. The dune slopes will range from about 1 on 4 to 1 on 7, depending on grain size and wind velocity.

(f) More than one lift of fence can be filled within a year, if the fill rate is closely observed. The rate of fill is not constant and varies with local conditions. A fence may nearly fill during a short period of high wind velocities. If the next lift of fence is erected shortly after the filling of the existing fence, it also may be filled within the same season.

(g) Installation time and positioning of the succeeding lifts of sand fence depend on the objectives, i.e. to increase the dune height, the width of the dune base, or both. Dune height is increased by erecting succeeding lifts of fence at the crest of the existing dune. (See Figure 6-31.) The effective height increase gained by positioning the fence at the crest is nearly 3 feet with a 4-foot fence as shown by the second lift in Figure 6-31. Note that the effective height gained from the third lift is much less. The third lift was initially erected at the crest of the dune shown by the 24-month profile. Dry, high winds occurred for several days following installation. Turbulence at the dune crest eroded so much sand from the base of the fence that support posts had to be reset to keep the fence upright. Thus the effective height was reduced to 1 foot.

Dune width is increased by erecting succeeding lifts of fence parallel to and away from the existing fence. The second lift is placed shoreward or landward of the existing fence depending on the direction the dune is to be constructed. The offset distance between fence lines should be about

SCHEDULE FENCE ERECTION

Time (Months)	Lift Number
0	1
12	2
24	3

SAND VOLUME
(cu. yds. / lin. ft. of beach)

Time (Months)	Cumulative	Interval
0	0	0
12	3.4	3.4
24	6.1	2.7
36	10.4	4.3
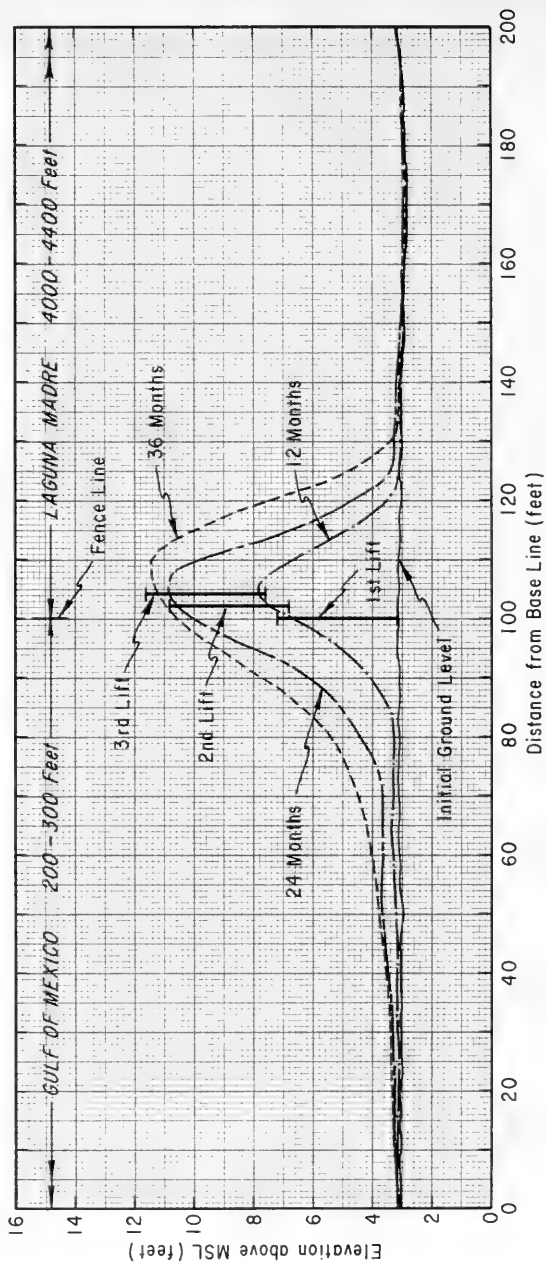
Figure 6-31. Sand Fence Dune -- Padre Island, Texas
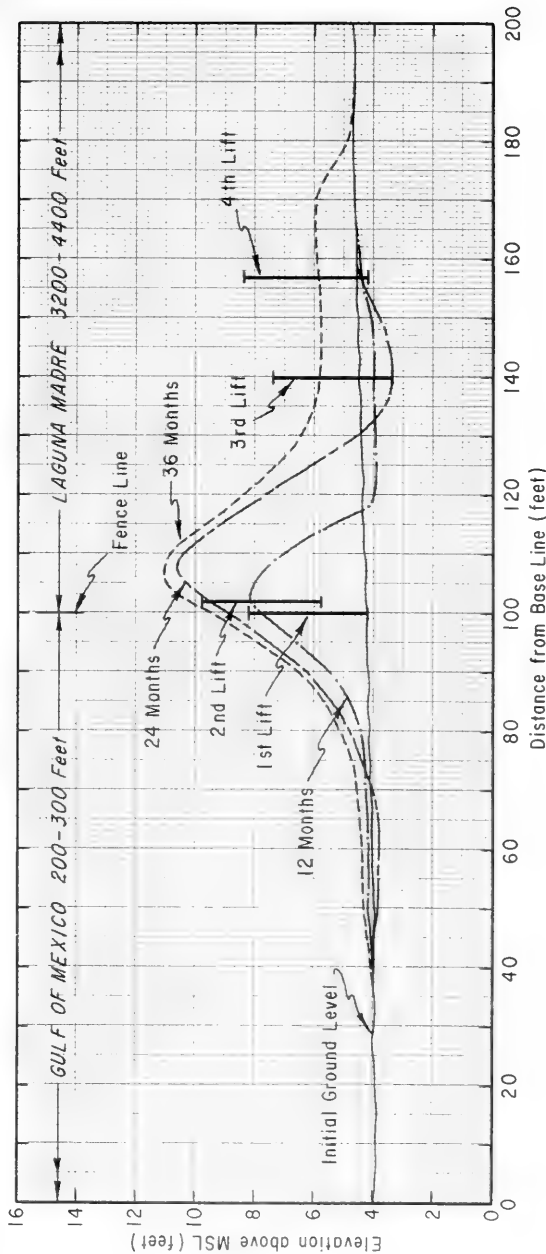
Figure 6-32. Sand Fence Dune -- Padre Island, Texas

four times the fence height. A 4-foot fence requires fence lines to be 16 feet apart, see third and fourth lifts in Figure 6-32. This arrangement is most efficient in trapping sand, and forms a more uniform dune. Positioning the second lift on the slope of the existing dune will increase both its height and width. The actual sequence of installation of the fence may alternate between a position on the crest, along the slope, or offset to the existing dune.

(h) The trapping capacity of the initial installation and succeeding lifts of a 4-foot high sand fence averages between 2 and 3 cubic yards per linear foot. (See Figures 6-31 and 6-32.)

(i) CERC's experience has been that on the average 6 man-hours were required to erect 235 feet of wooden, picket-type fence or 185 feet of fabric fence when a six-man crew had materials available at the site and used a mechanical posthole digger.

(j) Unless maintained, dunes created by fencing are short-lived, because of corrosion of wire, deterioration of wood (Figure 6-33), and vandalism.

(k) Junk cars should not be used for dune building. They are more expensive and less effective than fencing. (Gage, 1970.) Junk cars mar the beauty of a beach, and create a safety hazard.

Figure 6-33. Sand Fence Deterioration Due to Exposure and Storms

(1) The best way to maintain a fence-constructed dune is to plant it with vegetation.

6.44 DUNE CONSTRUCTION - VEGETATION

Few plant species survive in the harsh beach environment. Those that thrive along beaches are adapted to conditions that include abrasive and accumulating sand, exposure to full sunlight, high surface temperatures, occasional inundation by salt water, and drought. The plants that do survive are long-lived, rhizomatous or stoloniferous perennials with extensive root systems, stems capable of rapid upward growth through accumulating sand, and tolerance of salt spray. Although only a few plant species have these essential characteristics, one or more suitable species of beach-grasses occur along most of the beaches of the United States.

The most frequently used beach grasses are American beach grass (*Ammophila breviligulata*) along the Mid- and Upper-Atlantic coast and in the Great Lakes region (Jagschitz and Bell, 1966b; Woodhouse and Hanes, 1967; Woodhouse, 1970); European beach grass (*Ammophila arenaria*) along the Pacific Northwest and California coast (Brown and Hafenrichter, 1948; McLaughlin and Brown, 1942; Kidby and Oliver, 1965; USDA, 1967) sea oats (*Uniola paniculata*), along the South Atlantic and Gulf coast (Woodhouse, Seneca, and Cooper, 1968: Woodard, et al., 1971); panic beach grasses (*Panicum amarum*) and (*amarulum*) along the Atlantic and Gulf coasts (Woodhouse, 1970; Woodard, et al., 1971.)

Transplanting techniques for most species of beach grass are well developed. Transplanting is recommended for areas adjacent to the beach berm and for critical areas - sites subject to erosion. Most critical areas require densely spaced transplants to ensure successful stabilization. A mechanical transplanter mounted on a tractor is recommended for flat or moderate slopes. (See Figure 6-34.) Steep and irregular slopes must be planted by hand.

Seeding is practical only when protection from eroding and drying winds can be provided by mulching or frequent irrigation, and is therefore not applicable to most beach areas. Beach grass seeds are not available from commerical sources, and must be wild harvested during the fall for spring seeding.

Table 6-1 summarizes much of the information about transplanting and sand-trapping ability of the beach grasses. Additional factors for successful transplanting are harvesting and processing of transplants, proper placement of dune, and planting transplants.

6.441 Harvesting and Processing. The plants should be dug with care so that most roots remain attached to the plants. The clumps should be separated into transplants having the desired number of culms (stems). Plants should be cleaned of most dead vegetation and trimmed to a length of 18 to 20 inches to facilitate mechanical transplanting. Plants dug while dormant and held in cold storage may be used for late spring plantings.

Figure 6-34. Mechanical Transplanting of American Beachgrass

6.442 <u>Spacing</u>. The vulnerability of a site to erosion determines transplant spacing and culm number. The more vulnerable a site is to erosion, the greater the number of culms per transplant and the closer the plant spacing. (See Table 6-1.) Also, if dense first-year growth is essential, plant spacing should not exceed 18 inches.

6.443 <u>Nutrients</u>. Where field tested, beach grasses have responded to supplemental nutrients by increased foliage production. This in turn, provides greater sand-trapping capacity. Rates of fertilizer are provided in Table 6-1. If first-year growth is satisfactory, the fertilizer program may be reduced to fewer applications and less fertilizer. Response of beach grasses to slow-release fertilizers has been varied, and results are inconclusive. (Augustine, et al., 1964; Hawk and Sharp; 1967; Woodhouse and Hanes, 1967.)

6.444 <u>Seed</u>. American beachgrass can be seeded only on protected sites. Seeding is less expensive than transplanting. However, costs for harvesting, chilling and storing seed, plus costs of mulching after seeding, if required, reduce the cost difference. Harvest in the fall from a good stand of American beach grass should yield about 32 pounds of seed to the acre. (Jagschitz, 1960.) After harvest the seed should be chilled at 40°F under moist conditions for 3 to 4 weeks in the northern part of its geographic zone and 2 weeks or less in the southern part. (Seneca, 1969,

Table 6-1. Beach Grass Planting Summary

Element	Species			
	Beach Grass			Sea Oats*
	American	European	Par⁚c	
Planting Season				
Late fall to early winter	yes	yes	yes	no
Mid-Winter	yes	yes	optimum	optimum
Late winter to early spring	optimum	optimum	optimum	yes
Early spring to mid-spring	yes	yes	yes	no
Available Source				
Transplants				
Commercial	yes	yes	no	no
Wild-harvest	yes	yes	yes	yes
Seed				
Commercial	no	no	no	no
Wild-harvest	yes	yes	yes	yes
Planting Density (maximum and minimum values) (Stem number x plant center spacing in inches)				
Eroding site	5 x 6 − 3 x 18†	5 x 6 − 3 x 18	1 x 6 − 1 x 18	3 x 12 − 1 x 18
Noneroding site	3 x 18 − 1 x 36	3 x 18 − 1 x 36	1 x 18 − 1 x 48	1 x 18 − 1 x 48
Fertilizer—MPK‡				
Rate lbs./acre (annual)	200-60-0	40-0-0	NFT§	NFT
Frequency (applications/year)	3	1	NFT	NFT
Average Annual Sand-Trapping Rate (cubic yards per lineal foot of beach)				
Padre Island, Texas	NA‖	NA	3 (2)	3 (3)
Core Banks, N.C.	2 (7)£	NA	NFT	1 (5)
Ocracoke Island, N.C.	2 (7)	NA	NFT	NFT
Clatsop Spit, Oregon	NA	5 (33)	NA	NA
Annual Rate of Increase in Dune Dimensions (feet)				
Lateral	7 (7)	NFT	NFT	1 (3)
Elevation	1 (7)	0.7 (33)	2 (2)	2 (3)

* Illegal to harvest in some states.

† 5 x 6 − 3 x 18 is 5 stems on 6-inch centers to 3 stems on 18-inch centers.

‡ NPK — Nitrogen Phosphorus Potassium.

§ NFT — Not Field Tested.

‖ NA — Not Applicable.

£ Number in parenthesis represents years of record.

Seneca and Cooper, 1971.) After cold treatment, the seed should be dried
and stored under cool, dry conditions until planting. Seeding date should
coincide with temperatures best for germination--65°F night, and 85°F days.
Best growth of seedlings occurs with daytime temperatures between 80°F and
90°F. (Seneca and Cooper, 1971.)

6.445 Disease and Stress. Beach grasses vary in their tolerance to
drought, heat, cold, disease, and parasites. Plantings of a species out-
side its natural geographic zone are vulnerable during periods of environ-
mental stress. American beach grass is more susceptible to scale infesta-
tion when exposure to sand blasting is reduced. Deteriorating stands of
American beach grass, due to scale infestation (*Eriococcus carolinea*),
have been identified from New Jersey to North Carolina. (Campbell and
Fuzy, 1972.) South of its natural geographic zone (Nags Head, North
Carolina), American beach grass is susceptible to heat (Seneca and Cooper,
1971), and a fungal infection (Marasius blight) is prevalent. (Lucas,
et al., 1971.)

South of Virginia, mixed species plantings are desirable and necessary.
The slow natural invasion (6 to 10 years) of sea oats into American beach
grass dunes (Woodhouse, Seneca and Cooper, 1968), may be hastened by mixed
species plantings. Thus with better vegetation cover, the chance of over-
topping during storms is reduced.

Sea oats and panic beach grass occur together throughout much of their
natural geographic zone. Mixed plantings of sea oats and beach grass are
recommended since they produce a thick cover and more dune profile.

6.446 Planting Width. Plant spacing and sand movement must be considered
in determining planting width. When little sand is moved for trapping,
and plant spacing is dense, nearly all sand is caught along the seaward
edge of the dune and a narrow-based dune is formed. If the plant spacing
along the seaward edge is less dense under similar conditions of sand
movement, a wider based dune will be formed. However, the rate of plant
growth limits the time in which the less dense plant spacing along the
seaward edge will be effective. The following example illustrates the
interrelationship of planting width, plant spacing, sand volume, and rate
of plant growth. American beach grass planted on the Outer Banks of North
Carolina at 18 inches and outer spacing of 24 to 36 inches accumulated
sand over a larger part of the width of the planting for the first two
seasons. By the end of the second season, the plant cover was so extensive
along the seaward face of the dune that most sand was being trapped within
the first 25 feet of the dune.

American beach grass typically spreads outward by rhizomatous (under-
ground stem) growth, and when planted in a band parallel to the shoreline
will grow seaward while trapping sand. Thus, a dune can build toward the
beach from the original planting. Seaward movement of the dune crest in
North Carolina is shown in Figures 6-35 and 6-36. This phenomenon has not
occurred with the sea oats plantings in south Texas (Figure 6-37) or Core
Banks, North Carolina. (See Figure 6-38.)

Figure 6-35. American Beachgrass Dune -- Ocracoke Island, North Carolina

SAND VOLUME
(cu. yds./ lin. ft. of beach)

Time (Months)	Cumulative	Interval
0	0	0
24	5.1	5.1
51	9.0	3.9
80	15.6	6.6

6-47
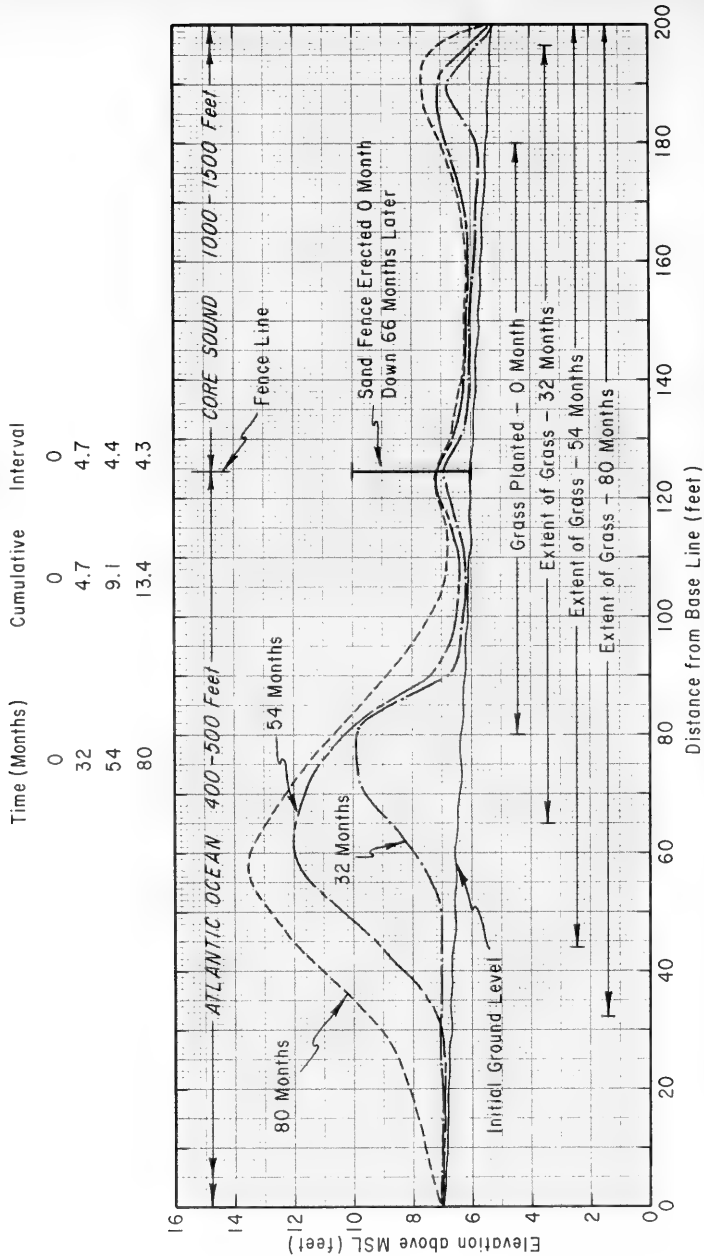
Figure 6-36. American Beachgrass with Sand Fence -- Core Banks, North Carolina

SAND VOLUME
(cu. yds. / lin. ft. of beach)

Time (Months)	Cumulative	Interval
0	0	0
32	4.7	4.7
54	9.1	4.4
80	13.4	4.3
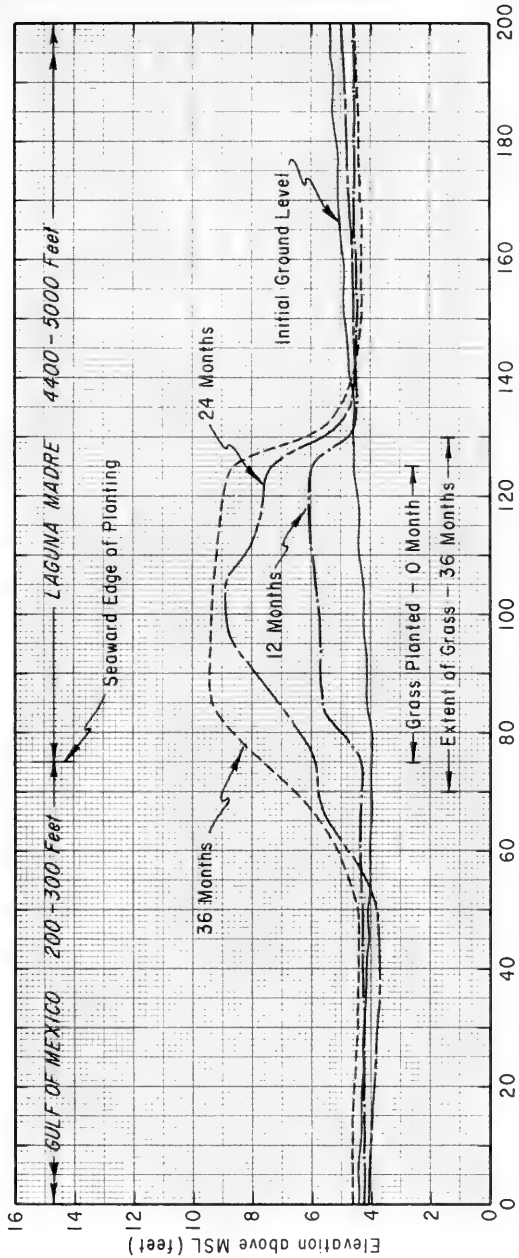
Figure 6-37. Sea Oats Dune -- Padre Island, Texas

SAND VOLUME
(cu. yds./ lin. ft. of beach)

Time (Months)	Cumulative	Interval
0	0	0
22	2.0	2.0
36	3.1	1.1
55	5.6	2.5
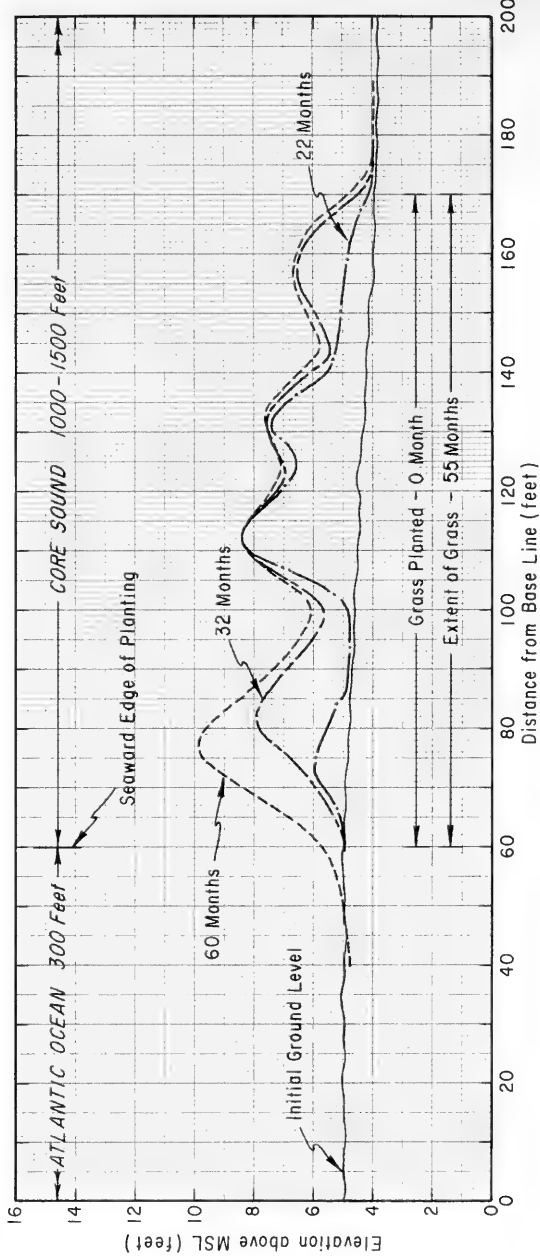
Figure 6-38. Sea Oats Dune -- Core Banks, North Carolina

The rate of spread for American beach grass has averaged about 3 feet per year on the landward side of the dune and 7 feet per year on the seaward slope of the dune as long as sand was available for trapping. (See Figures 6-35 and 6-36.) The rate of spread of sea oats is considerably less, 1 foot or less per year.

Figure 6-35 shows an experiment to test the feasibility of increasing the dune base by a sand fence in a grass planting. The fence was put in the middle of the 100-foot wide planting. (See Figure 6-39.) Some sand was trapped while the American beach grass began its growth, but afterwards little sand was trapped by this fence. Figure 6-36 shows how the central part of the planting had a limited increase in elevation due to the reduced amount of sand reaching it. The seaward edge of the dune trapped nearly all of the beach sand during onshore winds. The landward edge of the dune trapped the sand transported by offshore winds blowing over the unvegetated area landward of the dune.

6.447 <u>Trapping Capacity</u>. Periodic cross-section surveys were made of the plantings to determine the volume of trapped sand, and to document the profile of the developing dune. The annual average rate of sand trapped is 2 to 3 cubic yards per linear foot of beach by American beach grass in North Carolina, (Figures 6-35, 6-36), and by sea oats (Figures 6-37 and 6-40), and panic beach grass in Texas. The annual average rate of sand trapped by sea oats in North Carolina is 1 cubic yard. (See Figure 6-38.)

European beach grass annual trapping rate on Clatsop Spit, Oregon, has averaged about 5 cubic yards. Although surveys were not taken until nearly 30 years after planting (Kidby and Oliver, 1965), the initial trapping rates must have been greater. (See Figure 6-41.)

These rates are much less than the rates of vigorous grass plantings. Small plantings (100 feet square) of American beach grass trapping sand from all directions have trapped as much as 16 cubic yards per linear foot of beach in a period of 15 months on Core Banks, North Carolina. (Savage and Woodhouse, 1969.) While this figure may exaggerate the volume of sand available for dune construction over a long beach, it does indicate the potential trapping capacity of American beach grass. Similar data for sea oats or panic beach grass are not available. However, observations on the rate of dune growth on Padre Island, Texas following Hurricane Beulah (September 1967) indicate that the trapping capacity of sea oats and panic beach grass is greater then the 3 cubic yard annual rate observed for the planted dunes. This suggests that dune growth in most areas is limited by the amount of sand transported off the beach rather than by the trapping capacity of the beach grasses.

6.448 <u>Dune Elevation</u>. The crest elevation of the constructed dunes is 12 feet MSL on Ocracoke Island (Figure 6-35), 13 feet MSL on Core Banks (Figure 6-36), 10 feet MSL on Padre Island (Figure 6-37) and 37 feet MSL on Clatsop Spit (Figure 6-41). This is an increase of nearly 8 feet for dunes in North Carolina, 6 feet on Padre Island, and 27 feet on Clatsop Spit.
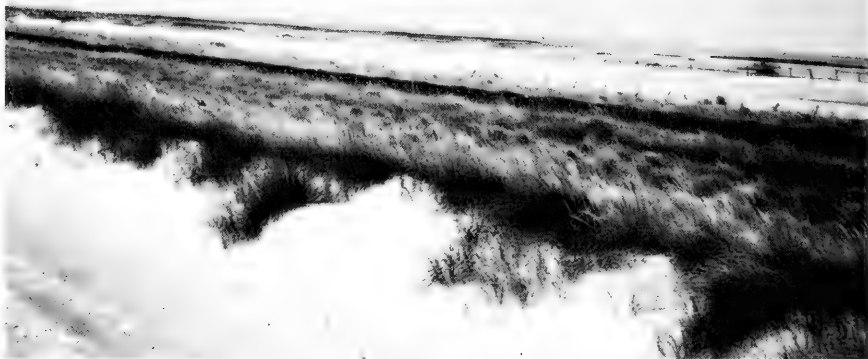
Figure 6-39. American Beach Grass Planting with Sand Fence, Core Banks, N.C. (32 months after planting)

Figure 6-40. Sea Oats Planting South Padre Island, Texas (38 months after planting)
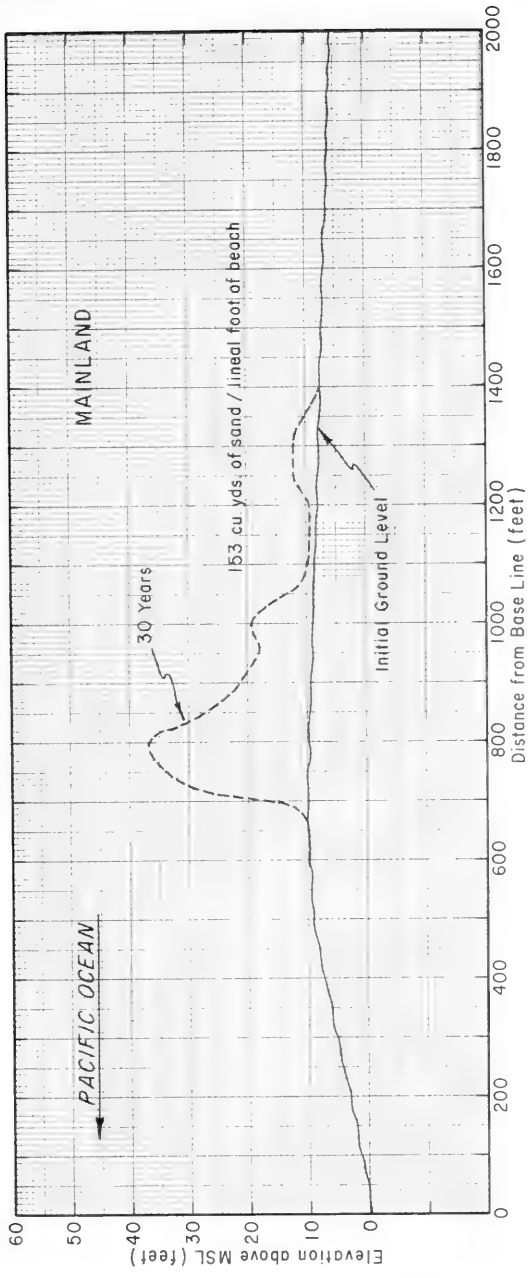
Figure 6-41. European Beachgrass Dune -- Clatsop Spit, Oregon

The average annual increment in elevation for 40 cross-sections on Ocracoke Island since 1964 is 1.01 feet. The average on Core Banks is less--0.17 feet for 18 cross-sections since 1965. The elevation increment for 20 cross sections on Clatsop Spit is 0.7 feet per year for 33 years. Undoubtedly the latter average was much higher during the first 5 to 10 years, but survey information is lacking. For the first 3 years on Padre Island, the average increase in elevation has been 2 feet per year.

6.449 Cost Factors. Survival rate of transplants may be increased by increasing the number of culms per transplant. This increase in survival rate does not offset the increase in cost to harvest multiculm transplants. It is less expensive to reduce plant spacing if factors other than erosion (such as drought) affect survival rate.

Harvesting, processing, and transplanting of sea oats requires one man-hour per 130 hills, panic beach grass requires one man-hour per 230 hills. For example, a 50-foot wide, 1-mile long planting of sea oats on 24-inch centers requires about 500 man-hours for harvesting, processing, and transplanting if plants are locally available. Using a mechanical transplanter, 400 to 600 hills can be planted per man-hour.

Nursery production of transplants is recommended unless, easily harvested wild plants of quality are locally available. Nursery plants are easier to harvest than wild stock. Commercial nurseries are now producing American and European beach grass.

6.5 SAND BYPASSING

Several techniques have been used for mechanically bypassing sand at littoral barriers. The type of littoral barriers--breakwaters and jetties --determines the method of sand bypassing that should be employed. The four types of littoral barrier where sand transfer systems have been used are illustrated in Figure 6-42. The basic methods of sand bypassing are: Fixed bypassing plants, floating bypassing plants, and land-based vehicles. Various features combining types of littoral barriers and methods of bypassing are illustrated by descriptions of selected projects.

6.51 FIXED BYPASSING PLANTS

Fixed bypassing plants have been used at the following Type I (Fig. 6-42) inlet improvements in the United States: Rudee Inlet, Virginia Beach, Virginia; South Lake Work Inlet, Florida; and Lake Worth Inlet, Florida.

In other countries, fixed bypassing plants were used at Salina Cruz, Mexico, (U.S. Army, Beach Erosion Board, 1951), Durban, Natal, South Africa, (U.S. Army, Beach Erosion Board, 1956.) Both were located at breakwaters on the updrift sides of harbor entrances. The Salina Cruz plant rapidly became land-locked, and was abandoned in favor of other methods of channel maintenance. (U.S. Army, Beach Erosion Board 1952,
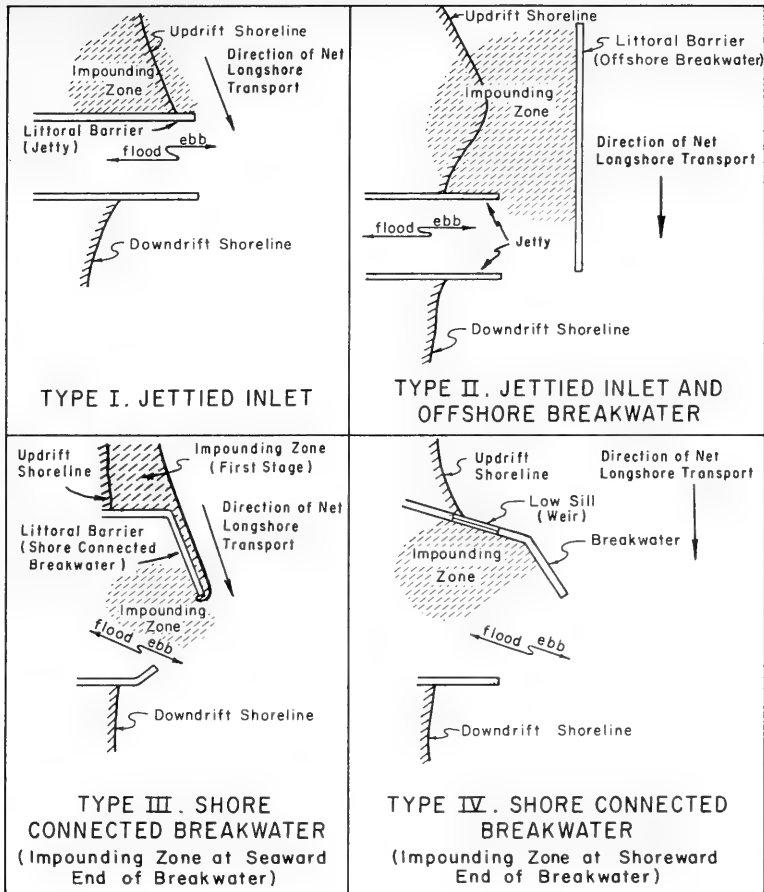
(Watts, 1965)

Figure 6-42. Types of Littoral Barriers where Sand-Transfer Systems have been used

1955.) At Durban, the plant bypassed about 200,000 cubic yards of sand per year from 1950 to 1954; afterward the amount decreased. The plant was removed in 1959 when not enough littoral drift reached it. No apparent reduction in maintenance dredging of the harbor entrance channel took place during the 9 years of bypassing operations. Starting in 1960, the material dredged from the channel was pumped to the beach to the north by a pump-out arrangement from the dredge and booster pumps along the beach.

6.511 South Lake Worth Inlet, Florida. (Watts, 1953). South Lake Worth Inlet, about 15 miles south of Lake Worth Inlet and about 10 miles south of Palm Beach, was dredged, and two entrance jetties were constructed in 1927. The primary purpose of this inlet was to create a circulation of water in the south end of Lake Worth, to lessen a stagnant water condition. The inlet channel also permits passage of craft drawing up to 6 or 8 feet. It is 125 feet wide and 600 feet long. The entrance jetties are 250 feet long. Their top elevation is 12 feet above mean low water. After jetties were built, the downdrift beach south of the inlet eroded. Construction of a seawall and groin field failed to stabilize the shoreline. A fixed sand bypassing plant began operation in 1937. (See Figure 6-43.) The initial plant was designed to bypass enough sand over 2 years to fill the groins and protect the seawall. Design capacity did not include consideration of total longshore transport. The plant consisted of an 8-inch suction line, a 6-inch centrifugal pump driven by a 65-horsepower diesel engine, and about 1,200 feet of 6-inch discharge line that crossed the inlet on a highway bridge. The outfall was located on the beach south of the south jetty.

The plant, with a capacity of about 55 cubic yards of sand per hour, pumped an average of 48,000 cubic yards of sand a year for 4 years. The net north-to-south longshore transport rate was estimated to be about 225,000 cubic yards a year. After 5 years (1937-1941), the beach was partially restored for more than a mile downcoast. During the next 3 years (1942-1945), pumping was discontinued, and the beach south of the inlet severely eroded. In 1945, the plant resumed operation, and the shore immediately south of the inlet was stabilized. To reduce shoaling in the inlet channel, the size of the bypassing plant was increased to an 8-inch pump with a 27-horsepower diesel engine with a capacity of about 80 cubic yards of sand per hour. This plant bypassed about one-third of the available littoral drift. The remainder, about 150,000 cubic yards, was transported by waves and currents to the offshore zone, the middleground shoal, and the downdrift shore.

6.512 Lake Worth Inlet, Florida. (Zermuhlen, 1958, and Middleton, 1959). Lake Worth Inlet is at the north limit of Palm Beach, Florida. The fixed bypassing plant is a two-level, reinforced concrete structure near the end of the north jetty. (See Figure 6-44.) On the lower level (1 foot below MLW) are a centrifugal dredge pump, a 400-horsepower electric motor, and a power transformer. The upper level houses controls and ventilating equipment. The pump has a 12-inch suction and 10-inch discharge, and is designed to handle 15 percent solids at more than 60 percent efficiency. Design capacity was about 170 cubic yards per hour. The suction line is

(December 1955)
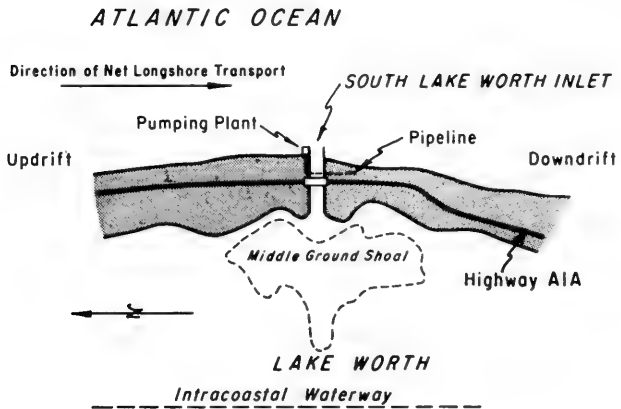
Figure 6-43. Fixed Bypassing Plant - South Lake Worth Inlet, Florida
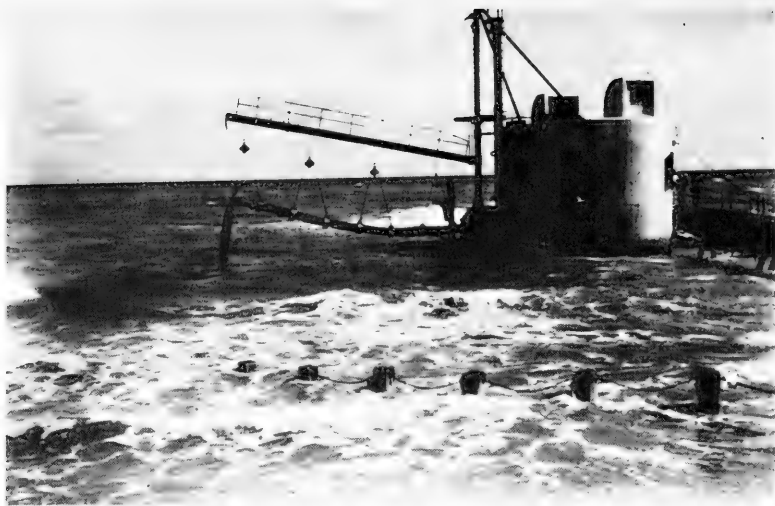
(Circa, 1961)
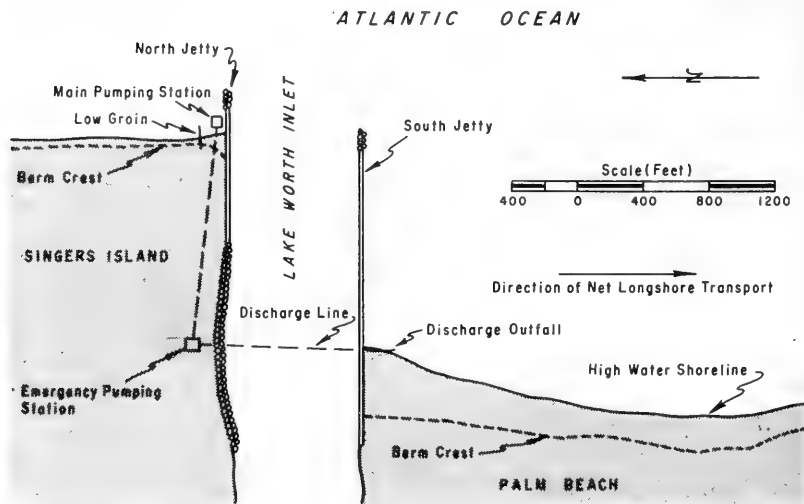
Figure 6-44. Fixed Bypassing Plant - Lake Worth Inlet, Florida

6-58

supported by a 30-foot movable boom. The discharge line is 1,750 feet long, and is made of steel pipe with a 1/2-inch wall thickness, except for an 800-foot section of wire-reinforced rubber hose submerged line that crosses the navigation channel. This section can be removed during channel maintenance. Safety features were installed to reduce the possibility of clogging the submerged discharge line.

The plant began operating in August, 1958. It was estimated that 71,400 cubic yards of sand were bypassed in 451 hours of operation during 8 months, or a rate of about 100,000 cubic yards per year, almost half of the estimated annual littoral transport rate.

6.52 FLOATING BYPASSING PLANTS

All four types of littoral barriers (Figure 6-42) have used floating plants for harbor and inlet improvements. Floating bypassing plant operations have been used at the following places:

TYPE I
Port Hueneme, California

TYPE II
Channel Islands Harbor, California
Ventura Marina, California

TYPE III
Fire Island Inlet, New York
Santa Barbara, California
Oceanside Harbor, California

TYPE IV
Hillsboro Inlet, Florida
Masonboro Inlet, North Carolina
Ponce de Leon Inlet, Florida
East Pass, Florida
Perdido Pass, Alabama

6.521 Port Hueneme, California. (Savage, 1957). This harbor is about 7 miles south-southeast of the mouth of the Santa Clara River. The harbor, constructed in 1940, was acquired by the U.S. Navy in 1942. The 35-foot-deep entrance channel is protected by two converging rubble-mound jetties. (See Figure 6-45.) Littoral drift moves southeast at a rate estimated between 800,000 and 1,200,000 cubic yards a year. (Herron, 1960.) Although the west jetty impounded a substantial amount of sand, its greatest effect was to divert the sand into the Hueneme Canyon, thus preventing this material from reaching the shores southeast of Port Hueneme. Before harbor construction, the downdrift shore was exceptionally stable. After construction, the rate of erosion was about 1,200,000 cubic yards per year from 1940 to 1953. In 1953 an emergency project was started at this harbor to reduce downdrift erosion by nourishing the downdrift beaches.

(Circa, 1953)
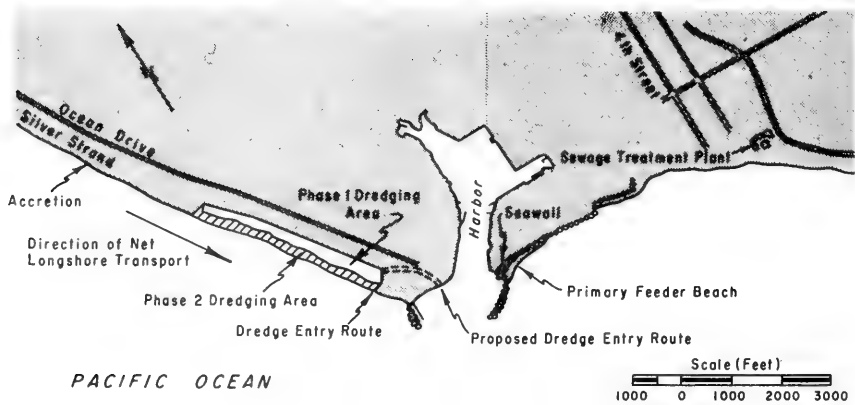
Figure 6-45. Sand Bypassing - Port Hueneme, California

6-60

Sand trapped by the updrift jetty was pumped to the downdrift beach through a floating pipeline dredge. The dredging procedure used was unique. The outer strip of the impounded beach was used to protect the dredge from wave action during the initial phase. Land equipment excavated a hole in the beach, and then a small pipeline dredge enlarged the hole enough to permit a larger dredge to enter from the open sea. The larger dredge completed the Phase 1 dredging, leaving a protective strip of beach for the final operation. In dredging the barrier strip of beach, cuts were made from the Phase 1 area to the mean lower low water line at an angle of about 60 degrees to the shoreline. These diagonal cuts gave the dredge more protection from waves than perpendicular cuts.

Since it was necessary to close the dredge entrance channel to prevent erosion of the protective barrier, water had to be pumped into the Phase 1 dredging area to supply the dredge. This problem might have been avoided had the proposed entry route from inside the harbor been used and left open during Phase 1 dredging, rather than the entry route from the open sea. (See Figure 6-45.)

From August 1953 to June 1954, 2,033,000 cubic yards of sand were bypassed to two downdrift feeder beaches through a discharge line submerged across the harbor entrance. A survey indicated an erosion rate downdrift from the harbor of about 2 million cubic yards from June 1955 to June 1956. Subsequent development of Channel Island Harbor, discussed below, provided periodical nourishment to the downdrift beaches.

6.522 <u>Channel Islands Harbor, California</u>. This harbor, designed to shelter about 1,100 private small craft, was constructed about a mile northwest of the entrance channel to Port Hueneme. (See Figure 6-46.)

The design objectives of the littoral barrier were to trap nearly all of the southward moving littoral drift, to prevent losses of drift into the Hueneme Canyon, to prevent shoaling of the harbor entrance, and to protect a floating dredge from waves. The sand bypassing operations transfered dredged sand across both the Channel Islands Harbor entrance and the Port Hueneme entrance to the eroded shore downdrift (southeast) of Port Hueneme (U.S. Army Engineer District, Los Angeles, 1957). The general plan is shown in Figure 6-46.

The project consisted of an offshore breakwater and two entrance jetties. The breakwater, 2,300 feet long and located at the 30-foot
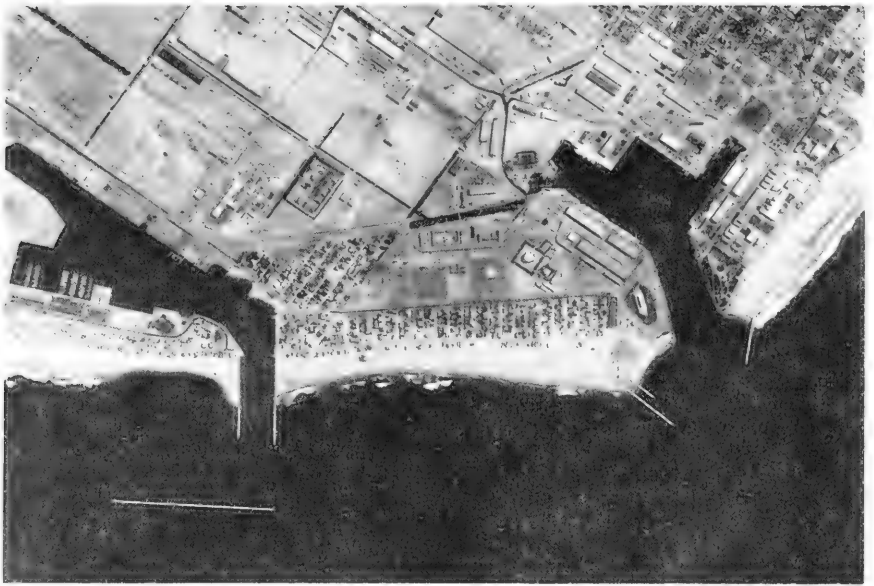
(September 1965)
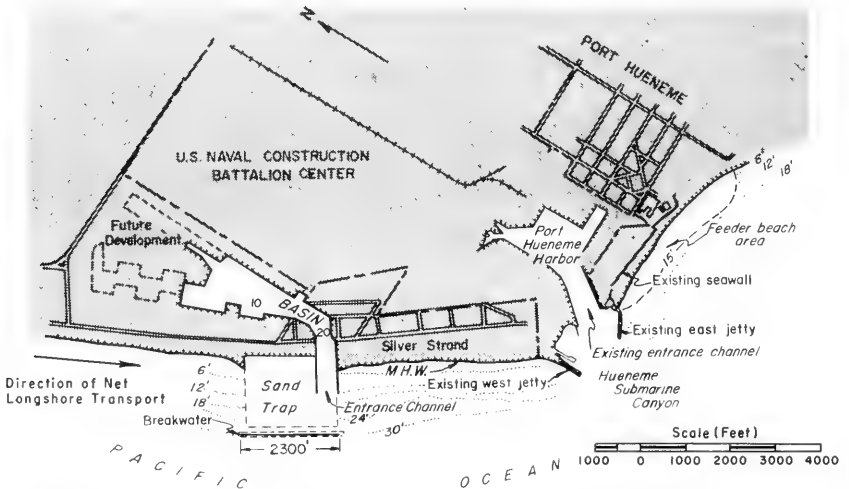
Figure 6-46. Sand Bypassing - Channel Islands Harbor, California.
The photo was taken just after 3 million cubic yards
had been dredged from the trap

6-62

contour, is a rubble-mound structure with a crest elevation 14 feet above mean lower low water. Its location and orientation enable it to trap almost all of the downcoast littoral drift. The breakwater provides protection from waves for the dredge and for the small craft entering the harbor. The rubble-mound entrance jetties have a crest elevation of 14 feet above mean lower low water, and extend to about the 14-foot isobath. They prevent shoaling of the entrance channel which has a project depth of 20 feet.

A floating dredge has cleaned the trap periodically since 1960. In 1960-61, dredging of the sand trap, the entrance channel, and the first phase of harbor development provided about 6 million cubic yards of sand. In 1963, 2 million cubic yards were dredged; in 1965, 3 million cubic yards were transferred. In the Port Hueneme operation (Section 6.521), 2 million cubic yards were transferred in 1953. This total of 13 million cubic yards had stabilized the eroded downdrift shores by 1965. Since 1965, bypassing has continued at intervals of about 2 years.

6.523 Santa Barbara, California. (Wiegel, 1959). The Santa Barbara sand bypassing operation was necessitated by the construction of a 2,800-foot breakwater, completed in 1928, to protect the harbor. (See Figure 6-47.) The breakwater resulted in accretion on the updrift side (west) and erosion on the downdrift side (east). Bypassing was started in 1935 by hopper dredges which dumped about 202,000 cubic yards in 22 feet of water about 1,000 feet offshore. Surveys showed that this sand was not moved to the beach. The next bypassing was done in 1938 by pipeline dredge. A total of 584,700 cubic yards of sand was deposited in the feeder beach area shown in Figure 4-47. This feeder beach was successful in reducing erosion downdrift of the harbor, and the operation was continued by placing 4,475,000 cubic yards periodically from 1940 to 1952.

The city of Santa Barbara decided in 1957, not to remove the shoal at the seaward end of the breakwater, because it provided additional protection to the inner harbor. A channel is being maintained around the inshore end of the shoal by a small floating dredge. Wave and weather conditions limit operations to about 72 percent of the time. With a capacity of about 1,600 cubic yards per 8-hour shift, dredging is adequate on a yearly basis, but inadequate to prevent some shoaling of the channel during storms.

(August 1965)
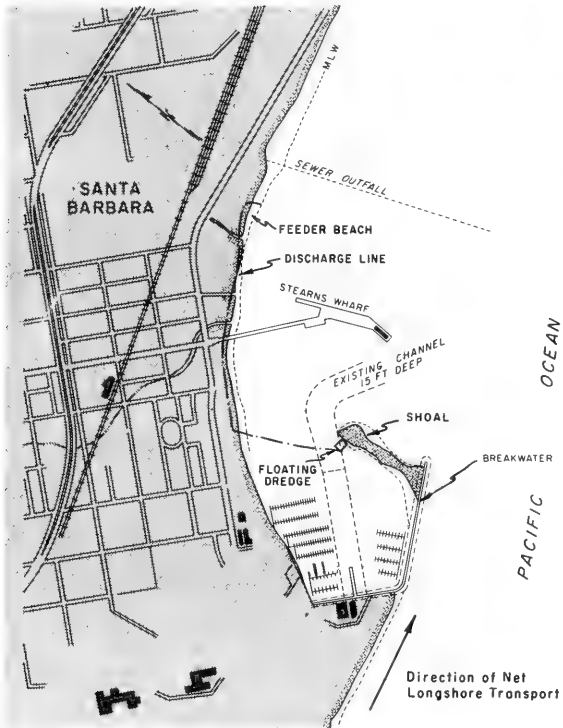
Figure 6-47. Sand Bypassing - Santa Barbara, California

6-64

6.524 Hillsboro Inlet, Florida. (Hodges, 1955). This inlet is about 36 miles north of Miami Beach. Sand bypassing operations have been by a pipeline dredge. (See Figure 6-48.) This method is well suited for this location, because the littoral material moving to the south is impounded in an area sheltered by a rock reef and rubble-mound jetty. The rock reef and jetty form what has been termed a *sand spillway*. Dredging the sand behind the spillway and depositing it on the downdrift beach has helped keep the inlet open and has provided nourishment to the downdrift beach. Experience has indicated that about 75,000 cubic yards of sand should be bypassed each year. This plan is the original *weir jetty*, and forms the basis for the Type IV design concept.

6.525 Masonboro Inlet, North Carolina. (Magnuson, 1966, Rayner and Magnuson, 1966, U.S. Army Engineer District, Wilmington 1970.) This inlet is the southern limit of Wrightsville Beach, North Carolina. An improvement to stabilize the inlet and navigation channel, and to bypass nearly all of the littoral drift has been partly constructed. The part completed in 1966, comprised the north jetty and deposition basin. (See Figure 6-49.) The jetty consists of an inner section 1,700 feet long of concrete sheet piles, of which 1,000 feet is the weir or spillway section, and a rubble-mound outer section 1,900 feet long. The elevation of the weir section (about half-tide level) was established low enough to pass the littoral drift, but high enough to protect a dredge in the deposition basin, and to control tidal currents in and out of the inlet. The elevation appears to be suitable for this location where the mean tidal range is about 4 feet. The basin was dredged to a depth of 16 feet, mean low water, and 367,000 cubic yards of sand were removed. It was planned to redredge the basin at 2-year intervals, and deposit the material to nourish and stabilize downdrift shores. A south jetty, intended to prevent material from entering the channel during periods of longshore transport reversal, has not been built. Without the south jetty, sand that enters the inlet from the south has caused a northward migration of the channel into the deposition basin and against the north jetty. Because migration of the channel has caused navigation problems, model studies are presently in progress to establish the final design of the inlet including the alignment and dimensions of the south jetty.

6.526 Perdido Pass, Alabama. This weir-jetty project was completed in 1969. (See Figure 6-50.) Since the direction of longshore transport is westward, the east jetty included a weir section 1,000 feet long at an elevation 1/2 foot above mean low water. The diurnal tidal range is about 1.2 feet. A deposition basin was dredged between the weir adjacent to the 12-foot-deep channel. Scour along the basin side of the concrete sheet pile weir was remedied by placing a rock toe on the weir. Nearly all the littoral drift crosses the weir. The deposition basin filled so rapidly that the fill encroached on the channel. Redredging of the basin was necessary in 1971.

6.527 Other Floating Plant Projects. Other sand bypassing projects using floating dredges are at the following locations:
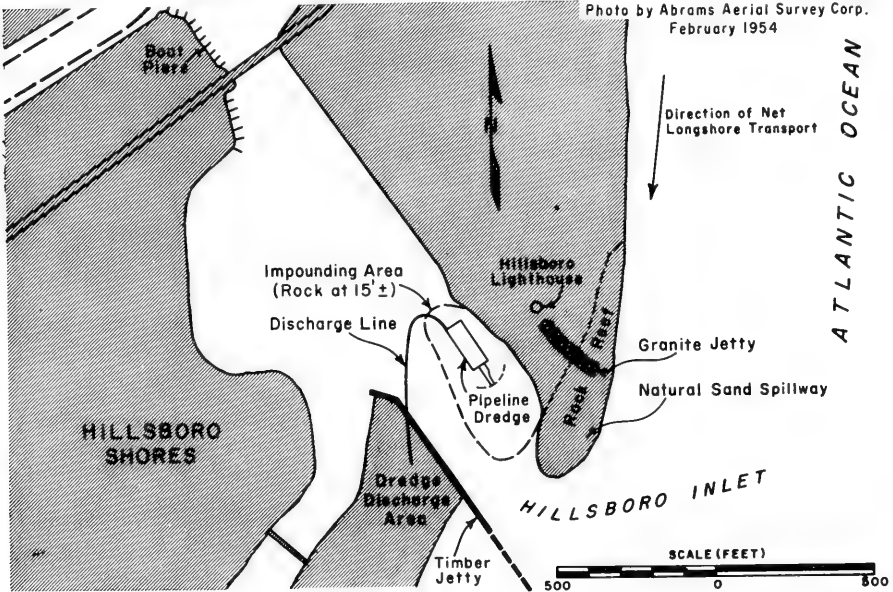
Figure 6-48. Sand Bypassing - Hillsboro Inlet, Florida

(August 1971)
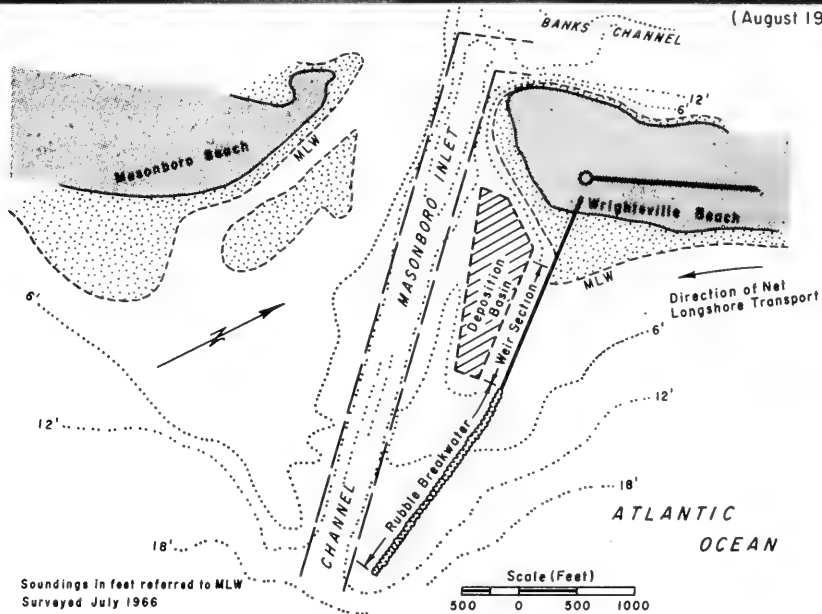
Figure 6-49. Sand Bypassing - Masonboro Inlet, North Carolina

(October 1970)
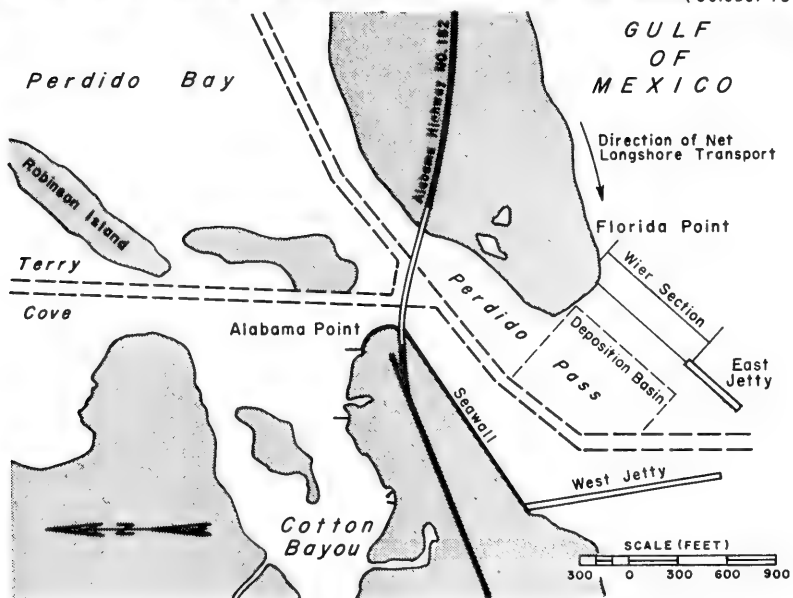
Figure 6-50. Sand Bypassing - Perdido Pass, Alabama
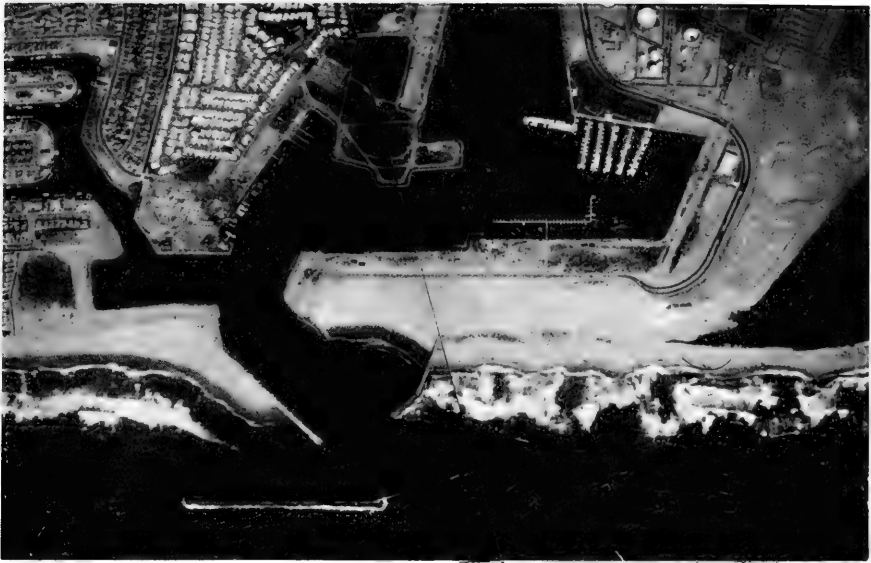
(March 1972)
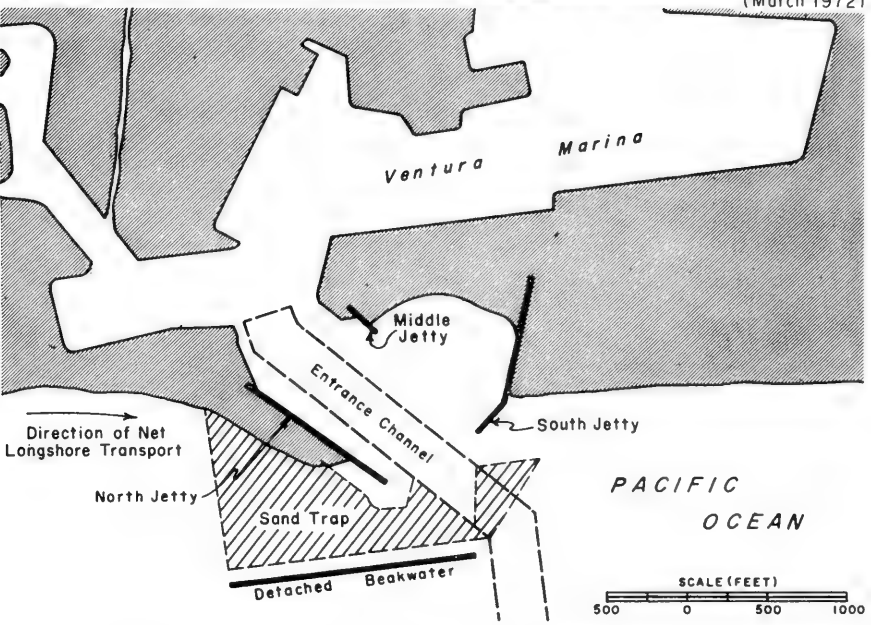
Figure 6-51. Sand Bypassing - Ventura Marina, California
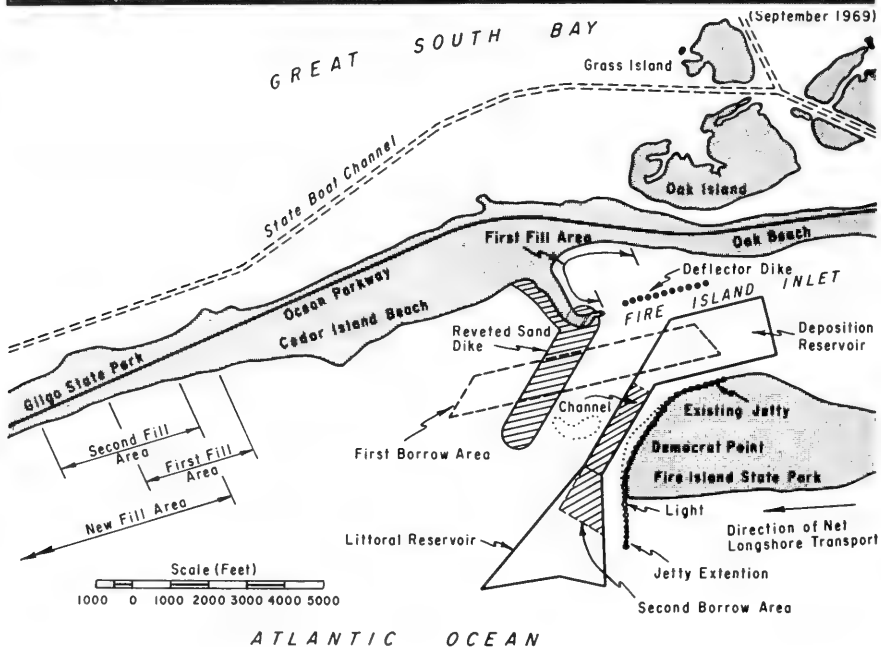
Figure 6-52. Sand Bypassing - Fire Island Inlet, New York

6-70

(Circa, 1968)
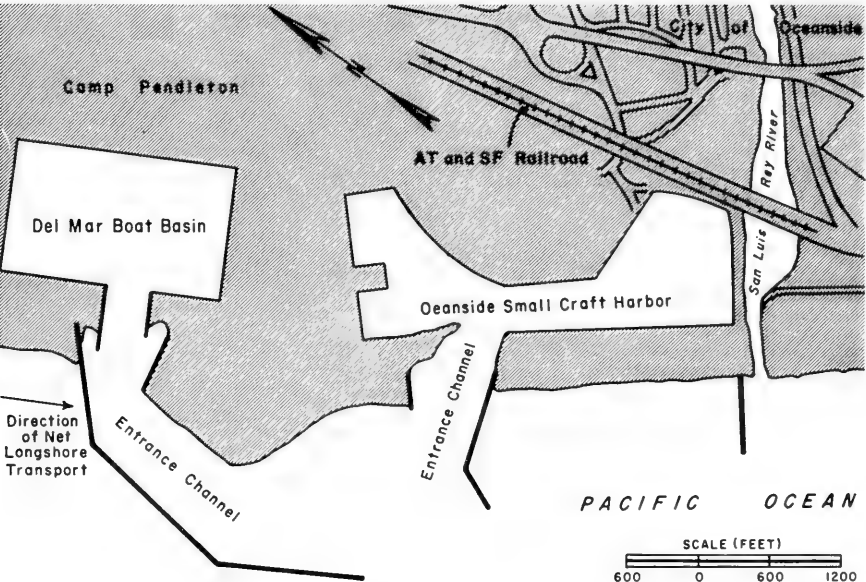
Figure 6-53.   Sand Bypassing - Oceanside Harbor, California

6-71

(April 1971)
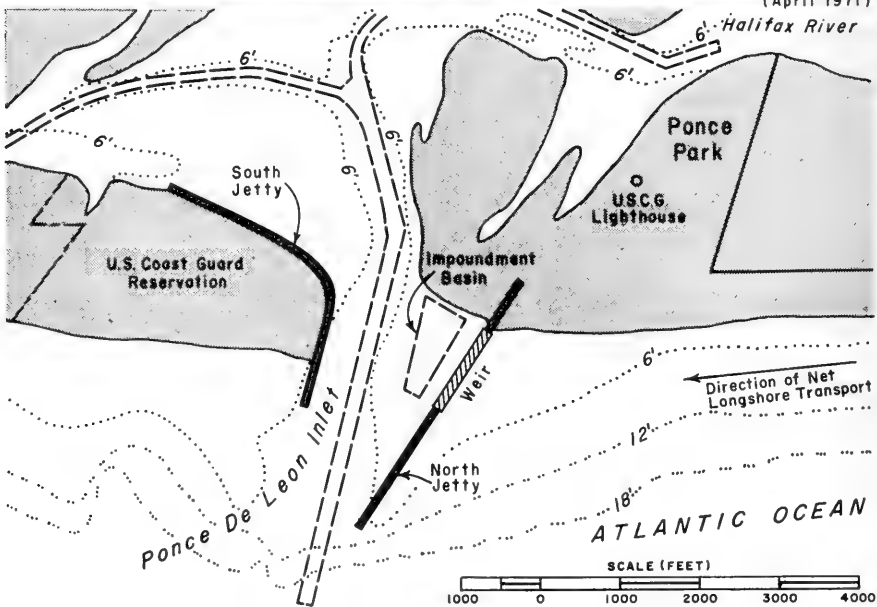
Figure 6-54. Sand Bypassing - Ponce de Leon Inlet, Florida, just south of Daytona Beach

(March 1972)
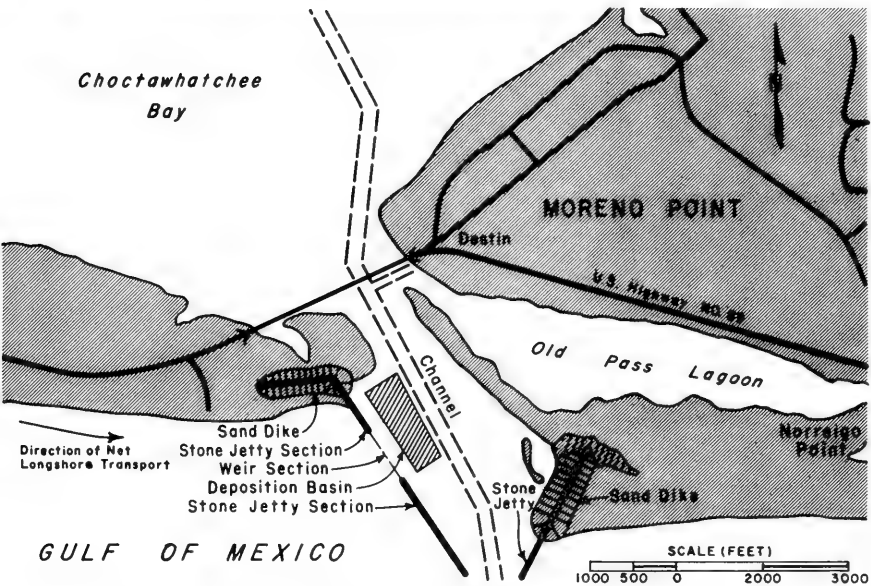
Figure 6-55. Sand Bypassing - East Pass, Florida

(Circa, July 1958)
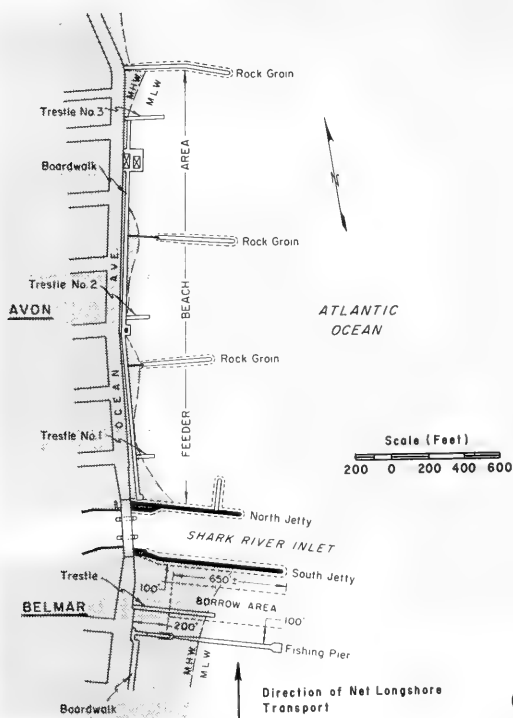
(Angas, 1960)

Figure 6-56. Sand Bypassing - Shark River Inlet, New Jersey

6-74

Excavating sand from the borrow area

(Angas, 1960)

Sand dumped on the beach is distributed by wave action at high water

Figure 6-57.   Sand Bypassing - Shark River Inlet, New Jersey

6.53 LAND-BASED VEHICLES

A bypassing operation at Shark River Inlet, New Jersey (Angas, 1960) used land-based vehicles. The project consisted of removing 250,000 cubic yards of sand from an area 225 feet south of the south jetty and placing this material along 2,500 feet of beach on the north side of the inlet. (See Figures 6-56 and 6-57.) On the south side of the inlet a trestle was built in the borrow area to a point beyond the low water line allowing trucks access from the highway to a crane with a 2 1/2-yard bucket. (See Figure 6-57.) Three shorter trestles were built north of the inlet from which the sand was dumped on the beach allowing wave action to distribute it to downdrift beaches.

6.6 GROINS

6.61 TYPES

As described in Section 5.6, groins are classified principally as to permeability, height and length. Groins built of common construction materials can be made permeable or impermeable, and high or low in profile. The materials used are stone, concrete, timber, and steel. Asphalt and sand-filled nylon bags have also been used to a limited extent. Various structural types of groins built with different construction materials are illustrated in Figures 6-58 through 6-63.

6.611 Timber Groins. A common type of timber groin is an impermeable structure composed of sheet piles supported by wales and round piles. Some permeable timber groins have been built, by leaving spaces between the sheeting. A typical timber groin is shown in Figure 6-58. The round timber piles forming the primary structural support should be at least 12 inches in diameter at the butt. Stringers or wales, bolted to the piling, should be at least 8 by 10 inches, preferably cut and drilled before being pressure treated with creosote. The sheet piles are usually either of the Wakefield, tongue and groove, or ship-lap type, supported in a vertical position between the wales and secured to the wales with nails. All timbers and piles used for marine construction should be given the maximum recommended pressure treatment of creosote or creosote and coal-tar solution.

6.612 Steel Groins. A typical design for a timber-steel sheet-pile groin is shown in Figure 6-59. Steel sheet-pile groins have been constructed with straight web, arch web, or Z piles. Some have been made permeable by cutting openings in the piles. The interlock type of joint of steel sheet-piles provides a sandtight connection. The selection of the type
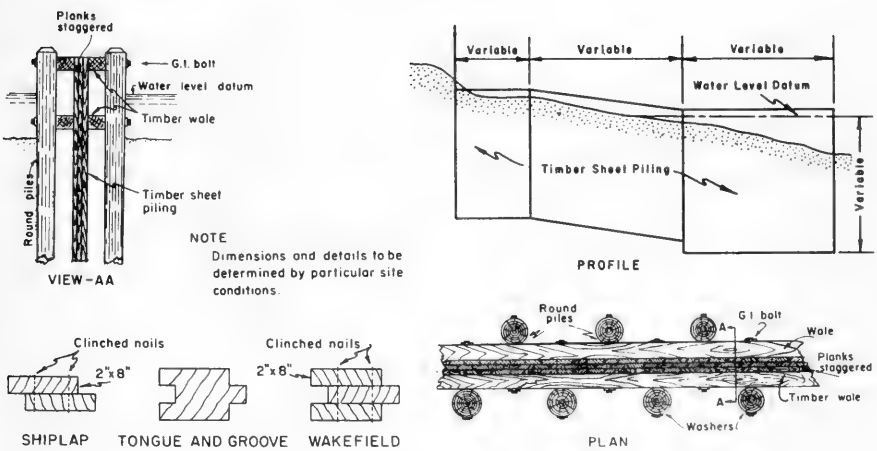
Figure 6-58.   Timber Sheet - Pile Groin

(1958)

SECTION A-A

STRAIGHT WEB PILE

ARCH WEB PILE

Z PILE

PROFILE

PLAN

NOTE:
Dimensions and details to be determined by particular site conditions.
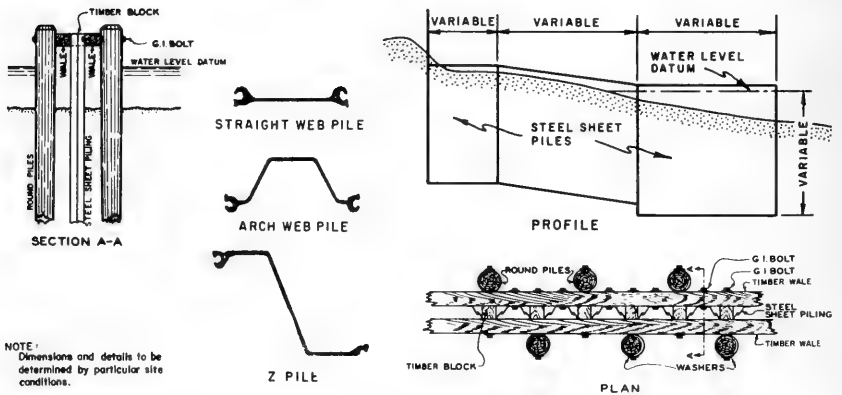
Figure 6-59. Timber-Steel Sheet-Pile Groin

Evanston, Illinois (before 1960)

SECTION A—A
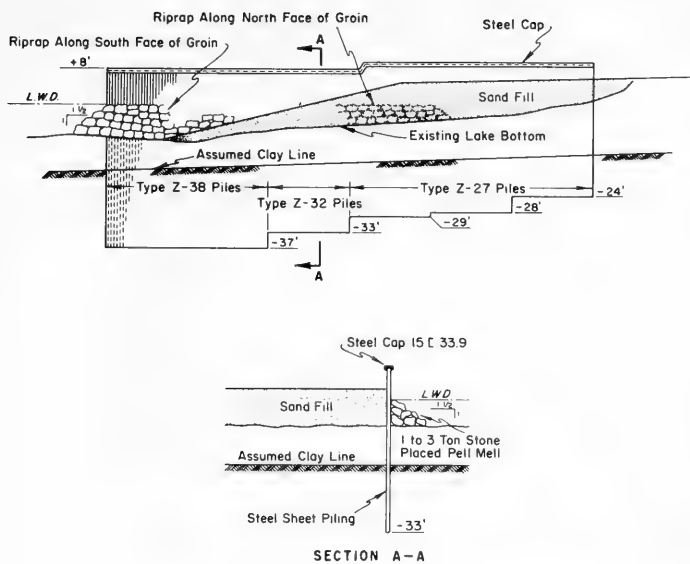
Figure 6-60.   Cantilever Steel Sheet-Pile Groin

6-79

Presque Isle, Pennsylvania (October 1965)
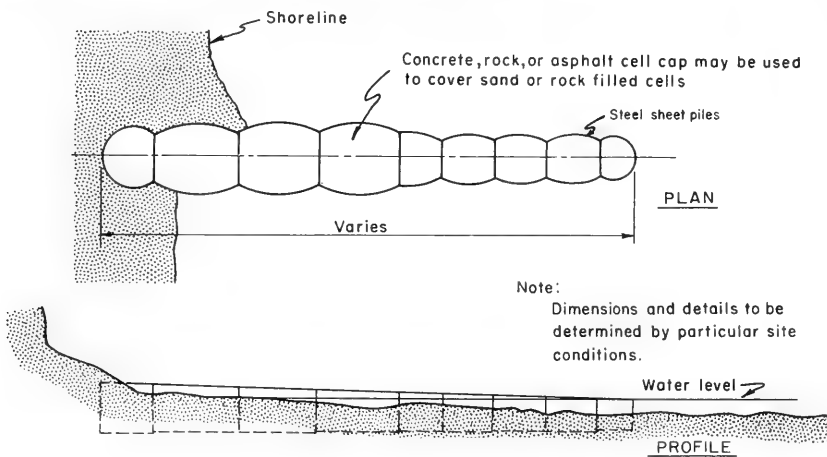
Figure 6-61.   Cellular Steel Sheet-Pile Groin

6-80

Seal Beach, California (July 1959)
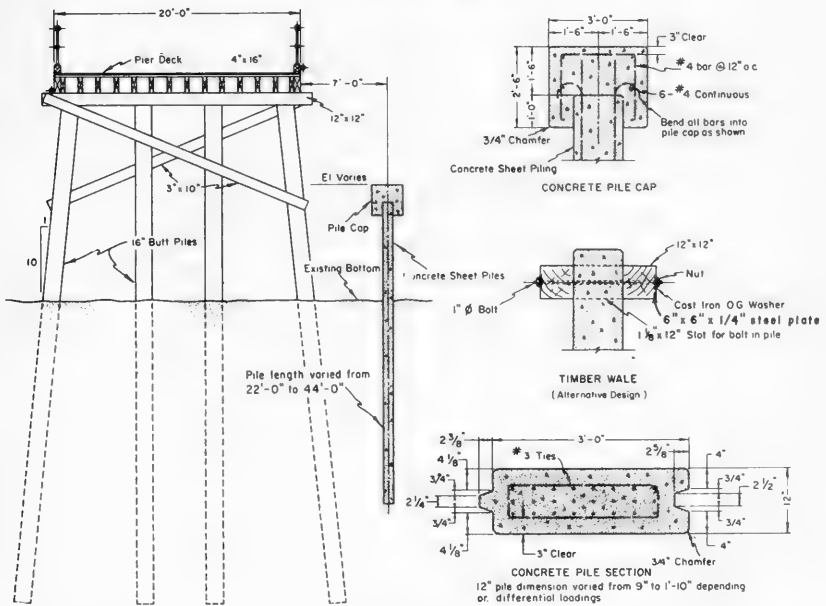
Figure 6-62. Prestressed Concrete Sheet-Pile Groin

Long Island, New York (circa 1971)

PROFILE

NOTE: Dimensions and details to be determined by particular site conditions

CROSS-SECTION
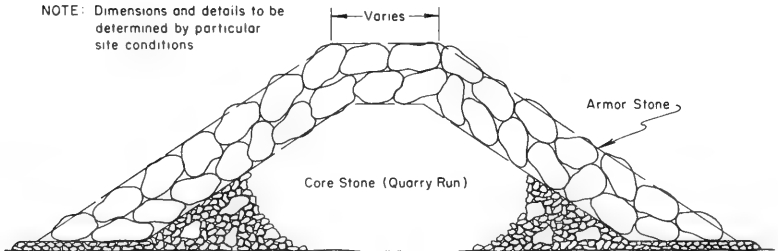
Figure 6-63. Rubble-Mound Groin

6-82

of sheet-piles depends on the earth forces to be resisted. Where the forces are small, straight web piles can be used. Where forces are great, deep-web Z piles should be used. The timber-steel sheet-pile groins are constructed with horizontal timber or steel wales along the top of the steel sheet-piles, and vertical round timber piles or brace piles are bolted to the outside of the wales for added structural support. The round piles may not always be required with the Z pile, but ordinarily are used with the flat or arch web sections. The round pile and timbers should be creosoted to maximum treatment for use in waters with marine borers.

Figure 6-60 illustrates the use of a cantilever steel sheet-pile groin. A groin of this type may be used where the wave attack and earth loads are moderate. In this structure, the sheet-piles are the basic structural members; they are restrained at the top by a structural steel channel welded to the piles.

The cellular type of steel sheet-pile groin is used on the Great Lakes where adequate pile penetration cannot be obtained for foundation. A typical cellular type groin is shown in Figure 6-61. This groin is comprised of cells of varying sizes, each consisting of semicircular walls connected by cross diaphragms. Each cell is filled with sand or stone to provide structural stability. Concrete, asphalt, or stone caps are used to retain the fill material.

6.613 Concrete Groins. Previously, the use of concrete in groins was generally limited to permeable-type structures that permitted passage of sand through the structure. Many of these groins designs are discussed by Portland Cement Association (1955) and Berg and Watts (1967). A more recent development in the use of concrete for groin construction is illustrated in Figure 6-62. This groin is an impermeable, prestressed concrete-pile structure with a cast-in-place concrete cap. At a more recent installation at Masonboro Inlet, North Carolina, a double timber wale was used as a cap to provide greater flexibility.

6.614 Rubble-Mound Groins. Rubble-mound groins are constructed with a core of quarry-run material including fine material to make them sand-tight, and covered with a layer of armor stone. The armor stone should weigh enough to be stable against the design wave. A typical rubble-mound groin is illustrated in Figure 6-63.

If permeability of a rubble-mound groin is a problem, the voids between stones can be filled with concrete or asphalt grout. This sealing also increases the stability of the entire structure against wave action. In January 1963, asphalt grout was used to seal a rubble-mound groin at Asbury Park, New Jersey, with apparent success. (Asphalt Institute, 1964, 1965, 1969.)

6.615 Asphalt Groins. Experimentation in the U.S. with asphalt groins began in 1948 at Wrightsville Beach, North Carolina. During the next decade, sand-asphalt groins were built at Fernandina Beach, Florida,

Ocean City, Maryland (Jachowski, 1959), Nags Head, North Carolina, and Harvey Cedars, Long Beach Island, New Jersey.

The behavior of sand-ashpalt groins, of the type used to date demonstrates definite limitations of their effectiveness. This is partly due to the limitation of extending the structures beyond the low waterline, and early structural failure of the section seaward of the beach berm crest. The failure in this zone is the result of normal seasonal variability of the shoreface and consequent undermining of the structure foundation. Modification of the design as to mix, dimensions, and sequence of construction may reveal a different behavior.

6.62 SELECTION OF TYPE

After planning has indicated that the use of groins is practicable, the selection of groin type is based on varying interrelated factors.

No universal type of groin can be prescribed because of the wide variation in conditions at each location. A thorough investigation of foundation materials is essential to selection. Borings or probings should be taken to determine the subsurface conditions for penetration of piles. Where foundations are poor or where little penetration is possible, a gravity-type structure such as a rubble or a cellular steel sheet-pile groin should be considered. Where penetration is good, a cantilever-type of structure of concrete, timber, or steel sheet-piles should be considered.

Availability of materials affects the selection of the type of groin because of costs. The economic life of the material and the annual cost of maintenance to attain that economic life are also selection factors. The first costs of timber and steel sheet-pile groins, in that order, are often less than for other types of construction. Concrete sheet-pile groins are generally more expensive than either timber or steel, but may cost less than a rubble-mound groin. However, concrete and rubble-mound groins require less maintenance, and have a much longer life than do the timber or steel sheet-pile groins. These factors, the amount of funds available for initial construction, the annual charges, and the period during which protection will be required, must all be studied before deciding on a particular type.

6.7 JETTIES

6.71 TYPES

The principal construction materials are stone, concrete, steel, and timber. Asphalt has occasionally been used as a binder. Some structural types of jetties are illustrated in Figures 6-64 through 6-66.

6.711 Rubble-Mound Jetties. The rubble-mound structure is a mound of stones of different sizes and shapes either dumped at random or placed in courses. Side slopes and stone sizes are designed so that the structure

Santa Cruz, California (1963)

CHANNEL SIDE   SEAWARD SIDE

A-Stone   Avg. 10 ton, Min. 7 ton
B-Stone   50% > 6000#, min. 4000#
C-Stone   4000# to 4" 50% > 500#
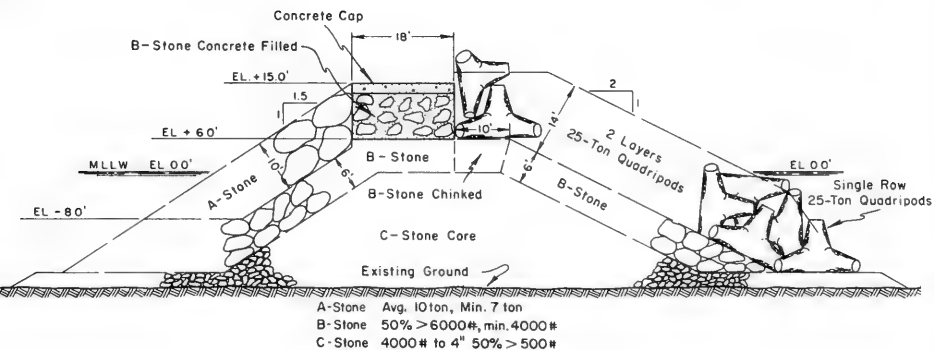
Figure 6-64.   Quadripod-Rubble-Mound Jetty

6-85

Humboldt Bay, California (1971)
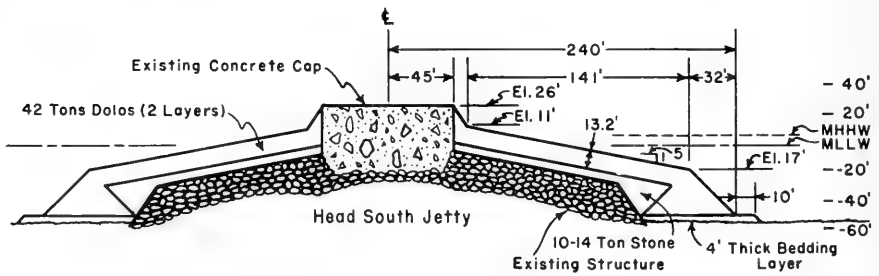
(after Magoon and Shimizu, 1971)

Figure 6-65.   Dolos-Rubble-Mound Jetty

Grand Marais Harbor, Michigan (before 1965)
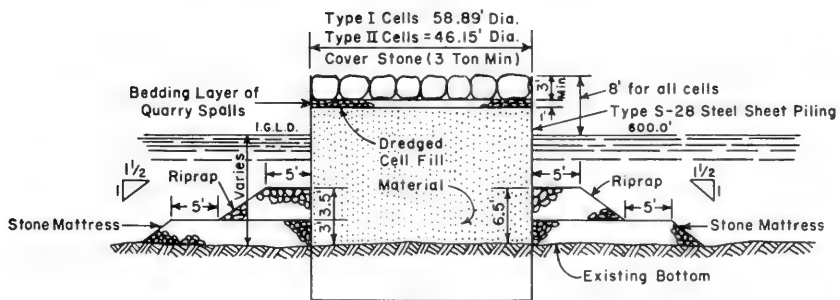
Figure 6-66. Cellular Steel Sheet-Pile Jetty

will resist the expected wave action. Rubble-mound jetties illustrated in Figures 6-64 and 6-65 are adaptable to any depth of water and most foundation conditions. Rubble-mound structures are used extensively. Chief advantages are: settlement of the structure results in readjustment of component stones, and increased stability, rather than in failure of the structure, damage is easily repaired, and rubble absorbs rather than reflects wave action. Chief disadvantages are: the large quantity of material required, the high first cost if satisfactory material is not locally available, and the wave energy propagated through the structure if the core is not high and impermeable.

Where rock armor units in adequate quantities or size are not economically available, concrete armor units are used. Section 7.376, Concrete Armor Units, discusses the shapes that have been tested and are available. Figure 6-64 illustrates the use of Quadripod armor units on the rubble-mound jetty at Santa Cruz, California. Figure 6-65 illustrates the use of the more recently developed Dolos armor unit where 42- and 43-ton dolos were used to rehabilitate the seaward end of the Humboldt Bay jetties against 40-foot breaking waves. (Magoon and Shimizu, 1971).

6.712 Sheet-Pile Jetties. Timber, steel and concrete sheet-piles have been used for jetty construction where waves are not severe. Steel sheet-piles are used for jetties in various ways. These include: a single row of piling with or without pile buttresses, a single row of sheet-piles arranged so that the row of piles acts as a buttressed wall; double walls of sheet-piles held together with tie rods with the space between the walls filled with stone or sand, usually separated into compartments by cross walls if sand is used; and cellular steel sheet-pile structures which are modifications of the double-wall type. An example of a cellular steel sheet-pile jetty is shown in Figure 6-66.

Cellular steel sheet-pile structures require little maintenance and are suitable for construction in depths to 40 feet on all types of foundations. Steel sheet-pile structures are economical and may be constructed quickly, but are vulnerable to storm damage during construction. If stone is used to fill the structure, the life will be longer than with sand filling, because holes that corrode through the web have to be big before the stone will leach out. Corrosion is the principal disadvantage of steel in sea water. Sand and water action abrade corroded metal and leave fresh steel exposed. The life of piles in this environment may not exceed 10 years. However, if corrosion is left undisturbed, piles may last more than 35 years. Plastic protective coatings and electrical cathodic protection have effectively extended the life of steel sheet-piles.

6.8 BREAKWATERS--SHORE-CONNECTED

6.81 TYPES

In exposed locations, breakwaters are generally some variation of a rubble-mound structure. In less severe exposures, both cellular steel

and concrete caissons have been used. Figures 6-67 through 6-70 illustrate structural types of shore-connected breakwaters used for harbor protection.

6.811 **Rubble-Mound Breakwaters**. The rubble-mound breakwaters in Figures 6-67 and 6-68 are adaptable to almost any depth, and can be designed to withstand severe waves.

Figure 6-67 illustrates the first use in the U.S. of tetrapod armor units. The Crescent City, California, Breakwater was extended in 1957 using two layers of 25-ton tetrapods. (Deignan, 1959.)

Figure 6-68 illustrates the use of tribar armor units on a rubble-mound structure. The 18-ton tribars were used to rehabilitate the 2,150-foot Nawiliwili breakwater in 1959. (Palmer, 1960.) In 1965, 35- and 50-ton tribars were used in the repair of the East Breakwater at Kahului, Hawaii.

6.812 <u>Stone-Asphalt Breakwaters</u>. (Kerkhoven, 1965 and Asphalt Institute, 1969). At Ijmuiden, the entrance to the port of Amsterdam, The Netherlands, the existing breakwaters were extended in 1964 to provide better protection and enable larger ships to enter the port. (See Figure 6-69.) The southern breakwater was extended 6,890 feet, and now projects 8,340 feet into the open sea to a depth of about 60 feet. These breakwaters had to be heavily protected to withstand wave attack. The Rijkswaterstaat (a government agency of The Netherlands) decided to construct rubble breakwaters in the open sea with a core of heavy stone blocks weighing 660 to 2,200 pounds. Since such blocks were not heavy enough to be stable against prevailing wave attack, a protective cover was needed. Application of a normal sand mastic grouting of the stone core was not possible because the dimensions of the stones and consequently the interstices were too large. A new material called stone-asphalt was developed to protect the stone core.

The stone-asphalt contained 60 to 80 percent by weight stones 2 to 20 inches in size, and 20 to 40 percent by weight asphaltic concrete mix with a maximum stone size of 2 inches. The stone-asphalt mix was pourable and required no compaction.

During construction the stone core was protected with about 1 ton of stone-asphalt grout per square yard of surface area. For this application the composition was modified, so that it was possible to obtain some penetration into the surface layer of the stone core. This stone-asphalt grout was effective and demonstrated the outstanding properties of this material for protection against wave attack.

The final protection of the stone core was a layer or revetment of stone asphalt about 7 feet thick. The structure side slopes are 1 on 2 above water and 1 on 1.75 under water. (See Figure 6-69.)

The stone-asphalt was manufactured by a double mixing procedure. An asphaltic concrete type of mix was made in a normal hot mix plant and then

Cresent City, California (1957)

SEAWARD SIDE   HARBOR SIDE
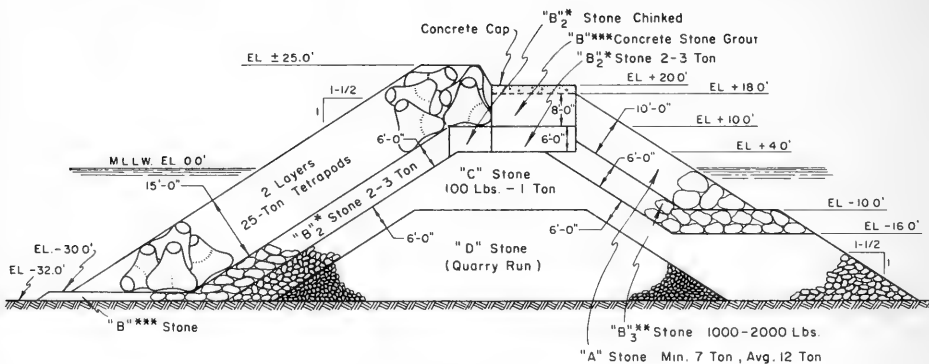
* "B$_2$" – One ton variation to 7 ton max

** "B$_3$" – 1/2 ton to 1 ton min. – 7 ton max. as available.

*** "B" – 1 ton to 7 tons or to suit depth conditions at seaward toe.

Figure 6-67. Tetrapod-Rubble-Mound Breakwater

6-90
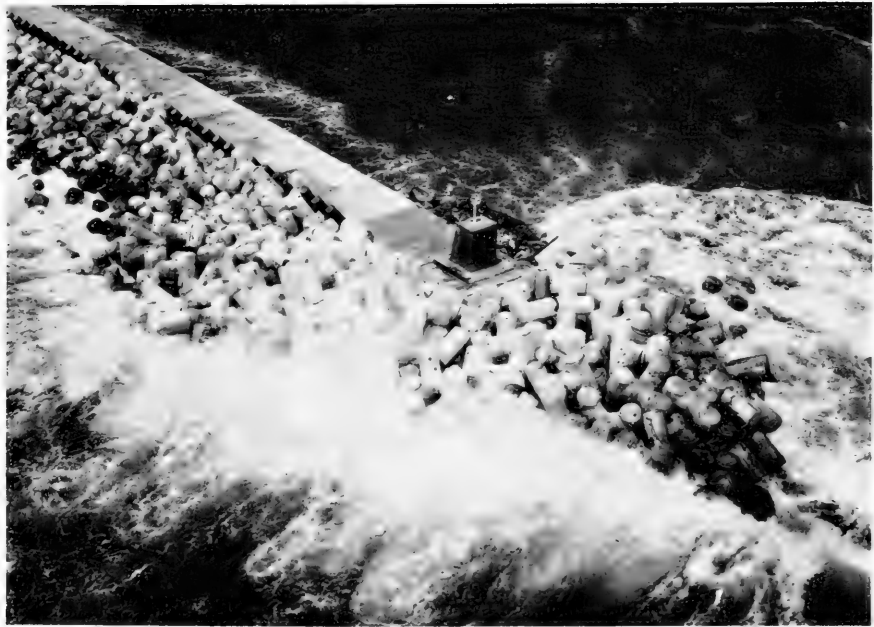
Nawiliwili, Kauai, Hawaii (1959)
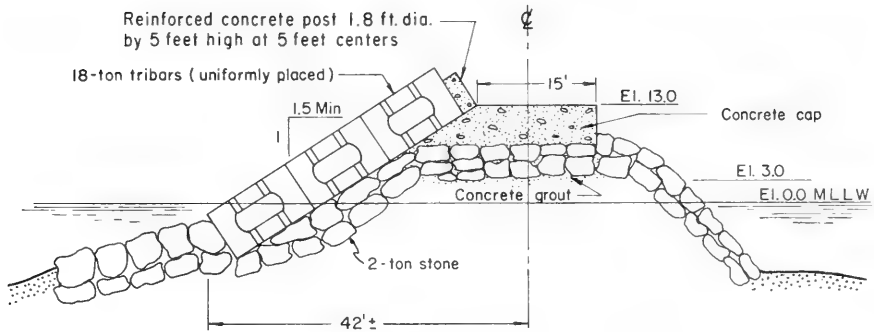
Figure 6-68. Tribar-Rubble-Mound Breakwater

Ijmuiden, The Netherlands (1964)

NORTH SEA

COAST LINE

EXTENSION OF
NORTHERN BREAKWATER

LOCKS

SCALE
0   1
                    km

EXTENSION OF
SOUTHERN BREAKWATER

COAST LINE

7 METRES

CEMENT-CONCRETE CROWN ELEMENT
SAND-MASTIC-GROUTED RUBBLE

STONE ASPHALT
ABOVE WATER

FIRST PROTECTION OF STONE CORE WITH
A RELATIVELY THIN LAYER OF STONE ASPHALT GROUT

MEAN WATER LEVEL   1   2

STONE ASPHALT
UNDER WATER   1 1¾   STONE
                  STONE ASPHALT   (300/1000 kg)

SCALE
0   10 METRES   (after Asphalt Institute, 1969)

Figure 6-69.   Stone Asphalt Breakwater

6-92

blended with dried and preheated stones. Because of the special mixing plant and equipment necessary, this material can be used only on large projects. At Ijmuiden, specially designed 22-ton vehicles transported the stone-asphalt mix to buckets of the same capacity. These buckets were lifted by crane for placing the mix either above or under water. (See Figure 6-69.) A specially designed plot system was used to ensure accurate placement of the mix. Because large amounts were dumped at one time, cooling was slow, and successive batches flowed together to form one monolithic revetment.

Extension of the breakwaters started in 1964. By the completion of the project in 1967, about 1 million tons of stone asphalt had been used.

To date regular maintenance has been required to deal with settlements in the stone-asphalt revetment, especially during the summer, but it is expected that a steadily decreasing amount of maintenance will be required.

6.813 Cellular Steel Sheet-Pile Breakwaters. These breakwaters have been used where storm waves are not too severe. The shores of the Great Lakes have moderately high wave exposure. A cellar steel sheet-pile and steel sheet-pile breakwater installation at Port Sanilac, Michigan, is illustrated in Figure 6-70.

Cellular steel sheet-pile structures require little maintenance and are suitable for construction in depths up to about 40 feet and into various types of sedimentary foundations. Steel sheet-pile structures have advantages of economy and speed of construction, but are vulnerable to storm damage during construction. Corrosion is the principal disadvantage of steel in sea water.

6.814 Concrete Caisson Breakwaters. Breakwaters of this type are built of reinforced concrete shells, that are floated into position, settled on a prepared foundation, filled with stone or sand for stability, and then capped with concrete or stones. These structures may be constructed with or without parapet walls for protection against wave overtopping. In general, concrete caissons have a reinforced concrete bottom, although open-bottom concrete caissons have been used. The open-bottom type is closed with a temporary wooden bottom that is removed after the caisson is placed on the foundation. The stone used to fill the compartments combines with the foundation material to provide additional resistance against horizontal movement.

Figure 6-71 illustrates the patented perforated type of caisson breakwater. (Jarlan, 1961.) The installation at Baie Comeau, Quebec (Stevenson, 1963), utilizes the caisson as a wharf on the harbor side. The holes or perforations on the seaward side reduce the undesirable conditions of a smooth vertical face wall (wave overtopping and wave reflection) by partly dissipating the wave energy within the wave chamber (Marks, 1967), (Marks and Jarlan, 1969), (Terrett, et al., 1969), (Richey and Sollitt, 1969.)
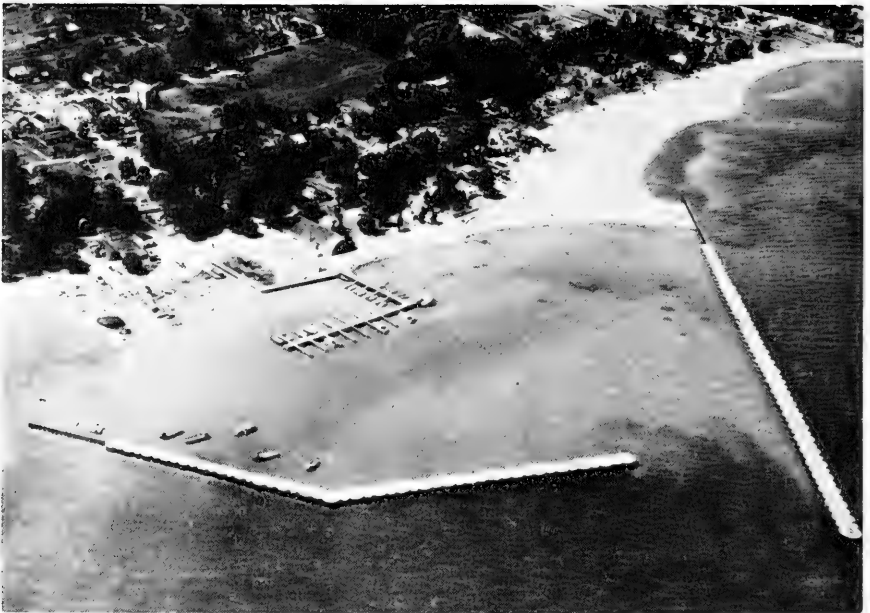
Port Sanilac, Michigan (July 1963)
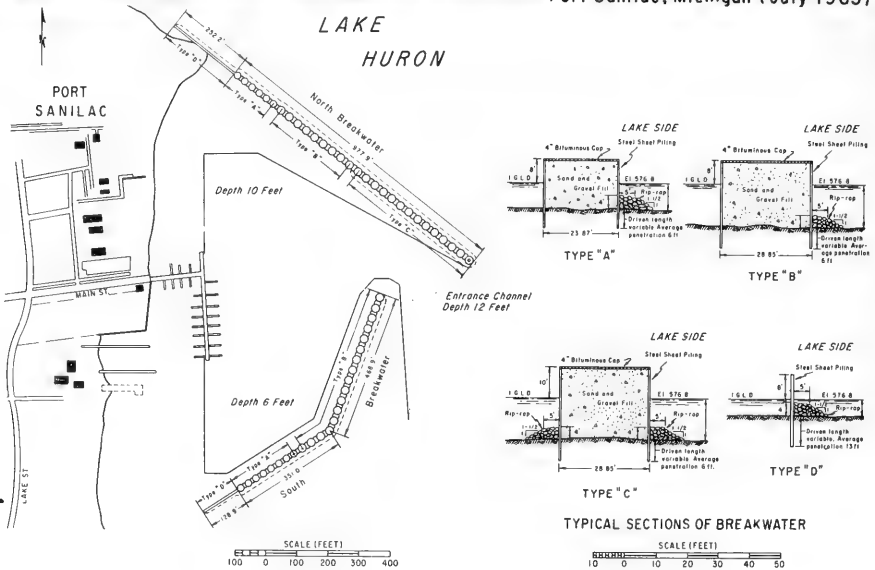
Figure 6-70. Cellular Steel Sheet-Pile and Sheet-Pile Breakwater

Baie Comeau, Quebec, Canada (August 1962)
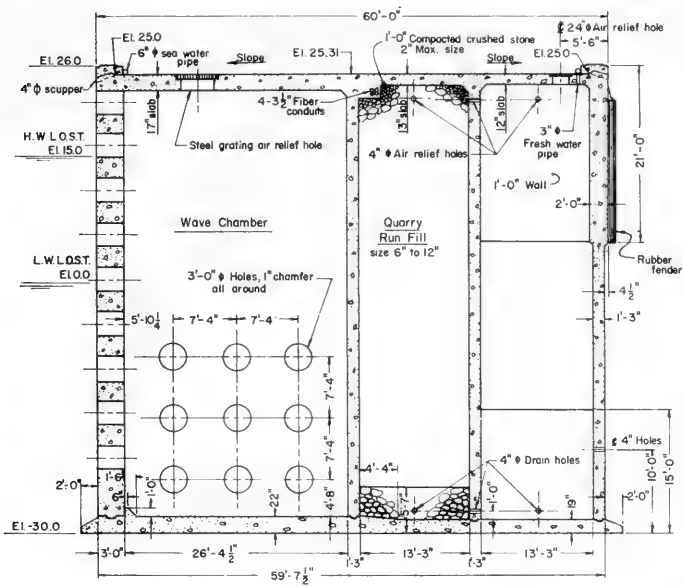
Figure 6-71.   Perforated Caisson Breakwater

Caissons are generally suitable for depths from about 10 to 35 feet. The foundation must support the structure and withstand scour, and usually consists of a mat or mound of rubble stone. (See Section 7.38.) Where foundation conditions dictate, piles may be used to support the structure. Heavy riprap is usually placed along the base of the caissons to protect against scour, horizontal displacement, or weaving when the caisson is supported on piles.

6.9   BREAKWATERS--OFFSHORE

6.91 TYPES

Offshore breakwaters can also be classified into two types: rubble-mound and cellular steel sheet-pile. Selection of the type for a given location is dependent on the comparative cost which is dependent on the depth of water, availability of material and wave action. For open ocean exposure, rubble-mound structures are usually required; for less severe exposure, as in the Great Lakes, the cellular steel sheet-pile structure may be a better choice. Figures 6-46 and 6-51 illustrate the use of rubble-mound offshore breakwaters to trap littoral material, to protect a floating dredge, and to protect the harbor entrance.

Figure 6-72 illustrates the structural details of the rubble-mound breakwater at Marina Del Rey, Venice, California.

Probably the most notable offshore breakwater complex in this country is the 8 1/2-mile-long Los Angeles-Long Beach breakwater built between 1899 and 1949. Other offshore breakwaters are located at Santa Monica, California, built in 1934; Venice, California, built in 1905; and Winthrop Beach, Massachusetts, built in 1933.

6.10 CONSTRUCTION MATERIALS

The selection of materials in the structural design of shore protective works depends on the environmental conditions of the shore area. Discussions of criteria that should be applied to materials commonly used follow.

6.101   Concrete. Proper quality concrete is required for satisfactory performance in a marine environment. The quality is obtainable by use of good concrete design and construction practices. The concrete should have low permeability, provided by the water-cement ratio recommended for the exposure conditions; adequate strength; air-entrainment, a necessity in freezing climate; adequate cover over reinforcing steel; durable aggregates and proper type of portable cement for the exposure condition. Factors affecting durability of concrete in a marine environment have been reported by Mather (1957). The requirements for durable concrete, consisting of water-cement ratio, air-entrainment, durable aggregate and type of portland cement are discussed in an engineering manual (U.S. Army, Office, Chief of Engineers, 1971b). Details of reinforcing steel are discussed in an engineering manual (U.S. Army, Office, Chief of Engineers, 1971a).

6-96

Marina Del Rey, Venice, California (before 1966)

"A"   Stone — 16 tons or greater

"A-1" Stone — 13 tons or greater

"A-2" Stone — 8 tons or greater.

"A-3" Stone — 6 tons or greater.

"A-4" Stone — 500 lbs. to 8 tons

"B" Stone — Core stone varies from quarry-run stone
              to pieces of 1 ton to 4 tons

"C" Stone — Core stone varies from quarry-waste to
              pieces of 1,500 lbs. to 4 tons.
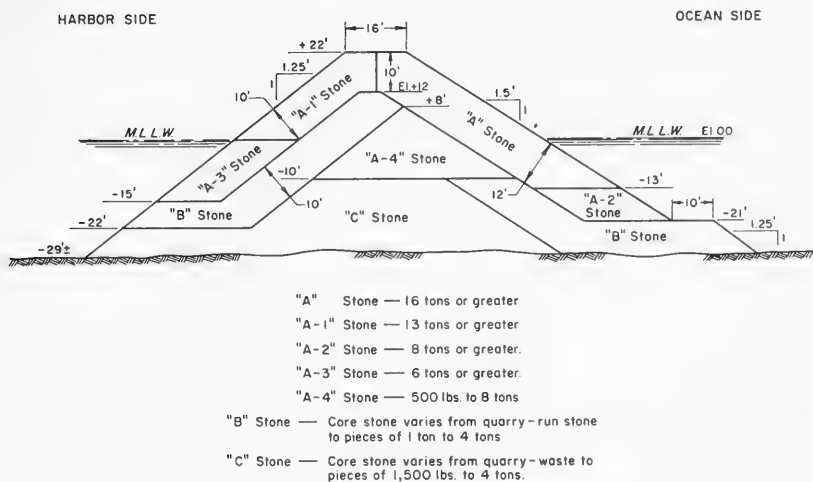
Figure 6-72.   Rubble-Mound Breakwater

6-97

6.102 Steel. Where steel is exposed to weathering, allowable working stresses must be reduced to account for corrosion and abrasion. Certain steel chemical formulations are available which offer greater corrosion resistance in the splash zone.

6.103 Timber. Allowable stresses for timber should be those for timbers more or less continuously damp or wet. These working stresses are discussed in U.S. Department of Commerce publications dealing with American lumber standards.

6.104 Stone. Stone for protective structures should be sound, durable, and hard. It should be free from laminations, weak cleavages, and undesirable weathering, and should be of such character that it will not disintegrate from the action of air, sea water, or in handling and placing. All stone should be angular quarrystone. The greatest dimension should be no greater than three times the least dimension. All stone should conform to the following test designations: apparent specific gravity, ASTM C 127; and abrasion, ASTM C 131. Density is in pounds per cubic foot (solid cubic foot without voids). In general, it is desirable to use stone with a high specific gravity to decrease the volume of material required in the structure.

6.11 MISCELLANEOUS DESIGN PRACTICES

Experience with the deterioration of concrete, steel and timber in shore structures may be summarized in the following guidelines:

(a) Within the tidal zone, the elimination of as much bracing as is practicable is desirable; maximum deterioration occurs in that zone.

(b) Round members, because of a smaller surface area and better flow characteristics, generally have a longer life than other shapes.

(c) All steel
(c) All steel or concrete deck framing should be located above normal spray level.

(d) Untreated timber piles should not be used unless protected from marine-borer attack.

(e) The most effective injected preservative appears to be creosote oil with a high phenolic content. For piles subject to marine-borer attack, a maximum penetration and retention of creosote and creosote and coal-tar solutions is recommended in accordance with standards of the American Wood-Preservers Association.

(f) Boring and cutting of piles after treatment should be avoided. Where unavoidable, cut surfaces should receive field treatment.

(g) Untreated timber piles encased in a gunite armor and properly sealed at the top will give economical service.

(h) The lower the water-cement ratio, the more durable the con-
crete will be in salt water.

(i) Coarse and fine aggregates must be selected carefully for
density of gradin, and to avoid unfavorable chemical reaction with the
cement.

(j) Maintenance of enough concrete cover over all reinforcing
steel during casting is very important.

(k) Smooth form work and rounded corners improve the durability
of concrete structures.

(l) Steel in and above the tidal range will last longer if pro-
tected by coatings of concrete, corrosion-resistant metals or organic and
inorganic paints (epoxies, vinyls, phenolics, etc).

REFERENCES AND SELECTED BIBLIOGRAPHY

ANGAS, W.M., "Sand By-Passing Project for Shark River Inlet," *Journal of the Waterways and Harbors Division*, ASCE, Vol. 86, WW3, No. 2599, Sept. 1960.

ASPHALT INSTITUTE, "Sentinel Against the Sea," *Asphalt*, Jan. 1964.

ASPHALT INSTITUTE, "Battering Storms Leave Asphalt Jetty Unharmed," *Asphalt*, Oct. 1965.

ASPHALT INSTITUTE, "Asbury Park's Successful Asphalt Jetties," *Asphalt Jetties*, Information Series No. 149, Jan. 1969.

AUGUSTINE, M.T., et al., "Response of American Beachgrass to Fertilizer," *Journal of Soil and Water Conservation*, Vol. 19, No. 3, 1964, pp. 112-115.

BAGNOLD, R.A., *The Physics of Blown Sand and Desert Dunes*, William Morrow, New York, 1942, 265 pp.

BARR, D.A., "Jute-Mesh Dune Forming Fences," *Journal of the Soil Conservation Service of New South Wales*, Vol. 22, No. 3, 1966, pp. 123-129.

BERG, D.W., and WATTS, G.M., "Variations in Groin Design," *Journal of the Waterways and Harbors Division*, ASCE, Vol. 93, WW2, No. 5241, 1967, pp. 79-100.

BLUMENTHAL, K.P., "The Construction of a Drift Sand Dyke on the Island Rottumerplatt," *Proceedings of the Ninth Coastal Engineering Conference*, ASCE, Ch. 23, 1965, pp. 346-367.

BROWN, R.L., and HAFENRICHTER, A.L., "Factors Influencing the Production and Use of Beachgrass and Dunegrass Clones for Erosion Control: I. Effect of Date of Planting," *Journal of Agronomy*, Vol. 40, No. 6, 1948, pp. 512-521.

CAMPBELL, W.V., and FUZY, E.A., "Survey of the Scale Insect Effect on American Beachgrass," *Shore and Beach*, Vol. 40, No. 1, 1972, pp. 18-19.

DEIGNAN, J.E., "Breakwater at Crescent City, California," *Journal of the Waterways and Harbors Division*, ASCE, Vol. 85, WW3, No. 2174, 1959.

DUANE, D.B., and MEISBURGER, E.P., "Geomorphology and Sediments of the Nearshore Continental Shelf, Miami to Palm Beach, Florida," TM-29, U.S. Army, Corps of Engineers, Coastal Engineering Research Center, Washington, D.C., Nov. 1969.

ESCOFFIER, F.F., and DOLIVE, W.L., "Shore Protection in Harrison County, Mississippi," *The Bulletin of the Beach Erosion Board*, Vol. 8, No. 3, July 1954.

FISHER, C.H., "Mining the Ocean for Beach Sand," *Proceedings of the Conference on Civil Engineering in the Oceans*, II, ASCE, 1969, pp. 717-723.

GAGE, B.O., "Experimental Dunes of the Texas Coast", MP 1-70, U.S. Army, Corps of Engineers, Coastal Engineering Research Center, Washington, D.C., Jan. 1970.

HALL, J.V., Jr., "Wave Tests of Revetment Using Machine-Produced Interlocking Blocks," *Proceedings of the 10th Coastal Engineering Conference*, ASCE, Ch. 60, 1967, pp. 1025-1035.

HAWK, V.B., and SHARP, W.C., "Sand Dune Stabilization Along the North Atlantic Coast," *Journal of Soil and Water Conservation*, Vol. 22, No. 4, 1967, pp. 143-146.

HERRON, W.J., Jr. "Beach Erosion Control and Small Craft Harbor Development at Point Hueneme," *Shore and Beach*, Vol. 28, No. 2, Oct. 1960, pp. 11-15.

HODGES, T.K. "Sand By-Passing at Hillsboro Inlet, Florida," *Bulletin of the Beach Erosion Board*, Vol. 9, No. 2, Apr. 1955.

JACHOWSKI, R.A. "Behavior of Sand-Asphalt Groins at Ocean City, Maryland," MP 2-59, U.S. Army, Corps of Engineers, Beach Erosion Board, Washington, D.C., May 1959.

JAGSCHITZ, J.A., "Research to Rebuild and Stabilize Sand Dunes in Rhode Island," *Shore and Beach*, Vol. 28, No. 1, 1960, pp. 32-35.

JAGSCHITZ, J.A., and BELL, R.S., "Restoration and Retention of Coastal Dunes with Fences and Vegetation," Bull. No. 382, Agricultural Experiment Station, University of Rhode Island, Kingston, R.I., 1966a.

JAGSCHITZ, J.A., and BELL, R.S., "American Beachgrass (Establishment--Fertilization--Seeding)," Bull. No. 383, Agricultural Experiment Station, University of Rhode Island, Kingston, R.I., 1966b.

JARLAN, G.L.E., "A Perforated Vertical Wall Breakwater," *The Dock and Harbour Authority*, Vol. 41, No. 486, Apr. 1961, pp. 394-398.

JARLAN, G.L.E. "Note on the Possible Use of a Perforated Vertical-Wall Breakwater," Unpublished Manuscript, Hydraulic Laboratory, National Research Council, Ottawa, Canada.

KERKHOVEN, R.E., "Recent Developments in Asphalt Techniques for Hydraulic Applications in the Netherlands," *Proceedings of the Association of Asphalt Paving Technologists*, Vol. 34, 1965.

KIDBY, H.A., and OLVER, J.R., "Erosion and Accretion Along Clatsop Spit," *Coastal Engineering, Santa Barbara Specialty Conference*, ASCE, 1965, pp. 647-672.

KRUMBEIN, W.C., and JAMES, W.R., "A Lognormal Size Distribution Model for Estimating Stability of Beach Fill Material," TM-16, U.S. Army, Corps of Engineers, Coastal Engineering Research Center, Washington, D.C., Nov. 1965.

LUCAS, L.T., et al, "Marasmius Blight, A New Disease of American Beachgrass," *Plant Disease Reporter*, Vol. 55, No. 7, 1971, pp. 582-585.

MAGNUSON, N.C., "Planning and Design of a Low-Weir Section Jetty at Masonboro Inlet, North Carolina," *Coastal Engineering, Santa Barbara Specialty Conference*, ASCE, Ch. 36, 1966, pp. 807-820.

MAGOON, O.T., and SHIMIZU, N., "Use of Dolos Armor Units in Rubble-Mound Structures, e.g., for Conditions in the Arctic," *Proceedings from the First International Conference on Port and Ocean Engineering Under Arctic Conditions*, Technical University of Norway, Trondheim, Norway, Vol. II, 1971, pp. 1089-1108 (also CERC Reprint R. 1-73).

MARKS, W., "A Perforated Mobile Breakwater for Fixed and Floating Applications," *Proceedings of the 10th Conference on Coastal Engineering*, ASCE, Vol. 2, 1967, pp. 1079-1129.

MARKS, W., and JARLAN, G.L.E., "Experimental Studies on a Fixed Perforated Breakwater," *Proceedings of the 11th Conference on Coastal Engineering*, ASCE, Vol. 2, 1969, pp. 1121-1140.

MATHER, B., "Factors Affecting Durability of Concrete in Coastal Structures," TM-96, U.S. Army, Corps of Engineers, Beach Erosion Board, June 1957.

MAURIELLO, L.J., "Experimental Use of Self-Unloading Hopper Dredge for Rehabilitation of an Ocean Beach," *Proceedings of the World Dredging Conference*, 1967, pp. 367-396.

McLAUGHLIN, W.T., and BROWN, R.L., "Controlling Coastal Sand Dunes in the Pacific Northwest," Cir. No. 660, U.S. Department of Agriculture, Washington, D.C., Sept. 1942, pp. 1-46.

MEISBURGER, E.P., "Geomorphology and Sediments of the Inner Continental Shelf, Chesapeake Bay Entrance," TM-38, U.S. Army, Corps of Engineers, Coastal Engineering Research Center, Washington, D.C., June 1972.

MEISBURGER, E.P., and DUANE, D.B., "Geomorphology and Sediments of the Inner Continental Shelf, Palm Beach to Cape Kennedy, Florida," TM-34, U.S. Army, Corps of Engineers, Coastal Engineering Research Center, Washington, D.C., Feb. 1971.

MIDDLETON, S.R., "Installation and Operation of Fixed Sand Bypassing Plant at Lake Worth Inlet, Florida," *Shore and Beach*, Vol. 27, No. 9., June 1959.

PALMER, R.Q., "Breakwaters in the Hawaiian Islands," *Proceedings of the American Society of Civil Engineers,* Waterways and Harbors Division, ASCE, Vol. 86, WW2, No. 2507, 1960.

PORTLAND CEMENT ASSOCIATION, *"Concrete Shore Protection,"* 2nd ed., 1955, (1st ed., 1939).

RAYNER, A.C. and MAGNUSON, N.C. "Stabilization of Masonboro Inlet," *Shore and Beach,* Vol. 34, No. 2, 1966, pp. 36-41.

RICHEY, E.P., and SOLLITT, C.K., "Wave Attenuation by a Porous Walled Breakwater," *Proceedings of the Conference on Civil Engineering in the Oceans--II,* ASCE, 1969, pp. 903-928.

SAVAGE, R.P., "Sand Bypassing at Port Hueneme, California," TM-92, U.S. Army, Corps of Engineers, Beach Erosion Board, Washington, D.C., Mar. 1957.

SAVAGE, R.P., "Experimental Study of Dune Building with Sand Fences," *Proceedings of the Eighth Conference on Coastal Engineering,* ASCE, Council on Wave Research, 1962, pp. 380-396.

SAVAGE, R.P., and WOODHOUSE, W.W., Jr., "Creation and Stabilization of Coastal Barrier Dunes," *Proceedings of the 11th Conference on Coastal Engineering,* ASCE, 1969, pp. 671-700.

SENECA, E.D., "Germination Response to Temperature and Salinity of Four Dune Grasses from the Outer Banks of North Carolina," *Ecology,* Vol. 50, 1969, pp. 45-53.

SENECA, E.D., and COOPER, A.W., "Germination and Seedling Response to Temperature, Daylength, and Salinity by *Ammophila breviligulata* from Michigan and North Carolina," *Botanical Gazette,* Vol. 132, No. 3, 1971, pp. 203-215.

STEVENSTON, C.A., "Set a Wave to Catch a Wave," *Canadian Consulting Engineer,* June 1963.

TERRETT, F.L., OSORIO, J.D.C., and LEAN, G.H., "Model Studies of a Perforated Breakwater," *Proceedings of the 11th Conference on Coastal Engineering,* ASCE, Vol. 2, 1969, pp. 1104-1120.

U.S. ARMY, CORPS OF ENGINEERS, "Bypassing Littoral Drift at a Harbour Entrance," *The Bulletin of the Beach Erosion Board,* Vol. 5, No. 3, July 1951.

U.S. ARMY, CORPS OF ENGINEERS, "Sand Bypassing Plant at Salina Cruz, Mexico," *The Bulletin of the Beach Erosion Board,* Vol. 6, No. 2, Apr. 1952.

U.S. ARMY, CORPS OF ENGINEERS, "Status of Sand Bypassing Plant at Salina Cruz Harbor, Isthmus of Tehantepec, Mexico," *The Bulletin of the Beach Erosion Board*, Vol. 9, No. 1, Jan. 1955.

U.S. ARMY, CORPS OF ENGINEERS, "Beach Erosion at Durban, South Africa," *The Bulletin of the Beach Erosion Board*, Vol. 10, No. 2, July 1956.

U.S. ARMY, CORPS OF ENGINEERS, "General Design for Harbor and Shore Protection Works Near Port Hueneme, California," California Region, Engineer District, Los Angeles, Calif., 1957.

U.S. ARMY, CORPS OF ENGINEERS, "Cooperative Research and Data Collection Program of Coast of Southern California, Cape San Martin to Mexican Boundary, Three-Year Report, 1967-69," Beach Erosion Control Report, California Region, Engineer District, Los Angeles, Calif., 1970.

U.S. ARMY, CORPS OF ENGINEERS, "Study on Use of Hopper Dredges for Beach Nourishment," Hopper Dredge Improvement Program, No. 10, North Atlantic Region, Engineer District, Philadelphia, Pa., 1967.

U.S. ARMY, CORPS OF ENGINEERS, "Details of Reinforcement--Hydraulic Structures," EM 1110-2-2103, Office, Chief of Engineers, May 1971a.

U.S. ARMY, CORPS OF ENGINEERS, "Standard Practice for Concrete," EM 1110-2-2000, Office, Chief of Engineers, Nov. 1971b.

U.S. ARMY, CORPS OF ENGINEERS, "Carolina Beach and Vicinity, North Carolina; Combined Report on an Interim Hurricane Survey and Cooperative Beach Erosion Control Study," South Atlantic-Gulf Region, Engineer District, Wilmington, N.C., 1961.

U.S. ARMY, CORPS OF ENGINEERS, "Atlantic Intracoastal Waterway Between Norfolk, Virginia and the St. Johns River, Florida, Wilmington District," South Atlantic-Gulf Region, Engineer District, Wilmington, N.C., 1970.

U.S. DEPARTMENT OF AGRICULTURE, "Sand Dune Control Benefits Everbody: The Bodega Bay Story," Soils Conservation Service Pamphlet, Portland, Oreg., 1967.

VALLIANOS, LIMBERIOS, "Recent History of Erosion at Carolina Beach, North Carolina," *Proceedings of the 12th Coastal Engineering Conference*, ASCE, Vol. 2, Ch. 77, 1970, pp. 1223-1242.

WATTS, G.M., "A Study of Sand Movement at South Lake Worth Inlet, Florida," TM-42, U.S. Army, Corps of Engineers, Beach Erosion Board, Washington, D.C., Oct. 1953.

WATTS, G.M., "Behavior of Beach Fill at Ocean City, New Jersey," TM-77, U.S. Army, Corps of Engineers, Beach Erosion Board, Washington, D.C., Mar. 1956.

WATTS, G.M., "Behavior of Beach Fill and Borrow Area at Harrison County, Mississippi," TM-107, U.S. Army, Corps of Engineers, Beach Erosion Board, Washington, D.C., Aug. 1958.

WATTS, G.M., "Behavior of Beach Fill at Virginia Beach, Virginia," TM-113, U.S. Army, Corps of Engineers, Beach Erosion Board, Washington, D.C., June 1959.

WATTS, G.M., "Trends in Sand By-Passing Systems," *Coastal Engineering, Santa Barbara Specialty Conference,* ASCE, Ch. 34, 1966, pp. 779-804.

WIEGEL, R.L., "Sand By-Passing at Santa Barbara, California," *Journal of the Waterways and Harbors Division,* ASCE, Vol. 85, WW2, June 1959.

WOODARD, D.W., et al, "The Use of Grasses for Dune Stabilization Along the Gulf Coast with Initial Emphasis on the Texas Coast," Report No. 114, Gulf Universities Research Corporation, Galveston, Tex., 1971, (for the U.S. Army, Coastal Engineering Research Center).

WOODHOUSE, W.W., Jr., "Use of Vegetation for Dune Stabilization," *Proceedings of the Coastal Processes and Shore Protection Seminar,* Coastal Plains Center for Marine Development Services, Wilmington, N.C., Seminar Series No. 1, 1970, pp. 36-39.

WOODHOUSE, W.W., Jr. and HANES, R.E., "Dune Stabilization with Vegetation on the Outer Banks of North Carolina," TM-22, U.S. Army, Corps of Engineers, Coastal Engineering Research Center, Washington, D.C., Aug. 1967.

WOODHOUSE, W.W., Jr., SENECA, E.D., and COOPER, A.W., "Use of Sea Oats for Dune Stabilization in the Southeast," *Shore and Beach,* Vol. 36, No. 2, 1968, pp. 15-21.

ZURMUHLEN, F.H., "The Sand Transfer Plant at Lake Worth Inlet," *Proceedings of the Sixth Conference on Coastal Engineering,* ASCE, Council of Wave Research, 1958.

STRUCTURAL DESIGN -
PHYSICAL FACTORS

PRAIA BAY, TERCEIRA, AZORES – 2 March 1970

STRUCTURAL DESIGN - PHYSICAL FACTORS

7.1   WAVE CHARACTERISTICS

Wind-generated waves produce the most critical forces to which coastal structures are subjected (except for seismic sea waves). A structure exposed to wave action should be designed to withstand the highest wave expected at the structure, if such a design is economically justified. Economic evaluations depend on frequency of occurrence of extreme events such as, height and duration of extreme waves, damage potential of high waves, and permissible risk. Wave characteristics are normally determined for deep water, and then propagated shoreward to the structure. Deepwater significant wave height H_O and significant wave period T_S may be determined if wind speed, wind duration, and fetch length are known.   (See Sections 3.5 and 3.6) This information, with water-level data, is used with refraction analyses to determine wave conditions at the site.

Wave conditions at a structure site at any time depend critically on the water level. Consequently, a design stillwater level (SWL) or range of water levels must be established in determining wave forces on a structure. Structures may be subjected to radically different types of wave action as the water level at the site varies. A given structure might be subjected to nonbreaking, breaking, and broken waves during different stages of a tidal cycle. The wave action a structure is subjected to may also vary along its length at a given time. This is true for structures oriented perpendicular to the shoreline such as groins and jetties. The critical section of these structures may be shoreward of the seaward end of the structure depending on structure crest elevation, tidal range, and bottom profile.

Detailed discussion of the effects of astronomical tides and wind-generated surges in establishing water levels is presented in Chapter 3, WAVE AND WATER LEVEL PREDICTIONS. In Chapter 7, it is assumed that the methods of Chapter 3 have been applied to determine design water levels.

The wave height usually obtained from statistical analysis of synoptic weather charts is the significant height, H_S. Assuming a Rayleigh wave-height distribution, H_S may be further defined in approximate relation to other height parameters of the statistical wave-height distribution:

$$H_{1/3} \text{ or } H_S = \text{average of highest } 1/3 \text{ of all waves,}$$

$$H_{10} \approx 1.27 \ H_S = \text{average of highest 10 percent of all waves} \quad (7\text{-}1)$$

$$H_1 \approx 1.67 \ H_S = \text{average of highest 1 percent of all waves} \quad (7\text{-}2)$$

7.11 DETERMINATION OF WAVE CONDITIONS

All wave data applicable to the project site should be evaluated for possible use as design criteria. Visual observation of storm waves, while difficult to confirm, may provide an indication of wave height, period, direction, storm duration, and frequency of occurrence. Instrumentation has been developed for recording wave height and period at a point. Instrumentation for recording wave direction is presently in the development stage, thus direction data must be obtained from visual observations. Wave direction is usually necessary for design analysis. If reliable visual shore or ship observations of wave direction are not available, hindcast procedures (Sec. 3.5, SIMPLIFIED WAVE PREDICTION MODELS) must be used. Where reliable, statistical deepwater wave data are available, these can provide the necessary shallow-water wave data. If wave data are not directly available at the site, the best available procedure must be employed, with sound engineering judgment, to transform available deepwater and extreme offshore wave data to the structure site. (See Section 2.238, Wave Energy and Power, and Sections 2.3, WAVE REFRACTION, and 2.4, WAVE DIFFRACTION.)

7.12 SELECTION OF DESIGN WAVE

The choice of a design wave height depends on whether the structure is subjected to the attack of nonbreaking, breaking, or broken waves and on the geometrical and porosity characteristics of the structure. (Jackson, 1968a.) Once wave characteristics are known, the next step is to determine if wave height at the site is controlled by water depth. (See Section 2.6, BREAKING WAVES.) The type of wave action experienced by a structure may vary with position along the structure, and with water level and time at a given structure section. For this reason, wave conditions should be determined at various points along a structure and for various water levels. Critical wave conditions that result in maximum forces on structures like groins and jetties may be found at a location other than the seaward end of the structure. The possibility of such conditions should be considered in establishing design waves and water levels.

If breaking in shallow water does not limit wave height, a non-breaking wave condition exists. For nonbreaking waves, the design height is selected from a statistical height distribution. The selected design height depends on whether the structure is defined as *rigid, semirigid,* or *flexible.* As a rule of thumb, the design wave is selected as follows. For *rigid* structures, such as cantilever steel sheet-pile walls, where a high wave within the wave train might cause faulure of the entire structure, the design wave is normally based on H_1, the average height of the highest 1 percent of all waves. For *semirigid* structures, the design wave is selected from a range of H_{10} to H_1. Steel sheet-pile cell structures are semirigid, and can absorb wave pounding; therefore, a design wave height of H_{10} may be used. For *flexible* structures, such as rubble-mound or riprap structures, the design height is usually the significant height H_s. Waves higher than H_s impinging on flexible

structures seldom create serious damage for short durations of extreme wave action. When an individual stone or armor unit is displaced by a high wave, smaller waves of the train may move it to a more stable position on the slope.

Damage to rubble-mound structures is usually progressive, and an extended period of destructive wave action is required before a structure ceases to provide protection. It is therefore necessary in selecting a design wave to consider both frequency of occurrence of damaging waves and economics of construction, protection, and maintenance. On the Atlantic and Gulf coasts of the United States, hurricanes may provide the design criteria. The frequency of occurrence of the design hurricane at any site may range from once in 20 to once in 100 years. It may be uneconomical to build a structure that would withstand the hurricane conditions without damage, hence H_s may be a more reasonable design wave height. On the North Pacific coast of the United States, the weather pattern is more uniform; severe storms are likely each year. The use of H_s as a design height under these conditions could result in extensive annual damage and frequent maintenance because of the higher frequency and duration of waves greater than H_s in the spectrum. Here, a higher design wave of about H_{10} may be advisable. Selection of the design height between H_s and H_{10} is based on the following factors:

(a) degree of structure damage allowable and associated maintenance costs,

(b) availability of armor materials, and

(c) comparative alternate size or type of armor unit and their costs.

7.121 <u>Breaking Waves</u>. Selection of a design wave height also depends on whether a structure is subject to attack by breaking waves. It has been commonly assumed that a structure sited at a water depth d_s (measured at design water stage), will be subjected to breaking waves if $d_s \leq 1.3$ H where H = design wave height. Study of the breaking process indicates that this assumption is not always valid. The breaking point is defined as the point where foam first appears on the wave crest, where the front face of the wave first becomes vertical, or where the wave crest first begins to curl over the face of the wave. (See Section 2.6, BREAKING WAVES.) The breaking point is an intermediate point in the breaking process between the first stages of instability and the area of complete breaking. Therefore, the depth that initiates breaking directly against a structure is actually some distance seaward of the structure and not necessarily the depth at the structure toe. The presence of a structure on a beach also modifies the breaker location and height. Jackson (1968a), has evaluated the effect of rubble structures on the breaking process. Additional research is required to fully evaluate the influence of structures.

Hedar (1965) suggested that the breaking process extends over a distance equal to half the shallow-water wavelength. This wavelength is based on the depth at this seaward position. On flat slopes, the resultant height of a wave breaking against the structure varies only a small amount with nearshore slope. A slope of 1 on 15 might increase the design breaking wave height by 20 to 80 percent depending on deepwater wavelength or period. Galvin (1968,69) indicated a relationship between the distance traveled by a plunging breaker and the wave height at breaking H_b. The relationship between the breaker travel distance x_p and the breaker height H_b depends on the nearshore slope and was expressed by Galvin (1969) as:

$$x_p = \tau_p H_b = (4.0 - 9.25\ m)\ H_b \tag{7-3}$$

where m is the nearshore slope (ratio of vertical to horizontal distance) and $\tau_p = (4.0 - 9.25\ m)$ is the dimensionless plunge distance. (See Figure 7-1.)
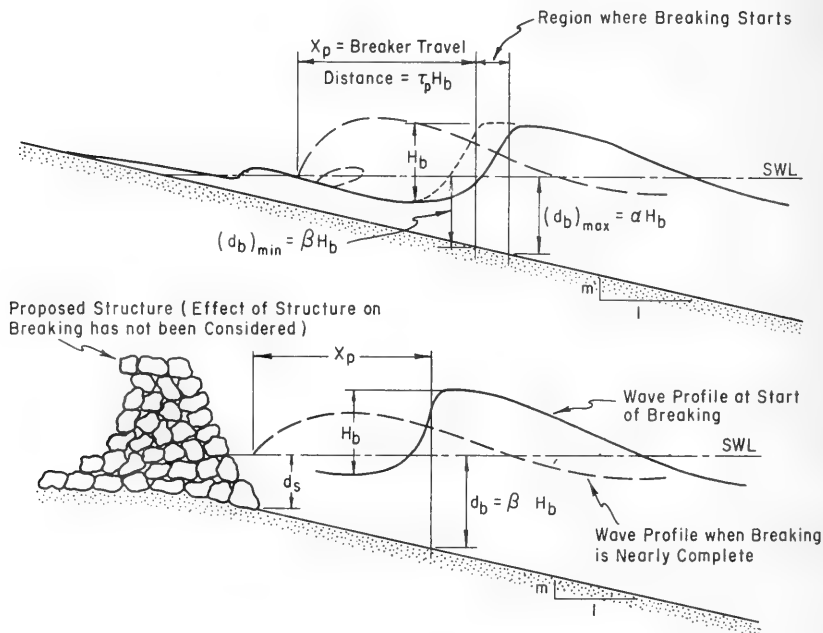
Figure 7-1. Definition of Breaker Geometry

7-4

Analysis of experimental data shows that the relationship between depth at breaking d_b and breaker height H_b is more complex than indicated by the equation $d_b = 1.3\, H_b$. Consequently, the expression $d_b = 1.3\, H_b$ *should not be used* for design purposes. The dimensionless ratio d_b/H_b varies with nearshore slope m and incident wave steepness H_b/gT^2 as indicated in Figure 7-2. Since experimental measurements of d_b/H_b exhibit scatter, even when made in laboratory flumes, two sets of curves are presented in Figure 7-2. The curve of α vs. H_b/gT^2 represents an upper limit of experimentally observed values of d_b/H_b hence $\alpha = (d_b/H_b)_{max}$. Similarly, β is an approximate lower limit of measurements of d_b/H_b; therefore, $\beta = (d_b/H_b)_{min}$. Figure 7-2 can be used with Figure 7-3 to determine the water depth in which an incident wave of known period and unrefracted deepwater height will break.

* * * * * * * * * * * * * * EXAMPLE PROBLEM * * * * * * * * * * * * * * * *

GIVEN: A wave with period T = 10 seconds, and an unrefracted deepwater height of H'_o = 5 feet advancing shoreward over a nearshore slope of m = 0.050 (1:20).

FIND: The range of depths where breaking may start.

SOLUTION: The breaker height can be found in Figure 7-3. Calculate,

$$\frac{H'_o}{gT^2} = \frac{5}{32.2\,(10)^2} = 0.00155 ,$$

and enter the figure to the curve for an m = 0.05 or 1:20 slope. H_b/H'_o is read from the figure

$$\frac{H_b}{H'_o} = 1.65 .$$

Therefore,

$$H_b = 1.65\ H'_o = 1.65\,(5.0) = 8.3 \text{ ft} .$$

H_b/gT^2 may now be computed.

$$\frac{H_b}{gT^2} = \frac{8.3}{(32.2)\,(10)^2} = 0.0026 .$$

Entering Figure 7-2 with the computed value of H_b/gT^2 the value of α is found to be 1.51 and the value of β for a beach slope of 0.050 is 0.93. Then,

$$\left(d_b\right)_{max} = \alpha H_b = 1.51\,(8.3) = 12.5 \text{ ft} ,$$

and

$$\left(d_b\right)_{min} = \beta H_b = 0.93\,(8.3) = 7.7 \text{ ft} .$$

NOTE: When results of computations are used in subsequent problems or steps of the same problem, the number of significant digits carried is the number of digits that can be read on a slide rule. Final answers should be rounded to reflect the accuracy of the original given data and assumptions.
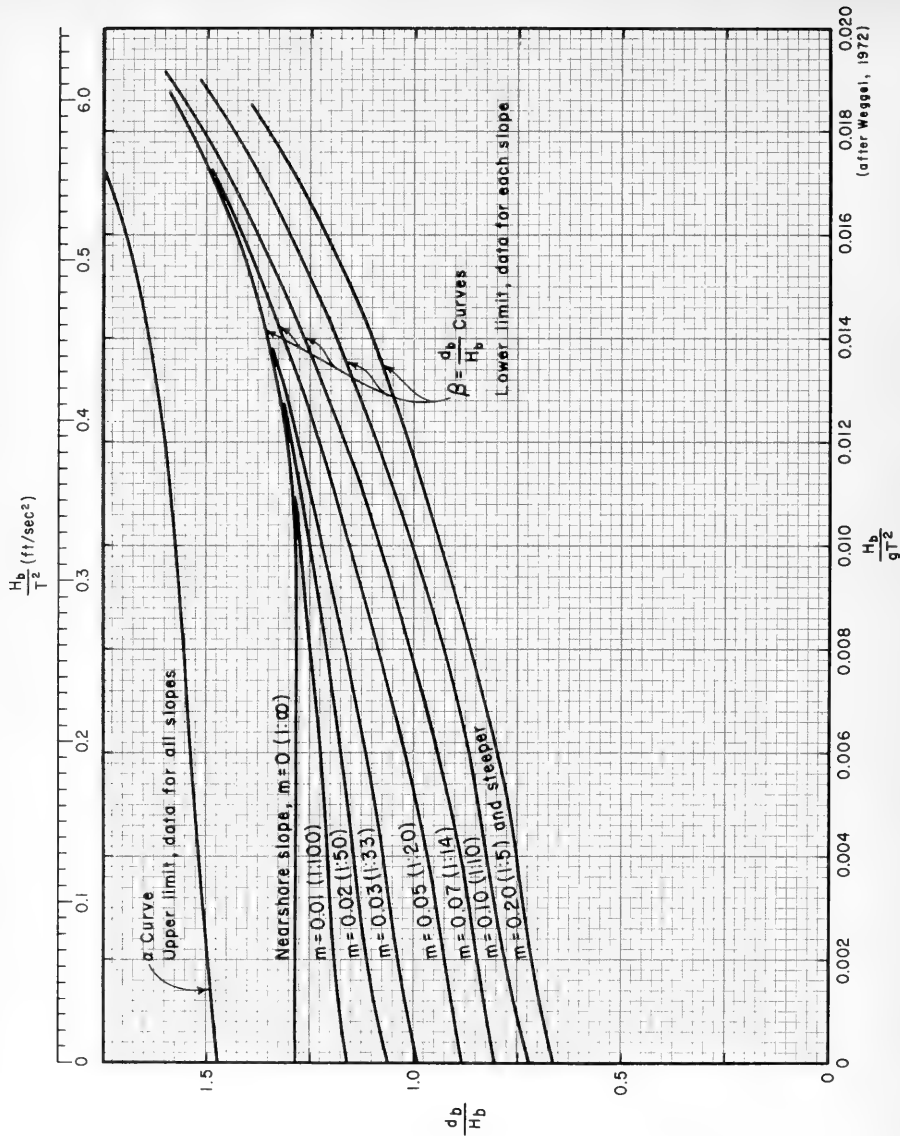
Figure 7-2. α and β Versus H_b/gT^2
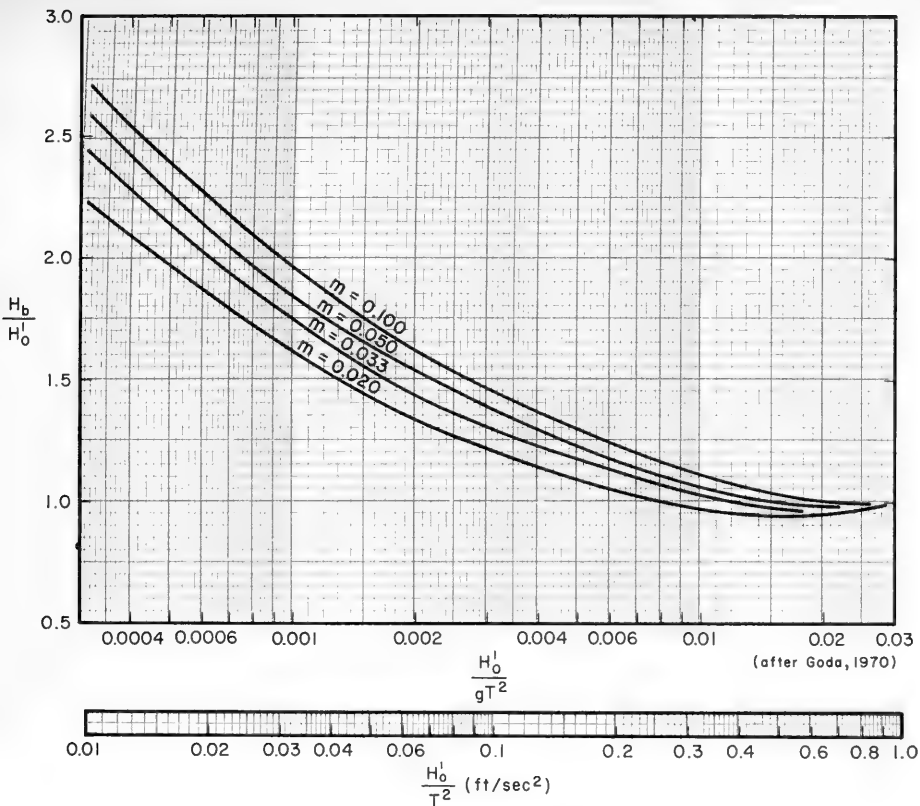
Figure 7-3. Breaker Height Index, H_b/H_o' Versus Deep Water
Wave Steepness, H_o'/gT^2

7-7

Where wave characteristics are not significantly modified by the presence of structures, incident waves generally will break when the depth is slightly greater than $(d_b)_{min}$. As wave-reflection effects of shore structures begin to influence breaking, depth of breaking increases, and the region of breaking moves farther seaward. As illustrated by the example, a structure sited on a 1 on 20 slope under action of the given incident wave ($H_o' = 5.0$ feet, $T = 10$ seconds) could be subjected to waves breaking directly on it, if the depth at the structure toe were between $(d_b)_{min} = 7.7$ feet and $(d_b)_{max} = 12.5$ feet.

* *

7.122 Design Breaker Height. When designing for a breaking wave condition, it is desirable to determine the maximum breaker height to which the structure might reasonably be subjected. The design breaker height H_b depends on the depth of water some distance seaward from the structure toe where the wave first begins to break. This depth varies with tidal stage. The design breaker height depends, therefore, on critical design depth at the structure toe, slope on which structure is built, incident wave steepness, and distance traveled by the wave during breaking.

Assuming that the design wave is one that plunges on the structure, design breaker height may be determined from:

$$H_b = \frac{d_s}{\beta - m\tau_p} , \tag{7-4}$$

where d_s is depth at the structure toe; β is the ratio of breaking depth to breaker height d_b/H_b; m is the nearshore slope, and τ_p is the dimensionless plunge distance x_p/H_b from Equation 7-3.

The magnitude of β to be used in Equation 7-4 cannot be directly evaluated since it depends on breaking wave steepness that cannot be known until H_b is evaluated. To aid in finding H_b, Figure 7-4 has been derived from Equations 7-3 and 7-4 using β values from Figure 7-2. If maximum design depth at the structure and incident wave period are known, design breaker height can be obtained using Figure 7-4.

* * * * * * * * * * * * * * * EXAMPLE PROBLEM * * * * * * * * * * * * * * * *

GIVEN:

(a) Design depth structure toe, $d_s = 7.5$ feet.

(b) Slope in front of structure is 1 on 20, or m = 0.050.

(c) Range of wave periods to be considered in design

$$T = 6 \text{ sec (minimum)}$$
$$T = 10 \text{ sec (maximum)}$$

FIND: Maximum breaker height against the structure for the maximum and minimum wave periods.

7-8
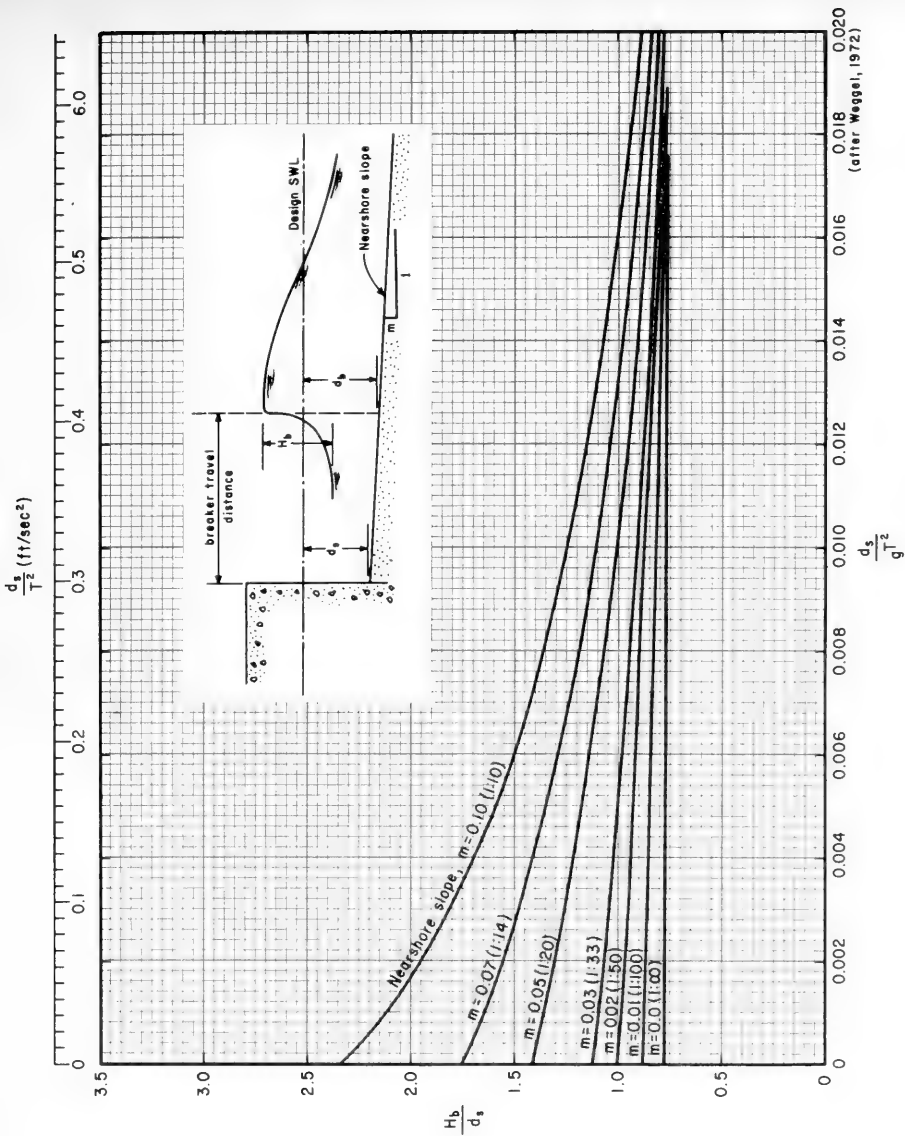
Figure 7-4. Dimensionless Design Breaker Height Versus Relative Depth at Structure

7-9

SOLUTION:

Computations are shown for the 6-second wave; only the final results for the 10-second wave are given.

From the given information, compute d_s/gT^2.

$$\frac{d_s}{gT^2} = \frac{7.5}{(32.2)(6)^2} = 0.0065 \ . \qquad (T = 6 \text{ sec.})$$

Enter Figure 7-4 with the computed value of d_s/gT^2 and determine value of H_b/d_s from the curve for a slope of m = 0.050.

$$\frac{d_s}{gT^2} = 0.0065 \ ; \ \frac{H_b}{d_s} = 1.12 \ . \qquad (T = 6 \text{ sec.})$$

Note that H_b/d_s is not identical with H_b/d_b where d_b is the depth at breaking and d_s is the depth at the structure. In general, because of nearshore slope, $d_s < d_b$; therefore $H_b/d_s > H_b/d_b$.

For the example, breaker height can now be computed from,

$$H_b = 1.12 \, d_s = 1.12 \, (7.5) = 8.40 \text{ ft} \ . \qquad (T = 6 \text{ sec.})$$

For the 10-second wave a similar analysis gives,

$$H_b = 1.30 \, d_s = 1.30 \, (7.5) = 9.75 \text{ ft} \ . \qquad (T = 10 \text{ sec.})$$

As illustrated by the example problem, longer period waves result in higher design breakers; therefore, the greatest breaker height which could possibly occur against a structure for a given design depth and nearshore slope is found by entering Figure 7-4 with $d_s/gT^2 = 0$ (infinite period). For the example problem,

$$\frac{d_s}{gT^2} = 0 \ ; \ \frac{H_b}{d_s} = 1.41 \ (m = 0.050),$$

$$H_b = 1.41 \, d_s = 1.41 \, (7.5) = 10.6 \textbf{ ft} \ .$$

* *

It is often of interest to know the deepwater wave height associated with the design breaker height obtained from Figure 7-4. Comparison of the design associated deepwater wave height determined from Figure 7-4 with actual deepwater wave statistics characteristic of the site will give some indication of how often the structure could be subjected to breakers as high as the design breaker. Deepwater height may be found in Figure 7-5 and information obtained by a refraction analysis. (See Section 2.3, WAVE REFRACTION.) Figure 7-5 is based on observations by Iversen (1952a, 1952b), as modified by Goda (1970), of periodic waves breaking on impermeable, smooth, uniform laboratory slopes. Figure 7-5 is a modified form of Figure 7-3.
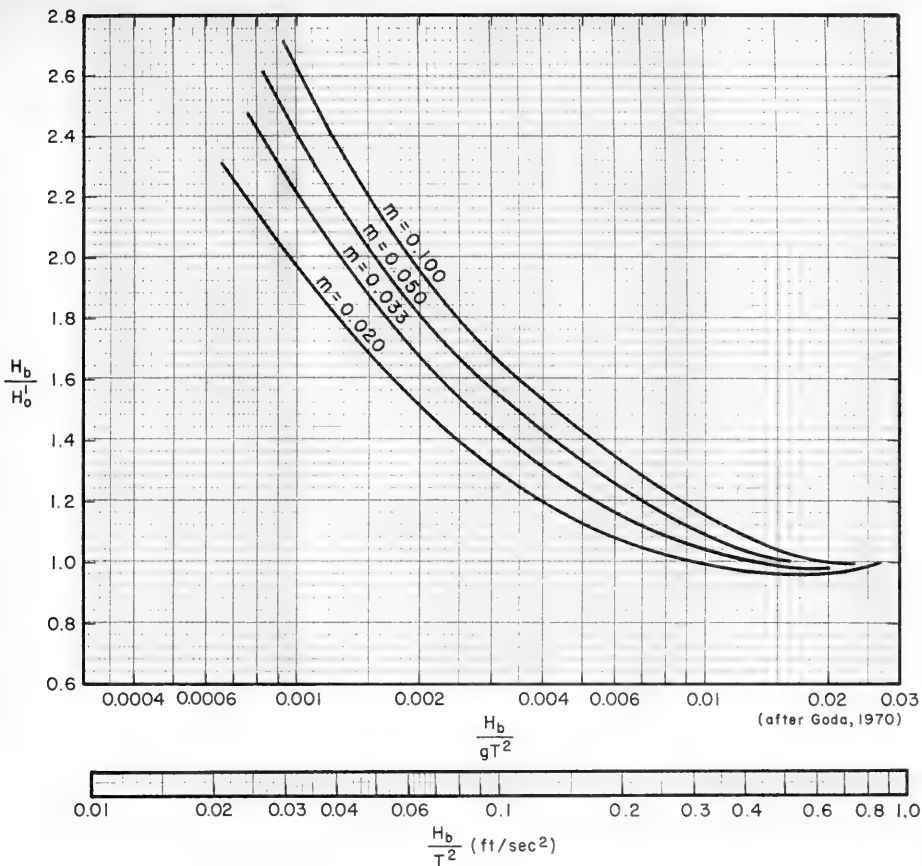
Figure 7-5. Breaker Height Index, H_b/H_o' Versus H_b/gT^2

GIVEN:

(a) $H_b = 8.4$ ft ,   (T = 6 sec.)

   and

                   $H_b = 9.8$ ft . (see previous example)   (T = 10 sec.)

(b)   Assume that refraction analysis of the structure site gives,

$$K_R = \sqrt{\frac{b_o}{b}} = 0.85 , \qquad (T = 6 \text{ sec.})$$

   and

$$K_R = 0.75 , \qquad (T = 10 \text{ sec.})$$

for a given deepwater direction of wave approach. See Section 2.3, WAVE REFRACTION.)

FIND: The deepwater height H_o of the waves resulting in the given breaker heights H_b.

SOLUTION: Calculate H_b/gT^2 for each wave condition to be investigated.

$$\frac{H_b}{gT^2} = \frac{8.4}{(32.2)(6)^2} = 0.0072. \qquad (T = 6 \text{ sec.})$$

With the computed value of H_b/gT^2 enter Figure 7-5 to the curve for a slope of m = 0.05 and determine H_b/H_o' which may be considered an ultimate shoaling coefficient or the shoaling coefficient when breaking occurs.

$$\frac{H_b}{gT^2} = 0.0072 \; ; \; \frac{H_b}{H_o'} = 1.19 . \qquad (T = 6 \text{ sec.})$$

With the value of H_b/H_o' thus obtained and with the value of K_R obtained from a refraction analysis, the deepwater wave height resulting in the design breaker may be found with Equation 7-5.

$$H_o = \frac{H_b}{K_R \left(H_b/H_o' \right)} . \qquad (7\text{-}5)$$

H_o is the actual deepwater wave height, while H_o' is the wave height in deep water if no refraction occurred (H_o' = unrefracted, deepwater height). Where the bathymetry is such that significant wave energy

is dissipated by bottom friction as the waves travel from deep water to the structure site, the computed deepwater height should be *increased* accordingly. See Section 3.7, HURRICANE WAVES, for a discussion of wave height attenuation by bottom friction.

Applying Equation 7-5 to the example problem gives:

$$H_o = \frac{8.4}{(0.85)(1.19)} = 8.3 \text{ ft} .$$ (T = 6 sec.)

A similar analysis for the 10-second wave gives,

$$H_o = 8.3 \text{ ft} .$$ (T = 10 sec.)

A wave advancing from the direction for which refraction was analyzed, and with a height in deep water greater than the computed H_o, will break at a distance greater than x_b feet in front of the structure. Waves with a deepwater height less than the H_o computed above could break directly against the structure; however, the corresponding breaker height will be less than the *design breaker height determined from Figure 7-4.*

* *

7.123 <u>Nonbreaking Waves</u>. Since statistical hindcast wave data are normally available for deepwater conditions $(d > L_o/2)$ or for depth conditions some distance from the shore, refraction analysis is necessary to determine wave characteristics at a nearshore site. (See Section 2.3, **WAVE REFRACTION.**) Where the Continental Shelf is broad and shallow, as in the Gulf of Mexico, it is advisable to allow for a large energy loss due to bottom friction (Savage, 1953), (Bretschneider, 1954a, b). (See Section 3.7, HURRICANE WAVES.)

General procedures for developing the height and direction of the design wave by use of refraction diagrams follow:

From the site, draw a set of *refraction fans* for the various waves that might be expected (use wave period increments of no more than 2 seconds), and determine refraction coefficients by the method given in Section 2.3, WAVE REFRACTION. Tabulate refraction coefficients determined for the selected wave periods and for each deepwater direction of approach. The statistical wave data from synoptic weather charts or other sources may then be reviewed to determine if waves having directions and periods with large refraction coefficients will occur frequently.

The deepwater wave height, adjusted by refraction and shoaling coefficients, that gives the highest significant wave height at the structure would indicate direction of approach and period of the design wave. The inshore height so determined is the design significant wave height. A typical example of such an analysis is shown in Table 7-1.

Table 7-1. Determination of Design Wave Heights

1	2	3	4	5
Direction	Significant Deepwater Wave Height (ft.)	Wave Period (sec.)	Combined Refraction and Shoaling Coefficients* ($K_R K_s$)	Refracted Wave Height to Nearest One-half Foot (ft.)
NW	15	8	0.20	3.0
		10	0.14	2.0
		12	0.08	1.0
WNW	12	8	0.30	3.5
		10	0.24	3.0
		12	0.18	2.0
W	10	10	0.60	6.0
		12	0.62	6.0
		14	0.40	4.0
		16	0.50	5.0
WSW	10	10	1.20	12.0†
		12	1.00	10.0
		14	0.70	7.0
		16	0.70	7.0
SW	8	12	1.44	12.0†
		14	1.18	9.5
		16	0.80	6.5

* Refraction coefficient, $K_R = \sqrt{b_o / b}$ at design water level.

Shoaling coefficient, $K_s = H / H_o'$ at design water level.

† Adopted as the significant design wave height.

NOTES

Columns 1, 2 and 3 are taken from the statistical wave data as determined from synoptic weather charts.

Column 4 is determined from the relative distances between two adjacent orthogonals in deep water and shallow water, and the shoaling coefficient.

Column 5 is the product of columns 2 and 4.

In this example, although the highest significant deepwater waves approached from directions ranging from W to NW, the refraction study indicated that higher inshore significant waves may be expected from more southerly directions.

The accuracy of determining the shallow-water design wave by a refraction analysis is decreased by highly irregular bottom conditions. For irregular bottom topography, field observations including the use of aerial photos or hydraulic model tests may be required to obtain valid refraction information.

7.124 <u>Bathymetry Changes at Structure Site</u>. The effect of a proposed structure on conditions influencing wave climate in its vicinity should also be considered. The presence of a structure might cause significant deepening of the water immediately in front of it. This deepening, resulting from scour during storms may increase the design depth and consequently the design breaker height if a breaking wave condition is assumed for design. If the material removed by scour at the structure is deposited offshore as a bar, it may provide protection to the structure by causing large waves to break farther seaward. Experiments by Russell and Inglis (1953), van Weele (1965), Kadib (1962, 1963), and Chesnutt (1971), provide information for estimating changes in depth. A general rule for estimating the scour at the toe of a wall is given in Section 5.28.

7.125 <u>Summary - Evaluating the Marine Environment</u>. The design process of evaluating wave and water level conditions at a structure site is summarized in Figure 7-6. The path taken through the figure will generally depend on the type, purpose, and location of a proposed structure and on the availability of data. Design depths and wave conditions at a structure can usually be determined concurrently. However, applying these design conditions to structural design requires evaluation of water levels and wave conditions that can reasonably be assumed to occur simultaneously at the site. Where hurricanes cross the coast, high water levels resulting from storm surge and extreme wave action generated by the storm occur together, and usually provide critical design conditions. Design water levels and wave conditions are needed for refraction and diffraction analyses, and these analyses must follow establishment of design water levels and design wave conditions.

The frequency of occurrence of adopted design conditions and the frequency of occurrence and duration of reasonable combinations of water level and wave action are required for an adequate economic evaluation of any proposed shore protection scheme.

7.2 <u>WAVE RUNUP, OVERTOPPING AND TRANSMISSION</u>

7.21 <u>WAVE RUNUP</u>

The vertical height above the stillwater level to which water from an incident wave will run up the face of a structure determines the required structure height, if wave overtopping cannot be permitted.
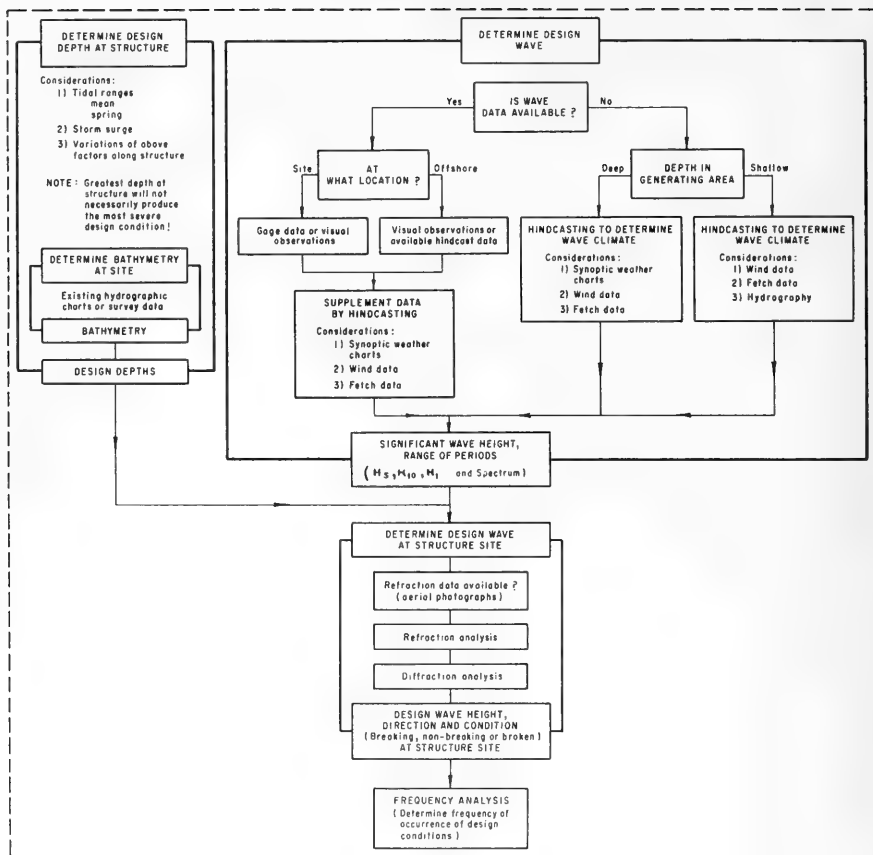
Figure 7-6. Logic Diagram for Evaluation of Marine Environment

Runup depends on structure shape and roughness, water depth at structure toe, bottom slope in front of a structure, and incident wave characteristics. Because of the large number of variables involved, a complete description is not available of the runup phenomenon in terms of all possible ranges of the geometric variables and wave conditions. Numerous laboratory investigations have been conducted, but mostly for runup on smooth, impermeable slopes. Hall and Watts (1953) investigated runup of solitary waves on impermeable slopes; Saville (1956) investigated runup by periodic waves. Dai and Kamel (1969) investigated the runup and rundown of waves on rubble breakwaters. Savage (1958) studied effects of structure roughness and slope permeability. Miller (1968) investigated runup of undular and fully broken waves on three beaches of different roughnesses. LeMéhauté (1963) and Freeman and LeMéhauté (1964) studied long-period wave runup analytically. Keller, et al. (1960), Ho and Meyer (1962), and Shen and Meyer (1963) studied the motion of a fully broken wave and its runup on a sloping beach.

Figures 7-8 through 7-13 summarize results for small-scale laboratory tests of wave runup on smooth impermeable slopes. (Saville, 1958a.) The curves are in dimensionless form for the relative runup R/H'_O as a function of deepwater wave steepness and structure slope, where R is the runup height measured (vertically) from the SWL and H'_O is the *unrefracted deepwater wave height*. (See Figure 7-7 for definitions.) Results predicted by Figures 7-8 through 7-12 are probably less than the runup on prototype structures because of a scale effect due to the inability to scale roughness effects in small-scale laboratory tests. *Runup values from Figure 7-8 through 7-12 can be adjusted for scale effects by using Figure 7-13.*
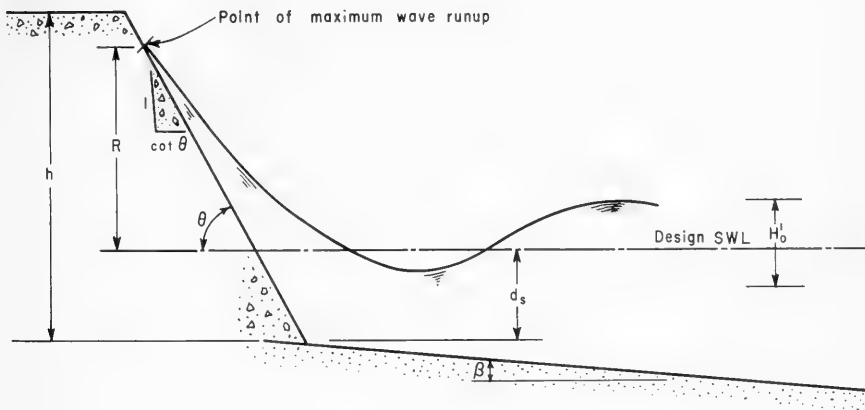
Figure 7-7. Definition Sketch, Wave Runup and Overtopping
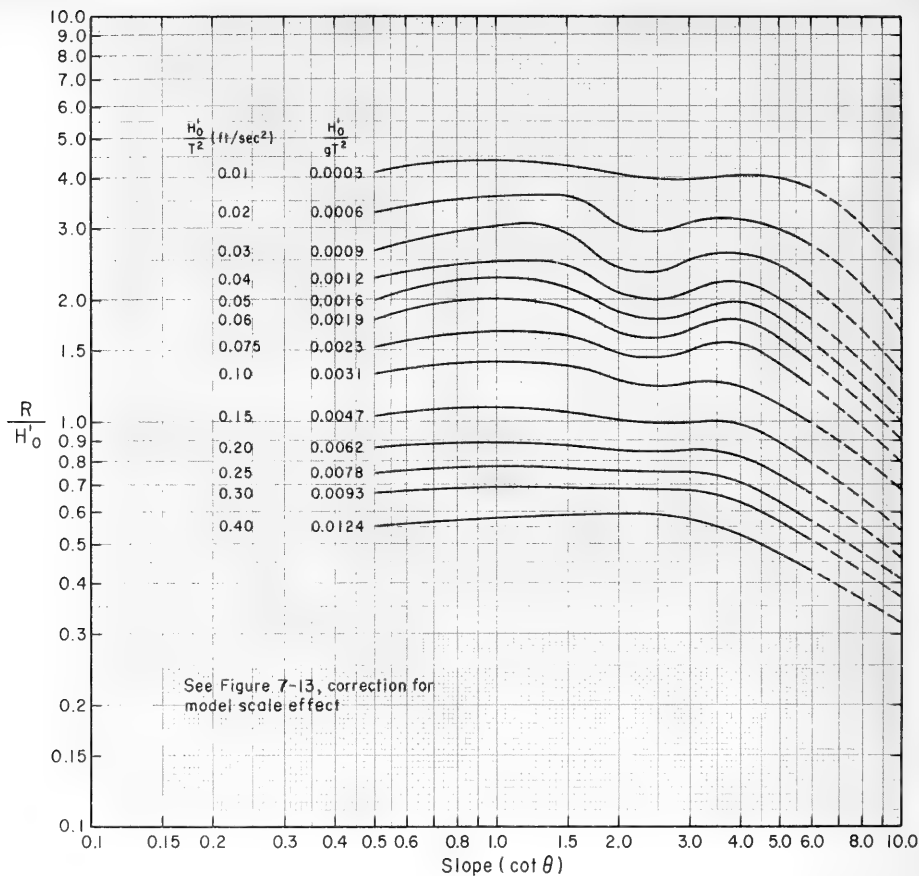
Figure 7-8. Wave Runup on Smooth, Impermeable Slopes, $d_s/H_0' = 0$
(Structure Fronted by a 1:10 Slope)
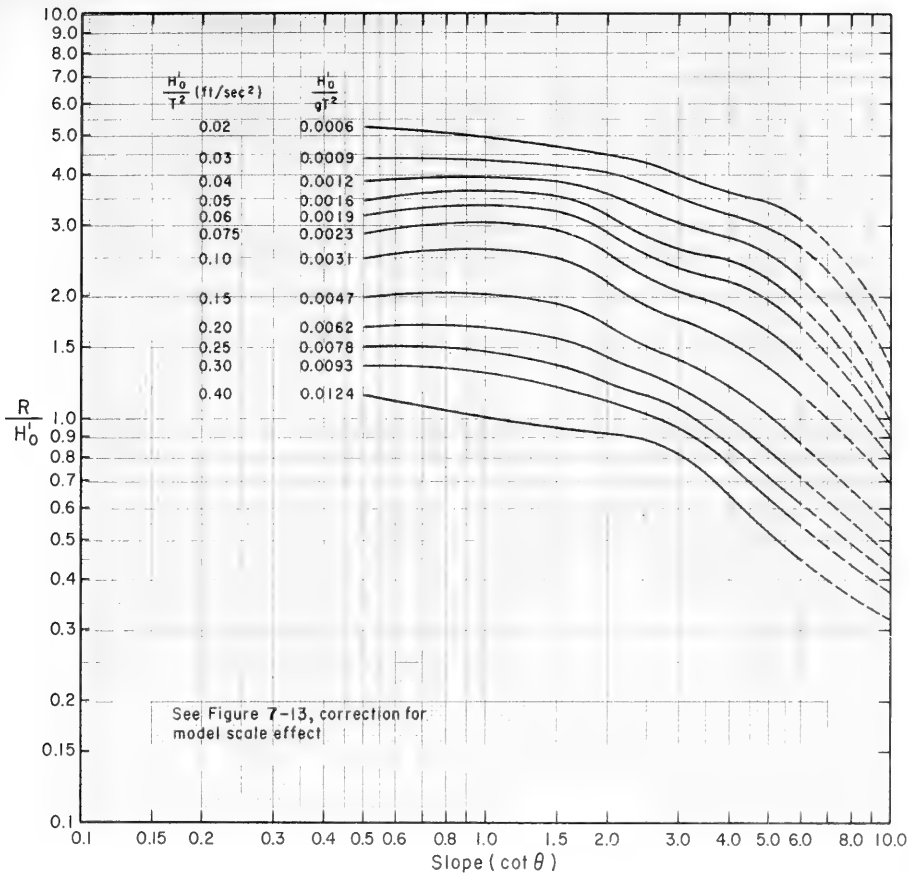
Figure 7-9. Wave Runup on Smooth, Impermeable Slopes, $d_S / H_0' \approx 0.45$
(Structure Fronted by a 1:10 Slope)
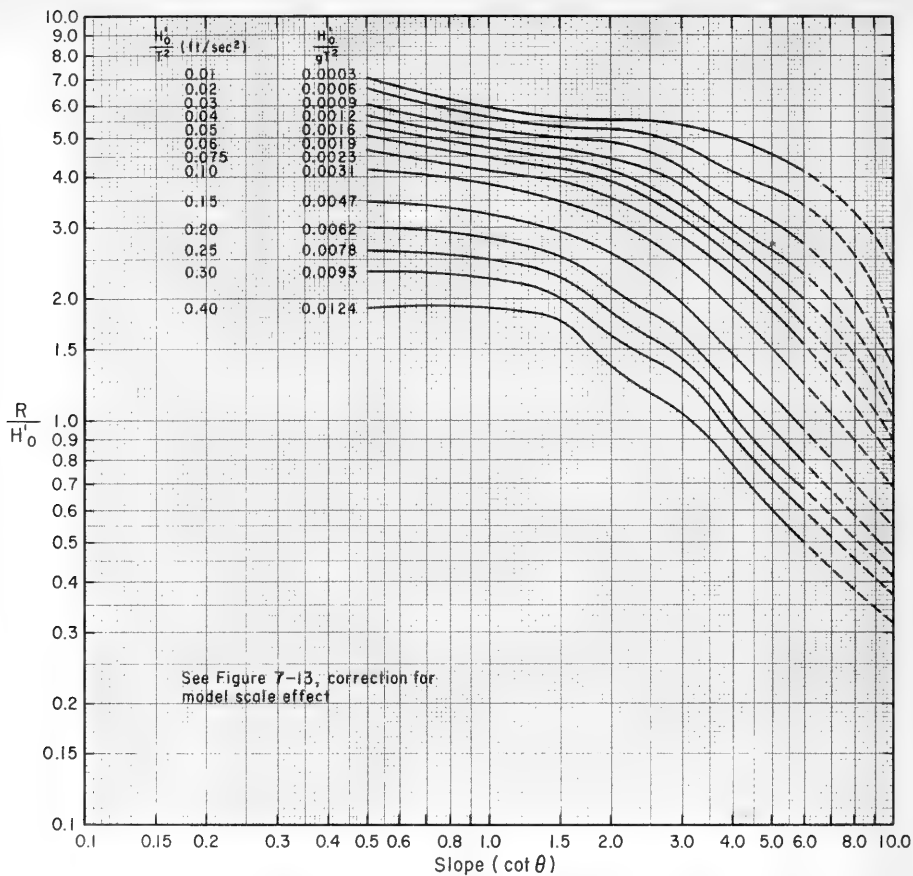
Figure 7-10. Wave Runup on Smooth, Impermeable Slopes, $d_s/H_0' \approx 0.80$
(Structure Fronted by a 1:10 Slope)

The chart axes and key:

Y-axis: $\dfrac{R}{H_0'}$, ranging from 0.1 to 10.0

X-axis: Slope ($\cot\theta$), ranging from 0.1 to 10.0

$\dfrac{H_0'}{T^2}$ (ft/sec^2)	$\dfrac{H_0'}{gT^2}$
0.01	0.0003
0.02	0.0006
0.03	0.0009
0.04	0.0012
0.05	0.0016
0.06	0.0019
0.075	0.0023
0.10	0.0031
0.15	0.0047
0.20	0.0062
0.25	0.0078
0.30	0.0093
0.40	0.0124
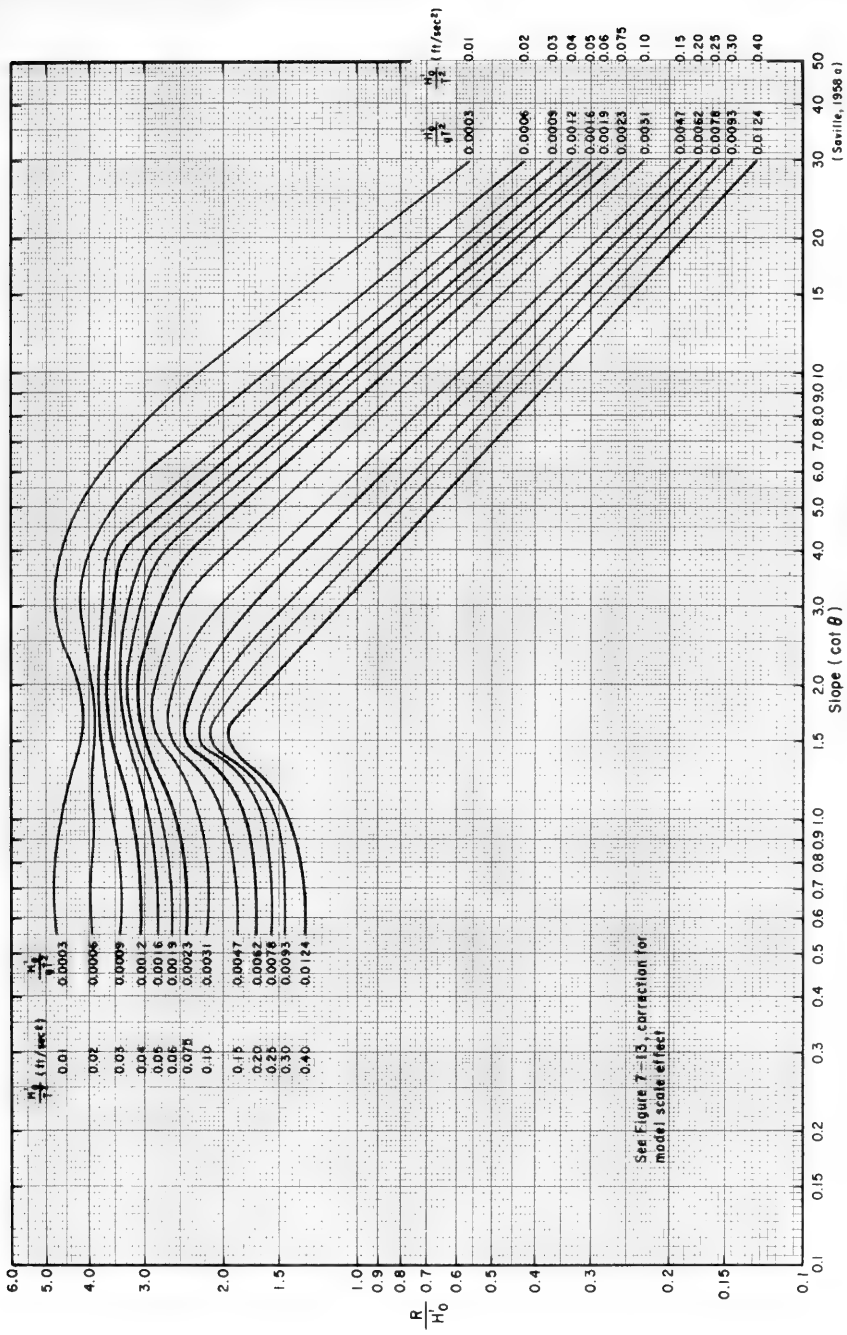
See Figure 7-13, correction for model scale effect

7-20

Figure 7-11. Wave Runup on Smooth, Impermeable Slopes, $d_S/H_0' \approx 2.0$

(Saville, 1958 a)
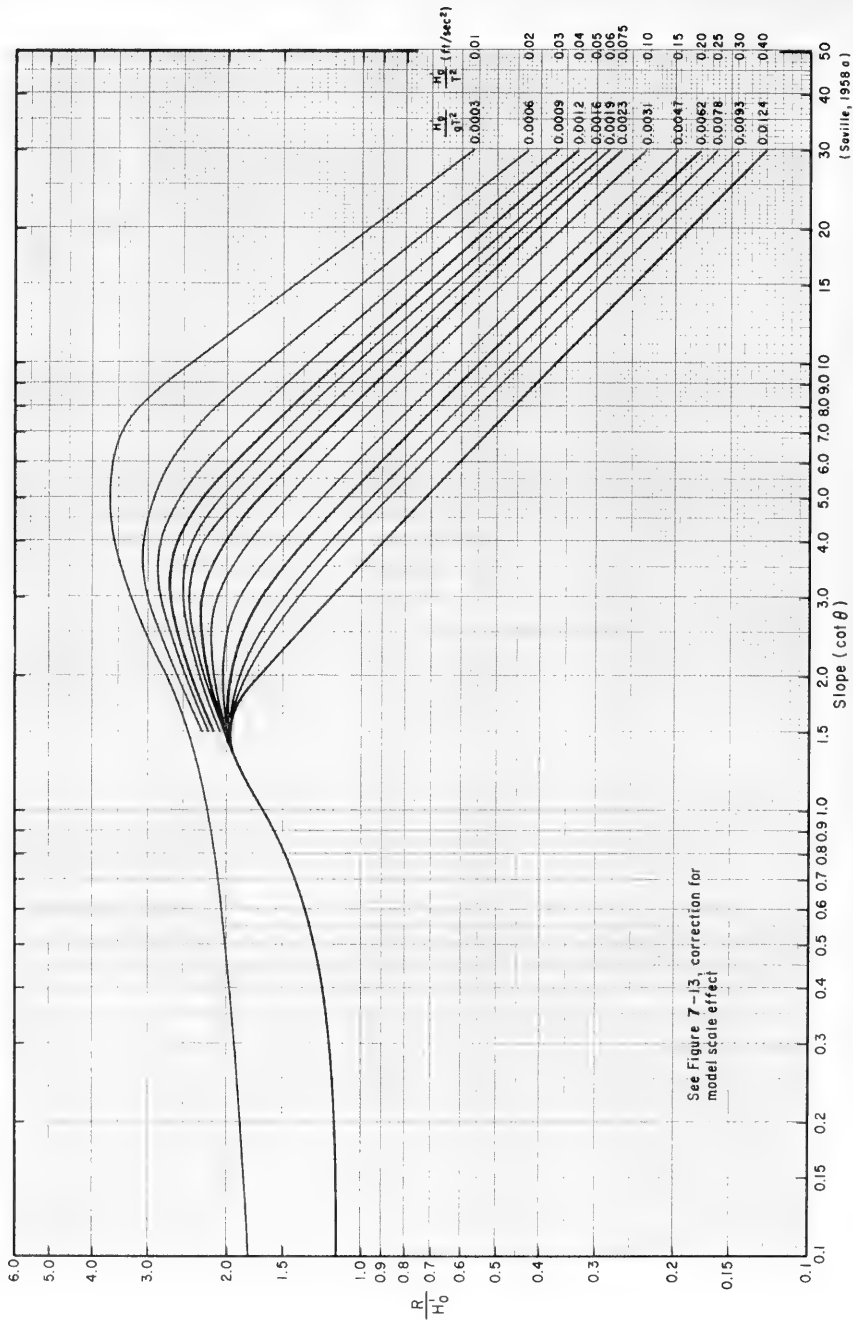
Figure 7-12. Wave Runup on Smooth, Impermeable Slopes, $d_s/H_0' \geq 3.0$
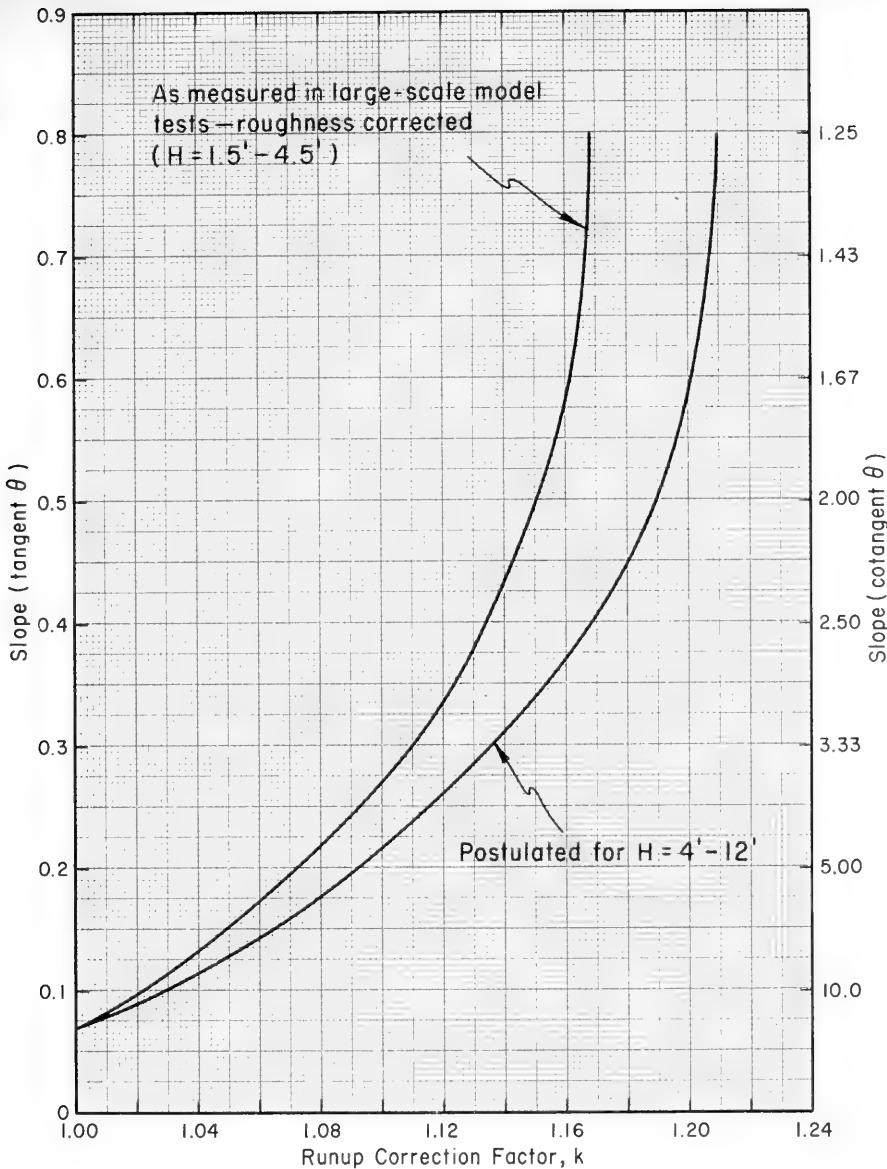
Figure 7-13. Runup Correction for Scale Effects

Runup on impermeable structures having riprap slopes and runup on vertical, stepped, curved and Galveston-type recurved seawalls have been studied on laboratory-scale models by Saville (1955, 56). The results are shown in Figures 7-14 through 7-18. Effects of using graded riprap on the face of an impermeable structure (as opposed to riprap of uniform size for which Figure 7-15 was obtained) are presented in Figure 7-19 for a 1 on 2 graded riprap slope. Wave rundown for the same slope is also presented in Figure 7-19. Runup on *permeable rubble slopes* as a function of structure slope and H_o'/gT^2 is compared with runup on smooth slopes in Figure 7-20. Corrections for scale effects, using the curves in Figure 7-13 should be applied to runup values obtained from Figures 7-8 through 7-12 and 7-14 through 7-18. The values of runup obtained from Figures 7-19 and 7-20 are assumed directly applicable to prototype structures without correction for scale effects.

The use of the figures to estimate wave runup is illustrated by the following example.

* * * * * * * * * * * * * * * EXAMPLE PROBLEM * * * * * * * * * * * * * * * *

GIVEN: An impermeable structure has a smooth slope of 1 on 2.5 and is subjected to a design wave, H = 7 ft. measured at a gage located in a depth d = 15 ft. Design period is T = 8 sec. Design depth at structure toe at high water is d_s = 10 ft. (Assume no change in the refraction coefficient between the structure and the wave gage.)

FIND:

(a) The height above the SWL to which the structure must be built to prevent overtopping by the design wave.

(b) The reduction in required structure height if uniform-sized riprap is placed on the slope.

SOLUTION:

(a) Since the runup curves are for deepwater height H_o' the shallow water wave height H = 7 ft. must be converted to an equivalent deepwater value. Using the depth where the wave height is measured, calculate,

$$\frac{d}{L_o} = \frac{d}{5.12 \, T^2} = \frac{15}{5.12 \, (8)^2} = 0.0458 .$$

From Table C-1, Appendix C, for

$$\frac{d}{L_o} = 0.0458 ,$$

$$\frac{H}{H_o'} = 1.039 .$$

7-24
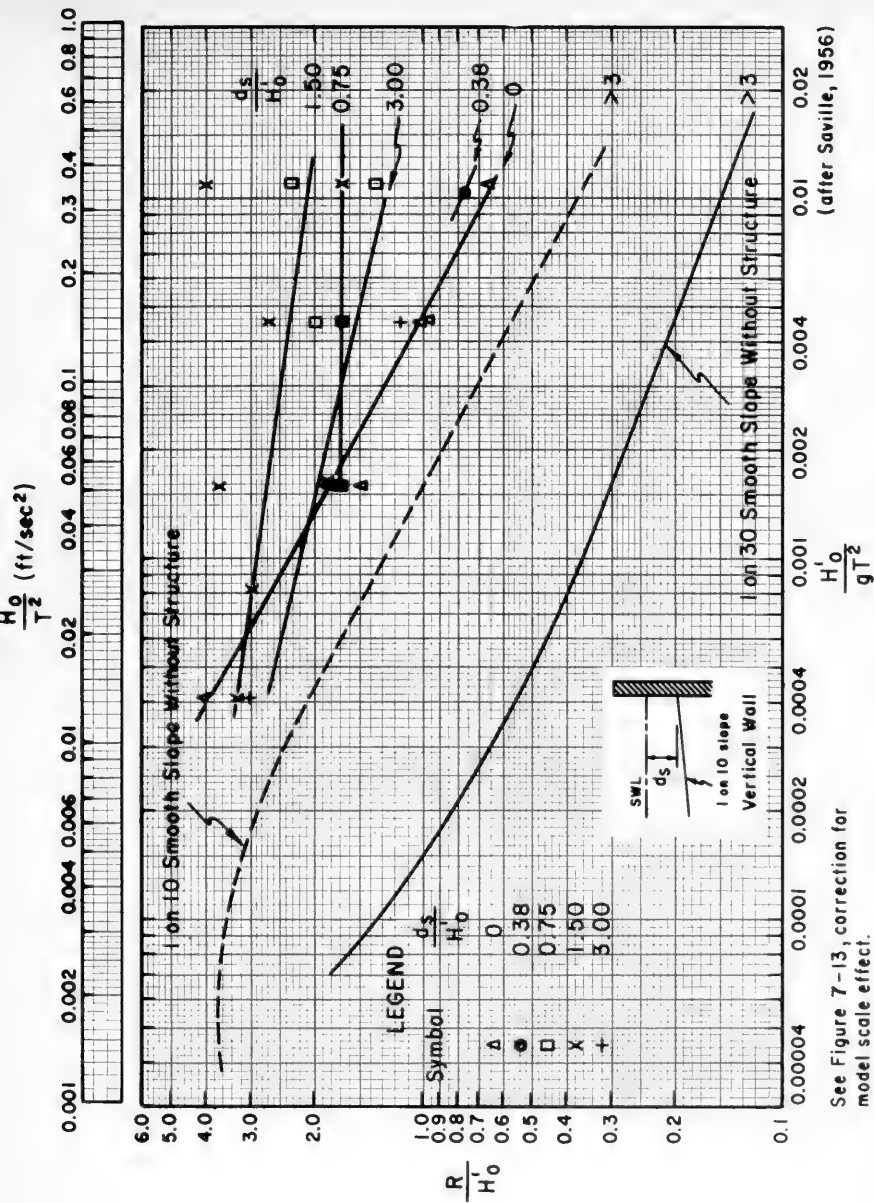
Figure 7-14. Wave Runup on Impermeable, Vertical Wall versus H_O'/gT^2

7-25
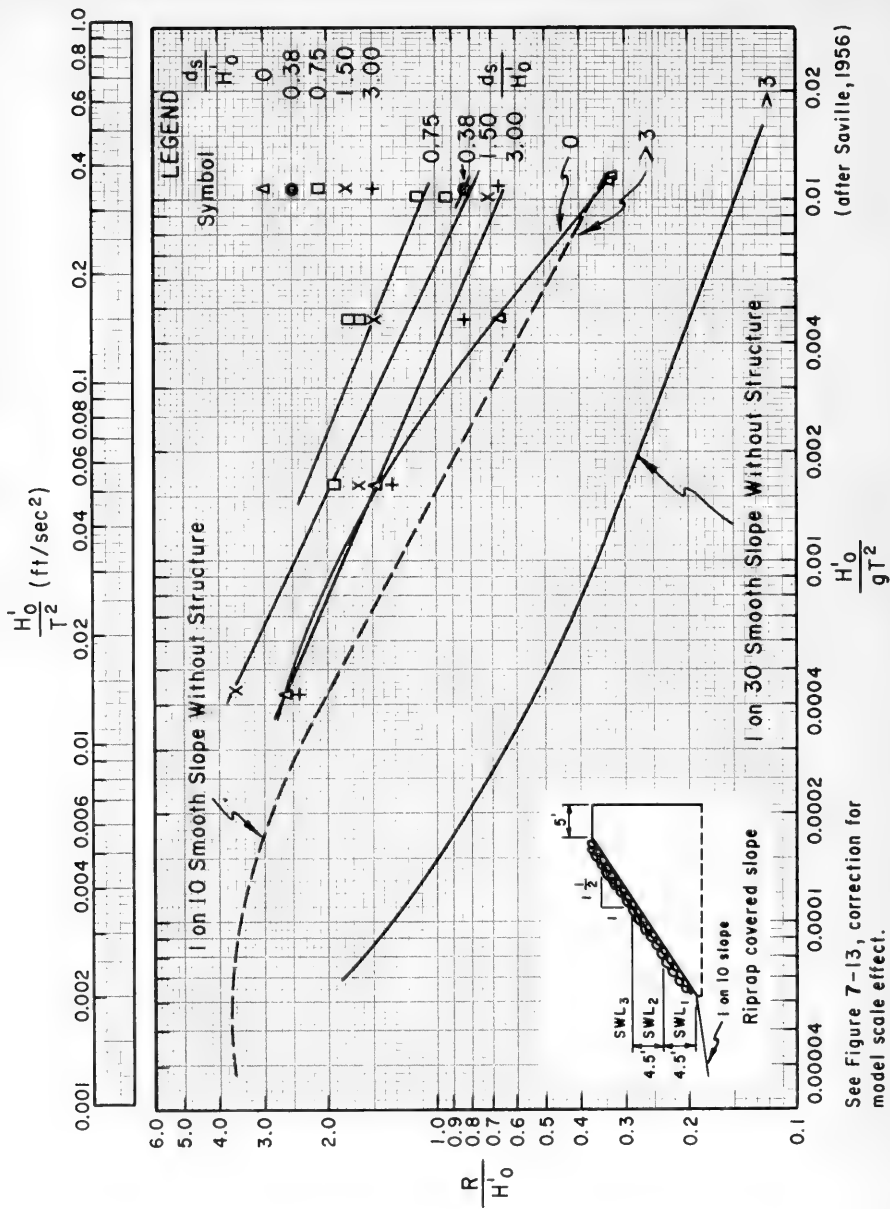
Figure 7-15. Wave Runup on Impermeable, Riprap, 1:1.5 Slope versus H'_O/gT^2

7-26
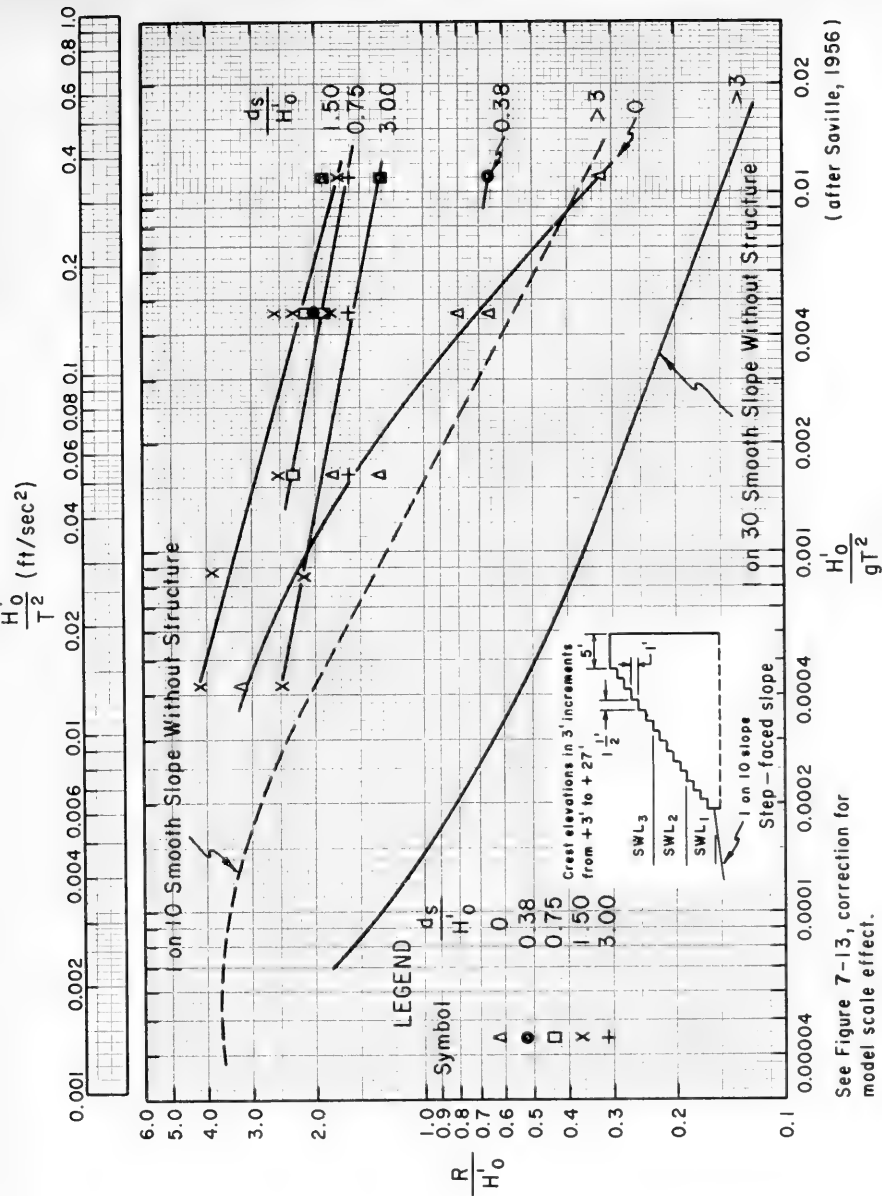
Figure 7-16. Wave Runup on Impermeable, Stepped, 1:1.5 Slope versus H'_O/gT^2
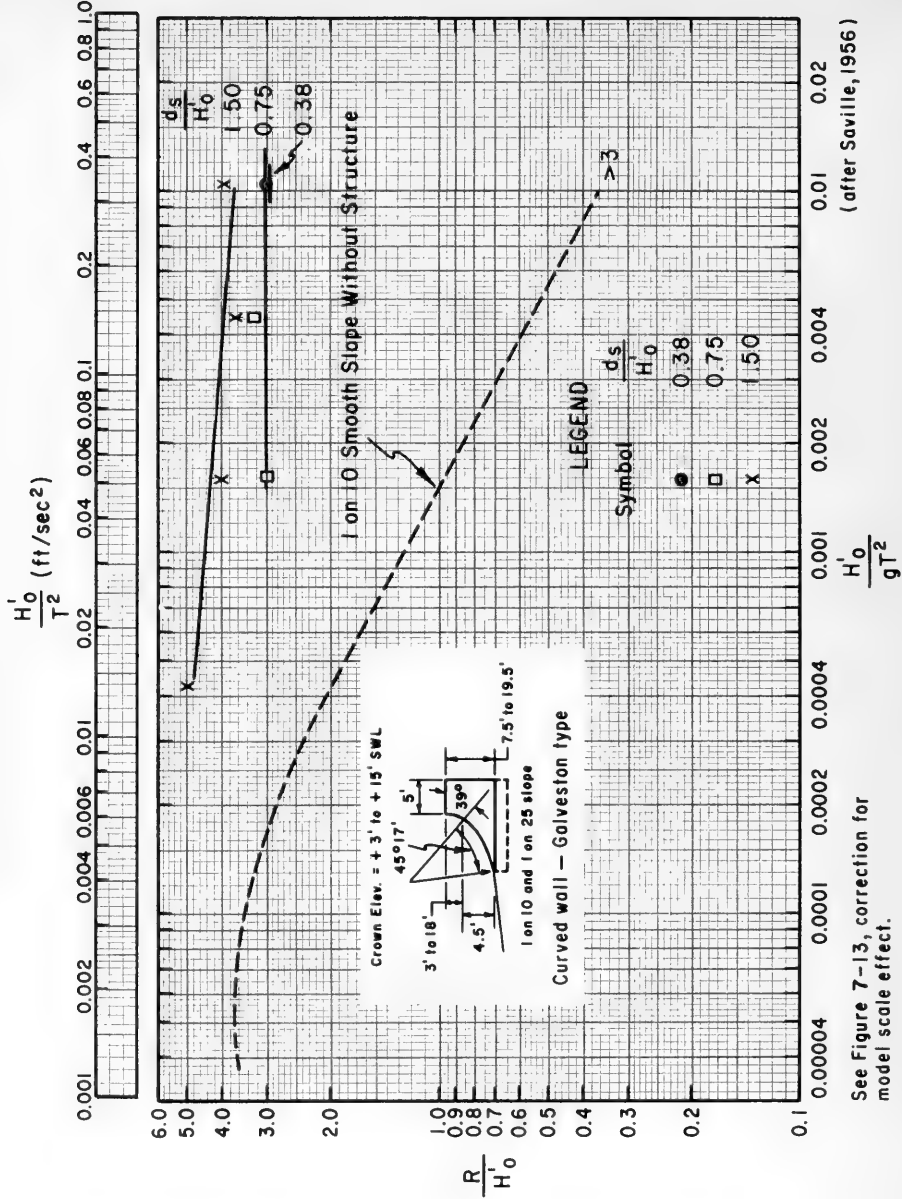
(after Saville, 1956)

7-27

Figure 7-17. Wave Runup on Impermeable Seawall versus H'_O/gT^2
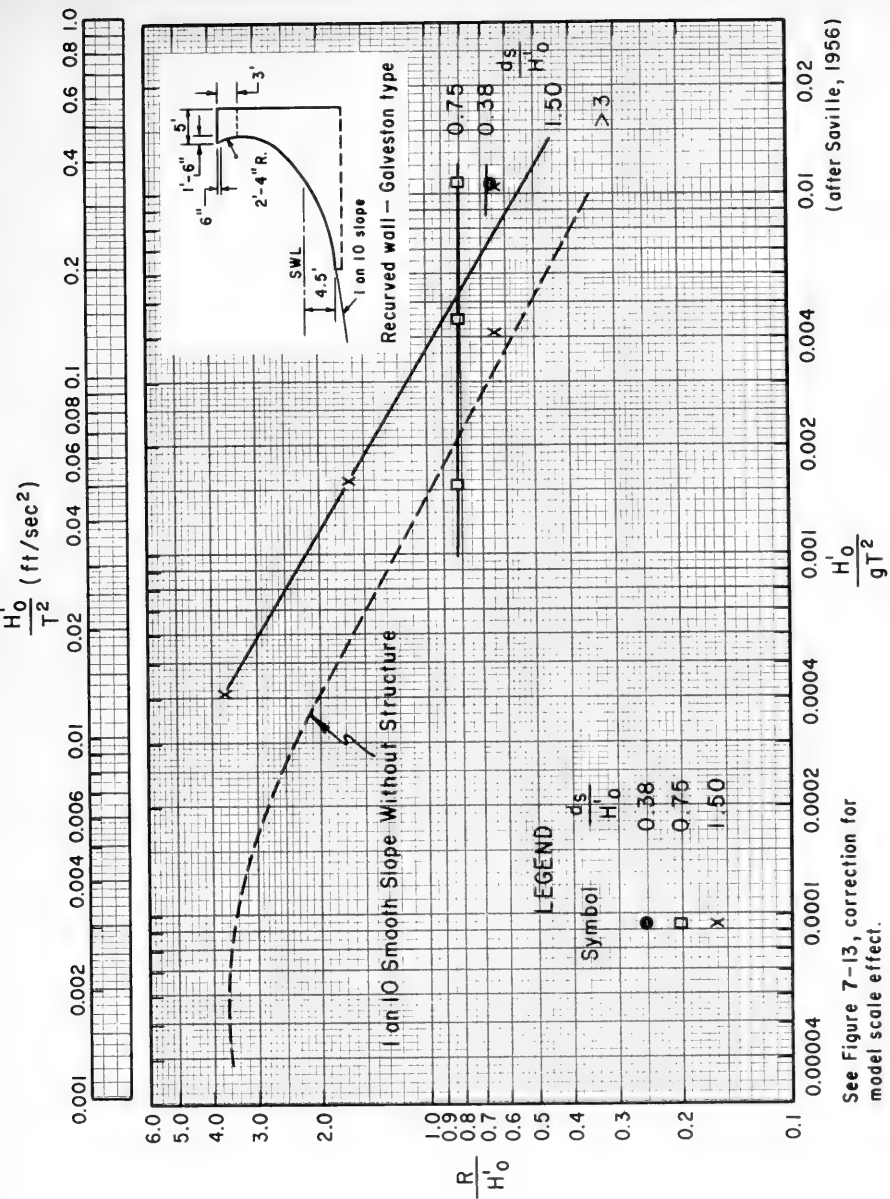
Figure 7-18. Wave Runup on Recurved (Galveston type) Seawall versus H_O'/gT^2

7-29
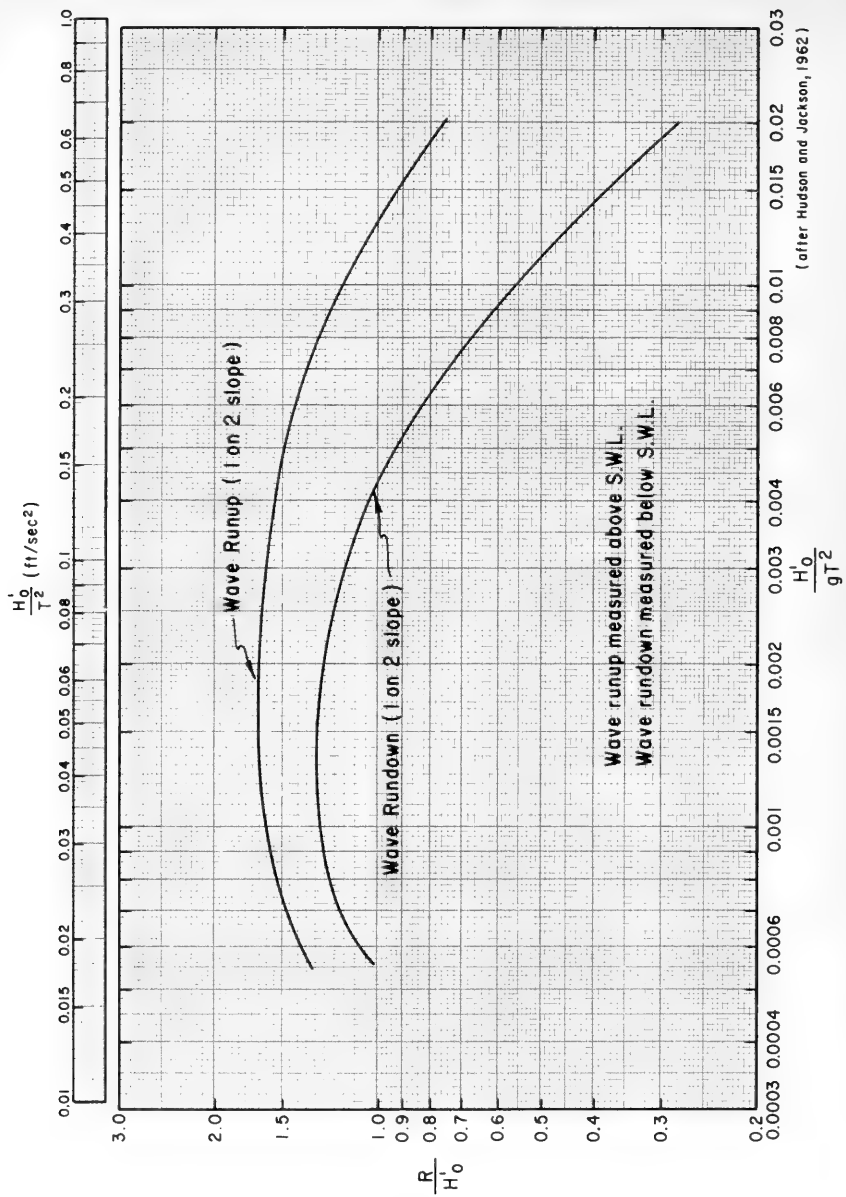
Figure 7-19. Wave Runup and Rundown on Graded Riprap, 1:2 Slope, Impermeable Base, Versus H_0'/gT^2 (data for $d_s/H_0' > 3.0$)
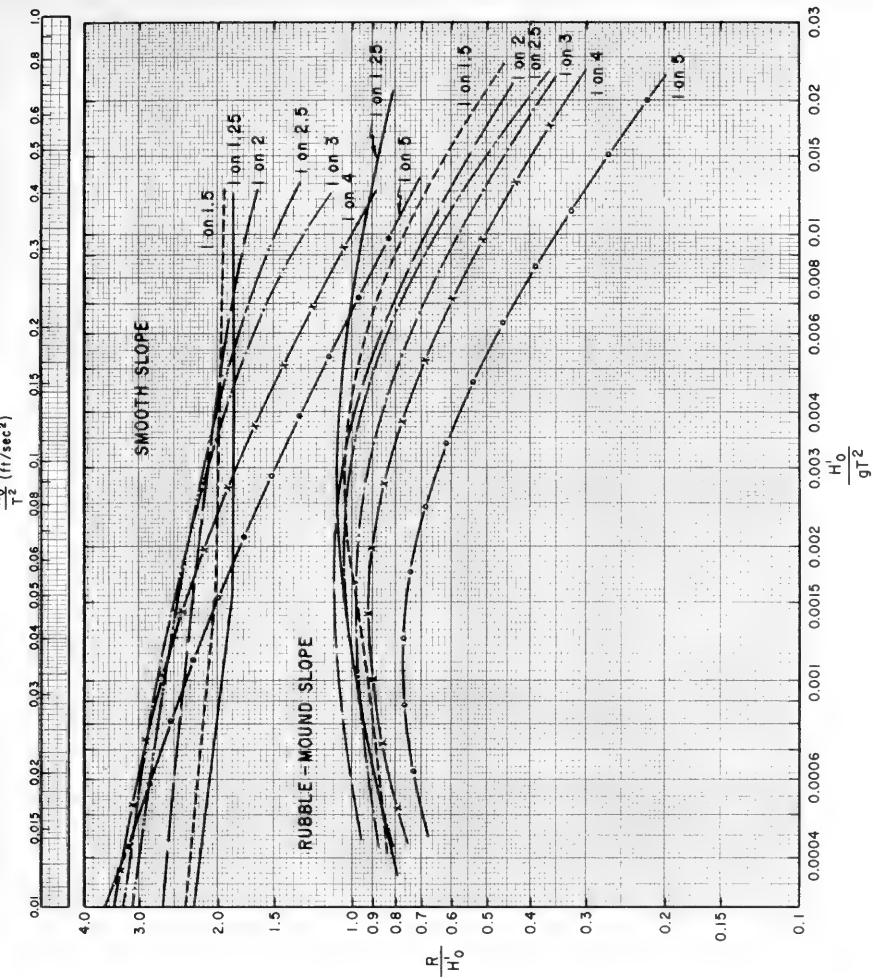
Figure 7-20. Comparison of Wave Runup on Smooth Slopes with Runup on Permeable Rubble Slopes (data for $d_s/H_0' > 3.0$)

Therefore

$$H_o' = \frac{H}{1.039} = \frac{7}{1.039} = 6.74 \text{ ft}.$$

To determine the runup, calculate

$$\frac{H_o'}{gT^2} = \frac{6.74}{32.2\,(8)^2} = 0.0033,$$

and using the depth at the structure toe,

$$d_s = 10 \text{ ft},$$

$$\frac{d_s}{H_o'} = \frac{10}{6.74} = 1.48.$$

Interpolating between Figures 7-10 and 7-11, for a 1 on 2.5 slope,

Figure 7-10 $\dfrac{d_s}{H_o'} = 0.80 \qquad \dfrac{R}{H_o'} = 2.8,$

Interpolated Value $\dfrac{d_s}{H_o'} = 1.48 \qquad \dfrac{R}{H_o'} \approx 2.7,$

Figure 7-11 $\dfrac{d_s}{H_o'} = 2.0 \qquad \dfrac{R}{H_o'} = 2.7.$

The runup, *uncorrected for scale effects*, is

$$R = 2.7\,\left(H_o'\right),$$

$$R = 2.7\,(6.74) = 18.2 \text{ ft}.$$

The scale correction factor k can be found from Figure 7-13. The slope in terms of $m = \tan\theta$ is

$$\tan\theta = \frac{1}{2.5} = 0.40.$$

The corresponding correction factor for a wave height, $H_o' = 6.74$ ft. is,

$$k = 1.17.$$

Therefore, the corrected runup is

$$R = 1.17\,(18.2) = 21.3 \text{ ft}.$$

(b) Riprap on a slope decreases the maximum runup. Hydraulic model studies for the range of possible slopes have not been conducted; however, Figure 7-15 can be used with Figures 7-10 and 7-11 to estimate the percent reduction of runup resulting from adding riprap to a 1 on 1.5 slope and to apply that reduction to structures with different slopes. From an analysis similar to the above, the runup, *uncorrected for scale effects*, on a 1 on 1.5 smooth, impermeable slope is,

$$\left[\frac{R}{H_o'}\right]_{smooth} = 3.1.$$

From Figure 7-15 (riprap), entering with $H_o'/gT^2 = 0.0033$ and using the curve for $d_s/H_o' = 1.5$ which is closest to the actual value of

$$\frac{d_s}{H_o'} = 1.48 \ ,$$

$$\left[\frac{R}{H_o'}\right]_{riprap} = 1.5 \ .$$

The reduction in runup is therefore

$$\frac{\left[R/H_o'\right]_{riprap}}{\left[R/H_o'\right]_{smooth}} = \frac{1.5}{3.1} = 0.48 \ .$$

Applying this correction to the runup calculated for the 1 on 2.5 slope in the preceding part of the problem,

$$R_{riprap} = 0.48 \, R_{smooth} = 0.48 \, (21.3) = 10.3 \text{ ft} \ .$$

Since the scale-corrected runup (21.3 ft.) was multiplied by the factor 0.48, the correction for scale effects is included in the 10.3 ft. runup value. This technique gives a reasonable estimate of runup on riprapped slopes when model test results for the actual structure slope are not available.

* *

Saville (1958a) presented a method for determining runup on composite slopes using experimental results obtained for constant slopes. The method assumes that a composite slope can be replaced by a hypothetical, uniform slope running from the bottom, at the point where the incident wave breaks, up to the point of maximum runup on the structure. Since the point of maximum runup is the answer sought, a method of successive approximations is used. Calculation of runup on a composite slope is illustrated by the following example problem for a smooth-faced levee.

7-33

The method is equally applicable to any composite slope. The resultant runup for slopes composed of different types of surface roughness may be calculated by using a proportionate part of various surface roughnesses of the composite slope on the hypothetical slope. The composite-slope method should not be used where beach berms are wider than $L/4$, where L is the design wavelength for the structure. In the case where a wide berm becomes flooded or the water depth increased by wave setup (see Sections 3.8 and 3.85) such as a reef, the wave runup is based on the water depth on the berm or reef.

* * * * * * * * * * * * * * * EXAMPLE PROBLEM * * * * * * * * * * * * * * * *

GIVEN: A smooth-faced levee (cross section shown in Figure 7-21) is sub-
jected to a design wave having a period $T = 8$ sec. and an equivalent deepwater height $H_O' = 5$ ft. The depth at the structure toe is $d_s = 4$ ft.

FIND: Using the composite-slope method, determine the maximum runup on the levee face by the design wave.

SOLUTION: The runup on a 1 on 3 slope is first calculated to determine whether the runup will exceed the berm elevation. Calculate,

$$\frac{d_s}{H_o'} = \frac{4}{5} = 0.8,$$

and

$$\frac{H_o'}{gT^2} = \frac{5}{32.2 \, (8)^2} = 0.0024 \ .$$

From Figure 7-10 for

$$\frac{d_s}{H_o'} = 0.8,$$

with

$$\cot (\theta) = \frac{1}{\tan \theta} = 3,$$

and

$$\frac{H_o'}{gT^2} = 0.0024 \ ,$$

$$\frac{R}{H_o'} = 2.8 \ .$$

This runup is corrected for scale effects by using Figure 7-13 with $\tan \theta = 0.33$ and $H \approx 5$ ft. A correction factor of $k = 1.15$ is obtained, and

$$R = 2.8 \ k \ H_o' = 2.8 \, (1.15) \, (5),$$

$$R = 16.1 \ \text{ft} .$$

which is 10.1 feet above the berm elevation. (See Figure 7-21.) Therefore, the composite-slope method must be used.
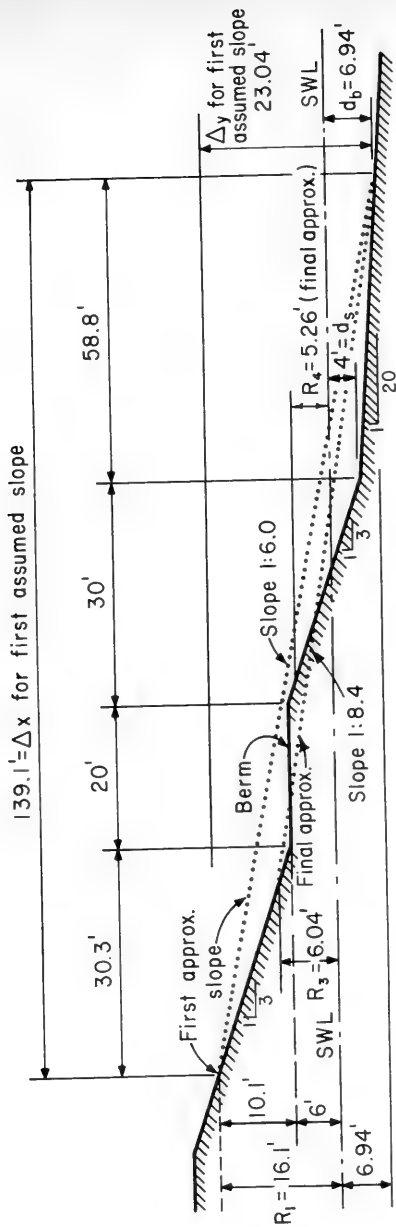
Figure 7-21. Calculation of Runup for Composite Slope, Example of a Levee Cross Section

7-35

The breaker depth for the given design wave is first determined. With

$$\frac{H'_o}{gT^2} = 0.0024 ,$$

calculate,

$$\frac{H'_o}{L_o} = 2\pi \frac{H'_o}{gT^2} = 6.28 \, (0.0024) = 0.015 .$$

Enter Figure 7-3 with $H'_o/gT^2 = 0.0024$, using the curve for the given slope of $m = 0.050$ (1:20), and find

$$\frac{H_b}{H'_o} = 1.46 .$$

Therefore,

$$H_b = 1.46 \, (5) = 7.30 \text{ ft } .$$

Calculate,

$$\frac{H_b}{gT^2} = \frac{7.30}{32.2 \, (8)^2} = 0.00354 .$$

Then, from Figure 7-2, from the curve for $m = 0.05$,

$$\frac{d_b}{H_b} = 0.95 ,$$

and

$$d_b = 0.95 \, H_b = 0.95 \, (7.30) = 6.94 .$$

Therefore, the wave will break a distance $(6.94-4.0)/0.05 = 58.8$ ft. in front of the structure toe.

The runup value calculated above is a first approximation to the actual runup, and is used to calculate a hypothetical slope that is used to determine the second approximation to the runup. The hypothetical slope is taken from the point of maximum runup on the structure to the bottom at the breaker location (the upper dotted line on Figure 7-22). Then,

$$\Delta x = 58.8' + 30' + 20' + 30.3' = 139.1 \text{ ft } ,$$

and, the change in elevation is

$$\Delta y = 6.94 + 16.1 = 23.04 \text{ ft } ,$$

and therefore

$$\cot \theta = \frac{\Delta x}{\Delta y} = \frac{(139.1)}{(23.04)} \approx 6.0 .$$

7-36

This slope may now be used with the runup curves (Figures 7-10 and 7-11) to determine a second approximation to the actual runup. Calculate d_s/H_o' using the breaker depth d_b,

$$\frac{d_b}{H_o'} = \frac{6.94}{5} = 1.39 .$$

Interpolating between Figures 7-10 and 7-11, for

$$\frac{H_o'}{gT^2} = 0.0024 ,$$

$$\frac{R}{H_o} = 1.55 .$$

Correcting for scale effects using Figure 7-13,

$$k = 1.07 ,$$

and

$$R = 1.55 (1.07) 5 \approx 8.3 \text{ ft.}$$

A new hypothetical slope as shown in Figure 7-22 can now be calculated using the second runup approximation to determine Δx and Δy. A third approximation for the runup can then be obtained. This procedure is continued until the difference between two successive approximations is nearly zero. The sequence of runup approximations for the example problem is

$$R_1 = 16.1 \text{ ft} ,$$
$$R_2 = 8.3 \text{ ft} ,$$
$$R_3 = 6.04 \text{ ft} ,$$
$$R_4 = 5.26 \text{ ft} ,$$
$$R_5 = 6 + \text{ ft} .$$

and the steps in the calculations are shown graphically in Figure 7-22. The number of computational steps could have been decreased if a better first guess of the hypothetical slope had been made.

* *

7.22 WAVE OVERTOPPING

It may be too costly to design structures to preclude overtopping by the largest waves of a wave spectrum. If the structure is a levee or dike, the required capacity of pumping facilities to dewater a shoreward area will depend on the rate of wave overtopping and water contributed by local rains and stream inflow. Incident wave height and period are important
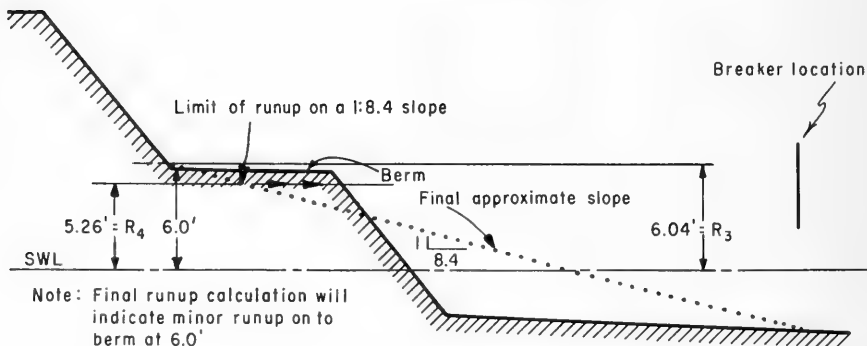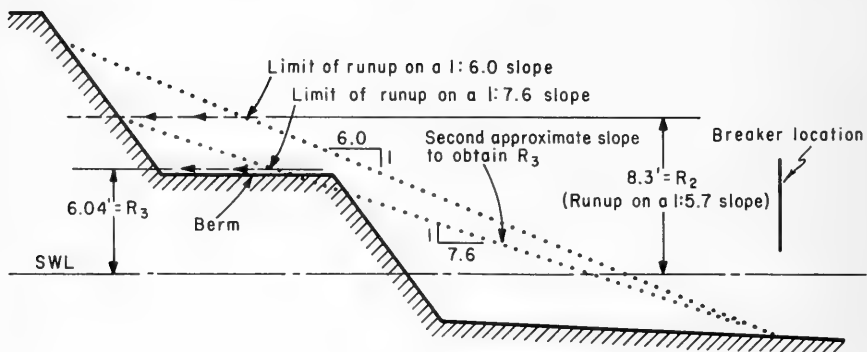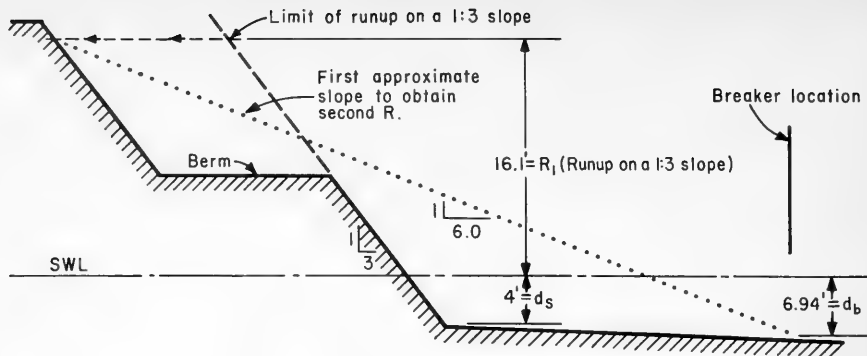
Figure 7-22. Successive Approximations to Runup on a Composite Slope -- Example Problem

factors, as are wind speed and direction with respect to the structure axis. The volume rate of wave overtopping depends on structure height, water depth at the structure toe, structure slope, and whether the slope face is smooth, stepped, or riprapped. Saville and Caldwell (1953) and Saville (1955) investigated overtopping rates and runup heights on small-scale laboratory models of structures. Larger scale model tests have also been conducted for Lake Okeechobee levee sections (Saville, 1958b.) A reanalysis of Saville's data indicates that the overtopping rate per unit length of structure can be expressed by,

$$Q = \left(g \, Q_o^* \, H_o'^3\right)^{1/2} \, e^{-\left[\frac{0.217}{\alpha} \, \tanh^{-1}\left(\frac{h-d_s}{R}\right)\right]},$$

in which   (7-6)

$$0 \leq \frac{h-d_s}{R} < 1.0 ,$$

or equivalently by,

$$Q = \left(g \, Q_o^* \, H_o'^3\right)^{1/2} \, e^{-\left[\frac{0.1085}{\alpha} \, \log_e\left(\frac{R+h-d_s}{R-h+d_s}\right)\right]},$$

in which   (7-7)

$$0 \leq \frac{h-d_s}{R} < 1.0 ,$$

where Q is the overtopping rate (volume/unit time) per unit structure length, g is the gravitational acceleration, H_o' is the equivalent deepwater wave height, h is the height of the structure crest above the bottom, d_s is the depth at the structure toe, R is the runup on the structure that would occur if the structure were high enough to prevent overtopping corrected for scale effects (Section 7.21, WAVE RUNUP), and α and Q_o^* are empirically determined coefficients that depend on incident wave characteristics and structure geometry. Approximate values of α and Q_o^* as functions of wave steepness H_o'/gT^2 and relative height d_s/H_o' for various slopes and structure types are given in Figures 7-23 through 7-31. The numbers beside the indicated points are values of α and Q_o^* (Q_o^* in parentheses on the figures) that, when used with Equation 7-6 or 7-7, predict measured overtopping rates. Equations 7-6 and 7-7 are valid only for $0 \leq (h-d_s) < R$. When $(h-d_s) \geq R$ the overtopping rate is taken as zero.

It is known that onshore winds increase the overtopping rate at a barrier. The increase depends on wind velocity and direction with respect to the axis of the structure and structure slope and height. As a guide, calculated overtopping rates may be multiplied by a wind correction factor given by

$$k' = 1.0 + W_f \left(\frac{h-d_s}{R} + 0.1\right) \sin \theta , \qquad (7-8)$$
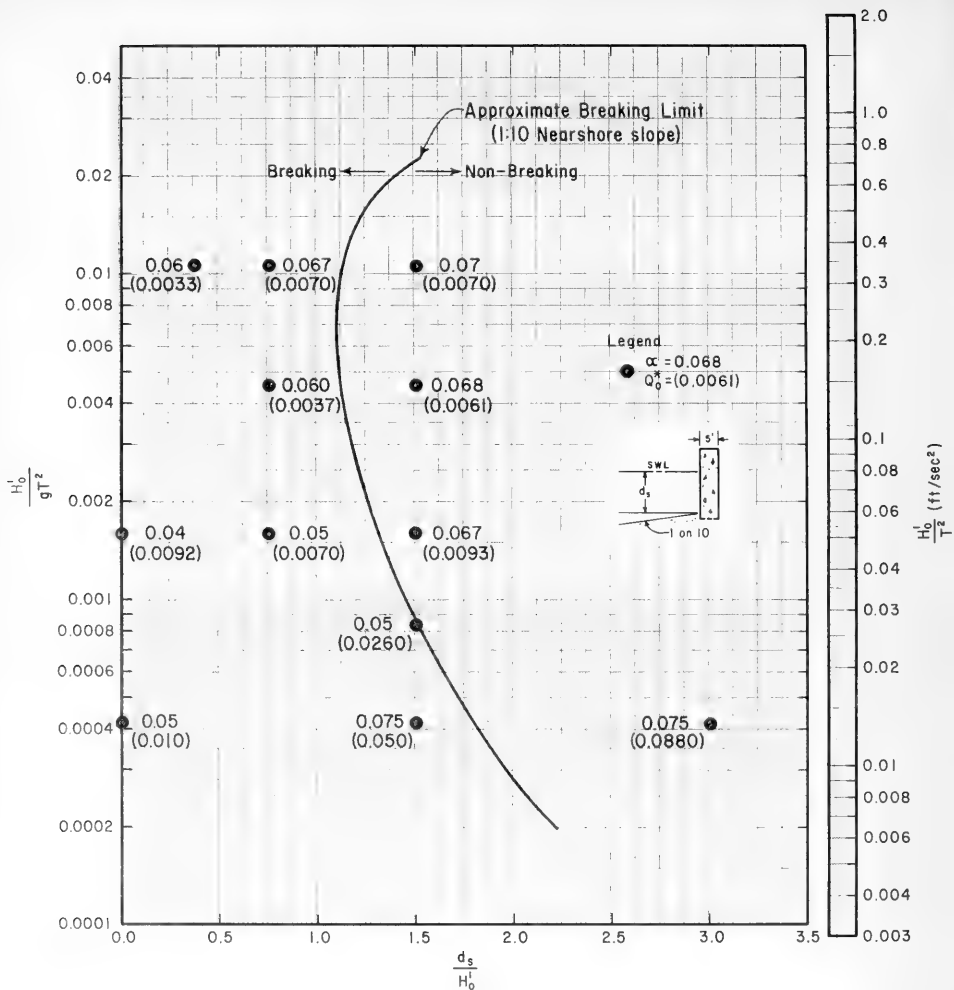
Figure 7-23. Overtopping Parameters, α and Q_0^* (Smooth Vertical Wall on a 1:10 Nearshore Slope)

7-40
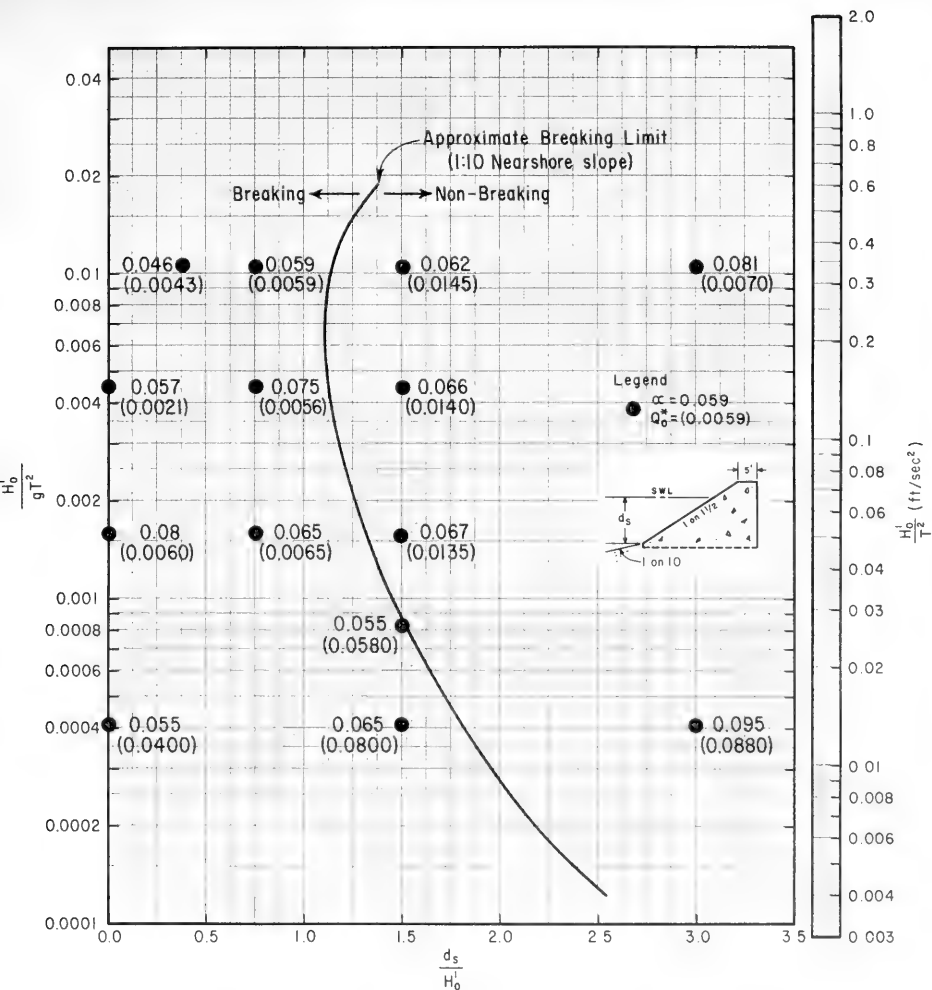
Figure 7-24. Overtopping Parameters, α and Q_0^* (Smooth 1:1-1/2
Structure Slope on a 1:10 Nearshore Slope)
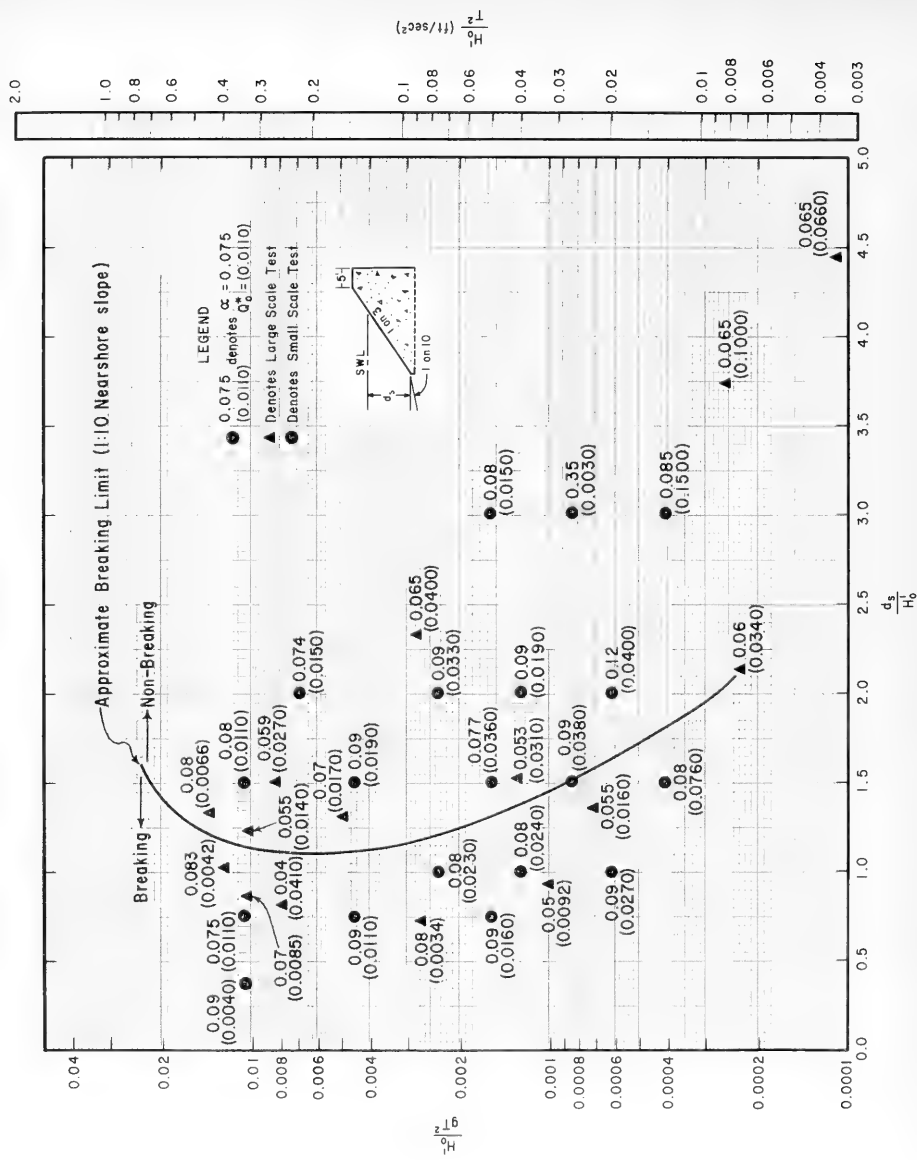
Figure 7-25. Overtopping Parameters, α and Q_0^* (Smooth 1:3 Structure Slope on a 1:10 Nearshore Slope)

7-42
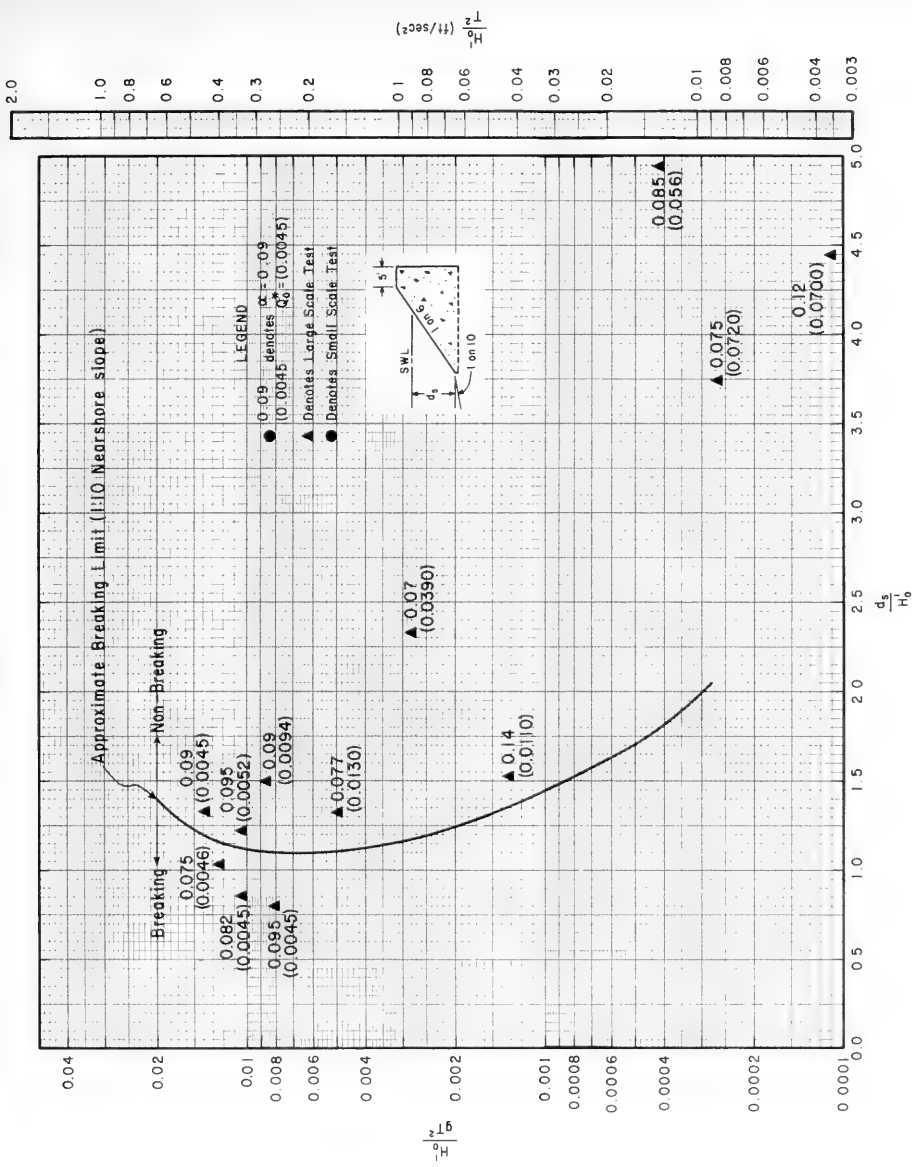
Figure 7-26. Overtopping Parameters, α and Q_0^* (Smooth 1:6 Structure Slope on a 1:10 Nearshore Slope)
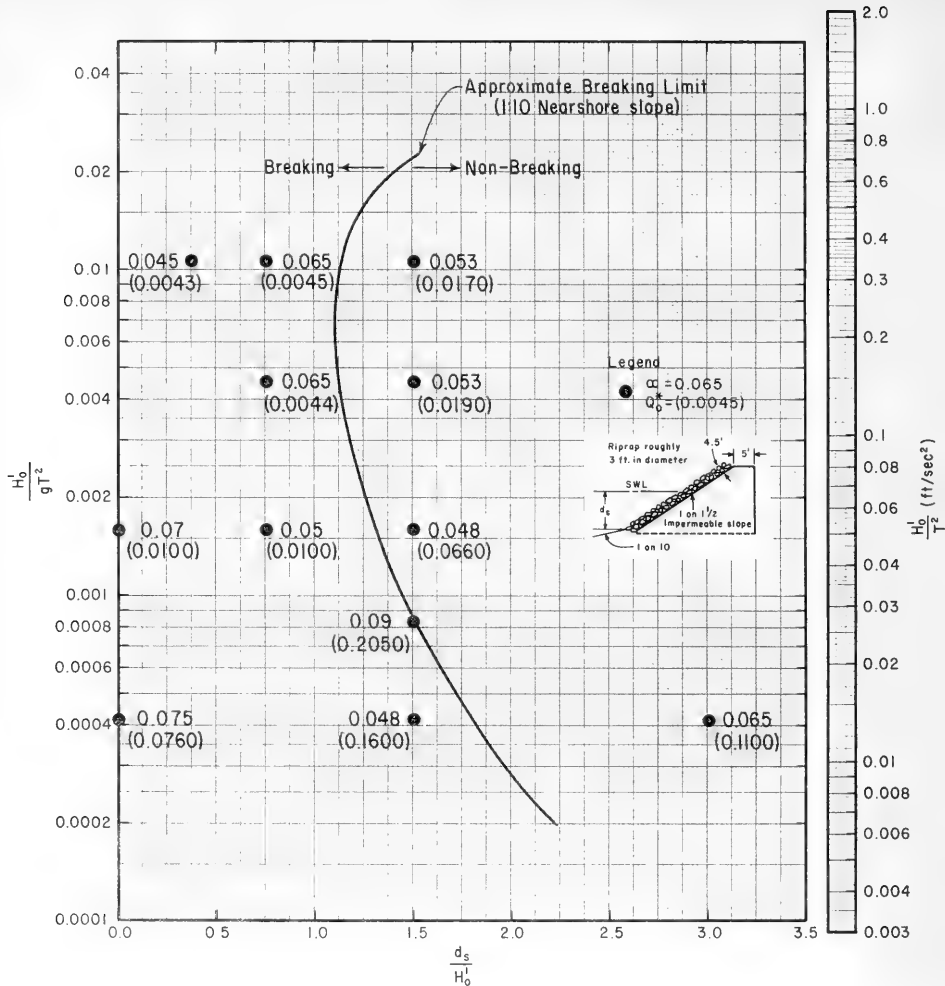
Figure 7-27. Overtopping Parameters, α and Q_0^* (Riprapped 1:1-1/2 Structure Slope on a 1:10 Nearshore Slope)
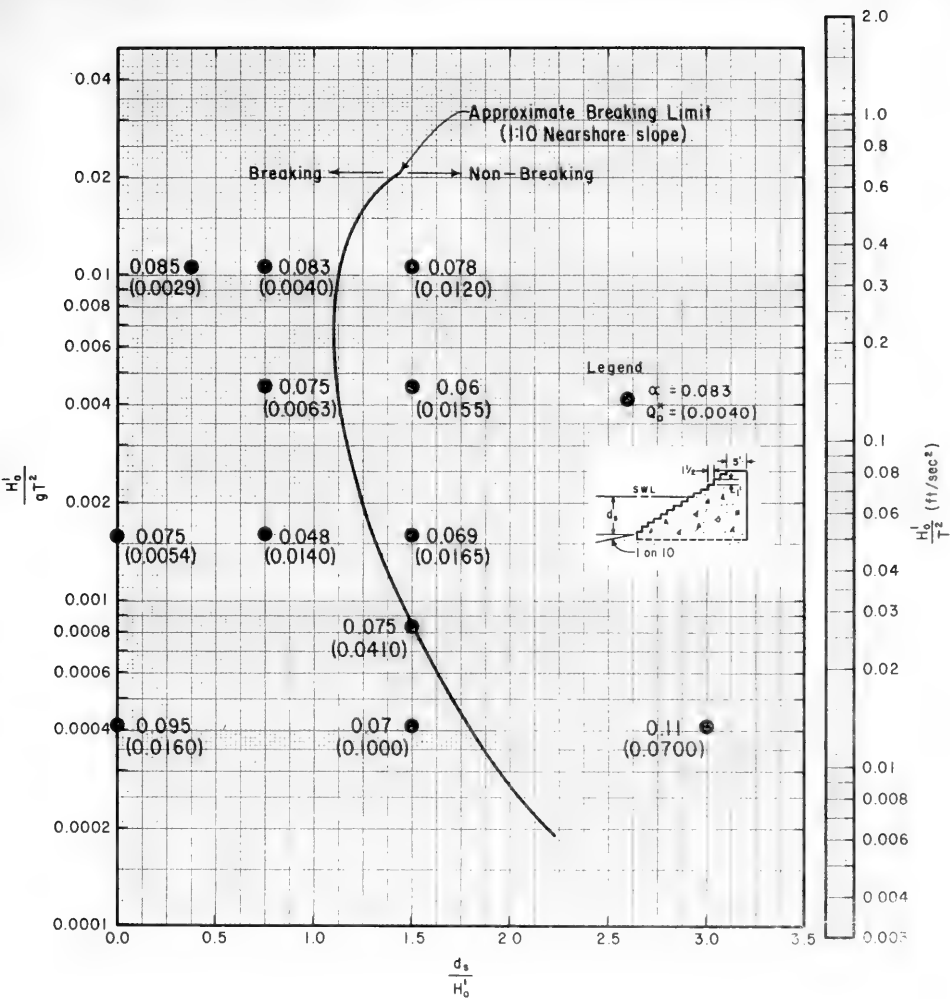
Figure 7-28. Overtopping Parameters, α and Q_0^x (Stepped 1:1-1/2 Structure Slope on a 1:10 Nearshore Slope)
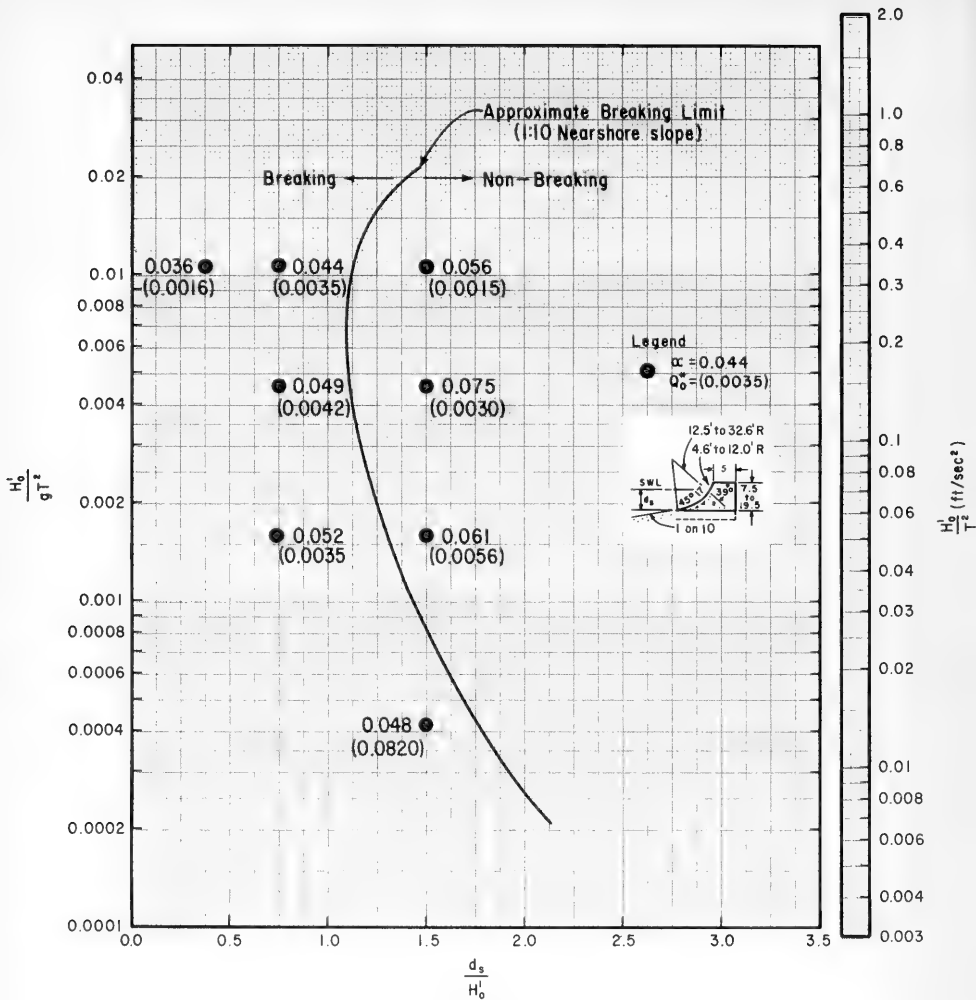
Figure 7-29. Overtopping Parameters, α and Q_0^* (Curved Wall on a 1:10 Nearshore Slope)
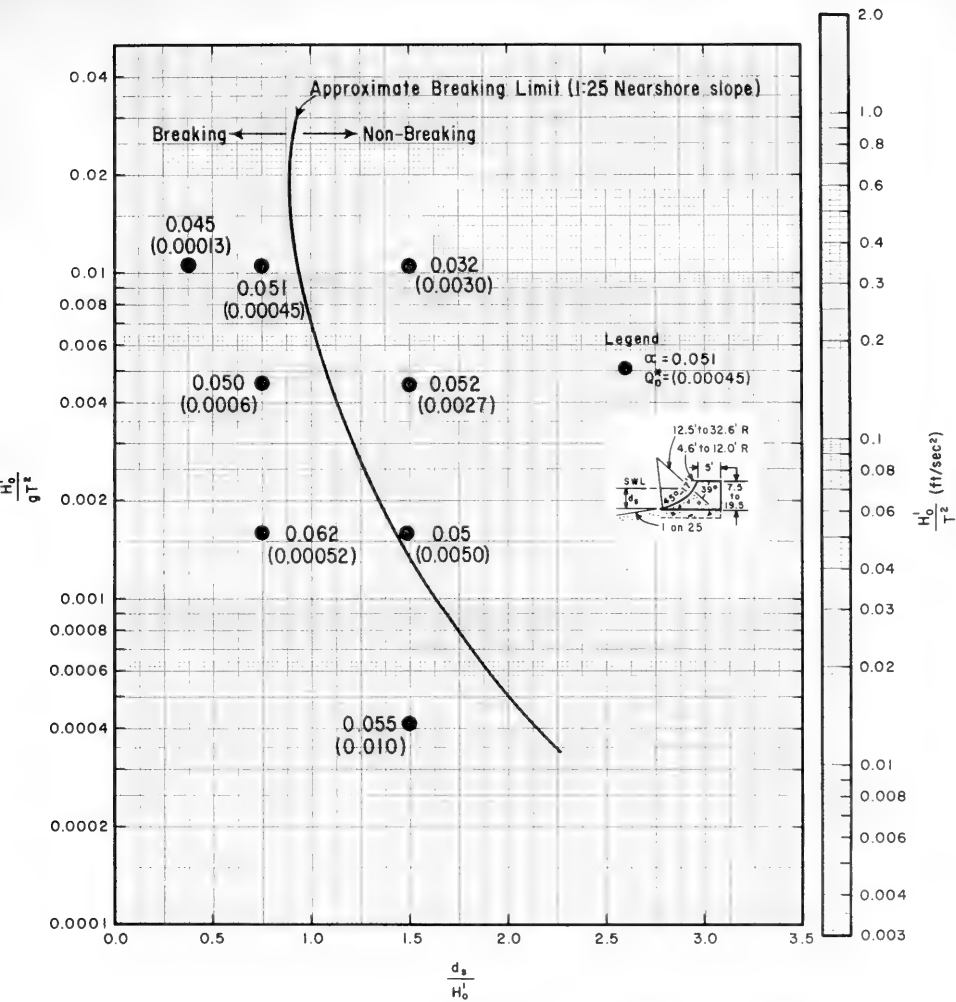
Figure 7-30. Overtopping Parameters, α and Q_0^* (Curved Wall on a 1:25 Nearshore Slope)

7-47
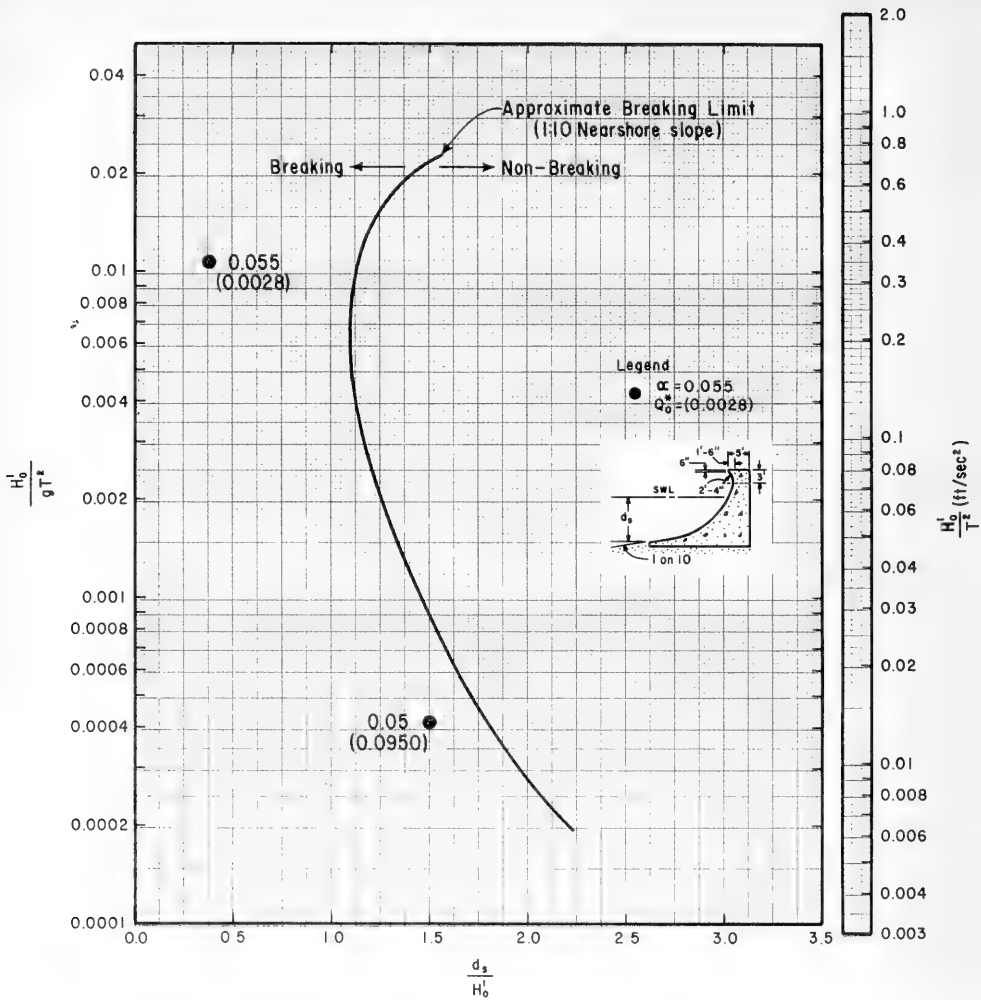
Figure 7-31. Overtopping Parameters, α and Q_0^* (Recurved Wall on a 1:10 Nearshore Slope)

7-48

where W_f is a coefficient depending on wind speed, and θ is the structure slope ($\theta = 90°$ for Galveston walls). For onshore wind speeds of 60 mph or greater $W_f = 2.0$ should be used. For a wind speed of 30 mph, $W_f = 0.5$; when no onshore winds exist, $W_f = 0$. Interpolation between values of W_f given for 60, 30, and 0 mph will give values of W_f for intermediate wind speeds. Equation 7-8 is unverified, but is believed to give a reasonable estimate of the effects of onshore winds of significant magnitude. For a wind speed of 30 mph, the correction factor k' varies between 1.0 and 1.55 depending on the values of $(h-d_s)/R$ and $\sin \theta$.

Values of α and Q_o^* larger than those in Figures 7-23 through 7-31 should be used if a more conservative (higher) estimate of overtopping rates is required.

Calculation of wave overtopping rates is illustrated by the following example.

* * * * * * * * * * * * * * EXAMPLE PROBLEM * * * * * * * * * * * * * * * *

GIVEN: An impermeable structure with a smooth slope of 1 on 2.5 is subjected to waves having a deepwater height $H_o' = 5$ ft. and a period $T = 8$ sec. The depth at the structure toe is $d_s = 10$ ft; crest elevation is 5 ft. above SWL. Onshore winds of 35 mph are assumed.

FIND: Estimate the overtopping rate for the given wave.

SOLUTION: Determine the runup for the given wave and structure. Calculate,

$$\frac{d_s}{H_o'} = \frac{10}{5} = 2.0 \ ,$$

$$\frac{H_o'}{gT^2} = \frac{5}{32.2\,(8)^2} = 0.0024.$$

From Figure 7-11, since

$$\frac{d_s}{H_o'} \text{ is } 2.0 \ ,$$

$$\frac{R}{H_o'} = 2.9 \text{ (uncorrected for scale effect)} \ .$$

Since $H'_o = 5$ ft., from Figure 7-13 the runup correction factor k' is approximately 1.17. Therefore,

$$\frac{R}{H'_o} = 1.17 \, (2.9) = 3.4 \; ,$$

and

$$R = 3.4 \; H'_o = (3.4) \, (5) = 17.0 \text{ ft.}$$

The values of α and Q_o^* for use in Equation 7-6 can be found by interpolation between Figures 7-24 and 7-25. From Figure 7-25 for a 1 on 3 slope for small-scale data,

$$\left.\begin{array}{l} \alpha = 0.09 \\[18pt] Q_o^* = 0.033 \end{array}\right\} \text{at} \; \frac{d_s}{H'_o} = 2.0 \; \text{and} \; \frac{H'_o}{gT^2} = 0.0024 \; .$$

Also from Figure 7-25 for larger scale data,

$$\left.\begin{array}{l} \alpha = 0.065 \\[18pt] Q_o^* = 0.040 \end{array}\right\} \text{at} \; \frac{d_s}{H'_o} = 2.33 \; \text{and} \; \frac{H'_o}{gT^2} = 0.0028 \; .$$

Note that these values were selected for a point close to the actual values for the problem, since no large-scale data are available exactly at

$$\frac{d_s}{H'_o} = 2.0 \, ,$$

and

$$\frac{H'_o}{gT^2} = 0.0024 \; .$$

From Figure 7-24 for small-scale data on a 1 on 1.5 slope,

$$\left.\begin{array}{l} \alpha = 0.067 \\[18pt] Q_o^* = 0.0135 \end{array}\right\} \text{at} \; \frac{d_s}{H'_o} = 1.5 \; \text{and} \; \frac{H'_o}{gT^2} = 0.0016 \; .$$

Large-scale data are not available for a 1 on 1.5 slope. Since larger values of α and Q_o^* give larger estimates of overtopping, interpolation by eye between the data for a 1 on 3 slope and a 1 on 1.5 slope gives approximately,

$$\alpha = 0.08 \, ,$$

$$Q_o^* = 0.035 \, .$$

From Equation 7-6,

$$Q = \left(g\, Q_o^* H_o'^3\right)^{\frac{1}{2}} e^{-\left[\frac{0.217}{\alpha} \tanh^{-1}\left(\frac{h-d_s}{R}\right)\right]},$$

$$Q = \left[(32.2)\,(0.035)\,(5)^3\right]^{\frac{1}{2}} e^{-\left[\frac{0.217}{0.08} \tanh^{-1}\left(\frac{h-d_s}{R}\right)\right]}$$

The value of

$$\frac{h-d_s}{R} \text{ is } \frac{15-10}{17.0} = 0.294 .$$

To evaluate $\tanh^{-1}\left[(h-d_s)/R\right]$ find 0.294 in column 4 of either Table C-1 or C-2, Appendix C, and read the value of $\tanh^{-1}\left[(h-d_s)/R\right]$ from column 3. Therefore,

$$\tanh^{-1}\,(0.294) \approx 0.31 .$$

Calculating the exponent,

$$\frac{0.217\,(0.31)}{0.08} = 0.84 ;$$

therefore,

$$Q = 11.9\, e^{-0.84} = 11.9\,(0.431) = 5.1 \ \text{ft}^3/(\text{sec-ft}).$$

For an onshore wind velocity of 35 mph, the value of W_f is found by interpolation.

$$30 \text{ mph; } W_f = 0.5 ,$$

$$35 \text{ mph; } W_f = 0.75,$$

$$60 \text{ mph; } W_f = 2.0.$$

From Equation 7-8,

$$k' = 1 + W_f \left(\frac{h-d_s}{R} + 0.1\right) \sin\theta ,$$

where

$$W_f = 0.75,$$

$$\frac{h-d_s}{R} = 0.3 ,$$

$$\theta = \tan^{-1}\left(\frac{1}{2.5}\right) \approx 22° ,$$

and

$$\sin 22° = 0.37 .$$

Therefore,

$$k' = 1 + 0.75 \ (0.3 + 0.1) \ 0.37 = 1.11 \ ,$$

and the corrected overtopping rate is,

$$Q_c = k'Q \ ,$$

$$Q_c = 1.11 \ (5.1) = 5.7 \ \text{ft}^3/(\text{sec-ft}).$$

The total volume of water overtopping the structure is obtained by multiplying Q_c by the length of the structure and by the duration of the given wave conditions.

* *

7.23 WAVE TRANSMISSION

When incident waves hit a breakwater, wave energy will be either reflected from, dissipated on, or transmitted through the structure. The way incident wave energy is partitioned between reflection, dissipation and transmission depends on incident wave characteristics (period, height and water depth), breakwater type (rubble or smooth faced, permeable or impermeable), and the geometry of the structure (slope, crest elevation relative to SWL, and crest width). Ideally, harbor breakwaters should reflect or dissipate all wave energy approaching from the sea, and dissipate any wave energy approaching from the harbor. (See Section 2.5, WAVE REFLECTION.) Transmission of wave energy over or through a breakwater should be eliminated to prevent damaging waves and resonance within a harbor. When a permeable or low-crested breakwater must be considered, an estimate of the transmitted wave height is necessary.

For impermeable structures, crest elevation and crest width are important in determining transmitted wave heights. Jeffreys (1944) and Fuchs (1951) studied the transmission of waves over impermeable, submerged breakwaters (crest elevation below the SWL) using linear, small-amplitude wave theory. Because of the small-amplitude assumption, their equations predict no wave transmission when the structure crest elevation is at the SWL. For finite-amplitude waves, energy is transmitted over breakwaters by overtopping even if the crest is above the SWL but below the limit of maximum runup. (See Section 7.21, WAVE RUNUP.)

Jeffreys (1944) theoretically analyzed transmission of waves over an offshore bar which is similar to transmission of wave energy over a

wide, submerged, impermeable breakwater. His equation for the transmission coefficient, ratio of transmitted wave height to incident wave height H_t/H_i, is given by

$$\frac{H_t}{H_i} = \frac{1}{\sqrt{1 + \left[\left(\frac{0.25\ d_s}{d_s - h}\right)^{\frac{1}{2}} - \left(\frac{0.25\ d_s - 0.25\ h}{d_s}\right)^{\frac{1}{2}}\right]^2 \sin^2\left[\frac{2\pi b}{\sqrt{gT}}\left(\frac{1}{d_s - h}\right)^{\frac{1}{2}}\right]}} \quad (7\text{-}9)$$

where d_s is the depth below the SWL at the structure toe, h is the height of the structure above bottom, b is crest width, g is acceleration of gravity, and T is wave period. The development of Equation 7-9 does not consider energy dissipation, and therefore does not consider waves breaking on the structure or energy loss by friction. In addition, the equation is valid only for shallow-water waves when $d/gT^2 < 0.00155$, and should not be used when $h/d > 0.8$. When crest width is small relative to structure height (say $b/h \leq 0.5$) the value of H_t/H_i given by the equation may be too large.

Fuchs (1951) presented an equation for calculating wave transmission over a rigid, thin vertical barrier by considering power transmission across the barrier. The equation is based on linear wave theory, and cannot be used when transmission is by overtopping. Fuchs' equation is

$$\frac{H_t}{H_i} = \sqrt{1 - \frac{(4\pi h/L) + \sinh(4\pi h/L)}{\sinh\left(4\pi d_s/L\right) + \left(4\pi d_s/L\right)}}, \quad (7\text{-}10)$$

and is assumed valid in water of any depth, provided the wavelength L corresponds to the depth d_s. In shallow water, Equation 7-10 reduces to

$$\frac{H_t}{H_i} = \sqrt{1 - \frac{h}{d_s}}, \quad (7\text{-}11)$$

for

$$\frac{d_s}{gT^2} < 0.00155,$$

and in deep water Equation 7-10 reduces to

$$\frac{H_t}{H_i} = \sqrt{1 - e^{-\left[\frac{4\pi(d_s - h)}{L}\right]}}, \quad (7\text{-}12)$$

for

$$\frac{d_s}{gT^2} > 0.0793.$$

For $0.00155 < d_s/gT^2 < 0.0793$ Equation 7-10 must be used.

When submergence of a crest is small ($h/d_s \geq 0.8$ for shallow water) or when transmission is by overtopping, the results of hydraulic model studies must be used to evaluate transmission coefficients. The range of d_s/gT^2 values included in numerous laboratory investigations are summarized in Figure 7-32. Figures 7-33 through 7-35 show some experimental results obtained by Saville (1963) for an impermeable rubble-mound breakwater. Interpolation between curves permits an estimate of wave heights on the leeward side of similar prototype structures. If experimental results in Figure 7-32 are used to determine wave transmission, transmission coefficients obtained by several investigators should be computed and compared for the appropriate value of d_s/gT^2 whenever possible.

Figures 7-36 and 7-37 show experimental values of the transmission coefficient for the permeable rubble-mound breakwater sections investigated by Saville. Higher transmission coefficients result for permeable structures than for similar impermeable structures, since part of any incident wave energy is transmitted through a permeable structure in addition to the energy transmitted over it. Because of the difficulty of modeling permeability in laboratory studies, transmission coefficients obtained by interpolation between the curves of Figures 7-36 and 7-37 should be considered as *estimates* of the true transmission coefficient. The data shown in Figures 7-36 and 7-37 can be supplemented by the experimental results of Jackson (1966), Hudson and Jackson (1966), Dai and Jackson (1966), and Davidson (1969) for wave transmission through typical rubble breakwater sections.

The use of Equations 7-9 and 7-10 and Figures 7-33 through 7-37 to obtain transmitted wave heights is illustrated by the following example problems.

* * * * * * * * * * * * * * EXAMPLE PROBLEM * * * * * * * * * * * * * * *

GIVEN: A design wave with H = 6 ft, T = 8 sec and a submerged impermeable breakwater with a crest width of b = 30 ft. Depth in front of the structure is d_s = 15 ft, the height of the crest above bottom is 10 ft, and seaward and landward slopes are 1 on 2.

FIND: Wave height on the leeward side of the breakwater assuming no energy dissipation at the structure.

SOLUTION: Calculate:

$$\frac{d_s}{gT^2} = \frac{15}{(32.2)(8)^2} = 0.0073 ,$$

which is greater than $d_s/gT^2 = 0.00155$, hence the wave is not a shallow-water wave and Equation 7-9 cannot be used. Assuming that

7-54
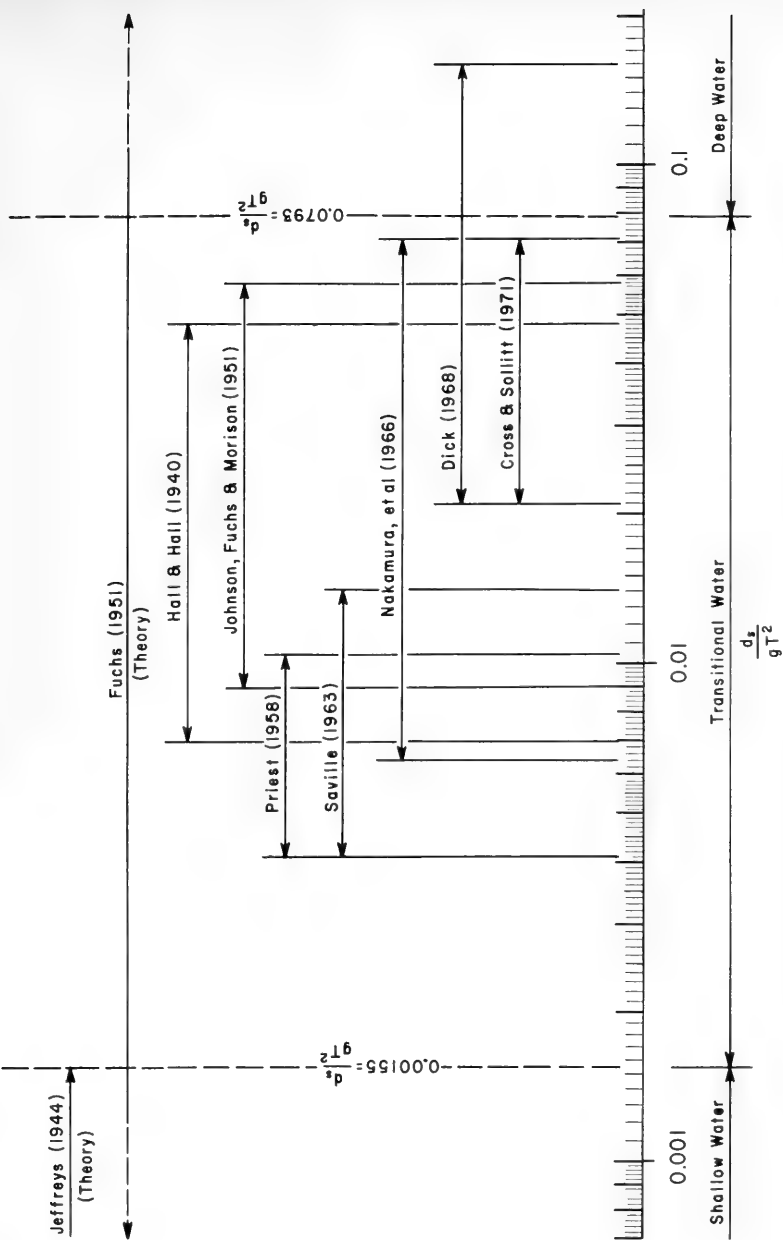
Figure 7-32. Wave Transmission over Submerged and Overtopped Structures, Range of d_S/gT^2 Studied by Various Investigators

7-55
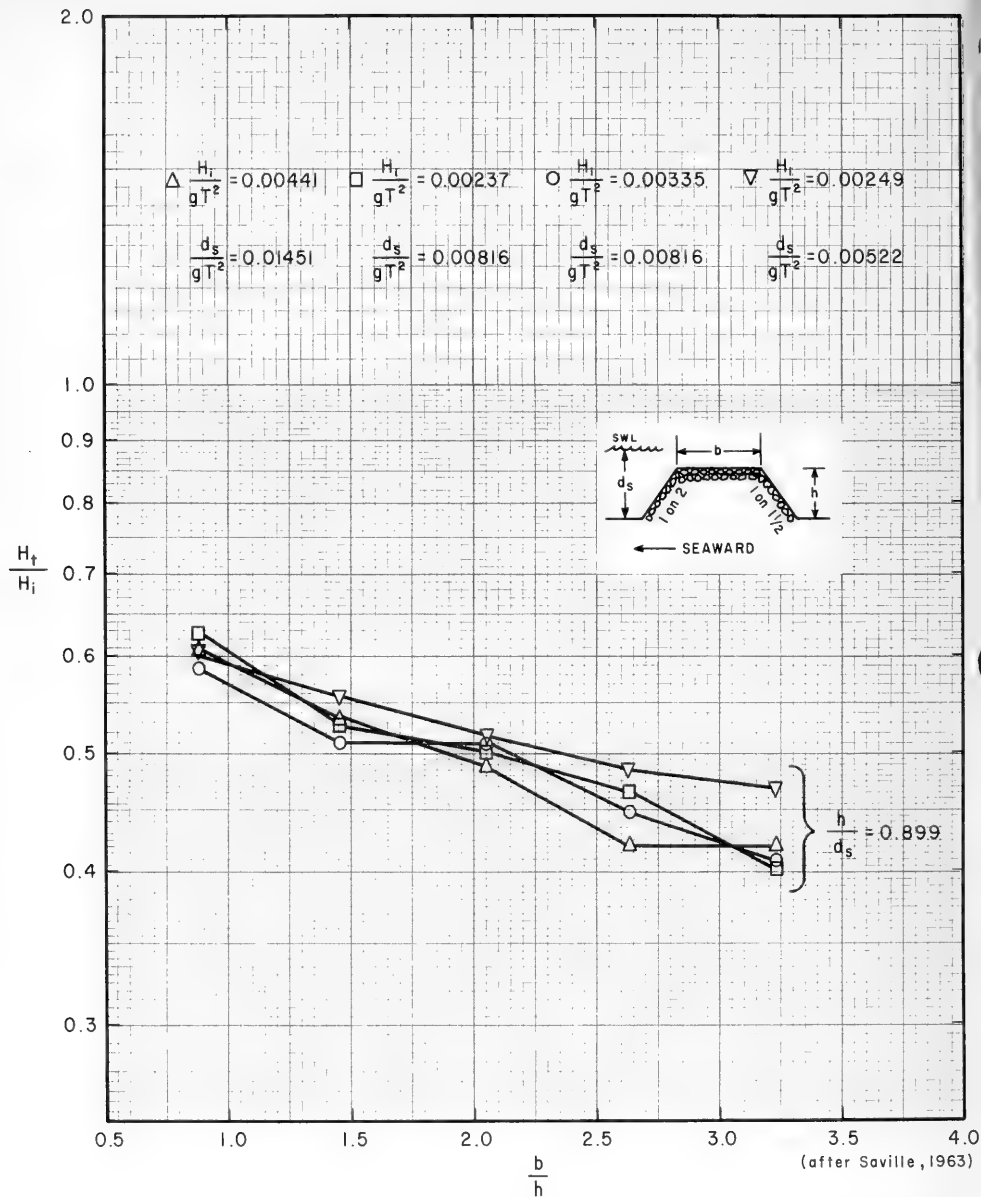
Figure 7-33. Wave Transmission, Impermeable Rubble-mound Breakwater
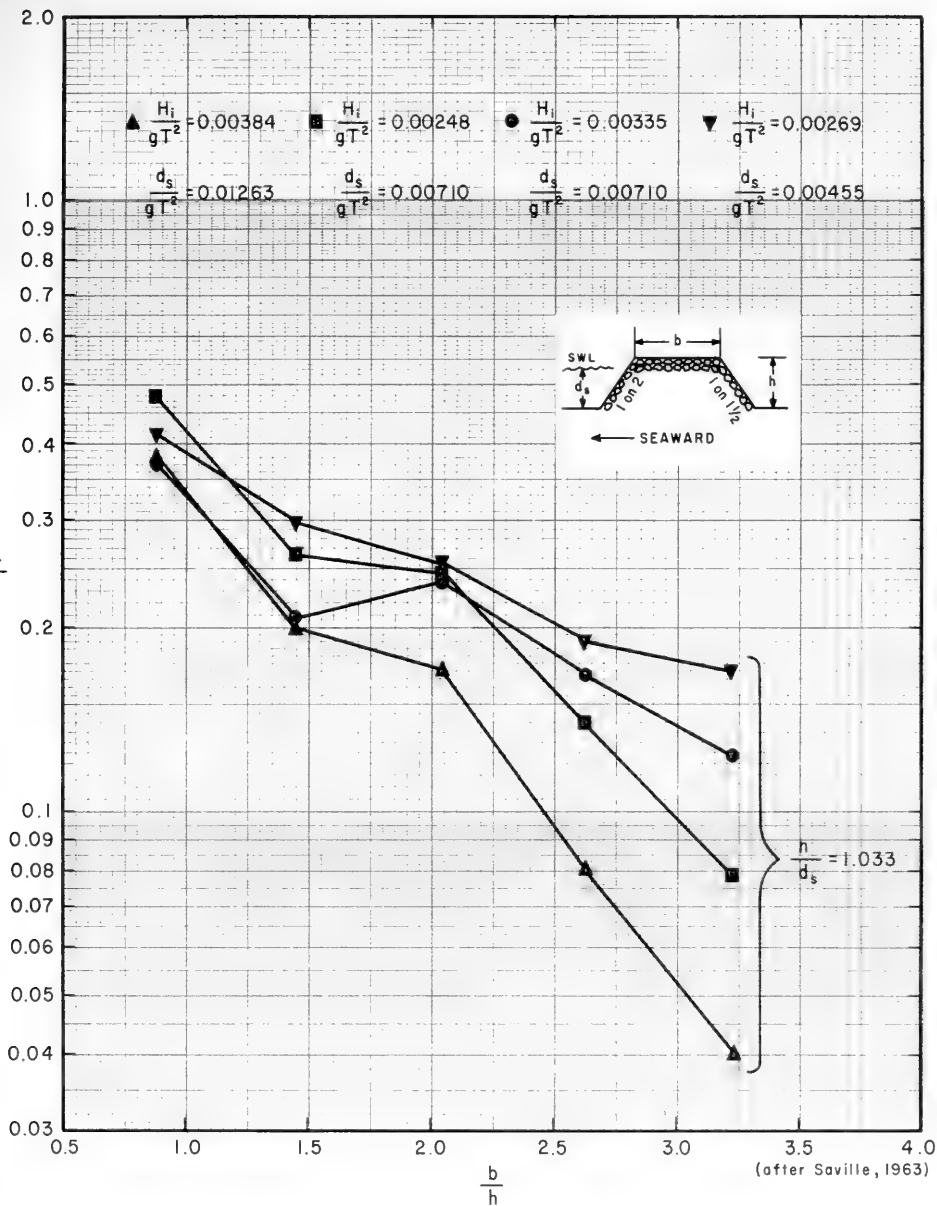
Figure 7-34. Wave Transmission, Impermeable Rubble-mound Breakwater

7-57
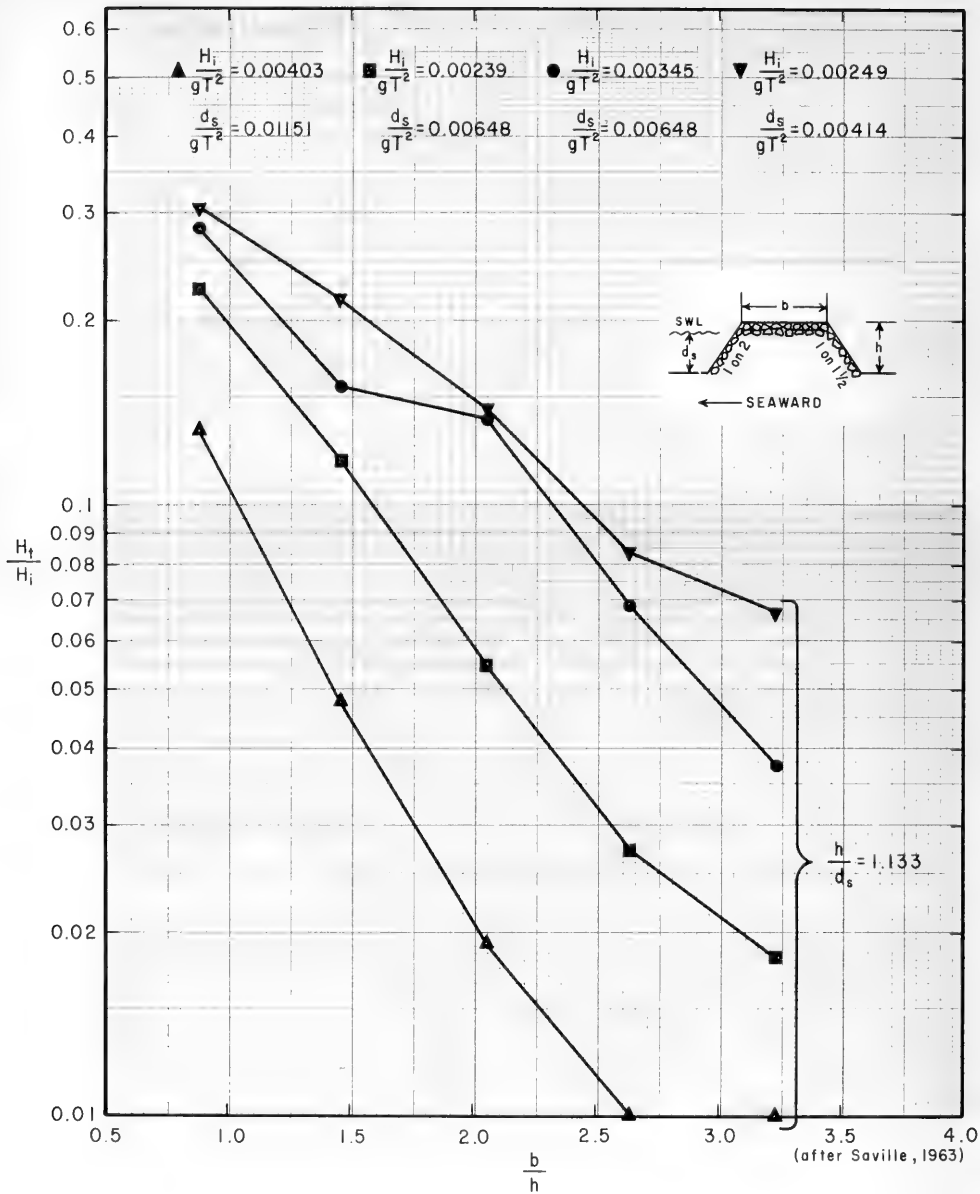
Figure 7-35. Wave Transmission, Impermeable Rubble-mound Breakwater
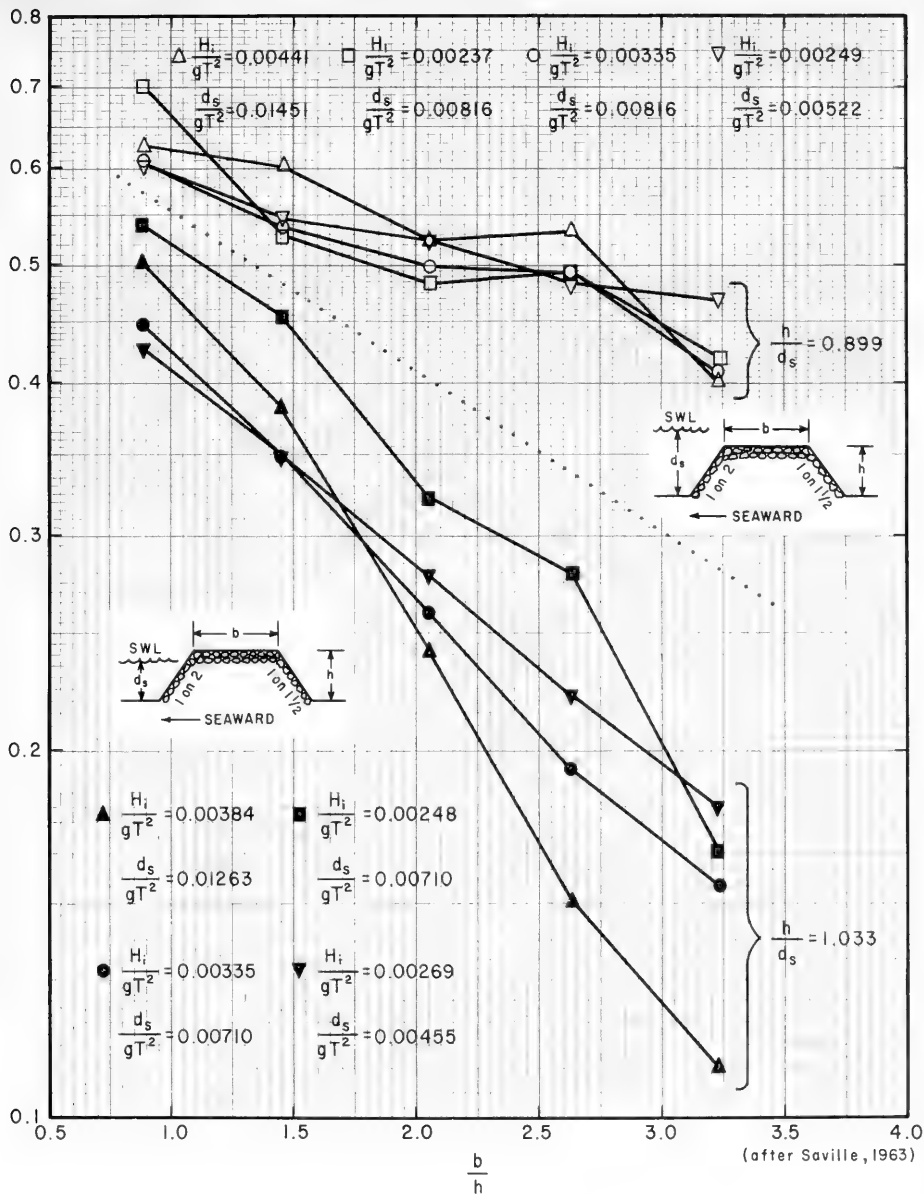
Figure 7-36. Wave Transmission, Permeable Rubble-mound Breakwater
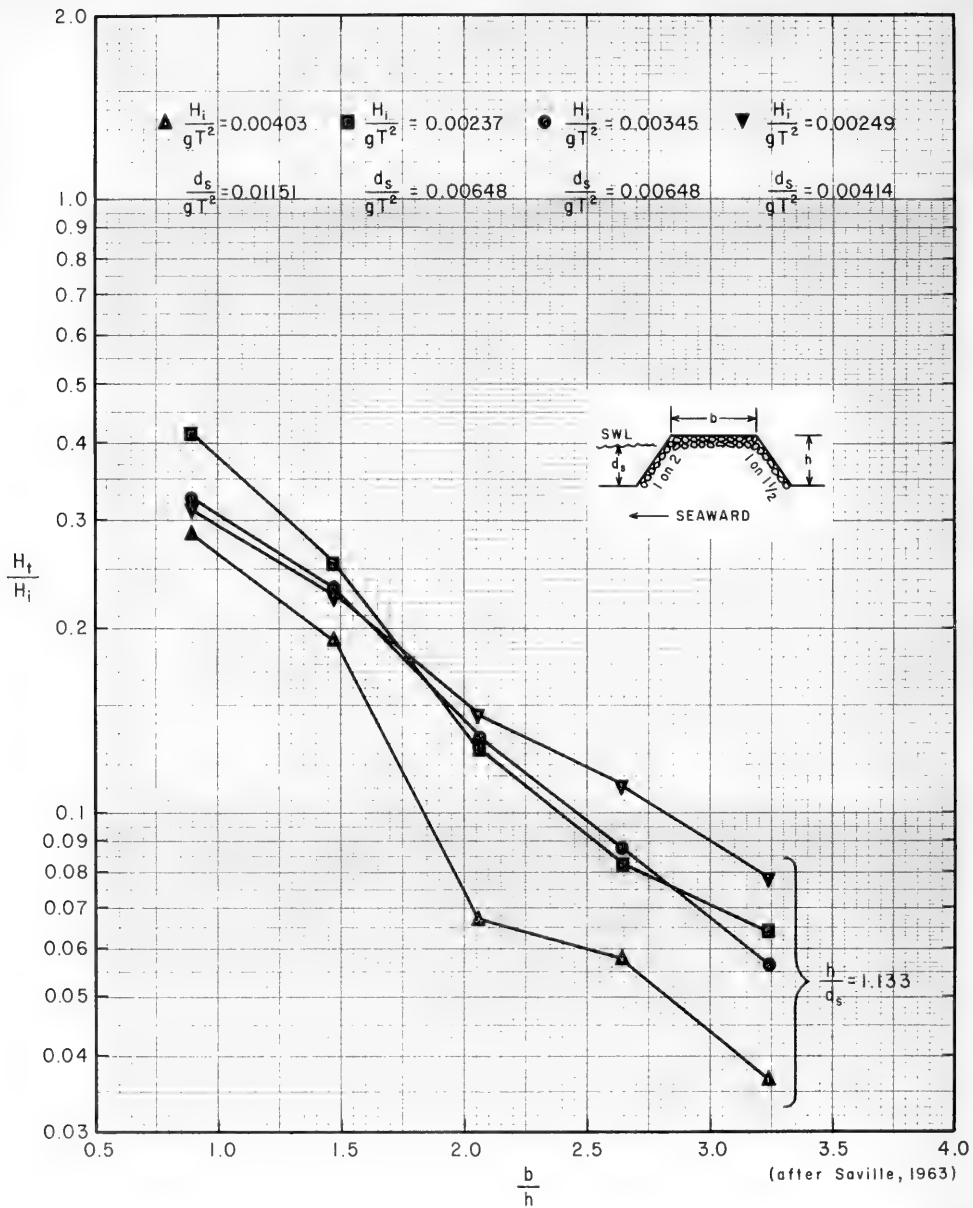
Figure 7-37. Wave Transmission, Permeable Rubble-mound Breakwater

the structure is a rigid, thin barrier, calculate L in a depth d_s = 15 ft. using Equation 7-10.

$$L_o = \frac{gT^2}{2\pi} = 5.12\,(8)^2 = 328 \text{ ft.,}$$

and

$$\frac{d_s}{L_o} = \frac{15}{328} = 0.0458 .$$

From Table C-1, Appendix C, setting d_s = d,

$$\frac{d}{L} = 0.0896, \quad \frac{4\pi d}{L} = 1.127, \quad \sinh\left(\frac{4\pi d}{L}\right) = 1.378,$$

and calculate,

$$\frac{4\pi h}{L} = \frac{h}{d}\left(\frac{4\pi d}{L}\right) = \frac{10}{15}\,(1.127) = 0.751 .$$

Find 0.751 in Column 9 of Table C-1, Appendix C and read sinh $(4\pi d/L)$ from Column 10. Hence,

$$\sinh\left(\frac{4\pi h}{L}\right) = 0.825 .$$

From Equation 7-10,

$$\frac{H_t}{H_i} = \sqrt{1 - \frac{\left(4\pi h/L\right) + \sinh\left(4\pi h/L\right)}{\sinh\left(4\pi d_s/L\right) + \left(4\pi d_s/L\right)}} ,$$

$$\frac{H_t}{H_i} = \sqrt{1 - \frac{(0.751) + (0.825)}{(1.378) + (1.127)}} ,$$

$$\frac{H_t}{H_i} = \sqrt{1 - \frac{1.576}{2.505}} = \sqrt{0.370} = 0.609 .$$

The transmitted wave height is

$$H_t = 0.609\ H_i ,$$

$$H_t = 0.609\,(6) = 3.67 \text{ ft.,}$$

say

$$H_t = 3.5 \text{ ft.}$$

The calculated value can be assumed to exceed the true value, since the finite structure crest width will decrease the transmitted wave height and some energy dissipation will occur.

* *

GIVEN: A design wave with $H = 6$ ft and $T = 8$ sec is incident on a rubble structure with a cross section as shown in Figure 7-34, situated in a depth $d_s = 10$ ft. The crest of the structure is $b = 10$ ft wide and is 1 ft above the SWL.

FIND:

(a) The height of the wave transmitted over the structure by over-topping if the structure is permeable.

(b) The reduction in transmitted wave height if an impermeable core is included in the structure.

SOLUTION: Calculate: $h = d_s$ + crest height above SWL $= 10 + 1 = 11$ feet, then,

$$\frac{b}{h} = \frac{10}{11} = 0.909 \ ,$$

$$\frac{h}{d_s} = \frac{11}{10} = 1.1 \ ,$$

$$\frac{H_i}{gT^2} = \frac{6}{(32.2)(8)^2} = 0.0029 \ ,$$

$$\frac{d_s}{gT^2} = \frac{10}{(32.2)(8)^2} = 0.0048 \ .$$

For a permeable structure, find the corresponding H_t/H_i values for $b/h = 0.909$ by interpolating between $h/d_s = 1.033$ in Figure 7-36 and $h/d_s = 1.133$ in Figure 7-37, and using the curve for $H_i/gT^2 = 0.00269$ and $d_s/gT^2 = 0.00455$ in Figure 7-36 and the curve for $H_i/gT^2 = 0.00249$ and $d_s/gT^2 = 0.00414$ in Figure 7-37. For $h/d_s = 1.033$ from Figure 7-36, $H_t/H_i = 0.44$ and for $h/d_s = 1.133$ from Figure 7-37, $H_t/H_i = 0.31$; therefore,

$$\frac{H_t}{H_i} \approx 0.35 \ .$$

Hence,

$$H_t = (0.35) H_i = 0.35 (6) = 2.1 \ \text{ft.}$$

By a similar analysis for an impermeable breakwater, using Figures 7-34 and 7-35,

$$\frac{H_t}{H_i} \approx 0.33,$$

and

$$H_t = (0.33)\, H_i = 0.33\,(6) = 1.98 \text{ ft. , say 2 ft.}$$

The presence of an impermeable core in this instance does not provide a significant decrease in transmitted wave height. Most of the wave energy is transmitted by overtopping for the example conditions.

* *

7.3 WAVE FORCES

The study of wave forces on coastal structures can be classified in two ways; (a) by the type of structure on which the forces act and (b) by the type of wave action against the structure. Fixed coastal structures can generally be classified as one of three types: (a) pile supported structures such as piers and offshore platforms, (b) wall type structures such as seawalls, bulkheads, revetments and some breakwaters, and (c) rubble structures such as many groins, revetments, jetties and breakwaters. Individual structures are often combinations of these three types. The types of waves that can act on these structures are nonbreaking, breaking or broken waves. Figure 7-38 illustrates the subdivision of wave force problems by structure type and by type of wave action, and indicates nine types of force determination problems encountered in design.
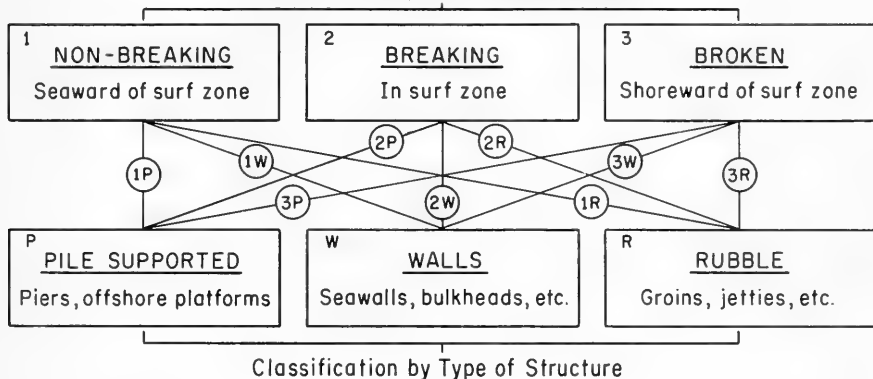
Figure 7-38. Classification of Wave Force Problems by Type of Wave Action and by Structure Type

7-63

Rubble structure design does not require differentiation between all three types of wave action; problem types shown as 1R, 2R, and 3R on the figure need consider only nonbreaking and breaking wave design. Horizontal forces on pile-supported structures resulting from broken waves in the surf zone are usually negligible, and are not considered. Determination of breaking and nonbreaking wave forces on piles is presented in Section 7.31, FORCES ON PILES. Nonbreaking, breaking and broken wave forces on vertical (or nearly vertical) walls are considered in Sections 7.32, NONBREAKING WAVE FORCES ON WALLS, 7.33, BREAKING WAVE FORCES ON VERTICAL WALLS, and 7.34, BROKEN WAVES. Design of rubble structures is considered in Section 7.37, STABILITY OF RUBBLE STRUCTURES.

7.31 FORCES ON PILES

7.311 Introduction. Frequent use of pile-supported coastal and offshore structures makes the interaction of waves and piles of significant practical importance. The basic problem is to predict forces on a pile due to the wave-associated flow field. Because wave-induced flows are complex, even in the absence of structures, solution of the complex problem of wave forces on piles relies on empirical coefficients to augment theoretical formulations of the problem.

Variables important in determining forces on circular piles subjected to wave action are shown in Figure 7-39. Variables describing nonbreaking, monochromatic waves are the wave height H, water depth d, and either wave period T, or wavelength L. Water particle velocities and accelerations in wave-induced flows directly cause the forces. For vertical piles, the horizontal fluid velocity u and acceleration du/dt and their variation with distance below the free surface are important. The pile diameter D and a dimension describing pile roughness elements ε are important variables describing the pile. In this discussion, the effect of the pile on the wave-induced flow is assumed negligible. Intuitively, this assumption implies that the pile diameter D must be small with respect to the wavelength L. Significant fluid properties include the fluid density ρ and the kinematic viscosity ν. In dimensionless terms, the important variables can be expressed by:

$$\frac{H}{gT^2} = \text{dimensionless wave steepness,}$$

$$\frac{d}{gT^2} = \text{dimensionless water depth,}$$

$$\frac{D}{L} = \text{ratio of pile diameter to wavelength (assumed small),}$$

$$\frac{\epsilon}{D} = \text{relative pile roughness,}$$

and

$$\frac{HD}{T\nu} = \text{a form of the Reynolds' number.}$$

Given the orientation of a pile in the flow field, the total wave force acting on the pile can be expressed as a function of these variables. The variation of force with distance along the pile depends on the mechanism by which the forces arise, that is, how the water particle velocities and accelerations cause the forces. The following analysis relates the local force, acting on a section of pile element of length dz to the local fluid velocity and acceleration that would exist at the center of the pile, if the pile were not present. Two dimensionless force coefficients, an inertia or mass coefficient C_M and a drag coefficient C_D, are used to establish the wave-force relationships. These coefficients are determined by experimental measurements of force, velocity, and acceleration or by measurements of force and water surface profiles with accelerations and velocities inferred by assuming an appropriate wave theory.

The following discussion initially assumes that the force coefficients C_M and C_D are known, and illustrates the calculation of forces on vertical cylindrical piles subjected to monochromatic waves. A discussion of the selection of C_M and C_D follows in Section 7.315, Selection of Hydrodynamic Force Coefficients, C_D and C_M. Experimental data are available primarily for the interaction of nonbreaking waves and vertical cylindrical piles. Only general guidelines are given for the calculation of forces on noncircular piles.
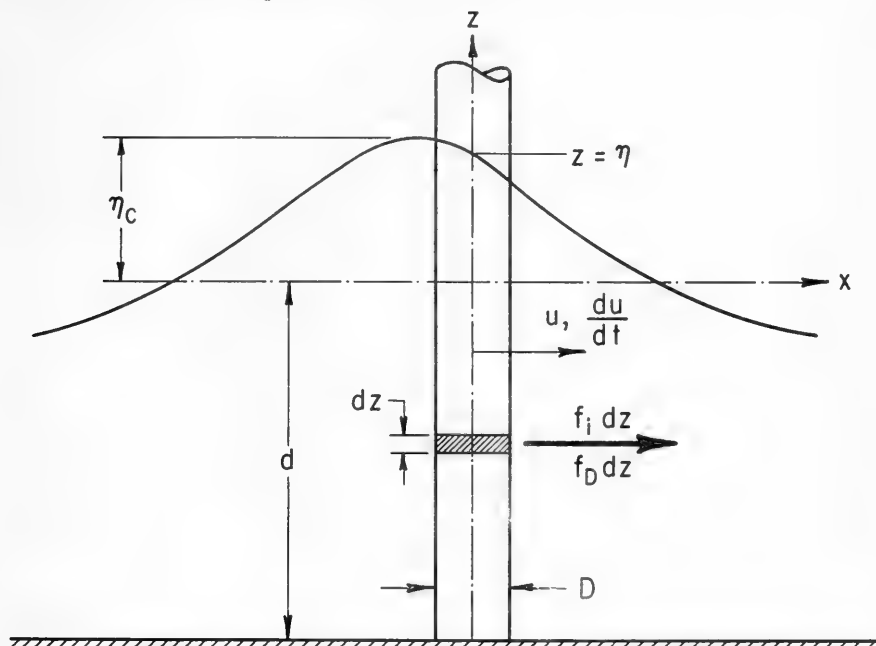
Figure 7-39. Definition Sketch of Wave Forces on a Vertical Cylinder

7-65

7.312 Vertical Cylindrical Piles and Nonbreaking Waves - (Basic Concepts).
By analogy to the mechanism by which fluid forces on bodies occur in uni-
directional flows, Morison et al. (1950) suggested that the horizontal
force per unit length of a vertical cylindrical pile may be expressed as,
(See Figure 7-39 for definitions.)

$$f = f_i + f_D = C_M \, \rho \, \frac{\pi D^2}{4} \frac{du}{dt} + C_D \, \frac{1}{2} \, \rho \, D \, u|u|, \tag{7-13}$$

where,

f_i = inertial force per unit length of pile,

f_D = drag force per unit length of pile,

ρ = density of fluid (2 slugs/ft^3 for sea water),

D = diameter of pile,

u = horizontal water particle velocity at the axis of the pile, (calculated as if the pile were not there)

$\dfrac{du}{dt}$ = total horizontal water particle acceleration at the axis of the pile, (calculated as if the pile were not there)

C_D = hydrodynamic force coefficient, the "Drag" coefficient,

and

C_M = hydrodynamic force coefficient, the "Inertia" or "Mass" coefficient.

The term f_i is of the form obtained from an analysis of force on a body in an accelerated flow of an ideal nonviscous fluid. The term f_D is the drag force exerted on a cylinder in a steady flow of a real viscous fluid (f_D is proportional to u^2 and acts in the direction of the velocity u; for flows that change direction this is expressed by writing u^2 as $u|u|$). Although these remarks support the soundness of the formulation of the problem as that given by Equation 7-13, it should be realized that *expressing total force by the terms* f_i *and* f_D *is an assumption* justi-
fied only if it leads to sufficiently accurate predictions of wave force.

From the definitions of u and du/dt, given in Equation 7-13 as the values of these quantities at the axis of the pile, it is seen that the influence of the pile on the flow field a short distance away from the pile has been neglected. Based on linear wave theory, MacCamy and Fuchs (1954) analyzed theoretically the problem of waves passing a circular

cylinder. Their analysis assumes an ideal nonviscous fluid, and leads therefore to a force having the form of f_i. Their result, however, is valid for all ratios of pile diameter to wavelength, D/L_A, and shows the force to be about proportional to the acceleration du/dt for small values of D/L_A (L_A is the Airy approximation of wavelength). Taking their result as indicative of how small the pile should be for Equation 7-13 to apply, the restriction is obtained that

$$\frac{D}{L_A} < 0.05. \tag{7-14}$$

Figure 7-40 shows the relative wavelength L_A/L_o and pressure factor K versus d/gT^2 for the Airy wave theory.

* * * * * * * * * * * * * * * EXAMPLE PROBLEM * * * * * * * * * * * * * * * *

GIVEN: A wave with a period of T = 5 sec., and a pile with a diameter D = 1 ft. in 5 ft. of water.

FIND: Can Equation 7-13 be used to find the forces?

SOLUTION:

$$L_o = 5.12\, T^2 = 5.12\,(25) = 128 \text{ ft.},$$

$$\frac{d}{gT^2} = \frac{5}{32.2\,(5)^2} = 0.0062 \ ,$$

which, using Figure 7-40, gives

$$\frac{L_A}{L_o} = 0.47$$

$$L_A = 0.47\, L_o = 0.47\,(128) = 60 \text{ ft.},$$

$$\frac{D}{L_A} = \frac{1}{60} = 0.017 < 0.05 \ .$$

Since D/L_A satisfies Equation 7-14, force calculations may be based on Equation 7-13.

* *

The result of the example problem indicates that the restriction expressed by Equation 7-14 will seldom be violated for pile force calculations. However, this restriction is important when calculating forces on dolphins, caissons, and similar large structures that may be considered special cases of piles.
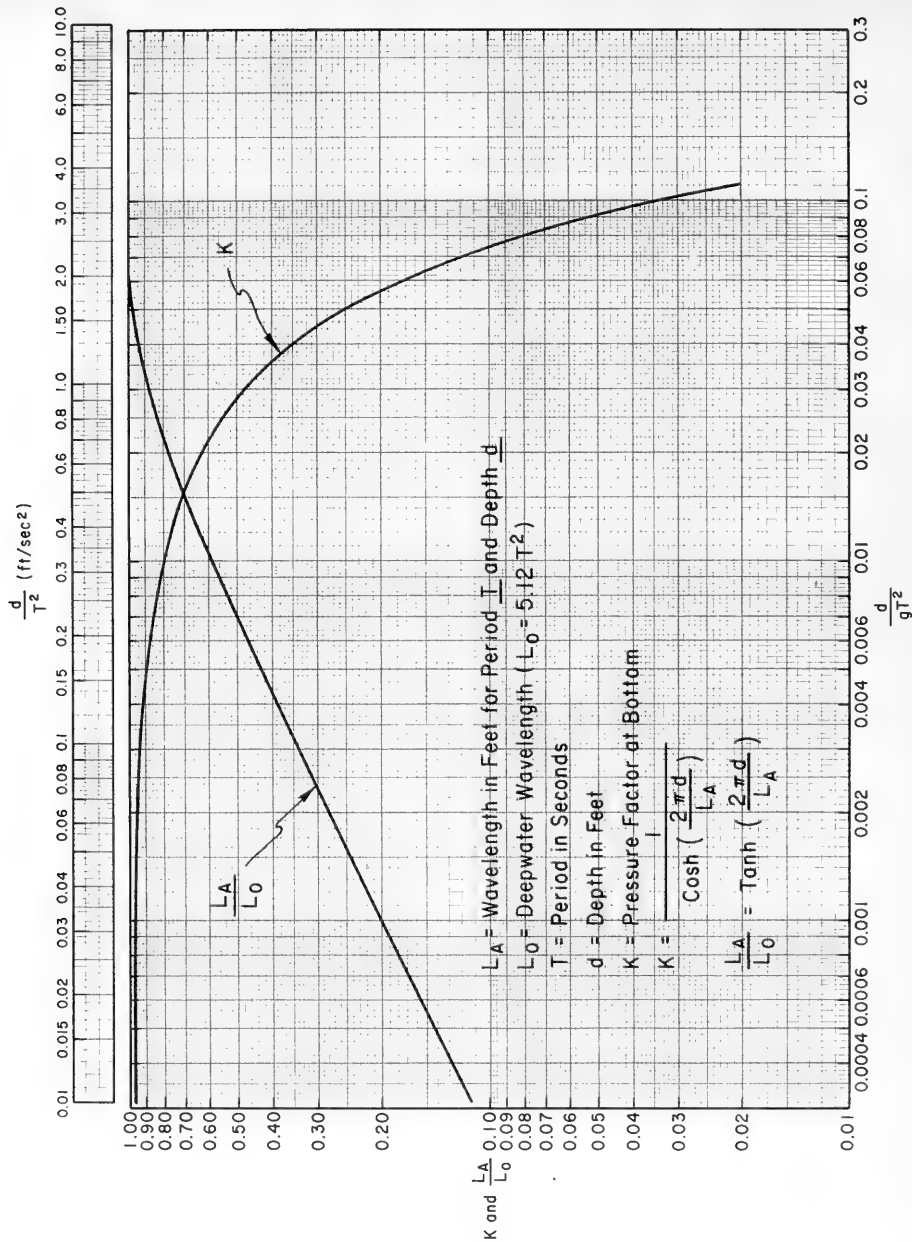
Figure 7-40. Relative Wavelength and Pressure Factor Versus d/gT^2 (Airy Wave Theory)

L_A = Wavelength in Feet for Period T and Depth d

L_0 = Deepwater Wavelength ($L_0 = 5.12\, T^2$)

T = Period in Seconds

d = Depth in Feet

K = Pressure Factor at Bottom

$$K = \frac{1}{Cosh\left(\frac{2\pi d}{L_A}\right)}$$

$$\frac{L_A}{L_0} = Tanh\left(\frac{2\pi d}{L_A}\right)$$

Two typical problems arise in the use of Equation 7-13.

(1) Given the water depth d the wave height H and period T, which wave theory should be used to predict the flow field?

(2) For a particular wave condition, what are appropriate values of the coefficients C_D and C_M ?

7.313 Calculation of Forces and Moments. *It is assumed in this section that the coefficients C_D and C_M are known and are constants.* (For the selection of C_D and C_M see Section 7.315, Selection of Hydrodynamic Force Coefficients C_D and C_M.) To use Equation 7-13, assume that the velocity and acceleration fields associated with the design wave can be described by Airy wave theory. With the pile at x = 0, as shown in Figure 7-39, the equations from Chapter 2 for surface elevation, (Equation 2-10), horizontal velocity (Equation 2-13), and acceleration (Equation 2-15), are

$$\eta = \frac{H}{2} \cos\left(\frac{2\pi t}{T}\right),$$

(7-15)

$$u = \frac{H}{2} \frac{gT}{L} \frac{\cosh\left[2\pi(z+d)/L\right]}{\cosh\left[2\pi d/L\right]} \cos\left(\frac{2\pi t}{T}\right),$$

(7-16)

$$\frac{du}{dt} \approx \frac{\partial u}{\partial t} = \frac{g\pi H}{L} \frac{\cosh\left[2\pi(z+d)/L\right]}{\cosh\left[2\pi d/L\right]} \sin\left(-\frac{2\pi t}{T}\right).$$

(7-17)

Introducing these expressions in Equation 7-13 gives

$$f_i = C_M \; \rho g \; \frac{\pi D^2}{4} \; H \left[\frac{\pi}{L} \frac{\cosh\left[2\pi(z+d)/L\right]}{\cosh\left[2\pi d/L\right]}\right] \sin\left(-\frac{2\pi t}{T}\right),$$

(7-18)

$$f_D = C_D \; \frac{1}{2} \; \rho g \; D \; H^2 \left[\frac{gT^2}{4L^2} \left(\frac{\cosh\left[2\pi(z+d)/L\right]}{\cosh\left[2\pi d/L\right]}\right)^2\right] \left|\cos\left(\frac{2\pi t}{T}\right)\right| \cos\left(\frac{2\pi t}{T}\right). \quad (7\text{-}19)$$

Equations 7-18 and 7-19 show that the two force components vary with elevation on the pile z and with time t. The inertia force f_i is maximum for sin (- 2πt/T) = 1, or for t = - T/4 for Airy wave theory. Since t = 0 corresponds to the wave crest passing the pile, the inertia force attains its maximum value T/4 sec. *before* passage of the wave crest. The maximum value of the drag force component f_D coincides with passage of the wave crest when t = 0.

Variation in magnitude of the maximum inertia force per unit length of pile with elevation along the pile is, from Equation 7-18, identical to the variation of particle acceleration with depth. The maximum value is largest at the surface z = 0 and decreases with depth. The same is true for the drag force component f_D ; however, the decrease with depth is more rapid since the attenuation factor, cosh[2π(z+d)/L]/cosh[2πd/L],

7-69

is squared. For a quick estimate of the variation of the two force components relative to their respective maxima, the curve labeled $K = 1/\cosh[2\pi d/L]$ in Figure 7-40 may be used. The ratio of the force at the bottom to the force at the surface is equal to K for the inertia forces, and to K^2 for the drag forces.

The design wave will usually be too high for Airy theory to provide an accurate description of the flow field. Nonlinear theories in Chapter 2 showed that wavelength and elevation of wave crest above stillwater level depend on wave steepness and the *wave height – water depth* ratio. The influence of steepness on crest elevation η_c and wavelength is presented graphically in Figures 7-41 and 7-42. The use of these figures is illustrated by the following examples.

* * * * * * * * * * * * * * * EXAMPLE PROBLEM * * * * * * * * * * * * * * * * *

GIVEN: Depth $d = 15$ ft., wave height $H = 10$ ft., and wave period $T = 10$ sec.

FIND: Crest elevation above stillwater level, wavelength, and relative variation of force components along the pile.

SOLUTION: Calculate,

$$\frac{d}{gT^2} = \frac{15}{32.2\,(10)^2} = 0.0047 \ ,$$

$$\frac{H}{gT^2} = \frac{10}{32.2\,(10)^2} = 0.0031 \ .$$

From Figure 7-40,

$$L_A = 0.41\ L_o = (0.41)\,(5.12)T^2 = 210\ \text{ft.,}$$

$$K = 0.9 \ .$$

From Figure 7-41,

$$\eta_c = 0.845\ H = 8.45\ \text{ft.}$$

From Figure 7-42,

$$L = 1.165\ L_A = 245\ \text{ft.}$$

and

$$K = \frac{f_{i\,(z\,=\,-d)}}{f_{i\,(z\,=\,0)}} = 0.9 \ ,$$

$$K^2 = \frac{f_{D\,(z\,=\,-d)}}{f_{D\,(z\,=\,0)}} = 0.81 \ .$$

7-70
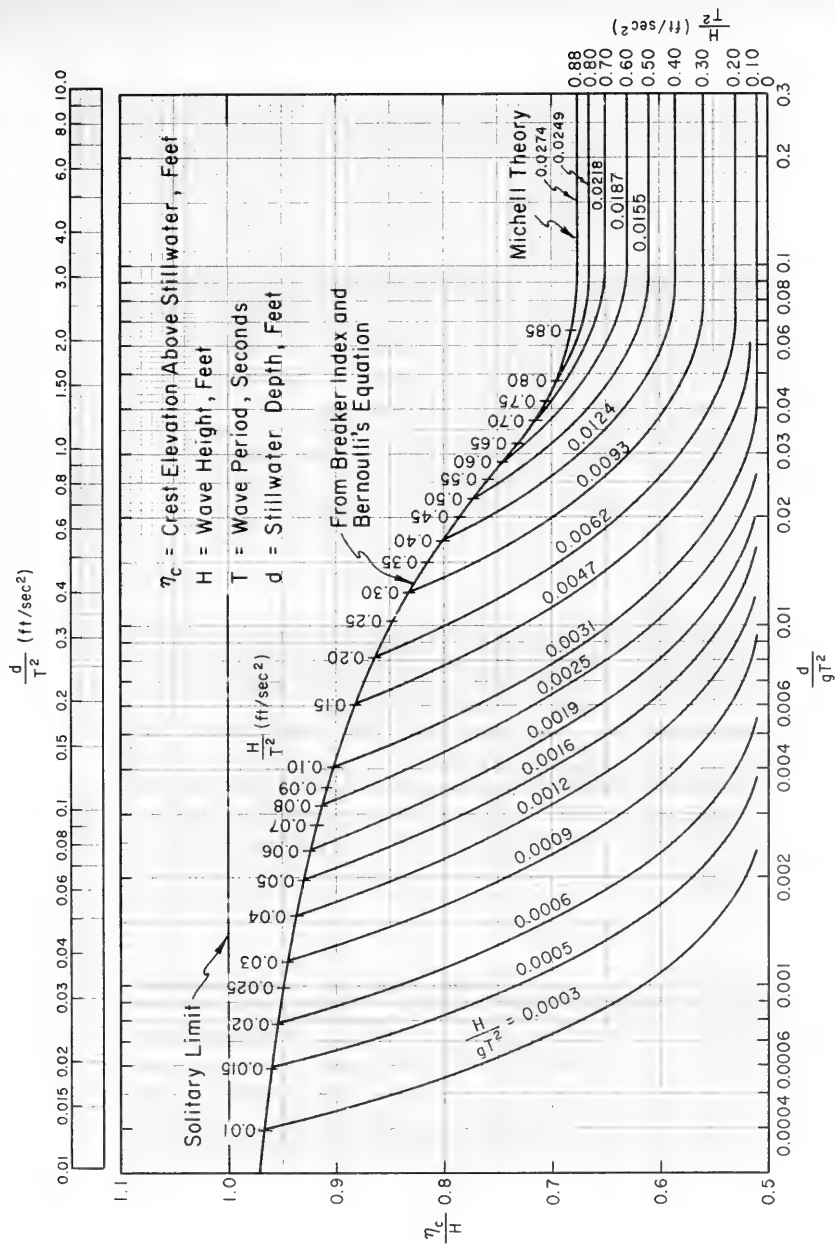
Figure 7-41. Ratio of Crest Elevation above Stillwater Level to Wave Height

7-71
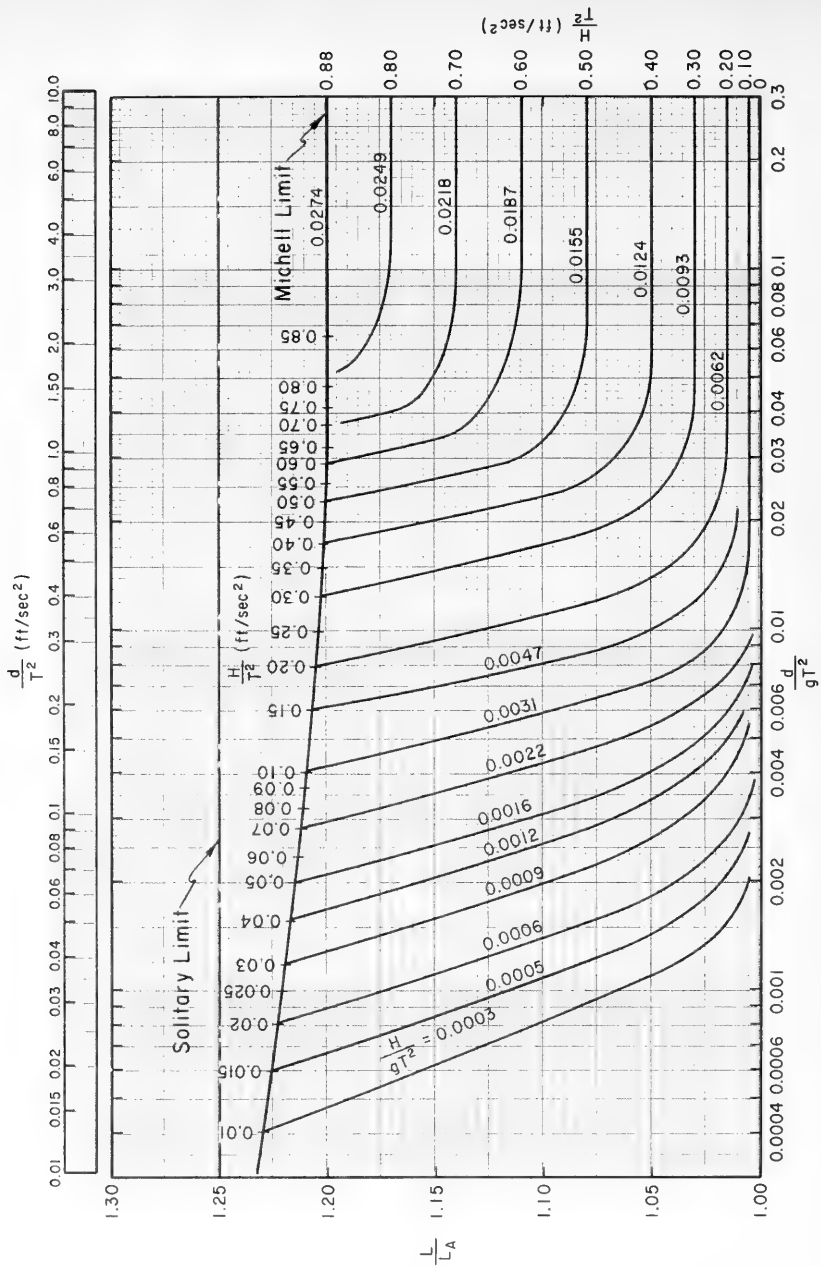
Figure 7-42. Wave Length Correction Factor for Finite Amplitude Effects

7-72

Note the large increase in η_c above the Airy estimate of $H/2 = 5.0$ ft. and the relatively small change of drag and inertia forces along the pile. The wave condition approaches that of a long wave or shallow-water wave.

* *

* * * * * * * * * * * * * * EXAMPLE PROBLEM * * * * * * * * * * * * * * * *

GIVEN: Same wave conditions as preceding problem $H = 10$ ft. and $T = 10$ sec.; however, the depth $d = 100$ ft.

FIND: Crest elevation above stillwater level, wavelength, and the relative variation of force components along the pile.

SOLUTION: Calculate,

$$\frac{d}{gT^2} = \frac{100}{32.2\,(10)^2} = 0.031\ ,$$

$$\frac{H}{gT^2} = \frac{10}{32.2\,(10)^2} = 0.0031\ .$$

From Figure 7-40,

$$L_A = 0.89\ L_o = 0.89\,(5.12)\,T^2 = 455\ \text{ft.},$$

$$K = 0.46\ .$$

From Figure 7-41,

$$\eta_c = 0.52\ H = 5.2\ \text{ft.}$$

From Figure 7-42,

$$L = 1.01\ L_A = 460\ \text{ft.}$$

and

$$K = \frac{f_i\,(z = -d)}{f_i\,(z = 0)} = 0.46.$$

$$K^2 = \frac{f_D\,(z = -d)}{f_D\,(z = 0)} = 0.21\ .$$

Note the large decrease in forces with depth. The wave condition approaches that of a deepwater wave.

* *

For force calculations, an appropriate wave theory should be used to calculate u and du/dt. Skjelbria, et al. (1960) have prepared tables based on Stokes' fifth-order wave theory. For a wide variety of given wave conditions, i.e., water depth, wave period and wave height, these tables may be used to obtain the variation of f_i and f_D with time (values are given for time intervals of $2\pi t/T = 20°$) and position along the pile (values given at intervals of 0.1 d). Similar tables based on Dean's numerical stream-function theory (Dean, 1965) are to be published by CERC in 1973. (Dean, 1973.)

For structural design of a single vertical pile, it is often unnecessary to know in detail the distribution of forces along the pile. Total horizontal force acting on the pile and total moment of forces about the mudline $z = -d$ are of primary interest. These may be obtained by integration of Equation 7-13.

$$F = \int_{-d}^{\eta} f_i \ dz + \int_{-d}^{\eta} f_D \ dz = F_i + F_D, \tag{7-20}$$

$$M = \int_{-d}^{\eta} (z+d) f_i \ dz + \int_{-d}^{\eta} (z+d) f_D \ dz = M_i + M_D. \tag{7-21}$$

In general form these quantities may be written

$$F_i = C_M \ \rho g \ \frac{\pi D^2}{4} \ H \ K_i, \tag{7-22}$$

$$F_D = C_D \ \frac{1}{2} \ \rho g \ D \ H^2 \ K_D, \tag{7-23}$$

$$M_i = C_M \ \rho g \ \frac{\pi D^2}{4} \ H \ K_i \ d \ S_i = F_i \ d \ S_i, \tag{7-24}$$

$$M_D = C_D \ \frac{1}{2} \ \rho g \ D \ H^2 \ K_D \ d \ S_D = F_D \ d \ S_D. \tag{7-25}$$

in which C_D and C_M have been assumed constant, and where K_i, K_D, S_i and S_D are dimensionless. When using Airy theory (Equations 7-18 and

7-74

7-19), the integration indicated in Equations 7-20 and 7-21 may be performed if the upper limit of integration is zero instead of η. This leads to

$$K_i = \frac{1}{2} \tanh\left(\frac{2\pi d}{L}\right) \sin\left(-\frac{2\pi t}{T}\right), \tag{7-26}$$

$$K_D = \frac{1}{8}\left(1 + \frac{4\pi d/L}{\sinh[4\pi d/L]}\right) |\cos\left(\frac{2\pi t}{T}\right)| \cos\left(\frac{2\pi t}{T}\right) \tag{7-27}$$

$$= \frac{1}{4} n |\cos\left(\frac{2\pi t}{T}\right)| \cos\left(\frac{2\pi t}{T}\right).$$

$$S_i = 1 + \frac{1 - \cosh[2\pi d/L]}{(2\pi d/L)\sinh[2\pi d/L]}, \tag{7-28}$$

$$S_D = \frac{1}{2} + \frac{1}{2n}\left(\frac{1}{2} + \frac{1 - \cosh[4\pi d/L]}{(4\pi d/L)\sinh[4\pi d/L]}\right). \tag{7-29}$$

where $n = C_g/C$ has been introduced to simplify the expressions. From Equations 7-26 and 7-27, the maximum values of the various force and moment components may be written

$$F_{im} = C_M \rho g \frac{\pi D^2}{4} H K_{im}, \tag{7-30}$$

$$F_{Dm} = C_D \frac{1}{2} \rho g D H^2 K_{Dm}, \tag{7-31}$$

$$M_{im} = F_{im} d S_i, \tag{7-32}$$

$$M_{Dm} = F_{Dm} d S_D. \tag{7-33}$$

where K_{im} and K_{Dm} according to Airy theory, are obtained from Equations 7-26 and 7-27 taking $t = -T/4$ and $t = 0$, respectively, and S_i and S_D are given by Equations 7-28 and 7-29 respectively.

Equations 7-30 through 7-33 are general. Using Dean's stream-function theory (Dean, 1973), the graphs in Figures 7-43 through 7-46 have been prepared and may be used to obtain K_{im}, K_{Dm}, S_{im} and S_{Dm}. S_i and S_D, as given in Equations 7-28 and 7-29 for Airy theory, are independent of wave phase angle θ and thus are equal to the maximum values. For stream-function and other finite amplitude theories S_i and S_D depend on phase angle; Figures 7-45 and 7-46 give maximum values, S_{im} and S_{Dm}. The degree of nonlinearity of a wave can be described by the ratio of wave height to the breaking height, which may be obtained from Figure 7-47 as illustrated by the following example.
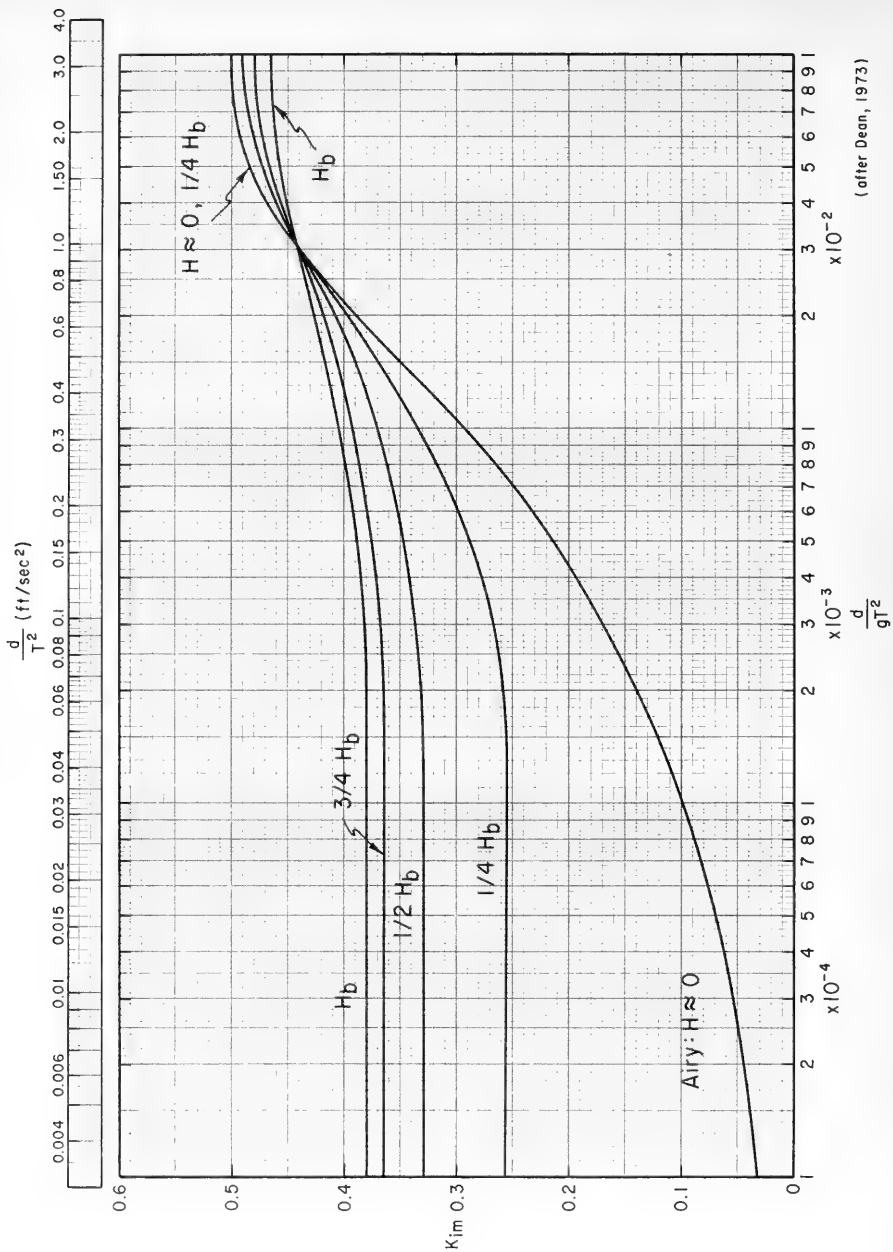
Figure 7-43. K_{im} Versus Relative Depth, d/gT^2

(after Dean, 1973)

7-76

Figure 7-44. K_{Dm} Versus Relative Depth, d/gT^2

(after Dean, 1973)

7-77
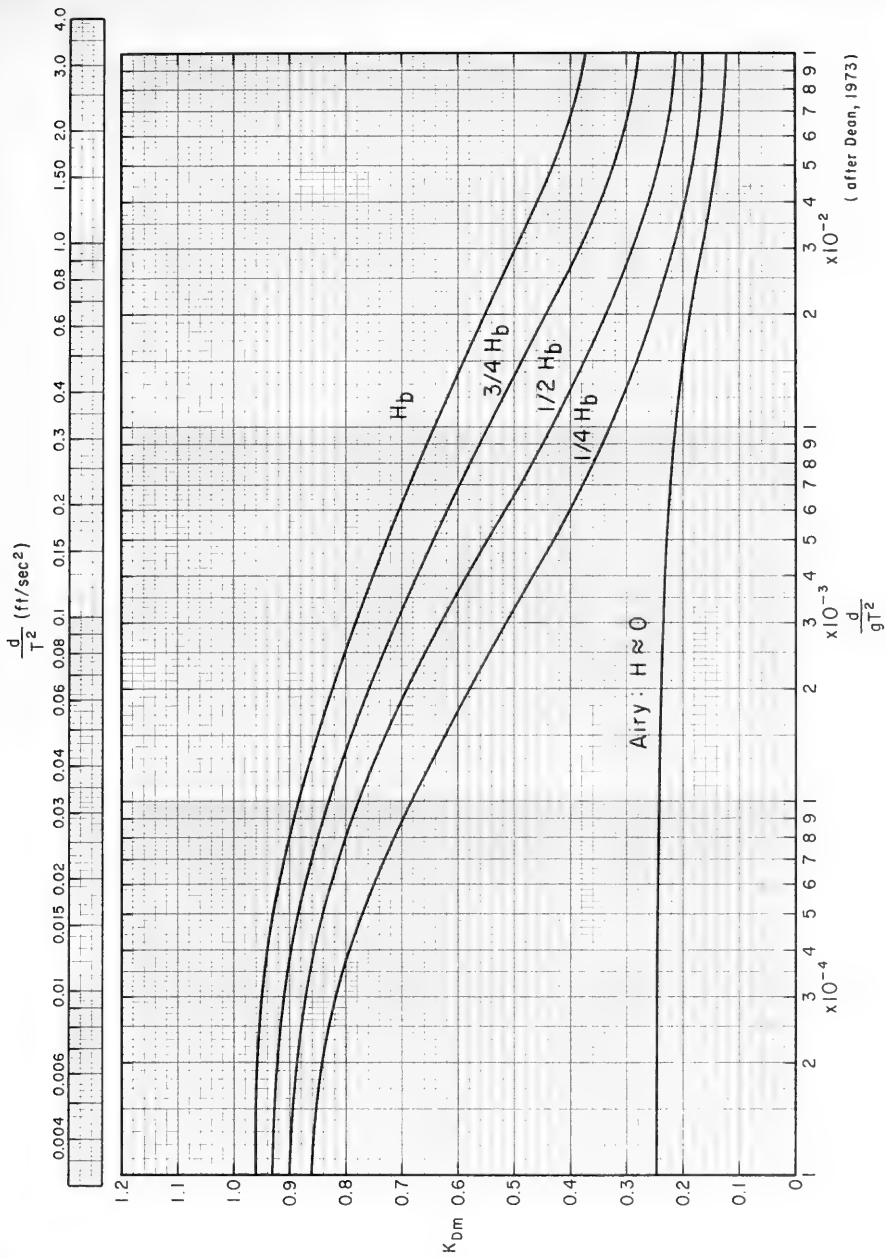
Figure 7-45. Inertia Force Moment Arm, S_{im}, Versus Relative Depth, d/gT^2
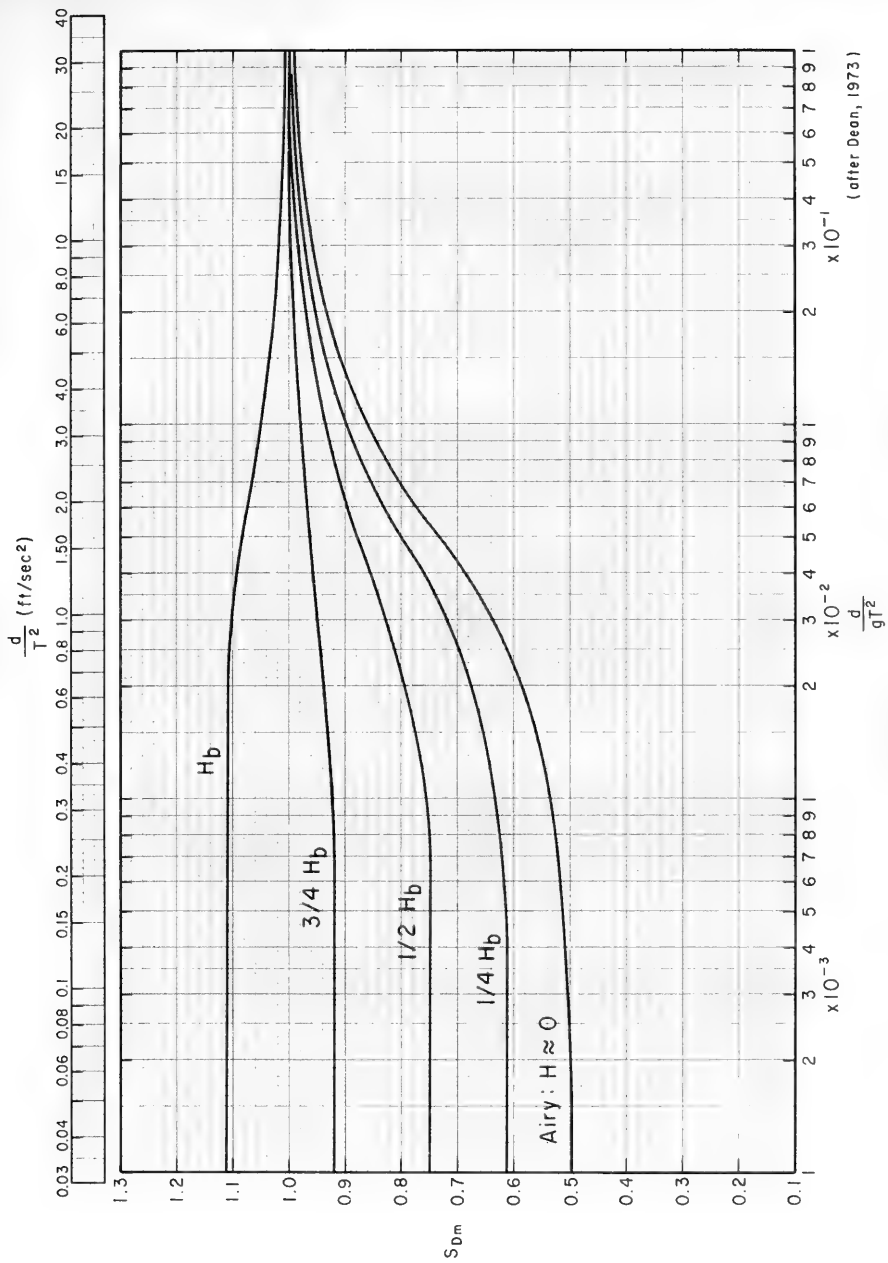
Figure 7-46. Drag Force Moment Arm, S_{Dm}, Versus Relative Depth, d/gT^2

(after Dean, 1973)

* * * * * * * * * * * * * * EXAMPLE PROBLEM * * * * * * * * * * * * * * *

GIVEN: A design wave $H = 10$ ft. with a period $T = 8$ sec. in a depth $d = 40$ ft.

FIND: The ratio of wave height to breaking height.

SOLUTION: Calculate,

$$\frac{d}{gT^2} = \frac{40}{(32.2)(8)^2} = 0.0194.$$

Enter Figure 7-47 with $d/gT^2 = 0.0194$ to the curve marked *Breaking Limit* and read,

$$\frac{H_b}{gT^2} = 0.015.$$

Therefore,

$$H_b = 0.015 \ gT^2 = 0.015 (32.2)(8)^2 = 30.1 \text{ ft.}$$

The ratio of the design wave height to the breaking height is

$$\frac{H}{H_b} = \frac{10}{30.1} = 0.33.$$

* *

By using Equations 7-30 through 7-33 with Figures 7-43 through 7-46, the maximum values of the force and moment components can be found. To estimate the maximum total force F_m Figures 7-48 through 7-51 by Dean (1965a) may be used. The figure to be used is determined by calculating,

$$W = \frac{C_M D}{C_D H}, \qquad (7-34)$$

and the maximum force is calculated by

$$F_m = \phi_m \ wC_D H^2 D, \qquad (7-35)$$

where ϕ_m is the coefficient read from the figures. Similarly, the maximum moment M_m can be determined from Figures 7-52 through 7-55 which are also based on Dean's stream-function theory. (Dean, 1965a.) The figure to be used is again determined by calculating W by Equation 7-34 and the maximum moment about the mud line $(z = -d)$ is found from

$$M_m = \alpha_m \ wC_D H^2 Dd, \qquad (7-36)$$

where α_m is the coefficient read from the figures.

Calculation of the maximum force and moment on a vertical cylindrical pile is illustrated by the following example.
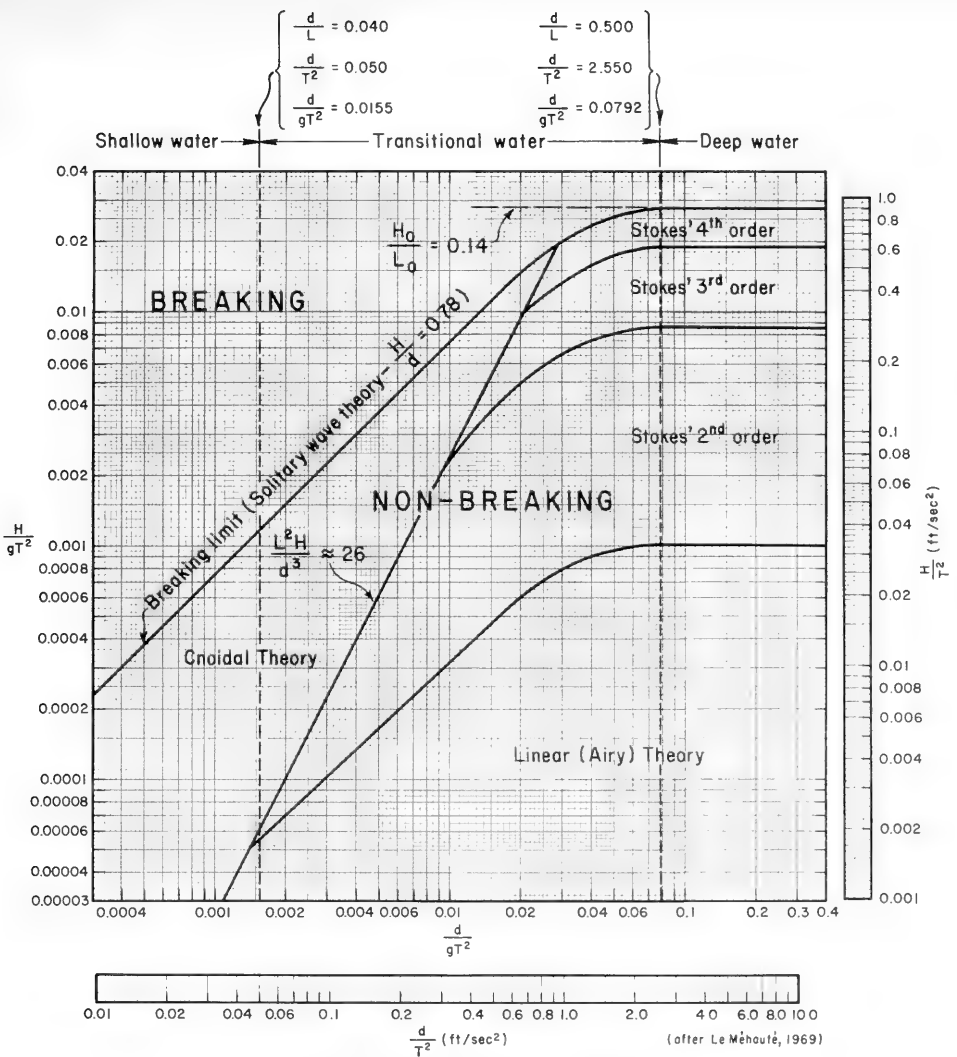
Figure 7-47. Breaking Wave Height and Regions of Validity of Various Wave Theories

7-81
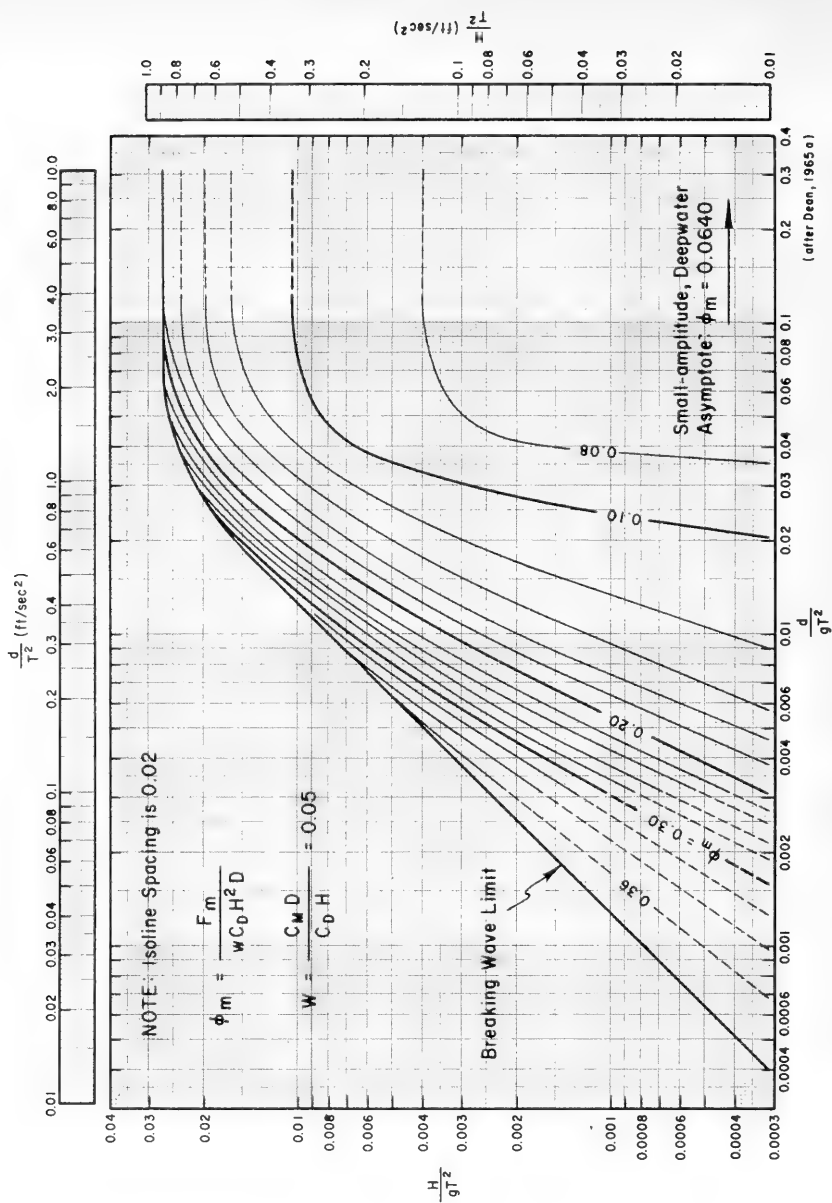
Figure 7-48. Isolines of ϕ_m Versus H/gT^2 and d/gT^2 ...... (W = 0.05)
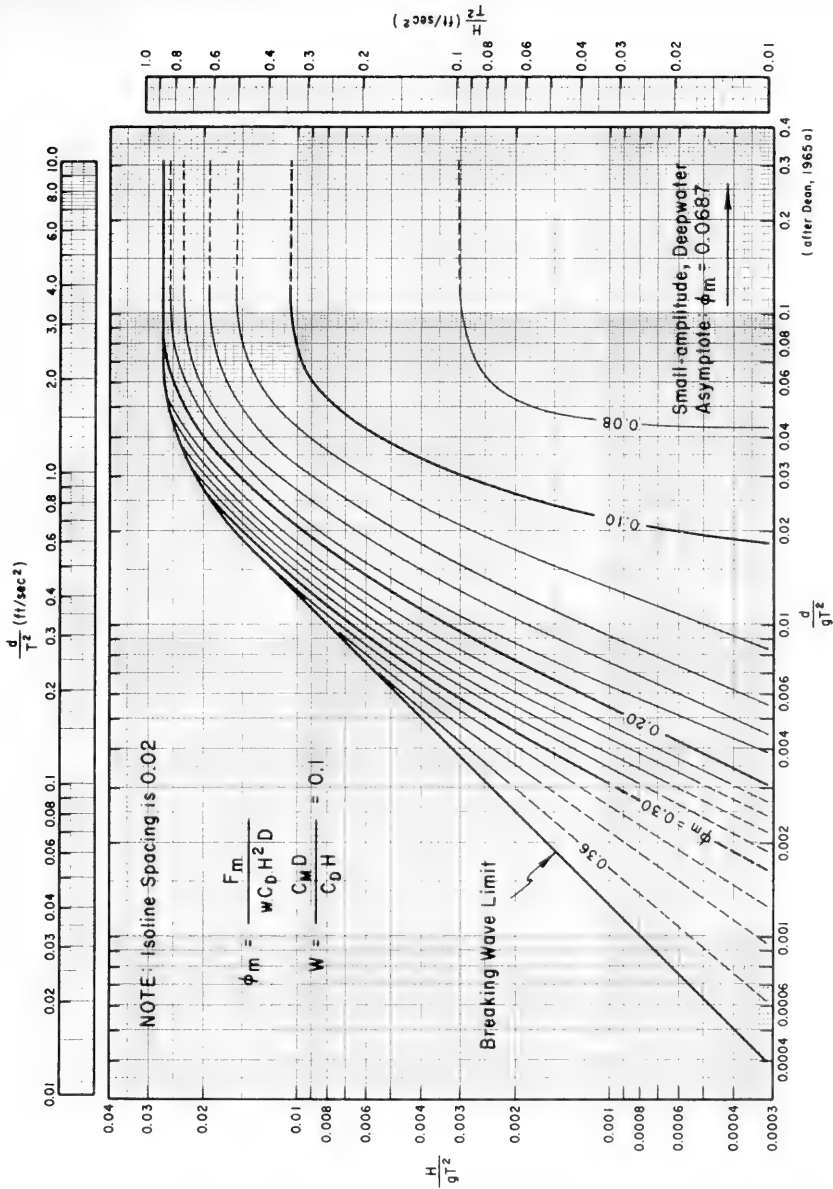
Figure 7-49. Isolines of ϕ_m Versus H/gT^2 and d/gT^2 ...... (W = 0.1)

7-83
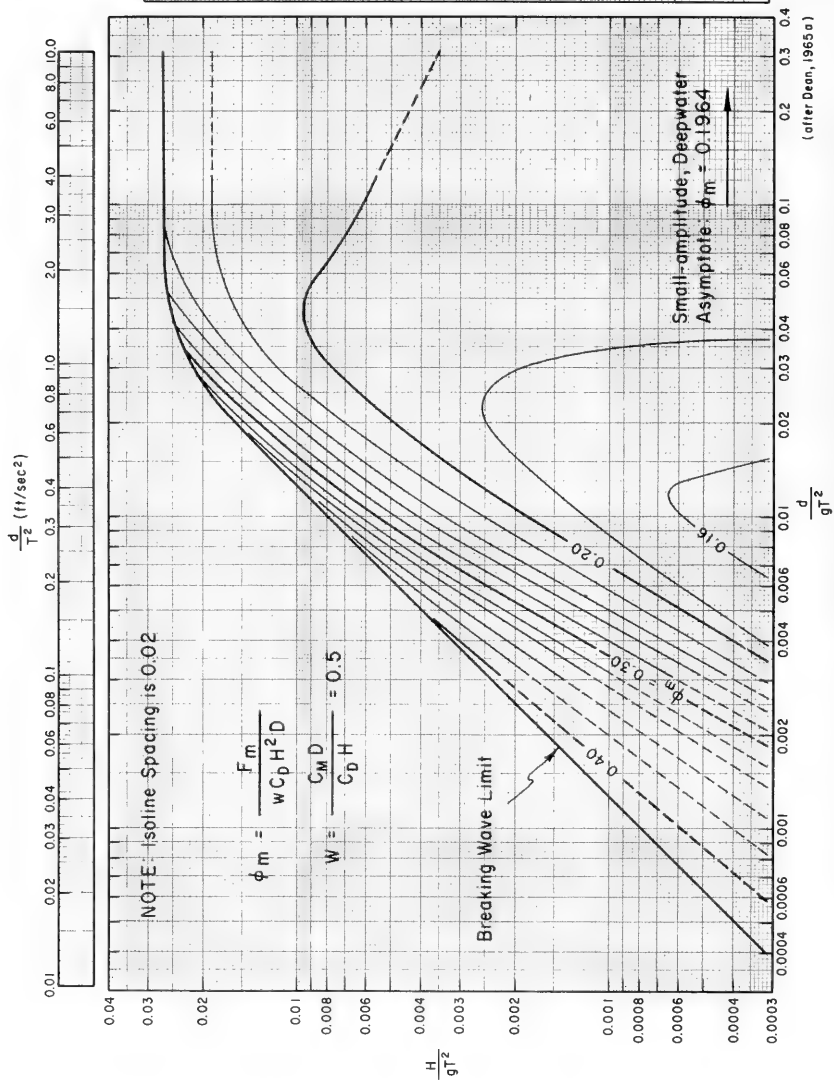
Figure 7-50. Isolines of ϕ_m Versus H/gT^2 and d/gT^2 ..... (W = 0.5)
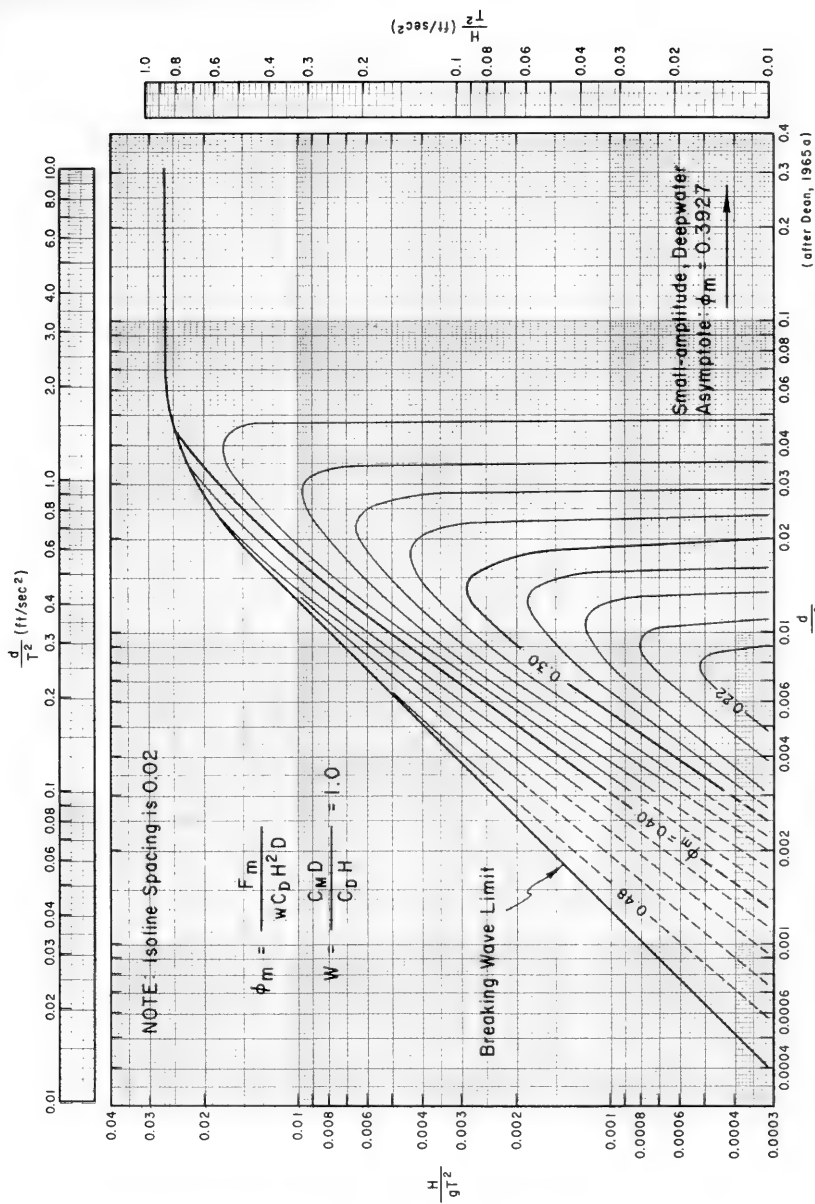
Figure 7-51. Isolines of ϕ_m Versus H/gT^2 and d/gT^2 ..... (W = 1.0)
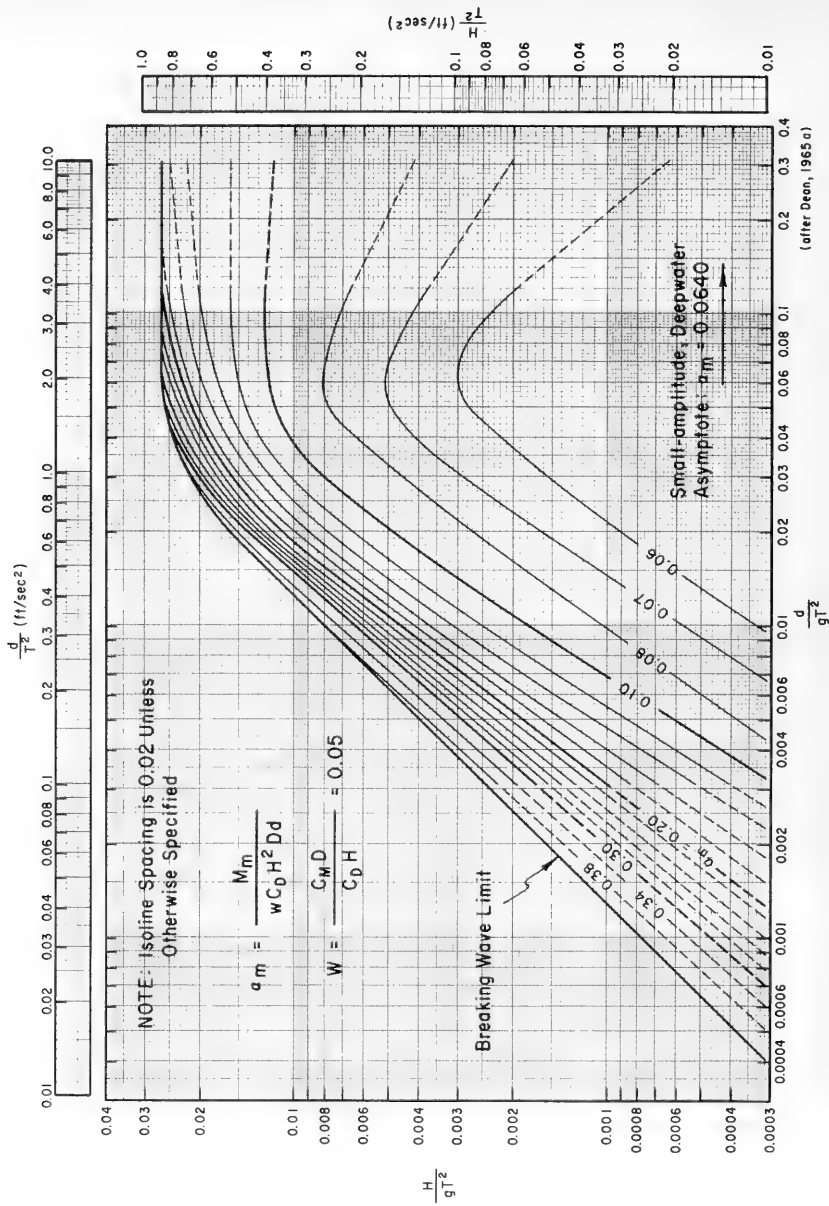
Figure 7-52. Isolines of α_m Versus H/gT^2 and d/gT^2 ..... ($W = 0.05$)

7-86
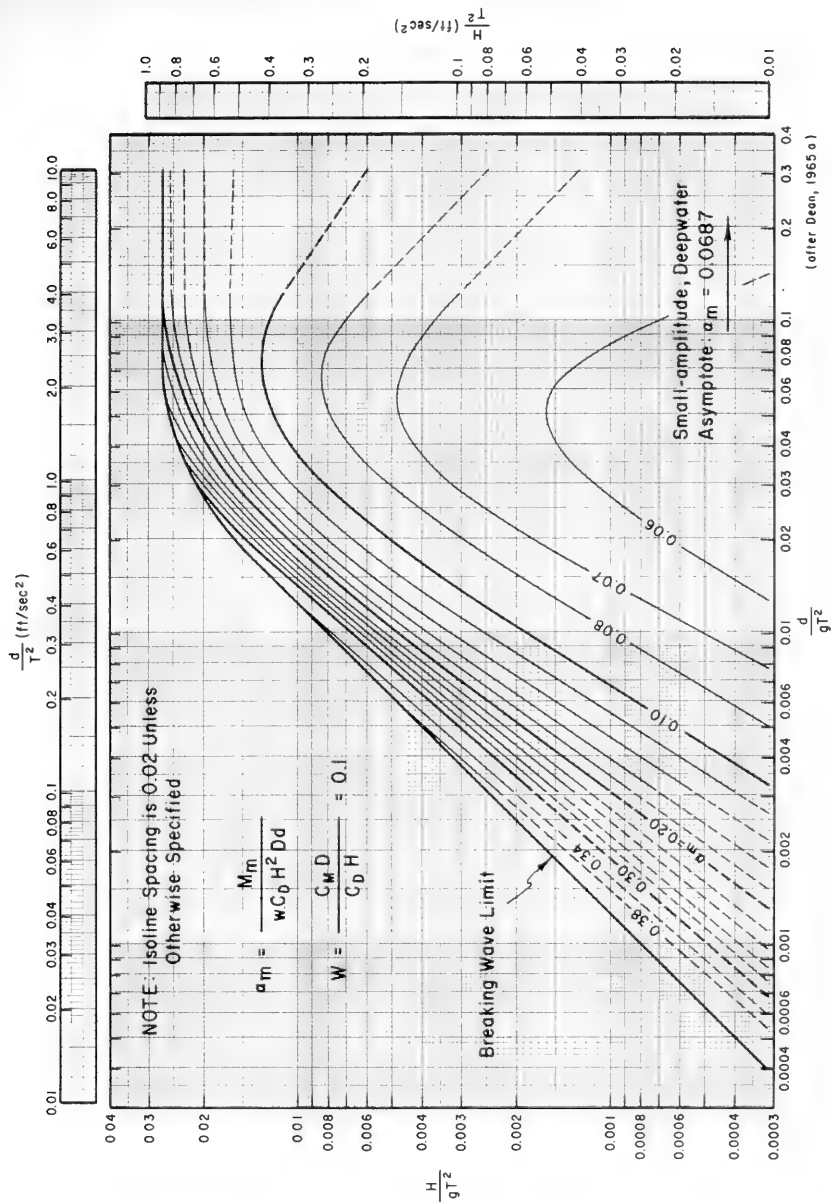
Figure 7-53. Isolines of α_m Versus H/gT^2 and d/gT^2 ..... (W = 0.1)
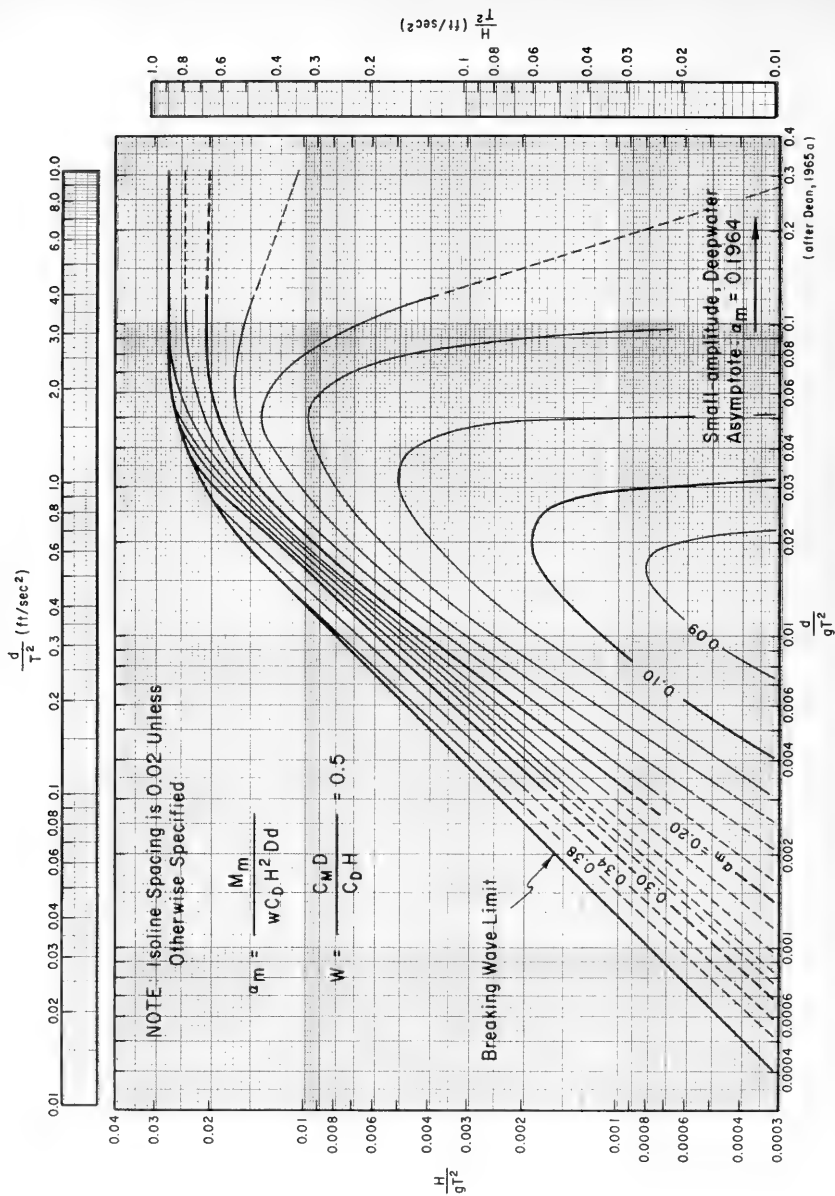
Figure 7-54. Isolines of α_m Versus H/gT^2 and d/gT^2 ..... (W = 0.5)

7-88
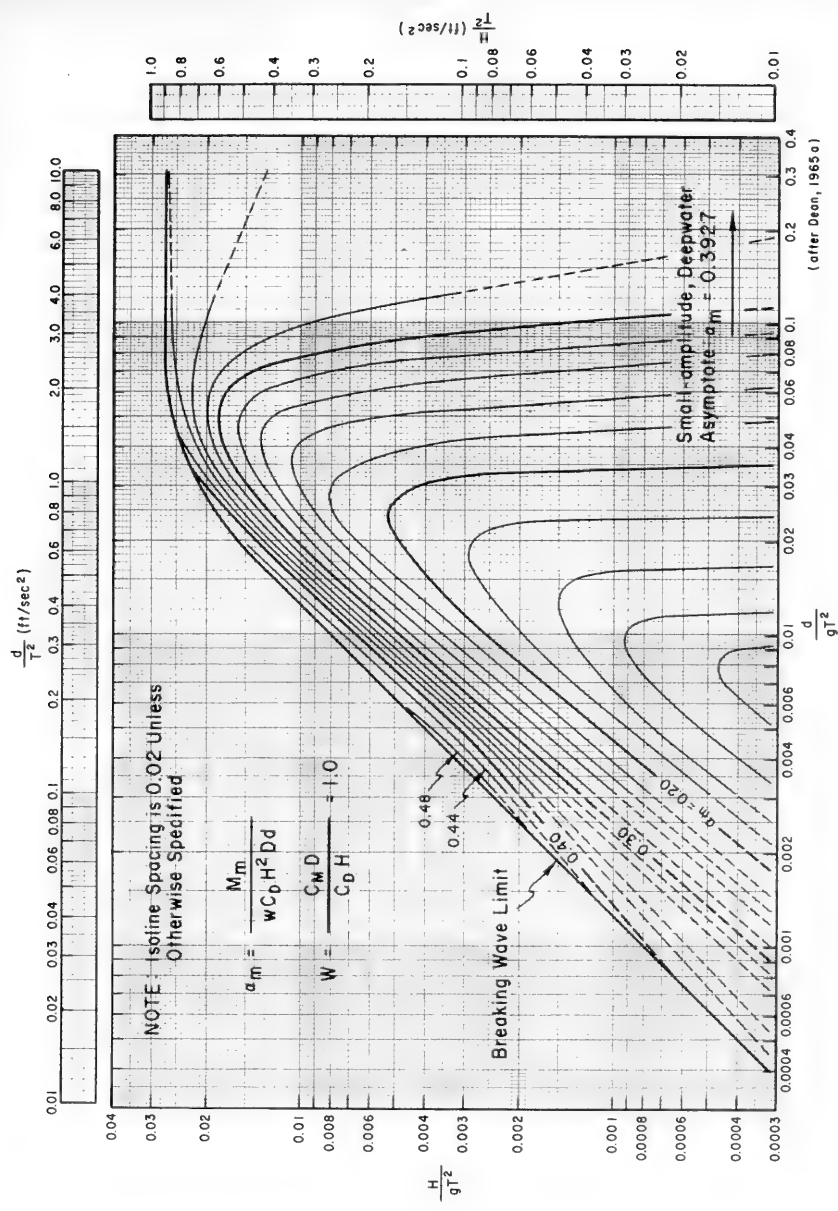
Figure 7-55. Isolines of a_m Versus H/gT^2 and d/gT^2 ..... (W=1.0)

GIVEN: A design wave with height H = 10 ft. and period T = 10 sec. 'acts on a vertical circular pile with a diameter D = 1 ft. in depth d = 15 ft. Assume that C_M = 2.0 and C_D = 0.7. Selection of C_M and C_D is discussed in Section 7.315.

FIND: The maximum total horizontal force and the maximum total moment around the mudline of the pile.

SOLUTION: Calculate,

$$\frac{d}{gT^2} = \frac{15}{(32.2)(10)^2} = 0.00466,$$

and enter Figure 7-47 to the breaking limit curve and read,

$$\frac{H_b}{gT^2} = 0.00357.$$

Therefore,

$$H_b = 0.00357 \; gT^2 = 0.00357 \,(32.2)\,(10^2) = 11.5 \text{ ft.,}$$

and

$$\frac{H}{H_b} = \frac{10}{11.5} = 0.87.$$

From Figures 7-43 and 7-44, using d/gT^2 = 0.00466 and H = 0.87 H_b, interpolating between curves H = H_b and H = 3/4 H_b to find, K_{im} and K_{Dm}:

$$K_{im} = 0.38,$$

$$K_{Dm} = 0.70.$$

From Equation 7-30:

$$F_{im} = C_M \; \rho g \; \frac{\pi D^2}{4} \; H \; K_{im},$$

$$F_{im} = (2)\,(2)\,(32.2) \; \frac{\pi \, 1^2}{4} \;(10)\,(0.38) = 384 \text{ lbs.}$$

and from Equation 7-31:

$$F_{Dm} = C_D \; \frac{1}{2} \; \rho g \; D \; H^2 \; K_{Dm},$$

$$F_{Dm} = (0.7)\,(0.5)\,(2)\,(32.2)\,(1)\,(10)^2\,(0.7) = 1,580 \text{ lbs.}$$

7-90

From Equation 7-34, compute

$$W = \frac{C_M D}{C_D H} = \frac{(2.0)(1)}{(0.7)(10)} = 0.29.$$

Interpolation between Figures 7-49 and 7-50 for ϕ_m is required. Calculate

$$\frac{H}{gT^2} = \frac{10}{(32.2)(10)^2} = 0.0031,$$

and recall that

$$\frac{d}{gT^2} = 0.00466$$

Find the point on Figures 7-49 and 7-50 corresponding to the computed values of H/gT^2 and d/gT^2 and determine ϕ_m.

Figure 7-49 $W = 0.1$; $\phi_m = 0.35,$

Interpolated Value $W = 0.29$; $\phi_m \approx 0.365,$

Figure 7-50 $W = 0.5$; $\phi_m = 0.38.$

From Equation 7-35, the maximum force is

$$F_m = \phi_m \ wC_D H^2 D,$$

$$F_m = 0.365 (64)(0.7)(10)^2 (1) = 1,635 \text{ lbs.}$$

say

$$F_m = 1,600 \text{ lbs.}$$

To calculate the inertia moment component, enter Figure 7-45 with

$$\frac{d}{gT^2} = 0.00466,$$

and $H = 0.87\ H_b$ interpolate between $H = H_b$ and $H = 3/4\ H_b$ to find,

$$S_{im} = 0.81.$$

Similarly from Figure 7-46 for the drag moment component, determine

$$S_{Dm} = 1.02.$$

7-91

Therefore from Equation 7-32,

$$M_{im} = F_{im}\ d\ S_{im} = 384\,(15)\,(0.81) = 4{,}670\ \text{lb.-ft.},$$

and from Equation 7-33,

$$M_{Dm} = F_{Dm}\ d\ S_{Dm} = 1{,}580\,(15)\,(1.02) = 24{,}170\ \text{lb.-ft.}$$

The value of α_m is found by interpolation between Figures 7-53 and 7-54 using W = 0.29, $H/gT^2 = 0.0031$ and $d/gT^2 = 0.00466$.

Figure 7-53 $\qquad\qquad$ W = 0.1 ; α_m = 0.34,

Interpolated Value $\qquad$ W = 0.29 ; $\alpha_m \approx$ 0.35,

Figure 7-54 $\qquad\qquad$ W = 0.5 ; α_m = 0.36.

The maximum total moment about the mudline is found from Equation 7-36.

$$M_m = \alpha_m\ w\ C_D H^2 D d,$$

$$M_m = 0.35\,(64)\,(0.7)\,(10)^2\,(1)\,(15) = 23{,}520\ \text{lb.-ft.}$$

say

$$M_m = 23{,}500\ \text{lb.-ft.}$$

The moment arm, measured from the bottom, is the maximum total moment M_m divided by the maximum total force F_m; therefore,

$$\frac{M_m}{F_m} = \frac{23{,}520}{1{,}635} = 14.1\ \text{ft.}$$

If it is assumed that the upper 2 feet of the bottom material lacks significant strength, or if it is assumed that scour of 2 feet occurs, the maximum total horizontal force is unchanged, but the lever arm is increased by about 2 feet. The increased moment can be calculated by increasing the moment arm by 2 feet and multiplying by the maximum total force. Thus the maximum moment is estimated to be

$$\left(M_m\right)_{2\,ft.\ below\ mudline} = (14.1 + 2)\,F_m = 16.1(1{,}635) = 26{,}320\ \text{lb.-ft.},$$

say

$$\left(M_m\right)_{2\,ft.\ below\ mudline} = 26{,}300\ \text{lb.-ft.}$$

* *

* * * * * * * * * * * * * * EXAMPLE PROBLEM * * * * * * * * * * * * * * * *

GIVEN: A design wave with height H = 10 ft. and period T = 10 sec. acts on a vertical circular pile with a diameter D = 1 ft. in a depth d = 100 ft. Assume C_M = 2.0 and C_D = 1.2

<u>FIND:</u> The maximum total horizontal force and the moment around the mudline of the pile.

<u>SOLUTION:</u> The procedure used is identical to that of the preceding problem. Calculate,

$$\frac{d}{gT^2} = \frac{100}{(32.2)(10)^2} = 0.031.$$

and enter Figure 7-47 to the breaking-limit curve and read

$$\frac{H_b}{gT^2} = 0.0205.$$

Therefore

$$H_b = 0.0205 \, gT^2 = 0.0205 \, (32.2)(10)^2 = 66 \, \text{ft.,}$$

and

$$\frac{H}{H_b} = \frac{10}{66} = 0.15 \, .$$

From Figures 7-43 and 7-44, using $d/gT^2 = 0.031$ and interpolating between $H \approx 0$ and $H = 1/4 \, H_b$, for $H = 0.15 \, H_b$,

$$K_{im} = 0.44,$$

$$K_{Dm} = 0.20 \, .$$

From Equation 7-30,

$$F_{im} = C_M \, \rho g \, \frac{\pi D^2}{4} \, H \, K_{im},$$

$$F_{im} = 2.0 \, (2)(32.2) \, \frac{\pi(1)^2}{4} \, (10)(0.44) = 445 \, \text{lbs.}$$

and from Equation 7-31,

$$F_{Dm} = C_D \, \frac{1}{2} \, \rho g D H^2 \, K_{Dm},$$

$$F_{Dm} = 1.2 \, (0.5)(2)(32.2)(1)(10)^2 \, (0.20) = 773 \, \text{lbs.}$$

Compute W from Equation 7-34,

$$W = \frac{C_M D}{C_D H} = \frac{2.0 \, (1.0)}{1.2 \, (10)} = 0.16 \, .$$

Interpolation between Figures 7-49 and 7-50 for ϕ_m gives

$$\phi_m = 0.11 .$$

From Equation 7-35 the maximum total force is

$$F_m = \phi_m \, w \, C_D \, H^2 D ,$$

$$F_m = 0.11 \, (64) \, (1.2) \, (10)^2 \, (1.0) = 845 \text{ lbs.}$$

say

$$F_m = 850 \text{ lbs.}$$

From Figures 7-45 and 7-46, for $H = 0.15 \, H_b$,

$$S_{im} = 0.57 ,$$

and

$$S_{Dm} = 0.69 .$$

From Equation 7-32,

$$M_{im} = F_{im} \, d \, S_{im} = 445 \, (100) \, (0.57) = 25{,}370 \text{ lb.-ft.,}$$

and from Equation 7-33,

$$M_{Dm} = F_{Dm} \, d \, S_{Dm} = 773 \, (100) \, (0.69) = 53{,}340 \text{ lb.-ft.}$$

Interpolation between Figures 7-53 and 7-54 with $W = 0.16$ gives

$$\alpha_m = 0.076 .$$

The maximum total moment about the mudline from Equation 7-36 is,

$$M_m = \alpha_m \, w \, C_D H^2 Dd ,$$

$$M_m = 0.076 \, (64) \, (1.2) \, (10)^2 \, (1.0) \, (100) = 58{,}370 \text{ lb.-ft.,}$$

say

$$M_m = 58{,}400 \text{ lb.-ft.}$$

If calculations show the pile diameter to be too small, noting that F_{im} is proportional to D^2 and F_{Dm} is proportional to D will allow adjustment of the force for a change in pile diameter. For example, for the same wave conditions and a 2-foot-diameter pile the forces become,

$$F_{im} \, (D = 2 \text{ ft.}) = F_{im} \, (D = 1 \text{ ft.}) \, \frac{(2)^2}{(1)^2} = 445 \, (4) = 1{,}780 \text{ lbs.,}$$

$$F_{Dm} \, (D = 2 \text{ ft.}) = F_{Dm} \, (D = 1 \text{ ft.}) \, \frac{2}{1} = 773 \, (2) = 1{,}546 \text{ lbs.}$$

7-94

The new value of W from Equation 7-34 is

$$W = \frac{C_M D}{C_D H} = \frac{2.0 \, (2.0)}{1.2 \, (10)} = 0.33 \; ,$$

and the new values of ϕ_m and α_m are,

$$\phi_m = 0.15 \; ,$$

and

$$\alpha_m = 0.093 \; .$$

Therefore, from Equation 7-35,

$$\left(F_m\right)_{2' \, diam.} = \phi_m \, w \, C_D H^2 D \; ,$$

$$\left(F_m\right)_{2' \, diam.} = 0.15 \, (64) \, (1.2) \, (10)^2 \, (2) = 2,300 \text{ lbs.},$$

and from Equation 7-36,

$$\left(M_m\right)_{2' \, diam.} = \alpha_m \, w \, C_D H^2 Dd \; ,$$

$$\left(M_m\right)_{2' \, diam.} = 0.093 \, (64) \, (1.2) \, (10)^2 \, (2) \, (100) = 142,800 \text{ lb.-ft.},$$

say

$$\left(M_m\right)_{2' \, diam.} = 143,000 \text{ lb.-ft.}$$

* *

7.314 Transverse Forces Due to Eddy Shedding (Lift Forces). In addition to drag and inertia forces that act in the direction of wave advance, transverse forces may arise. Because they are similar to aerodynamic lift force, transverse forces are often termed *lift forces*, although they do not act vertically but perpendicular to both wave direction and the pile axis. Transverse forces result from vortex or eddy shedding on the downstream side of a pile. Eddies are shed alternately from one side of the pile and then from the other resulting in a laterally oscillating force.

Laird, et al. (1960) and Laird (1962) studied transverse forces on rigid and flexible oscillating cylinders. In general, lift forces were found to depend on the dynamic response of the structure. For structures with a natural frequency of vibration about twice the wave frequency, a dynamic coupling between the structure motion and fluid motion occurs, resulting in large lift forces. Transverse forces have been observed 4.5 times greater than the drag force.

For rigid structures, however, transverse forces equal to the drag force is a reasonable upper limit. *This upper limit pertains only to rigid structures.* Larger lift forces can occur when there is dynamic interaction between waves and the structure. For a discussion see Laird (1962). The design procedure and discussion that follow pertain only to rigid structures.

7-95

Chang (1964), in a laboratory investigation, found that eddies are shed at a frequency twice the wave frequency. Two eddies were shed after passage of the wave crest (one from each side of the cylinder), and two on the return flow after passage of the trough. The maximum lift force is proportional to the square of the horizontal wave-induced velocity in much the same way as the drag force. Consequently, for design estimates of the lift force, Equation 7-37 may be used.

$$F_L = F_{Lm} \cos 2\theta = C_L \frac{\rho g}{2} DH^2 K_{Dm} \cos 2\theta. \qquad (7-37)$$

where F_L is the lift force, F_{Lm} is the maximum lift force, $\theta = (2\pi x/L - 2\pi t/T)$, and C_L is empirical lift coefficient analogous to the drag coefficient in Equation 7-31. Chang found that C_L depends on the Keulegan-Carpenter (1956) number $\bar{u}_{max} T/D$ where $\bar{u}_{max}$ is the maximum horizontal velocity averaged over the depth. When this number is less than 3, no significant eddy shedding occurs, and no lift forces arise. As $\bar{u}_{max} T/D$ increases, C_L increases until it is approximately equal C_D (for rigid piles only). Bidde (1970, 1971) investigated the ratio of the maximum lift force to the maximum drag force F_{Lm}/F_{Dm} which is nearly equal to C_L/C_D if there is no phase difference between the lift and drag force (this is assumed by Equation 7-37). Figure 7-56 illustrates the dependence of C_L/C_D on $\bar{u}_{max} T/D$. Both Chang and Bidde found little dependence of C_L on Reynolds Number $R_e = \bar{u}_{max} D/\nu$ for the ranges of R_e investigated. The range of R_e investigated is significantly lower than the range to be anticipated in the field, hence the data presented should be interpreted merely as a guide in estimating C_L and then F_L.

The use of Equation 7-37 and Figure 7-56 to estimate lift forces is illustrated by the following example.

* * * * * * * * * * * * * * EXAMPLE PROBLEM * * * * * * * * * * * * * * * *

GIVEN: A design wave with height, H = 10 ft. and period, T = 10 sec. acts on a vertical circular pile with a diameter, D = 1 ft., in a depth, d = 15 ft. Assume $C_M = 2.0$ and $C_D = 0.7$.

FIND: The maximum traverse (lift) force acting on the pile and the approximate time variation of the transverse force assuming that Airy theory adequately predicts the velocity field. Also estimate the maximum total force.
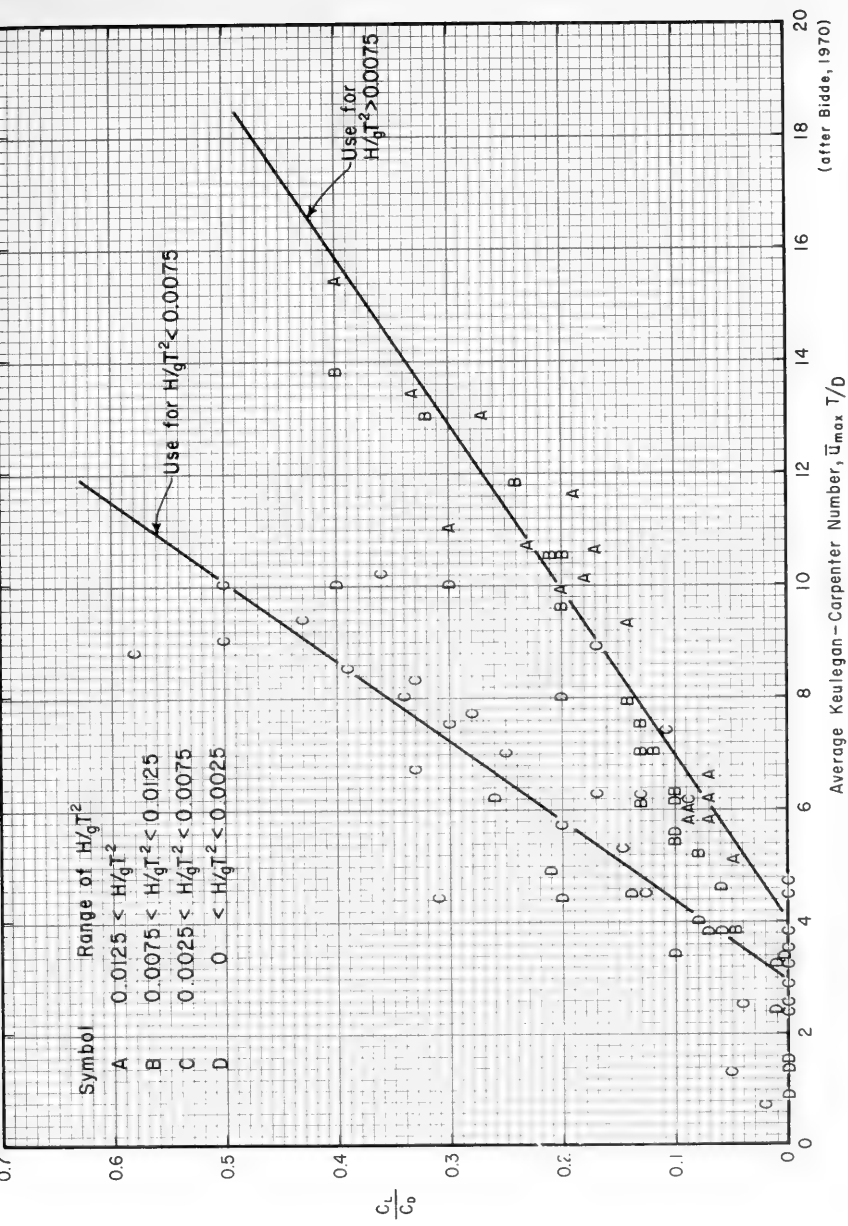
Figure 7-56. Variation of C_L / C_D with Keulegan-Carpenter Number and H/gT^2

(after Bidde, 1970)

7-97

SOLUTION: Calculate,

$$\frac{H}{gT^2} = \frac{10}{(32.2)(10)^2} = 0.0031,$$

$$\frac{d}{gT^2} = \frac{15}{(32.2)(10)^2} = 0.0047,$$

and the average Keulegan-Carpenter number $\overline{u}_{max}$ T/D using the maximum horizontal velocity at the SWL and at the bottom to obtain $\overline{u}_{max}$. Therefore, from Equation 7-16 with z = -d,

$$\left(u_{max}\right)_{bottom} = \frac{H}{2} \frac{gT}{L_A} \frac{1}{\cosh\left[2\pi d / L_A\right]},$$

$$\left(u_{max}\right)_{bottom} = \frac{10}{2} \frac{(32.2)(10)}{215} (0.89) = 6.66 \text{ ft./sec.,}$$

where L_A is found from Figure 7-40 by entering with d/gT^2 and reading $L_A/L_O = 2\pi L_A/gT^2 = 0.42$. Also, $1/\cosh[2\pi d/L]$ is the K value on Figure 7-40. Then, from Equation 7-16 with z = 0,

$$\left(u_{max}\right)_{SWL} = \frac{H}{2} \frac{gT}{L_A},$$

$$\left(u_{max}\right)_{SWL} = \frac{10}{2} \frac{(32.2)(10)}{215} = 7.49 \text{ ft./sec.}$$

The average velocity is therefore,

$$\overline{u}_{max} = \frac{\left(u_{max}\right)_{bottom} + \left(u_{max}\right)_{SWL}}{2},$$

$$\overline{u}_{max} = \frac{6.66 + 7.49}{2} = \frac{14.15}{2} = 7.08 \text{ ft./sec.,}$$

and the average Keulegan-Carpenter number is

$$\frac{\overline{u}_{max} T}{D} = \frac{7.08(10)}{1} = 70.8.$$

The computed value of $\overline{u}_{max}$ T/D is well beyond the range of Figure 7-56, and the lift coefficient should be taken to be equal to the drag coefficient (*for a rigid structure*). Therefore,

$$C_{L_{max}} = C_D = 0.7.$$

7-98

From Equation 7-37,

$$F_L = C_L \frac{\rho g}{2} D H^2 K_{Dm} \cos 2\theta = F_{Lm} \cos 2\theta.$$

The maximum transverse force F_{Lm} occurs when $\cos 2\theta = 1.0$. Therefore,

$$F_{Lm} = 0.7 \frac{(2)(32.2)}{2} (1)(10)^2 (0.7) = 1,580 \text{ lbs.,}$$

where K_{Dm} is found as in the preceding examples. For the example problem the maximum transverse force is equal to the drag force.

Since the inertia component of force is small (preceding example), an estimate of the maximum force can be obtained by vectorially adding the drag and lift forces. Since the drag and lift forces are equal and perpendicular to each other, the maximum force in this case is simply,

$$F_{max} \approx \frac{F_{Lm}}{\cos 45°} = \frac{1580}{0.707} = 2,230 \text{ lbs.,}$$

which occurs about when the crest passes the pile.

The time variation of lift force as given by,

$$F_L = 1,580 \cos 2\theta,$$

is shown in Figure 7-57.

* *

7.315 Selection of Hydrodynamic Force Coefficients C_D and C_M. Values of C_M, C_D and safety factors given in the sections that follow are suggested values only. Selection of C_M, C_D and safety factors for a given design must be dictated by the wave theory used and the purpose of the structure. Values given here are intended for use with the design curves and equations given in preceding sections for preliminary design and for checking design calculations. More accurate calculations require the use of appropriate wave tables such as those of Dean (1973) or Skjelbria, et al. (1960) along with the appropriate C_M and C_D.

a. Factors influencing C_D. The variation of drag coefficient C_D with Reynolds Number R_e for steady flow conditions is shown in Figure 7-58. The Reynolds Number is defined by,

$$R_e = \frac{u D}{\nu}, \tag{7-38}$$
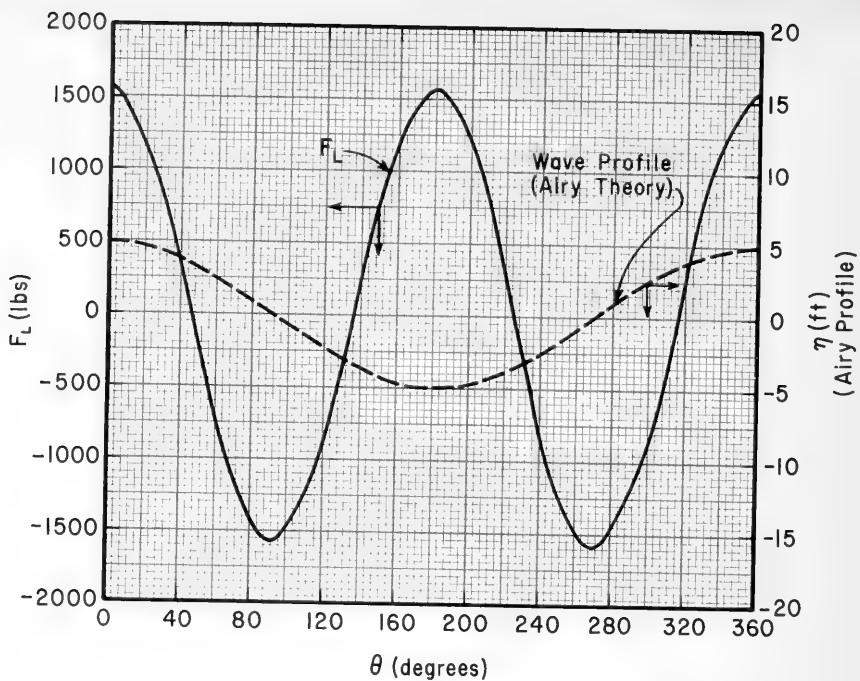
Figure 7-57. Variation of Transverse Lift Force and Wave Profile
(Airy Theory)

7-100
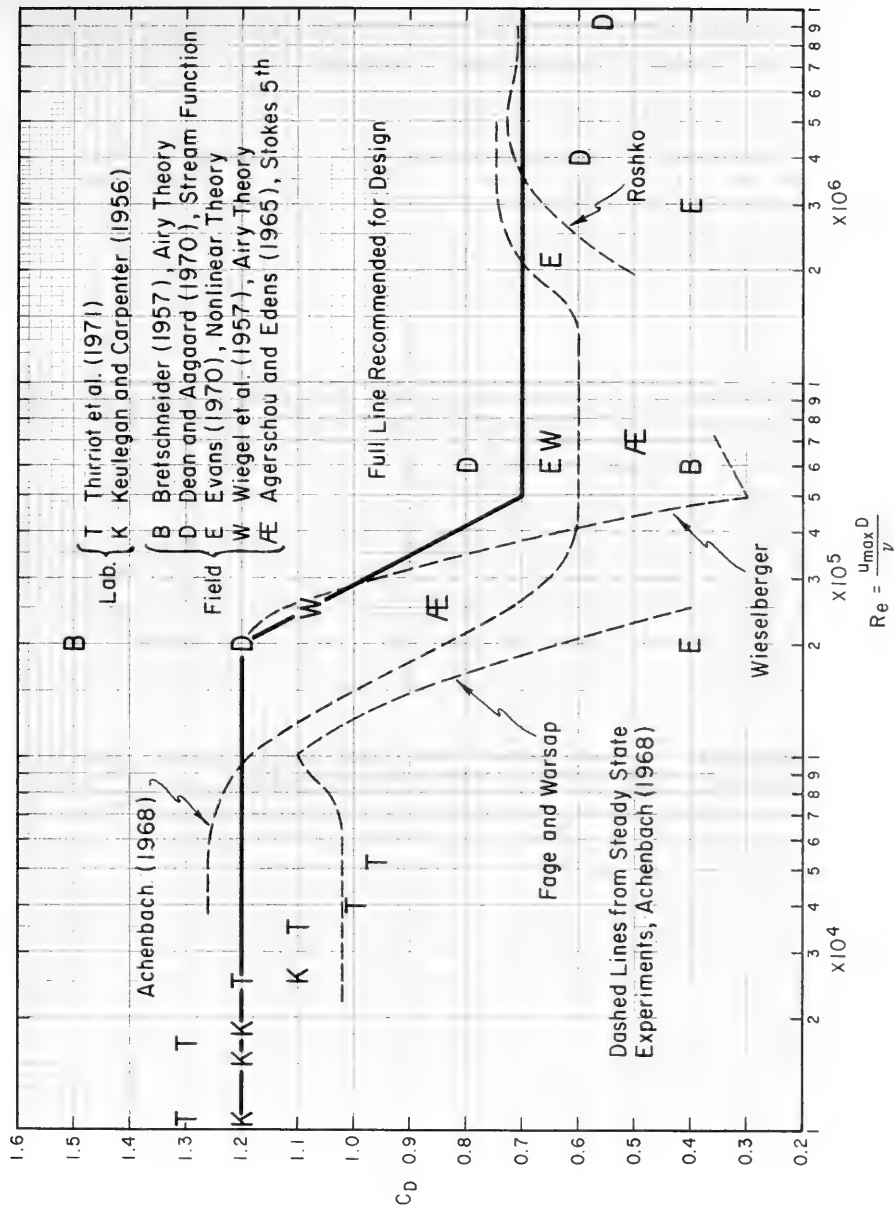
Figure 7-58. Variation of Drag Coefficient, C_D, with Reynolds Number, R_e

7-101

where

   u = velocity,

   D = pile diameter,

   ν = kinematic viscosity (approximately 1.0×10^{-5} ft.^{2}/sec. for sea water.)

Results of steady state experiments are indicated by dashed lines. (Achenbach, 1968.) Taking these results, three ranges of R_e exist:

   (1) Subcritical; $R_e < 1 \times 10^5$ where C_D is relatively constant (≈ 1.2),

   (2) Transitional; $1 \times 10^5 < R_e < 4 \times 10^5$ where C_D varies, and

   (3) Supercritical; $R_e > 4 \times 10^5$; where C_D is relatively constant ($\approx 0.6 - 0.7$).

Thus, depending on the value of the Reynolds number, the results of steady state experiments show that the value of C_D may change by about a factor of 2.

    The steady-flow curves shown in Figure 7-58 show that the values of R_e defining the transitional region vary from investigator to investigator. Generally, the value of R_e at which the transition occurs depends on the roughness of the pile and the ambient level of turbulence in the fluid. A rougher pile will experience the transition at a smaller R_e. In the subcritical region, the degree of roughness has an insignificant influence on the value of C_D. However, in the supercritical region, the value of C_D increases with increasing surface roughness. The variation of C_D with surface roughness is given in Table 7-2.

    The preceding discussion was based on experimental results obtained under steady, unidirectional flow conditions. To apply these results to the unsteady oscillatory flow conditions associated with waves, it is necessary to define a Reynolds number for the wave motion. As Equation 7-16 shows, the fluid velocity varies with time and with position along the pile. In principle, an instantaneous value of the Reynolds number could be calculated, and the corresponding value of C_D used. However the accuracy with which C_D is determined hardly justifies such an elaborate procedure.

    Keulegan and Carpenter (1956), in a laboratory study of forces on a cylindrical pile in oscillatory flow, found that over most of a wave cycle the value of the drag coefficient remained about constant. Since the maximum value of the drag force occurs when the velocity is a maximum, it seems justified to use the maximum value of the velocity u_{max} when

Table 7-2. Steady Flow Drag Coefficients for Supercritical Reynolds' Numbers

Surface of 3-Foot-Diameter Cylinder	Average Drag Coefficient $R_e = 1 \times 10^6$ to 6×10^6
Smooth (polished)	0.59
Bitumastic,* glass fiber, and felt wrap	0.61
Bitumastic, glass fiber, and felt wrap (damaged)	0.66
Number 16 grit sandpaper (approximately equivalent to a vinyl-mastic coating on a 1- to 2-foot-diameter cylinder)	0.76
Bitumastic, glass fiber, and burlap wrap (approximately equivalent to bitumastic, glass fiber, and felt wrap on a 1- to 2-foot-diameter cylinder)	0.78
Bitumastic and oyster shell coating (approximately equivalent to light fouling on a 1- to 2-foot-diameter cylinder)	0.88
Bitumastic and oyster shell with concrete fragments coating (approximately equivalent to medium barnacle fouling on a 1- to 2-foot-diameter cylinder)	1.02

Blumberg and Rigg, 1961

*Bitumastic is a composition of asphalt and filler (as asbestos shorts) used chiefly
as a protective coating on structural metals exposed to weathering or corrosion.
(Webster's Third)

calculating a wave Reynolds number. Furthermore, since the flow near the stillwater level contributes most to the moment around the mudline, the location at which u_{max} is determined is chosen to be $z = 0$. Thus, wave Reynolds number is

$$R_e = \frac{u_{max} D}{\nu} ,$$ (7-39)

where ν = kinematic viscosity of the fluid ($\nu \approx 1.0 \times 10^{-5}$ for salt water), u_{max} = maximum horizontal velocity at $z = 0$, determined from Airy theory, is given by

$$u_{max} = \frac{\pi H}{T} \frac{L_o}{L_A} .$$ (7-40)

The ratio L_A/L_o can be obtained from Figure 7-40.

An additional parameter, the importance of which was cited by Keulegan and Carpenter (1956), is the ratio of the amplitude of particle motion to pile diameter. Using Airy theory, this ratio A/D can be related to a period parameter = $(u_{max} T)/D$ (introduced by Keulegan and Carpenter) by,

$$\frac{A}{D} = \frac{1}{2\pi} \frac{u_{max} T}{D} .$$ (7-41)

When $z = 0$ Equation 7-41 gives

$$A = \frac{H}{2} \frac{1}{\tanh\left[2\pi d/L\right]} = \frac{H}{2} \frac{L_o}{L_A} .$$ (7-42)

The ratio L_A/L_o is from Figure 7-40.

In a recent laboratory study by Thirriot, et al. (1971), it was found that for

$$\frac{A}{D} > 10 , \quad C_D \approx C_D \text{ (steady flow)} ;$$

$$1 < \frac{A}{D} < 10 , \quad C_D > C_D \text{ (steady flow)} .$$

Combining this with Equation 7-42, the steady state value of C_D should apply to oscillatory motion, provided

$$\frac{A}{D} = \frac{H}{2D} \frac{L_o}{L_A} > 10 ,$$ (7-43)

7-104

or equivalently,

$$\frac{H}{D} > 20 \frac{L_A}{L_o}$$ (7-44)

* * * * * * * * * * * * * * EXAMPLE PROBLEM * * * * * * * * * * * * * * *

GIVEN: A design wave with height, H = 10 ft., period, T = 10 sec. in a depth, d = 15 ft. acts on a pile of diameter, D = 1 ft.

FIND: Is the condition expressed by the inequality of Equation 7-44 satisfied?

SOLUTION: Calculate,

$$\frac{d}{gT^2} = 0.00466 \ .$$

From Figure 7-40:

$$\frac{L_A}{L_o} = 0.41$$

Then,

$$\frac{H}{D} = \frac{10}{1} = 10 > 20 \frac{L_A}{L_o} = 8.2 \ .$$

Therefore, the inequality is satisfied and the steady state C_D can be used.

* *

Thirriot, et al. (1971) found that the satisfaction of Equation 7-44 was necessary only when $R_e < 4 \times 10^4$. For larger Reynolds numbers, they found C_D approximately equal to the steady flow C_D, regardless of the value of A/D. It is therefore unlikely that the condition imposed by Equation 7-44 will be encountered in design. However, it is important to realize the significance of this parameter when interpreting data of small-scale experiments. The average value of all the C_D's obtained by Keulegan and Carpenter (1956) is $(C_D)_{avg} = 1.52$. The results plotted in Figure 7-58 (Thirriot, et al., 1971) that account for the influence of A/D show that $C_D \approx 1.2$ is a more representative value for the range of Reynolds numbers covered by the experiments.

To obtain experimental values for C_D for large Reynolds numbers, field experiments are necessary. Such experiments require simultaneous measurement of the surface profile at or near the test pile and the forces acting on the pile. Values of C_D (and C_M) obtained from prototype-scale experiments depend critically on the wave theory used to estimate fluid flow fields from measured surface profiles.

* * * * * * * * * * * * * * EXAMPLE PROBLEM * * * * * * * * * * * * * * * * *

GIVEN: When the crest of a wave, with H = 10 ft. and T = 10 sec., passes a pile of D = 1 ft., in 15 ft. of water, a force $F = F_{Dm} = 1,500$ lbs. is measured.

FIND: The appropriate value of C_D.

SOLUTION: From Figure 7-44 as in the problem of the preceding section, $K_{Dm} = 0.7$ when $H = 0.87 H_b$. The measured force corresponds to F_{Dm}, therefore, rearranging Equation 7-31,

$$C_D = \frac{F_{Dm}}{(1/2)\rho g\, D\, H^2\, K_{Dm}}$$

$$C_D = \frac{1500}{(1/2)(2)(32.2)(1)(10)^2(0.7)} = 0.66$$

If Airy theory had been used $(H \approx 0)$, Figure 7-44 with $d/gT^2 = 0.0047$ would give $K_{Dm} = 0.235$ and therefore

$$\left(C_D\right)_{Airy} = \left[\left(C_D\right)_{H=0.87\,H_b}\right] \frac{\left(K_{Dm}\right)_{H=0.87\,H_b}}{\left(K_{Dm}\right)_{Airy\,(H\approx 0)}} = 0.66\,\frac{0.7}{0.235} = 1.96 \ .$$

* *

* * * * * * * * * * * * * * EXAMPLE PROBLEM * * * * * * * * * * * * * * * * *

GIVEN: Same conditions as preceding example, but with a wave height, H = 50 ft., a depth, d = 100 ft., and $F = F_{Dm} = 30,000$ lbs.

FIND: The appropriate value of C_D.

SOLUTION: From Figure 7-47 $H_b = 66$ ft; then $H/H_b = 50/66 = 0.76$. Entering Figure 7-44 with $d/gT^2 = 0.031$, $K_{Dm} = 0.38$ is found. Therefore, from Equation 7-31,

$$C_D = \frac{F_{Dm}}{1/2\,\rho g\, D\, H^2\, K_{Dm}}$$

$$C_D = \frac{30,000}{1/2\,(2)(32.2)(1)(50)^2(0.38)} = 0.98 \ .$$

If Airy theory had been used $K_{Dm} = 0.17$, and

$$\left(C_D\right)_{Airy} = \left[\left(C_D\right)_{H=0.76 H_b}\right] = \frac{\left(K_{Dm}\right)_{H=0.76 H_b}}{\left(K_{Dm}\right)_{Airy\ (H \approx 0)}} = (0.98) \frac{(0.38)}{(0.17)} = 2.19 \ .$$

Some of the difference between the two values of C_D is because the SWL (instead of the wave crest) was the upper limit of the integration performed to obtain K_{Dm} for Airy theory. The remaining difference is because Airy theory is unable to describe accurately the water-particle velocities of finite-amplitude waves.

* *

The two examples show the influence of the wave theory used on the value of C_D determined from a field experiment. Since the determination of wave forces is the inverse problem, i.e., C_D and wave conditions known, *it is important in force calculations to use a wave theory that is equivalent to the wave theory used to obtain the value of* C_D *(and* C_M*)*. A wave theory that accurately describes the fluid motion should be used in the analysis of experimental data to obtain C_D (and C_M) and in design calculations.

Results obtained by several investigators for the variation of C_D with Reynolds number are indicated in Figure 7-58. The solid line is generally conservative, and is recommended for design along with Figures 7-44 and 7-46 with the Reynolds number defined by Equation 7-38.

* * * * * * * * * * * * * * EXAMPLE PROBLEM * * * * * * * * * * * * * * * * *

<u>DETERMINE:</u> Were the values of C_D used in the preceding example problems reasonable?

<u>SOLUTION:</u> For the first example with H = 10 ft., T = 10 sec., d = 15 ft. and D = 1 ft., from Equation 7-40,

$$u_{max} = \left(\frac{\pi H}{T} \frac{L_o}{L_A}\right) \ ,$$

$$u_{max} = \frac{\pi 10}{10} \frac{1}{0.41} = 7.66 \ \text{ft./sec.}$$

From Equation 7-39,

$$R_e = \frac{u_{max} D}{\nu}$$

$$R_e = \frac{(7.66)(1)}{1 \times 10^{-5}} = 7.66 \times 10^5 \ .$$

7-107

From Figure 7-58, $C_D = 0.7$, which is the value used in the preceding example.

For the example with H = 50 ft., T = 10 sec., d = 100 ft., and D = 1 ft., from Equation 7-40,

$$u_{max} = \frac{\pi(10)}{(10)} \frac{(1)}{(0.9)} = 3.5 \text{ ft./sec.}$$

From Equation 7-39,

$$R_e = \frac{(3.5)(1)}{(1 \times 10^{-5})} = 3.5 \times 10^5.$$

From Figure 7-58, $C_D = 0.9$ which is less than the value of $C_D = 1.2$ used in the force calculation. Consequently, the force calculation gave a high force estimate.

* *

b. Factors Influencing C_M. MacCamy and Fuchs (1954) found by theory that for small ratios of pile diameter to wavelength,

$$C_M = 2.0 . \tag{7-45}$$

This is identical to the result obtained for a cylinder in accelerated flow of an ideal or nonviscous fluid. (Lamb, 1932.) The theoretical prediction of C_M can only be considered an estimate of this coefficient. The effect of a real viscous fluid, which accounted for the term involving C_D in Equation 7-41, will drastically alter the flow pattern around the cylinder, and invalidate the analysis leading to $C_M = 2.0$. The factors influencing C_D also influence the value of C_M.

No quantitative dependence of C_M on Reynolds number has been established, although Bretschneider (1957) indicated a decrease in C_M with increasing R_e. However for the range of Reynolds numbers ($R_e < 3 \times 10^4$) covered by Keulegan and Carpenter (1956), the value of the parameter A/D plays an important role in determining C_M. For A/D < 1 they found $C_M \approx 2.0$. Since for small values of A/D the flow pattern probably deviates only slightly from the pattern assumed in the theoretical development, the result of $C_M = 2.0$ seems reasonable. A similar result was obtained by Jen (1968) who found $C_M \approx 2.0$ from experiments when A/D < 0.4. For larger A/D values that are closer to actual design conditions, Keulegan and Carpenter found a minimum $C_M \approx 0.8$, for A/D ≈ 2.5, and found that C_M increased from 1.5 to 2.5 for 6 < A/D < 20.

Just as for C_D, Keulegan and Carpenter showed that C_M was nearly constant over a large part of the wave period, therefore supporting the initial assumption of constant C_M and C_D.

Table 7-3 presents values of C_M reported by various investigators. The importance of considering which wave theory was employed when determining C_D from field experiments is equally important when dealing with C_M.

Based on the information in Table 7-3, the following choice of C_M is recommended for use in conjunction with Figures 7-43 and 7-44:

$$\left. \begin{array}{ll} C_M = 2.0, & \text{when } R_e < 2.5 \times 10^5, \\[2ex] C_M = 2.5 - \dfrac{R_e}{5 \times 10^5}, & \text{when } 2.5 \times 10^5 < R_e < 5 \times 10^5, \\[2ex] C_M = 1.5, & \text{when } R_e > 5 \times 10^5. \end{array} \right\} \quad (7\text{-}46)$$

with R_e defined by Equation 7-39.

Table 7-3. Experimentally Determined Values of C_M

Investigator	Approximate R_e	C_M *	Type of Experiment and Theory Used
Keulegan and Carpenter (1956)	$< 3 \times 10^4$	1.5 to 2.5	Oscillatory laboratory flow (A/D 6)
Bretschneider (1957)	1.6×10^5 to 2.3×10^5	2.26 to 2.02	Field experiments
	3.8×10^5 to 6×10^5	1.74 to 1.23	Linear Theory
Wilson (1965)	large ($> 5 \times 10^5$)	1.53	Field experiment, spectrum
Skjelbreia (1960)	large ($> 5 \times 10^5$)	1.02 ± 0.53	Field experiments, Stokes' Fifth Order Theory
Dean and Aagaard (1970)	2×10^5 to 2×10^6	1.2 to 1.7	Field experiments, Stream-function Theory
Evans (1970)	large ($> 5 \times 10^5$)	1.76 ± 1.05	Field experiments, Numerical Wave Theory or Stokes' Fifth Order Theory
Wheeler (1970)	large ($> 5 \times 10^5$)	1.5	Field experiments, Modified spectrum analysis using $C_D = 0.6$ and $C_M = 1.5$ the standard deviation of the calculated peak force was 33 percent

* Range or mean ± standard deviation.

The values of C_M given in Table 7-3 show that Skjelbria (1960), Dean and Aagaard (1970) and Evans (1970), used almost the same experimental data, and yet estimated different values of C_M. The same applies to their determination of C_D, but while the recommended choice of C_D from Figure 7-58 is generally conservative, from Equation 7-46 the recommended choice of C_M for $R_e > 5 \times 10^5$ corresponds approximately to the average of the reported values. This possible lack of conservatism, however, is not significant since the inertia force component is generally smaller than the drag force component for design conditions. From Equations 7-30 and 7-31 the ratio of maximum inertia force to maximum drag force becomes

$$\frac{F_{im}}{F_{Dm}} = \frac{\pi}{2} \frac{C_M}{C_D} \frac{D}{H} \frac{K_{im}}{K_{Dm}} \qquad (7\text{-}47)$$

For example, if $C_M \approx 2\, C_D$ and a design wave corresponding to $H/H_b = 0.75$ is assumed, the ratio F_{im}/F_{Dm} may be written (using Figures 7-43 and 7-44 as

$$\frac{F_{im}}{F_{Dm}} \approx \begin{cases} 1.25\, \dfrac{D}{H} & \text{(shallow-water waves)} \\[2ex] 5.35\, \dfrac{D}{H} & \text{(deepwater waves)} \end{cases} \qquad (7\text{-}48)$$

Since D/H will generally be smaller than unity for a design wave, the inertia-force component will be much smaller than the drag-force component for shallow-water waves, and the two force components will be of comparable magnitude only for deepwater waves.

7.316 Example Problem and Discussion of Choice of a Safety Factor.

* * * * * * * * * * * * * * EXAMPLE PROBLEM * * * * * * * * * * * * * * *

GIVEN: A design wave with height, H = 35 ft. and period, T = 12 sec, acts on a pile with diameter, D = 4 ft. in water of depth, d = 85 ft.

FIND: The wave force on the pile.

SOLUTION: Compute,

$$\frac{H}{gT^2} = \frac{35}{(32.2)\,(12)^2} = 0.00755 \ ,$$

and

$$\frac{d}{gT^2} = \frac{85}{(32.2)\,(12)^2} = 0.0183 \ .$$

From Figure 7-40, for $d/gT^2 = 0.0183$,

$$\frac{L_A}{L_o} = 0.75 \; ,$$

and

$$L_A = 0.75 \; L_o = 0.75 \; \frac{gT^2}{2\pi} = 0.75 \; \frac{(32.2)\,(12)^2}{2\pi} = 554 \; \text{ft.}$$

From Figure 7-41, for $d/gT^2 = 0.0183$,

$$\frac{\eta_c}{H} = 0.68 \; ,$$

and therefore,

$$\eta_c = 0.68 \; H = 0.68 \, (35) = 23.8 \; \text{ft.,}$$

say

$$\eta_c = 24 \; \text{ft.}$$

The structure supported by the pile must be 24 feet above the still-water line to avoid uplift forces on the superstructure by the given wave.

Calculate, from Equation 7-14,

$$\frac{D}{L_A} = \frac{4}{554} = 0.0072 < 0.05 \; .$$

Therefore Equation 7-13 is valid.

From Figure 7-47,

$$\frac{H_b}{gT^2} = 0.014 \; \text{ft./sec}^2,$$

$$\frac{H}{H_b} = \left(\frac{H}{gT^2} \middle/ \frac{H_b}{gT^2} \right) = \frac{0.00755}{0.014} = 0.54 \; .$$

From Figures 7-43 through 7-46,

$$K_{im} = 0.405$$

$$K_{Dm} = 0.37$$

$$S_{im} = 0.62$$

$$S_{Dm} = 0.82 \; .$$

7-111

From Equations 7-39 and 7-40,

$$u_{max} = \frac{\pi H}{T} \left(\frac{L_o}{L_A} \right) = \frac{\pi \ 35}{12} \ \frac{1}{0.75} = 12.2 \ \text{ft./sec.,}$$

and

$$R_e = \frac{u_{max} D}{\nu} = \frac{(12.2)(4)}{1 \times 10^{-5}} = 4.88 \times 10^6 .$$

From Figure 7-58,

$$C_D = 0.7 \ ,$$

and from Equation 7-46, with $R_e > 5 \times 10^5$,

$$C_M = 1.5 \ .$$

Therefore,

$$F_{im} = C_M \ \rho g \ \frac{\pi D^2}{4} \ H \ K_{im} ,$$

$$F_{im} = (1.5)(2)(32.2) \ \frac{\pi (4)^2}{4} \ (35)(0.405) = 17,200 \ \text{lbs.,}$$

$$F_{Dm} = C_D \ \frac{1}{2} \ \rho g \ D \ H^2 \ K_{Dm} ,$$

$$F_{Dm} = (0.7)(0.5)(2)(32.2)(4)(35)^2 (0.37) = 40,800 \ \text{lbs.,}$$

$$M_{im} = F_{im} \ d \ S_{im} = (17,200)(85)(0.62) = 906,000 \ \text{ft. lbs.,}$$

$$M_{Dm} = F_{Dm} \ d \ S_{Dm} = (40,800)(85)(0.82) = 2,840,000 \ \text{ft. lbs.}$$

From Equation 7-34,

$$W = \frac{C_M D}{C_D H} = \frac{1.5 \ (4)}{0.7 \ (35)} = 0.245 \ .$$

Interpolating between Figures 7-49 and 7-50 with $H/gT^2 = 0.00755$ and $d/gT^2 = 0.0183$,

$$\phi_m = 0.20 \ .$$

Therefore, from Equation 7-35,

$$F_m = \phi_m \ w \ C_D \ H^2 D,$$

$$F_m = (0.20)(64)(0.7)(35)^2 \ (4) = 43,900 \ \text{lbs.}$$

Interpolating between Figures 7-53 and 7-54 gives

$$\alpha_m = 0.16 \ .$$

Therefore, from Equation 7-36,

$$M_m = \alpha_m \ w \ C_D \ H^2 \ Dd \ ,$$

$$M_m = (0.16)(64)(0.7)(35)^2(4)(85) = 2,985,000 \ \text{lb.-ft.},$$

say

$$M_m = 2,990,000 \ \text{lb.-ft.}$$

* *

Before designing the pile or performing the foundation analysis, a safety factor is usually applied to calculated forces. It seems pertinent to indicate (Bretschneider, 1965) that the design wave is often a large wave, with little probability of being exceeded during the life of the structure. Also, since the experimentally determined values of C_M and C_D show a large scatter, values of C_M and C_D could be chosen so that they would rarely be exceeded. Such an approach is quite conservative. For the recommended choice of C_M and C_D when used with the generalized graphs, the results of Dean and Aagaard (1970) show that predicted peak force deviated from measured force by at most ±50 percent.

When the design wave is unlikely to occur, it is recommended that a safety factor of 1.5 be applied to calculated forces and moments and that this nominal force and moment be used as the basis for structural and foundation design for the pile.

Some design waves may occur frequently. For example, maximum wave height could be limited by the depth at the structure. *If the design wave is likely to occur, a larger safety factor, say greater than 2, may be applied* to account for the uncertainty in C_M and C_D.

In addition to the safety factor, changes occurring during the expected life of the pile should be considered in design. Such changes as scour at the base of the pile and added pile roughness due to marine growth may be important. For flow conditions corresponding to super-critical Reynolds numbers (Table 7-3) the drag coefficient C_D will increase with increasing roughness.

The design procedure presented above is a static procedure; forces are calculated and applied to the structure statically. The dynamic nature of forces from wave action must be considered in the design of some offshore structures. When a structure's natural frequency of

oscillation is such that a significant amount of energy in the wave spectrum is available at that frequency, the dynamics of the structure must be considered. In addition, stress reversals in structural members subjected to wave forces may cause failure by fatigue. If fatigue problems are anticipated, the safety factor should be increased or allowable stresses should be decreased. Evaluation of these considerations is beyond the scope of this manual.

Corrosion and fouling of piles also require consideration in design. Corrosion decreases the strength of structural members. Consequently, corrosion rates over the useful life of an offshore structure must be estimated, and the size of structural members increased accordingly. Watkins (1969) provides some guidance in the selection of corrosion rates of steel in seawater. Fouling of a structural member by marine growth increases the roughness and effective diameter of the member, and increases forces on the member. Guidance on selecting a drag coefficient C_D can be obtained from Table 7-2. However, the increased diameter must be carried through the entire design procedure to determine forces on a fouled member.

7.317 Calculation of Forces and Moments on Groups of Vertical Cylindrical Piles. To find the maximum horizontal force and the moment around the mudline for a group of piles supporting a structure, the approach presented in Section 7.312 must be generalized. Figure 7-59 shows an example group of piles subjected to wave action. The design wave concept assumes a two-dimensional (long crested) wave; hence the x-direction is chosen as the direction of wave propagation. Choosing a reference pile located at x = 0, the x-coordinate of each pile in the group may be determined from,

$$x_n = \ell_n \cos\alpha_n, \tag{7-49}$$

where the subscript n refers to a particular pile, and ℓ_n and α_n are as defined in Figure 7-59. If the distance between any two adjacent piles is large enough, the forces on a single pile will be unaffected by the presence of the other piles. The problem is simply one of finding the maximum force on a series of piles.

In Section 7.312, the force variation in a single vertical pile as a function of time was found. If the design wave is assumed to be a wave of permanent form (i.e. it does not change form as it propagates), the variation of force at a particular point with time is the same as the variation of force with distance at an instant in time. By introducing the phase angle

$$\theta = \frac{2\pi x}{L} - \frac{2\pi t}{T}, \tag{7-50}$$

where L is wavelength, the formulas given in Section 7.313 (equations 7-18 and 7-19) for a pile located at x = 0 may be written in general form by introducing θ, defined by $2\pi x/L - 2\pi t/T$ in place of $-2\pi t/T$.
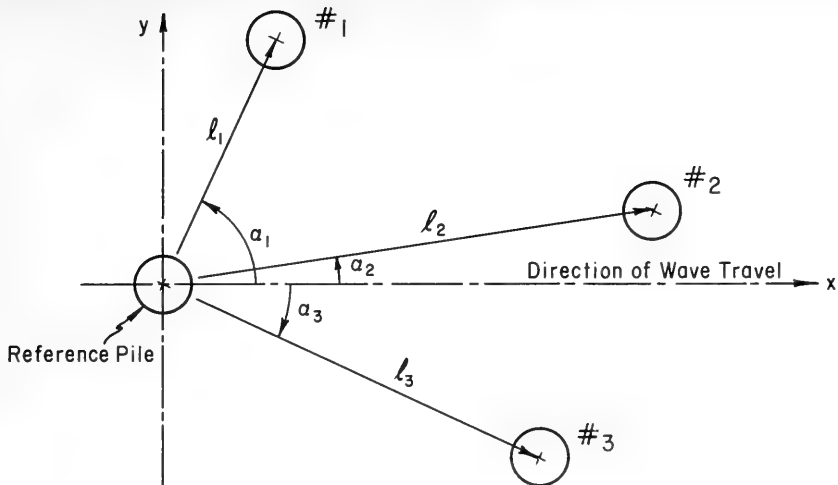
Figure 7-59. Definition Sketch - Calculation of Wave Forces on a Group of Piles that are Structurally Connected

Using tables (Skjelbreia, et al., 1960, and Dean, 1973), it is possible to calculate the total horizontal force $F(x)$ and moment around the mudline $M(x)$ as a function of distance from the wave crest x.   By choosing the location of the reference pile at a certain position $x = x_r$ relative to the design wave crest the total force, or moment around the mudline, is obtained by summation,

$$F_{Total} = \sum_{n=0}^{N-1} F\left(x_r + x_n'\right),$$ (7-51)

$$M_{Total} = \sum_{n=0}^{N-1} M\left(x_r + x_n\right).$$ (7-52)

where

N = total number of piles in the group,

$x_o = 0,$

x_n = from Equation 7-49,

x_r = location of reference pile relative to wave crest.

Repeating this procedure for various choices of x_r it is possible to determine the maximum horizontal force and moment around the mudline for the pile group.

$F_D(\theta)$ is an even function, and $F_i(\theta)$ is an odd function, hence

$$F_D(\theta) = F_D(-\theta), \tag{7-53}$$

and

$$F_i(\theta) = -F_i(-\theta). \tag{7-54}$$

and calculations need only be done for $0 \le \theta \le \pi$ radians. Equations 7-53 and 7-54 are true for any wave that is symmetric about its crest, and are therefore applicable if the wave tables of Skjelbria, et al. (1960) and Dean (1973) are used. When these tables are used, the wavelength computed from the appropriate finite amplitude theory should be used to transform θ into distance from the wave crest, x.

The procedure is illustrated by the following examples. For simplicity, Airy theory is used and only maximum horizontal force is considered. The same computation procedure is used for calculating maximum moment.

* * * * * * * * * * * * * * EXAMPLE PROBLEM * * * * * * * * * * * * * * * *

GIVEN: A design wave with height, H = 35 ft. and period, T = 12 sec. in a depth, d = 85 ft. acts on a pile with a diameter, D = 4 ft. (assume Airy theory to be valid).

FIND: The variation of the total force on the pile as a function of distance from the wave crest.

SOLUTION: From an analysis similar to that in Section 7.315,

$$C_D = 0.7,$$

and

$$C_M = 1.5 .$$

From Figures 7-43 and 7-44 using the curve for Airy theory with

$$\frac{d}{gT^2} = \frac{85}{32.2\,(12)^2} = 0.0183 ,$$

$$K_{im} = 0.378 ; \; K_{Dm} = 0.195,$$

and from Equations 7-30 and 7-31,

$$F_{im} = 1.5\,(2)\,(32.2)\,\frac{\pi(4)^2}{4}\,(35)\,(0.378) = 16{,}100 \;\; \text{lbs.},$$

$$F_{Dm} = 0.7\,(0.5)\,(2)\,(32.2)\,(4)\,(35)^2\,(0.195) = 21{,}500 \;\; \text{lbs.}$$

Combining Equations 7-22 and 7-26 gives

$$F_i = F_{im}\,\sin\theta ,$$

and combining Equations 7-23 and 7-27 gives

$$F_D = F_{Dm} \cos \theta \, | \cos \theta |,$$

where

$$\theta = \frac{2\pi x}{L} - \frac{2\pi t}{T}.$$

The wavelength can be found from Figure 7-40,

$$L \approx L_A = 554 \text{ ft.}$$

From Table 7-4 or Figure 7-60 the maximum force on the example pile occurs when $20° < \theta < 40°$, and is about $F_m \approx 25,000$ lbs.

Table 7-4. Example Calculation of Wave Force Variation with Phase Angle

θ (deg.)	x (ft.)	$F_i = F_{im} \sin \theta$ (lbs.)	$F_D = F_{Dm} \lvert \cos \theta \rvert \cos \theta$ (lbs.)	$F(\theta) = F_i + F_D$ (lbs.)	$F(-\theta) = F_D - F_i$ (lbs.)
0	0	0	21,500	21,500	21,500
20	30.8	5,500	19,000	24,500	13,500
40	61.6	10,350	12,600	22,950	2,250
60	92.4	13,950	5,370	19,220	−8,580
80	123.2	15,850	650	16,500	−15,200
100	154.0	15,850	−650	15,200	−16,500
120	184.8	13,950	−5,370	8,580	−19,220
140	215.6	10,350	−12,600	−2,250	−22,950
160	246.4	5,500	−19,000	−13,500	−24,500
180	277.2	0	−21,500	−21,500	−21,500

* *

* * * * * * * * * * * * * * EXAMPLE PROBLEM * * * * * * * * * * * * * * *

GIVEN: Two piles each with a diameter, D = 4 ft., spaced 100 ft. apart are acted on by a design wave having a height, H = 35 ft., a period, T = 12 sec. in a depth, d = 85 ft. The direction of wave approach makes an angle of 30° with a line joining the pile centers.

FIND: The maximum horizontal force experienced by the pile group and the location of the reference pile with respect to the wave crest (phase angle) when the maximum force occurs.

SOLUTION: The variation of total force on a single pile with phase angle θ was computed from Airy theory for the preceding problem and is given in Figure 7-60 and Table 7-4. Figure 7-60 will be used
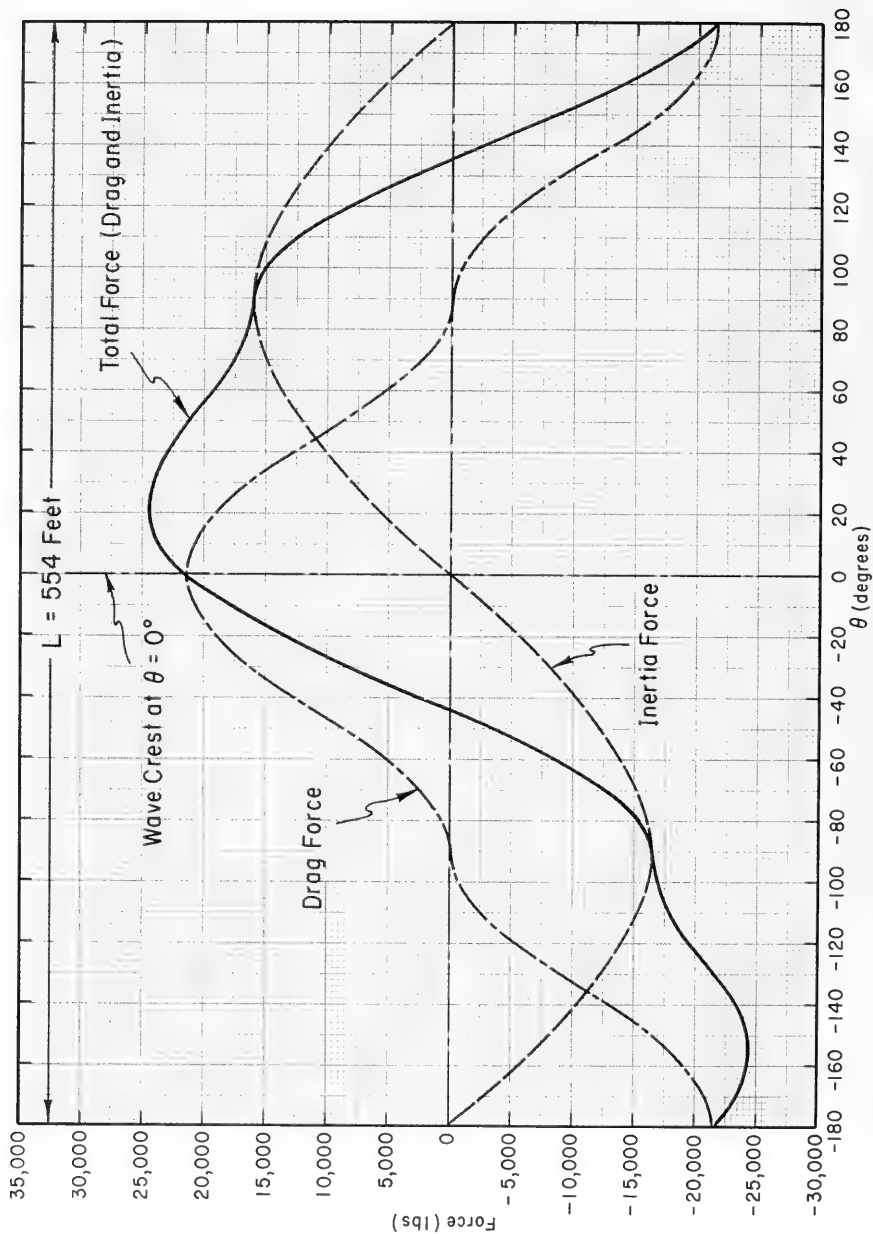
Figure 7-60. Example Variation of Drag, Inertia and Total Wave Forces with Phase Angle, θ, for a Circular Pile

7-118

to compute the maximum horizontal force on the two-pile group. Compute the phase difference between the two piles by Equation 7-49,

$$x_n = \ell_n \cos \alpha_n = 100 \, (\cos 30°),$$

$$x_n = 86.6 \text{ ft.}$$

From the previous example problem, $L \approx L_A = 554$ ft. for $d = 85$ ft. and $T = 12$ secs. Then from the expression,

$$\frac{x}{L} = \frac{\theta_n}{2\pi} \,,$$

$$\theta_n = \frac{2\pi x}{L} = \frac{2\pi \, (86.6)}{554} = 0.982 \text{ radians},$$

or

$$\theta_n = \frac{360° \, (86.6)}{554} = 56.3° \,.$$

Figure 7-60 can be shifted by 56.3° to represent the variation of force on the second pile with phase angle as shown in Figure 7-61. The total horizontal force is the sum of the two curves ($F_m = 42,000$ lbs). The same procedure can be used for any number of piles with one curve for each pile. Table 7-4 can be used similarly simply by offsetting the force values by an amount equal to 56.3°. The procedure is also applicable to moment computations.

Figure 7-61 shows the maximum force to be about 42,000 lbs. when the wave crest is about 8° or [(8°/360°) 554] $\approx$ 12 ft. in front of the reference pile.

Because Airy theory does not accurately describe the flow field of finite amplitude waves, a correction to the computed maximum force as determined above could be applied. This correction factor for structures of minor importance might be taken as the ratio of maximum total force on a single pile for an appropriate finite-amplitude theory to maximum total force on the same pile as computed by Airy theory. For the example, the forces on a single pile are (from preceding example problems),

$$\left(F_m\right)_{\textit{finite amplitude}} = 43,900 \text{ lbs.} \,,$$

and

$$\left(F_m\right)_{\textit{Airy}} = 25,000 \text{ lbs.}$$
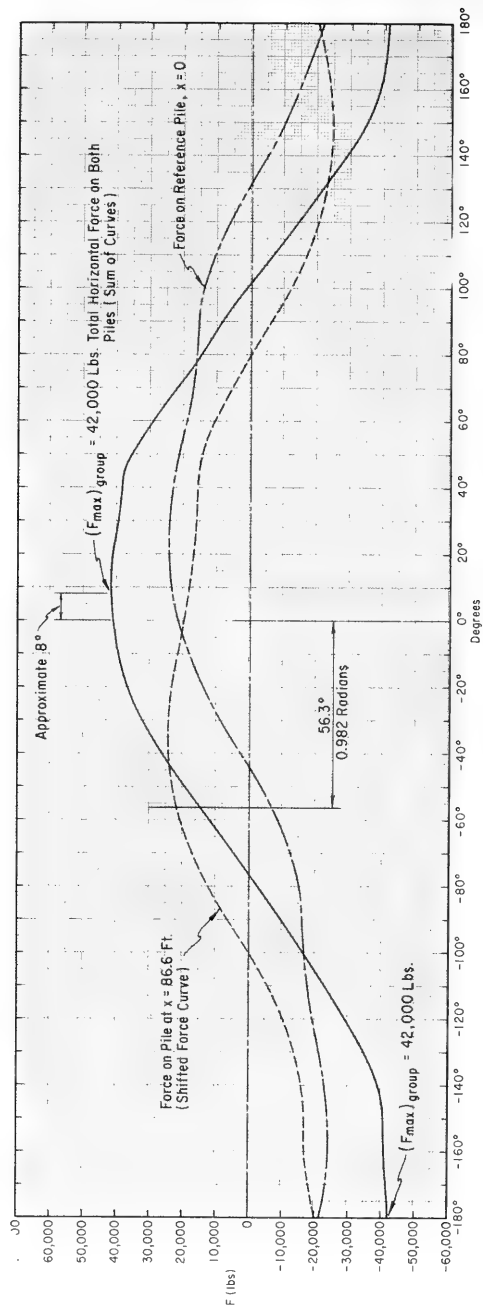
Figure 7-61. Example Calculation of Total Force on a Two-Pile Group

Therefore, the total force on the 2-pile group, corrected for the finite amplitude design wave, is given by,

$$[F_{Total}]_{2\text{-}piles} = \frac{(F_m)_{finite\ amplitude}}{(F_m)_{Airy}} [F_{Total}]_{2\text{-}piles}$$

(corrected for finite amplitude design wave)

(computed from Airy theory)

$$[F_{Total}]_{2\text{-}piles} = \frac{43,900}{25,000} (42,000) = 73,750 \text{ lbs., say } 73,800 \text{ lbs.}$$

* *

This approach is an approximation, and should be limited to rough calculations for checking purposes only. The use of tables of finite amplitude wave properties (Skjelbria, et al., 1960 and Dean, 1973) is recommended for design calculations.

As the distance between piles becomes small relative to the wavelength, maximum forces and moments on pile groups may be conservatively estimated by adding the maximum forces or moments on each pile.

The assumption that piles are unaffected by neighboring piles is not valid when distance between piles is less than three times the pile diameter. A few investigations evaluating the effects of nearby piles are summarized by Dean and Harleman (1966).

7.318 Calculation of Forces on a Nonvertical Cylindrical Pile. A single, nonvertical pile subjected to the action of a two-dimensional design wave traveling in the + x direction is shown in Figure 7-62. Since forces are perpendicular to the pile axis, it is reasonable to calculate forces by Equation 7-13 using components of velocity and acceleration perpendicular to the pile. Experiments (Bursnall and Loftin, 1951) indicate this approach may not be conservative, since the drag force component depends on resultant velocity rather than on the velocity component perpendicular to the pile axis. To consider these experimental observations, the following procedure is recommended for calculating forces on nonvertical piles.

For a given location on the pile (x_o, y_o, z_o in Figure 7-62), the force per unit length of pile is taken as the horizontal force per unit length of a fictitious vertical pile at the same location.

* * * * * * * * * * * * * * EXAMPLE PROBLEM * * * * * * * * * * * * * * * * *

GIVEN: A pile with diameter D = 4 ft. at an angle of 45° with the horizontal in the x-z plane is acted on by a design wave with height H = 35 ft., period T = 12 sec. in a depth d = 85 ft.
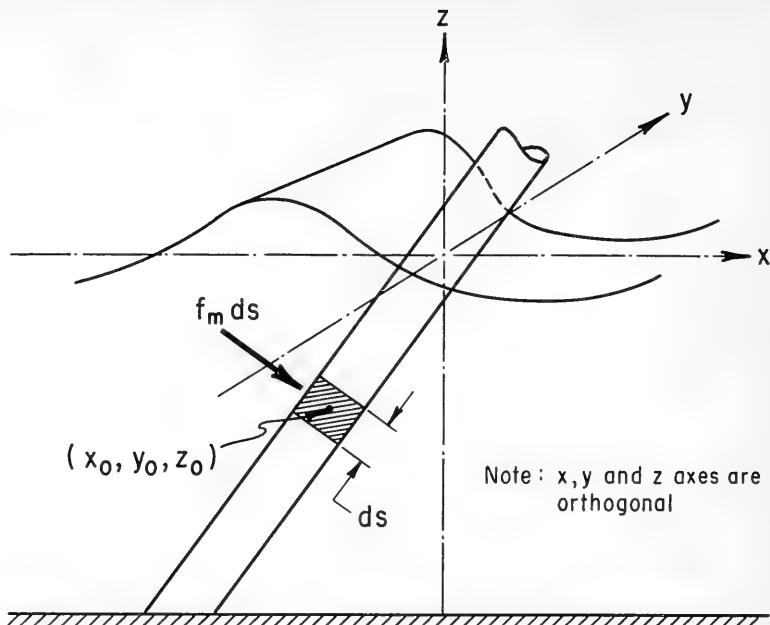
Figure 7-62. Definition Sketch - Calculation of Wave Forces on a Nonvertical Pile

FIND: The maximum force per unit length on the pile 30 ft. below the SWL (z = -30 ft.).

SOLUTION: For simplicity, Airy theory is used. From preceding examples, $C_M = 1.5$, $C_D = 0.7$, and $L = L_A = 554$ feet.

From Equation 7-18, with sin $(-2\pi t/T) = 1.0$,

$$f_{im} = C_M \; \rho g \; \frac{\pi D^2}{4} \; H \; \frac{\pi}{L} \; \frac{\cosh[2\pi(d+z)/L]}{\cosh[2\pi d/L]} \; ,$$

$$f_{im} = 1.5 \, (2) \, (32.2) \, \frac{\pi(4)^2}{4} \, (35) \, \frac{\pi}{554} \, (0.8) = 193 \; \text{lbs./ft.}$$

From Equation 7-19, with cos $(2\pi t/T) = 1.0$,

$$f_{Dm} = C_D \; \frac{\rho g}{2} \; DH^2 \; \frac{gT^2}{4L^2} \left[\frac{\cosh[2\pi(d+z)/L]}{\cosh[2\pi d/L]} \right]^2 ,$$

$$f_{Dm} = 0.7 \, \frac{(2)(32.2)}{(0.5)} \, (4) \, (35)^2 \, \frac{(32.2)(12)^2}{(4)(554)^2} \, (0.8)^2 = 267 \; \text{lb./ft.}$$

7-122

The maximum force can be assumed to be given by

$$f_m = f_{Dm} \frac{F_m}{F_{Dm}} ,$$

where F_m and F_{Dm} are given by Equations 7-35 and 7-31. Substituting these equations into the above gives

$$f_m = f_{Dm} \frac{\phi_m\ wC_D\ H^2D}{C_D(\rho g/2)H^2DK_{Dm}} = f_{Dm} \frac{2\phi_m}{K_{Dm}} .$$

From Equation 7-34,

$$W = \frac{C_M D}{C_D H} = \frac{1.5\,(4)}{0.7\,(35)} = 0.245 .$$

Interpolating between Figures 7-49 and 7-50 with $H/gT^2 = 0.00755$ and $d/gT^2 = 0.0183$, it is found that $\phi_m = 0.20$

From a preceding problem,

$$\frac{H}{H_b} = 0.54 .$$

Enter Figure 7-44 with $d/gT^2 = 0.0183$ and using the curve labeled $1/2\ H_b$ read

$$K_{Dm} = 0.35 .$$

Therefore,

$$f_m = f_{Dm} \frac{2\phi_m}{K_{Dm}} ,$$

$$f_m = 267 \frac{2\,(0.20)}{0.35} = 305\ \text{lb./ft.}$$

say

$$f_m = 300\ \text{lb./ft.}$$

The maximum horizontal force per unit length at $z = -30$ ft. on the fictitious vertical pile is $f_m = 300$ lbs./ft. This is also taken as the maximum force per unit length perpendicular to the actual inclined pile.

* *

7-123

7.319 Calculation of Forces and Moments on Cylindrical Piles Due to Breaking Waves. Forces and moments on vertical cylindrical piles due to breaking waves can, in principle, be calculated by a procedure similar to that outlined in Section 7.312 by using the generalized graphs with $H = H_b$. This approach is recommended for waves breaking in deep water. (See Section 2.6, BREAKING WAVES.)

For waves in shallow water, the inertia force component is small compared to the drag force component. The force on a pile is therefore approximately

$$F_m \approx F_{Dm} = C_D \frac{1}{2} \rho g D H^2 K_{Dm} \qquad (7\text{-}55)$$

Figure 7-44, for shallow-water waves with $H = H_b$, gives $K_{Dm} = 0.96 \approx 1.0$; consequently the total force may be written

$$F_m = C_D \frac{1}{2} \rho g D H_b^2 \qquad (7\text{-}56)$$

From Figure 7-46, the corresponding lever arm is $d_b S_{Dm} \approx d_b$ (1.11) and the moment about the mudline becomes

$$M_m = F_m \left(1.11 \, d_b\right) \qquad (7\text{-}57)$$

Small-scale experiments ($R_e \approx 5 \times 10^4$ by Hall, 1958) indicate that

$$F_m \approx 1.5 \, \rho g D H_b^2 \qquad (7\text{-}58)$$

and

$$M_m \approx F_m \, H_b \qquad (7\text{-}59)$$

Comparison of Equation 7-56 with Equation 7-58 shows that the two equations are identical if $C_D = 3.0$. This value of C_D is 2.5 times the value obtained from Figure 7-58. ($C_D = 1.2$ for $R_e \approx 5 \times 10^4$.) From Section 2.6, since H_b generally is smaller than (1.11) d_b, it is conservative to assume the breaker height approximately equal to the lever arm, 1.11 d_b. *Thus, the procedure outlined in Section 7.312 may also be used for breaking waves in shallow water. However, C_D should be the value obtained from Figure 7-58 multiplied by 2.5.*

Since the Reynolds number generally will be in the supercritical region, where according to Figure 7-58, $C_D = 0.7$ it is recommended to calculate breaking wave forces using

$$\left(C_D\right)_{breaking} = 2.5 \, (0.7) = 1.75 \qquad (7\text{-}60)$$

The above recommendation is based on limited information; however, large-scale experiments by Ross (1959) partially support its validity.

For shallow-water waves near breaking, the velocity near the crest approaches the celerity of wave propagation. Thus, as a first approximation the horizontal velocity near the breaker crest is

$$u_{crest} \approx \sqrt{g \, d_b} \approx \sqrt{g \, H_b} \, , \tag{7-61}$$

where H_b is taken approximately equal to d_b, the depth at breaking. Using Equation 7-61 for the horizontal velocity, and taking $C_D = 1.75$, the force per unit length of pile near the breaker crest becomes

$$f_{Dm} \approx C_D \frac{1}{2} \rho D u_{crest}^2 \approx 0.88 \, \rho g \, D H_b \, . \tag{7-62}$$

Table 7-5 is a comparison between the result calculated from Equation 7-62 with measurements by Ross (1959) on a 1-foot diameter pile $(R_e \approx 1.3 \times 10^6)$.

Table 7-5. Comparison of Measured and Calculated Breaker Force*

Breaker Height (ft.)	f_{Dm} † (lbs./ft.)	f_{Dm} ‡ (lbs./ft.)
3.7	207	220
3.8	213	250
4.1	230	125
4.2	235	170
4.2	235	280
4.9	275	250

* Values given are force per unit length of pile near breaker crest.
† Calculated from Equation 7-62.
‡ Measured by Ross, 1959.

Based on this comparison, the choice of $C_D = 1.75$ for $R_e > 5 \times 10^5$ appears justified for calculating forces and moments due to breaking waves in shallow water.

7.3110 Calculation of Forces on Noncircular Piles. The basic force equation (Equation 7-13) can be generalized for piles of other than circular cross section, if the following substitutions are made

$$\frac{\pi D^2}{4} = \text{volume per unit length of pile} \, , \tag{7-63}$$

where

$\quad\quad\quad D$ = area perpendicular to flow direction per unit length of pile.

Substituting the above quantities for a given noncircular pile cross section, Equation 7-13 may be used. The coefficients K_{im}, etc., depend only on the flow field, and are independent of pile cross-section geometry; therefore, the generalized graphs are still valid. However, the hydrodynamic coefficients C_D and C_M, depend strongly on the cross-section shape of the pile. If values for C_D and C_M corresponding to the type of pile to be used are available, the procedure is identical to the one presented in previous sections.

Keulegan and Carpenter (1956) performed tests on flat plate in oscillating flows. Equation 7-13 in the form applicable for a circular cylinder, with D taken equal to the width of the plate gave

and

$$\left.\begin{array}{c} 3 < C_M < 4.5 \\[2mm] 1.8 < C_D < 2.7 \end{array}\right\} \text{ for } \frac{A}{D} > 10 \qquad (7\text{-}64)$$

The fact that C_D approaches the value of 1.8 as A/D (Equation 7-43) increases is in good agreement with results obtained under steady flow conditions. (Rouse, 1950.)

The following procedure is proposed for estimating forces on piles having sharp-edged cross sections for which no empirical data are available for values of C_M and C_D.

a. The width of the pile measured perpendicular to the flow direction is assumed to be the diameter of an equivalent circular cylindrical pile, D.

b. The procedures outlined in the preceding sections are valid, and the formulas are used as if the pile were of circular cross section with diameter D.

c. The hydrodynamic coefficients are chosen within the range given by Equation 7-64, i.e., $C_M \approx 3.5$ and $C_D \approx 2.0$.

This approach is approximate, and should be used with caution. More accurate analyses require empirical determination of C_M and C_D for the pile geometry under consideration.

Forces resulting from action of broken waves on piles are much smaller than forces due to breaking waves. When pile-supported structures are constructed in the surf zone, lateral forces from the largest wave breaking on the pile should be used for design. (See Section 7.12.) While breaking-wave forces in the surf zone are great per unit length of pile, the pile length actually subjected to wave action is usually short, hence resulting in a small total force. Pile design in this region is usually governed primarily by vertical loads acting along the pile axis.

7.32 NONBREAKING WAVE FORCES ON WALLS

7.321 <u>General</u>. In an analysis of wave forces on structures, a distinction is made between the action of *nonbreaking, breaking,* and *broken* waves. (See Section 7.12, SELECTION OF DESIGN WAVE.) Forces due to nonbreaking waves are primarily hydrostatic. Broken and breaking waves exert an additional force due to the dynamic effects of turbulent water and the compression of entrapped air pockets. Dynamic forces may be much greater than hydrostatic forces. Therefore, structures located where waves break are designed for greater forces than those exposed only to nonbreaking waves.

7.322 <u>Nonbreaking Waves</u>. Typically, shore structures are located in depths where waves will break against them. However, in protected regions or where the fetch is limited, and when depth at the structure is greater than about 1.5 times the maximum expected wave height, nonbreaking waves may occur.

Sainflou (1928) proposed a method for determining the pressure due to nonbreaking waves. The advantage of his method has been ease of application, since the resulting pressure distribution may be reasonably approximated by a straight line. Experimental observations by Rundgren (1958), have indicated Saniflou's method overestimates the nonbreaking wave force for steep waves. The higher order theory by Miche (1944), as modified by Rundgren (1958), to consider the wave reflection coefficient of the structure, appears to best fit experimentally measured forces on vertical walls. Design curves presented here have been developed from the Miche-Rundgren equations.

7.323 <u>Miche-Rundgren: Nonbreaking Wave Forces</u>. Wave conditions at a structure and seaward of a structure (when no reflected waves are shown) are depicted in Figure 7-63. The wave height that would exist at the structure if the structure were not present is the incident wave height, H_i. The wave height that actually exists at the structure is the sum of H_i, and the height of the wave reflected by the structure, H_r. The wave reflection coefficient, χ, is defined as the ratio of H_r to H_i ($\chi = H_r/H_i$). Wave height at the wall, H_w, is given as

$$H_w = H_i + H_r = (1 + \chi)\, H_i \qquad (7\text{-}65)$$

If reflection is complete, and the reflected wave has the same amplitude as the incident wave, then $\chi = 1$, and the height of the *clapotis* or *standing wave* at the structure will be $2H_i$. See Figure 7-63 for definition of terms associated with a clapotis at a vertical wall. The height of the clapotis crest above the bottom is given by

$$y_c = d + h_o + \frac{1 + \chi}{2}\, H_i \qquad (7\text{-}66)$$

The height of the clapotis trough above the bottom is given by,

$$y_t = d + h_o - \frac{1 + \chi}{2}\, H_i \qquad (7\text{-}67)$$

7-127
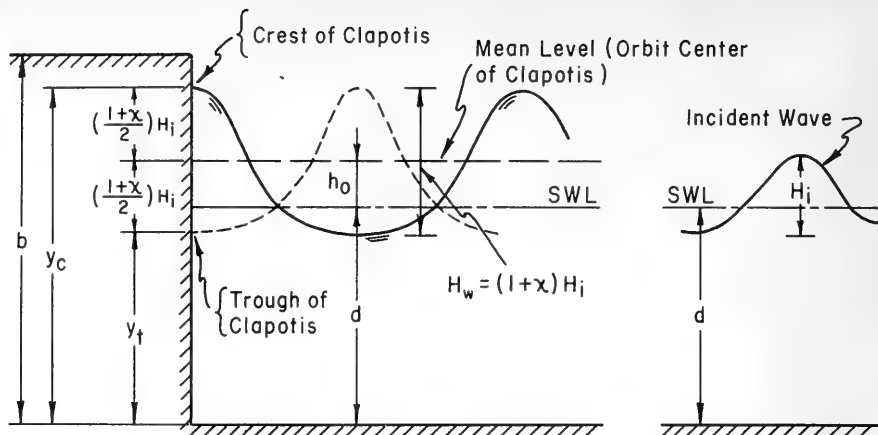
d = Depth from Stillwater Level

H_i = Height of Original Free Wave (In Water of Depth, d)

χ = Wave Reflection Coefficient

h_0 = Height of Clapotis Orbit Center (Mean Water Level at Wall) Above the Stillwater Level (See Figures 7-65 and 7-68)

y_c = Depth from Clapotis Crest = $d + h_0 + \left(\dfrac{1+\chi}{2} \right) H_i$

y_t = Depth from Clapotis Trough = $d + h_0 - \left(\dfrac{1+\chi}{2} \right) H_i$

b = Height of Wall

Figure 7-63. Definition of Terms--Nonbreaking Wave Forces

The reflection coefficient, and consequently clapotis height and wave force, depends on the geometry and roughness of the reflecting wall and possibly on wave steepness and the "wave height-to-water depth" ratio. Domzig (1955), and Greslou and Mahe (1954), have shown that the reflection coefficient decreases with both increasing wave steepness and "wave height-to-water-depth" ratio. Goda and Abe (1968) indicate that for reflection from smooth vertical walls this effect may be due to measurement techniques, and could be only an apparent effect. Until additional research is available, it should be assumed that smooth vertical walls completely reflect incident waves and $\chi = 1$. Where wales, tiebacks or other structural elements increase the surface roughness of the wall by retarding vertical motion of the water, a lower value of χ may be used. A lower value of χ also may be assumed when the wall is built on a rubble base or when rubble has been placed seaward of the structure toe. *Any value of χ less than 0.9 should not be used for design purposes.*

Pressure distributions of the crest and trough of a clapotis at a vertical wall are shown in Figure 7-64. When the crest is at the wall, pressure increases from zero at the free water surface to $wd + p_1$ at the bottom, where p_1 is given as

$$p_1 = \left(\frac{1 + \chi}{2}\right) \frac{w H_i}{\cosh(2\pi d/L)} \tag{7-68}$$
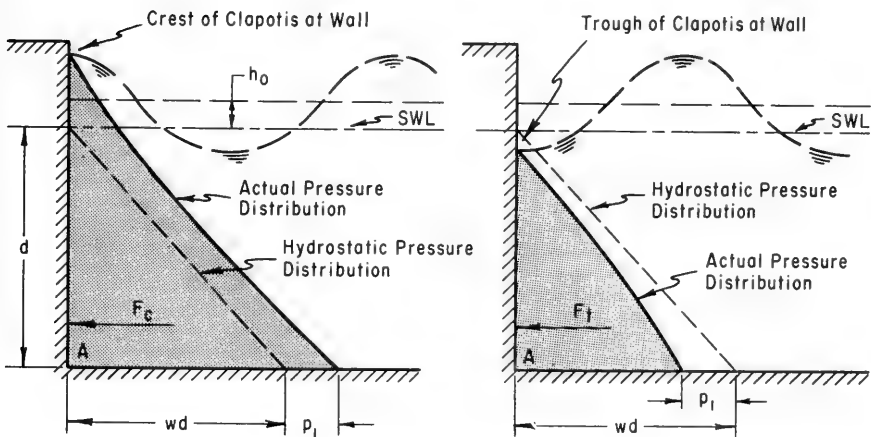
Figure 7-64. Pressure Distributions - Nonbreaking Waves

7-129

When the trough is at the wall, pressure increases from zero at the water surface to $wd - p_1$ at the bottom. The approximate magnitude of wave force may be found if the pressure is assumed to decrease linearly from the free surface to the bottom when either the crest or trough is at the wall. Figures 7-65 through 7-70 permit a more accurate determination of forces and moments resulting from a nonbreaking wave at a wall. Figures 7-65, 7-66, and 7=67 show the dimensionless height of the clapotis orbit center above stillwater level, dimensionless horizontal force, and dimensionless moment about the bottom of the wall for a reflection coefficient, $\chi = 1$. Figures 7-68 through 7-70 represent identical dimensionless parameters for $\chi = 0.9$. The use of the figures to determine forces and moments is illustrated in the following example.

* * * * * * * * * * * * * * * EXAMPLE PROBLEM * * * * * * * * * * * * * * * *

GIVEN:

(a) Smooth-faced vertical wall ($\chi = 1.0$).

(b) Wave height at structure if structure were not there, $H_i = 5.0$ feet.

(c) Depth at structure, $d = 10.0$ feet.

(d) Range of wave periods to be considered in design,
    $T = 6$ sec. (minimum) $T = 10$ sec. (maximum)

FIND: The nonbreaking wave force and moments against a vertical wall resulting from the given wave conditions.

SOLUTION: Details of the computations are given for only the 6-second wave. From the given information, compute H_i/d and H_i/gT^2 for the design condition:

$$\frac{H_i}{d} = \frac{5.0}{10.0} = 0.5 , \quad \frac{H_i}{gT^2} = \frac{5.0}{32.2 \, (6)^2} = 0.0043 . \quad (T = 6 \text{ sec.})$$

Enter Figure 7-65 (because the wall is smooth) with the computed value of H_i/gT^2, and determine the value of h_o/H_i from the curve for $H_i/d = 0.5$. (If the wave characteristics fall outside of the dashed line, the structure will be subjected to breaking or broken waves, and the method for calculating breaking wave forces should be used.)

For $\dfrac{H_i}{gT^2} = 0.0043,$ $\qquad\qquad$ $\dfrac{h_o}{H_i} = 0.70.$ $\qquad\qquad$ (T = 6 sec.)

Therefore,

$$h_o = 0.70 \, (H_i) = 0.70 \, (5.0) = 3.5 \text{ ft.} \qquad (T = 6 \text{ sec.})$$

7-130
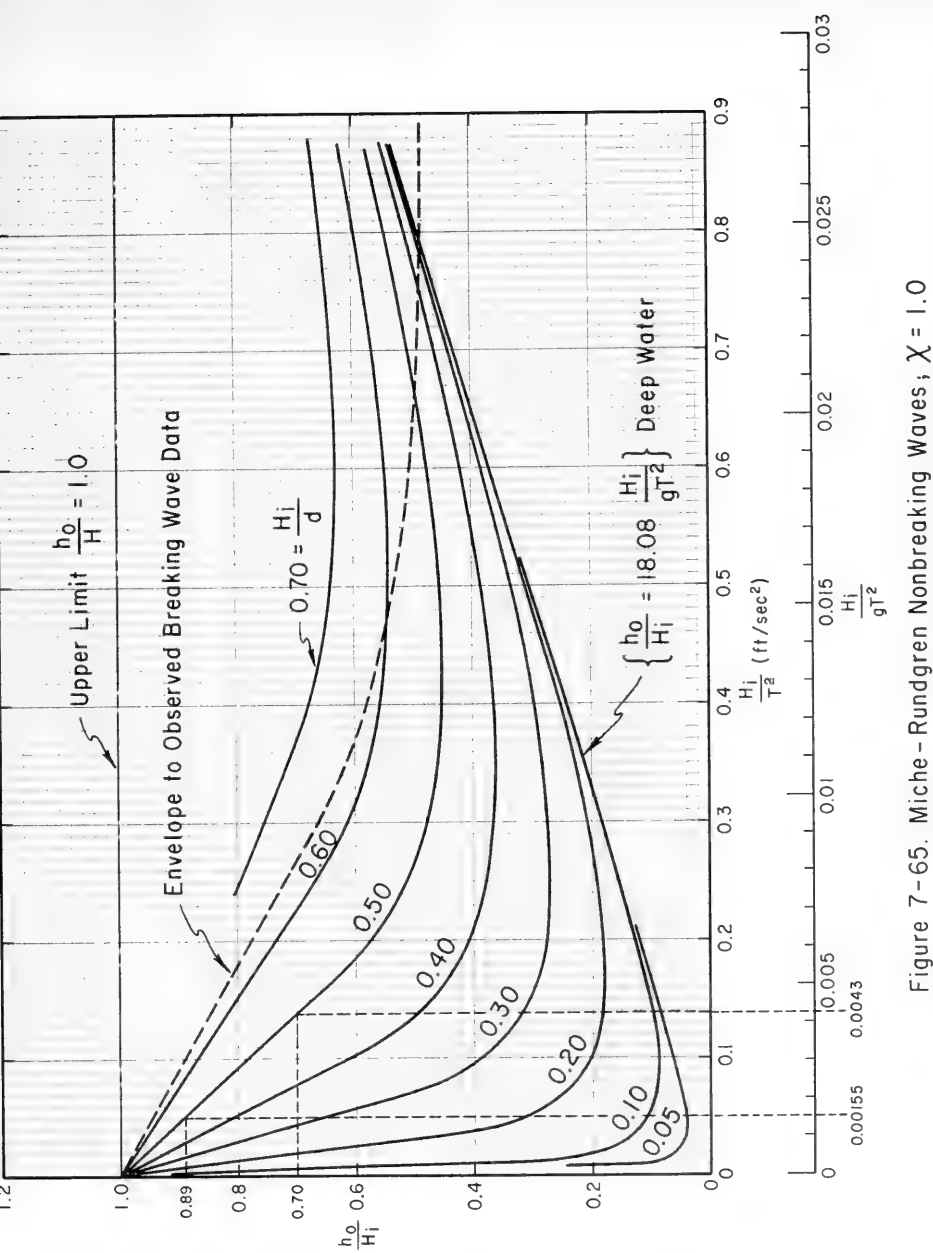
Figure 7-65. Miche-Rundgren Nonbreaking Waves; $X = 1.0$
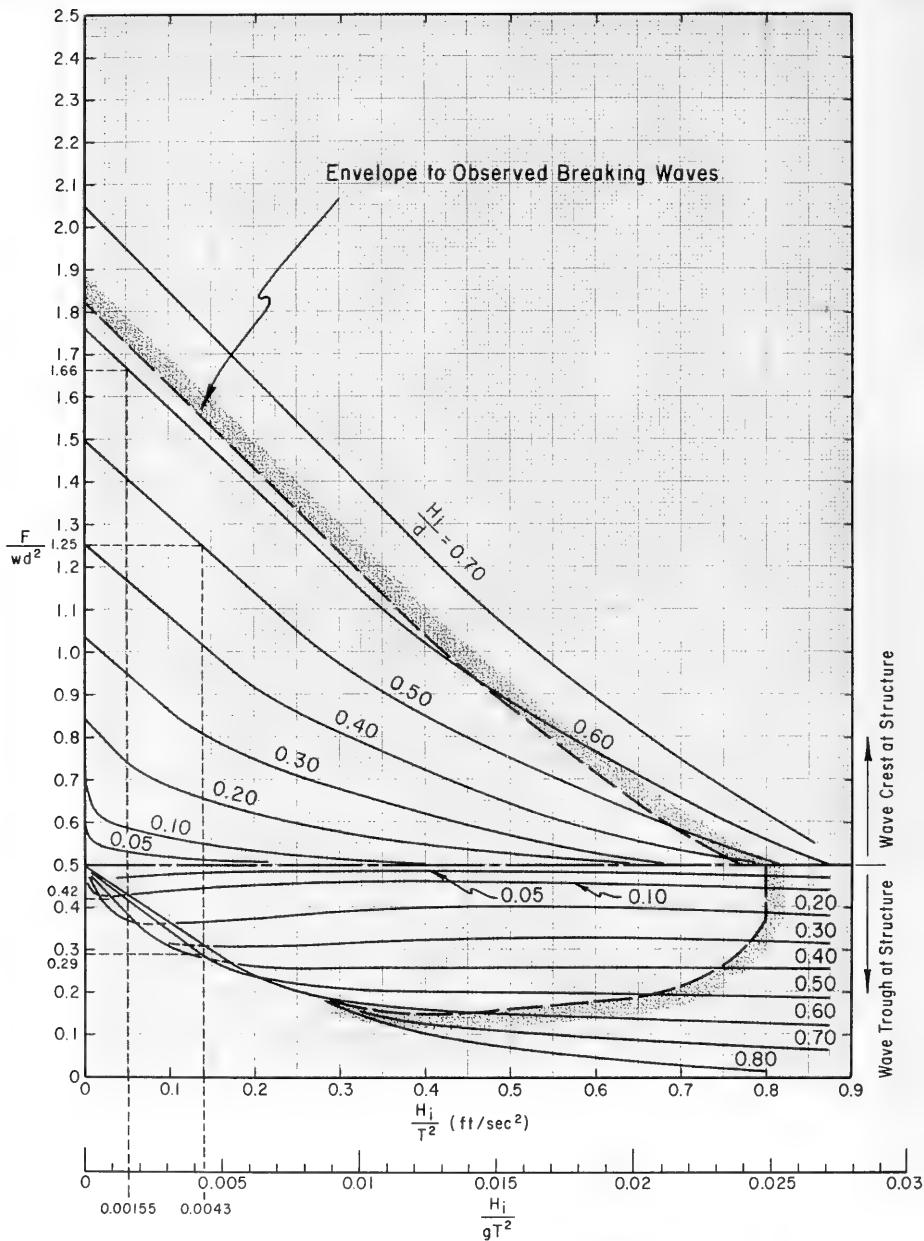
Figure 7-66. Miche-Rundgren Nonbreaking Wave Forces; $\chi = 1.0$
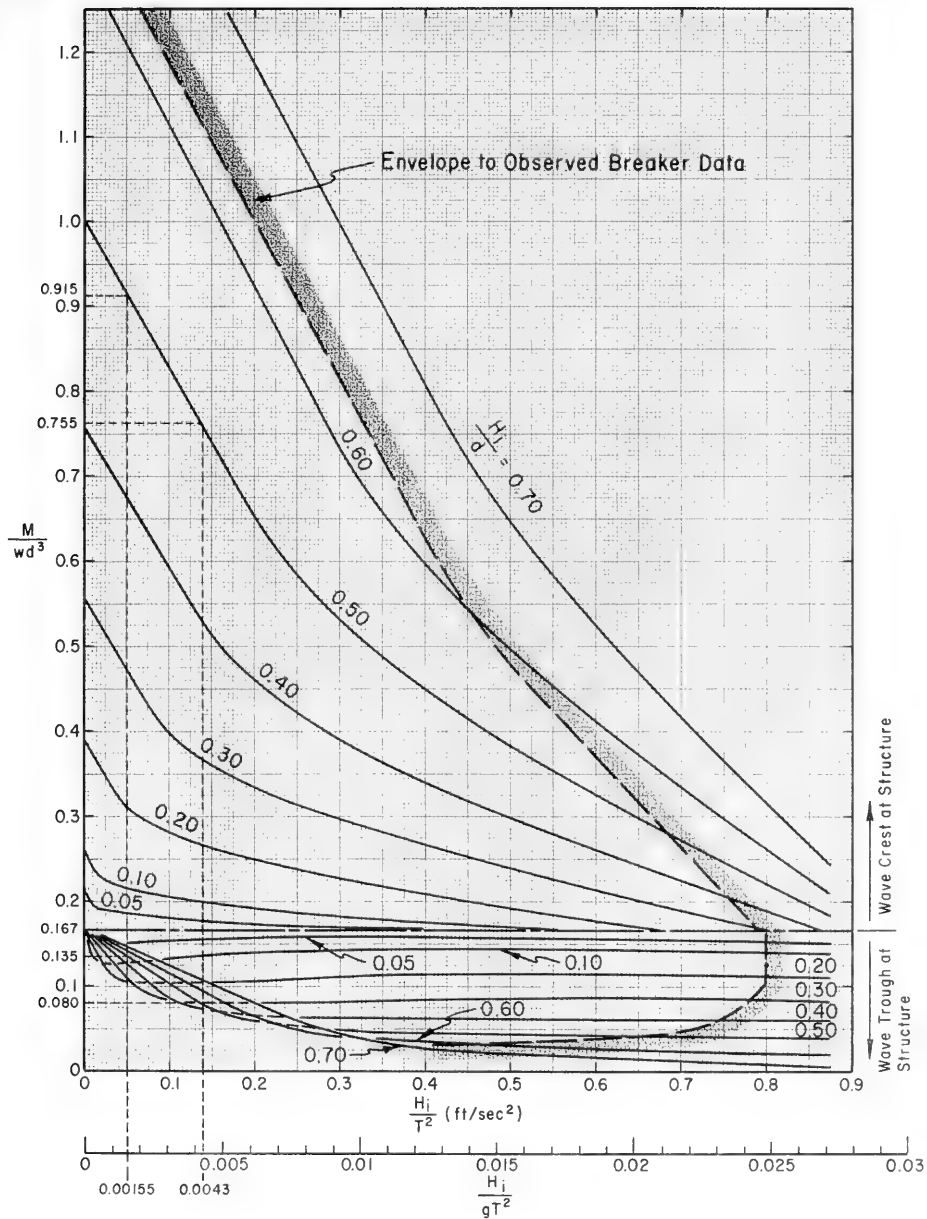
Figure 7-67. Miche-Rundgren Nonbreaking Wave Moment; $\chi = 1.0$
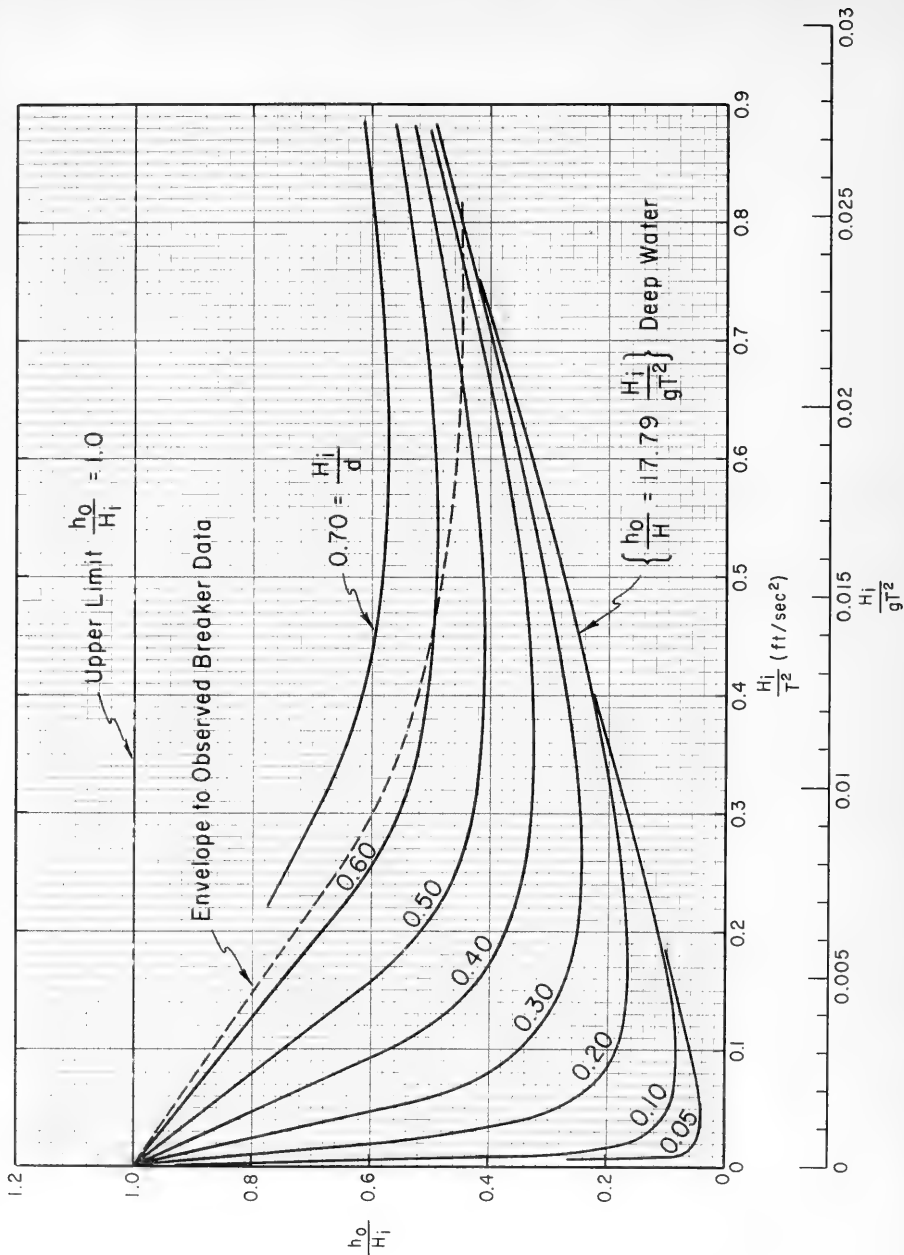
Figure 7-68. Miche-Rundgren Nonbreaking Waves; $\chi = 0.9$.
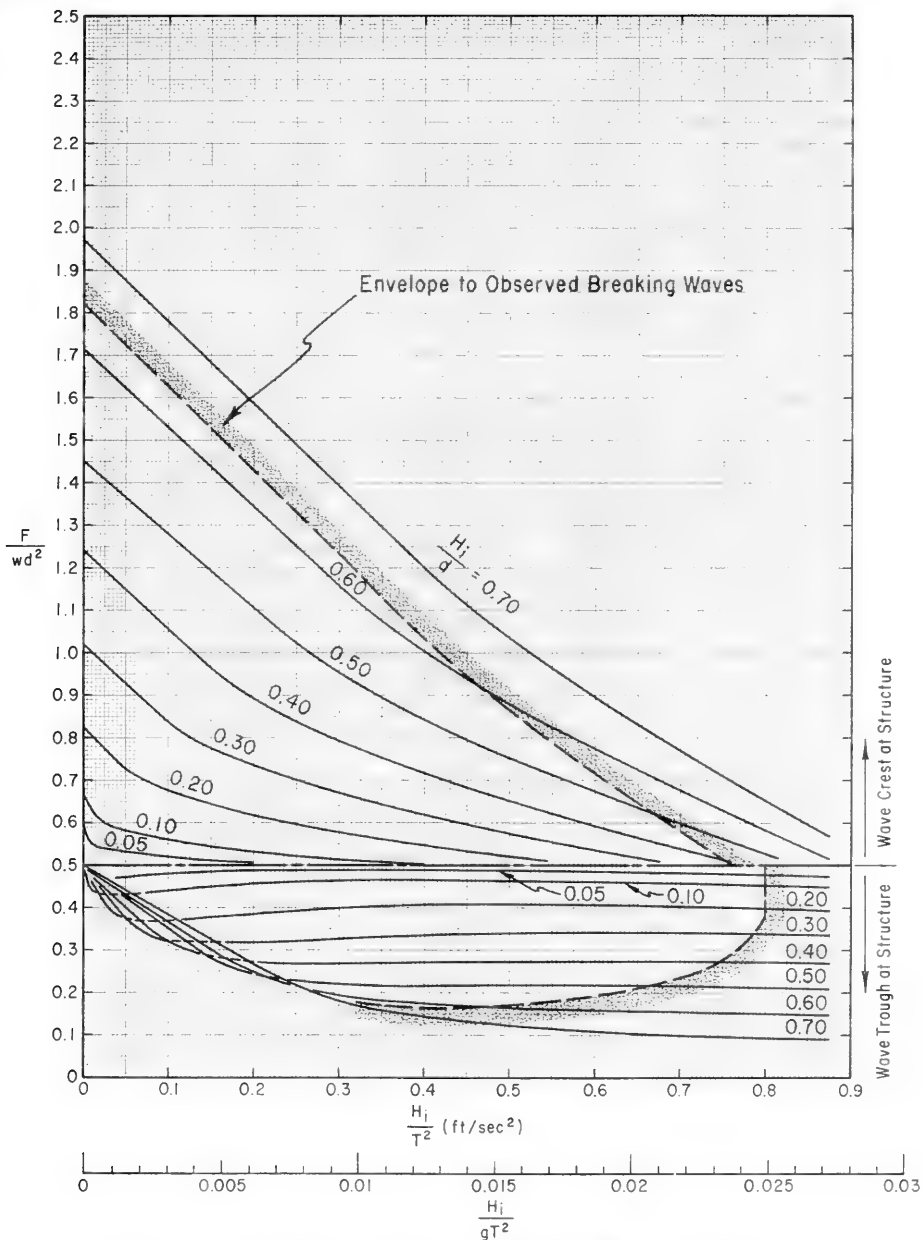
Figure 7-69. Miche-Rundgren Nonbreaking Wave Forces; $\chi = 0.9$
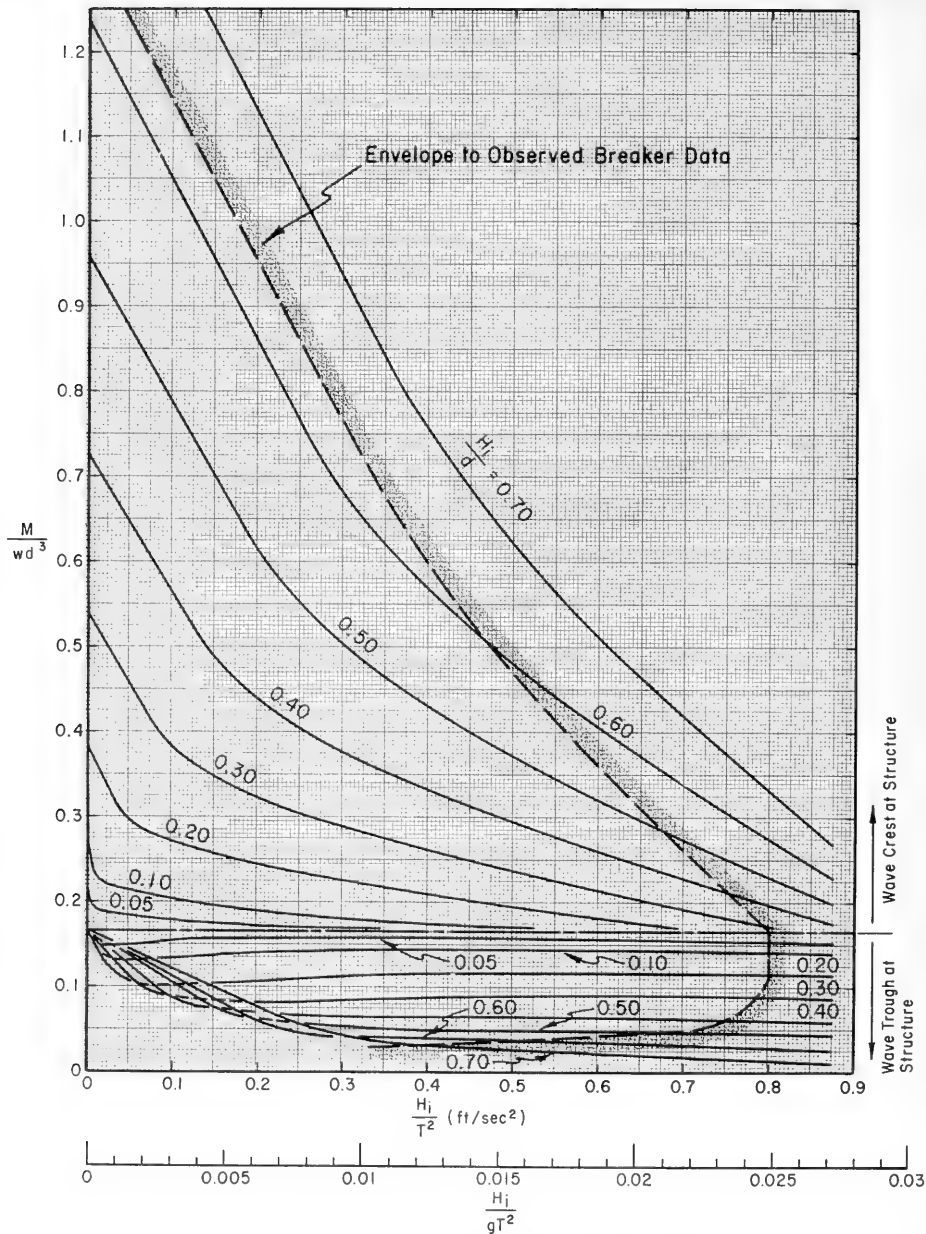
Figure 7-70. Miche-Rundgren Nonbreaking Wave Moment; $\chi = 0.9$

The height of the free surface above the bottom y, when the wave crest and trough are at the structure, may be determined from Equations 7-66 and 7-67,

$$y_c = d + h_o + \left(\frac{1+\chi}{2}\right) H_i \, ,$$

and

$$y_t = d + h_o - \left(\frac{1+\chi}{2}\right) H_i \, ,$$

$$y_c = 10 + 3.50 + (1)(5) = 18.5 \text{ ft.} ,$$
$$y_t = 10 + 3.50 - (1)(5) = 8.5 \text{ ft.}$$

$$(T = 6 \text{ sec.})$$

A similar analysis for the 10-second wave gives

$$y_c = 19.5 \text{ ft.} ,$$
$$y_t = 9.5 \text{ ft.}$$

$$(T = 10 \text{ sec.})$$

The wall would have to be about 20 feet high if it were not to be over-topped by a 5-foot high wave having a period of 10 seconds.

The horizontal wave forces may be evaluated using Figure 7-66. Entering the figure with the computed value of H_i/gT^2, the value of F/wd^2 can be determined from either of two curves of constant H_i/d. The upper family of curves (above $F/wd^2 = 0.5$) will give the dimensionless force when the crest is at the wall, F_c/wd^2; the lower family of curves (below $F/wd^2 = 0.5$) will give the dimensionless force when the trough is at the wall, F_t/wd^2. For the example problem, with $H_i/gT^2 = 0.0043$, and $H_i/d = 0.50$,

$$\frac{F_c}{wd^2} = 1.25; \ \frac{F_t}{wd^2} = 0.29 \, . \qquad\qquad (T = 6 \text{ sec.})$$

Therefore, assuming a weight per unit volume of 64.0 lbs./ft.^{3} for sea water,

$$F_c = 1.25 \, (64) \, (10)^2 = 8,000 \text{ lbs./ft.} ,$$
$$F_t = 0.29 \, (64) \, (10)^2 = 1,860 \text{ lbs./ft.}$$

$$(T = 6 \text{ sec.})$$

The horizontal line in Figure 7-66 ($F/wd^2 = 0.5$) represents the horizontal hydrostatic force against a wall in still water of depth, d. For the example problem, if the water depth on the leeward side of the wall is also 10 feet and there is no wave action, the maximum seaward acting horizontal force will be $F_c = 0.5 \, wd^2$. Therefore, the net horizontal force will be,

$$F_{net} = 1.25 \, (64) \, (10)^2 - 0.5 \, (64) \, (10)^2 ,$$
$$F_{net} = (1.25 - 0.5) \, (64) \, (10)^2 = 4,800 \text{ lbs./ft.} \qquad (T = 6 \text{ sec.})$$

If waves act on both sides of the structure, the maximum net horizontal force will occur when the clapotis crest acts against one side when the trough acts against the other. Hence the maximum horizontal force will be $F_c - F_t$, with F_c and F_t determined for the appropriate wave conditions. Assuming for the example problem that the wave action is identical on both sides of the wall,

$$F_{net} = 1.25\,(64)\,(10)^2 - 0.29\,(64)\,(10)^2$$

$$F_{net} = (1.25 - 0.29)\,(64)\,(10)^2 = 6,144 \text{ lbs./ft.}$$

say

$$F_{net} = 6,100 \text{ lbs./ft.} \qquad\qquad (T = 6 \text{ sec.})$$

The moment about point A at the bottom of the wall (Fig. 7-64) may be determined from Figure 7-67. The procedures are identical to those given for the dimensionless forces. However, in this case the horizontal line, $M/wd^3 = 0.167$ indicates the hydrostatic moment about the toe resulting from still water of depth d. Continuing the example problem, from Figure 7-67, with $H_i/gT^2 = 0.0043$ and $H_i/d = 0.50$

$$\frac{M_c}{wd^3} = 0.755 \;;\; \frac{M_t}{wd^3} = 0.80 \qquad\qquad (T = 6 \text{ sec.})$$

Therefore,

$$M_c = 0.755\,(64)\,(10)^3 = 48,300 \;\frac{\text{lb.-ft.}}{\text{ft.}}$$

$$\qquad\qquad (T = 6 \text{ sec.})$$

$$M_t = 0.080\,(64)\,(10)^3 = 5,120 \;\frac{\text{lb.-ft.}}{\text{ft.}}$$

When there is still water of depth d on the leeward side, the maximum moment

$$M_{net} = M_c - 0.167\,wd^3 .$$

Therefore, the resultant moment about A is

$$M_{net} = 0.755\,(64)\,(10)^3 - 0.167\,(64)\,(10)^3$$

$$M_{net} = (0.755 - 0.167)\,(64)\,(10)^3 = 37,600 \;\frac{\text{lb.-ft.}}{\text{ft.}} \quad (T = 6 \text{ sec.})$$

The maximum moment when there is wave action on the leeward side of the structure will be $M_c - M_t$ with M_c and M_t evaluated for the appropriate wave conditions. For the example problem, if identical wave conditions prevail on both sides of the structure

$$M_{net} = (0.755 - 0.080)\,(64)\,(10)^3 = 43,200 \;\frac{\text{lb.-ft.}}{\text{ft.}} \quad (T = 6 \text{ sec.})$$

Figures 7-68, 7-69, and 7-70 are used in a similar manner to determine forces and moments on a structure which has a reflection coefficient of $\chi = 0.9$.

* *

7-138

7.324 <u>Wall of Low Height</u>. It is often not economically feasible to design a structure to provide a nonovertopping condition by the design wave. Consequently, it is necessary to evaluate the force on a structure where the crest of the design clapotis is above the top of the wall as shown in Figure 7-71. The resulting pressure distribution is shown by the shaded area, and the force resulting from it is F'. The magnitude of F' is proportional to F, the force that would act against the wall if it extended up to the crest of the clapotis (the force determined from Figures 7-66 or 7-69). The relationship between F' and F is given by

$$F' = r_f F, \tag{7-69}$$

where r_f is a force reduction factor given by

$$r_f = \frac{b}{y}\left(2 - \frac{b}{y}\right) \qquad \text{when} \qquad \frac{b}{y} < 1.0 ,$$

and

$$r_f = 1.0 \qquad \text{when} \qquad \frac{b}{y} \geq 1.0 , \tag{7-70}$$

where b and y are defined in Figure 7-71. The relationship between r_f and b/y is shown in Figure 7-72.
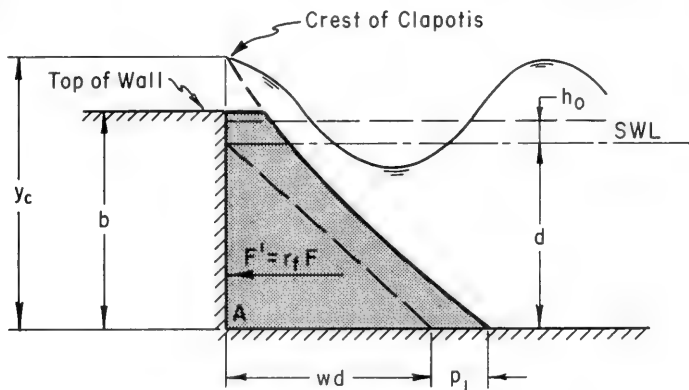
Figure 7-71. Wall of Low Height - Pressure Distribution

Similarly, the reduced moment about point A is given by

$$M' = r_m M, \tag{7-71}$$

where the moment reduction factor r_m is given by

$$r_m = \left(\frac{b}{y}\right)^2 \left(3 - 2\,\frac{b}{y}\right) \qquad \text{when} \qquad \frac{b}{y} < 1.0 ,$$

and

$$r_m = 1.0 \qquad \text{when} \qquad \frac{b}{y} \geq 1.0 \; 1 . \tag{7-72}$$

7-139
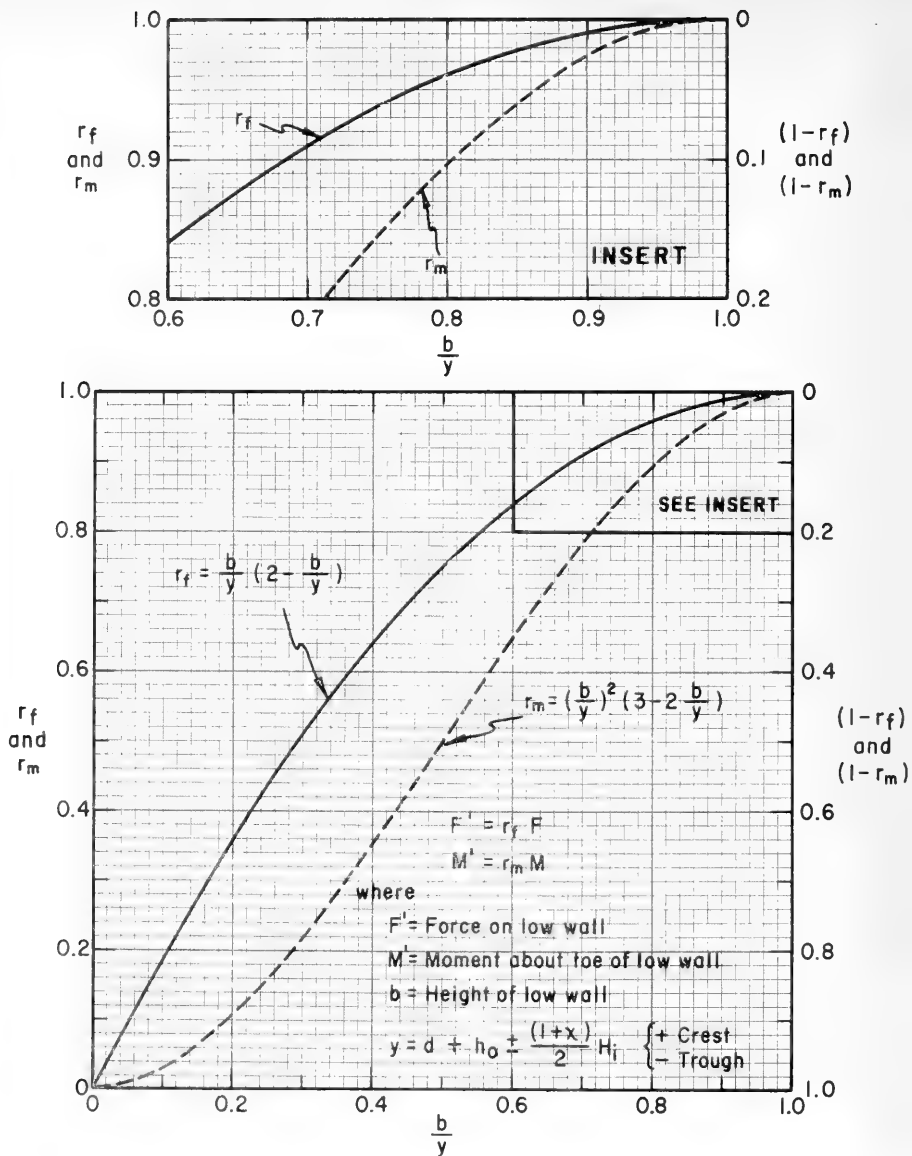
Figure 7-72. Force and Moment Reduction Factors

7-140

The relationship between r_m and b/y is also shown in Figure 7-72. Equations 7-69 through 7-72 are valid, when either the wave crest or wave trough are at the structure, provided the correct value of y is used.

* * * * * * * * * * * * * * EXAMPLE PROBLEM * * * * * * * * * * * * * * * *

GIVEN:

   (a) Wall height, b = 16.0 feet.

   (b) Incident wave height, H_i = 5.0 feet.

   (c) Depth at structure toe, d = 10.0 feet.

   (d) Wave period,

      T = 6 sec. (minimum), T = 10 sec. (maximum)

FIND: Determine the reduced wave force and moment on the given vertical wall.

SOLUTION: From the example problems in Section 7.323,

$$y_c = 18.50 \text{ ft.,}$$
$$y_t = 8.50 \text{ ft.}$$

$$(T = 6 \text{ sec.})$$

Compute b/y for each case

$$\frac{b}{y_c} = \frac{16.0}{18.50} = 0.865.$$

$$(T = 6 \text{ sec.})$$

$$\frac{b}{y_t} = \frac{16.0}{8.50} = 1.88 > 1.0.$$

Entering Figure 7-72 with the computed value of b/y, determine the values of r_f and r_m from the appropriate curve. For the wave with T = 6 sec.,

$$\frac{b}{y_c} = 0.865 ; \quad \text{therefore,} \quad r_f = 0.981 ; r_m = 0.950,$$

and

$$\frac{b}{y_t} > 1.0 ; \quad \text{therefore,} \quad r_f = 1.0 ; r_m = 1.0 .$$

Reduced forces and moments may be calculated from Equations 7-69 and 7-71 using the values of F and M found in the example problem of the previous section; for T = 6 sec.

$$F_c' = 0.981 \ (8,000) = 7,850 \ \text{lbs./ft.};$$

$$M_c' = 0.950 \ (48,300) = 45,900 \ \frac{\text{lb.-ft.}}{\text{ft.}},$$

$$F_t' = 1.0 \ (1,860) = 1,860 \ \text{lbs./ft.};$$

$$M_t' = 1.0 \ (5,120) = 5,120 \ \frac{\text{lb.-ft.}}{\text{ft.}}.$$

Again assuming that the wave action on both sides of the structure is identical, so that the maximum net horizontal force and maximum over-turning moment occurs when a clapotis crest is on one side of the structure and a trough is on the other side

$$F_{net}' = F_c' - F_t' = 7,850 - 1,860 = 5,990 \ \text{lbs./ft.},$$

say   (T = 6 sec.)

$$F_{net}' = 6,000 \ \text{lbs./ft.},$$

and

$$M_{net}' = M_c' - M_t' = 45,900 - 5,120 = 40,730 \ \frac{\text{lb.-ft.}}{\text{ft.}},$$

say   (T = 6 sec.)

$$M_{net}' = 41,000 \ \frac{\text{lb.-ft.}}{\text{ft.}}.$$

A similar analysis for the 10-second wave gives,

$$F_{net}' = 6,065 \ \text{lbs./ft.},$$

(T = 10 sec.)

$$M_{net}' = 44,700 \ \frac{\text{lbs.-ft.}}{\text{ft.}}.$$

* *

7.325 _Wall on Rubble Foundation._ Forces acting on a vertical wall built on a rubble foundation are shown in Figure 7-73, and may be computed in a manner similar to computing the forces acting on a low wall if the comple-ments of the force and moment reduction factors are used. As shown in Figure 7-73, the value of b which is used for computing b/y _is the_ _height of the rubble base and not the height of the wall above the_ _foundation._ The equation relating the reduced force F" against the wall on a rubble foundation with the force F which would act against a wall extending the entire depth is,

$$F'' = \left(1 - r_f\right) \ F. \tag{7-73}$$

The equation relating the moments is,

$$M_A'' = (1 - r_m) M \qquad (7\text{-}74)$$

where M_A'' is the moment about the bottom (point A on Figure 7-73). Usually, the moment desired is that about point B which may be found from

$$M_B'' = (1 - r_m) M - b (1 - r_f) F$$

or $\qquad\qquad\qquad\qquad\qquad\qquad\qquad\qquad\qquad\qquad\qquad$ (7-75)

$$M_B'' = M_A'' - bF''$$

The values of $(1 - r_m)$ and $(1 - r_f)$ may be obtained directly from Figure 7-72.
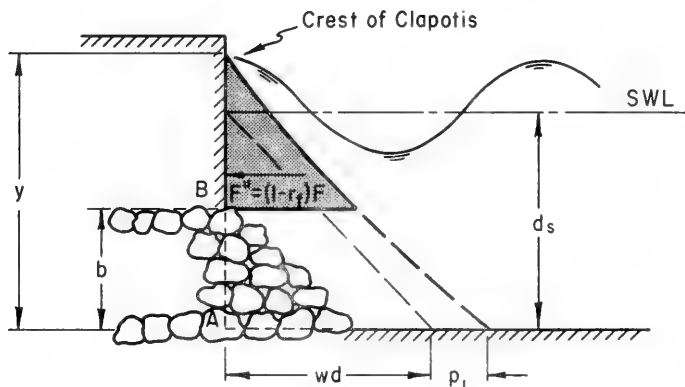
Figure 7-73. Wall on Rubble Foundation - Pressure Distribution

* * * * * * * * * * * * * * EXAMPLE PROBLEM * * * * * * * * * * * * * * * *

GIVEN:

  (a) A smooth-faced vertical wall on a rubble base.

  (b) Height of rubble foundation, b = 9 ft.

  (c) Incident wave height, Hi = 5 ft.

  (d) Design depth at the structure, d = 10 ft.

  (e) Wave period,

        T = 6 sec. (minimum),   T = 10 sec. (maximum)

7-143

FIND: Determine the force and overturning moment on the given wall on a rubble foundation.

SOLUTION: For this example problem Figures 7-65 through 7-67 are used to evaluate h_o, F and M even though a rubble base will reduce the wave reflection coefficient of a structure by dissipating some incident wave energy. Values of h_o, F, and M used in this example, have been determined in the example problem of Section 7.323,

$$y_c = 18.5 \text{ ft.}$$
$$(T = 6 \text{ sec.})$$
$$y_t = 8.5 \text{ ft.}$$

Compute b/y for each case, remembering that b now represents the height of the foundation.

$$\frac{b}{y_c} = \frac{9.0}{18.50} = 0.486$$
$$(T = 6 \text{ sec.})$$
$$\frac{b}{y_t} = \frac{9.0}{8.50} = 1.058 > 1.0$$

Enter Figure 7-72 with the computed values of b/y and determine corresponding values of $(1 - r_f)$ and $(1 - r_m)$. For the 6-second wave,

$$\frac{b}{y_c} = 0.486 ; \ (1 - r_f) = 0.264 ; (1 - r_m) = 0.521$$

and

$$\frac{b}{y_t} > 1.0 ; \ (1 - r_f) = 0.0 ; \ (1 - r_m) = 0.0$$

From Equation 7-73,

$$F_c'' = 0.264 \ (8,000) = 2,100 \text{ lbs./ft.}$$
$$(T = 6 \text{ sec.})$$
$$F_t'' = 0.0 \ (1,860) = 0 \text{ lbs./ft.}$$

For the 10-second wave, a similar analysis gives,

$$F_c'' = 2,620 \text{ lbs./ft.}$$
$$(T = 10 \text{ sec.})$$
$$F_t'' \approx 0 \text{ lbs./ft.}$$

The overturning moments about point A are, from Equation 7-74,

$$\left(M_A''\right)_c = 0.521 \ (45,900) = 23,900 \ \frac{\text{lb.-ft.}}{\text{ft.}}$$
$$(T - 6 \text{ sec.})$$
$$\left(M_A''\right)_t = 0.0 \ (5,120) = 0 \ \frac{\text{lb.-ft.}}{\text{ft.}}$$

7-144

and for the 10-second wave,

$$\left(M_A''\right)_c = 32,000 \; \frac{\text{lb.-ft.}}{\text{ft.}},$$

$$\left(M_A''\right)_t = 43 \; \frac{\text{lb.-ft.}}{\text{ft.}} .$$

(T = 10 sec.)

The overturning moments about point B are obtained from Equation 7-75,

$$\left(M_B''\right)_c = 23,900 - 9.0 \; (2,100) = 5,000 \; \frac{\text{lb.-ft.}}{\text{ft.}},$$

$$\left(M_B''\right)_t \approx 0 \; \frac{\text{lb.-ft.}}{\text{ft.}} ,$$

(T = 6 sec.)

and for the 10-second wave,

$$\left(M_B''\right)_c = 8,400 \; \frac{\text{lb.-ft.}}{\text{ft.}},$$

$$\left(M_B''\right)_t \approx 0 \; \frac{\text{lb.-ft.}}{\text{ft.}} .$$

(T = 10 sec.)

As in the examples in Sections 7.323 and 7.324, various combinations of appropriate wave conditions for the two sides of the structure can be assumed and resulting moments and forces computed.

* *

7.33 BREAKING WAVE FORCES ON VERTICAL WALLS

Waves breaking directly against vertical-face structures exert high, short duration, dynamic pressures that act near the region where the wave crests hit the structure. These impact or shock pressures have been studied in the laboratory by Bagnold (1939), Denny (1951), Ross (1955), Nagai (1961 b), Carr (1954), Leendertse (1961), Kamel (1968), Weggel (1968), and Weggel and Maxwell (1970 a, and b). Some measurements on full-scale breakwaters have been made by deRouville, et al., (1938). Wave tank experiments by Bagnold (1939) led to an explanation of the phenomenon. Bagnold found that impact pressures occur at the instant that the vertical, front face of a breaking wave hits the wall and only when a plunging wave entraps a cushion of air against the wall. Because of this critical dependence on wave geometry, high impact pressures are infrequent against prototype structures. However, the possibility of high impact pressures must be recognized, and considered in design. The high impact pressures are short (of the order of hundredths of a second), and their importance in the design of breakwaters against sliding or overturning is questionable. However, lower dynamic forces which last longer are important.

7.331 Minikin Method: Breaking Wave Forces. Minikin (1955, 1963)
developed a design procedure based on observations of full-scale break-
waters and the results of Bagnold's study. Minikin's method can give
wave forces that are extremely high, as much as 15 to 18 times those
calculated for nonbreaking waves. Therefore, the following procedures
should be used with caution, and only until a more accurate method of
calculation is found.

The maximum pressure assumed to act at the SWL is given by

$$p_m = 101 \ w \ \frac{H_b}{L_D} \ \frac{d_s}{D} \ (D + d_s), \tag{7-76}$$

where p_m is the maximum dynamic pressure, H_b is the breaker height,
d_s is the depth at the toe of the wall, D is the depth one wavelength
in front of the wall, and L_D is the wavelength in water of depth D.
The distribution of dynamic pressure is shown in Figure 7-74. The
pressure decreases parabolically from p_m at the SWL to zero at a distance
of $H_b/2$ above and below the SWL. The force represented by the area under
the dynamic pressure distribution is

$$R_m = \frac{p_m H_b}{3}$$

(force resulting from dynamic component of pressure) (7-77)

and the overturning moment about the toe is

$$M_m = R_m d_s = \frac{p_m H_b d_s}{3}$$

(moment resulting from dynamic component of pressure) (7-78)

The hydrostatic contribution to the force and overturning moment must be
added to the results obtained from Equations 7-77 and 7-78 to determine
total force and overturning moment.

The Minikin formula was originally derived for composite breakwaters
comprised of a concrete superstructure founded on a rubble substructure.
Strictly, D and L_D in Equation 7-76 are the depth and wavelength at the
toe of the substructure; d_s is the depth at the toe of the vertical wall
(i.e., the distance from the SWL down to the crest of the rubble substruc-
ture). For caisson and other vertical structures where no substructure is
present, the formula has been adapted by using the depth at the structure
toe as d_s; D and L_D are the depth and wavelength a distance one wave-
length seaward of the structure. Consequently, the depth D can be found
from

$$D = d_s + L_d \ m, \tag{7-79}$$

where L_d is the wavelength in a depth equal to d_s, and m is the near-shore slope. The forces and moments resulting from the hydrostatic pressure must be added to the dynamic force and moment computed above. The triangular hydrostatic pressure distribution is shown in Figure 7-74; the pressure is zero at the breaker crest (taken at $H_b/2$ above the SWL), and increases linearly to $w(d_s + H_b/2)$ at the toe of the wall.

The total force is

$$R_t = R_m + \frac{w\left(d_s + \frac{H_b}{2}\right)^2}{2} = R_m + R_s, \qquad (7-80)$$

and the total moment about the toe is,

$$M_t = M_m + \frac{w\left(d_s + \frac{H_b}{2}\right)^3}{6} = M_m + M_s. \qquad (7-81)$$

The last terms on the right side of Equations 7-80 and 7-81 (R_s and M_s) are the hydrostatic contributions.
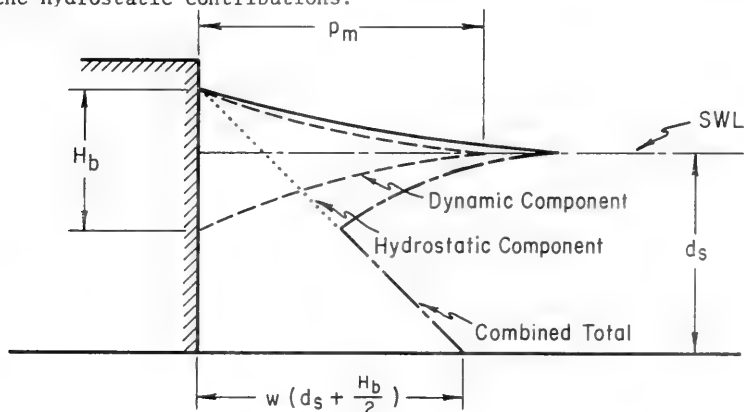
Figure 7-74. Minikin Wave Pressure Diagram

Calculations to determine the force and moment on a vertical wall are illustrated by the following example.

* * * * * * * * * * * * * * EXAMPLE PROBLEM * * * * * * * * * * * * * * * *

GIVEN: A vertical wall, 14 feet high is sited in sea water with d_s = 7.5 feet. The wall is built on a bottom slope of 1:20 (m = 0.05). Reasonable wave periods range from T = 6 sec. to T = 10 sec.

7-147

FIND:

    (a)   The maximum pressure, horizontal force and overturning moment about the toe of the wall for the given slope, and

    (b)   the maximum pressure, horizontal force, and overturning moment for the 6-second wave if the slope were 1:100.

SOLUTION:

    (a)   From the example problem in Section 7.122, the maximum breaker height for a design depth of 7.5 feet, a slope of 0.05, and wave periods of 6- and 10-seconds are

$$H_b = 8.4 \text{ ft.}, \qquad\qquad\qquad (T = 6 \text{ sec.})$$

$$H_b = 9.8 \text{ ft.} \qquad\qquad\qquad (T = 10 \text{ sec.})$$

The wavelength at the wall in water 7.5 feet deep can be found with the aid of Table C-1, Appendix C. (The following calculations are for the 6-second wave.) First calculate the wavelength in deep water $(T = 6 \text{ sec.})$,

$$L_o = \frac{gT^2}{2\pi} = 5.12\,(6)^2 = 184 \text{ ft.}$$

Then

$$\frac{d}{L_o} = \frac{7.5}{184} = 0.0408,$$

and from Table C-1, Appendix C,

$$\frac{d}{L} = 0.084,$$

and

$$.\, L_d = 89.1 \text{ ft.}$$

From Equation 7-79

$$D = d_s + L_d\, m = 7.5 + 89.1\,(0.05) = 11.96 \text{ ft.},$$

and using Table C-1, as above,

$$\frac{D}{L_o} = 0.0650 \,;\, \frac{D}{L_D} = 0.1091,$$

hence

$$L_D = \frac{D}{D/L_D} = \frac{11.96}{0.1091} = 109 \text{ ft.},$$

say

$$L_D = 110 \text{ ft.}$$

Equation 7-76 can now be used to find p_m.

$$P_m = 101 \; w \; \frac{H_b}{L_D} \; \frac{d_s}{D} \; (D + d_s),$$

$$P_m = 101 \, (64) \; \frac{8.4}{109.6} \; \frac{7.5}{11.96} \; (11.96 + 7.5) \; ,$$

$$= 6{,}050 \; \text{lbs./ft.} \qquad\qquad (T = 6 \; \text{sec.})$$

A similar analysis for the 10-second wave gives,

$$P_m = 3{,}300 \; \text{lbs./ft.}^2 \qquad\qquad (T = 10 \; \text{sec.})$$

The above values can be obtained more rapidly by using Figure 7-75, a graphical representation of the above procedure. To use the figure, calculate for the 6-second wave,

$$\frac{d_s}{gT^2} = \frac{7.5}{32.2 \, (6)^2} = 0.0065.$$

Enter Figure 7-75 with the calculated value of d_s/gT^2, using the curve for $m = 0.05$, and read the value of p_m/wH_b.

$$\frac{P_m}{wH_b} = 11.3.$$

Using the calculated values of H_b,

$$P_m = 11.3 \; w \; H_b = 11.3 \, (64) \, (8.4) = 6{,}075 \; \text{lbs./ft.}^2 \; , \quad (T = 6 \; \text{sec.})$$

For the 10-second wave,

$$P_m = 5.3 \; w \; H_b = 5.3 \, (64) \, (9.8) = 3{,}300 \; \text{lbs./ft.}^2 \qquad (T = 10 \; \text{sec.})$$

The force can be evaluated from Equation 7-77

$$R_m = \frac{P_m H_b}{3} = \frac{6{,}050 \, (8.4)}{3} = 16{,}900 \; \text{lbs./ft.} \; , \qquad (T = 6 \; \text{sec.})$$

and

$$R_m = 11{,}500 \; \text{lbs./ft.} \qquad\qquad (T = 10 \; \text{sec.})$$
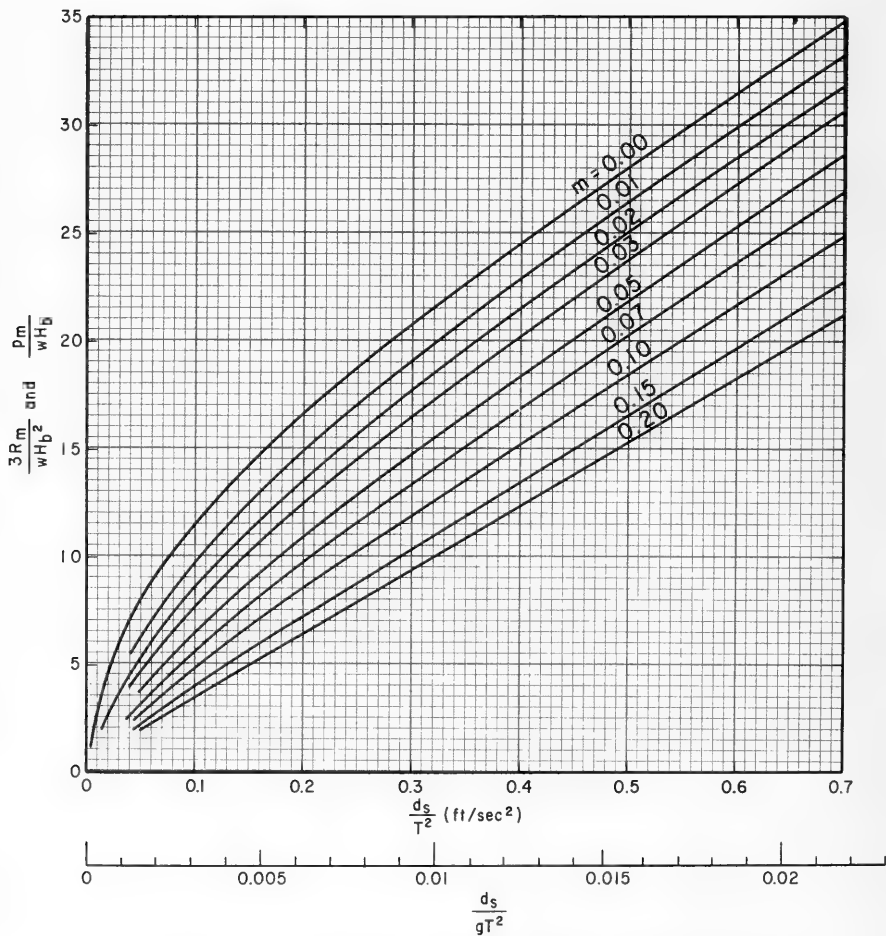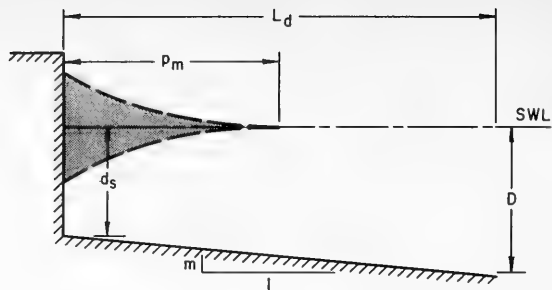
Figure 7-75. Dimensionless Minikin Wave Pressure and Force

The overturning moments are given by Equation 7-78 as,

$$M_m = R_m d_s = 16,900 \, (7.5) = 126,800 \, \frac{\text{ft.-lbs.}}{\text{ft.}} \, , \qquad\qquad (T = 6 \text{ sec.})$$

and

$$M_m = 86,300 \, \frac{\text{ft.-lbs.}}{\text{ft.}} \, . \qquad\qquad (T = 10 \text{ sec.})$$

For the example, the total forces, including the hydrostatic force from Equations 7-80 and 7-81,

$$R_t = R_m + R_s \, ,$$

$$R_t = 16,900 + \frac{64 \left(7.5 + \dfrac{8.4}{2}\right)^2}{2} = 16,900 + 4,380 = 21,280 \text{ lbs./ft.}$$

say

$$R_t = 21,300 \text{ lbs./ft.} \qquad\qquad (T = 6 \text{ sec.})$$

$$R_t = 16,400 \text{ lbs./ft.} \qquad\qquad (T = 10 \text{ sec.})$$

Then

$$M_t = M_m + M_s \, ,$$

$$M_t = 126,800 + \frac{64 \left(7.5 + \dfrac{8.4}{2}\right)^3}{6} = 126,800 + 17,100 \, ,$$

$$M_t = 143,900 \, \frac{\text{lb.-ft.}}{\text{ft.}} \, , \qquad\qquad (T = 6 \text{ sec.})$$

say

$$M_t = 144,000 \, \frac{\text{lb.-ft.}}{\text{ft.}} \, , $$

and

$$M_t = 106,600 \, \frac{\text{ft.-lb.}}{\text{ft.}} \, . \qquad\qquad (T = 10 \text{ sec.})$$

7-151

(b) If the nearshore slope is 1:100 (m = 0.01), the maximum breaker heights must be recomputed using the procedure of Section 7.122. For a 6-second wave on a 0.01 slope the results of an analysis similar to the preceding gives,

$$H_b = 6.3 \text{ ft.} \ \left(d_b = 7.7 \text{ ft.} > d_s\right),$$

$$p_m = 6,050 \text{ lbs./ft.}^2 \ , \qquad\qquad (T = 6 \text{ sec.})$$

and

$$R_m = 12,700 \text{ lbs./ft.}$$

The resulting maximum pressure is about the same as for the wall on a 1:20 sloping beach ($p_m = 6,075$ lbs./ft.^{2}); however, the dynamic force is less against the wall on a 1:100 slope than against the wall on a 1:20 slope, because the maximum possible breaker height reaching the wall is lower on a flatter slope.

* *

7.332 __Wall On a Rubble Foundation.__ The dynamic component of breaking wave force on a vertical wall built on a rubble substructure can be estimated with either Equation 7-76 or Figure 7-76. The procedure for calculating forces and moments is similar to that outlined in the example problem of the preceding section. However, the ratio d_s/D is used instead of the nearshore slope when using Figure 7-76. Minikin's equation was originally derived for breakwaters of this type. For expensive structures, hydraulic models should be used to evaluate forces.

7.333 __Wall of Low Height.__ When the top of a structure is lower than the crest of the design breaker, the dynamic and hydrostatic components of wave force and overturning moment can be corrected by using Figures 7-77 and 7-78. Figure 7-77 is a Minikin force reduction factor to be applied to the dynamic component of the breaking wave force equation,

$$R'_m = r_m R_m . \qquad\qquad (7\text{-}82)$$

Figure 7-78 gives a dimensionless moment reduction factor a for use in the equation

$$M'_m = d_s R_m - \left(d_s + a\right) \ \left(1 - r_m\right) R_m , \qquad\qquad (7\text{-}83)$$

or

$$M'_m = R_m \ \left[r_m \ \left(d_s + a\right) - a\right] . \qquad\qquad (7\text{-}84)$$

7-152
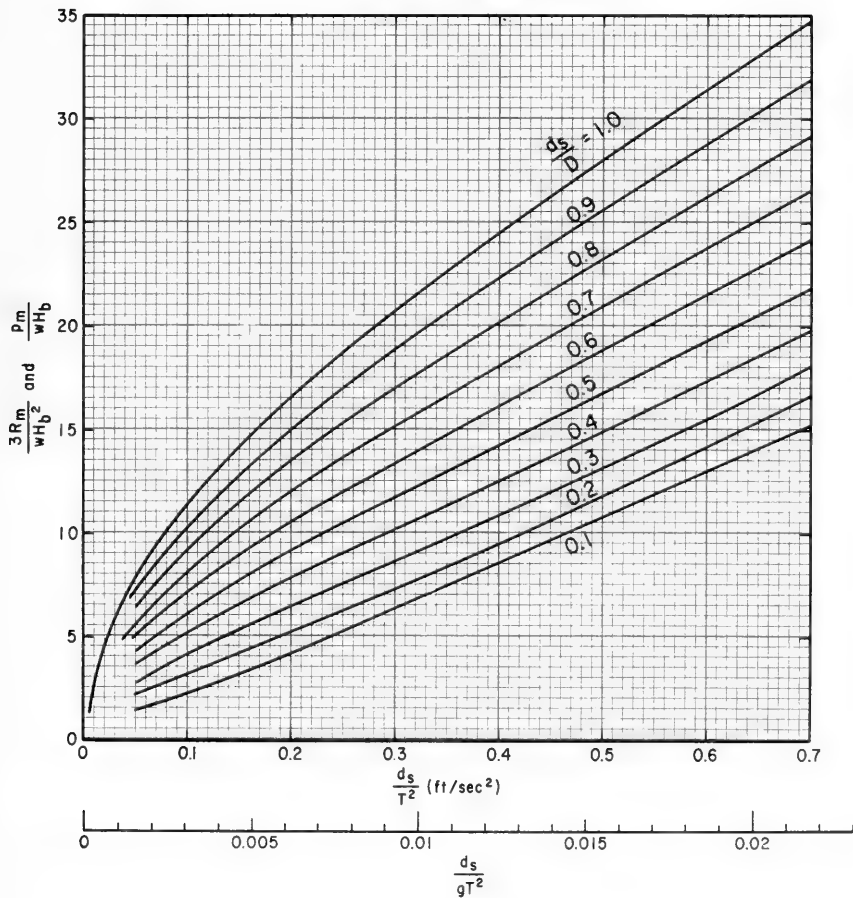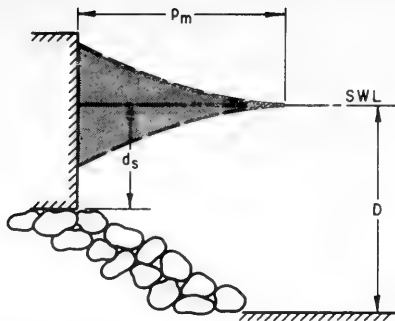
Figure 7-76. Dimensionless Minikin Wave Pressure and Force
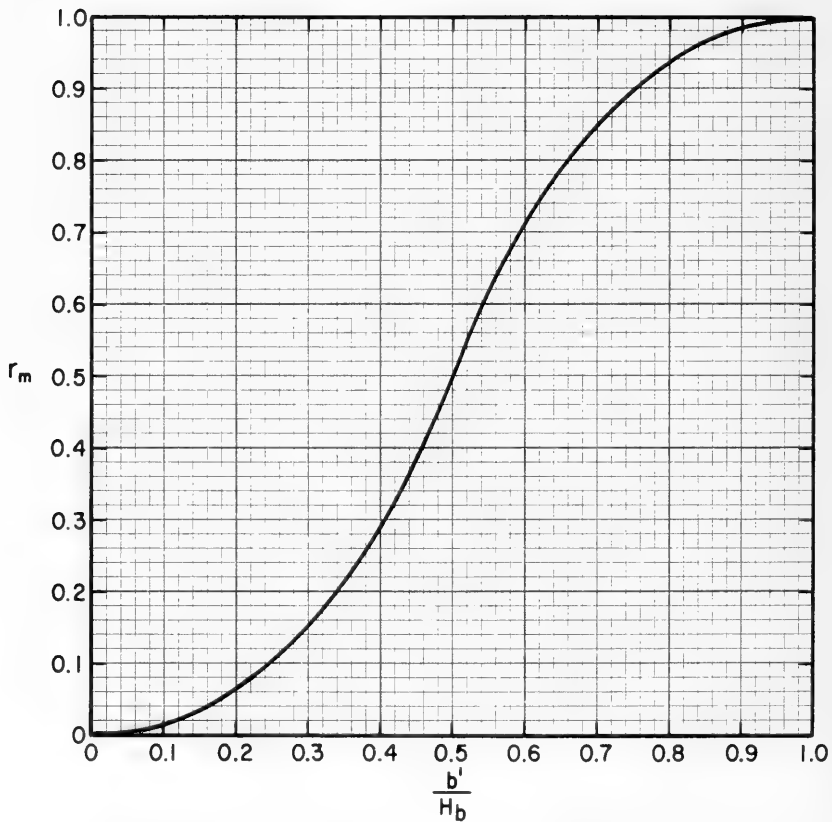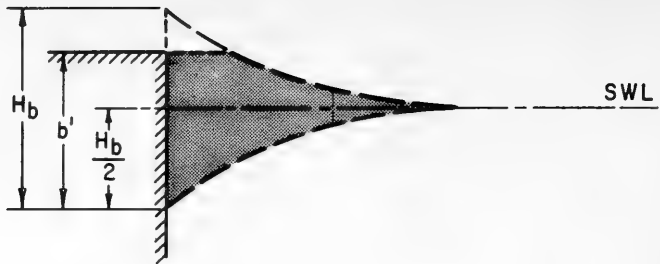
Figure 7-77. Minikin Force Reduction Factor

$$M_m' = d_s R_m - (d_s + a)(1 - r_m) R_m$$
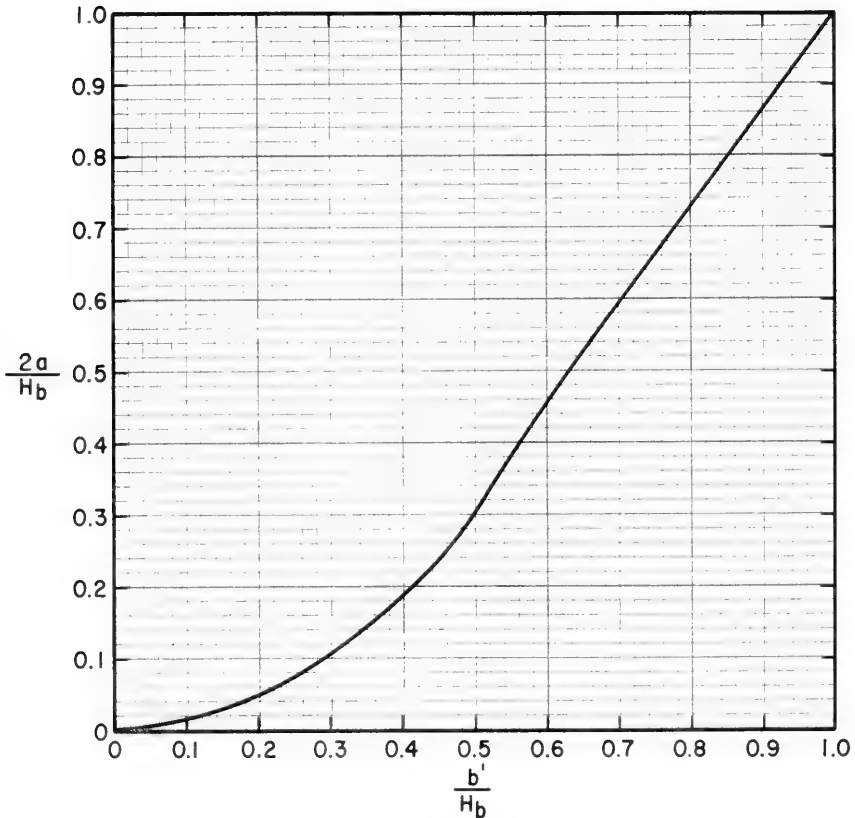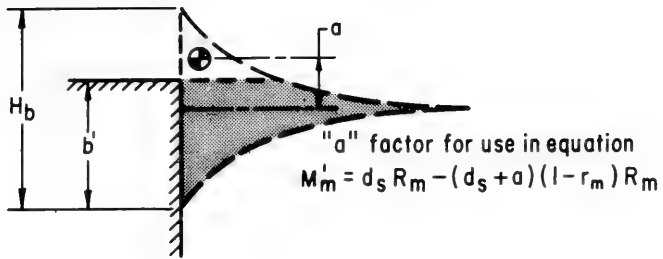
Figure 7-78. Minikin Moment Reduction for Low Wall

GIVEN:

   (a) A vertical wall 10 feet high in a water depth of $d_s = 7.5$ feet on a nearshore slope of 1:20 (m = 0.05), and

   (b) design wave periods of T = 6 sec. and T = 10 sec.

FIND: Determine the reduced force and overturning moment because of the reduced wall height.

SOLUTION: Calculations of the breaker heights, unreduced forces and moments are given in preceding example problems. From the preceding problems,

$$H_b = 8.4 \text{ ft. },\qquad \left(d_b = 8.9 \text{ ft.} > d_s\right) ,$$

$$R_m = 16,900 \text{ lbs./ft. },$$

$$M_m = 126,800 \ \frac{\text{lb.-ft.}}{\text{ft.}} \qquad\qquad (T = 6 \text{ sec.})$$

and

$$H_b = 9.8 \text{ ft. },\qquad \left(d_b = 9.2 \text{ ft.} > d_s\right),$$

$$R_m = 11,500 \text{ lbs./ft. },$$

$$M_m = 86,300 \ \frac{\text{lbs.-ft.}}{\text{ft.}} \quad . \qquad\qquad (T = 10 \text{ sec.})$$

For the breaker with a period of 6 seconds, the height of the breaker crest above the bottom is

$$\left(d_s + \frac{H_b}{2}\right) = \left(7.5 + \frac{8.4}{2}\right) = 11.7 \text{ ft.}$$

The value of b' as defined in Figure 7-77 is 6.7 feet (i.e., the breaker height H_b minus the height obtained by subtracting the wall crest elevation from the breaker crest elevation). Calculate

$$\frac{b'}{H_b} = \frac{6.7}{8.4} = 0.798 \ . \qquad\qquad (T = 6 \text{ sec.})$$

From Figure 7-77,

$$r_m = 0.94 \ ,$$

therefore from Equation 7-82,

$$R'_m = r_m R_m = 0.94 \, (16,900) = 15,900 \text{ lbs.} \qquad (T = 6 \text{ sec.})$$

From Figure 7-78, entering with $b/H'_b = 0.798$,

$$\frac{2a}{H_b} = 0.73 \ ,$$

hence

$$a = \frac{0.73 \, (8.4)}{2} = 3.07 \ ,$$

and from Equation 7-84,

$$M'_m = R_m \left[r_m \left(d_s + a \right) - a \right] = 16,900 \, [0.94 \, (7.5 + 3.07) - 3.07] \ .$$

$$M'_m = 16,900 \, [6.87] = 116,000 \ \frac{\text{lb.-ft.}}{\text{ft.}} \ . \qquad (T = 6 \text{ sec.})$$

A similar analysis for the maximum breaker with a 10-second period gives

$$r_m = 0.90 \ ,$$

$$a = 3.28 \text{ ft.} \ ,$$

$$R'_m = 10,350 \text{ lbs./ft.} \ ,$$

$$M'_m = 73,800 \ \frac{\text{lb.-ft.}}{\text{ft.}} \ . \qquad (T = 10 \text{ sec.})$$

The hydrostatic part of the force and moment can be computed from the hydrostatic pressure distribution shown in Figure 7-74 by assuming the hydrostatic pressure to be zero at $H_b/2$ above SWL, and taking only that portion of the area under the pressure distribution which is below the crest of the wall.

* *

7.34. BROKEN WAVES

Shore structures may be located so that even under severe storm and tide conditions waves will break before striking the structure. No studies have yet been made to relate forces of broken waves to various

wave parameters, and it is necessary to make simplifying assumptions about the waves to estimate design forces. If more accurate force estimates are required, model tests are necessary.

It is assumed that immediately after breaking the water mass in a wave moves forward with the velocity of propagation attained before breaking; that is, upon breaking, the water particle motion changes from oscillatory to translatory motion. This turbulent mass of water then moves up to and over the stillwater line dividing the area shoreward of the breakers into two parts, seaward and landward of the stillwater line. For a conservative estimate of wave force, it is assumed that neither wave height nor wave velocity decreases from the breaking point to the stillwater line, and that after passing the stillwater line the wave will run up roughly twice its height at breaking, with both velocity and height decreasing to zero at this point. Wave runup can be estimated more accurately from the procedure outlined in Section 7.21, WAVE RUNUP.

Model tests have shown that for waves breaking at a shore approximately 78 percent of the breaking wave height H_b is above the stillwater level. (Wiegel, 1964.)

7.341 <u>Wall Seaward of Stillwater Line</u>. Walls located seaward of the stillwater line are subjected to wave pressures that are partly dynamic and partly hydrostatic. (See Figure 7-79.)
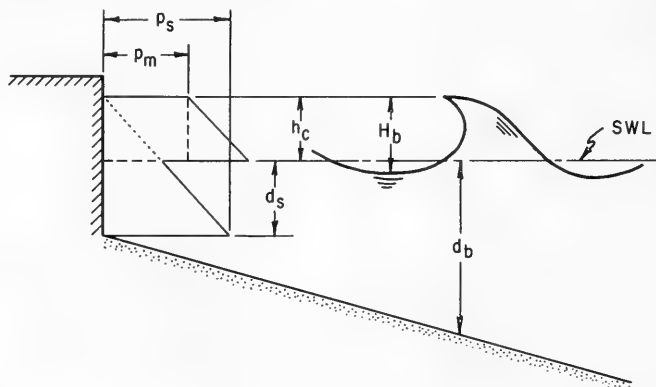
Figure 7-79.   Wave Pressures from Broken Waves: Wall Seaward of
                Stillwater Line

Using the approximate relationship $C = \sqrt{gd_b}$ for the velocity of wave propagation C where g is the acceleration of gravity and d_b is the

breaking wave depth, wave pressures on a wall may be approximated in the following manner:

The dynamic part of the pressure will be

$$p_m = \frac{wC^2}{2g} = \frac{wd_b}{2} , \qquad (7\text{-}85)$$

where w is the unit weight of water. If the dynamic pressure is uniformly distributed from the stillwater level to a height h_c above SWL, where h_c is given by

$$h_c = 0.78 \ H_b , \qquad (7\text{-}86)$$

then the dynamic component of the wave force is given by

$$R_m = p_m h_c = \frac{wd_b h_c}{2} , \qquad (7\text{-}87)$$

and the overturning moment caused by the dynamic force by

$$M_m = R_m \left(d_s + \frac{h_c}{2}\right) , \qquad (7\text{-}88)$$

where d_s is the depth at the structure.

The hydrostatic component will vary from zero at a height h_c above SWL to a maximum at the wall base. This maximum will be given by,

$$p_s = w \left(d_s + h_c\right) . \qquad (7\text{-}89)$$

The hydrostatic force component will therefore be

$$R_s = \frac{w \left(d_s + h_c\right)^2}{2} , \qquad (7\text{-}90)$$

and the overturning moment will be,

$$M_s = R_s \frac{\left(d_s + h_c\right)}{3} = \frac{w \left(d_s + h_c\right)^3}{6} . \qquad (7\text{-}91)$$

The total force on the wall is the sum of the dynamic and hydrostatic components; therefore,

$$R_t = R_m + R_s \qquad (7\text{-}92)$$

and

$$M_t = M_m + M_s \qquad (7\text{-}93)$$

7-159

7.342 Wall Shoreward of Stillwater Line. For walls landward of the still-
water line as shown in Figure 7-80 the velocity v' of the water mass at
the structure at any location between the SWL and the point of maximum
wave runup may be approximated by,

$$v' = C \left(1 - \frac{x_1}{x_2}\right) = \sqrt{gd_b} \left(1 - \frac{x_1}{x_2}\right) , \qquad (7\text{-}94)$$

and the wave height h' above the ground surface by,

$$h' = h_c \left(1 - \frac{x_1}{x_2}\right) , \qquad (7\text{-}95)$$

where

x_1 = distance from the stillwater line to the structure,

x_2 = distance from the stillwater line to the limit of wave uprush;
$x_2 = 2H_b \cot \beta = 2H_b/m$ Note: (The actual wave runup as found
from the method outlined in Section 7.21 could be substituted
for the value $2H_b$.) β = the angle of beach slope, and $m = \tan \beta$.
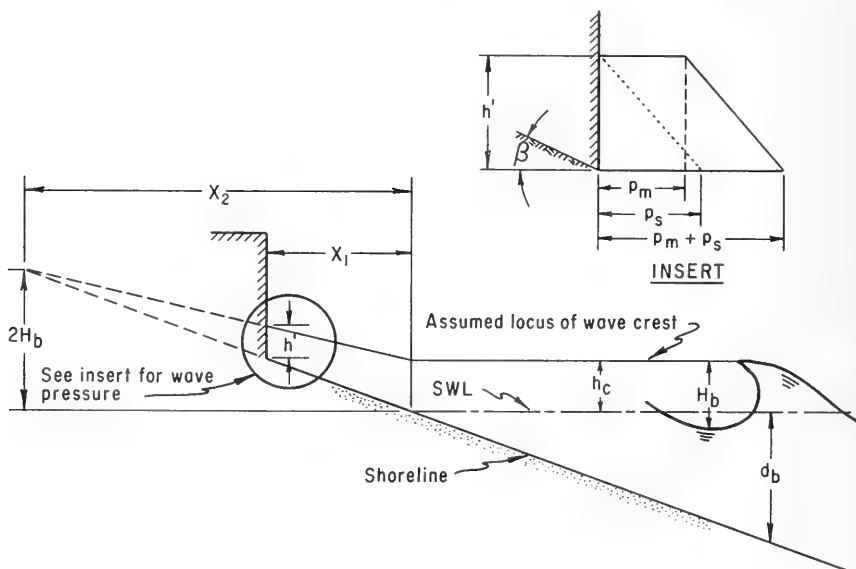
Figure 7-80. Wave Pressures from Broken Waves: Wall Landward
of Stillwater Line

An analysis similar to that for structures located seaward of the still-water line gives for the dynamic pressure,

$$p_m = \frac{wv'^2}{2g} = \frac{wd_b}{2} \left(1 - \frac{x_1}{x_2}\right)^2 . \qquad (7\text{-}96)$$

The dynamic pressure is assumed to act uniformly over the height h, hence the dynamic component of force is given by,

$$R_m = p_m h' = \frac{wd_b h_c}{2} \left(1 - \frac{x_1}{x_2}\right)^3 \qquad (7\text{-}97)$$

and the overturning moment by,

$$M_m = R_m \frac{h'}{2} = \frac{wd_b h_c^2}{4} \left(1 - \frac{x_1}{x_2}\right)^4 \qquad (7\text{-}98)$$

The hydrostatic force component is given by,

$$R_s = \frac{wh'^2}{2} = \frac{wh_c^2}{2} \left(1 - \frac{x_1}{x_2}\right)^2 \qquad (7\text{-}99)$$

and the moment resulting from the hydrostatic force by,

$$M_s = R_s \frac{h'}{3} = \frac{wh_c^3}{6} \left(1 - \frac{x_1}{x_2}\right)^3 \qquad (7\text{-}100)$$

The total forces and moments are the sums of the dynamic and hydrostatic components; therefore, as before,

$$R_t = R_m + R_s \qquad (7\text{-}101)$$

and,

$$M_t = M_m + M_s \qquad (7\text{-}102)$$

The pressures, forces and moments computed by the above procedure will be *approximations* since the assumed wave behavior is simplified. Where structures are located landward of the stillwater line the preceding equations will not be exact, since the runup criterion was assumed to be a fixed fraction of the breaker height. However, the assumptions should result in a high estimate of the forces and moments.

GIVEN: The elevation at the toe of a vertical wall is 2 feet above the mean lower low water (MLLW) datum. Mean higher high water (MHHW) is 4.3 feet above MLLW and the beach slope is 1:20. Breaker height is H_b = 9.0 ft., wave period is T = 6 sec.

FIND:

(a) The total force and moment if the SWL is at MHHW. (Wall seaward of stillwater line.)

(b) The total force and moment if the SWL is at MLLW. (Wall landward of stillwater line.)

SOLUTION:

(a) The breaking depth d_b can be found from Figure 7-2. Calculate,

$$\frac{H_b}{gT^2} = \frac{9.0}{32.2\,(6)^2} = 0.0078 \ ,$$

and the beach slope,

$$m = \tan\beta = \frac{1}{20} = 0.05 \ .$$

Enter Figure 7-2 with $H_b/gT^2 = 0.0078$ and using the curve for m = 0.05, read,

$$\frac{d_b}{H_b} = 1.10 \ ,$$

Therefore,

$$d_b = 1.10\ H_b = 1.10\,(9.0) = 9.9 \text{ ft.}$$

From Equation 7-86,

$$h_c = 0.78\ H_b = 0.78\,(9.0) = 7.02 \text{ ft.}$$

The dynamic force component from Equation 7-87 is

$$R_m = \frac{wd_b h_c}{2} = \frac{64\,(9.9)\,(7.02)}{2} = 2,200 \text{ lbs./ft.}$$

and the moment from Equation 7-88 is

$$M_m = R_m\left(d_s + \frac{h_c}{2}\right) = 2,200\left(2.3 + \frac{7.02}{2}\right) = 12,900 \ \frac{\text{lb.-ft.}}{\text{ft.}} \ ,$$

where $d_s = 2.3$ is the depth at the toe of the wall when the SWL is at MHHW. The hydrostatic force and moment are given by Equations 7-90 and 7-91,

$$R_s = \frac{w(d_s + h_c)^2}{2} = \frac{64(2.3 + 7.02)^2}{2} = 2,780 \text{ lbs./ft.},$$

$$M_s = R_s \frac{(d_s + h_c)}{3} = 2,780 \frac{2.3 + 7.02}{3} = 8,640 \frac{\text{lb.-ft.}}{\text{ft;}} .$$

The total force and moment are therefore,

$$R_t = R_m + R_s = 2,200 + 2,780 = 4,980 \text{ lbs./ft.},$$

$$M_t = M_m + M_s = 12,900 + 8,640 = 21,540 \frac{\text{lb.-ft.}}{\text{ft.}} .$$

(b) When the SWL is at MLLW, the structure is landward of the still-water line. The distance from the stillwater line to the structure x_1 is given by the difference in elevation between the SWL and the structure toe divided by the beach slope,

$$x_1 = \frac{2.0}{0.05} = 40 \text{ ft.}$$

The limit of wave runup is approximately,

$$x_2 = \frac{2H_b}{m} = \frac{2(9.0)}{0.05} = 360 \text{ ft.}$$

The dynamic component of force from Equation 7-97 is,

$$R_m = \frac{wd_b h_c}{2} \left(1 - \frac{x_1}{x_2}\right)^3 = \frac{64(9.9)(7.02)}{2} \left(1 - \frac{40}{360}\right)^3 = 1,560 \text{ lbs./ft.},$$

and the moment from Equation 7-98 is,

$$M_m = \frac{wd_b h_c^2}{4} \left(1 - \frac{x_1}{x_2}\right)^4 = \frac{64(9.9)(7.02)^2}{4} \left(1 - \frac{40}{360}\right)^4 = 4,870 \frac{\text{lb.-ft.}}{\text{ft.}} .$$

The hydrostatic force and moment from Equations 7-99 and 7-100 are,

$$R_s = \frac{wh_c^2}{2} \left(1 - \frac{x_1}{x_2}\right)^2 = \frac{64(7.02)^2}{2} \left(1 - \frac{40}{360}\right)^2 = 1,250 \text{ lbs./ft.},$$

and

$$M_s = \frac{wh_c^3}{6} \left(1 - \frac{x_1}{x_2}\right)^3 = \frac{64(7.02)^3}{6} \left(1 - \frac{40}{360}\right)^3 = 2,590 \frac{\text{lb.-ft.}}{\text{ft.}} .$$

Total force and moment is given by,

$$R_t = R_m + R_s = 1,560 + 1,250 = 2,810 \text{ lbs./ft.}$$

$$M_t = M_m + M_s = 4,870 + 2,590 = 7,460 \frac{\text{lb.-ft.}}{\text{ft.}}$$

* *

7.35 EFFECT OF ANGLE OF WAVE APPROACH

When *breaking* or *broken waves* strike the vertical face of a structure such as a groin, bulkhead, seawall or breakwater at an oblique angle, the *dynamic component of the pressure* or force will be less than for breaking or broken waves that strike perpendicular to the structure face. The force may be reduced by the equation,

$$R' = R \sin^2 \alpha \qquad (7\text{-}103)$$

where α is the angle between the axis of the structure and the direction of wave advance, R' is the reduced dynamic component of force, R is the dynamic force that would occur if the wave hit perpendicular to the structure. The development of Equation 7-103 is given in Figure 7-81. *Force reduction by Equation 7-103 should be applied only to the dynamic wave-force component of breaking or broken waves and should not be applied to the hydrostatic component. The reduction is not applicable to rubble structures.* The maximum force does not act along the entire length of a wall simultaneously; consequently, the average force per unit length of wall will be lower.

7.36 EFFECT OF A NONVERTICAL WALL

Formulas previously presented for breaking and broken wave forces may be used for structures with nearly vertical faces.

If the face is sloped backward as in Figure 7-82 (a), the horizontal component of the dynamic force due to waves breaking either on or seaward of the wall should be reduced to,

$$R'' = R' \sin^2 \theta \qquad (7\text{-}104)$$

where θ is defined in Figure 7-82. The vertical component of the dynamic wave force may be neglected in stability computations. For design calculations, forces on stepped structures as in Figure 7-82 (b) may be computed as if the face were vertical, since the dynamic pressure is about the same as computed for vertical walls. Curved nonreentrant face structures (Fig. 7-82 (c)) and reentrant curved face walls (Fig. 7-82 (d)) may also be considered as vertical.
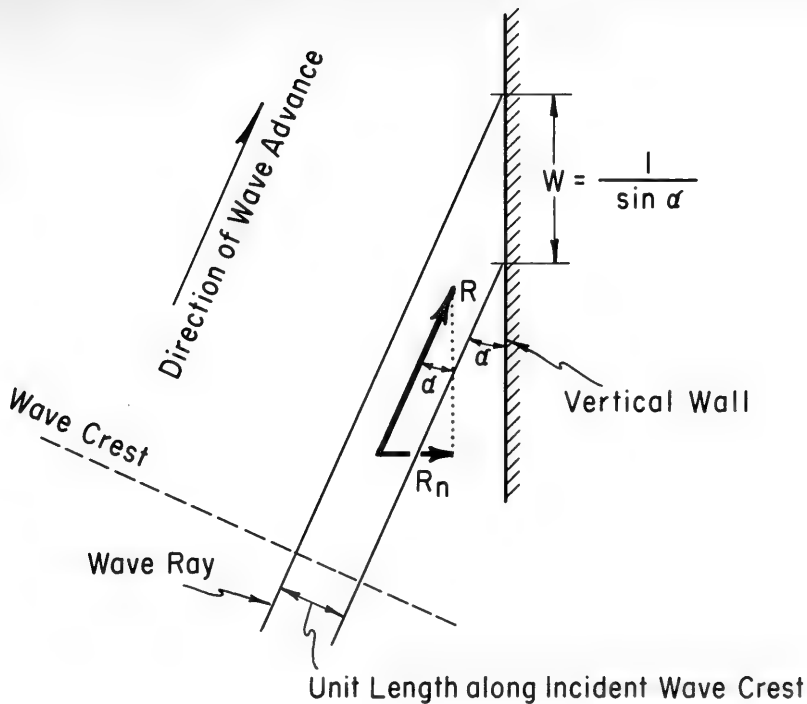
R = Dynamic Force Per Unit Length of Wall if Wall were Perpendicular to Direction of Wave Advance

R_n = Component of R Normal to Actual Wall. $R_n = R \sin \alpha$

W = Length Along Wall Affected by a Unit Length of Wave Crest. $W = 1/\sin \alpha$

R' = Dynamic Force Per Unit Length of Wall

$$R' = \frac{R_n}{W} = \frac{R \sin \alpha}{1/\sin \alpha} = R \sin^2 \alpha$$

$$R' = R \sin^2 \alpha$$

Figure 7-81. Effect of Angle of Wave Approach--Plan View
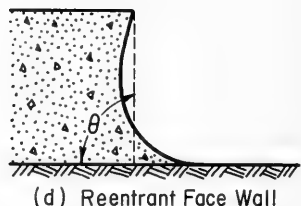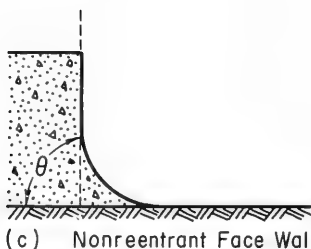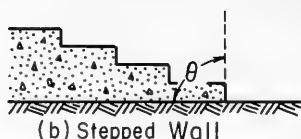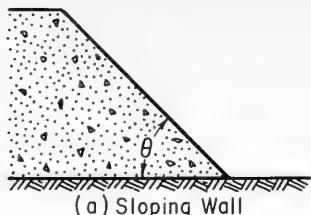
Figure 7-82. Wall Shapes

* * * * * * * * * * * * * * EXAMPLE PROBLEM * * * * * * * * * * * * * * * *

GIVEN: A structure in water, d_s = 7.5 ft. on a 1:20 nearshore slope is subjected to breaking waves, H_b = 8.4 ft., and period T = 6 secs. The angle of wave approach is, α = 80° and the wall has a shoreward sloping face of 10 (vertical) on 1 (horizontal).

FIND:

(a) The reduced total horizontal wave force.

(b) The reduced total overturning moment about the toe (neglect the vertical component of the hydrostatic force).

SOLUTION: From the example problem of Section 7.331 for the given wave conditions,

$$R_m = 16,900 \text{ lbs./ft.}$$

$$M_m = 126,800 \frac{\text{lb.-ft.}}{\text{ft.}}$$

$$R_s = 4,380 \text{ lbs./ft.}$$

and

$$M_s = 17,100 \frac{\text{lb.-ft.}}{\text{ft.}}$$

7-166

Applying the reduction of Equation 7-103 for the angle of wave approach, with

$$R_m = R ,$$

$$R' = R_m \sin^2 \alpha = 16,900 \, (\sin 80°)^2 ,$$

$$R' = 16,900 \, (0.985)^2 = 16,400 \, \text{lbs./ft.}$$

Similarly,

$$M' = M_m \sin^2 \alpha = 126,800 \, (\sin 80°)^2 ,$$

$$M' = 126,800 \, (0.985)^2 = 123,000 \, \frac{\text{lb.-ft.}}{\text{ft.}} .$$

Applying the reduction for a nonvertical wall, the angle the face of the wall makes with the vertcal is,

$$\theta = \arctan (10) \approx 84° .$$

Applying Equation 7-104,

$$R'' = R' \sin^2 \theta = 16,400 \, (\sin 84°)^2 ,$$

$$R'' = 16,400 \, (0.995)^2 = 16,200 \, \text{lbs./ft.}$$

Similarly for the moment,

$$M'' = M' \sin^2 \theta = 123,000 \, (\sin 84°)^2 ,$$

$$M'' = 123,000 \, (0.995)^2 = 121,800 \, \frac{\text{lb.-ft.}}{\text{ft.}} .$$

The total force and overturning moment are given by the sums of the reduced dynamic components and the unreduced hydrostatic components. Therefore,

$$R_t = 16,200 + 4,400 = 20,600 \, \text{lb./ft.} ,$$

$$M_t = 121,800 + 17,100 = 138,900 \, \frac{\text{lb.-ft.}}{\text{ft.}} .$$

* *

7.37   STABILITY OF RUBBLE STRUCTURES

7.371   General.   A rubble structure is composed of several layers of random-shaped and random-placed stones, protected with a cover layer of selected armor units of either quarry stones or specially shaped concrete units.   Armor units in the cover layer may be placed in an orderly manner

to obtain good wedging or interlocking action between individual units, or they may be placed at random. Present technology does not provide guidance to determine the forces required to displace individual armor units from the cover layer. Armor units may be displaced either over a large area of the cover layer sliding down the slope *en masse*, or individual armor units may be lifted and rolled either up or down the slope. Empirical methods have been developed that, if used with care, will give a satisfactory determination of the stability characteristics of these structures, when under attack by storm waves.

A series of basic decisions must be made in designing a rubble structure. Those decisions are discussed in succeeding sections.

7.372 **Design Factors.** A primary factor influencing wave conditions at a structure site is the bathymetry in the general vicinity of the structure. Depths will partly determine whether a structure is subjected to breaking, nonbreaking, or broken waves for a particular design wave condition. (See Section 7.1, WAVE CHARACTERISTICS.)

Variation in water depth along the structure axis must also be considered as it affects wave conditions, being more critical where breaking waves occur than where the depth may allow only nonbreaking waves or waves that overtop the structure.

When waves impinge on rubble structures, they may:

(a) break completely, projecting a jet of water roughly perpendicular to the slope,

(b) partially break with a poorly defined jet, or

(c) establish an oscillatory motion of the water particles up or down the structure slope, similar to the motion of a clapotis at a vertical wall.

The design wave for a rubble structure is usually the significant wave. Damage from waves higher than the significant wave is progressive, but the displacement of several individual armor units will not necessarily result in the complete loss of protection. A logic diagram for the evaluation of the marine envrionment is presented in Figure 7-6, and summarizes factors involved in selecting the design water depth and wave conditions to be used in the analysis of a rubble structure.

7.373 **Hydraulics of Cover Layer Design.** Until about 1930, design of rubble structures was based only on experience and general knowledge of site conditions. Empirical formulas subsequently developed are generally expressed in terms of the stone weight required to withstand design wave conditions. These formulas have been partially substantiated in model studies. They are guides, and must be used with experience and engineering judgment.

Following work by Iribarren (1938, 1950), comprehensive investigations were made by Hudson (1953, 1959, 1961 a, and 1961 b) at the U.S. Army Engineer Waterways Experiment Station (WES), and a formula was developed to determine the stability of armor units on rubble structures. The stability formula, based on the results of extensive small-scale model testing and some preliminary verification by large-scale model testing is

$$W = \frac{w_r \, H^3}{K_D \, (S_r - 1)^3 \, \cot \theta} \qquad (7\text{-}105)$$

where

W = weight in pounds of an individual armor unit in the primary cover layer. (When the cover layer is two quarry stones in thickness, the stones comprising the primary cover layer can range from about 0.75 W to 1.25 W with about 75 percent of the individual stones weighing more than W. The maximum weight of individual stones depends on the size or shape of the unit. The unit should not be of such a size as to extend an appreciable distance above the average level of the slope.)

w_r = unit weight (saturated surface dry) of armor unit, lbs./ft.^{3},

H = design wave height at the structure site in feet. (See Section 7.372.),

S_r = specific gravity of armor unit, relative to the water at the structure, $(S_r = w_r/w_w)$.

w_w = unit weight of water, fresh water = 62.4 lbs./ft.^{3}, sea water = 64.0 lbs./ft.^{3},

θ = angle of structure slope measured from horizontal in degrees,

and

K_D = stability coefficient that varies primarily with the shape of the armor units, roughness of the armor unit surface, sharpness of edges and degree of interlocking obtained in placement. (See Table 7-6.)

Equation 7-105 is intended for conditions when the crest of the structure is high enough to prevent major overtopping. Also the slope of the cover layer will be partly determined on the basis of stone sizes economically available. Cover layer slopes steeper than 1 on 1.5 are not recommended by the Corps of Engineers. Figures 7-83 through 7-86 provide a graphical solution of Equation 7-105.

Table 7-6. Suggested K_D Values for Use in Determining Armor Unit Weight

			No-Damage Criteria and Minor Overtopping				
Armor Units	n *	Placement	Structure Trunk		Structure Head		
			K_D §		K_D		Slope
			Breaking wave	Nonbreaking wave	Breaking wave	Nonbreaking wave	$\cot \theta$
Quarrystone							
Smooth rounded	2	random	2.1	2.4	1.7	1.9	1.5 to 3.0
Smooth rounded	>3	random	2.8	3.2	2.1	2.3	||
Rough angular	1	random †	†	2.9	†	2.3	||
Rough angular	2	random	3.5	4.0	2.9 / 2.5 / 2.0	3.2 / 2.8 / 2.3	1.5 / 2.0 / 3.0
Rough angular	>3	random	3.9	4.5	3.7	4.2	||
Rough angular	2	special ‡	4.8	5.5	3.5	4.5	||
Tetrapod and Quadripod	2	random	7.2	8.3	5.9 / 5.5 / 4.0	6.6 / 6.1 / 4.4	1.5 / 2.0 / 3.0
Tribar	2	random	9.0	10.4	8.3 / 7.8 / 7.0	9.0 / 8.5 / 7.7	1.5 / 2.0 / 3.0
Dolos	2	random	22.0 ¶	25.0 ¶	15.0 / 13.5	16.5 / 15.0	2.0 £ / 3.0
Modified Cube	2	random	6.8	7.8	——	5.0	||
Hexapod	2	random	8.2	9.5	5.0	7.0	||
Tribar	1	uniform	12.0	15.0	7.5	9.5	||
Quarrystone (K_{RR}) Graded angular	–	random	2.2	2.5			

* n is the number of units comprising the thickness of the armor layer.

† The use of single layer of quarrystone armor units subject to breaking waves is not recommended, and only under special conditions for nonbreaking waves. When it is used, the stone should be carefully placed.

‡ Special placement with long axis of stone placed perpendicular to structure face.

§ Applicable to slopes ranging from 1 on 1.5 to 1 on 5.

\|\| Until more information is available on the variation of K_D value with slope, the use of K_D should be limited to slopes ranging from 1 on 1.5 to 1 on 3. Some armor units tested on a structure head indicate a K_D-slope dependence.

¶ Data only available for 1 on 2 slope.

£ Slopes steeper than 1 on 2 not recommended at the present time.
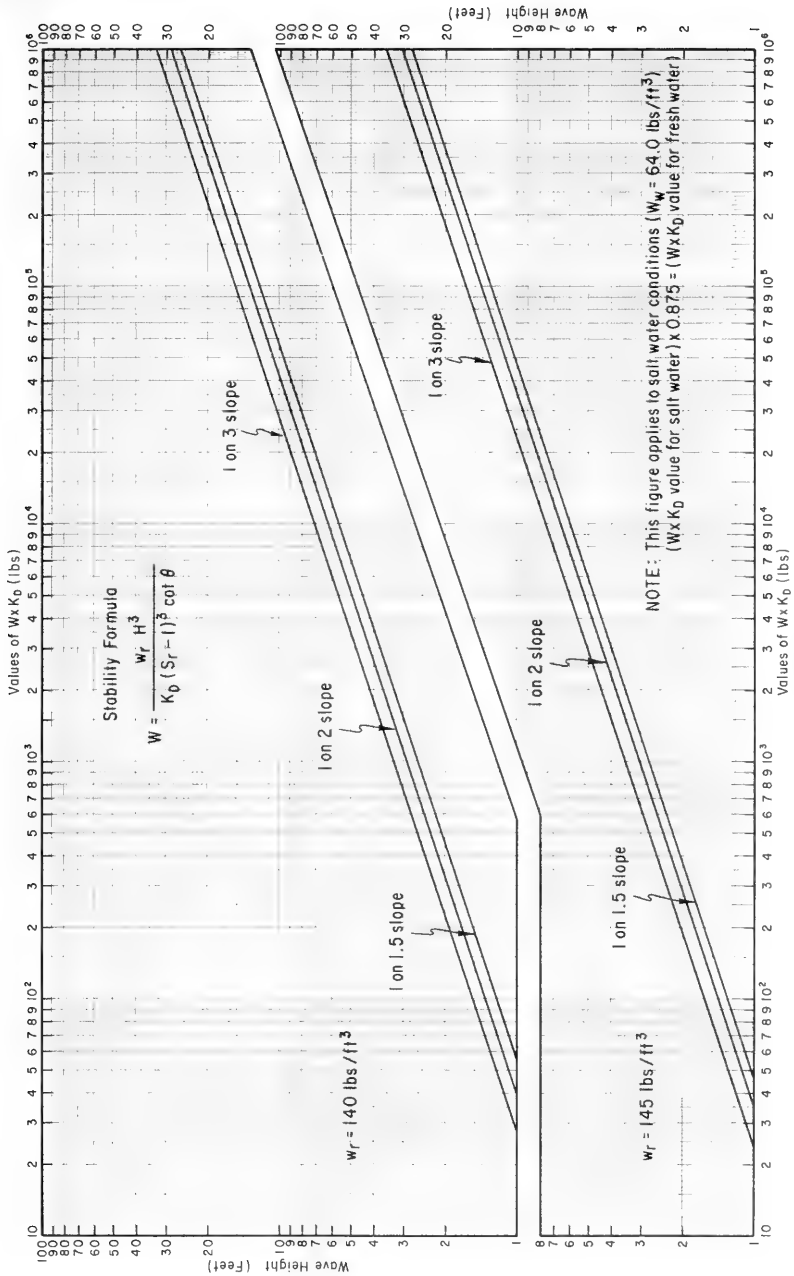
Figure 7-83 Weight of Armor Units x K_D Versus Wave Height for Various Slope Values (w_r = 140 lbs /ft³ and 145 lbs /ft³)
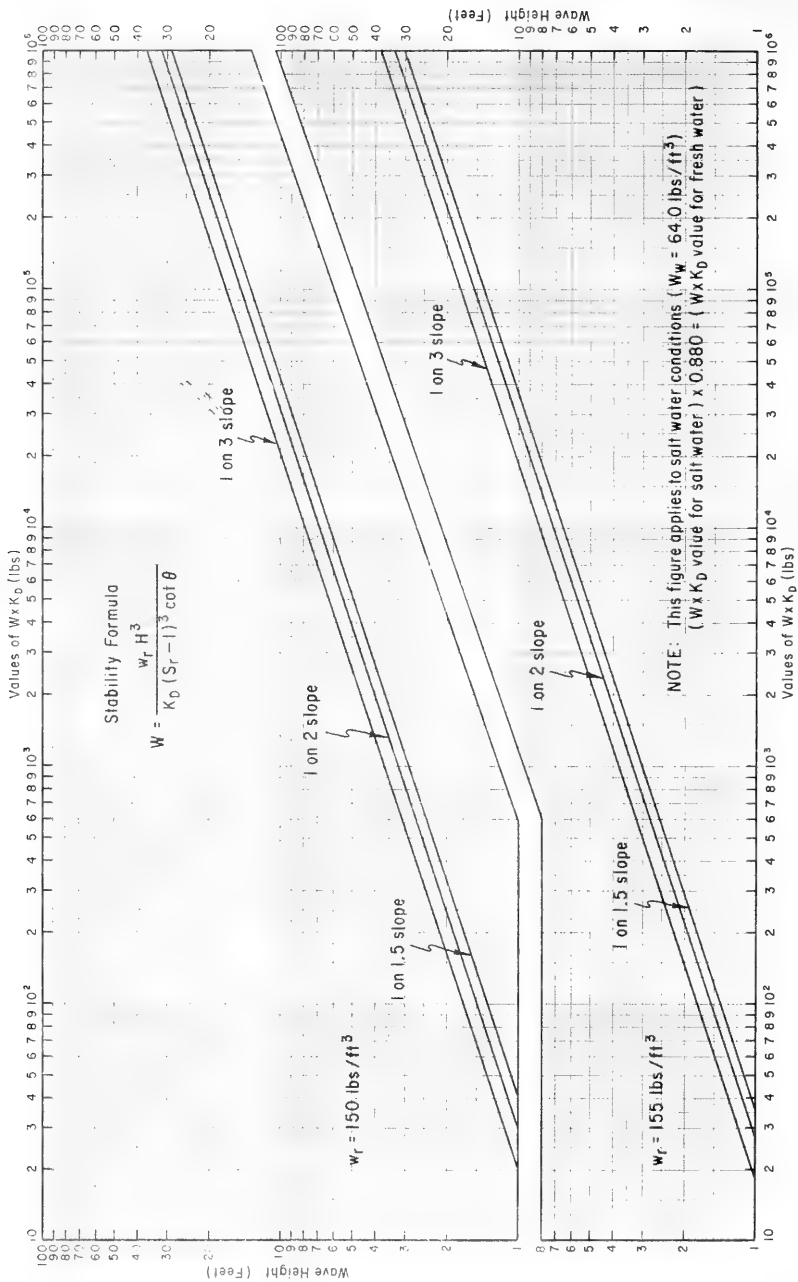
Figure 7-84. Weight of Armor Units x K_D Versus Wave Height for Various Slope Values ($w_r = 150$ lbs/ft^3 and 155 lbs/ft^3)
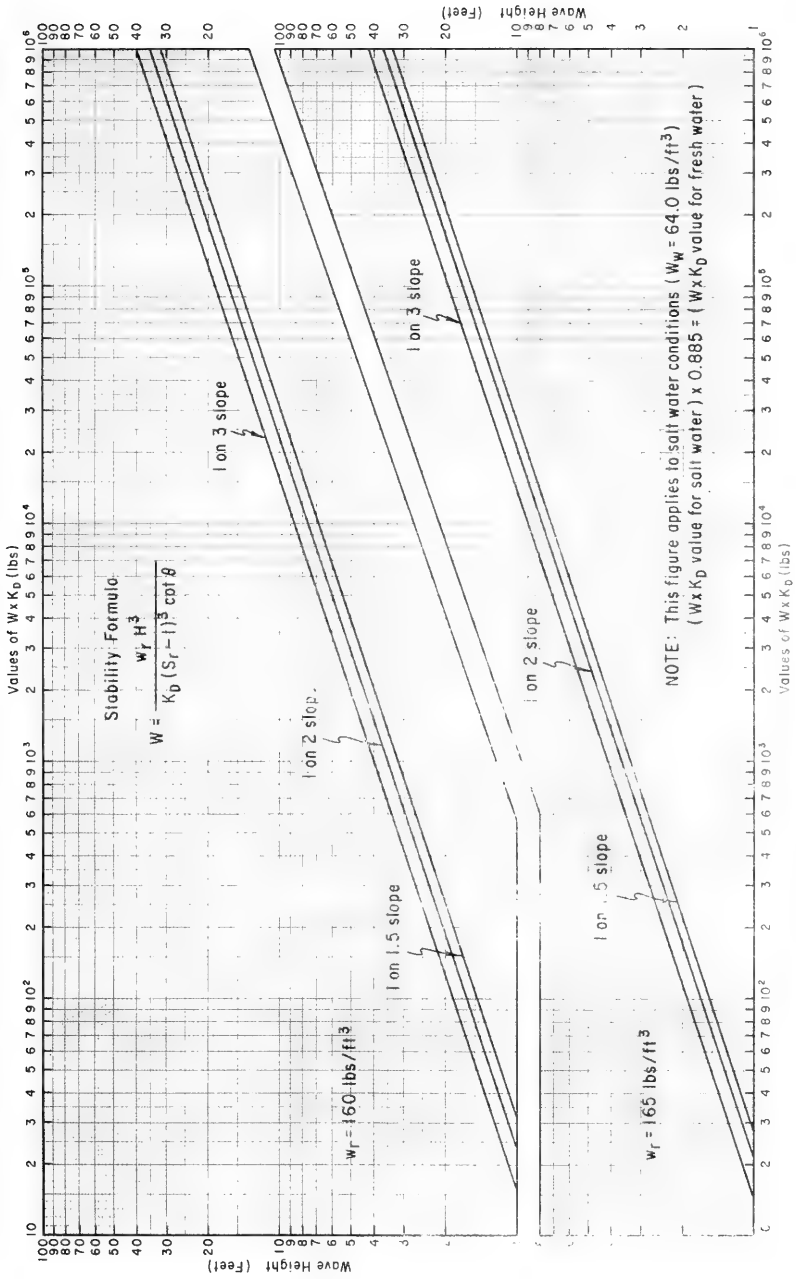
Figure 7-85. Weight of Armor Units ID Versus Wave Height for Various Slope Values (w_r = 160 lbs/ft³ and 165 lbs/ft³)

Stability Formula

$$W = \frac{w_r H^3}{K_D (S_r - 1)^3 \cot \theta}$$

NOTE: This figure applies to salt water conditions (w_w = 64.0 lbs/ft³) ($W \times K_D$ value for salt water) x 0.885 = ($W \times K_D$ value for fresh water)

7 - 71
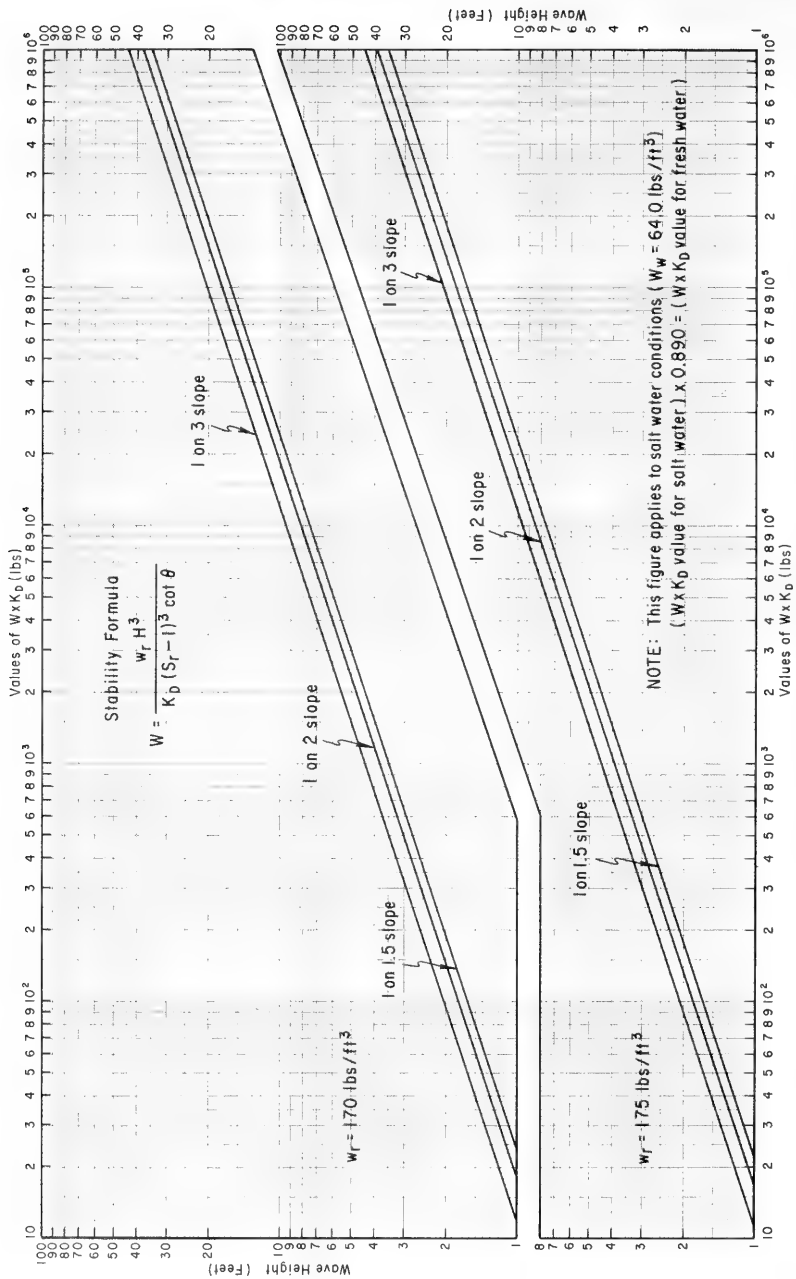
Figure 7-86. Weight of Armor Units x K_D Versus Wave Height for Various Slope Values (w_r = 170 lbs/ft^3 and 175 lbs/ft^3)

Stability Formula

$$W = \frac{w_r H^3}{K_D (S_r - 1)^3 \cot \theta}$$

NOTE: This figure applies to salt water conditions (W_w = 64.0 lbs/ft^3).
($W \times K_D$ value for salt water) x 0.890 = ($W \times K_D$ value for fresh water.)

Equation 7-105 determines the weight of an armor unit of nearly uniform size. For a graded riprap armor stone, Hudson and Jackson (1962) have modified the equation to:

$$W_{50} = \frac{w_r\ H^3}{K_{RR}\ (S_r - 1)^3\ \cot\theta} \qquad (7\text{-}106)$$

The symbols are the same as defined for Equation 7-105 except that W_{50} is the weight of the 50-percent size in the gradation. The maximum weight of graded rock is 3.6 W_{50}; the minimum is 0.22 W_{50}. K_{RR} is a stability coefficient for angular graded riprap, similar to K_D. Values of K_{RR} are shown in Table 7-6. These values allow for 5 percent damage. (Hudson and Jackson, 1962.)

Use of graded riprap cover layers is generally more applicable to revetments than to breakwaters or jetties. A limitation for the use of graded riprap is that the design wave height should be less than about 5 feet. For waves higher than 5 feet, it is usually more economical to use the more uniform-size armor units as indicated in Equation 7-105.

7.374 Selection of Stability Coefficient. The dimensionless stability coefficient K_D in Equation 7-105 accounts for all variables other than structure slope, wave height, unit weight of armor units, and the specific gravity of water at the site (i.e., fresh or salt water). These variables include:

(1) Shape of armor units,

(2) number of layers of armor units,

(3) manner of placing armor units,

(4) surface roughness and sharpness of edges of armor units (degree of interlocking of armor units),

(5) type of wave attacking structure (breaking or nonbreaking),

(6) part of structure (trunk or head),

(7) angle of incidence of wave attack,

(8) model scale (Reynolds number),

(9) unit weight of armor units,

(10) distance below stillwater level that the armor units extend down the face slope,

(11) size and porosity of underlayer material,

7-175

(12)   core height relative to stillwater level,

    (13)   crown type (concrete cap or armor units over the crown and
           extending down the back slope),

    (14)   crown elevation above stillwater level relative to wave height,
           and

    (15)   crest width.

Hudson (1959, 1961 a, and b) and Hudson and Jackson (1959) have conducted
numerous laboratory tests with a view to establishing values of K_D for
various conditions of some of the variables. They have found that for a
given geometry of rubble structure, the most important variables listed
above with respect to the magnitude of K_D are those from (1) through (8).
While the angle of wave approach may be important in the stability of
armor units especially when the waves are breaking directly on the struc-
ture, sufficient information is not available to provide firm guidance on
angle effect of the stability coefficient. The data of Hudson and Jackson
comprise the basis for selecting K_D, although a number of limitations in
the application of laboratory results to prototype conditions must be
recognized. These are:

    (1)   Laboratory waves were monochromatic and did not reproduce the
variable conditions of nature. Laboratory studies by Ouellet (1972) and
Rogan (1969) have shown that action of irregular waves (wave spectrum) on
model rubble structures can be modeled by monochromatic waves if the mono-
chromatic wave height corresponds to the significant wave height of the
spectrum. The validity of this comparison depends somewhat on the shape
of the wave spectrum, with the best agreement for a narrow band spectrum
(narrow range of frequencies or periods) when the wave heights are dis-
tributed according to a Rayleigh distribution. (See Section 3.2.)

    (2)   Preliminary analysis of large-scale tests has indicated that
the scale effect is probably unimportant, and can be made negligible by
the proper selection of linear scale for the tests (Reynolds Number,
$R_e \geq 6 \times 10^4$).

    (3)   The degree of interlocking obtained in the special placement
of armor units in the laboratory is unlikely to be duplicated in the pro-
totype. Above the water surface in prototype construction, it is possi-
ble to place armor units with a high degree of interlocking. Below the
water surface, the same quality of interlocking can rarely be attained.
It is therefore advisable to use data obtained from random placement in
the laboratory as a basis for K_D values.

    (4)   Numerous tests have been performed for nonbreaking waves, but
only limited tests are available for plunging waves. Limited test re-
sults for breaking waves indicate that the K_D value for breaking waves
is proportional the K_D value for nonbreaking waves. Therefore, K_D
values for armor units not tested for breaking waves have been obtained
by applying a reduction factor to the K_D value for nonbreaking waves.

(5) Under similar wave conditions, the head of a rubble structure normally sustains more extensive and frequent damage than the trunk of the structure. Under all wave conditions, a segment of the slope of the rounded head of the structure is subject to overtopping. A part of the head is usually subject to direct wave attack regardless of wave direction. A wave trough on the lee side coincident with maximum runup on the windward side will create a high static head for flow through the structure.

Based on available data and the discussion above, Table 7-6 presents recommended values for K_D. Because of the limitations discussed, values in the table provide little or no safety factor. The experience of the field engineer may be utilized to adjust the K_D value indicated in Table 7-6, but deviation to less conservative values should be fully evaluated. A two-unit armor layer is recommended. If a one-unit armor layer is considered, the K_D values for a single layer should be obtained from Table 7-6. The indicated K_D values are less for a single-stone layer than for a two-stone layer, and will require heavier armor stone to ensure stability. More care must be taken in the placement of a single armor layer to ensure that armor units provide an adequate cover for the underlayer and that there is a high degree of interlock with adjacent armor units.

These coefficients were derived from large- and small-scale tests that used many various shapes and sizes of both natural and artificial armor units. Values are reasonably definitive, and are recommended for design.

The values given in Table 7-6 are indicated as no-damage criteria, but actually consider up to 5 percent damage. If some degree of damage to the cover layer is acceptable, slightly larger values of K_D can be used for design. The deliberate selection of a larger value of K_D than recommended in Table 7-6 may be partly justified by the fact that settlement of the structure and readjustment of the interlocking between armor units can result in a more stable structure than the original structure. It is possible that structural damage will occur to individual concrete armor units during movement and rekeying of the units. However, a structure designed to resist waves of a moderate storm, but which may suffer damage without complete destruction during a severe storm, will have a lower annual cost than one designed to be completely stable for larger waves. Values of K_D as a function of percent damage to the rubble structure have been determined for several of the armor unit shapes. (See Table 7-7.) These values, together with statistical data concerning the frequency of occurrence of waves of different heights, should be used to determine the annual cost as a function of the acceptable percent damage without endangering the functional characteristics of the structure.

Table 7-7 shows the results of damage tests where $H/H_{D=0}$ and K_D are functions of the percent damage D for various armor units. H is the significant wave height corresponding to damage D. $H_{D=0}$ is the

significant wave height corresponding to 0- to 5-percent damage, gener-
ally referred to as no-damage condition. K_D is the stability coeffi-
cient for the respective armor unit and damage condition.

Table 7-7. $H/H_{D=0}$ and K_D as a Function of Cover-Layer Damage and Type of Armor Unit

Unit		Damage (D) in Percent						
		0 to 5	5 to 10	10 to 15	15 to 20	20 to 30	30 to 40	40 to 50
Quarrystone (smooth)	$H/H_{D=0}$	1.00	1.08	1.14	1.20	1.29	1.41	1.54
	K_D	2.4	3.0	3.6	4.1	5.1	6.7	8.7
Quarrystone (rough)	$H/H_{D=0}$	1.00	1.08	1.19	1.27	1.37	1.47	1.56
	K_D	4.0	4.9	6.6	8.0	10.0	12.4	15.0
Tetrapods & Quadripods	$H/H_{D=0}$	1.00	1.09	1.17	1.24	1.32	1.41	1.50
	K_D	8.3	10.8	13.4	15.9	19.2	23.4	27.8
Tribar	$H/H_{D=0}$	1.00	1.11	1.25	1.36	1.50	1.59	1.64
	K_D	10.4	14.2	19.4	26.2	35.2	41.8	45.9

Breakwater Trunk, n = 2, Random Placed Armor Units, Nonbreaking Waves, and Minor Overtopping Conditions.

The percent damage is based on the volume of armor units displaced
from the zone of active armor unit removal for a specific significant
wave height. This zone, as defined by Jackson (1968 a), extends from
the middle of the breakwater crest down the seaward face to a depth
equivalent to one zero-damage wave height $H_{D=0}$ below the stillwater
level. Once damage occurred, testing was continued for the specified
wave condition until slope equilibrium was established or armor unit
displacement ceased.

The following example illustrates the ways in which Table 7-7 may
be used.

* * * * * * * * * * * * * * EXAMPLE PROBLEM * * * * * * * * * * * * * * * * *

GIVEN: Rough two-layer quarrystone breakwater designed for nonbreaking
wave and minor overtopping from a no-damage design wave of $H_{D=0}$ = 8
feet and a K_D = 4.0.

FIND:

(a) Anticipated percent damage from a wave height H = 9 feet,

(b) anticipated percent damage from using a value of K_D = 8.2 in the
stability analysis instead of K_D = 4.0, and

(c) appropriate values of wave height, H and stability coefficient,
K_D for acceptable 30- to 40-percent damage.

7-178

SOLUTION:

(a) Calculate,

$$\frac{H}{H_{D=0}} = \frac{9}{8} = 1.13 .$$

Using Table 7-7, the value of $H/H_{D=0}$ for rough quarrystone falls between 5- to 10-percent and 10- to 15-percent damage, therefore the anticipated damage for a 9-foot wave would be about 10 percent.

(b) Table 7-7, using a value of $K_D = 8.2$ for rough quarrystone, shows a percent damage range of 15 to 20 percent.

(c) From Table 7-7 for D = 30 to 40 percent,

$$\frac{H}{H_{D=0}} = 1.47,$$

or

$$H = 8 (1.47) = 11.8 \text{ ft.}$$

and

$$K_D = 12.6.$$

Therefore if the structure were designed for a wave height, $H_{D=0} = 8$ feet and a no-damage stability coefficient $K_D = 4.0$ and subsequently attacked by waves $H = 11.8$ feet, the anticipated damage to the structure's armor layer could be between 30 and 40 percent. On the other hand, if the structure were only designed for a 5.4-foot wave ($H_{D=0}$), but an 8-foot wave could occur, then 30- to 40-percent damage should be anticipated from the 8-foot wave.

If the structure were designed for H = 8 feet and $K_D = 12.6$ instead of the no-damage value of $K_D = 4.0$, 30- to 40-percent damage could be anticipated as the result of the occurrence of an 8-foot wave.

* *

7.375 Importance of Unit Weight of Armor Units. The basic equation used for design of armor units for rubble structures indicates that the unit weight w_r of quarrystone or concrete is important. Designers should carefully evaluate the advantages of increasing unit weight of concrete armor units to effect savings in the structure cost. Brantzaeg (1966) cautioned that variations in unit weight should be limited within a range --say 120 lbs./ft.^{3} to 180 lbs./ft.^{3} Unit weight of quarry-stone available from a particular quarry will likely vary over a narrow range of values. The unit weight of concrete containing normal aggregates is usually between 140 pcf and 155 pcf. It can be made higher or lower through the use of special heavy or light weight aggregates that are usually available but are more costly than normal aggregates. The unit weight obtainable from a given set of materials and mixture proportions can be computed from

Method CRD-3 of the Handbook for Concrete and Cement published by the U.S. Army Engineers Waterways Experiment Station. Figure 7-87 illustrates the effect of varying the value of the unit weight w_r on the weight of the armor unit W in Equation 7-105. The weight factor of armor unit f is the ratio of,

$$\frac{w_r}{\left(\dfrac{w_r}{w_w} - 1\right)^3} \text{ to } \frac{150}{\left(\dfrac{150}{64} - 1\right)^3}$$

The effect of varying the unit weight of concrete is illustrated by the following example problem.

* * * * * * * * * * * * * * EXAMPLE PROBLEM * * * * * * * * * * * * * * *

GIVEN: A 36-ton concrete armor unit is required for the protection of a rubble-mound structure against a given wave height. This weight was determined using a unit weight of concrete w_r = 145 lbs./ft.^{3}

FIND: Determine the required weight of armor unit for w_r = 140 lbs./ft.^{3} and w_r = 170 lbs./ft.^{3} concrete.

SOLUTION: Using the lower curve in Figure 7-87, the weight factor for

$$f\left(w_r = 140 \text{ lbs./ft.}^3\right) = 1.38 ,$$

$$f\left(w_r = 145 \text{ lbs./ft.}^3\right) = 1.18 ,$$

$$f\left(w_r = 170 \text{ lbs./ft.}^3\right) = 0.62 .$$

Thus for, w_r = 140 lbs./ft.^{3},

$$W = 36 \times \frac{1.38}{1.18} = 42.1 \text{ tons} ,$$

say W = 42 tons.

and for W_r = 170 lbs./ft.^{3},

$$W = 36 \times \frac{0.62}{1.18} = 18.9 \text{ tons} ,$$

say W = 19 tons.

* *

7.376 Concrete Armor Units. Many different concrete shapes have been developed as armor units for rubble structures. The major advantage of concrete armor units is that they usually have a higher stability coefficient value, thus permitting the use of steeper structure side slopes or a lighter weight of armor unit. This has particular value when quarrystone of the required size is not available.
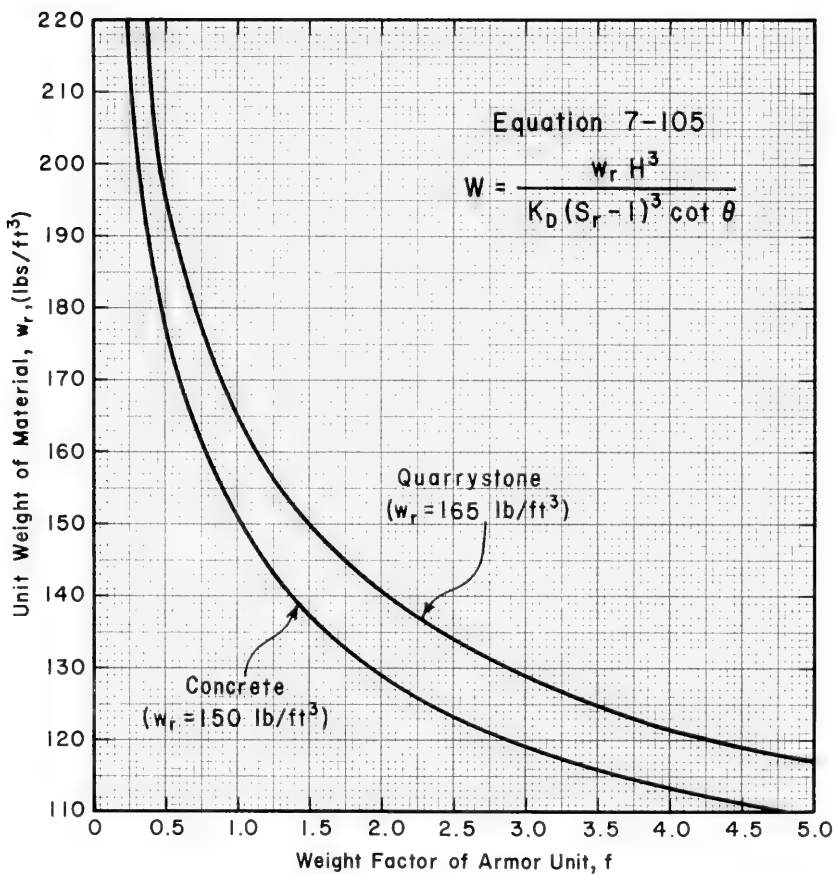
Figure 7-87. Effect of Unit Weight Changes on Required
Weight of Armor Unit

Table 7-8 lists the concrete armor units that have been cited in literature and shows where and when the unit was developed. One of the earlier non-block concrete armor units was the *tetrapod*. It was developed and patented in 1950 by Neyrpic, Inc., of France. The tetrapod is an unreinforced concrete shape with four truncated conical legs projecting radially from a center point. (See Figure 7-88.) International patent coverage requires a royalty be paid per cubic yard of concrete used in the unit. A general patent license agreement now exists between Neyrpic, and the U.S. Government regarding the royalty payment for use of tetrapods and quadripods.

Figure 7-89 provides volume, weight, thickness of layers, and dimensions of the tetrapod unit. The quadripod (⌐ig. 7-88) was developed and tested by the United States in 1959; details are shown in Figure 7-90.

In 1958, R. Q. Palmer, United States, developed and patented the *tribar*. This concrete shape consists of three cylinders connected by three radial arms. (See Figure 7-88.) The need for steel reinforced concrete in tribars depends on the techniques of placement and the size of the unit. Generally, when using land-based equipment, steel reinforcement is not required for units weighing less than 20 tons. Placing any type of armor unit from a floating plant subject to wave action can result in bumping of units resulting in overstress of the concrete. Some form of reinforcement may be required for tribars weighing about 10 tons or more when placed by floating equipment. Figure 7-91 provides tribar details on the volume, weight, thickness of layers and dimensions. According to the patent rights of the tribar, the U.S. Government is granted royalty-free use.

The *Dolos* armor unit was developed in 1963 by E. M. Merrifield, Republic of South Africa. (Merrifield and Zwamborn, 1968.) The Dolos is illustrated in Figure 7-88. This concrete unit closely resembles a ship anchor. Generally, reinforcement is not required for units weighing up to 20 tons, but for units over 20 tons reinforcement is required. (Magoon and Shimizu, 1971.) This armor unit is not patented in the United States. Detailed dimensions are shown in Figure 7-92.

As noted in Table 7-6, various other shapes have been tested by the Corps of Engineers. Other shapes are the *modified cube* and the *hexapod*. Details of the modified cube and hexapod are shown in Figures 7-93 and 7-94 respectively.

Projects using tetrapods, tribars, quadripods, and dolosse in the United States, are listed in Table 7-9.

7.377 Design of Structure Cross-Section. A rubble structure is normally comprised of a bedding layer and a core of quarry-run stone covered by one or more layers of larger stone and an exterior layer(s) of large quarrystone or concrete armor units. Typical rubble-mound cross sections for nonbreaking and breaking waves are shown in Figures 7-95

Table 7-8. Types of Concrete Armor Units

Name of Unit	Development of Unit	
	Country	Year
Akmon	Netherlands	1962
Bipod	Netherlands	1962
Cob	England	1969
*Cube	------------------	†
*Cube (modified)	United States	1959
*Dolos	South Africa	1963
Dom	Mexico	1970
Gassho Block	Japan	1967
Grabbelar	South Africa	1957
Hexaleg Block	Japan	-------
*Hexapod	United States	1959
Hollow Square	Japan	1960
Hollow Tetrahedron	Japan	1959
N-Shaped Block	Japan	1960
*Pelican Stool	United States	1960
*Quadripod	United States	1959
*Rectangular Block	------------------	†
Stabilopod	Romania	1965
Stabit	England	1961
*Sta-Bar	United States	1966
*Sta-Pod	United States	1966
Stalk Cube	Netherlands	1965
Svee Block	Norway	1961
*Tetrahedron (solid)	------------------	‡
*Tetrahedron (perforated)	United States	1959
Tetrapod	France	1950
Toskane	South Africa	1966
Tribar	United States	1958
Trigon	United States	1962
Tri-Long	United States	1968
Tripod	Netherlands	1962

* The units have been tested, some extensively, at the Waterways Experiment Station (WES).

† Cubes and rectangular blocks are known to have been used in masonry type breakwaters since early Roman times, and in rubble-mound breakwaters during the last two centuries. The cube was tested at WES as early as 1943.

‡ Solid tetrahedrons are known to have been used in hydraulic works for many years. This unit was tested at WES in 1959.
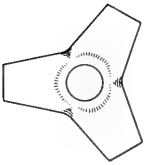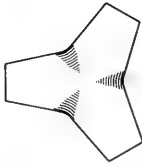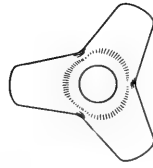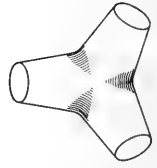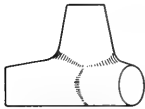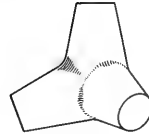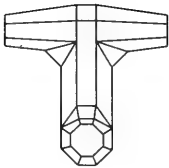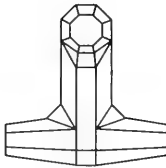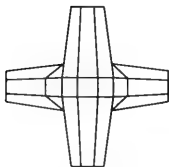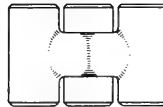
Figure 7-88. Concrete Armor Units

VOLUME OF INDIVIDUAL ARMOR UNITS (CU FT)

UNIT WEIGHT LB/CU FT	7.16	14.32	28.57	71.43	142.86	214.29	285.71	357.14	428.57	500.00	571.43
WEIGHT OF INDIVIDUAL ARMOR UNITS (TONS)											
140.0	0.50	1.00	2.00	5.00	10.00	15.00	20.00	25.00	30.00	35.00	40.00
149.6	0.53	1.07	2.14	5.34	10.68	16.02	21.36	26.70	32.04	37.38	42.71
156.0	0.56	1.11	2.23	5.57	11.14	16.71	22.29	27.86	33.43	39.00	44.57
162.0	0.58	1.16	2.31	5.79	11.57	17.36	23.14	28.93	34.71	40.50	46.29
AVERAGE MEASURED THICKNESS OF TWO LAYERS RANDOM PLACED (FT)											
	4.01	5.05	6.36	8.63	10.87	12.43	13.70	14.76	15.68	16.51	17.26
NUMBER OF ARMOR UNITS PER 1000 SQ FT (TWO LAYERS RANDOM PLACED)											
	290.10	176.40	111.10	60.42	37.94	29.02	24.02	20.70	18.41	16.64	15.18

DIMENSIONS OF ARMOR UNITS (FT)

SYMBOL	7.16	14.32	28.57	71.43	142.86	214.29	285.71	357.14	428.57	500.00	571.43
A	0.89	1.12	1.41	1.92	2.41	2.76	3.04	3.27	3.48	3.64	3.83
B	0.44	0.56	0.71	0.96	1.21	1.38	1.52	1.63	1.74	1.83	1.91
C	1.40	1.77	2.23	3.02	3.81	4.36	4.80	5.17	5.50	5.79	6.05
D	1.38	1.74	2.20	2.98	3.75	4.30	4.73	5.10	5.42	5.70	5.96
E	0.68	0.87	1.10	1.49	1.88	2.15	2.37	2.55	2.71	2.85	2.98
F	1.90	2.39	3.00	4.08	5.15	5.88	6.47	6.97	7.41	7.80	8.16
G	0.63	0.79	1.00	1.36	1.71	1.96	2.16	2.32	2.47	2.60	2.72
H	2.95	3.71	4.67	6.34	7.99	9.14	10.07	10.84	11.52	12.13	12.68
I	1.79	2.25	2.83	3.84	4.84	5.54	6.10	6.57	6.98	7.35	7.68
J	0.89	1.12	1.41	1.92	2.42	2.77	3.05	3.28	3.49	3.67	3.84
K	3.21	4.04	5.09	6.91	8.72	9.97	10.98	11.82	12.56	13.23	13.83
L	3.54	4.46	5.61	7.62	9.60	10.98	12.09	13.02	13.84	14.57	15.23

NOTE: DATA BASED ON TETRAPODS USED IN MODEL TESTS CONDUCTED AT THE WATERWAYS EXPERIMENT STATION

VOLUME OF INDIVIDUAL ARMOR UNIT = $0.280 H^3$

where:

A = 0.302 H
B = 0.151 H
C = 0.477 H
D = 0.470 H
E = 0.235 H
F = 0.644 H

G = 0.215 H
H = Overall dimension of unit
I = 0.606 H
J = 0.303 H
K = 1.091 H
L = 1.201 H
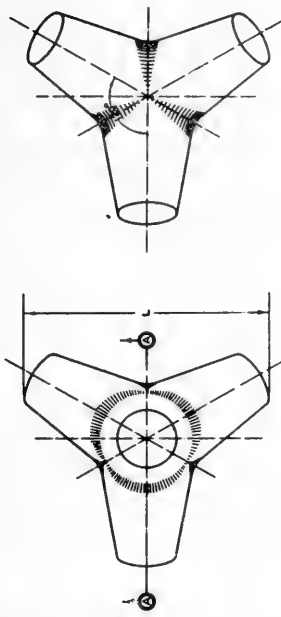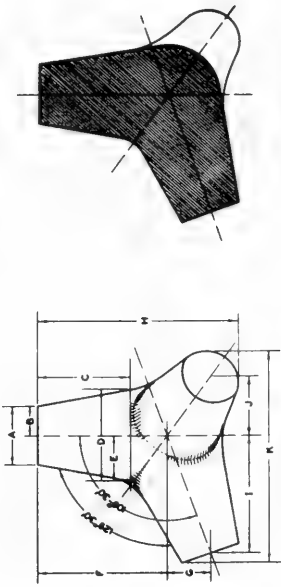
BOTTOM

SECTION—AA

PLAN

ELEVATION

Figure 7-89. Tetrapod Specifications

Figure 7-90. Quadripod Specifications

UNIT WEIGHT LB/CU FT	VOLUME OF INDIVIDUAL ARMOR UNITS (CU FT)										
	7.14	14.29	28.57	71.43	142.86	214.29	285.71	357.14	428.57	500.00	571.43
	WEIGHT OF INDIVIDUAL ARMOR UNITS (TONS)										
140.0	0.50	1.00	2.00	5.00	10.00	15.00	20.00	25.00	30.00	35.00	40.00
149.5	0.53	1.07	2.14	5.34	10.68	16.02	21.36	26.70	32.04	37.38	42.71
156.0	0.56	1.11	2.23	5.57	11.14	16.71	22.29	27.86	33.43	39.00	44.57
162.0	0.58	1.16	2.31	5.79	11.57	17.36	23.14	28.93	34.71	40.50	46.29
	THICKNESS OF TWO LAYERS PLACED PELL-MELL (FT)										
	3.66	4.61	5.81	7.86	9.93	11.37	12.51	13.48	14.33	15.08	15.77
	NUMBER OF ARMOR UNITS PER 1000 SQ FT (TWO LAYERS PLACED PELL-MELL)										
	261.05	164.44	103.59	56.30	35.37	27.04	22.30	19.26	17.15	15.41	14.15

DIMENSIONS OF ARMOR UNITS (FT)

SYMBOL											
A	0.93	1.17	1.48	2.00	2.52	2.88	3.17	3.42	3.63	3.82	4.01
B	0.46	0.58	0.74	1.00	1.26	1.44	1.59	1.71	1.82	1.92	2.00
C	1.20	1.61	2.03	2.76	3.48	3.98	4.38	4.72	5.03	5.28	5.52
D	1.30	1.74	2.19	2.97	3.74	4.28	4.71	5.08	5.40	5.68	5.94
E	0.65	0.87	1.09	1.49	1.87	2.14	2.36	2.54	2.70	2.84	2.97
F	1.97	2.48	3.13	4.25	5.35	6.12	6.74	7.26	7.72	8.12	8.49
H	2.43	3.07	3.86	5.24	6.61	7.57	8.33	8.97	9.53	10.03	10.49
I	1.97	2.48	3.13	4.25	5.35	6.12	6.74	7.26	7.72	8.12	8.49
J	0.99	1.24	1.56	2.12	2.67	3.06	3.37	3.63	3.85	4.06	4.25
	3.36	4.23	5.31	7.23	9.12	10.43	11.49	12.37	13.15	13.83	14.47
K	3.68	4.68	6.15	8.35	10.52	12.05	13.26	14.28	15.18	15.98	16.70

VOLUME OF INDIVIDUAL ARMOR UNIT = $0.495 G^3$

where:

A = 0.382 G   G = Overall height of unit
B = 0.191 G   H = 0.809 G
C = 0.526 G   I = 0.405 G
D = 0.566 G   J = 1.379 G
E = 0.283 G   K = 1.592 G
F = 0.809 G

BOTTOM

PLAN

ELEVATION

SECTION A-A

DIAMETER OF SEMICIRCLE adc = DIMENSION D
MAJOR AXIS OF SEMIELLIPSE adc = DIMENSION D
MINOR AXIS OF SEMIELLIPSE adc = DIMENSION A

NOTE: DATA BASED ON QUADRIPODS USED IN MODEL TESTS, CONDUCTED AT THE WATERWAYS EXPERIMENT STATION

Tribar Specifications

VOLUME OF INDIVIDUAL ARMOR UNITS (CU FT)

UNIT WEIGHT LB/CU FT	7.14	14.29	28.57	71.43	142.86	214.29	285.71	357.14	428.57	500.00	571.43
WEIGHT OF INDIVIDUAL ARMOR UNITS (TONS)											
140.0	0.50	1.00	2.00	5.00	10.00	15.00	20.00	25.00	30.00	35.00	40.00
149.5	0.53	1.07	2.14	5.34	10.68	16.02	21.36	26.70	32.04	37.38	42.71
156.0	0.56	1.11	2.23	5.57	11.14	16.71	22.29	27.86	33.43	39.00	44.57
162.0	0.58	1.16	2.31	5.79	11.57	17.36	23.14	28.93	34.71	40.50	46.29
AVERAGE MEASURED THICKNESS OF ONE LAYER PLACED UNIFORMLY (FT)											
	2.18	2.74	3.45	4.69	5.91	6.76	7.44	8.02	8.52	8.97	9.38
AVERAGE MEASURED THICKNESS OF TWO LAYERS PLACED PELL-MELL (FT)											
	3.85	4.85	6.11	8.30	10.46	11.97	13.17	14.19	15.08	15.87	16.60
NUMBER OF ARMOR UNITS PER 1000 SQ FT (ONE LAYER PLACED UNIFORMLY)											
	161.34	101.63	64.02	34.80	21.86	16.71	13.83	11.92	10.80	9.32	8.74
NUMBER OF ARMOR UNITS PER 1000 SQ FT (TWO LAYERS PLACED PELL-MELL)											
	247.88	156.12	98.35	53.45	33.58	25.67	21.25	18.31	16.28	14.63	13.43

DIMENSIONS OF ARMOR UNITS (FT)

SYMBOL											
A	1.05	1.32	1.66	2.25	2.84	3.25	3.58	3.85	4.09	4.31	4.51
B	0.52	0.66	0.83	1.13	1.42	1.62	1.79	1.93	2.05	2.15	2.25
C	1.25	1.58	1.99	2.70	3.41	3.90	4.29	4.62	4.91	5.17	5.41
D	1.78	2.24	2.82	3.83	4.82	5.52	6.08	6.55	6.96	7.33	7.66
E	1.09	1.37	1.72	2.34	2.95	3.38	3.72	4.00	4.25	4.48	4.68
F	3.22	4.06	5.11	6.93	8.74	9.97	11.01	11.86	12.60	13.26	13.87
G	2.09	2.63	3.32	4.51	5.68	6.50	7.15	7.70	8.19	8.62	9.01
H	0.52	0.66	0.83	1.13	1.42	1.62	1.79	1.93	2.05	2.15	2.25

NOTE: SHAPE AND DIMENSIONS OF UNIT WERE BASED ON THOSE USED IN MODEL TESTS. AT PRESENT TIME PATENTEE RECOMMENDS C = 1.25 A, AND FILLETS AT INTERSECTION OF HORIZONTAL AND VERTICAL MEMBERS WITH A RADIUS EQUAL TO A/4

SECTION A-A
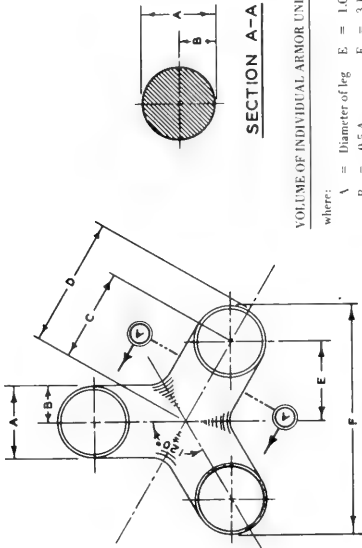
VOLUME OF INDIVIDUAL ARMOR UNIT = $6.48\,A^3$

where:

A = Diameter of leg	E = 1.08 A
B = 0.5 A	F = 3.16 A
C = 1.25 A	G = 2 A
D = 1.75 A	H = B = 0.5 A

PLAN
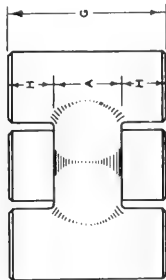
ELEVATION

Figure 7-91. Tribar Specifications

UNIT WEIGHT LB/CU FT	VOLUME OF INDIVIDUAL UNITS (CU FT)										
	7.14	14.29	28.57	71.43	142.86	214.29	285.71	357.14	428.57	500.00	571.43
	WEIGHT OF INDIVIDUAL ARMOR UNITS (TONS)										
140.0	0.50	1.00	2.00	5.00	10.00	15.00	20.00	25.00	30.00	35.00	40.00
149.5	0.53	1.07	2.14	5.34	10.68	16.02	21.36	26.70	32.04	37.38	42.71
156.0	0.56	1.11	2.23	5.57	11.14	16.71	22.29	27.86	32.43	39.00	44.57
162.0	0.58	1.16	2.31	5.79	11.57	17.36	23.14	28.93	34.71	40.50	46.29
	NUMBER OF ARMOR UNITS PER 1,000 SQ FT (TWO LAYERS RANDOM PLACED)										
	199.5	125.7	79.2	43.0	27.08	20.67	17.06	14.70	13.02	11.57	10.75
	AVERAGE MEASURED THICKNESS OF TWO LAYERS RANDOM PLACED (FT)										
	3.85	4.85	6.11	8.30	10.46	11.97	13.17	14.19	15.08	15.87	16.60
SYMBOL	DIMENSIONS OF ARMOR UNITS (FT)										
A	0.71	0.89	1.13	1.53	1.93	2.20	2.43	2.61	2.78	2.92	3.06
B	1.13	1.43	1.80	2.44	3.08	3.52	3.88	4.18	4.44	4.68	4.89
C	3.55	4.47	5.63	7.64	9.63	11.02	12.13	13.08	13.89	14.62	15.29
D	0.20	0.25	0.32	0.43	0.55	0.62	0.69	0.74	0.79	0.83	0.87

NOTE: SHAPE AND DIMENSIONS OF UNIT WERE BASED ON THOSE USED IN MODEL TESTS. AT PRESENT TIME INVENTOR RECOMMENDS B = 0.32 C TO 0.36 C DEPENDING ON THE WEIGHT OF THE INDIVIDUAL UNIT.

VOLUME OF INDIVIDUAL ARMOR UNIT = $0.16 \, C^3$

where:

A = 0.20 C   C = Overall dimension
B = 0.32 C   D = 0.057 C

SIDE
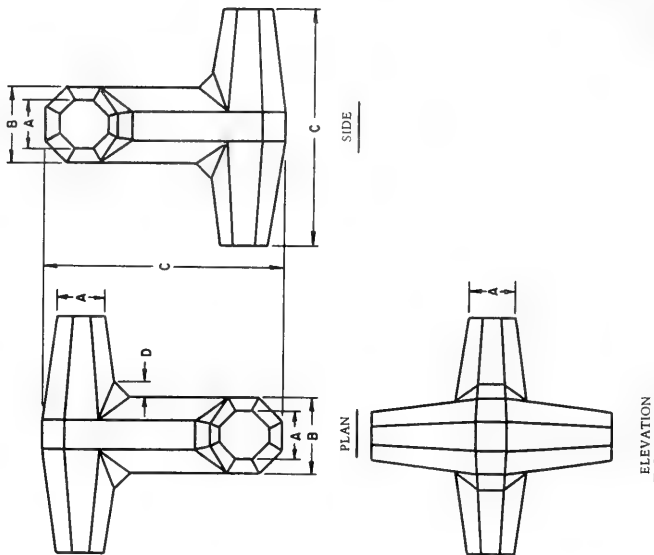
PLAN

ELEVATION

Figure 7-92. Dolos Specifications

VOLUME OF INDIVIDUAL ARMOR UNITS (CU FT)

UNIT WEIGHT LB/CU FT	7.14	14.29	28.57	71.43	142.86	214.29	285.71	357.14	428.57	500.00	571.43
WEIGHT OF INDIVIDUAL ARMOR UNITS (TONS)											
140.0	0.50	1.00	2.00	5.00	10.00	15.00	20.00	25.00	30.00	35.00	40.00
149.5	0.53	1.07	2.14	5.34	10.68	16.02	21.35	26.70	32.04	37.38	42.71
156.0	0.56	1.11	2.23	5.57	11.14	16.71	22.29	27.86	33.43	39.00	44.57
162.0	0.58	1.16	2.31	5.79	11.57	17.36	23.14	28.93	34.71	40.50	46.29
AVERAGE MEASURED THICKNESS OF ONE LAYER PLACED UNIFORMLY (FT)											
	2.16	2.72	3.42	4.65	5.86	6.70	7.38	7.95	8.44	8.89	9.29
AVERAGE MEASURED THICKNESS OF TWO LAYERS RANDOM PLACED (FT)											
	4.24	5.34	6.73	9.13	11.50	13.16	14.49	15.61	16.59	17.46	18.26
NUMBER OF ARMOR UNITS PER 1000 SQ FT (ONE LAYER PLACED UNIFORMLY)											
	220.26	138.75	87.40	47.50	29.84	22.81	18.89	16.27	14.47	13.00	11.94
NUMBER OF ARMOR UNITS PER 1000 SQ FT (TWO LAYERS RANDOM PLACED)											
	314.12	197.87	124.65	67.74	42.56	32.53	26.93	23.20	20.64	18.54	17.02
DIMENSIONS OF ARMOR UNITS (FT) — SYMBOL											
A	2.09	2.63	3.32	4.50	5.67	6.49	7.15	7.70	8.18	8.61	9.01
B	1.05	1.32	1.67	2.26	2.85	3.26	3.59	3.87	4.11	4.33	4.52
C	0.70	0.88	1.11	1.51	1.90	2.18	2.39	2.58	2.74	2.88	3.02
D	0.52	0.66	0.83	1.12	1.41	1.62	1.78	1.92	2.04	2.14	2.24

VOLUME OF INDIVIDUAL ARMOR UNIT = $0.781 A^3$

where:

A = Width of cube $C = 0.335 A$

$B = 0.502 A$ $D = 0.249 A$

NOTE: DATA BASED ON MODIFIED CUBES USED IN MODEL TESTS CONDUCTED AT THE WATERWAYS EXPERIMENT STATION.

Figure 7-93. Modified-Cube Specifications

VOLUME OF INDIVIDUAL ARMOR UNITS (CU FT)

UNIT WEIGHT LB/CU FT	7.14	14.29	25.57	71.43	142.86	214.29	285.71	357.14	428.57	500.00	571.43
					WEIGHT OF INDIVIDUAL ARMOR UNITS (TONS)						
140.0	0.50	1.00	2.00	5.00	10.00	15.00	20.00	25.00	30.00	35.00	40.00
149.5	0.53	1.07	2.14	5.34	10.68	16.02	21.36	26.70	32.04	37.38	42.71
156.0	0.56	1.11	2.23	5.57	11.14	16.71	22.29	27.86	33.43	39.00	44.57
162.0	0.58	1.16	2.31	5.79	11.57	17.36	23.14	28.93	34.71	40.50	46.29
AVERAGE MEASURED THICKNESS OF ONE LAYER PLACED UNIFORMLY (FT)											
	2.48	3.13	3.94	5.35	6.74	7.72	8.50	9.15	9.73	10.24	10.70
AVERAGE MEASURED THICKNESS OF TWO LAYERS RANDOM PLACED (FT)											
	4.43	5.58	7.03	9.54	12.02	13.76	15.15	16.32	17.34	18.26	19.09
NUMBER OF ARMOR UNITS PER 1000 SQ FT (ONE LAYER PLACED UNIFORMLY)											
	198.09	124.78	78.60	42.72	26.84	20.51	16.99	14.63	13.01	11.69	10.74
NUMBER OF ARMOR UNITS PER 1000 SQ FT (TWO LAYERS RANDOM PLACED)											
	328.40	206.86	130.31	70.82	44.49	34.01	28.16	24.26	21.56	19.38	17.60
DIMENSIONS OF ARMOR UNITS (FT)											
SYMBOL											
A	3.44	4.33	5.46	7.41	9.34	10.69	11.76	12.67	13.47	14.18	14.82
B	1.23	1.55	1.95	2.65	3.34	3.82	4.21	4.53	4.82	5.07	5.30
C	1.11	1.40	1.76	2.39	3.01	3.45	3.80	4.09	4.35	4.57	4.78
D	0.74	0.93	1.17	1.59	2.01	2.30	2.53	2.73	2.90	3.05	3.19

VOLUME OF INDIVIDUAL ARMOR UNIT = $0.176 A^3$

where:

A = Overall dimension of unit   C = 0.322 A

B = 0.357 A   D = 0.215 A

PLAN

ELEVATION

NOTE: DATA BASED ON HEXAPODS USED IN MODEL TESTS CONDUCTED AT THE WATERWAYS EXPERIMENT STATION.

Figure 7-94. Hexapod Specifications
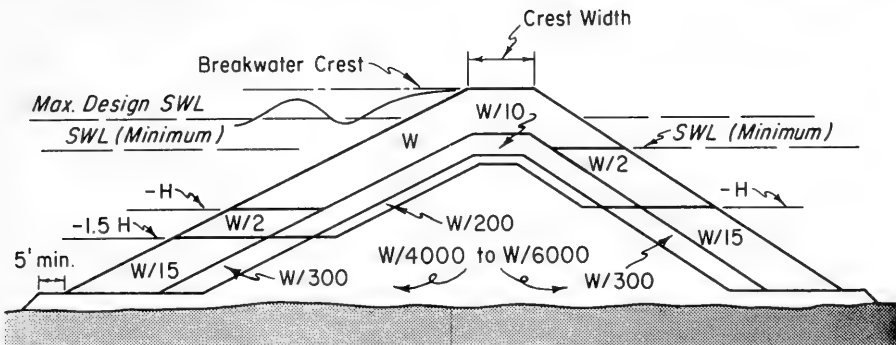
Idealized Multilayer Section

Rock Size	Layer	Rock Size Gradation (%)
W	Primary Cover Layer	125 to 75
W/2 and W/15	Secondary Cover Layer	125 to 75
W/10 and W/300	First Underlayer*	130 to 70
W/200	Second Underlayer	150 to 50
W/4000—W/6000	Core and Bedding and Filter Layer	170 to 30

*See Section 7.377g
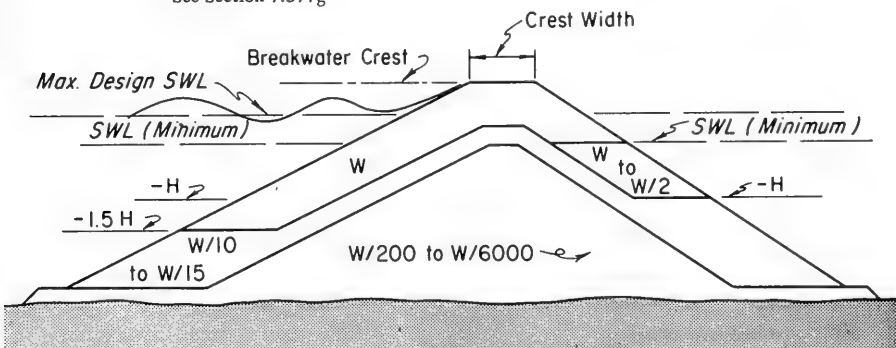
Recommended Three-layer Section

Figure 7-95. Rubble-Mound Section for Nonbreaking Wave Condition (zero to moderate overtopping conditions)

and 7-96. A logic diagram for the preliminary design of a rubble struc-
ture is shown in Figure 7-97. The design can be considered in three
phases: (1) structure geometry; (2) evaluation of construction tech-
nique; and (3) evaluation of design materials. A logic diagram for evalu-
ation of the preliminary design is shown in Figure 7-98.

Table 7-9. Concrete-Armor Projects in the United States

Date	Location	Structure	Armor Unit
1956	Crescent City, California	breakwater	25-ton tetrapods
1957	Kahului, Hawaii	breakwater	33-ton tetrapods
1958	Nawiliwili, Hawaii	breakwater	18-ton tribars
1958	Rincon Island, California	revetment	31-ton tetrapods
1963	Kahului, Hawaii	breakwater	19- to 50-ton tribars
1963	Santa Cruz, California	breakwater	28-ton quadripods
1963	Ventura, California	jetty	10.7-ton tribars
1971	Diablo Canyon, California	breakwater	21.5- to 36.5-ton tribars
1971	Humboldt Bay, California	jetty	42- to 43-ton dolosse

As part of the design analysis indicated in the logic diagram (Fig.
7-97), the following structure geometry should be investigated:

    (a)   crest elevation and width,
    (b)   concrete cap for rubble-mound structures,
    (c)   thickness of armor layer and underlayers, and
           number of armor units,
    (d)   bottom elevation of primary cover layer,
    (e)   structure head and lee side cover layer,
    (f)   secondary cover layer,
    (g)   underlayers, and
    (h)   bedding layer or filter blanket layer.

    a. Crest Elevation and Width. Overtopping of a rubble structure
such as a breakwater or jetty usually can be tolerated only if it does
not cause damaging waves behind the structure. Whether overtopping will
occur depends on the height of the crest of the structure relative to
the height of wave runup, R. Wave runup depends on wave characteristics,
structure slope, porosity, and roughness of the cover layer. If the
armor layer is chinked, or in other ways made smoother or less permeable
--as a graded riprap slope--the limit of maximum runup will be higher
than for rubble slopes. (See Section 7.21, and Figures 7-19 and 7-20.)
The selected crest elevation should be the lowest that provides the pro-
tection required. Excessive overtopping of a breakwater or jetty can
cause choppiness of the water surface behind the structure, and be detri-
mental to harbor operations. Operations such as mooring of small craft
and some types of commercial unloading require calm waters. Overtopping
of a rubble seawall or revetment can cause serious erosion behind the
structure and flooding of the backshore area. Overtopping of jetties
may be tolerated if it does not adversely affect the channel.
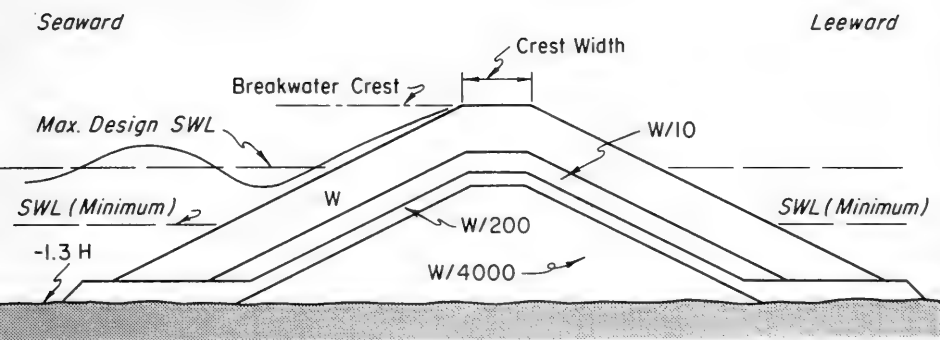
Idealized Multilayer Section

Rock Size	Layer	Rock Size Gradation (%)
W	Primary Cover Layer	125 to 75
W/10	First Underlayer*	130 to 70
W/200	Second Underlayer	150 to 50
W/4000	Core and Bedding and Filter Layer	170 to 30

*See Section 7.377g
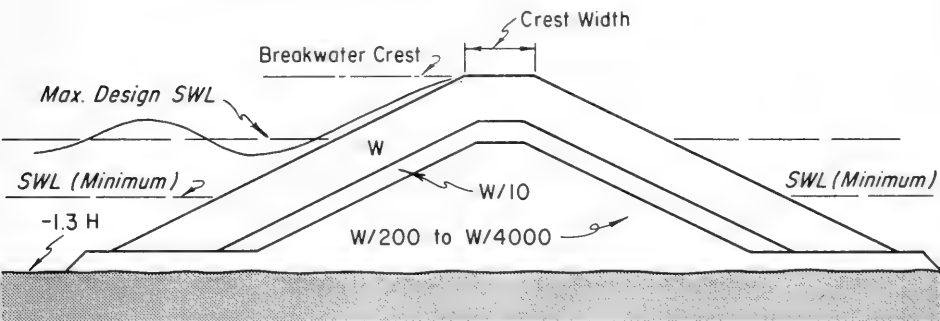
Recommended Three-layer Section

Figure 7-96.   Rubble-Mound Section for Breaking Wave Condition
(moderate overtopping)
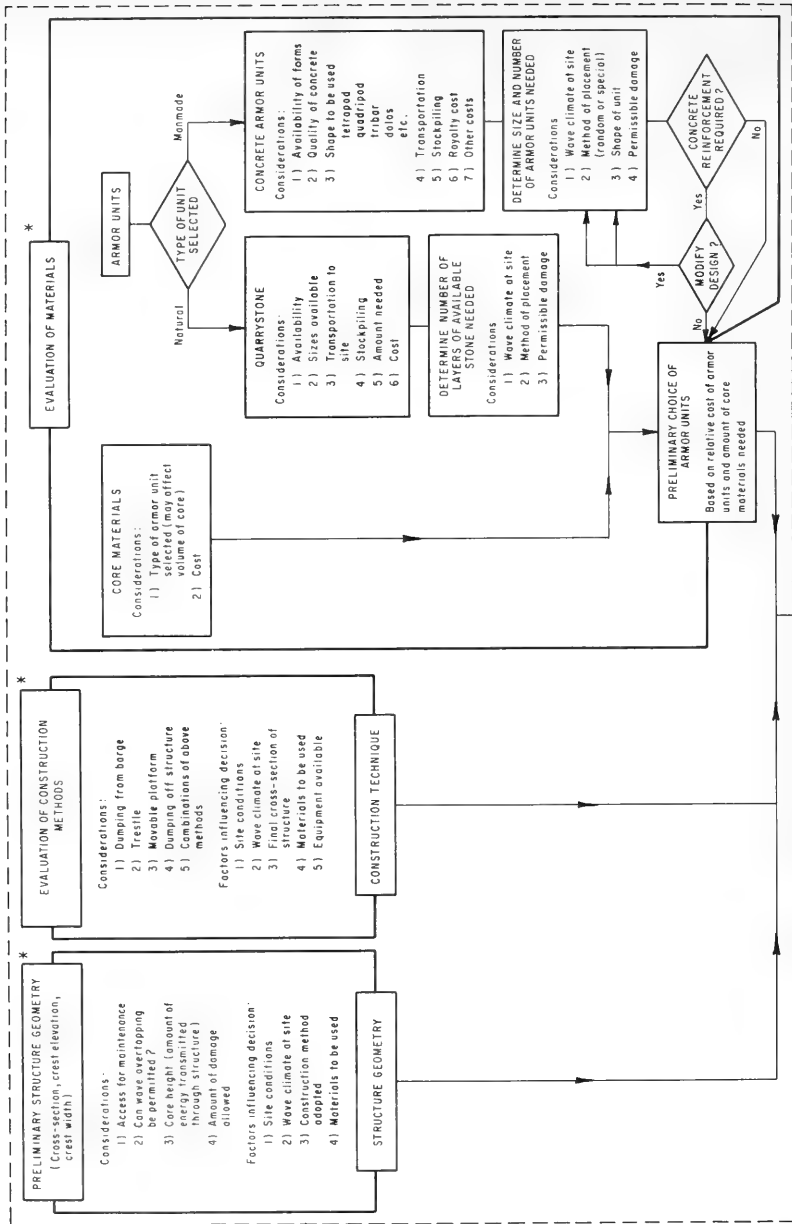
Figure 7-97. Logic Diagram for Preliminary Design of Rubble Structure

Figure 7-97

EVALUATION OF PRELIMINARY DESIGN (S)

FUNCTIONAL EVALUATION

(Does the structure provide the desired protection ?)

1) Sand barrier
2) Wave protection

Are model tests indicated ?

ECONOMIC EVALUATION

Considerations:
1) Material costs
2) Construction costs
3) Maintenance costs
4) Value of benefits
5) Intangible benefits (safety)

AESTHETIC AND ENVIRONMENTAL EVALUATION

Effect of structure on the environment

MODIFY LEVEL OF DESIGN AND REANALYZE DESIGN IF NECESSARY

(Increase or decrease allowable overtopping, raise or lower damage potential, change site and / or orientation, etc., to increase benefits and reduce costs)

EVALUATE PROMISING ALTERNATIVES

BENEFITS VERSUS COSTS

Benefits/Costs Too Low

ABANDON DESIGN

Benefits/Costs Adequate

FINAL DESIGN

(Based on policy, select alternative which has greatest benefit-cost ratio that increases net benefits)

Figure 7-98. Logic Diagram for Evaluation of Preliminary Design

The width of the crest depends greatly on the degree of allowable overtopping. Where there will be no overtopping, crest width is not critical. Little study has been made of crest width of a rubble structure subject to overtopping. As a general guide for overtopping conditions, the minimum crest width should equal the combined widths of three armor units (n = 3). Crest width may be obtained from the following equation.

$$B = nk_\Delta \left(\frac{W}{w_r}\right)^{1/3} , \qquad (7\text{-}107)$$

where,

B = crest width, ft.

n = number of stones (n = 3 is recommended minimum)

k_Δ = layer coefficient (Table 7-10)

W = weight of armor unit in primary cover layer, lbs.

w_r = unit weight of armor unit, lbs./ft^3.

The crest must be wide enough for construction and maintenance equipment operated from the structure.

Table 7-10. Layer Coefficient and Porosity for Various Armor Units

Armor Unit	n	Placement	Layer Coefficient k_Δ	Porosity (P) percent
Quarrystone (smooth)	2	random	1.02	38
Quarrystone (rough)	2	random	1.15	37
Quarrystone (rough)	>3	random	1.10	40
Cube (modified)	2	random	1.10	47
Tetrapod	2	random	1.04	50
Quadripod	2	random	0.95	49
Hexapod	2	random	1.15	47
Tribar	2	random	1.02	54
Dolos	2	random	1.00	63
Tribar	1	uniform	1.13	47
Quarrystone	graded	random	-------	37

b. Concrete Cap for Rubble-Mound Structures. Poured-in-place concrete has been added to the cover layer of rubble-mound jetties and breakwaters. Such use ranges from filling the interstices of stones on the cover layer, on the crest, and as far down the slopes as wave action permits, to casting large monolithic blocks of several hundred tons. This concrete may serve any of three purposes: (1) to strengthen the crest; (2) to increase the crest height; and (3) to provide roadway access along the crest for construction or maintenance purposes.

Massive concrete caps have been used with cover layers of precast concrete armor units. The cap provides a rigid backup to the top row of armor units at the crest. Instead of a concrete cap, solid or permeable parapets have been used. (See Figure 6-68.) The breakwater at Pria, Terceria, Azores was repaired using large quarrystone to support the primary tetrapod armor units instead of the concrete cap on the crest. Two rows of large armor stones were placed along the shoreward side of the crest to stabilize the top row of tetrapods. An inspection in March 1970 indicated that this placement has performed satisfactorily even though the structure has been subjected to wave overtopping.

To evaluate the need for a massive concrete cap for increasing structural stability against overtopping, consideration should be given to the cost of including a cap versus the cost of increasing dimensions to prevent overtopping and for construction and maintenance purposes. For a structure of concrete armor units subject to overtopping, a massive concrete cap is not necessary for structural stability when the difference in elevation between the crest and the limit of wave runup on the projected slope above the structure is less than 15 percent of the total wave runup, unless a substantial saving would result from the use of concrete. For this purpose, an all-rubble structure is preferable. Maintenance costs for an adequately designed rubble structure are likely to be lower than for any alternative composite type structure.

Experience indicates that concrete placed in the voids on the structure slopes has little structural value. By reducing slope roughness and surface porosity, the concrete increases wave runup. The effective life of the concrete is short, because the bond between concrete and stone is quickly broken by structure settlement. Such filling, increases maintenance costs. For a roadway, a concrete cap can usually be justified if frequent maintenance of armored slopes is anticipated.

c. Thickness of Armor Layer and Underlayers and Number of Armor Units. The thickness of the cover and underlayers and the number of armor units required can be determined from the following formulas:

$$r = n \, k_\Delta \left(\frac{W}{w_r}\right)^{1/3} \tag{7-108}$$

where r is the total layer thickness in feet, n is the number of layers of quarrystone or concrete armor units comprising the cover layer, W is the weight of individual armor units in pounds, and w_r is the unit weight in pounds per cubic foot.

$$N_r = A \, n \, k_\Delta \left(1 - \frac{P}{100}\right) \left(\frac{w_r}{W}\right)^{2/3} \tag{7-109}$$

where N_r is the required number of individual armor units for a given surface area, A is surface area in square feet, k_Δ is the layer coefficient, and P is the average porosity of the cover layer in percent.

Values of k_Δ and P, determined experimentally, are presented in Table 7-10. The average dimension for a range of quarrystone weights based on a unit weight of 165 pounds per cubic foot is shown in Table 7-11.

Table 7-11. Weight and Size Dimensions of Quarrystone

Weight (tons)	Dimen. (ft.)	Weight (lbs.)	Dimen. (ft.)	Weight (lbs.)	Dimen. (in.)	Weight (lbs.)	Dimen. (in.)	Weight (lbs.)	Dimen. (in.)
1	2.64	100	0.97	5	4.30				
2	3.33	200	1.23	10	5.42	0.5	2.00	0.025	0.74
3	3.81	300	1.40	15	6.21				
4	4.19	400	1.54	20	6.83	1.0	2.52	0.050	0.93
5	4.52	500	1.66	25	7.36				
6	4.80	600	1.77	30	7.82	1.5	2.88	0.075	1.06
7	5.05	700	1.86	35	8.23				
8	5.28	800	1.95	40	8.60	2.0	3.17	0.100	1.17
9	5.49	900	2.02	45	8.95				
10	5.69	1000	2.10	50	9.27	2.5	3.41	0.125	1.26
11	5.88	1100	2.16	55	9.57				
12	6.05	1200	2.23	60	9.85	3.0	3.63	0.150	1.34
13	6.21	1300	2.27	65	10.12				
14	6.37	1400	2.35	70	10.37	3.5	3.82	0.175	1.41
15	6.51	1500	2.40	75	10.61				
16	6.66	1600	2.45	80	10.84	4.0	3.99	0.200	1.47
17	6.79	1700	2.50	85	11.06				
18	6.92	1800	2.55	90	11.28	4.5	4.15	0.225	1.53
19	7.05	1900	2.60	95	11.48				
20	7.17	2000	2.64	100	11.63	5.0	4.30	0.250	1.59

NOTE: Average Dimension (ft.) is the solution for Equation 7-108, where n = 1, w_r = 165 lbs./ft.^{3} and k_Δ = 1.15 for quarrystone. (See Table 7-10.)

   d. Bottom Elevation of Primary Cover Layer. The armor units in the cover layer (the weights are obtained by Equation 7-105) should be extended downslope to an elevation below minimum SWL equal to the design wave height, H, when the structure is in a depth > 1.5H, as shown in Figure 7-95. When the structure is in a depth < 1.5H, armor units should be extended to the bottom as shown in Figure 7-96. Toe conditions at the intersections of slope with bottom may be critically unstable. Model studies should be made when economically feasible.

   e. Structure Head and Lee Side Cover Layer. Armoring of the head of a breakwater or jetty should be the same on the lee side slope as on the seaside slope for a distance of about 50 to 150 feet from the structure end. This distance depends on such factors as structure length and crest elevation at the seaward end.

Design of the lee side cover layer is based on the extent of wave overtopping, waves and surges acting directly on the lee slope, porosity of the structure, and differential hydrostatic head resulting in uplift forces which tend to dislodge the back slope armor units.

If the crest elevation is established to prevent possible overtopping, theoretically, the weight of armor units on the back slope cover layer should depend on the lesser wave action on the lee side and the porosity of the structure. When overtopping is anticipated, primary armor units should be extended down the back slope to minimum SWL. When both side slopes receive similar wave action (as with groins or jetties), both sides should be of similar design.

Lording and Scott (1971) tested an overtopped rubble-mound structure that was subjected to breaking waves in water levels up to the crest elevation. Maximum damage to the lee side armor units occurred with the stillwater level slightly below the crest and with waves breaking as close as two breaker heights from the toe of the structure. This would imply that waves were breaking over the structure and directly on the lee slope rather than on the seaward slope.

  f. Secondary Cover Layer. The weight of armor units in the secondary cover layer, between -H and -1.5H, should be greater than about one-half the weight of armor units in the primary cover layer. Below -1.5H, the weight requirements can be reduced to about W/15 for the same slope condition. (See Figure 7-95.) When the structure is located in shallow water (Fig. 7-96), that is depth $d \leq 1.3H$, armor units in the primary cover layer should be extended down the entire slope. The above ratios between the weights of armor units in the primary and secondary cover layers are applicable only when quarrystone units are used in the entire cover layer for the same slope. When precast concrete units are used in the primary cover layer, the weight of quarrystone in the other layers should be based on the equivalent weight, W of quarrystone armor units.

The secondary cover layer (Figs. 7-95 and 7-96) from -H to the bottom should be as thick or thicker than the primary cover layer. Thus, based on the preceding ratios between the armor weight, W in the primary cover layer and the quarrystone weight in the secondary cover layer, if $n = 2$ for the primary cover layer (two-quarrystones thick), then $n = 2.5$ for the secondary cover layer from -H to -1.5H, and $n = 5$ for that part of the secondary cover layer below -1.5H.

  g. Underlayers. The first underlayer (directly beneath the primary armor units) should have a minimum thickness of two quarrystones $(n = 2)$, and these should weigh about one-tenth the weight of the overlying armor units (W/10). (See Figure 7-95.) This applies where (a) cover layer and first underlayer are both quarrystone, (b) first underlayer is quarrystone and the cover layer is concrete armor units with a stability coefficient $K_D \leq 12$. When the cover layer is of armor units with $K_D \leq 20$, the first underlayer quarrystone should weigh about W/5

or one-fifth the weight of the overlying armor units. The second under-layer for this part of the structure should have a minimum thickness of two quarrystones; these should weigh about one-twentieth the weight of overlying quarrystones $(1/20 \times W/10 = W/200)$. The first underlayer for that part below $-1.5H$ should have a minimum of two thicknesses of quarrystone; these should weigh about one-twentieth the overlying second-ary armor unit $(1/20 \times W/15 = W/300)$. The second underlayer for that part below $-1.5H$, and the core material, can be as light as $W/6,000$, or quarry-run.

For a graded riprap cover layer, the weight of the first underlayer, if required, should be about $W_{50}/20$ to prevent the material from washing through the voids of the cover layer.

h. Bedding Layer or Filter Blanket. Foundation conditions for marine structures require thorough evaluation. Wave action against a rubble structure may scour the natural bottom and the foundation of the structure, even at depths usually considered unaffected by such action. A rubble structure may be protected from excessive settlement resulting from leaching, undermining, or scour, by the use of either a bedding layer or filter blanket. Depending on the weight of quarrystone used, a plastic filter cloth may be used instead of a bedding layer or with a thinner bedding layer.

It is advisable to use a bedding layer or filter blanket to protect the foundations of rubble-mound structures from undermining except; (a) where depths are greater than about three times the maximum wave height, (b) where the anticipated current velocities are too weak to move the average size of foundation material, or (c) where the foundation is a hard, durable material (such as bedrock).

When the foundation is a cohesive material, a filter blanket may not be required. However, a layer of quarry spalls or other crushed rock or gravel may be placed as a bedding layer or apron to reduce scour of the bottom or settlement of the structure. Foundations of coarse gravel may not require a filter blanket. When the rubble structure is founded on sand, a filter blanket should be provided to prevent waves and currents from removing sand through the voids of the rubble and thus causing settlement.

When large quarrystones are placed directly on a sand foundation at depths where waves and currents act on the bottom (as in the surf zone), the rubble will settle into the sand until it reaches the depth below which the sand will not be disturbed by the currents. Large amounts of rubble may be required to allow for the loss of rubble because of settle-ment. This, in turn, can provide a stable foundation.

Gradation requirements of a bedding layer depend principally on the size characteristic of the foundation material. However, quarry spalls, ranging in size from 1 to 50 pounds, will generally suffice. Layer thick-ness depends generally on the depth of water in which the material is to

7-200

be placed and the size of quarrystone used, but should not be less than 12 inches to ensure that bottom irregularities are completely covered. It is common practice to extend the bedding layer at least 5 feet beyond the toe of the cover stone. Details of typical rubble structures are shown in Chapter 6, STRUCTURAL FEATURES.

7.38 STABILITY OF RUBBLE FOUNDATIONS AND TOE PROTECTION

Forces of waves on rubble structures have been studied by several investigators. (See Section 7.37.) Brebner and Donnelly (1962) studied stability criteria for random-placed rubble of uniform shape and size used as foundation and toe protection at vertical-faced, composite structures. In their experiments, the shape and size of the rubble units were uniform, that is, subrounded to subangular beach gravel of 2.65 specific gravity. In practice, the rubble foundation and toe protection would be constructed with a core of dumped quarry-run material. The superstructure might consist of concrete or timber cribs founded on the core material. Finally, the apron and side slope of the core would be protected from erosion by a cover layer of armor units. The cover layer should have a minimum thickness of two armor units. An alternative method of constructing the superstructure would be to drive a pair of parallel-tied walls of steel sheet piling into the rubble core.

7.381 Design Wave Heights. For a composite breakwater with the superstructure resting directly on a rubble-mound foundation, structural integrity may depend on the ability of the foundation to resist the erosive scour by the highest waves. Therefore, for design of such structures, it is suggested that the selected design wave height H should be based on the following:

(1) For critical structures at open exposed sites where failure would be disastrous, and in the absence of reliable wave records, the design wave height H should be the average height of the highest 1 percent of all waves H_1 expected, based on the significant deepwater wave height H_O corrected for refraction and shoaling. (Early breaking might prevent the 1-percent wave from reaching the structure; if so, the maximum wave that could reach the structure should be taken for the design value of H.)

(2) For less critical structures, where some risk of exceeding design assumptions is allowable, wave heights between H_{10} and H_1 are acceptable.

The design wave for rubble toe protection is also between H_{10} and H_1.

7.382 Stability Number. The stability number is primarily affected by the depth of the rubble foundation and toe protection below the stillwater level d_1, and by the water depth at the structure site, d_s. The relation between the depth ratio, d_1/d_s, and N_s^3 is indicated in Figure 7-99. The cube value of the stability number has been used in the figure to facilitate its substitution in Equation 7-110.

7-201
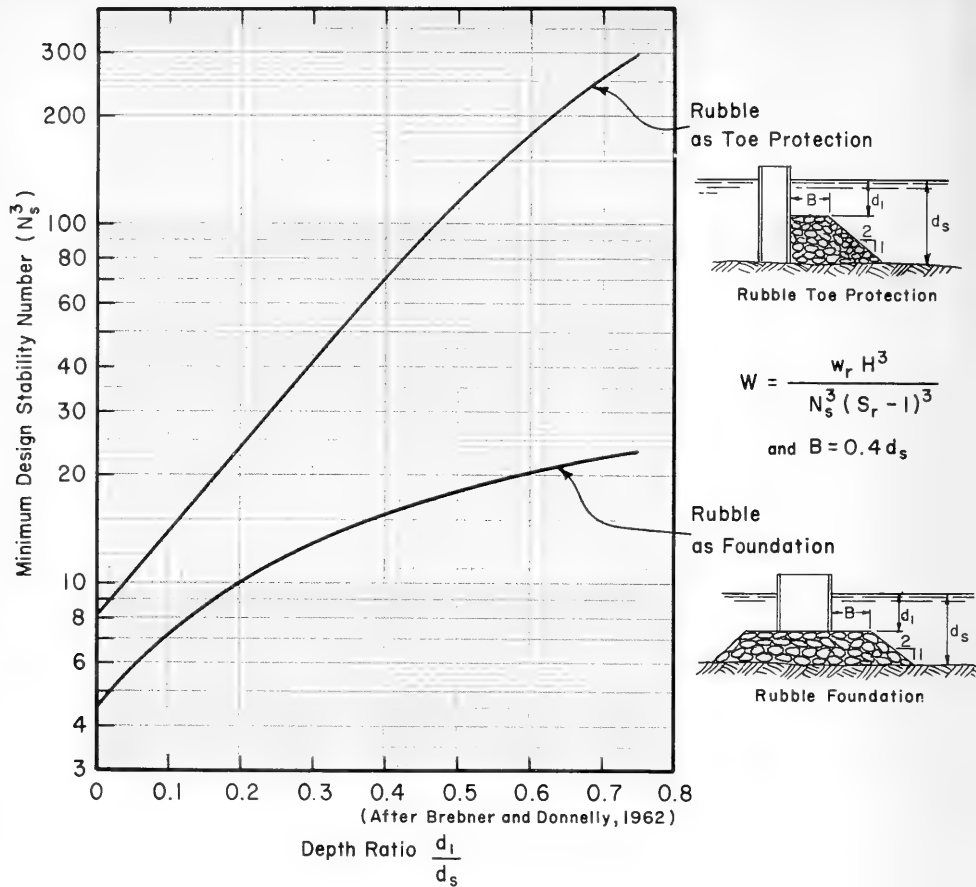
Figure 7-99. Stability Number for Rubble Foundation and
Toe Protection

7.383 **Armor Stone.** The equation used to determine the armor stone weight is a form of Equation 7-105,

$$W = \frac{w_r \, H^3}{N_s^3 \, (S_r - 1)^3} \, ,$$ (7-110)

where,

W = mean weight of individual armor unit, lbs.

w_r = unit weight of rock (saturated surface dry), lbs./ft.^{3}

H = design wave height (the incident wave height causing no damage to the structure).

S_r = specific gravity of rubble or armor stone relative to the water on which the structure is situated ($S_r = w_r/w_w$).

w_w = unit weight of water, fresh water = 62.4 lbs./ft.^{3} sea water = 64.0 lbs./ft.^{3}

N_s = design stability number for rubble foundations and toe protection. (See Figure 7-99.)

7.4 VELOCITY FORCES--STABILITY OF CHANNEL REVETMENTS

In the design of channel revetments, the armor stone along the channel slope should be able to withstand anticipated current velocities without being displaced. (Cox, 1958, and Cambell, 1966.) The maximum velocity of tidal currents in midchannel through a navigation opening as given by Sverdrup, Johnson. and Fleming (1942), can be approximated by the following formula:

$$V = \frac{4 \, \pi \, A \, h}{3 \, T \, S} \, ,$$ (7-111)

where V is the maximum velocity of tidal current at the center of the opening, T is the period of tide, A is the surface area of harbor basin, S is the cross-section area of openings, and h is the range of tide in the basin. The current in midchannel is about one-third swifter than at each side of the channel.

If the stable stone weight

$$W = \frac{\pi}{6} \, d_g^3 \, w_r \, ,$$ (7-112)

where d_g is the diameter of a stone sphere of equivalent weight, and

$$V = y \, \left(2_g\right)^{\frac{1}{2}} \, \left(\frac{w_r - w_w}{w_w}\right)^{\frac{1}{2}} \, (\cos \theta - \sin \theta)^{\frac{1}{2}} \, d_g^{\frac{1}{2}} \, ,$$ (7-113)

then combining the two equations for y = 1.20 (embedded stone) yields,

$$W = \frac{V^6 w_r w_w{}^3}{15.23 \times 10^5 \left(w_r - w_w\right)^3 \left(\cos \theta - \sin \theta\right)^3} , \qquad (7\text{-}114)$$

where

W = minimum weight of the stable stone, pounds

V = velocity of water acting directly on stone, feet per second

w_r = unit weight of stone, pounds per cubic foot

w_w = unit weight of water, pounds per cubic foot

g = acceleration of gravity, 32.2 feet per second^2

θ = angle of structure slope with the horizontal in the direction of flow

d_g = equivalent minimum stone diameter, feet

$$d_g = 1.24 \sqrt[3]{\frac{W}{w_r}} \qquad (7\text{-}115)$$

y = Isbash constant 1.20 and 0.86 for embedded and nonembedded stone, respectively.

A graphical solution of Equations 7-112 and 7-113 for the equivalent stone diameter and stone weight is shown in Figure 7-100. For salt water, the curve would be adjusted accordingly. The curves are considered applicable to conditions where turbulence is not excessive, and the stones are either embedded or nonembedded.

7.5 IMPACT FORCES

Impact forces are an important design consideration for shore structures, because of the increased use of thin flood walls and gated structures as part of hurricane protection barriers. High winds of a hurricane propelling small pleasure craft, barges and floating debris can cause great impact forces on a structure. Large floating ice masses also cause large horizontal impact forces. If site and functional conditions require the inclusion of impact forces in the design, other measures should be taken either to limit the depth of water against the face of the structure by providing a rubble-mound absorber against the face of the wall, or a partly submerged structure seaward of the structure that will ground floating masses, and eliminate the potential hazard and need for impact design consideration.

In many areas impact hazards may not occur, but where the potential exists (as for harbor structures), impact force should be evaluated from impulse-momentum considerations.

$$W = y (2g)^{\frac{1}{2}} \left(\frac{w_r - w_w}{w_w}\right)^{\frac{1}{2}} (\cos\theta - \sin\theta)^{\frac{1}{2}} d_g^{\frac{1}{2}}$$

$$W = \frac{\pi}{6} d_g^3 \ w_r \quad \text{where} \quad w_r = 165 \text{ lbs. per ft.}^3$$
$$w_w = 62.4 \text{ lbs. per ft.}^3$$

Example

Level Slope, Embedded Stone

V = 7 ft. per sec.

∴ d_g = 0.32 ft. or W = 2.8 lbs.

—— Embedded Stone (y = 1.20)

- - - Non Embedded Stone (y = 0.86)
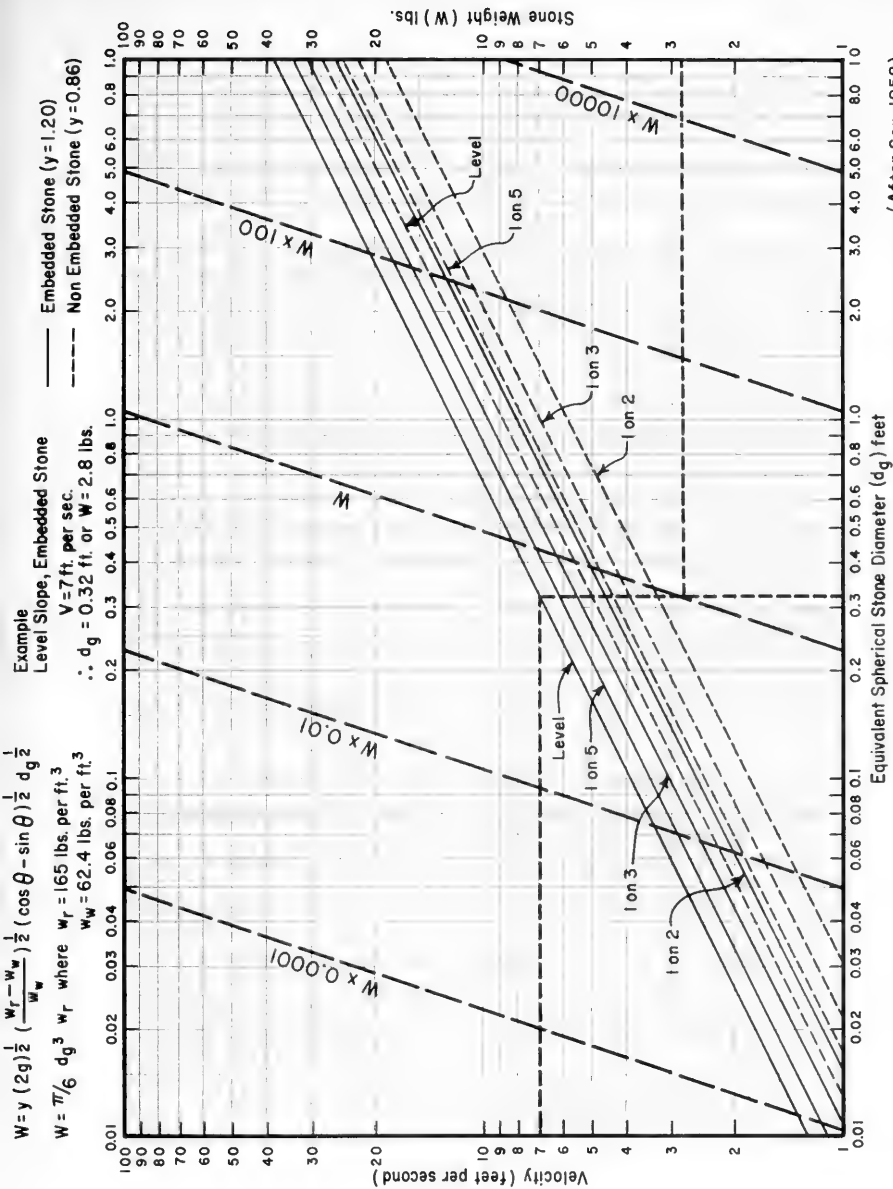
(After Cox, 1958)

Figure 7-100. Velocity versus Stone Weight and Equivalent Stone Diameter (w_w = 624 lbs./ft.³)

7-205

7.6 ICE FORCES

Ice forms are classified by terms that indicate manner of formation or effects produced. Usual classifications include: sheet ice, shale, slush, frazil ice, anchor ice, and agglomerate ice. (Striegl, 1952, Zumberg and Wilson, 1953, and Peyton, 1968.)

There are many ways ice can affect marine structures. In Alaska, great care must be exercised in predicting the different ways in which ice can exert forces on structures and restrict operations. Most situations in which ice affects marine structures are outlined in Table 7-12.

The amount of expansion of fresh water in cooling from 39°F. to 32°F. is 0.0132 percent. In changing from water at 32°F. to ice at 32°F. the amount of expansion is approximately 9.05 percent, or 685 times as great. A change of ice structure to denser form takes place when, with a temperature lower than -8°F., it is subjected to pressures greater than about 30,000 pounds per square inch. Excessive pressure, with temperatures above -8°F., causes the ice to melt. With the temperature below -8°F., the change to a denser form at high pressure results in shrinkage which relieves pressure. Thus, the probable maximum pressure that can be produced by water freezing in an enclosed space is 30,000 pounds per square inch.

Designs for dams include allowances for ice pressures of as much as 45,000 to 50,000 pounds per linear foot. The crushing strength of ice is about 400 pounds per square inch. Thrust per linear foot for various thicknesses of ice is about 28,800 pounds for 6 inches, 57,600 pounds for 12 inches, etc. Structures subject to blows from floating ice should be capable of resisting 10 to 12 tons per square foot (139 to 167 lbs./sq.in.) on the area exposed to the greatest thickness of floating ice.

Ice also expands when warmed from temperatures below freezing to a temperature of 32°F. without melting. Assuming a lake surface free of snow with an average coefficient of expansion of ice between -20°F. and 32°F. equaling 0.0000284, the total expansion of a sheet of ice a mile long for a rise in temperature of 50°F. would be 3.75 feet.

Normally, shore structures are subject to wave forces comparable in magnitude to the maximum probable pressure that might be developed by an ice sheet. As the maximum wave forces and ice thrust cannot occur at the same time, usually no special allowance is made for overturning stability to resist ice thrust. However, where heavy ice, either in the form of a solid ice sheet or floating ice fields may occur, adequate precautions must be taken to ensure that the structure is secure against sliding on its base. Ice breakers may be required in sheltered water where wave action does not require a heavy structure.

Floating ice fields when driven by a strong wind or current may exert great pressure on structures by piling up on them in large ice packs.

Table 7-12. Effect of Ice on Marine Structures

A. Direct Ice Forces on Structures.

   1. Horizontal Forces.

      a. Crushing ice failure of laterally moving floating ice sheets.

      b. Bending ice failure of laterally moving floating ice sheets.

      c. Impact by large floating ice masses.

      d. Plucking forces against riprap.

   2. Vertical Forces.

      a. Weight at low tide of ice frozen to structural elements.

      b. Buoyant uplift at high tide of ice masses frozen to structural elements.

      c. Vertical component of ice sheet bending failure introduced by ice breakers.

      d. Diaphram bending forces during water level change of ice sheets frozen to structural elements.

      e. Superstructure icing by ice spray.

   3. Second Order Effects.

      a. Motion during thaw of that ice frozen to structural elements.

      b. Expansion of entrapped water within structural elements.

      c. Jamming of rubble between structural framing members.

B. Indirect Ice Forces on Structures.

   1. Floating ice sheets impinging on moored ships.

   2. Unusual crane loads caused by the difficulty in maneuvering work boats in ice covered waters.

   3. Impact forces by ships during docking which are larger than might normally be expected.

   4. Abrasion and corollary corrosion of structural elements.

C. Low Risk but Catastrophic Considerations.

   1. Collision by a ship caught in fast-moving, ice-covered waters.

   2. Collision by extraordinarily large ice masses of very low probability of occurrence.

D. Operational Considerations.

   1. Problems of servicing offshore facilities in ice covered waters.

   2. Limits of ice cover severity during which ships can be moored to docks.

   3. Ship handling characteristics in turning basins and while docking and undocking.

   4. The extreme variability of ice conditions from year to year.

   5. The complacency to be expected by operators in anticipating 100-year occurrences in severity of ice conditions.

   6. The necessity of developing an ice operations manual to outline the operational limits for preventing the overstressing of structures.

Peyton, 1968

This condition must be given special attention in the design of small isolated structures. However, because of the flexibility of an ice field, pressures probably are not as great as those of a solid ice sheet in a confined area.

Ice formations at times cause considerable damage on shores in local areas, but their net effects are largely beneficial. Spray from winds and waves freezes on the banks and structures along the shore, covering them with a protective layer of ice. Ice piled on shore by wind and wave action does not, in general, cause serious damage to beaches, bulkheads, or protective riprap, but provides additional protection against severe winter waves. Ice often affects impoundment of littoral drift. Updrift source material is less erodible when frozen, and windrowed ice is a barrier to shoreward moving wave energy, therefore, the quantity of material reaching an impounding structure is reduced. During the winters of 1951-52, it was estimated that ice caused a reduction in rate of impoundment of 40 to 50 percent at the Fort Sheridan, Illinois, groin system.

Some abrasion of timber or concrete structures may be caused, and individual members may be broken or bent by the weight of the ice mass. Piling has been slowly pulled by the repeated lifting effect of ice freezing to the piles or attached members such as wales, and then being forced upward by a rise in water stage or wave action.

7.7 EARTH FORCES

Various texts on soil mechanics such as Andersen (1948), Hough (1957), and Terzaghi and Peck (1967), adequately discuss the subject. The forces exerted on a wall by soil backfill depend on the physical characteristics of the soil particles, the degree of soil compaction and saturation, the geometry of the soil mass, the movements of the wall caused by the action of the backfill and the foundation deformation. In wall design, since pressures and pressure distributions are indeterminate because of the factors noted, approximations of their influence must be made.

7.71 ACTIVE FORCES

When a mass of earth is held back by means of a retaining structure, a lateral force is exerted on the structure. If this is not effectively resisted, the earth mass will fail and a portion of it will move sideways and downward. The force exerted by the earth on the wall is called *active earth force*. Retaining walls are generally designed to allow minor rotation about the wall base to develop this active force, which is less than the *at-rest force* exerted if no rotation occurs. Coulomb developed the following active force equation:

$$P_a = \frac{wh^2}{2}\left[\frac{\csc\theta\ \sin(\theta-\phi)}{\sqrt{\sin(\theta+\delta)} + \sqrt{\dfrac{\sin(\phi+\delta)\ \sin(\phi-i)}{\sin(\theta-i)}}}\right]^2,\qquad (7\text{-}116)$$

where,

P_a = active force per unit length (lbs./linear ft. of wall)

w = unit weight of soil (lbs./ft.³)

h = height of wall or height of fill at wall if lower than wall (feet)

θ = angle between horizontal and back slope of wall (degrees)

i = angle of backfill surface from horizontal (degrees)

ϕ = internal angle of friction of the material (degrees)

δ = wall friction angle (degrees)

These symbols are further defined in Figure 7-101. Equation 7-116 may be reduced to that given by Rankine for the special Rankine conditions where δ is considered equal to i, and θ equal to 90° (vertical wall face). When, additionally, the backfill surface is level ($i = 0°$), the reduced equation is

$$P_a = \frac{wh^2}{2} \tan^2 \left(45° - \frac{\phi}{2}\right). \qquad (7\text{-}117)$$

Figure 7-102 shows that P_a from Equation 7-117 is applied horizontally.

Unit weights and internal friction angles for various soils are given in Table 7-13.

The resultant force for Equation 7-116 is inclined from a line perpendicular to the back of the wall by the angle of wall friction δ. (See Figure 7-101.) Values for δ can be obtained from Table 7-14, but should not exceed the internal friction angle of the backfill material ϕ, and for conservatism, should not exceed $(3/4)\phi$. (U.S. Army, Corps of Engineers, 1961.)

7.72 PASSIVE FORCES

If the wall resists forces that tend to compress the soil or fill behind it, then the earth must have enough internal resistance to transmit these forces. Failure to do this, will result in rupture; a part of the earth will move sideways and upward away from the wall. This resistance of the earth against outside forces is called *passive earth forces.*

The general equation for the passive force is

$$P_p = \frac{wh^2}{2} \left[\frac{\csc \theta \, \sin (\theta + \phi)}{\sqrt{\sin (\theta + \delta)} - \sqrt{\dfrac{\sin (\phi - \delta) \, \sin (\phi + i)}{\sin (\theta - i)}}} \right]^2 , \qquad (7\text{-}118)$$
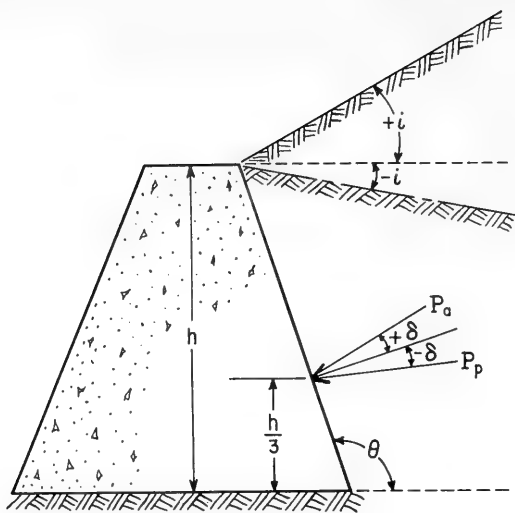
Figure 7-101. Definition Sketch for Coulomb Earth Force Equation
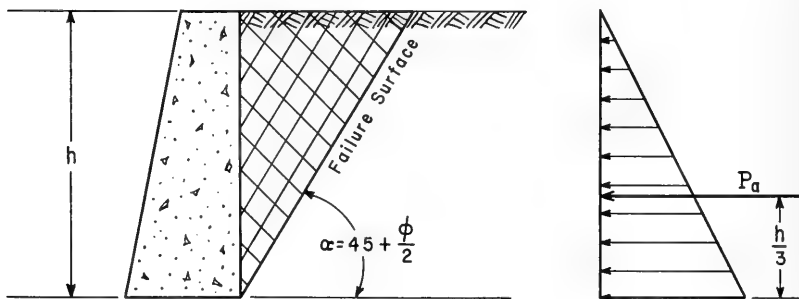
Figure 7-102. Active Earth Force for Simple Rankine Case

Table 7-13. Unit Weights and Internal Friction Angles of Soils

Classification	Dry Min. (loose)	Dry Max. (dense)	Wet Min. (loose)	Wet Max. (dense)	Submerged Min. (loose)	Submerged Max. (dense)
GRANULAR MATERIALS						
1. Uniform Materials						
Standard Ottawa SAND	92	110	93	131	57	69
Clean, uniform SAND (fine or Medium)	83	118	84	136	52	73
Uniform, inorganic SILT	80	118	81	136	51	73
2. Well-graded Materials						
Silty SAND	87	127	88	142	54	79
Clean, fine to coarse SAND	85	138	86	148	53	86
Micaceous SAND	76	120	77	138	48	76
Silty SAND and GRAVEL	89	146	90	155	56	92
MIXED SOILS						
1. Sandy or silty CLAY	60	135	100	147	38	85
2. Skip-graded silty CLAY with stones or rock fragments	84	140	115	151	53	89
3. Well-graded GRAVEL, SAND, SILT and CLAY mixture	100	148	125	156	62	94
CLAY SOILS						
1. CLAY (30 to 50 percent clay sizes)	50	112	94	133	31	71
2. Colloidal CLAY (-0.002 mm. ≥ 50 percent)	13	106	71	128	8	66
ORGANIC SOILS						
1. Organic SILT	40	110	87	131	25	69
2. Organic CLAY (30 to 50 percent clay sizes)	30	100	81	125	18	62

Classification	Friction Angle ϕ (degrees)	Density or Consistency	Unit Weight (lb/cu ft) Soil	Equivalent Fluid Active Case	Equivalent Fluid Passive Case
Coarse SAND or SAND and GRAVEL	45	compact	140	24	820
	38	firm	120	29	510
	32	loose	90	28	290
Medium SAND	40	compact	130	28	600
	34	firm	110	31	390
	30	loose	90	30	270
Fine SAND	34	compact	130	37	460
	30	firm	100	33	300
	28	loose	85	31	280
Fine, silty SAND or sandy SILT	32	compact	130	40	420
	30	firm	100	33	300
	28	loose	85	31	280
Fine, uniform SILT	30	compact	135	45	400
	28	firm	110	38	300
	26	loose	85	33	220
CLAY-SILT	20	medium	120	59	245
		soft	90	44	183
Silty CLAY	15	medium	120	71	204
		soft	90	53	153
CLAY	10	medium	120	84	170
		soft	90	53	153
CLAY	0	medium	120	120	120
		soft	90	90	90

(after Hough, 1957)

It should be noted that P_p is applied below the normal to the structure slope by an angle $-\delta$, whereas the active force is applied above the normal line by an angle $+\delta$. (See Figure 7-101.)

For the Rankine conditions given in Section 7.71, Equation 7-118 reduces to

$$P_p = \frac{wh^2}{2} \tan^2 \left(45° + \frac{\phi}{2}\right). \tag{7-119}$$

Equation 7-119 is satisfactory for use with a sheet-pile structure, assuming a substantially horizontal backfill.

Table 7-14. Coefficients and Angles of Friction

Surface, Stone - Brick - Concrete	Coefficient of Friction, μ	Angle of Wall Friction, δ
on Dry Clay	0.50	26°40'
on Wet or Moist Clay	0.33	18°20'
on Sand	0.40	21°50'
on Gravel	0.60	31°00'

NOTE: Angle of friction should be reduced by about 5 degrees if the wall fill will support train or truck traffic. The coefficient of friction, μ would equal the tangent of the new angle, δ.

7.73 COHESIVE SOILS

Sections 7.71 and 7.72 dealt with forces in cohesionless soil. A cohesive backfill may be necessary, and reduces the active force. However unless the soil can move continuously to maintain the cohesive resistance, it may relax. Thus, the wall should be designed for the active force in cohesionless soil.

7.74 STRUCTURES OF IRREGULAR SECTION

Earth force against structures of irregular section such as stepped-stone blocks or those having two or more back batters may be computed by Equations 7-116 and 7-118 by substituting an approximate average wall batter or slope to determine the angle, θ.

7.75 SUBMERGED MATERIAL

Forces due to submerged fills may be calculated by substituting the unit weight of the material reduced by buoyancy for value of w in the preceding equations, and then adding to the calculated forces the full hydrostatic force due to the water. Values of unit weight for dry, saturated, and submerged materials are indicated in Table 7-13.

7.76 UPLIFT FORCES

For design computations, uplift forces should be considered as full hydrostatic force for walls whose bases are below design water level or for walls with saturated backfill.

REFERENCES AND SELECTED BIBLIOGRAPHY

ACHENBACH, E., "Distribution of Local Pressure and Skin Friction Around a Circular Cylinder in Cross-Flow Up to Re = 5 x 10," *Journal of Fluid Mechanics*, Vol. 34, Part 4, 1968.

AGERSCHOU, H.A., and EDENS, J.J., "Fifth and First Order Wave-Force Coefficients for Cylindrical Piles," *Coastal Engineering, Santa Barbara Specialty Conference*, ASCE, 1965.

ANDERSEN, P., *Substructure Analysis and Design*, Ronald Press, New York, 1948.

BAGNOLD, R.A., "Interim Report on Wave Pressure Research," *Journal of the Institution of Civil Engineers*, Vol. 12, London, 1939.

BATTJES, J.A., "Runup Distributions of Waves Breaking on Sloping Walls," Report, Department of Civil Engineering, Delft, The Netherlands, 1969.

BATTJES, J.A., "Runup Distributions of Waves Breaking on Slopes," *Journal of the Waterways, Harbors and Coastal Engineering Division*, ASCE, Vol. 97, No. WW1, Proc. Paper 7923, 1971, pp. 91-114.

BIDDE, D.D., "Wave Forces on a Circular Pile Due to Eddy Shedding," HEL 9-16, Hydraulic Engineering Laboratory Research Report, University of California, Berkeley, Calif., 1970.

BIDDE, D.D., "Laboratory Study of Lift Forces on Circular Piles," *Journal of the Waterways, Harbors and Coastal Engineering Division*, ASCE, WW 4, Paper No. 8495, Nov. 1971.

BLUMBERG, R., and RIGG, A.M., "Hydrodynamic Drag at Super-Critical Reynolds Numbers," Paper Presented at *Petroleum Session, American Society of Mechanical Engineers*, Los Angeles, Calif., 1961.

BRANDTZAEG, A., "The Effect of Unit Weights of Rock and Fluid on the Stability of Rubble-Mound Breakwaters," *Proceedings of the 10th Conference on Coastal Engineering*, ASCE, Vol. II, 1966.

BREBNER, A., and DONNELLY, P., "Laboratory Study of Rubble Foundations for Vertical Breakwaters," Engineer Report No. 23, Queen's University at Kingston, Ontario, 1962.

BRETSCHNEIDER, C.L., "Modification of Wave Height Due to Bottom Friction, Percolation and Refraction," TM-45, U.S. Army, Corps of Engineers, Beach Erosion Board, Washington, D.C., Sept. 1954a.

BRETSCHNEIDER, C.L., "Field Investigations of Wave Energy Loss in Shallow Water Ocean Waves," TM-46, U.S. Army, Corps of Engineers, Beach Erosion Board, Washington, D.C., Sept. 1954b.

BRETSCHNEIDER, C.L., "Evaluation of Drag and Inertial Coefficients from Maximum Range of Total Wave Force," Technical Report No. 55-5, Department of Oceanography, Texas A&M University, College Station, Texas, 1957.

BRETSCHNEIDER, C.L., "On the Probability Distribution of Wave Force and an Introduction to the Correlation Drag Coefficient and the Correlation Inertial Coefficient," *Coastal Engineering, Santa Barbara Specialty Conference*, ASCE, 1965.

BURSNALL, W.J., and LOFTIN, L.K., "Experimental Investigation of the Pressure Distribution About a Yawed Cylinder in the Critical Reynolds Number Range," Technical Note 2463, National Advisory Committee for Aeronautics, 1951.

CAMBELL, F.B., "Hydraulic Design of Riprap," Misc. Paper No. 2-777, U.S. Army, Corps of Engineers, Waterways Experiment Station, Vicksburg, Miss., 1966.

CARR, J.H., "Breaking Wave Forces on Plane Barriers," Report No. E 11.3, Hydrodynamics Laboratory, California Institute of Technology, Pasadena, Calif., 1954.

CHANG, K.S., "Transverse Forces on Cylinders Due to Vortex Shedding in Waves," M.A. Thesis, Department of Civil Engineering, Massachusetts Institute of Technology, Cambridge, Mass., 1964.

CHESNUTT, C.B., "Scour of Simulated Gulf Coast Sand Beaches in Front of Seawalls and Dune Barriers," Report No. 139, Coastal and Ocean Engineering Division, Texas A&M University, College Station, Texas, 1971.

COX, R.G., "Velocity Forces on Submerged Rocks," Misc. Paper No. 2-265, U.S. Army, Corps of Engineers, Waterways Experiment Station, Vicksburg, Miss., 1958.

CROSS, R.H., and SOLLITT, C.K., "Wave Transmission by Overtopping," Technical Note 15, Department of Civil Engineering, Massachusetts Institute of Technology, Cambridge, Mass., 1971.

DAI, Y.B., and JACKSON, R.A., "Designs for Rubble-Mount Breakwaters, Dana Point Harbor, California," Misc. Paper No. 2-725, U.S. Army, Corps of Engineers, Waterways Experiment Station, Vicksburg, Miss., June 1966.

DAI, Y.B., and KAMEL, A.M., "Scale Effect Tests for Rubble-Mount Breakwaters," TR No. H-69-2, U.S. Army, Corps of Engineers, Waterways Experiment Station, Vicksburg, Miss., Dec. 1969.

DANEL, P., and GRESLOU, L., "The Tetrapod," *Proceedings of the Eighth Conference on Coastal Engineering*, ASCE, Council on Wave Research, The Engineering Foundation, 1963.

DAVIDSON, D.D., "Stability and Transmission Tests of Tribar Breakwater Section Proposed for Monterey Harbor, California," TR No. H-69-11, U.S. Army, Corps of Engineers, Waterways Experiment Station, Vicksburg, Miss., Sept. 1969.

DAVIDSON, D.D., "Proposed Jetty-Head Repair Sections, Humboldt Bay, California," TR H-71-8, U.S. Army, Corps of Engineers, Waterways Experiment Station, Vicksburg, Miss., 1971.

DEAN, R.G., "Stream Function Representation of Nonlinear Ocean Waves," *Journal of Geophysical Research*, Vol. 70, No. 18, 1965a.

DEAN, R.G., "Stream Function Wave Theory; Validity and Application," *Coastal Engineering, Santa Barbara Specialty Conference*, ASCE, Ch. 12, 1965.b.

DEAN, R.G., "Evaluation and Development of Water Wave Theories for Engineering Application," U.S. Army, Corps of Engineers, Coastal Engineering Research Center. (To be published in 1973).

DEAN, R.G., and AAGAARD, P.M., "Wave Forces: Data Analysis and Engineering Calculation Method," *Journal of Petroleum Technology*, Vol. 22, No. 3, 1970.

DEAN, R.G., and HARLEMAN, D.R.F., "Interaction of Structures and Waves," Ch. 8, *Estuary & Coastline Hydrodynamics*, A.T. Ippen, ed., McGraw-Hill, New York, 1966.

DE CASTRO, D.E., "Diques de escollera (Design of Rock-Fill Dikes)," *Revista de Obras Públicas*, Vol. 80, 1933.

DENNY, D.F., "Further Experiments on Wave Pressures," *Journal of the Institution of Civil Engineers*, Vol. 35, London, 1951

DICK, T.M., "On Solid and Permeable Submerged Breakwaters," C.E. Research Report No. 59, Department of Civil Engineering, Queens University, Kingston, Ontario, 1968.

DOMZIG, H., "Wellendruck und druckerzeugender Seegang," Mitteilungen der Hannoverschen Versuchsanstalt für Grundbau und Wasserbau, Hannover, West Germany, 1955.

ERGIN, A., and PORA, S., "Irregular Wave Action on Rubble-Mound Breakwaters," *Journal of the Waterways, Harbors and Coastal Engineering Division* ASCE, Vol. 97, No. WW2, Proc. Paper 8114, 1971, pp. 279-293.

EVANS, D.J., "Analysis of Wave Force Data," *Journal of Petroleum Technology*, Vol. 22, No. 3, 1970.

FREEMAN, J.C., and LÉMEHAUTÉ, B., "Wave Breakers on a Beach and Surges on a Dry Bed," *Journal of the Hydraulics Division*, ASCE, Vol. 90, 1964, pp. 187-216.

FUCHS, R.A., see Johnson, Fuchs and Morison (1951).

GALVIN, C.J., JR., "Horizontal Distance Traveled by a Breaking Wave," National Meeting on Transportation Engineering, ASCE, San Diego, Calif., Feb. 1968.

GALVIN, C.J., JR., "Breaker Travel and Choice of Design Wave Height," *Journal of the Waterways and Harbors Division*, ASCE, WW2, Vol. 95, Paper 6569, 1969.

GODA, Y., "A Synthesis of Breaker Indices," *Transactions of the Japanese Society of Civil Engineers*, Vol. 2, Pt. 2, 1970.

GODA, Y., and ABE, T., "Apparent Coefficient of Partial Reflection of Finite Amplitude Waves," Port and Harbor Research Institute, Japan, 1968.

GRESLOU, L., and MAHE, Y., "Etudé du coefficient de reflexion d'une houle sur un obstacle constitué par un plan incliné," *Proceeding of the Fifth Conference on Coastal Engineering*, ASCE, Grenoble, France, 1954.

HALL, J.V., and WATTS, G., "Laboratory Investigation of the Vertical Rise of Solitary Waves on Impermeable Slopes," TM-33, U.S. Army Corps of Engineers, Beach Erosion Board, Washington, D.C., Mar. 1953.

HALL, M.A., "Laboratory Study of Breaking Wave Forces on Piles," TM-106, U.S. Army, Corps of Engineers, Beach Erosion Board, Washington, D.C., Aug. 1958.

HALL, W.C., and HALL, J.V., "A Model Study of the Effect of Submerged Breakwaters on Wave Action," TM-1, U.S. Army, Corps of Engineers, Beach Erosion Board, Washington, D.C., May 1940.

HEDAR, PER ANDERS, "Rules for the Design of Rock-Fill Breakwaters and Revetments," *21st International Navigation Congress*, Stockholm, Section II, Subject 1, 1965.

HENSEN, W., "Modellversuche über den Wellenauflauf an Seedeichen im Wattengebiet," Mitteilungen der Hannoverschen Versuchsanstalt für Grundbau und Wasserbau, Franzius-Institut, Hannover, West Germany, 1954.

HO, D.V., and MEYER, R.E., "Climb of a Bore on a Beach-(1) Uniform Beach Slope," *Journal of Fluid Mechanics*, Vol. 14, 1962, pp. 305-318.

HOUGH, B.K., *Basic Soils Engineering*, Ronald Press, New York, 1957.

HUDSON, R.Y., "Wave Forces on Breakwaters," *Transactions of the American Society of Civil Engineers*, ASCE, Vol. 118, 1953, p. 653.

HUDSON, R.Y., "Design of Quarry-Stone Cover Layers for Rubble-Mound Breakwaters," RR No. 2-2, U.S. Army, Corps of Engineers, Waterways Experiment Station, Vicksburg, Miss., 1958.

HUDSON, R.Y., "Laboratory Investigations of Rubble-Mound Breakwaters," *Proceedings of the American Society of Civil Engineers*, ASCE, Waterways and Harbors Division, Vol. 85, No. WW3, Paper No. 2171, 1959.

HUDSON, R.Y., "Wave Forces on Rubble-Mound Breakwaters and Jetties," Misc. Paper 2-453, U.S. Army, Corps of Engineers, Waterways Experiment Station, Vicksburg, Miss., 1961a.

HUDSON, R.Y., "Laboratory Investigation of Rubble-Mound Breakwaters," *Transactions of the American Society of Civil Engineers*, ASCE, Vol. 126, Pt. IV, 1961b.

HUDSON, R.Y., and JACKSON, R.A., "Stability of Rubble-Mound Breakwaters," TM No. 2-365, U.S. Army, Corps of Engineers, Waterways Experiment Station, Vicksburg, Miss., 1953.

HUDSON, R.Y., and JACKSON, R.A., "Design of Tetrapod Cover Layer for a Rubble-Mound Breakwater, Crescent City Harbor, Cresent City, Calif.," TM No. 2-413, U.S. Army, Corps of Engineers, Waterways Experiment Station, Vicksburg, Miss., 1955.

HUDSON, R.Y., and JACKSON, R.A., "Design of Tribar and Tetrapod Cover Layers for Rubble-Mound Breakwaters," Misc. Paper 2-296, U.S. Army, Corps of Engineers, Waterways Experiment Station, Vicksburg, Miss., 1959.

HUDSON, R.Y., and JACKSON, R.A., "Design of Riprap Cover Layers for Railroad Relocation Fills, Ice Harbor and John Day Lock and Dam Projects; Hydraulic Model Investigation," Misc. Paper 2-465, U.S. Army, Corps of Engineers, Waterways Experiment Station, Vicksburg, Miss., 1962.

HUDSON, R.Y., and JACKSON, R.A., "Stability Tests of Proposed Rubble-Mound Breakwaters, Nassau Harbor, Bahamas," Misc. Paper No. 2-799, U.S. Army, Corps of Engineers, Waterways Experiment Station, Mar. 1966.

IPPEN, A.T., ed., *Estuary and Coastline Hydrodynamics*, McGraw-Hill, New York, 1966.

IRIBARREN CAVANILLES, R., "A Formula for the Calculation of Rock-Fill Dikes," *Revista de Obras Publicas*, 1938. (Translation in *The Bulletin of the Beach Erosion Board*, Vol. 3, No. 1, Jan. 1949.)

IRIBARREN CAVANILLES, R., and NOGALES Y OLANO, C., "Generalization of the Formula for Calculation of Rock Fill Dikes and Verification of its Coefficients," *Revista de Obras Publicas*, 1950, (Translation in *The Bulletin of the Beach Erosion Board*, Vol. 5, No. 1, Jan. 1951.)

IRIBARREN CAVANILLES, R., and NOGALES Y OLANO, C., "Report on Breakwaters," *18th International Navigation Congress*, Ocean Navigation Section, Question 1, Rome, 1953.

IVERSEN, H.W., "Laboratory Study of Breakers," Circular No. 521, U.S. National Bureau of Standards, Washington, D.C., 1952a.

IVERSEN, H.W., "Waves and Breakers in Shoaling Water," *Proceedings of the Third Conference on Coastal Engineering*, ASCE, Council on Wave Research, 1952b.

JACKSON, R.A., "Design of Quadripod Cover Layers for Rubble-Mound Break-waters," Misc. Paper 2-372, U.S. Army, Corps of Engineers, Waterways Experiment Station, Vicksburg, Miss., 1960.

JACKSON, R.A., "Designs for Rubble-Mound Breakwater Repair, Morro Bay Harbor, California," TR No. 2-567, U.S. Army, Corps of Engineers, Waterways Experiment Station, Vicksburg, Miss., 1961.

JACKSON, R.A., "Designs for Rubble-Mound Breakwater Construction, Tsoying Harbor, Taiwan," TR No. 2-640, U.S. Army, Corps of Engineers, Waterways Experiment Station, Vicksburg, Miss., 1964a.

JACKSON, R.A., "Designs for Rubble-Mound Breakwaters Repair, Kahului Harbor, Maui, Hawaii," TR 2-644, U.S. Army, Corps of Engineers, Waterways Experiment Station, Vicksburg, Miss., 1964b.

JACKSON, R.A., "Stability of Rubble-Mound Breakwaters, Nassau Harbor, Nassau, New Providence Bahamas," TR No. 2-697, U.S. Army, Corps of Engineers, Waterways Experiment Station, Vicksburg, Miss., 1965.

JACKSON, R.A., "Designs for Rubble-Mound Breakwater, Noyo Harbor, California," Misc. Paper No. 2-841, U.S. Army, Corps of Engineers, Waterways Experiment Station, Vicksburg, Miss., Aug. 1966.

JACKSON, R.A., "Stability of Proposed Breakwater, Burns Waterway Harbor, Indiana," TR No. 2-766, U.S. Army, Corps of Engineers, Waterways Expriment Station, Vicksburg, Miss., Mar. 1967.

JACKSON, R.A., "Limiting Heights of Breaking and Nonbreaking Waves on Rubble-Mound Breakwaters," TR No. H-68-3, U.S. Army, Corps of Engineers, Waterways Experiment Station, Vicksburg, Miss., June 1968a.

JACKSON, R.A., "Design of Cover Layers for Rubble-Mound Breakwaters Subjected to Nonbreaking Waves," RR No. 2-11, U.S. Army, Corps of Engineers, Waterways Experiment Station, Vicksburg, Miss., 1968b.

JACKSON, R.A., HUDSON, R.Y., and HOUSLEY, J.G., "Designs for Rubble-Mound Breakwater Repairs, Nawiliwili Harbor, Nawiliwili, Hawaii," Misc. Paper No. 2-377, U.S. Army, Corps of Engineers, Waterways Experiment Station, Vicksburg, Miss., 1960.

JEFFREYS, H., "Note on the Offshore Bar Problems and Reflection from a Bar," Wave Report No. 3, Great Britain Ministry of Supply, 1944.

JEN, Y., "Laboratory Study of Inertia Forces on a Pile," *Journal of the Waterways and Harbors Division*, ASCE, No. WW1, 1968.

JOHNSON, J.W., FUCHS, R.A., and MORISON, J.R., "The Damping Action of Submerged Breakwaters," *Transactions of the American Geophysical Union*, Vol. 32, No. 5, 1951, pp. 704-718.

KADIB, A.L., "Beach Profile as Affected by Vertical Walls," Hydraulic Engineering Laboratory, University of California, Berkeley, Calif., 1962. (also in TM-134, U.S. Army, Corps of Engineers, Beach Erosion Board, Washington, D.C., June 1963.)

KAMEL, A.M., "Water Wave Pressures on Seawalls and Breakwaters," R.R. No. 2-10, U.S. Army, Corps of Engineers, Waterways Experiment Station, Vicksburg, Miss., 1968.

KELLER, H.B., LEVINE, D.A., and WHITHAM, G.B., "Motion of a Bore Over a Sloping Beach," *Journal of Fluid Mechanics*, Vol. 7, 1960, pp. 302-315.

KEULEGAN, G.H., and CARPENTER, L.H., "Forces on Cylinders and Plates in an Oscillating Fluid," NBS Report No. 4821, National Bureau of Standards, Washington, D.C., 1956.

LAIRD, A.D.K., "Water Forces on Flexible, Oscillating Cylinders," *Journal of the Waterways and Harbors Division*, ASCE, Aug. 1962.

LAIRD, A.D.K., JOHNSON, C.H., and WALKER, R.W., "Water Eddy Forces on Oscillating Cylinders," *Journal of the Hydraulics Division*, ASCE, Nov. 1960.

LAMB, SIR HORACE, *Hydrodynamics*, Cambridge University Press, 6th ed., 1932.

LAMBE, T.W., and WHITMAN, R.V., *Soil Mechanics*, Series in Soil Engineering, Wiley, New York, 1969.

LEENDERTSE, J.J. "Forces Induced by Breaking Water Waves on a Vertical Wall," Technical Report 092, U.S. Naval Civil Engineering Laboratory, 1961.

LEMÉHAUTÉ, B., "Periodical Gravity Wave on a Discontinuity," *Journal of the Hydraulics Division*, ASCE, Vol. 86, No. HY 9, Part 1, 1960, pp. 11-41.

LEMÉHAUTÉ, B., "On Non-Saturated Breakers and the Wave Runup," *Proceedings of the Eighth Conference on Coastal Engineering*, ASCE, Mexico City, Council on Wave Research, 1963, pp. 77-92.

LEMÉHAUTÉ, B., "An Introduction to Hydrodynamics and Water Waves," Report No. ERL 118-POL3-1&2, U.S. Department of Commerce, Environmental Science Services Administration, Washington, D.C., July 1969.

LORDING, P.T., and SCOTT, J.R., "Armor Stability of Overtopped Breakwater," *Journal of the Waterways, Harbors and Coastal Engineering Division*, ASCE, Vol. 97, No. WW2, Proceedings Paper 8138, 1971, pp. 341-354.

MacCAMY, R.C., and FUCHS, R.A., "Wave Forces on Piles: A Diffraction Theory," TM-69, U.S. Army, Corps of Engineers, Beach Erosion Board, Washington, D.C., Dec. 1954.

MAGOON, O.T., and SHIMIZU, N., "Use of Dolos Armor Units in Rubble-Mound Structures, e.g., for Conditions in the Arctic," *Proceedings from the First International Conference on Port and Ocean Engineering Under Arctic Conditions*, Vol. II, Technical University of Norway, Trondheim, Norway, 1971, pp. 1089-1108.(also CERC Reprint 1-73).

MERRIFIELD, E.M., and ZWAMBORN, J.A., "The Economic Value of a New Break-Water Armor Unit," *Proceedings of the 10th Conference on Coastal Engineering*, ASCE, Tokyo, 1968, p. 885.

MICHE, R., "Mouvements ondulatoires de la mer in profondeur constante ou decroissante," *Annals des Ponts et Chaussees*, Paris, Vol. 114, 1944.

MILLER, R.L., "Experimental Determination of Runup of Undular and Fully Developed Bores," *Journal of the Geophysical Research*, Vol. 73, 1968, pp. 4497-4510.

MINIKIN, R.R., "Breaking Waves: A Comment on the Genoa Breakwater," *Dock and Harbour Authority*, London, 1955, pp. 164-165.

MINIKIN, R.R., *Winds, Waves and Maritime Structures: Studies in Harbour Making and in the Protection of Coasts*, 2nd rev. ed., Griffin, London, 1963, 294 pp.

MORRISON, J.R., et al., "The Force Exerted by Surface Waves on Piles," *Petroleum Transactions*, 189, TP 2846, 1950.

NAGAI, S., "Experimental Studies of Specially Shaped Concrete Blocks for Absorbing Wave Energy," *Proceedings of the Seventh Conference on Coastal Engineering*, ASCE, Council on Wave Research, The Engineering Foundation, 1961a.

NAGAI, S., "Shock Pressures Exerted by Breaking Waves on Breakwaters," *Transactions*, ASCE, Vol. 126, Part IV, No. 3261, 1961b.

NAGAI, S., "Stable Concrete Blocks on Rubble-Mound Breakwaters," *Proceedings of the American Society of Civil Engineers*, ASCE, Vol. 88, WW3, 1962, pp. 85-113.

NAKAMURA, M., SHIRAISHI, H., and SASAKI, Y., "Wave Damping Effect of Submerged Dike," *Proceedings of the 10th Conference on Coastal Engineering*, ASCE, Tokyo, Vol. 1, Ch. 17, 1966, pp. 254-267.

OUELLET, YVON, "Effect of Irregular Wave Trains on Rubble-Mound Break-waters," *Journal of the Waterways, Harbors and Coastal Engineering Division*, ASCE, Vol. 98, No. WW1, Proc. Paper 8693, 1972, pp. 1-14.

PAAPE, A., and WALTHER, A.W., "Akmon Armour Unit for Cover Layers of Rubble-Mound Breakwaters," *Proceedings of the Eighth Conference on Coastal Engineering*, ASCE, Council on Wave Research, 1962.

PALMER, R.Q., "Breakwaters in the Hawaiian Islands," *Proceedings of the American Society of Civil Engineers*, ASCE, Waterways and Harbors Division, Vol. 86, No. WW2, Paper No. 2507, 1960.

PECK, R.B., HANSON, W.E., and THORNBURN, T.H., *Foundation Engineering*, Wiley, New York, 1967.

PEYTON, H.R., "Ice and Marine Structure," *Ocean Industry Magazine*, Parts 1 - 3, Mar., Sept., and Dec., 1968.

PRIEST, M.S., "Reduction of Wave Height by Submerged Offshore Structures," Bulletin No. 34, Alabama Polytechnic Institute, Engineering Experiment Station, Auburn, Alabama, 1958.

REID, R.O., and BRETSCHNEIDER, C.L., "The Design Wave in Deep or Shallow Water, Storm Tide, and Forces on Vertical Piling and Large Submerged Objects," Department of Oceanography, Texas A&M University, College Station, Texas, 1953.

ROGAN, A.J., "Destruction Criteria for Rubble-Mound Breakwaters," *Proceedings of the 11th Coastal Engineering Conference*, ASCE, London, 1969, pp. 761-778.

ROLLINGS, A.P., "Stability of Crescent City Harbor Breakwater, Crescent City, California," Misc. Paper No. 2-171, U.S. Army, Corps of Engineers, Waterways Experiment Station, Vicksburg, Miss., 1956.

ROSS, C.W., "Laboratory Study of Shock Pressures of Breaking Waves," TM-59, U.S. Army, Corps of Engineers, Beach Erosion Board, Washington, D.C., Feb. 1955.

ROSS, C.W., "Large-Scale Tests of Wave Forces on Piling," TM-111, U.S. Army, Corps of Engineers, Beach Erosion Board, Washington, D.C., May 1959.

ROUSE, H., ed., *Engineering Hydraulics*, Wiley, New York, 1950.

ROUVILLE, A., de, BESSON, P., and PETRY, P., "État Actuel des Études Internationales sur les Efforts dus aux Lames," *Annals des Ponts et Chaussees*, Paris, Vol. 108, No. 2, 1938.

RUNDGREN, L., "Water Wave Forces," Bulletin No. 54, Royal Institute of Technology, Division of Hydraulics, Stockholm, Sweden, 1958.

RUSSELL, R.C.H., and INGLIS, C., "The Influence of a Vertical Wall on a Beach in Front of It," *Proceedings of the Minnesota International Hydraulics Convention*, International Association of Hydraulic Research, Minneapolis, 1953.

SAINFLOU, M., "Treatise on Vertical Breakwaters," *Annals des Ponts et Chaussees*, Paris, 1928. (Translated by W.J. Yardoff, U.S. Army Corps of Engineers.)

SAVAGE, R.P., "Laboratory Study of Wave Energy Losses by Bottom Friction and Percolation," TM-31, U.S. Army, Corps of Engineers, Beach Erosion Board, Washington, D.C., 1953.

SAVAGE, R.P., "Wave Runup on Roughened and Permeable Slopes," *Journal of the Waterways and Harbors Division*, ASCE, WW3, Paper No. 1640, 1958.

SAVILLE, T., JR., "Laboratory Data on Wave Runup and Overtopping on Shore Structures," TM-64, U.S. Army, Corps of Engineers, Beach Erosion Board, Washington, D.C., Oct. 1955.

SAVILLE, T., JR., "Wave Runup on Shore Structures," *Journal of the Waterways and Harbors Division*, WW2, Vol. 82, 1956.

SAVILLE, T., JR., "Wave Runup on Composite Slopes," *Proceedings of the Sixth Conference on Coastal Engineering*, ASCE, Council on Wave Research, 1958a.

SAVILLE, T., JR., "Large-Scale Model Tests of Wave Runup and Overtopping, Lake Okeechobee Levee Sections," Unpublished Manuscript, U.S. Army, Corps of Engineers, Beach Erosion Board, Washington, D.C., 1958b.

SAVILLE, T., JR., "Discussion: Laboratory Investigation of Rubble-Mound Breakwaters by R.Y. Hudson," *Journal of the Waterways and Harbors Division*, WW3, Vol. 86, 1960, p. 151.

SAVILLE, T., JR., "An Approximation of the Wave Runup Frequency Distribution," *Proceedings of the Eighth Conference on Coastal Engineering*, ASCE, Mexico City, Council on Wave Research, 1962, pp. 48-59.

SAVILLE, T., JR., "Hydraulic Model Study of Transmission of Wave Energy by Low-Crested Breakwater," Unpublished Memo for Record, U.S. Army, Corps of Engineers, Beach Erosion Board, Washington, D.C., Aug. 1963.

SAVILLE, T., JR., and CALDWELL, J.M., "Experimental Study of Wave Overtopping on Shore Structures," *Proceedings of the Minnesota International Hydraulics Convention*, Minneapolis, International Association of Hydraulic Research, 1953.

SAVILLE, T., JR., GARCIA, W.J., JR., and LEE, C.E., "Development of Breakwater Design," *Proceedings of the 21st International Navigation Congress*, Sec. 11, Subject 1, "Breakwaters with Vertical and Sloping Faces," Stockholm, 1965.

SHEN, M.C., and MEYER, R.E., "Climb of a Bore on a Beach, (3) Runup," *Journal of Fluid Mechanics*, Vol. 16, 1963, pp. 113-125.

SINGH, K.Y., "Stabit, A New Armour Block," *Proceedings of the 11th Conference on Coastal Engineering*, ASCE, Vol. II, 1968.

SKJELBRIA, L., et al., "Loading on Cylindrical Pilings Due to the Action of Ocean Waves," Contract NBy-3196, 4 Volumes, U.S. Naval Civil Engineering Laboratory, 1960.

STRIEGL, A.R., "Ice on the Great Lakes and its Engineering Problems," *Presented at a Joint Conference of the American Meteorological Society and the American Geophysical Union*, 1952.

SVEE, R.A., TRAETTEBERG, A., and TORUM, A., "The Stability Properties of the Svee-Block," *Proceedings of the 21st International Navigation Congress*, Sec. 11, Subject 1, Stockholm, 1965.

SVERDRUP, H.U., JOHNSON, M.W., and FLEMING, R.H., *The Oceans; Their Physics, Chemistry, and General Biology*, Prentice-Hall, Englewood Cliffs, N.J., 1942.

TANAKA, S., et al., "Experimental Report of Hollow Tetrahedron Blocks," Chisui Kogyo Co., Ltd., Osaka, Japan, 1966.

TERZAGHI, K., and PECK, R.B., *Soil Mechanics in Engineering Practice*, Wiley, New York, 1967.

THIRRIOT, C., LONGREE, W.D., and BARTHET, H., "Sur la Perte de Charge due a un Obstacle en Mouvement Periodique," *Proceedings of the 14th Congress of the International Association of Hydraulic Research*, 1971.

THOMSEN, A.L., WOHLT, P.E., and HARRISON, A.S., "Riprap Stability on Earth Embankments Tested in Large- and Small-Scale Wave Tanks," TM-37, U.S. Army, Corps of Engineers, Coastal Engineering Research Center, Washington, D.C., June 1972.

U.S. ARMY, CORPS OF ENGINEERS, "Stability of Rubble-Mound Breakwaters," Technical Memorandum No. 2-365, U.S. Army, Corps of Engineers, Waterways Experiment Station, Vicksburg, Miss., 1953.

U.S. ARMY, CORPS OF ENGINEERS, "Retaining Walls," *Engineer Manual, Engineering and Design*, EM 1110-2-2502, May 1961. (rev. 1965.)

WASSING, F., "Model Investigation on Wave Runup Carried Out in the Netherlands During the Past Twenty Years," *Proceedings of the Sixth Conference on Coastal Engineering*, ASCE, Council on Wave Research, 1957.

WATKINS, L.L., "Corrosion and Protection of Steel Piling in Seawater," TM-27, U.S. Army, Corps of Engineers, Coastal Engineering Research Center, Washington, D.C., May 1969.

WEELE, B., VAN, "Beach Scour Due to Wave Action on Seawalls," Report No. 45, Fritz Engineering Laboratory, Lehigh University, Bethlehem, Pa., 1965.

WEGGEL, J.R., "The Impact Pressures of Breaking Water Waves," Thesis presented to the University of Illinois, Urbana, Illinois, in partial fulfillment of the requirements for the degree of Doctor of Philosophy, (Unpublished, available through University Microfilms, Ann Arbor, Michigan).

WEGGEL, J.R., "Maximum Breaker Height," *Journal of the Waterways, Harbors and Coastal Engineering Division*, ASCE, Vol. 98, No. WW4, Paper 9384, 1972.

WEGGEL, J.R., "Maximum Breaker Height for Design," *Proceedings of the 13th Conference on Coastal Engineering*, Vancouver, B.C., 1973.

WEGGEL, J.R., and MAXWELL, W.H.C., "Numerical Model for Wave Pressure Distributions," *Journal of the Waterways, Harbors and Coastal Engineering Division*, ASCE, Vol. 96, No. WW3, Paper No. 7467, 1970a, pp. 623-642.

WEGGEL, J.R., and MAXWELL, W.H.C., "Experimental Study of Breaking Wave Pressures," *Preprint Volume of the Offshore Technology Conference*, Paper No. OTC 1244, 1970b.

WHEELER, J.D., "Method for Calculating Forces Produced by Irregular Waves," *Journal of Petroleum Technology*, Vol. 22, No. 3, 1970.

WIEGEL, R.L., *Oceanographical Engineering*, Prentice-Hall, Inc., Englewood Cliffs, New Jersey, 1964.

WIEGEL, R.L., BEEBE, K.E., and MOON, J., "Ocean Wave Forces on Circular Cylindrical Piles," *Journal of the Hydraulics Division*, ASCE, Vol. 83, No. HY2., 1957.

WILSON, B.W., "Analysis of Wave Forces on a 30-inch Diameter Pile Under Confused Sea Conditions," U.S. Army, Corps of Engineers, Coastal Engineering Research Center, Technical Memo No. 15, 1965.

ZUMBERG, J.H., and WILSON, J.T., "Effects of Ice on Shore Development," *Proceedings of the Fourth Conference on Coastal Engineering*, Chicago, Illinois, pp. 201-206, 1953.

CHAPTER 8

ENGINEERING ANALYSIS -
CASE STUDY

REDONDO - MALAGA COVE, CALIFORNIA — 23 January 1973

ENGINEERING ANALYSIS - CASE STUDY

8.1 INTRODUCTION

This chapter presents a series of calculations for the preliminary design of a hypothetical offshore island in the vicinity of Delaware Bay. It serves to illustrate the interrelationships between many types of problems encountered in coastal engineering. The text progresses from development of the physical environment through a preliminary design of several elements of the proposed structure.

For brevity, the design calculations are not complete; however, when necessary, the nature of additional work required to complete the design is indicated. It should be pointed out that a project of the scope illustrated here would require extensive model testing to verify and supplement the analysis. The design and analysis of such tests is beyond the scope of this manual. In addition, extensive field investigations at the island site would be required to establish the physical environment. These studies would include a determination of engineering and geological characteristics of local sediments, as well as measurement of waves and currents. The results of these studies would then have to be evaluated prior to beginning a final design.

While actual data for the Delaware Bay site were used when available, specific numbers used in the calculations should not be construed as directly applicable to other design problems in the Delaware Bay area. Calculations are presented as examples of the techniques presented in this manual.

General Problem Description

  A 300 acre artificial offshore island is pro-posed in the Atlantic Ocean just outside the mouth of Delaware Bay. It is required to develop char-acteristics of the physical environment at the proposed island site and to develop a preliminary design for the island. The calculations are pre-sented as follows:

Table of Contents   page no.

* References pertain to appropriate sections of <u>Shore Protection Manual</u> or to numbered references on page 8-132 of design calculations.

Design Problem _Physical Environment_

Site Description

The following pages present information on the general physical conditions at the proposed island site. Site plans showing the island location, surrounding shorelines and bathymetry are given.
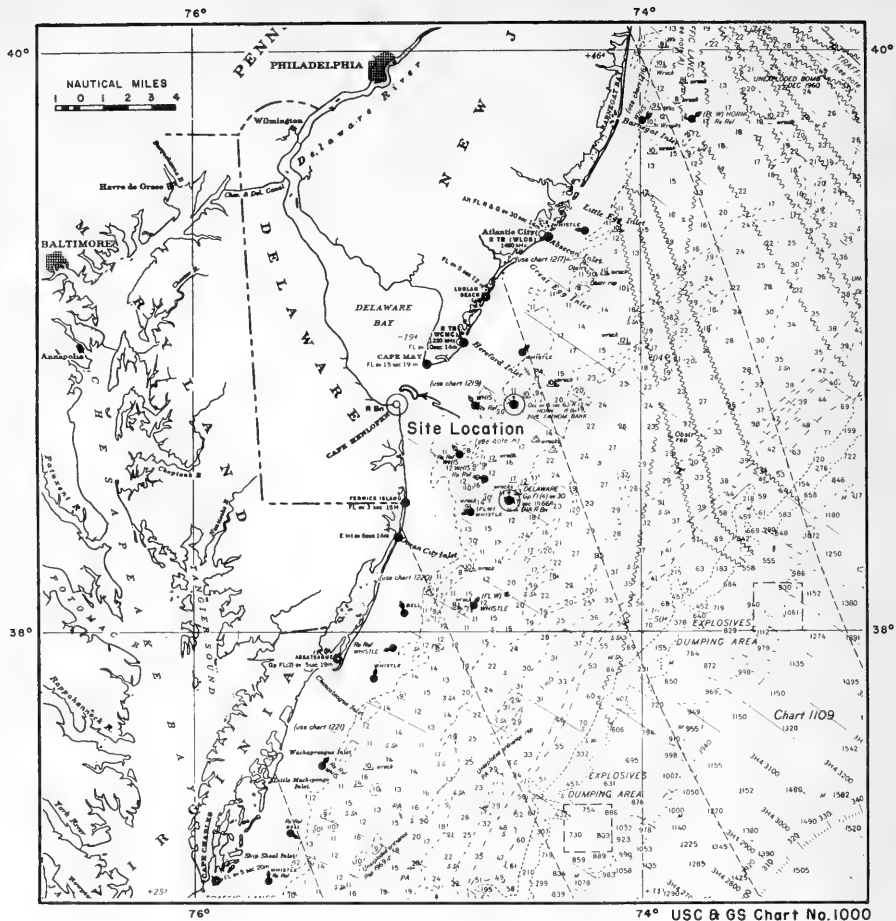
Note: The following pages present general descriptive
information about the site such as site plans and
bathymetry in the region of the island.

Figure 8-1.   Location Plan – Offshore Island
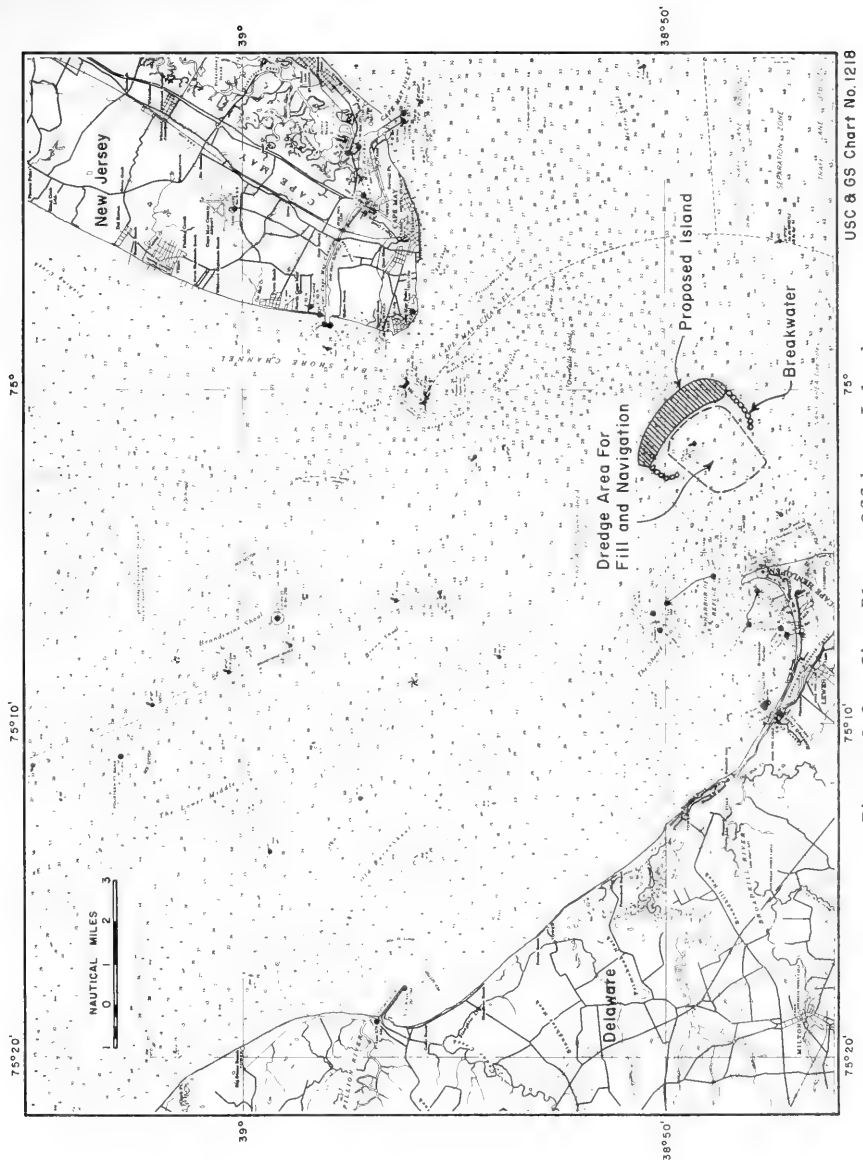
Figure 8-2. Site Plan – Offshore Island

USC & GS Chart No. 1218

New Jersey

Proposed Island

Breakwater

Dredge Area For
Fill and Navigation

Delaware

NAUTICAL MILES
0   1   2   3

8-5
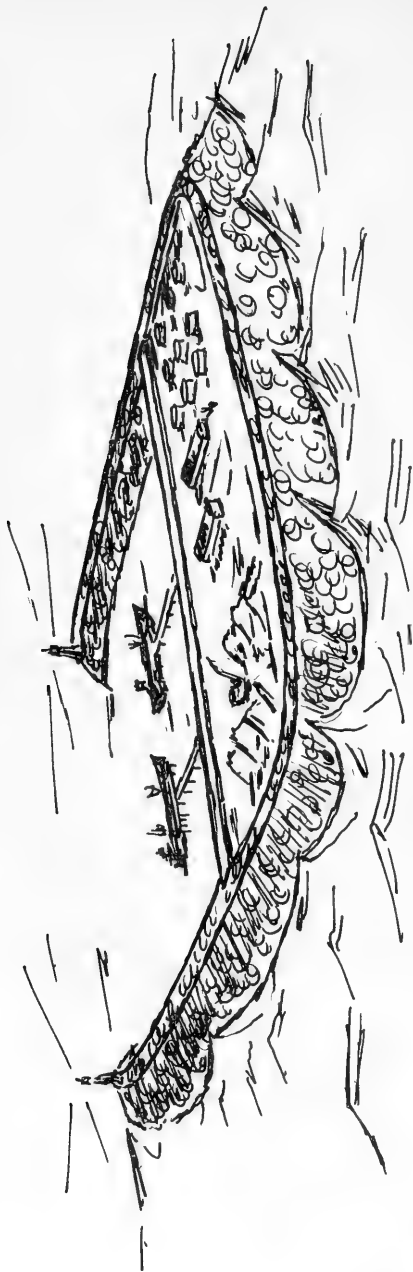
View Looking Northwest
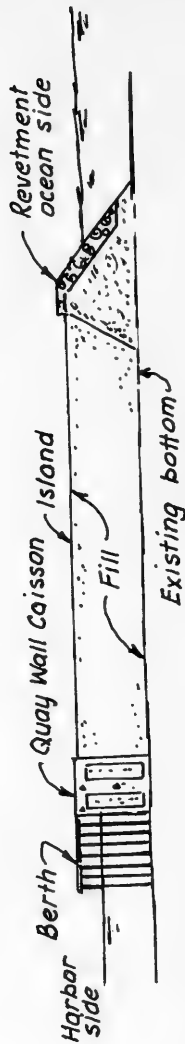
Section through Island

Figure 8-3. Perspective View and Section through Island

8-6
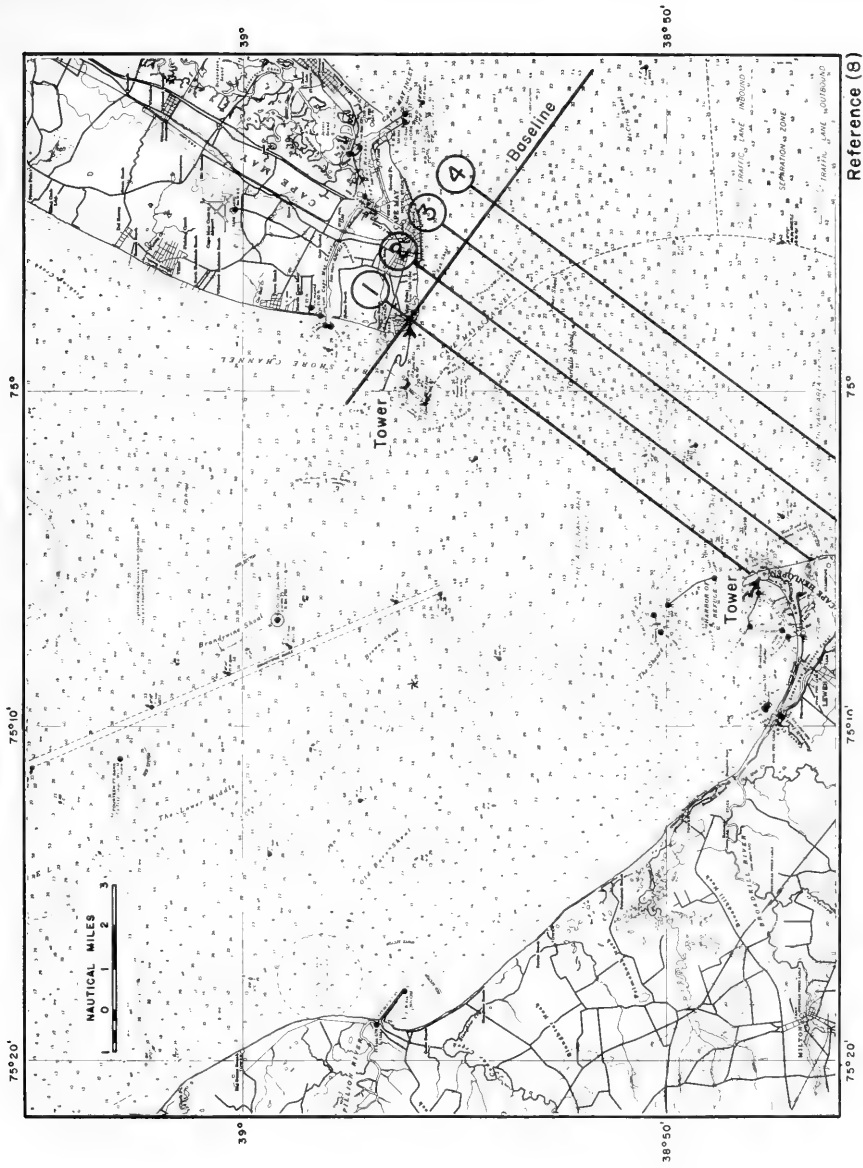
Figure 8-4. Location of Bottom Profiles

Reference (8)

8-7
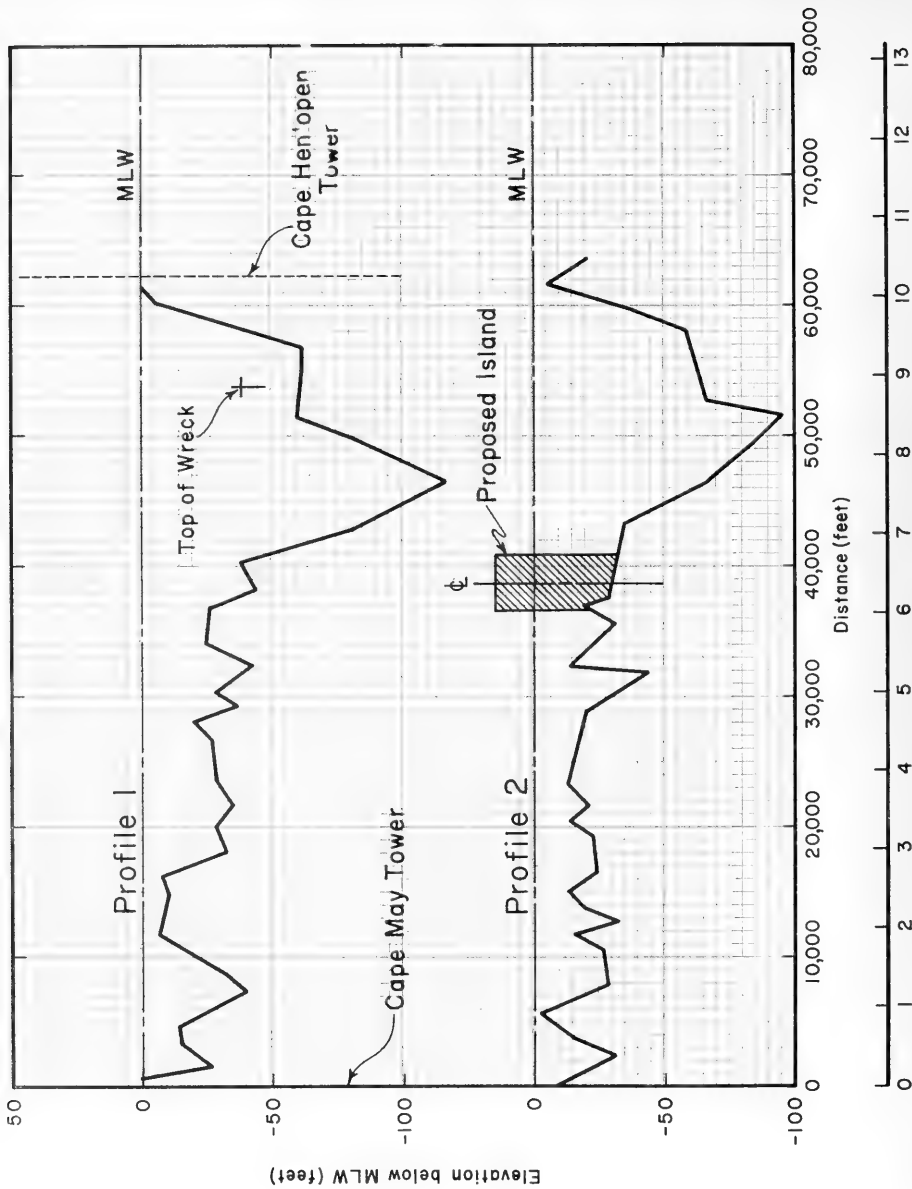
Figure 8-5. Bottom Profiles through Island Site
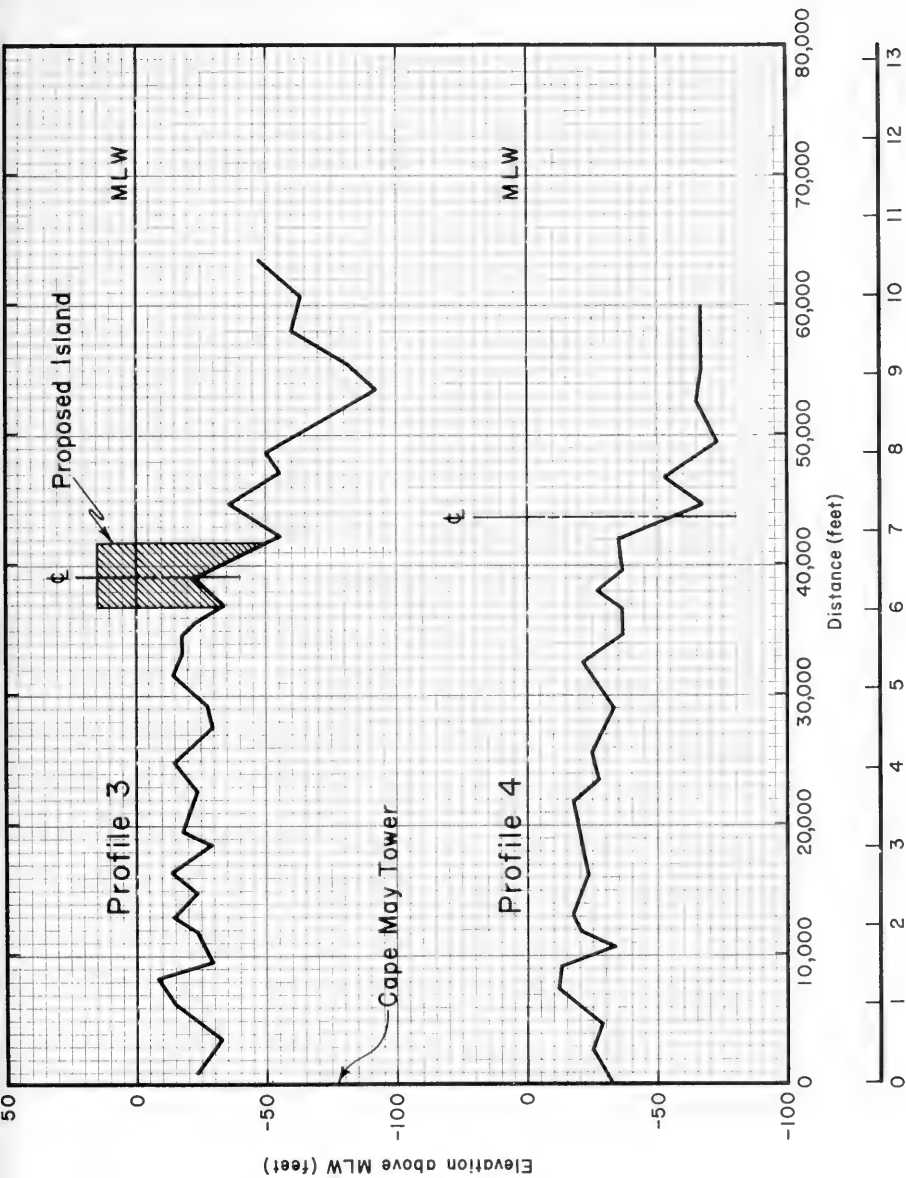
Figure 8-5. Continued—Bottom Profiles through Island Site

Water Levels – Storm Surge and Astronomical Tides

<div style="text-align:right">Chapter 3</div>

The following calculations establish design water levels at the island site using the methods of Chapter 3 and supplemented by data for the Delaware Bay Area given in References 5 & 16.

Estimate of Storm Surge – Nomograph Method

<div style="text-align:right">Sect. 3.865
b(1)(b)</div>

Note: The nomograph method can only provide a rough estimate for the present problem since the island site is in about 40 ft. of water in an estuary entrance. The nomograph method will give peak surge on the open coast (a high estimate for the island site).

Design Hurricanes   For illustrative purposes use hurricanes "A" & "B" given by Bretschneider in References 5 & 16.

Hurricane A

<div style="text-align:right">Refs. 5 & 16</div>

Radius to maximum winds = R = 33.5 n.m.

Central pressure Δp = 2.2 in. of mercury

Forward speed = V_F = 15 to 25 knots
(use V_F = 25 knots)

Maximum gradient wind,
$$U_{max.} = 0.868 \left\{ 73 \left(p_n - p_o \right)^{\frac{1}{2}} - R \left(0.575 f \right) \right\}$$

<div style="text-align:right">Eq. 3-35</div>

where for latitude 40°N,
$$f = 0.338$$
$$U_{max} = 0.868 \left\{ 73 \left(2.2 \right)^{\frac{1}{2}} - 33.5 \left(0.575 \right) \left(0.338 \right) \right\}$$

$$U_{max.} = 88.3 \text{ knots}$$
(102 mph)

Maximum sustained wind for V_F = 25 knots
$$U_R = 0.865 \, U_{max} + 0.5 \, V_F$$

<div style="text-align:right">Eq. 3-34</div>

$$U_R = 0.865 \left(88.3 \right) + 0.5 \left(25 \right) = 88.9 \text{ knots}$$
(102 mph)
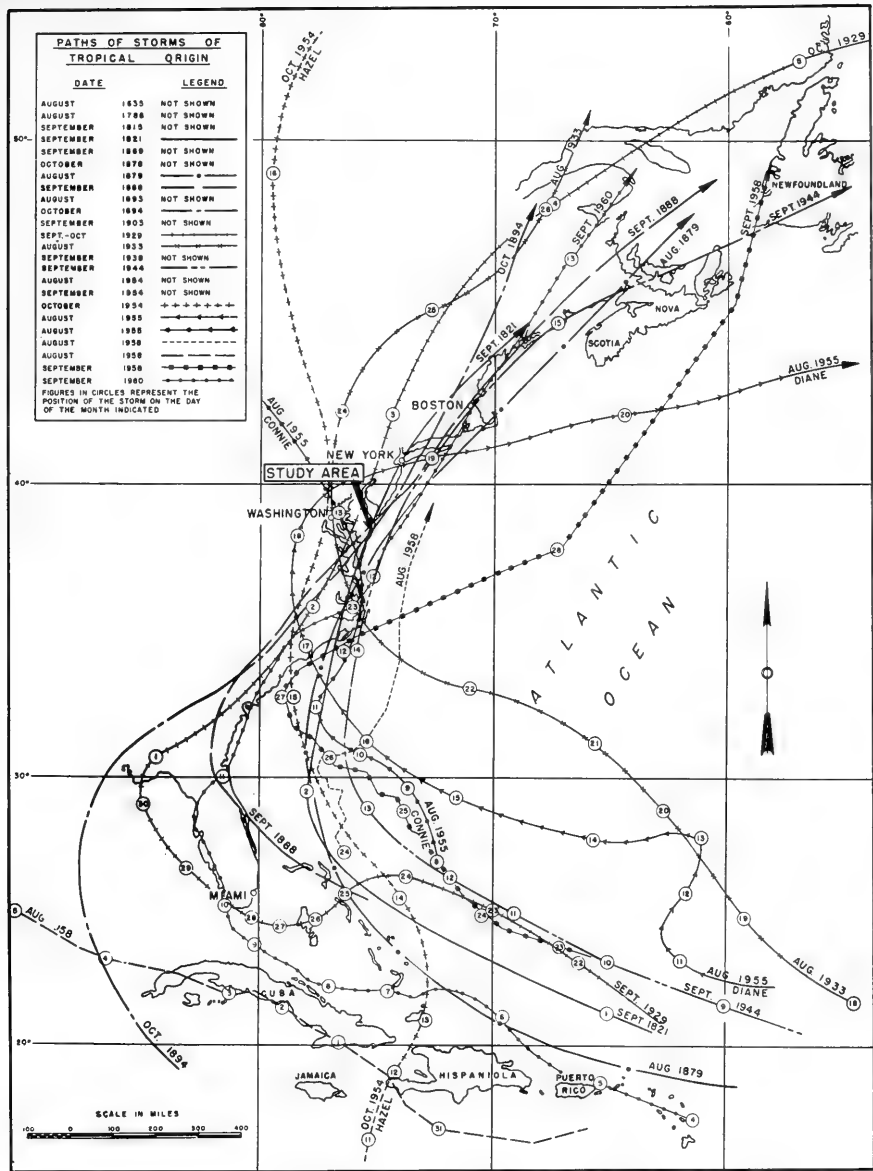
Figure 8-6. Hurricane Storm Tracks in the Delaware Bay Area

8-11

Nomograph Method (cont.)

Hurricane B

Refs. 5&16

$$R = 33.5 \text{ n.m.}$$
$$V_F = 25 \text{ knots}$$

U_{max} = 5 mph greater than hurricane A
  (5 mph = 4.34 knots)

Calculate Δp for U_{max} = 88.3 + 4.34 knots

$$U_{max} = 92.6 \text{ knots}$$
$$(107 \text{ mph})$$

Rearranging Eq 3-35,

$$\Delta p = \left\{ \frac{1}{73} \left[\frac{U_{max}}{0.868} + R(0.575f) \right] \right\}^2 \qquad \text{Eq. 3-35}$$

$$\Delta p = \left\{ \frac{1}{73} \left[\frac{92.6}{0.868} + 33.5(0.575)(0.338) \right] \right\}^2$$

$$\Delta p = 2.4 \text{ in. of mercury}$$

Peak Surge on Open Coast - Hurricane A

$$S_P = S_I F_S F_M \qquad \text{Eq. 3-78}$$

$\Delta p = 2.2$ in. of mercury
  (1 millibar = 0.0295 in. of mercury)

$$(\Delta p)_{millibars} = \frac{2.2 \text{ in.}}{0.0295 \text{ in/mb}} = 74.6 \text{ mb}$$

From Figure 3-51 for R = 33.5 n.m. = 38.5 mi.   Fig. 3-51

$$S_I = 16.5 \text{ ft.}$$

From Figure 3-53 for Cape May, N.J.   Fig. 3-53

$$F_S = 0.9$$

From Figure 3-54, assuming hurricane moves   Fig. 3-54
perpendicular to coast ($\psi = 90°$),
for $V_F = 25$ knots (28.8 mph)

$$F_M = 1.3$$

Peak Surge

$$S_P = S_I F_S F_M = 16.5(0.9)(1.3) = 19.3 \text{ ft.} \qquad \text{Eq. 3-78}$$

Page no :	13 of 133
Calculated by :	J. R. W.
Checked by :	R. H. J
Date :	2 Mar. 73

Design Problem _Physical Environment_

Nomograph Method (cont.)

Peak Surge on Open Coast – Hurricane B

$$S_I = 18.0 \text{ ft.}$$
$$F_S = 0.9$$
$$F_M = 1.30$$

$$S_P = S_I \, F_S \, F_M = 18.0 \, (0.9)(1.30) = 21.1 \text{ ft.}$$ Eq. 3-78

Note: The computed values of S_P are believed high for the island site since the island is in 40 ft. of water and at an estuary entrance; not at the coast as assumed by the nomograph method.

Estimate of Storm Surge – Reference 5   Ref. 5

Bretschneider (Ref 5) gives an empirical relationship between maximum sustained wind speed and surge height (both pressure and wind induced) at the Delaware Bay entrance. (Applicable only to Delaware Bay)

Equation 11 from Reference 5 for peak surge

$$(S_o)_{max} = 0.00085 \, U_R^2 \pm 10\%$$ Ref. 5 Eq. 11

$$(U_R \text{ in mph})$$

Hurricane A

$$U_R = 0.865 \, U_{max} + 0.5 \, V_F$$ Eq. 3-34

$$U_R = 0.865 \, (88.3) + 0.5 \, (25) = 88.9 \text{ knots}$$
$$(102 \text{ mph})$$

$$(S_o)_{max} = 0.00085 \, (102)^2 = 8.84 \text{ ft.}$$

$$\text{say } (S_o)_{max} = 9.0 \text{ ft.} \pm 1 \text{ ft.}$$

Hurricane B

$$(S_o)_{max} = 0.00085 \, (107)^2 = 9.7 \text{ ft.}$$

$$\text{say } (S_o)_{max} = 10.0 \text{ ft.} \pm 1 \text{ ft.}$$

Design Problem _Physical Environment_

Estimate of Storm Surge - Bathystrophic Method

Sect. 3.865 b(1)(a)

The figures on the following pages present the results of a detailed analysis of the storm surge at the entrance to Delaware Bay using the Bathystrophic Model. (Section 3.865 b(1)(a)

Summary of Storm Surge Estimates

Nomograph Method

Hurricane A $S_p = 19.3$ ft.

Hurricane B $S_p = 21.1$ ft.

Empirical Equation of Reference 5

Hurricane A $(S_o)_{max} = 9.0 \pm 1.0$ ft.

Hurricane B $(S_o)_{max} = 10.0 \pm 1.0$ ft.

Bathystrophic Method

Hurricane A $S_p = 11.1$ ft. [*]

Hurricane B $S_p = 12.1$ ft. [*]

---

[*] _Astronomical component subtracted._

Hurricane A $S_p = 13.07 - 2.0 \cong 11.1$ ft.

Hurricane B $S_p = 14.09 - 2.0 \cong 12.1$ ft.
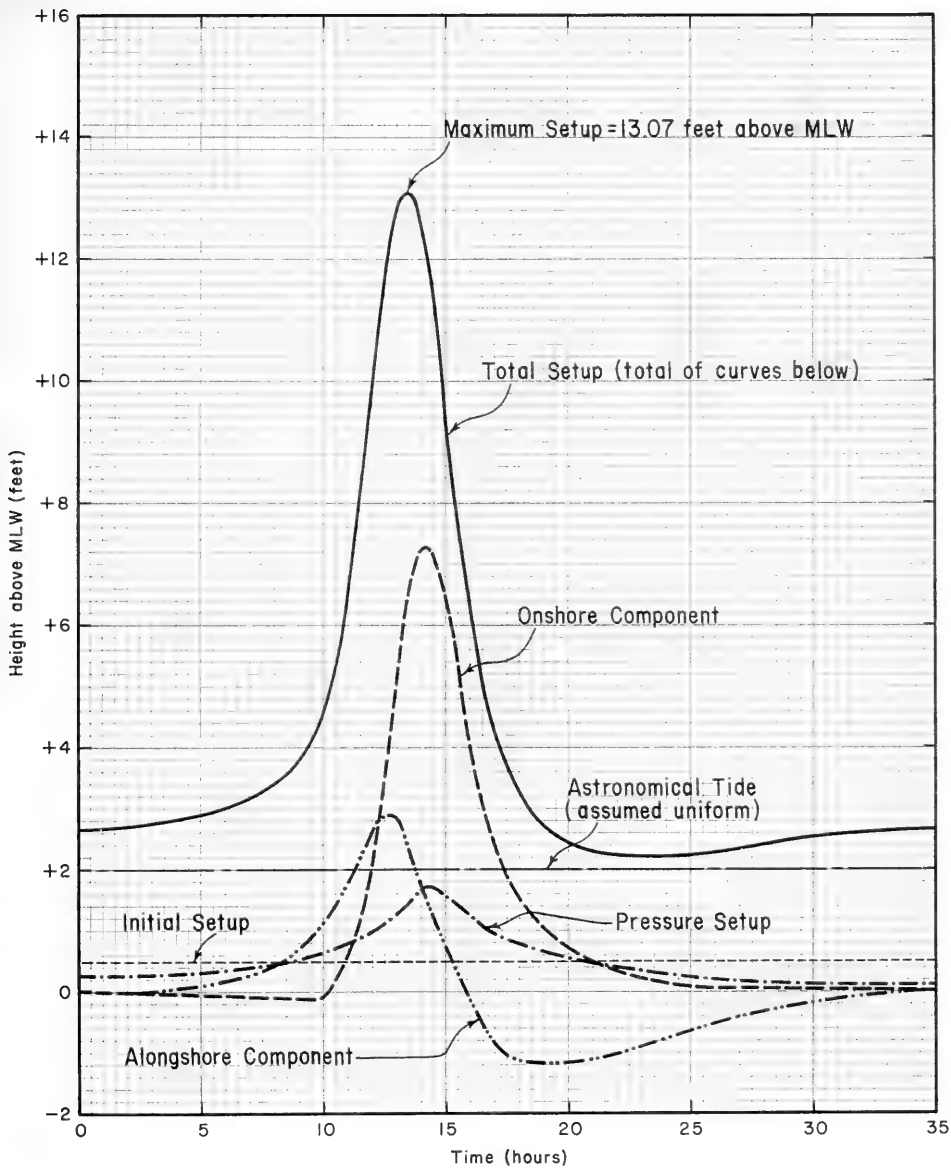
Figure 8-7. Bathystrophic Storm Surge Hydrograph
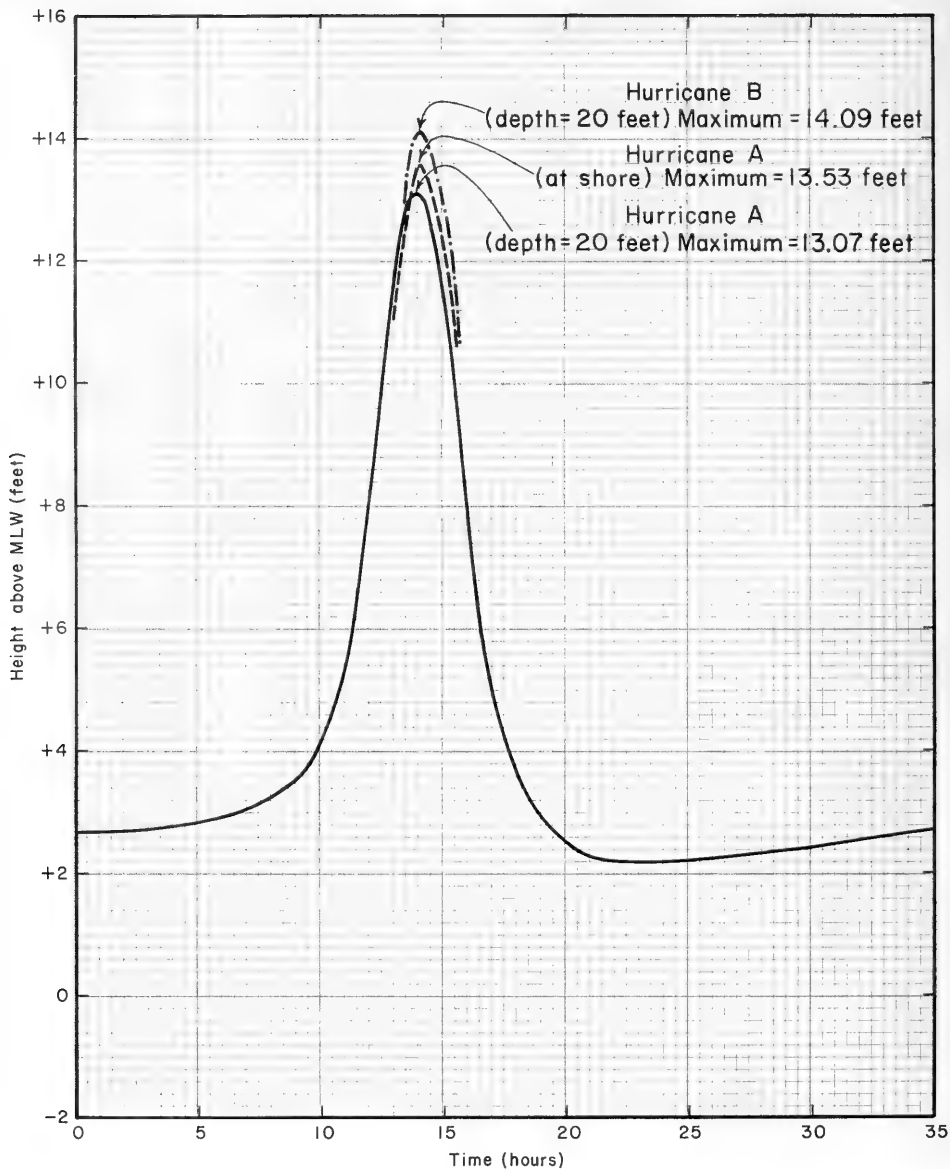
Figure 8-8. Bathystrophic Storm Surge Hydrograph – Comparison of Peak Surges

Design Problem _Physical Environment_

Observed Water Level Data – Breakwater Harbor
Lewes, Delaware

Sect. 3.81
Table 3-5
& Ref. 10

1. Length of Record: 1936 to present (1973)

2. Mean Tidal Range: 4.1 ft.

3. Spring Range: 4.9 ft.

4. Highest Observed Water Levels:
   a) Average yearly highest: 3.0 ft. above M.H.W.
   b) Highest observed: 5.4 ft. above M.H.W.
      (6 March 1962)

5. Lowest Observed Water Levels:
   a) Average yearly lowest: 2.5 ft. below M.L.W.
   b) Lowest observed: 3.0 ft. below M.L.W.
      (28 March 1955)

Graphical Summary
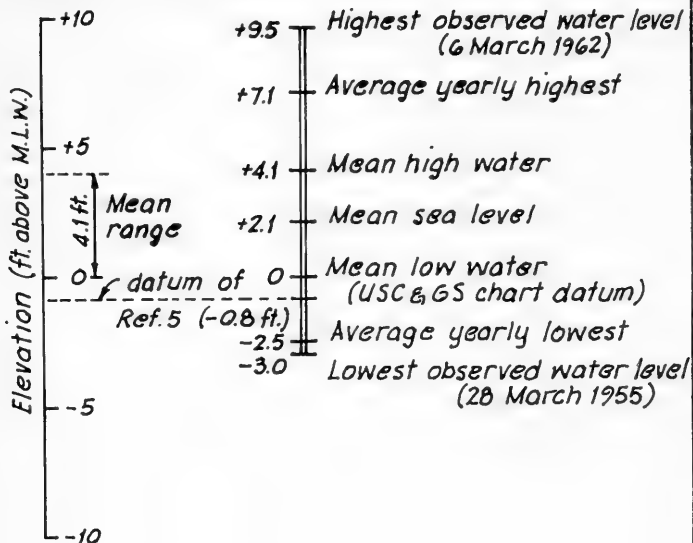
Analysis of Predicted Astronomical Tides

Ref. 10

Using the predicted high tides for Breakwater Harbor, Lewes, Delaware for the years 1962, 1967, 1968 and 1972, the probabilities that the water level will be above a given level at any time were generated (by computer) based on the following scheme.
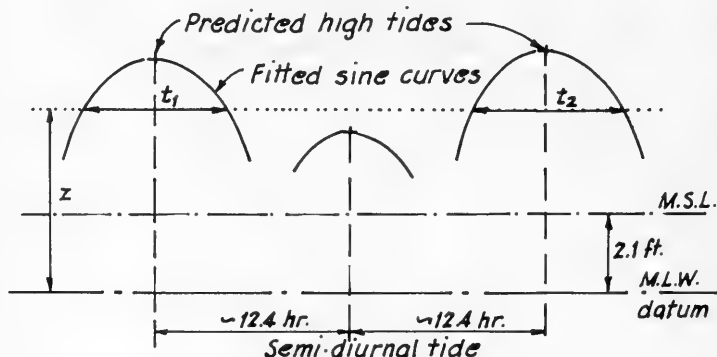
The probability the water level will be above z at any time is given by,

$$P(Z \geq z) = \frac{\sum t_i}{T_t}$$

where T_t is the length of the record analysed. and $\sum t_i$ is the amount of time the water level is above z. The results of the analysis are given on the following pages.

Based on this analysis, a water level above +5.0 ft. (M.L.W. datum) is exceeded 1.0 % of the time. (See Figure 8-9)

Astronomical Tide-Water Level Statistics
Based on Sine Curve Fit to Predicted
High Tides — Lewes, Delaware (1967)
(1967 data)

Elevation above MLW (z) feet	(1) Number of Hours per year	(2) Fraction of Time $P(Z \geq z)$
2.60000	3539.20154	0.40420
2.70000	3356.93503	.38338
2.80000	3162.84706	.36122
2.90000	2966.16526	.33875
3.00000	2750.04381	.31407
3.10000	2530.95381	.28905
3.20000	2307.68068	.26355
3.30000	2096.87811	.23948
3.40000	1897.91885	.21675
3.50000	1700.23383	.19418
3.60000	1537.76783	.17562
3.70000	1368.22078	.15626
3.80000	1217.94634	.13910
3.90000	1071.54007	.12238
4.00000	934.13571	.10668
4.10000	784.60798	.08961
4.20000	670.06012	.07652
4.30000	560.42541	.06400
4.40000	462.52767	.05282
4.50000	370.94314	.04236
4.60000	295.40660	.03374
4.70000	223.57539	.02553
4.80000	169.21023	.01932
4.90000	129.63847	.01481
5.00000	92.51881	.01057
5.10000	67.31568	.00769
5.20000	41.81988	.00478
5.30000	31.44437	.00359
5.40000	18.56210	.00212
5.50000	8.99619	.00103
5.60000	3.17861	.00036
5.70000	0.92306	.00011
5.80000	0.00064	.00000

(1) Number of hours per year water level above given elevation
(2) Fraction of time water level above given elevation
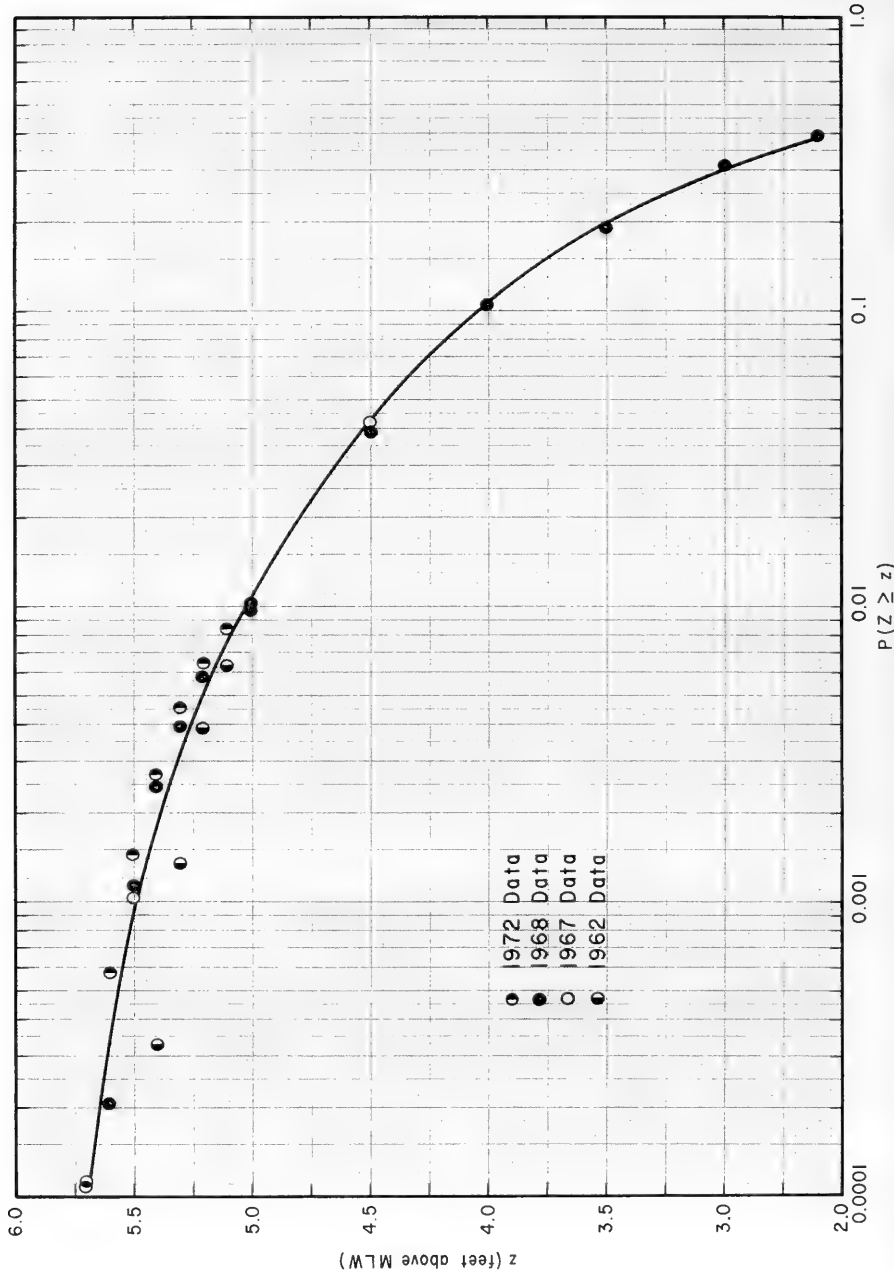
Figure 8-9. Astronomical Tides – Probability Water Level will be above a Given Level, Lewes, Delaware

Design Problem   Physical Environment

Design Water Level Summary

For purposes of the design problem the following water levels will be used. The criteria used here should not be assumed generally applicable since design water level criteria will vary with the scope and purpose of a particular project.

1. Astronomical tide: use + 5.0[†] ft (M.L.W.)

2. Storm surge: use + 11.0 ft.

3. Wave setup: (a function of wave conditions)   Sect. 3.85

                              16.0+ ft. (above M.L.W.)

† Exceeded 1.0% of time.

Tidal Currents at Delaware Bay Entrance   Refs. 9 & 10
(Surface Currents Only)
1948 values

Time	Velocity (knots)*	Velocity (ft./sec.)*	Direction (degrees N)
Flood-2 hr.	0.8	1.35	311°
-1 hr.	1.4	2.36	317°
Flood	1.6	2.70	309°
Flood +1 hr.	1.3	2.20	301°
+2 hr.	0.6	1.01	293°
+3 hr.	0.3	0.51	40°
Ebb -2 hr.	1.3	2.20	135°
-1 hr.	2.1	3.54	140°
Ebb	2.5	4.22	148°
Ebb +1 hr.	2.4	4.05	149°
+2 hr.	1.8	3.03	153°
+3 hr.	0.6	1.01	195°

* For spring tides

Example charts from Reference 9 and a summary of tidal current velocities are given on the following pages.
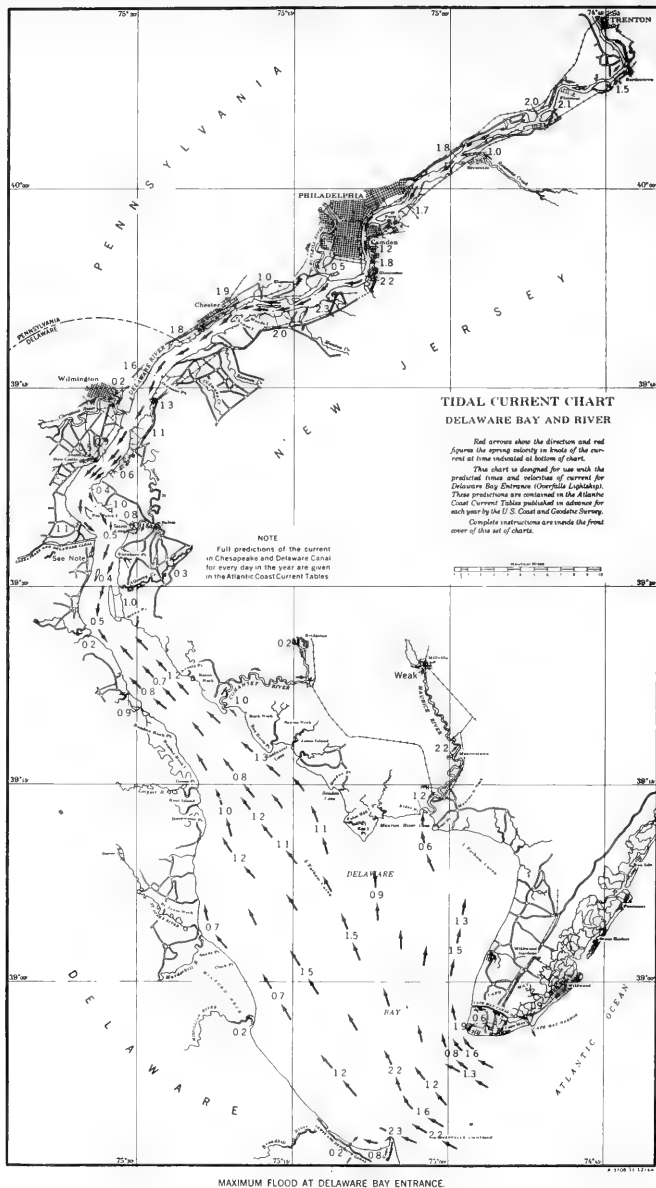
Figure 8-10.   Tidal Current Chart-Maximum Flood at Delaware Bay Entrance

MAXIMUM EBB AT DELAWARE BAY ENTRANCE.
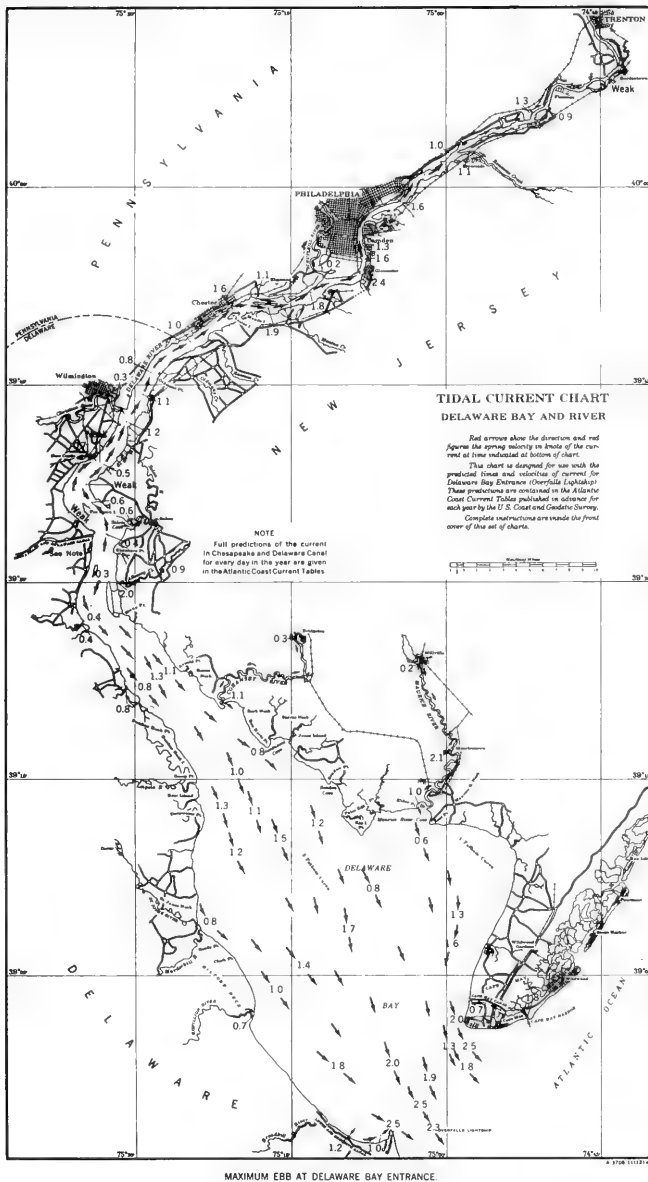
Figure 8-11. Tidal Current Chart-Maximum Ebb at Delaware Bay Entrance

8-23
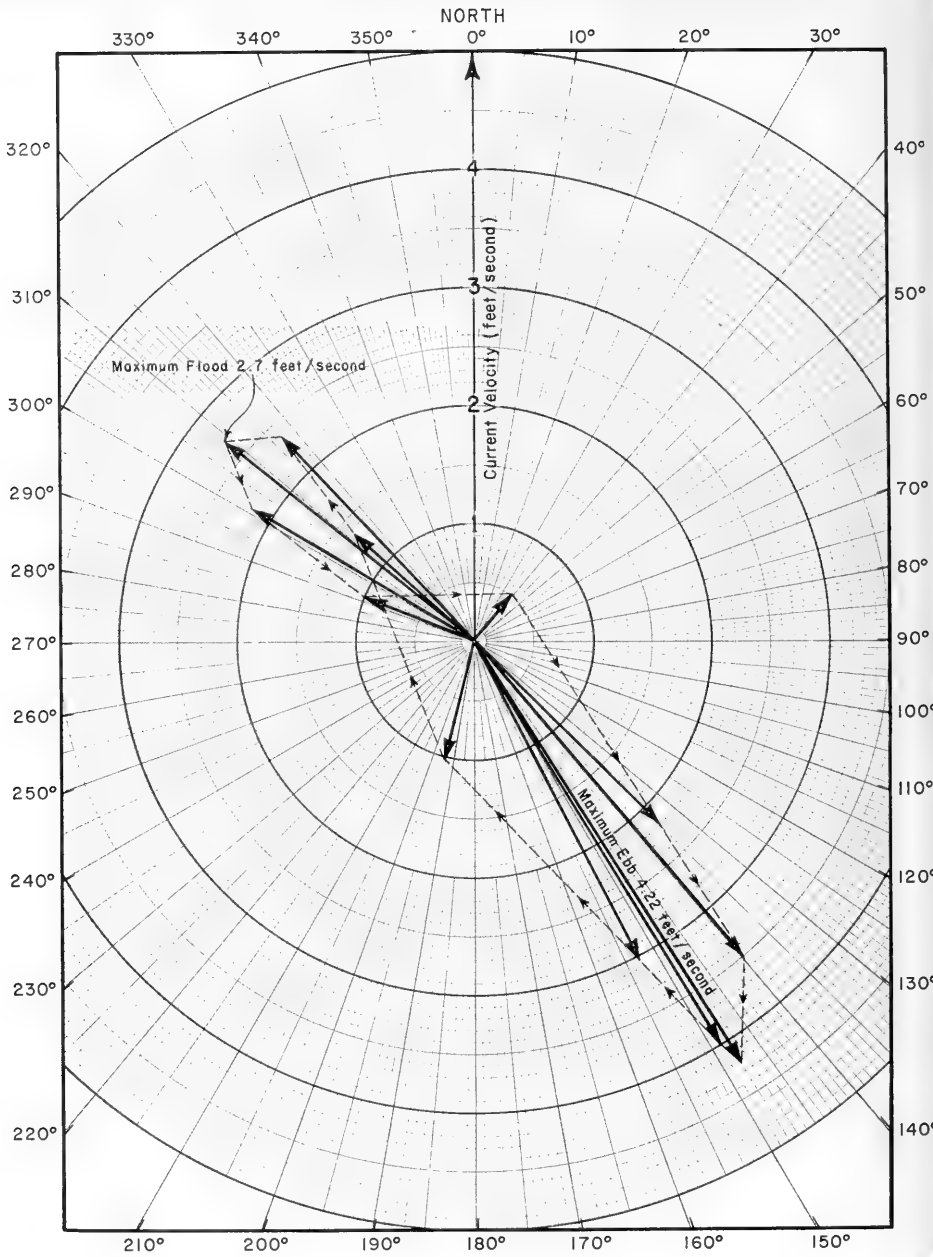
Figure 8-12. Polar Diagram of Tidal Currents at Island Site

8-24
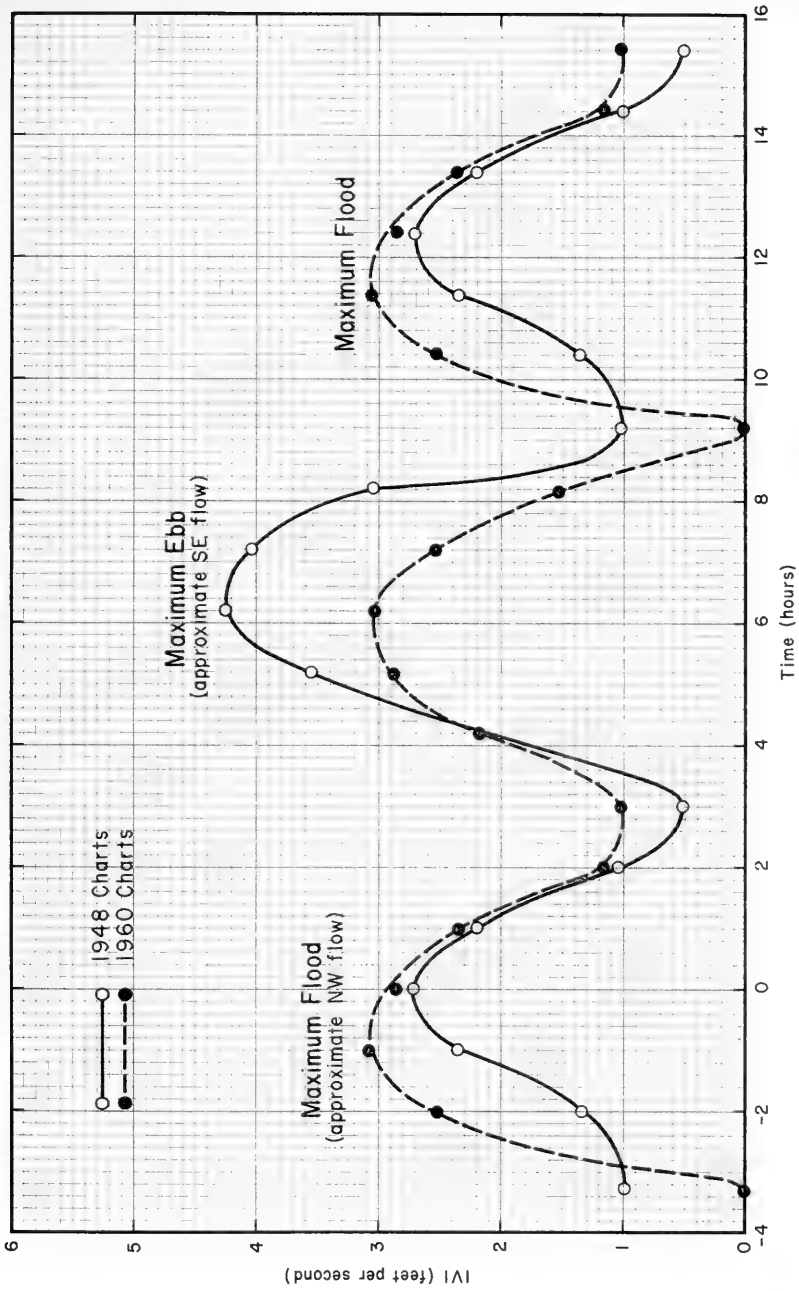
Figure 8-13. Time Variation of Tidal Current Speed at Island Site

8-25

Design Problem Physical Environment

Wave Conditions on Bay Side of Island

Sect. 3.6

Wave data on waves generated in Delaware Bay are not available for the island site. Consequently, wind data and limited fetch, shallow water wave forecasting techniques will be used to estimate wave conditions.

Calculation of Effective Fetch

Sect. 3.43
Fig. 3-29

(See Figure 8-14 on next page)

α * (degrees)	$\cos \alpha$	X_i ** (n.m.)	$X_i \cos \alpha$
$-42°$	0.743	9.2	6.8
$-36°$	0.809	11.6	9.4
$-30°$	0.866	13.0	11.3
$-24°$	0.914	15.5	14.2
$-18°$	0.951	21.8	20.7
$-12°$	0.978	25.5	25.0
$-6°$	0.995	27.9	27.7
$0°$	1.000	48.2	48.2
$+6°$	0.995	34.1	33.9
$+12°$	0.978	27.0	26.4
$+18°$	0.951	20.1	19.1
$+24°$	0.914	20.6	18.8
$+30°$	0.866	20.0	17.3
$+36°$	0.809	17.3	14.0
$+42°$	0.743	15.8	11.8
Totals	13.512		304.6

$$F_E = \frac{304.6}{13.512} = 22.54 \ n.m.$$

$$F_E = 22.54 \ n.m. \times 6080 \ \frac{ft.}{n.m} = 137,100 \ ft.$$

$$say \quad F_E = 140,000 \ ft.$$

* Angle measured clockwise from central radial.
** Distance along central radial in nautical miles.
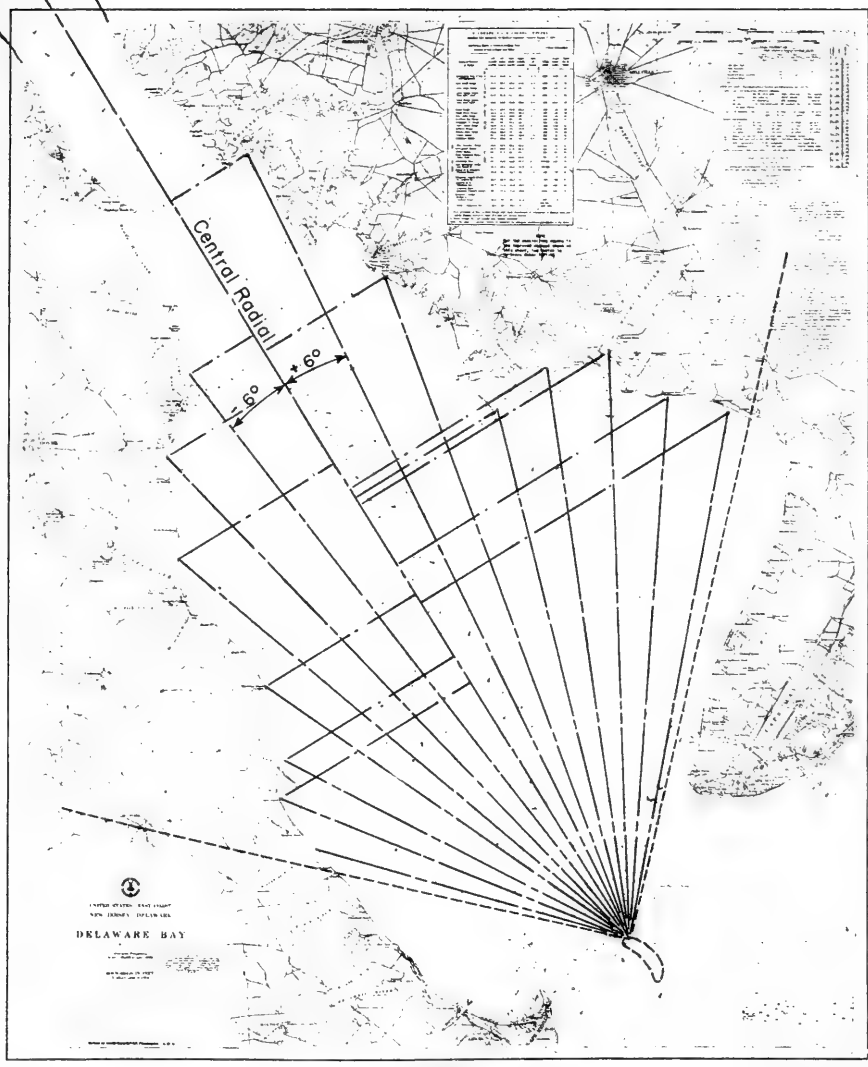
Figure 8-14. Calculation of Effective Fetch - Island Site at
Delaware Bay Entrance

Design Problem   Physical Environment

Wave Conditions on Bay Side of Island (cont.)

Significant Wave Height and Period as a Function   Sect. 3.61
of Wind Speed

Wind from N.N.W. along central radial.

Average Depth Along Central Radial
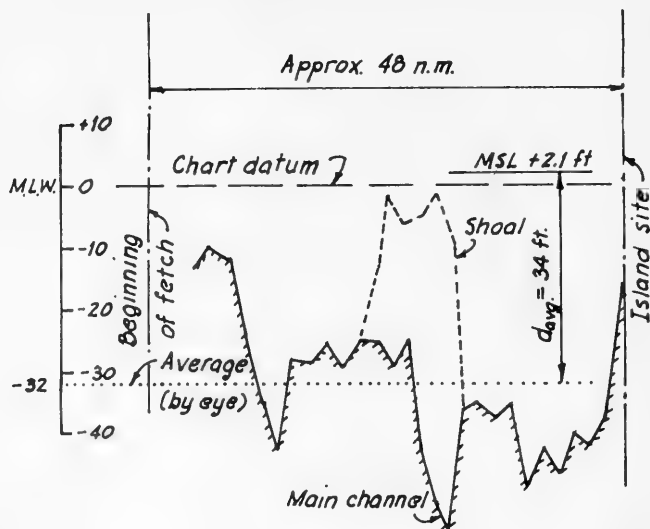
$$H_s = \frac{0.283\,U^2}{g}\tanh\left[0.530\left(\frac{gd}{U^2}\right)^{0.75}\right]\tanh\left[\frac{0.0125\left(\frac{gF}{U^2}\right)^{0.42}}{\tanh\left[0.530\left(\frac{gd}{U^2}\right)^{0.75}\right]}\right] \qquad Eq.\ 3\text{-}25$$

$$T_s = \frac{1.2\,(2\pi U)}{g}\tanh\left[0.833\left(\frac{gd}{U^2}\right)^{0.375}\right]\tanh\left[\frac{0.077\left(\frac{gF}{U^2}\right)^{0.25}}{\tanh\left[0.833\left(\frac{gd}{U^2}\right)^{0.375}\right]}\right] \qquad Eq.\ 3\text{-}26$$

Page no :	29 of 133
Calculated by :	J. R. W.
Checked by :	R. A. J
Date :	6 Mar. 73

Design Problem   _Physical Environment_

Wave Conditions on Bay Side of Island (cont.)

   Example Calculation

$$U = 50 \text{ mph} \quad (73.3 \text{ ft/sec.})$$
$$F_E = 140,000 \text{ ft.} \quad (26.52 \text{ miles})$$
$$d = 34 \text{ ft.}$$

$$\frac{gF}{U^2} = \frac{32.2\,(140,000)}{(73.3)^2} = 839.0$$

$$\frac{gd}{U^2} = \frac{32.2\,(34)}{(73.3)^2} = 0.204$$

$$H_s = \frac{0.283\,(73.3)^2}{32.2} \tanh\left[0.530(0.204)^{0.75}\right]\tanh\left[\frac{0.0125\,(839)^{0.42}}{\tanh\left[0.530(0.204)^{0.75}\right]}\right] \qquad Eq.\ 3\text{-}25$$

$$H_s = 47.2 \tanh\left[0.161\right]\tanh\frac{0.218}{\tanh\,(0.161)}$$

$$H_s = 6.52 \text{ ft.}$$

$$T_s = \frac{1.2\,(6.28)(73.3)}{32.2}\tanh\left[0.833(0.204)^{0.375}\right]\tanh\left[\frac{0.077(839)^{0.25}}{\tanh\left[0.833(0.204)^{0.375}\right]}\right] \qquad Eq.\ 3\text{-}26$$

$$T_s = 17.15 \tanh\left[0.833(0.551)\right]\tanh\left[\frac{0.414}{\tanh\left[0.833(0.551)\right]}\right]$$

$$T_s = 5.50 \text{ sec.}$$

  Note: See tabulation on next page.

Wave Conditions on Bay Side of Island (cont.)

$$F_E = 140,000 \text{ ft. } ; \quad d = 34 \text{ ft.}$$

U (mph)	U (ft./sec.)	H_s (ft.)	T_s (sec)
50	73.3	6.52	5.5
60	88.0	7.48	5.9
70	102.7	8.31	6.3
80	117.3	9.07	6.7
90	132.0	9.76	7.0
100	146.7	10.40	7.3
110	161.3	10.99	7.6

Eqns.
3-25
& 3-26

$8-30$
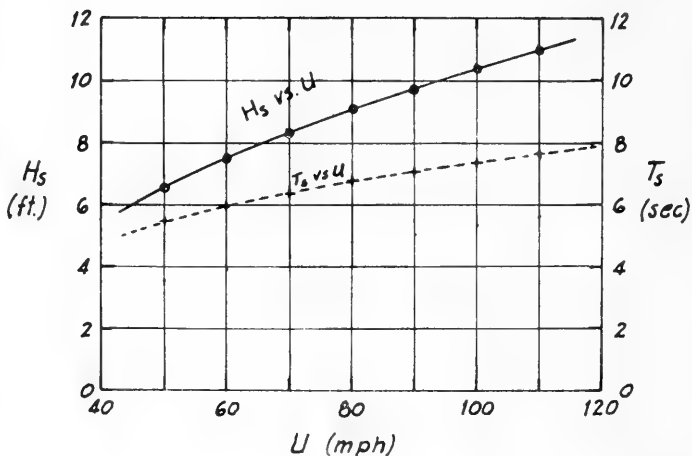
Wave Conditions on Bay Side of Island (cont.)

Frequency Analysis

Wind Data   Wind roses for the Delaware Bay area are given on the next page. Assume that sizeable waves occur primarily when wind is blowing along central radial from NW. This is the predominant wind direction for the Delaware Bay area. Wind is from the NW. approximately 16% of the time.

Ref. 14

   The maximum observed wind in 18 years of record was a 70 mph gale from the NW (daily maximum 5 minute wind speed)

Thom's Fastest-Mile-Wind Frequency

Ref. 8

In the absence of tabulated wind data (other than that given on the following page) the wind speed frequencies of Thom, adjusted for wind direction, will be used. Thom's wind speed frequencies are multiplied by 0.16 to adjust for direction. This assumes that winds from the NW are distributed the same as are winds when all directions are considered.

Thom's Wind Speeds - Delaware Bay Area

Quantile	Recurrence Interval (yrs)	Adjusted* Recurrence Interval (yrs)	U** (mph)
0.5	2	12.5	55
0.02	50	312.5	90
0.01	100	625.0	100

* Adjusted for direction (col. 2 divided by 0.16)
** Extreme fastest-mile-wind

Figure 8-15.   Wind Data in the Vicinity of Delaware Bay

Wave Conditions on Bay Side of Island (cont.)
Duration of Fastest-Mile-Wind

$$t = \frac{1 \text{ mile}}{U \text{ (mph)}} \cdot \frac{60 \text{ min.}}{hr.}$$

t = duration of wind in minutes

$$t \text{ (min.)} = \frac{60}{U \text{ (mph)}}$$
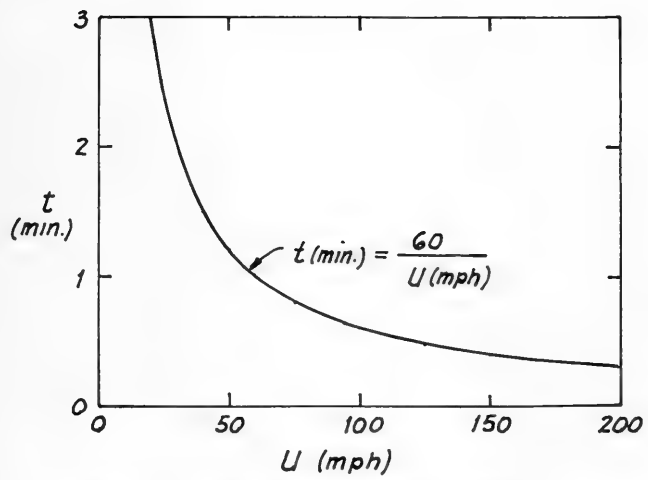
Note: Since the durations under consideration here are not sufficiently long to generate maximum wave conditions, Thom's wind data will result in a high estimate of wave heights and periods.

Dashed line on following page will be used to establish frequency of occurrence of given wave conditions. Calculated wave height recurrence intervals will be conservative.
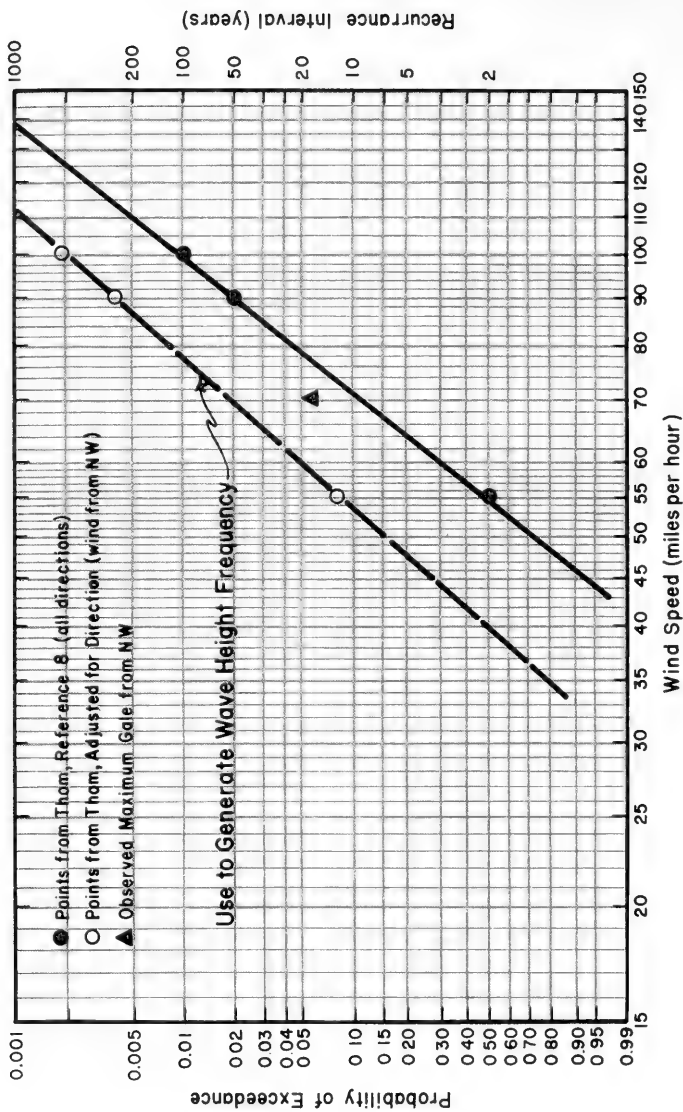
Figure 8-16. Probability Distribution of Maximum Wind Speed – Thom's Fastest Mile Wind

8-34

Design Problem Physical Environment

Wave Conditions on Bay Side of Island (cont.)

From dashed curve on previous page and graph on page 8-30 for H_s and T_s as a function of U.

Recurrence Interval (yrs)	Probability of Exceedance	U (mph)	H_s (ft.)	T_s (sec)
2	0.5	40	5.5	5.0
5	0.2	48	6.3	5.4
10	0.1	54	6.9	5.7
20	0.05	60	7.5	5.9
50	0.02	69	8.3	6.3
100	0.01	78	8.9	6.6
200	0.005	86	9.5	6.9

The computed wave heights plot as a straight line on log-normal probability paper (See Figure 8-17, next page).

Note: Economic considerations as well as the purpose of a given structure will determine the design wave conditions. The increased protection afforded by designing for a higher wave would have to be weighed against the increase in structure cost.

For the illustrative purposes of this problem, the significant wave height with a recurrence interval of 100 yrs. will be used.

Therefore, for design,

$$H_s = 8.9 \text{ ft.}$$

$$T_s = 6.6 \text{ sec.}$$

for waves generated in Delaware Bay.
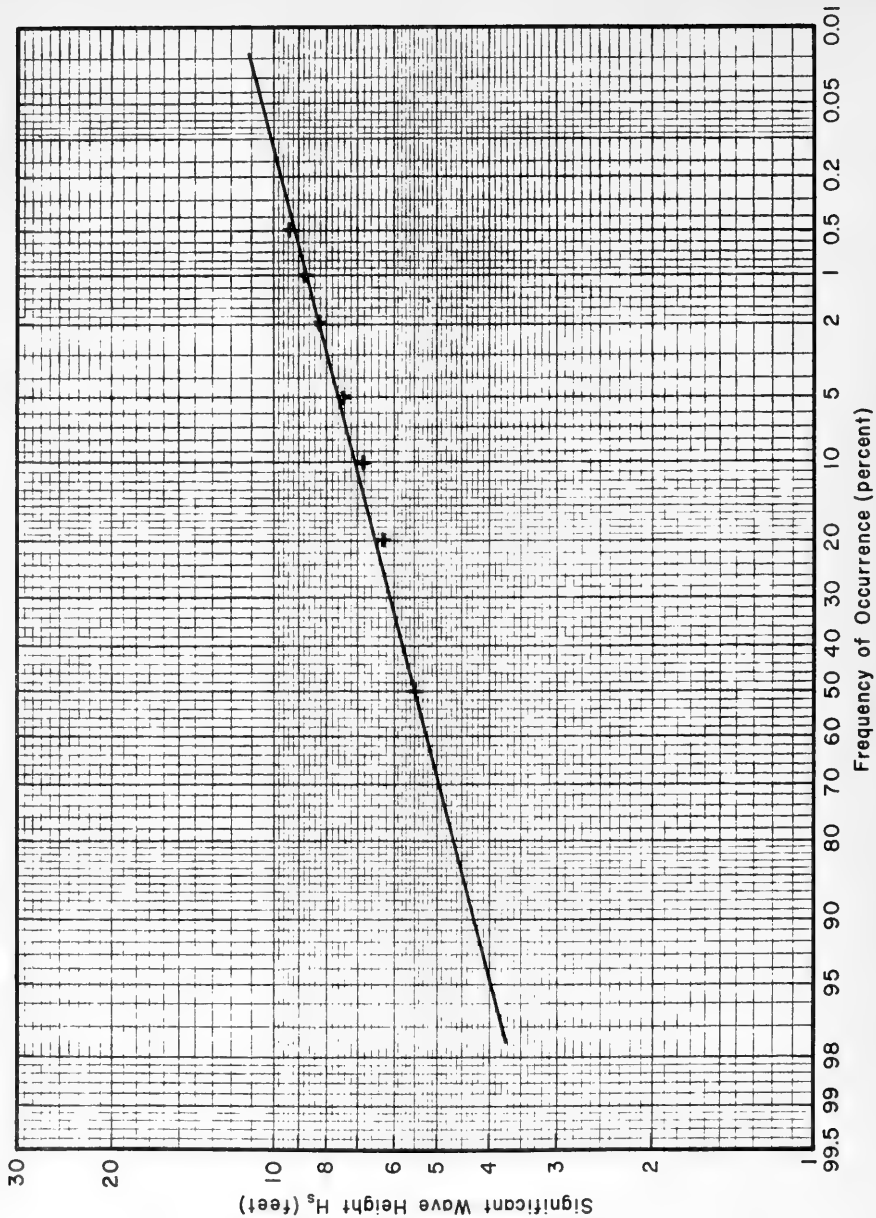
Figure 8-17. Frequency of Occurrence of Significant Wave Heights for Waves Generated in Delaware Bay

8-36

Wave Conditions on Ocean Side of Island

Ref. 7

     Hindcast wave statistics are available for several U.S. East Coast locations in Reference 7. Linear interpolation between the New York and Chesapeake Bay stations was used to determine statistics for the Delaware Bay region (see next page). Since the data are given for deep water, a refraction analysis is required to transform the statistics to the island site.

Idealized Refraction Analysis

Sect. 2.3

     For purposes of this problem, refraction by straight parallel bottom contours will be assumed.

Sect. 2.32

    Azimuth of shoreline $= 30°$ (See Figure 8-19)

Wave Directions

Direction of Wave Approach	Angle Between Wave Direction & Shoreline	
NNE	$-7.5°$	$(\alpha_o > 90°, neglect)$
NE	$+15.0°$	$* \alpha_o = 75°$
ENE	$+37.5°$	$\alpha_o = 52.5°$
E	$+60.0°$	$\alpha_o = 30.0°$
ESE	$+82.5°$	$\alpha_o = 7.5°$
SE	$+105.0°$	$\alpha_o = 15.0$
SSE	$+127.5°$	$\alpha_o = 37.5$
** S	$+150.0°$	$\alpha_o = 60.0$
SSW	$+172.5°$	$\alpha_o = 82.5°$
SW	$+195.0°$	$(\alpha_o > 90°, neglect)$

* α_o is the angle between the direction of wave approach and a normal to the shoreline.

** Used for typical refraction calculations given on following pages.

STATISTICAL WAVE HINDCAST FOR NORTH ATLANTIC COAST
ASSUMED STATION OFF DELAWARE BAY
(INTERPOLATED FROM NEW YORK HARBOR AND CHESAPEAKE BAY HINDCASTS)

Duration given in hours. Height and period groupings include lower value but not the upper.

Height (Feet)	Dir'n	4-6	6-8	8-10	10-12	12-14	14-16	16-18	18-20	20-22	22-24	Total
0.5-2	NE	22	88	514	430	16						1070
	ENE	48	640	1654	1388	68						3798
	E	118	866	1126	468	4	2					2584
	ESE	88	306	124	34							552
	SE	48	208	118	28	2						404
	SSE	14	124	32	14							184
	S	36	86	34	2	4						162
	SSW	16	6	2	2							24
	Tot.	390	2324	3602	2366	94	2					8778
2-4	WNW	8										10
	NE	56	24	126	346	294	38	4	2			890
	ENE	98	132	524	1152	846	132	16				2860
	E	148	180	386	626	236	38					1614
	ESE	110	80	148	114	46	8					500
	SE	58	50	44	102	64	6					324
	SSE	54	52	32	38	28						204
	S	46	28	38	32	8						152
	SSW	22	8	10	20	2	2					64
	SW	2										2
	Tot.	602	536	1302	2390	1534	224	20	2			6640
4-6	N	2										2
	WNW	12										22
	NE	46	38	54	96	122	100	30	4			490
	ENE	78	154	362	500	314	52					1614
	E	98	188	76	180	206	104					852
	ESE	44	86	38	46	52	22	2				290
	SE	32	50	6	12	52	32	4				188
	SSE	10	48	6	8	12						112
	S	14	18	6	10	8	2					58
	SSW	6	4			2						14
	SW	2										2
	Tot.	344	596	340	714	972	586	88	4			3644
6-8	N	2										2
	NNE	4	16	4								24
	NE	6	56	32	44	48	38	26	4			254
	ENE		118	32	72	162	328	80				828
	E	6	134	60	76	54	90	20				448
	ESE		68	28	14	22	24	2				148
	SE	2	40	6		12	20	24	2			106
	SSE		16	10		20	20	2	2			70
	S	2	24	10	6	4	16					60
	SSW	2	4	2			4					18
	SW	2										2
	Tot.	32	468	226	212	312	540	152	10			1952
8-10	NNE		10	12								22
	NE		26	30	42	16	32	24	12			150
	ENE		38	66	24	68	134	48	2			380
	E		56	56	48	26	38	36	2			230
	ESE	2	24	32	2	16	22	2				100
	SE		18	10	2	6	12	34	2			84
	SSE		12	6		6	10	34	2			74
	S		2	6	4		14	4				30
	SSW		4	2								10
	Tot.	2	190	224	62	138	262	182	20			1082
10-12	NNE		4	2								6
	NE		16	12	18	14	6	20	6			90
	ENE		12	66	28	28	46	40	14			230
	E		22	54	6	16	4	6	2	2		112
	ESE		8	2	4	4		6		2		32
	SE		6	2	2	2	4	26	2			44
	SSE		6	4		2	22	12				44
	S		6				4	8				30
	SSW			16								16
	Tot.		76	158	58	66	86	126	32	4		628
12-14	NNE		2									6
	NE			24	2	6	6	14	4	8		66
	ENE			38	10	20	16	20	12	2		120
	E			2	10	2	2	2				36
	ESE			14	6		18					38
	SE		6				6	4	4			22
	SSE			2			10	2	2			18
	S		4				6		6			16
	Tot.		10	128	32	30	64	46	38	10		348
14-16	NE			4		2	4	12	18			48
	ENE			8	18	14	8	16	12	6		82
	E		2	12	18							36
	ESE			8	2		6		8			16
	SE						6	2	8			10
	SSE			2		2	4					4
	S		2	34	46	22	22	30	30	24		200
	Tot.		2	34	46	22	22	30	30	24		200
16-18	NNE			2								2
	NE		8		6	2	2	4		4		26
	ENE				6	10	2	8	6	2		40
	E		8		10	4	2	10				28
	ESE				10	2			4	4		8
	SE				4				2			2
	SSW			18	32	14	6	22	14	10		114
	Tot.			18	32	14	6	22	14	10		114
18-20	NE				12	10	2	4	4			30
	ENE				14	6		6	8			34
	E		2		6		2	6				14
	ESE							2	4			4
	SE					2		2	2			4
	S					2			4			4
	SSW				4				4			100
	Tot.			4	32	20	4	18	22			100
20-25	NNE			2							4	4
	NE			2	16	10	4	4		2		40
	ENE				4	16	6	10	8	18		46
	E		2		6	4	2		2			4
	ESE				4				2			4
	SE							14	12	20		6
	Tot.			4	36	36	16	14	12	20	4	138
25-30	NNE					12						12
	NE			2		20				6	2	30
	Tot.			4		20	14			6	2	60
Total		**1370**	**4222**	**6040**	**5980**	**3270**	**1812**	**700**	**164**	**74**	**6**	**23,644**
Hrs. Calm												2,660
Total Hours in Period												26,304

Figure 8-18.   Wave and Swell Diagrams for a Location off
                Delaware Bay Entrance
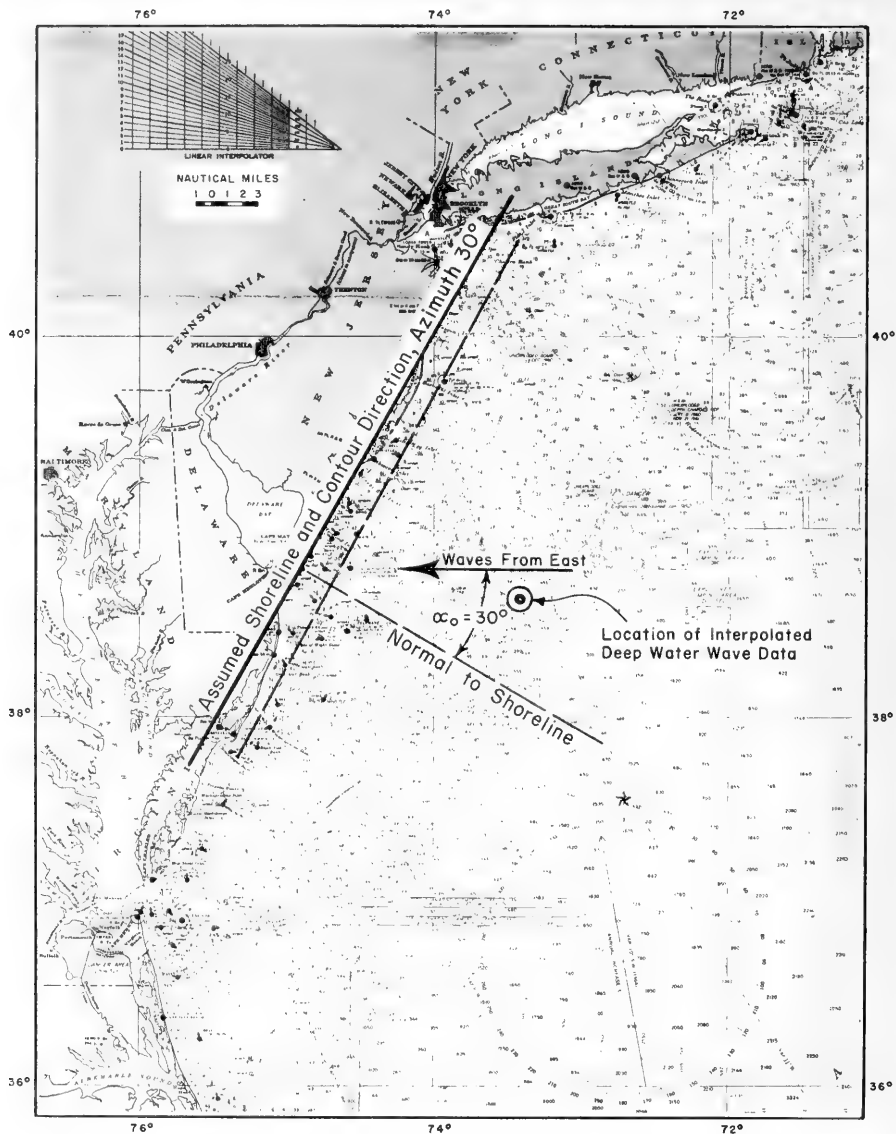
Figure 8-19. General Shoreline Alignment in Vicinity of
Delaware Bay for Refraction Analysis

Wave Conditions on Ocean Side of Island (cont.)

Typical Refraction Calculations

Depth at structure : Use 40.0 ft.

Shoaling coefficient

$$K_s = \frac{H}{H_o'} = \left\{ \frac{\coth\left(\frac{2\pi d}{L}\right)}{1 + \dfrac{4\pi d/L}{\sinh(4\pi d/L)}} \right\}^{\frac{1}{2}}$$

Eq. 2-44

equivalently,

$$K_s = \left\{ \frac{C_o}{2nC} \right\}^{\frac{1}{2}} = \left\{ \frac{gT^2}{4\pi n L} \right\}^{\frac{1}{2}}$$

Refraction coefficient and angle

$$\sin \alpha = \frac{C}{C_o} \sin \alpha_o$$

Eq. 2-78a

Note: Equation 2-78a is written between deep water and $d = 40$ ft since bottom contours and shoreline have been assumed straight and parallel.

For straight parallel bottom contours the expression for the refraction coefficient reduces to :

$$K_R = \left\{ \frac{b_o}{b} \right\}^{\frac{1}{2}} = \left\{ \frac{\cos \alpha_o}{\cos \alpha} \right\}^{\frac{1}{2}}$$

Recall,

$$L_o = \frac{gT^2}{2\pi} \quad \text{(deep water)}$$

Eq. 2-8

and

$$\frac{L}{L_o} = \frac{C}{C_o} = \tanh\left(\frac{2\pi d}{L}\right)$$

Eq. 2-11

Typical refraction-shoaling calculations are given on the next page. Calculations for various directions and for a range of periods follow.

Wave Conditions on Ocean Side of Island (cont.)

Example calculations for waves from South
(Angle between direction of wave approach and
normal to shoreline in deep water $= \alpha_o = 60°$)

T (sec)	L_o (ft)	d/L_o	H/H_o' (K_s)	C/C_o	α (degree)	K_R	$K_R K_s$ *
(1)	(2)	(3)	(4)	(5)	(6)	(7)	(8)
6	184	0.2174	0.9225	0.9065	51.7°	0.90	0.83
8	328	0.1220	0.9196	0.7634	41.4°	0.82	0.75
10	512	0.0781	0.9575	0.6431	33.8°	0.78	0.75
12	737	0.0543	1.009	0.5507	28.5°	0.75	0.76
14	1004	0.0398	1.065	0.4791	24.5°	0.74	0.79
16	1311	0.0305	1.122	0.4237	21.5°	0.73	0.82
18	1659	0.0241	1.177	0.3794	19.2°	0.73	0.86
20	2048	0.0195	1.233	0.3428	17.3°	0.72	0.89

Column (2) from Equation 2-8
     (3) 40 ft / column (2)
     (4) Equation 2-44 or Table C1, Appendix C.
     (5) Table C-1, Appendix C

$$C/C_o = \tanh\left(\frac{2\pi d}{L}\right)$$

     (6) Equation 2-78 a

     (7) $K_R = \left\{\dfrac{\cos \alpha_o}{\cos \alpha}\right\}^{\frac{1}{2}}$

     (8) Column (4) × column (7)

* $K_R K_s$ can also be obtained from Plate C-6,
     Appendix C.

Table of Breaker Angles and Refraction & Shoaling Coefficients

d = 40.00000 ft. α₀ = 52.50000° α₀ = .91630 radians

Block 1 — α₀ = 52.50000° = .91630 rad

	T=4sec	6	8	10	12	14	16	18	20	22	24sec
a (deg)	52.18646	45.95495	37.28015	30.67445	25.89852	22.35859	19.64969	17.51682	15.79675	14.38153	13.19739
α_o (rad)	.91083	.80207	.65066	.53537	.45201	.39023	.34295	.30573	.27571	.25101	.23034
K_r	.98934	.92232	.91963	.95750	1.00910	1.06496	1.12157	1.17749	1.23216	1.28536	1.33704
K_s	.99646	.93575	.87469	.84131	.82263	.81132	.80399	.79898	.79540	.79275	.79074
$K_r K_s$	.98584	.86307	.80439	.80555	.83012	.86403	.90173	.94079	.98006	1.01897	1.05725

(Example Calculations — box indicated around the T=18 and T=20 columns)

d = 40.00000 ft. α₀ = 60.00000° = 1.04720 rad

Block 2 — α₀ = 60.00000° = 1.04720 rad

	T=4sec	6	8	10	12	14	16	18	20	22	24sec
a (deg)	59.58441	51.68700	41.39121	33.84103	28.47583	24.53489	21.53509	19.18118	17.28722	15.73148	14.43134
α_o (rad)	1.03994	.90211	.72241	.59064	.49700	.42821	.37586	.33477	.30172	.27457	.25187
K_r	.98934	.92232	.91963	.95750	1.00910	1.06496	1.12157	1.17749	1.23216	1.28536	1.33704
K_s	.99379	.89806	.81638	.77588	.75420	.74137	.73316	.72759	.72364	.72073	.71853
$K_r K_s$	.98320	.82830	.75077	.74291	.76106	.78953	.82229	.85673	.89164	.92640	.96071

d = 40.00000 ft. α₀ = 75.00000° = 1.30900 rad

Block 3 — α₀ = 75.00000° = 1.30900 rad

	T=4sec	6	8	10	12	14	16	18	20	22	24sec
a (deg)	74.12387	61.06242	47.51627	38.39875	32.12634	27.59044	24.16806	21.49728	19.35626	17.60214	16.13899
α_o (rad)	1.29371	1.05574	.82932	.67018	.56071	.48154	.42181	.37520	.33783	.30722	.28168
K_r	.98934	.92232	.91963	.95750	1.00910	1.06496	1.12157	1.17749	1.23216	1.28536	1.33704
K_s	.97269	.73137	.61905	.57467	.55283	.54040	.53262	.52742	.52376	.52109	.51907
$K_r K_s$	.96232	.67456	.56929	.55025	.55786	.57550	.59737	.62103	.64536	.66979	.69402

d = 40.00000 ft. α₀ = 82.50000° = 1.43990 rad

Block 4 — α₀ = 82.50000° = 1.43990 rad

	T=4sec	6	8	10	12	14	16	18	20	22	24sec
a (deg)	80.84691	63.93134	49.19627	39.60867	33.08190	28.38437	24.84917	22.09470	19.88890	18.08302	16.57751
α_o (rad)	1.41104	1.11581	.85864	.69130	.57739	.49540	.43370	.38563	.34713	.31561	.28933
K_r	.98934	.92232	.91963	.95750	1.00910	1.06496	1.12157	1.17749	1.23216	1.28536	1.33704
K_s	.90584	.54500	.44693	.41161	.39469	.38518	.37927	.37533	.37257	.37055	.36904
$K_r K_s$	.89619	.50266	.41101	.39412	.39828	.41020	.42537	.44195	.45906	.47629	.49341

Table of Breaker Angles and Refraction & Shoaling Coefficients (Continued)

d=40.00000 ft   αo=7.500u0°   αb= .13090 radians

	T=4sec	6	8	10	12	14	16	18	20	22	24 sec
α= 7.46821°		6.79165	5.71929	4.81472	4.12088	3.58823	3.17148	2.83842	2.56701	2.34200	2.15265
α= .13034 rad		.11854	.09982	.08403	.07192	.06263	.05535	.04954	.04480	.04088	.03757
Ks= .98934		.92232	.91963	.95750	1.00910	1.06496	1.12157	1.17749	1.23216	1.28536	1.33704
Kr= .99996		.99923	.99820	.99747	.99700	.99669	.99648	.99632	.99621	.99613	.99606
KsKr= .98931		.92161	.91798	.95509	1.00608	1.06144	1.11762	1.17317	1.22750	1.28039	1.33178
		40.00000	15.00000		.26180						
		14.93531	11.39690	9.58040	8.12208	7.12880	6.29815	5.63506	5.09511	4.64773	4.27143
		.26067	.19891	.16721	.14298	.12442	.10992	.09835	.08893	.08112	.07455
		.98934	.91963	.95750	1.00910	1.06496	1.12157	1.17749	1.23216	1.28536	1.33704
		.99985	.99265	.98974	.98787	.98664	.98579	.98520	.98476	.98444	.98418
		.98919	.91287	.94768	.99686	1.05073	1.10563	1.16006	1.21339	1.26536	1.31589
		40.00000	30.00000		.52360						
		29.86070	22.44164	18.75493	15.97832	13.87138	12.23539	10.93482	9.87891	9.00592	8.27283
		.52117	.39168	.32734	.27887	.24210	.21355	.19085	.17242	.15718	.14439
		.98934	.91963	.95750	1.00910	1.06496	1.12157	1.17749	1.23216	1.28536	1.33704
		.99930	.96798	.95634	.94912	.94448	.94136	.93917	.93758	.93639	.93548
		.98865	.89018	.91570	.95776	1.00584	1.05580	1.10587	1.15525	1.20361	1.25078
		40.00000	37.50000		.65450						
		37.31496	27.69597	23.04532	19.58178	16.97131	14.95307	13.35327	12.05708	10.98703	10.08947
		.65127	.48339	.40222	.34177	.29621	.26098	.23306	.21044	.19176	.17609
		.98934	.91963	.95750	1.00910	1.06496	1.12157	1.17749	1.23216	1.28536	1.33704
		.99877	.94658	.92852	.91764	.91076	.90618	.90299	.90069	.89898	.89767
		.98812	.87050	.88907	.92599	.96992	1.01634	1.06327	1.10980	1.15552	1.20022

Design Problem   *Physical Environment*

Wave Conditions on Ocean Side of Island (cont.)
Summary of Refraction Analysis - d = 40.0 ft.
(Numbers given in Table are $K_s K_R$)

Direction	Wave Period (sec)								
	8	10	12	14	16	18	20	22	24
NE	0.569	0.550	0.558	0.576	0.597	0.621	0.645	0.670	0.694
ENE	0.804	0.806	0.830	0.864	0.902	0.941	0.980	1.02	1.06
E	0.890	0.916	0.958	1.01	1.06	1.11	1.16	1.20	1.25
ESE	0.918	0.955	1.01	1.06	1.12	1.17	1.23	1.28	1.33
SE	0.913	0.948	0.997	1.05	1.11	1.16	1.21	1.27	1.32
SSE	0.871	0.889	0.926	0.970	1.02	1.06	1.11	1.16	1.20
S	0.751	0.743	0.761	0.790	0.822	0.857	0.892	0.926	0.961
SSW	0.411	0.394	0.398	0.410	0.425	0.442	0.459	0.476	0.493

Refraction-shoaling coefficients are summarized graphically on next page.

Transformation of Wave Statistics by Refraction and Shoaling

The above refraction-shoaling coefficients will be used to transform the interpolated deepwater wave statistics given on page 8-38. The resulting statistics will only be an approximation since only the significant wave is considered in the analysis. The actual sea surface is made up of many wave periods or frequencies each of which results in a different refraction-shoaling coefficient. The analysis given here is only for the highest waves of the wave statistics on page 8-38. A more complete analysis would consider the entire table of statistics.
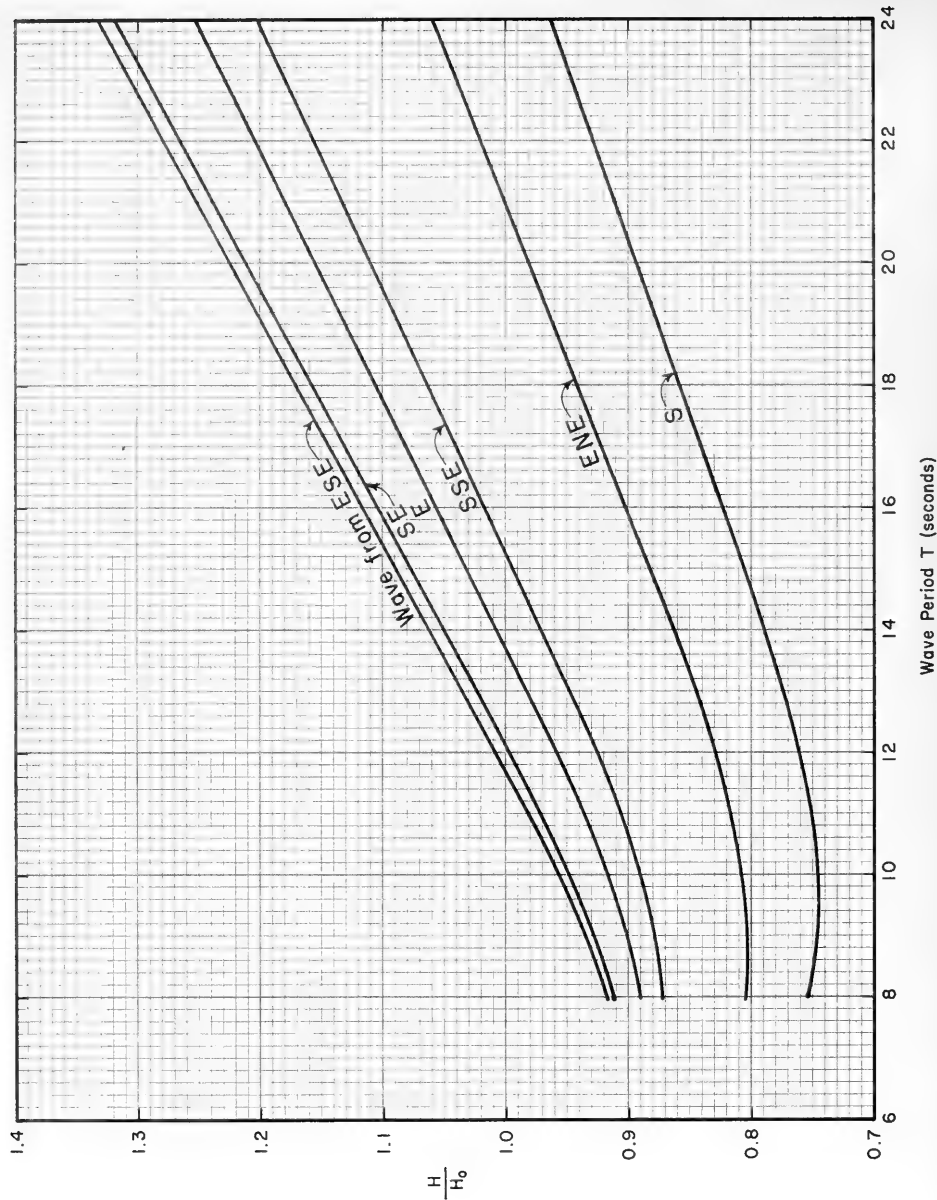
Figure 8-20. Refraction-Shoaling Coefficients as a Function of Wave Direction and Wave Period.

Wave Conditions on Ocean Side of Island (cont.)

Table of Transformed Wave Heights

Significant height & period in d = 40 ft.
(explanation of numbers in table on next page)

Deepwater Height & Direction	Wave Period (sec)							
	9	11	13	15	17	19	21	23
30 ft. NNE	–	– (2)	– (8)	–	–	–	–	–
NE	–	16.6	16.9 (12)	17.6	18.3	18.9	19.7	20.5
ENE	–	24.5 (2)	25.4 (20)	26.5	27.6	28.8	30.0 (6)	31.2 (2)
E	–	28.1	29.5 (8)	30.9	32.4	33.9	35.4	36.9
25 ft. NNE	–	–	–	–	–	–	–	–
NE	14.0	13.9 (16)	14.2 (10)	14.7 (4)	15.3 (4)	15.8	16.5 (2)	17.1 (4)
ENE	20.1	20.5 (4)	21.2 (16)	22.0 (6)	23.1 (10)	23.8 (8)	25.0 (18)	26.0
E	22.5 (2)	23.4 (6)	24.6 (4)	25.8 (2)	27.0	28.3 (2)	29.5	30.8
ESE	23.4	24.5 (4)	25.9	27.3	28.6	30.0	31.3	32.7
SE	23.3	24.3	25.6 (4)	27.0	28.3	29.6 (2)	31.0	32.3
SSE	22.0	22.6	23.7 (2)	24.8 (4)	26.0	27.2	28.3	29.5
20 ft. NNE	–	–	–	–	–	–	–	–
NE	11.2 (2)	11.1 (12)	11.4 (10)	11.7 (2)	12.2 (4)	12.6	13.1	13.6
ENE	16.1	16.4 (14)	16.9 (6)	17.6	18.4 (6)	19.2 (8)	20.0	20.8
E	18.0	18.7 (6)	19.7	20.6 (2)	21.6 (6)	22.6	23.6	24.6
ESE	18.7 (2)	19.6	20.7	21.8	22.8 (2)	24.0 (4)	25.0	26.2
SE	18.6	19.4	20.4 (2)	21.6	22.6	23.7 (2)	24.8	25.8
SSE	17.6	18.1	19.0 (2)	19.9	20.8	21.8	22.6	23.6
S	14.9	15.0	15.5	16.1	16.8	17.5 (4)	18.2	18.9
18 ft. NNE	– (2)	–	–	–	–	–	–	–
NE	10.1 (8)	10.0 (6)	10.2 (2)	10.5 (2)	11.0 (4)	11.4	11.8 (4)	12.3
ENE	14.5	14.7 (12)	15.2 (10)	15.8 (2)	16.6 (8)	17.3 (6)	18.0 (2)	16.9
E	16.2 (8)	16.8 (10)	17.7	18.5	19.4 (10)	20.3	21.2	22.1
ESE	16.8	17.6 (4)	18.6 (2)	19.6	20.5	21.6	22.5	23.5
SE	16.7	17.5	18.5	19.4	20.3	21.3 (4)	22.3 (4)	23.2
SSE	15.8	16.3	17.1	17.9	18.7	19.5	20.4	21.2
S	13.5	13.5	13.9	14.5	15.1	15.8 (2)	16.4	17.0
16 ft. NNE	–	–	–	–	–	–	–	–
NE	9.0 (4)	8.9 (8)	9.1 (2)	9.4 (4)	9.8 (12)	10.1	10.5 (18)	10.9
ENE	12.8 (8)	13.1 (18)	13.5 (14)	14.1 (8)	14.8 (16)	15.4 (12)	16.0 (6)	16.6
E	14.4 (12)	15.0 (18)	15.7 (4)	16.5	17.3	18.1	18.9	19.7
ESE	15.0 (8)	15.7 (2)	16.6	17.4 (6)	18.3	19.2	20.0	20.9
SE	14.9	15.5	16.4	17.2	18.1 (2)	19.0 (8)	19.8	20.6
SSE	14.0	14.5	15.2	15.9 (4)	16.6	17.4	18.1	18.9

Wave Conditions on Ocean Side of Island (cont.)

Explanation of numbers in table on preceding page.

1. Numbers represent transformed wave height. For example, a 30 ft high deep-water wave with a period of 23 sec. approaching from the ENE (in deep water) will be 31.2 ft high at the island site (in a depth, d = 40 ft.).

2. Numbers in parentheses represent the number of hours waves are below given height and above next lower height for given period and direction. For example, deepwater waves between 25 and 30 ft. in height with a period of 23 sec were experienced for 2 hours in the three years of hindcast data. Equivalently, the wave height at the structure site for the given deepwater wave statistics will be between 26.0 and 31.2 ft. for 2 hours.

Wave Conditions on Ocean Side of Island (cont.)

Number of hours wave height at structure
is in given height interval.

Wave Height at Structure (ft.)				
H ≥ 30ft.	25 to 30	20 to 25	18 to 20	16 to 18
0.46 *	1.54 *			
	6.00			
	7.34	0.65		
	1.90	18.10		
	1.16	0.84		
	1.55	0.44		
	0.32	1.68		
	0.46	3.53		
		1.13	0.87	
		6.60	1.39	
		18.00	–	
		6.59	3.40	
		2.72	3.27	
		4.46	11.53	
		0.49	3.51	
		3.92	0.08	
		3.76	0.24	
		4.34	1.66	
		1.11	0.89	
		3.67	0.33	
		4.00	–	
		2.00	–	
		2.00	–	
		4.36	1.63	
		0.57	1.43	
		0.42	1.57	
		2.26	1.74	
		3.68	0.32	
0.46 hr	20.27 hr.	101.32 hr.	33.86 hr.	Subtotals

Table continued on next page.

* Example: For waves = 30 ft. high, 23 sec. period from
ENE, from table, page 8-47, wave height at
structure is between 31.2 and 26.0 ft. for 2 hr.
Therefore, wave height is above 30 ft for $\frac{1.2}{5.2}$ (2)= 0.46 hr.

Design Problem Physical Environment

Wave Conditions on Ocean Side of Island (cont.)

Wave Height at Structure (ft.)				
H ≥ 30 ft.	25 to 30	20 to 25	18 to 20	16 to 18
* 0.46 hr.	* 20.27 hr.	* 101.32 hr.	* 33.86 hr	* 0 hr.
		1.57	0.43	
			5.05	2.95
			1.33	4.66
			1.05	0.95
			0.74	1.26
			–	2.00
			6.66	3.33
			2.21	3.79
			0.60	1.40
			3.47	4.52
0.46 hr.	20.27 hr.	102.89 hr.	55.4 hr.	Column not complete

Total hours in record: 26,304 hr.
(Includes 4,667 hrs. calm)

Height	Total hrs.	Frequency
H ≥ 30	0.46	0.0000175
H ≥ 25	20.73	0.000788
H ≥ 20	123.62	0.00470
H ≥ 18	179.02	0.00681
H ≥ 16	**	**

* Subtotal from previous page.
** Would require that above tables be extended to entire range of table on page 8-38.

Wave Conditions on Ocean Side of Island (cont.)

Deepwater Wave Statistics
(without consideration of direction)

Table page 8-38

Significant Wave Height (feet)	Cumulative Hours*	Probability of Exceedance
30	0	— **
25	60	0.00228
20	198	0.00753
18	298	0.01133
16	414	0.01573
14	614	0.02334
12	962	0.03657
10	1568	0.05961
8	2650	0.1007
6	4602	0.1749
4	8246	0.3135
2	14866	0.5652
0.5	23644	0.8989
0	26304	1.0

* Number of hours wave height will equal or exceed given value.

** 60 hrs / 26304 hrs in record = 0.00228

To obtain higher waves of spectrum:

$$H_{10} = 1.27 \, H_s$$

Eq. 7-1

$$H_1 = 1.67 \, H_s$$

Eq. 7-2

Note: Curves showing deepwater wave height statistics and transformed statistics are given on next page.
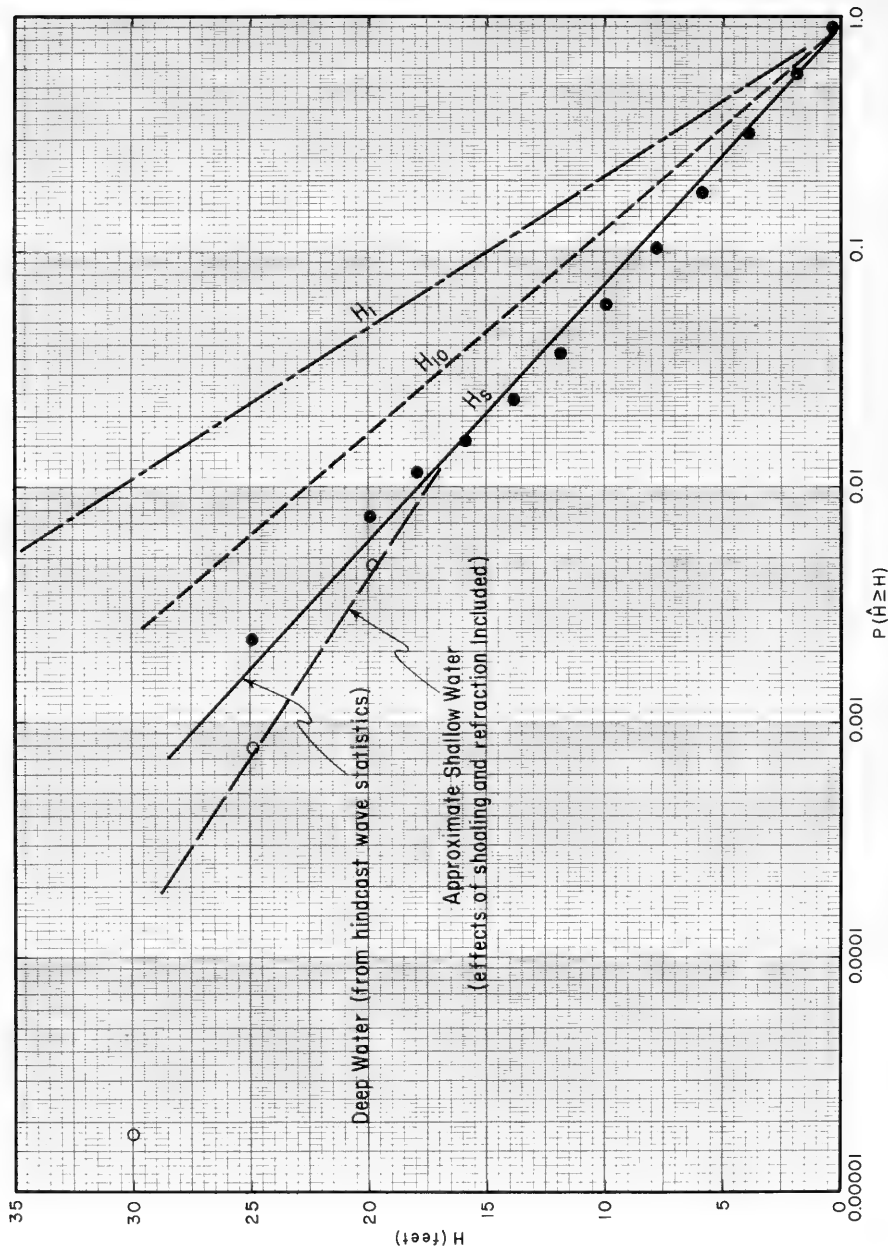
Figure 8-21. Frequency of Occurrence of Significant Wave Heights for Waves Generated in Ocean - Transformation by Refraction and Shoaling

8-52

Wave Conditions on Ocean Side of Island (cont.) | Sect. 3.73

Hurricane Waves

The waves associated with hurricane B of Reference 5 will be determined and routed across the continental shelf to the island site. | Ref. 5

Characteristics of Hurricane B

$$\Delta p = 2.4 \text{ in. of mercury}$$
$$R = 33.5 \text{ n.m.}$$
$$V_F = 25 \text{ knots}$$
$$U_{max} = 92.6 \text{ knots}$$
$$U_R = 0.865 \, U_{max} + 0.5 \, V_F = 92.6 \text{ knots} \qquad \text{Eq. 3-34}$$

Significant wave height at point of maximum winds in deep water.

$$H_0 = 16.5 \, e^{\frac{R\Delta P}{100}} \left[1 + \frac{0.208 \, \alpha \, V_F}{\sqrt{U_R}} \right] \qquad (\text{Assume } \alpha = 1.0) \qquad \text{Eq. 3-31}$$

$$H_0 = 16.5 \, e^{\frac{(33.5)(2.4)}{100}} \left[1 + \frac{0.208 \, (1.0)(25)}{\sqrt{92.6}} \right]$$

$$H_0 = 56.8 \text{ ft.}$$

Significant wave period at point of maximum winds.

$$T_S = 8.6 \, e^{\frac{R\Delta P}{200}} \left[1 + \frac{0.104 \, \alpha \, V_F}{\sqrt{U_R}} \right] \qquad \text{Eq. 3-32}$$

$$T_S = 8.6 \, e^{0.402} \left[1 + \frac{0.104 \, (1.0)(25)}{\sqrt{92.6}} \right]$$

$$T_S = 16.3 \text{ sec.}$$

Check by Equation 3-36,

$$T_S = 2.13 \sqrt{H_0} = 2.13 \sqrt{56.8} = 16.1 \text{ sec.} \qquad O.K. \qquad \text{Eq. 3-36}$$

Wave Conditions on Ocean Side of Island (cont.)

Hurricane Waves (cont.)

The relative distribution of wave heights within the hurricane can be obtained from Figure 3-34.

Calculation of Probable Maximum Wave

The time required for a length equal to the radius of maximum winds to pass a point if hurricane is moving with a forward speed equal to V_F.

$$t = \frac{R}{V_F} = \frac{33.5 \ n.m.}{25 \ knots} = 1.34 \ hrs \qquad \text{Eq. 3-37}$$

$$t = 1.34 \ hrs \times \frac{3600 \ sec.}{hr.} = 4824 \ sec.$$

The number of waves in 4824 sec.

$$N = \frac{t}{T_s} = \frac{4824 \ sec}{16.3 \ sec.} = 296 \ waves \qquad \text{Eq. 3-38}$$

From Equation 3-39 for $n=1$, the probable maximum wave is,

$$H_h = 0.707 \ H_o \sqrt{log_e \frac{N}{n}} \quad (Approximate) \qquad \text{Eq. 3-39}$$

$$H_{n=1} = 0.707 \ (56.8) \sqrt{log_e \ (296)}$$

$$H_{n=1} = 95.8 \ ft. \ (approximately)$$

Note: The above wave conditions are for deepwater conditions. Because of energy dissipation the wave heights will be lower at the island site. The hurricane will be routed across the continental shelf using the bottom profile given on next page (from Reference 5)
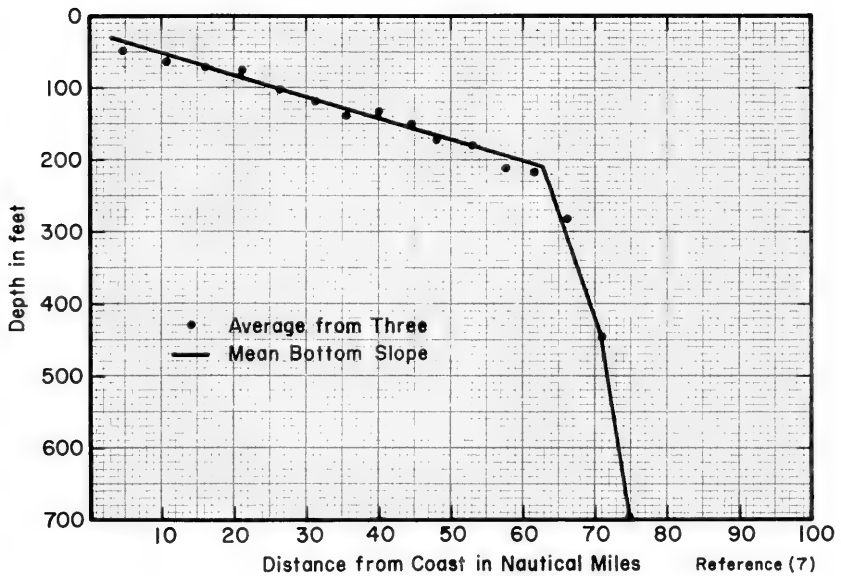
Figure 8-22.   Mean Bottom Profile from Deep Water to Mouth of
Delaware Bay

Wave Conditions on Ocean Side of Island (cont.)

Hurricane Waves (cont.)

Routing Hurricane Across Continental Shelf

Typical Calculations

Calculations for first row of table on page 8-61 following.

Column 1 :	Distance from coast in nautical miles	Fig. 8-22
Column 2 :	Depth below MLW at end of section.	Fig. 8-22

Column 3 : Depth at beginning of section to mean water surface (including astronomical tide and storm surge). The astronomical tide and storm surge are assumed to vary across the shelf as below.
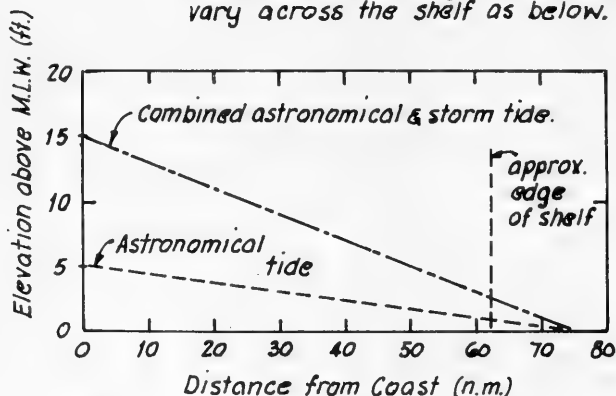
Note: These water surface elevations are _assumed_ to vary as shown for purposes of this example.

Column 4 : Depth at end of section to mean water surface.

Column 5 : Average depth in section = $\dfrac{d_1 + d_2}{2}$

Wave Conditions on Ocean Side of Island (cont.)

Hurricane Waves (cont.)

Column 6: Effective fetch, for first step

$$F_e = \left\{ \frac{H_o}{0.0555 \, U_R} \right\}^2 \quad \text{(Deep water)} \qquad Eq. \, 3\text{-}40$$

$$F_e = \left\{ \frac{56.8}{0.0555 \, (92.6)} \right\}^2 = 122 \ n.m.$$

For subsequent steps,

$$F_e = \left[\frac{H_o}{0.0555 \, (U_R)} \right]^2 + \Delta F \quad \begin{array}{l} \text{(always less} \\ \text{than or equal} \\ \text{to 122 n.m.)} \end{array} \qquad Eq. \, 3\text{-}40$$

Column 7: Deepwater wave height, given by

$$H_o = 0.0555 \, U_R \sqrt{F_e} \qquad Eq. \, 3\text{-}40$$

(Equation 3-40, rearranged)

$$H_o = 0.0555 \, (92.6) \sqrt{122} = 56.8 \ ft.$$

Column 8: Deepwater significant wave period,

$$T_o = 2.13 \sqrt{H_o} \qquad Eq. \, 3\text{-}36$$

$$T_o = 2.13 \sqrt{56.8} = 16.1 \ sec.$$

Column 9: From column 5 & column 8,

$$\frac{T_o^2}{\bar{d_T}} = \frac{(16.1)^2}{563} = 0.458 \ sec^2/ft.$$

Column 10: From Table 3-3, for $T_o^2/\bar{d_T} = 0.458$ Table 3-3
read $K_s = 0.981$

Column 11: Friction loss parameter,

$$A = \frac{f_f \, H_o \, K_s \, \Delta x}{(\bar{d_T})^2} \qquad Eq. \, 3\text{-}41$$

Wave Conditions on Ocean Side of Island (cont.)

Hurricane Waves (cont.)

where

f_f = friction factor = 0.01

Δx = reach length in ft.

$$5\,n.m. \times 6080\frac{ft.}{n.m.} = 30,400 \text{ ft.}$$

H_o from column 7

$\bar{d_T}$ from column 5

$$A = \frac{0.01\,(56.8)(0.981)(30,400)}{(563)^2} = 0.0534$$

Column 12: From Figure 3-35, for $A = 0.0534$ and $T_o^2/\bar{d_T} = 0.467$,

$$K_f = 1.0 \quad (by \ extrapolation)$$
(negligible energy dissipation)

Fig. 3-35

Column 13: Equivalent deepwater wave height

$$H_o' = K_f\,H_o$$

where K_f is from column 12.

$$H_o' = 1.0\,(56.8) = 56.8 \text{ ft.}$$

(Refraction coefficient, $K_R = 1.0$ has been assumed)

Column 14: Effective fetch for H_o', given by,

$$F_e' = \left\{ \frac{H_o'}{0.0555\,U_R} \right\}^2$$

Eq. 3-40

$$F_e' = \left\{ \frac{56.8}{0.0555\,(92.6)} \right\}^2 = 122 \text{ n.m.}$$

Design Problem Physical Environment

Wave Conditions on Ocean Side of Island (cont.)
Hurricane Waves (cont.)

Column 15: Significant period corresponding to H_o', from Equation 3-36,

$$T_o' = 2.13 \sqrt{H_o'}$$ Eq. 3-36

$$T_o' = 2.13 \sqrt{56.8} = 16.1 \text{ sec.}$$

Column 16: From columns 4 & 15,

$$\frac{(T_o')^2}{d_2} = \frac{(16.1)^2}{426} = 0.608 \text{ sec}^2/\text{ft.}$$

Column 17: From Table 3-3, with $(T_o')^2/d_2 = 0.608$,

$$K_{s2} = 0.956$$

Column 18: Significant wave height at end of reach (70 n.m. from coast)

$$H_s = K_{s2} H_o'$$

$$H_s = 0.956 (56.8) = 54.3 \text{ ft.}$$

Column 19: N = number of waves

$$N = \frac{4,824^*}{T_o'} = \frac{4824}{16.1} = 300 \text{ waves}$$ Eq. 3-38

Column 20: Probable maximum wave height, Equation 3-39 with $n=1$,

$$H_n = 0.707 \, H_s \sqrt{\log_e \frac{N}{n}}$$ Eq. 3-39

$$H_{n=1} = 0.707 (54.3) \sqrt{\log_e \frac{300}{1}} = 91.7 \text{ ft.}$$

(approximate)

---

* See page 8-54 of calculations.

Wave Conditions on Ocean Side of Island (cont.)
Hurricane Waves (cont.)

Column 21: Height of 10% wave (average height of the highest 10% of waves)

$$H_{10} = 1.27 \, H_s$$

Eq. 7-1

$$H_{10} = 1.27 \, (54.3) = 69.0 \text{ ft.}$$

Column 22: Height of 1% wave (average height of the highest 1% of waves)

$$H_1 = 1.67 \, H_s$$

Eq. 7-2

$$H_1 = 1.67 \, (54.3) = 90.7 \text{ ft.}$$

Note: Values given on next page were computed by slide rule and may differ in the last significant figure from calculations made by desk calculator.

Design Problem   _Physical Environment_

Wave Conditions on Ocean Side of Island (cont.)
Hurricane Routing Across Shelf

	(1) x n.m.	(2) d_x ft.	(3) d_l ft.	(4) d_2 ft.	(5) $\bar{d}_T$ ft.	(6) F_e n.m.	(7) H_o ft.	(8) T_o sec	(9) $T_o^2/\bar{d}_T$ sec²/ft	(10) K_s	(11) A
1	75	700	—	700	—	122	56.8	16.1	—	—	—
2	70	425	700	426	563	122	56.8	16.1	0.458	0.981	0.053
3	65	280	426	282	354	122	56.8	16.1	0.728	0.938	0.129
4	60	210	282	213	248	122	56.8	16.1	1.038	0.916	0.281
5	55	190	213	194	204	122	56.8	16.1	1.266	0.913	0.381
6	50	170	194	175	185	120	56.3	16.0	1.385	0.914	0.460
7	45	158	175	164	170	114	54.8	15.8	1.467	0.916	0.531
8	40	145	164	152	158	106	52.8	15.5	1.516	0.917	0.590
9	35	130	152	138	145	97	50.6	15.1	1.582	0.918	0.671
10	30	115	138	124	131	87	48.0	14.7	1.662	0.921	0.783
11	25	97	124	107	116	77	45.2	14.3	1.776	0.926	0.954
12	20	80	107	91	99	66	41.9	13.8	1.918	0.931	1.209
13	15	65	91	77	84	54	37.8	13.1	2.042	0.936	1.524
14	10	50	77	63	70	41	33.1	12.2	2.143	0.941	1.931
15	5	45	63	59	61	31	28.6	11.4	2.131	0.942	2.199
16	0	40	59	55	57	23	24.6	10.6	1.971	0.935	2.148

	(12) K_f	(13) H_o' ft.	(14) F_e' n.m.	(15) T_o' sec.	(16) $(T_o')^2/d_2$ sec²/ft.	(17) K_{s2}	(18) H_s ft.	(19) N	(20) $H_{n=1}$ ft.	(21) H_{10} ft.	(22) H_1 ft.
1	—	—	122	—	—	—	—	—	—	—	—
2	1.0	56.8	122	16.1	0.608	0.956	54.3	300	91.7	69.0	90.7
3	0.995	56.5	121	16.0	0.909	0.922	52.1	302	88.0	66.2	87.0
4	0.980	55.6	117	15.9	1.185	0.913	50.8	303	85.9	64.5	84.8
5	0.971	55.1	115	15.8	1.289	0.913	50.3	305	85.1	63.9	84.0
6	0.951	53.6	109	15.6	1.389	0.915	49.0	309	83.0	62.6	81.8
7	0.940	51.5	101	15.3	1.425	0.915	47.1	315	79.9	59.8	78.7
8	0.932	49.2	92	14.5	1.469	0.916	45.1	333	76.9	57.3	75.3
9	0.921	46.6	82	14.5	1.531	0.918	42.7	333	72.8	54.2	71.3
10	0.911	43.7	72	14.1	1.599	0.920	40.2	342	69.7	51.1	67.1
11	0.890	40.2	61	13.5	1.706	0.923	37.1	357	63.6	47.1	62.0
12	0.860	36.0	49	12.8	1.795	0.926	33.3	377	57.4	42.3	55.6
13	0.820	31.0	36	11.9	1.826	0.928	28.8	405	49.9	36.3	48.1
14	0.800	26.5	27	11.0	1.886	0.931	24.2	443	42.2	30.7	40.4
15	0.760	21.7	18	9.9	1.661	0.924	20.0	487	35.2	25.4	33.4
16	0.740	18.2	13	9.1	1.506	0.920	16.7	530	29.6	21.2	27.9

Wave Conditions on Ocean Side of Island (cont.)
Hurricane Waves (cont.)

Time Variation of Significant Wave Height
at Structure

Fig. 3-34

Distance of max. winds from coast r (n.m)	$\dfrac{r}{R}$ *	$\dfrac{H_s}{(H_s)_R}$ **	Time after landfall of max. winds $t = -\dfrac{r}{V_F} + 0.25$ **	H_s at site (ft.)
100	2.98	0.55	− 3.75	9.2
80	2.39	0.65	− 2.95	10.9
60	1.79	0.73	− 2.15	12.2
40	1.19	0.83	−1.35	13.9
20	0.60	0.95	− 0.55	15.9
0	0	1.00	+0.25	16.7
−20	−0.60	0.95	+ 1.05	15.9
−40	−1.19	0.83	+ 1.85	13.9
−60	−1.79	0.73	+ 2.65	12.2
−80	−2.39	0.65	+ 3.45	10.9
−100	−2.98	0.55	+ 4.25	9.2

* $R = 33.5$ n.m.

** Value of $(H_s)_R = 16.7$ ft

*** A time lag of 0.25 hr. has been assumed.

Note: Time variation of H_s only approximate.

Time after landfall of max. winds (hrs.)
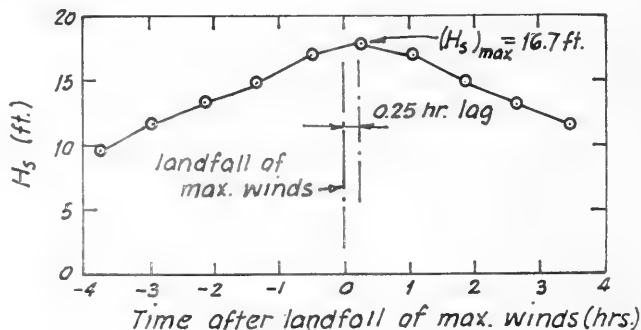
Design Problem _Preliminary Design_

Selection of Design Waves and Water Levels

The selection of design conditions is related to the economics of construction and annual maintenance costs to repair structure in the event of extreme wave action. These costs* are related to the probability of occurrence of extreme waves and high water levels. There will usually be some design wave height which will minimize the average annual cost (including amortization of first cost). This optimum design wave height will give the most economical design.

Design Wave Height
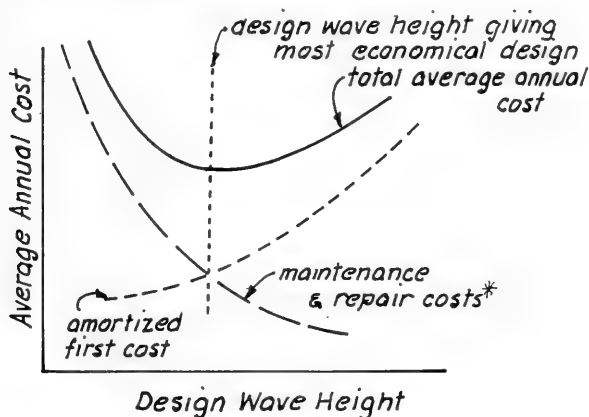
Intangible considerations such as the environmental consequences of a structural failure or the possibility of loss of life in the event of failure must also enter into the decision of selecting design conditions. These factors are related to the specific purpose of each structure.

Selected Design Conditions

The following design conditions are assumed for the illustrative purposes of this problem.

Water Levels (MLW datum)

1. Storm surge (less astronomical tide)

    Use   11.0 ft.

2. Astronomical tide (use water level exceeded 1% of time.)

    Use   5.0 ft.

3. Wave setup (assumed negligible since structure is in relatively deep water and not at beach)

Wave Conditions on Bay Side of Island

1. Use conditions with 100 yr recurrence interval.

    Use $H_s = 8.9$ ft.

    $T_s = 6.6$ sec.

Wave Conditions on Ocean Side of Island

1. Hurricane B waves

    $H_s = 16.7$ ft ; $T_s = 9.1$ sec.

2. From hindcast statistics (wave height exceeded 1% of time)

    $H_s = 17.5$ ft.

    Use $H_s = 18.0$ ft.

Design Problem _Preliminary Design_

Revetment Design – Ocean Side of Island

The ocean side of the island will be protected by a revetment using concrete armor units *

Type of Wave Action

The depth at the site required to initiate breaking of the 18 ft. design wave is:

For a slope in front of the structure

$$m = 0$$

$$H_b = 0.78 \, d_b$$

or $$d_b = \frac{H_b}{0.78} = \frac{18}{0.78} = 23.1 \text{ ft.}$$

Since the depth at the structure $(d_s \cong 40 \text{ ft})$ is greater than the computed breaking depth $(d_b = 23.1)$, the structure will be subjected to non-breaking waves.

Selection Between Alternative Designs

The choice of one cross section and/or armor unit type over another is primarily an economic decision requiring evaluation of the costs of various alternatives. A comparison of several alternatives follows:

Type of Armor Unit: Tribars vs. Tetrapods

Structure Slope: 1:1.5, 1:2, 1:2.5 and 1:3

Concrete Density: 150 lb/ft³, 160 lb/ft³ & 170 lb/ft³

---

* The use of concrete armor units will depend on the availability of suitable quarrystone and on the economics of using concrete as opposed to stone.

Design Problem Preliminary Design

Revetment Design (cont.)

Preliminary Cross Section
Modified from Figure 7-95
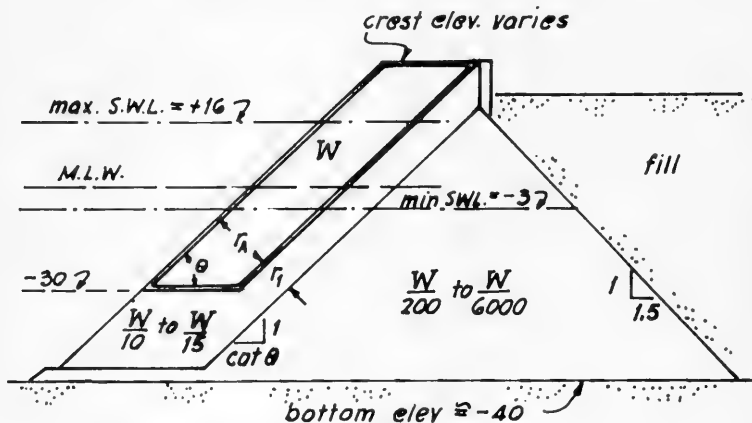
Crest Elevation

Established by maximum runup.

Runup estimate

$$H_s = 18 \ ft.$$
$$d = 56 \ ft.$$
$$T = ? \ (\text{use point on runup curve giving maximum runup})$$

$$\frac{d}{H_s} = \frac{56}{18} = 3.1 \quad \text{Use Figure 7-20}$$

$\cot \theta$	$(R/H_o')_{max}$	R ft.	Crest* elevation
1.5	1.05	18.9	use 36 ft.
2.0	1.10	19.8	use 38 ft.
2.5	1.05	18.9	use 36 ft.
3.0	1.00	18.0	use 34 ft.

* Waves over 18 ft. will result in some overtopping.

Revetment Design (cont.)

Armor Unit Size - Primary Cover Layer

Sect. 7.373

$$W = \frac{w_r H^3}{K_D (S_r - 1)^3 \cot\theta}$$

Eq. 7-105

H = design wave height = 18 ft.

w_r = unit weight of concrete
150 lb/ft³, 160 lb/ft³ and 170 lb/ft³

$\cot\theta$ = structure slope
1.5, 2.0, 2.5 and 3.0

$S_r = \frac{w_r}{w_w}$ = ratio of concrete unit weight to unit weight of water.

K_D = stability coefficient (depends on type of unit, type of wave action and structure slope)

The calculations that follow are for the structure trunk subjected to non-breaking wave action. Stability coefficients are obtained from Table 7-6.

Revetment Design (cont.)
Required Armor Unit Weights
Structure Trunk

Eq. 7-105

Type of Armor Unit	W_r (lb/ft³)	slope (cot θ)	K_D * (for n=2)	W (tons)	% damage for 1% wave **
Tribars	150	1.5	10.4	11.6	> 50%
		2.0		8.7	
		2.5		6.9	H_1 = 30 ft.
		3.0		5.8	
	160	1.5	10.4	8.9	> 50%
		2.0		6.6	
		2.5		5.3	H_1 = 30 ft.
		3.0		4.4	
	170	1.5	10.4	7.0	> 50%
		2.0		5.2	
		2.5		4.2	H_1 = 30 ft.
		3.0		3.5	
Tetrapods	150	1.5	8.3	14.5	> 50%
		2.0		10.9	
		2.5		8.7	H_1 = 30 ft.
		3.0		7.2	
	160	1.5	8.3	11.1	> 50%
		2.0		8.3	
		2.5		6.7	H_1 = 30 ft.
		3.0		5.6	
	170	1.5	8.3	8.8	> 50%
		2.0		6.6	
		2.5		5.3	H_1 = 30 ft.
		3.0		4.4	

* K_D from Table 7-6 for layer 2 units thick.

** Represents the damage under _sustained_ wave action of waves as high as the 1% wave, not the damage resulting from a few waves in the spectrum having a height equal to $H_1 = 1.67 H_s$

Revetment Design (cont.)

Volumes of Concrete - Primary Cover Layer

Structure Trunk

Type of Armor Unit	W_r (lb/ft³)	slope (cotθ)	Armor layer area/100 ft. of structure * (ft²)	W (tons)	Number of units required **	Volume of concrete/ 100 ft. of structure (ft³)
Tribars	150	1.5	11,860	11.6	380	57,700
		2.0	15,120	8.7	589	67,200
		2.5	17,720	6.9	797	71,800
		3.0	20,200	5.8	1022	77,700
	160	1.5	11,860	8.9	475	51,300
		2.0	15,120	6.6	741	59,300
		2.5	17,720	5.3	992	63,500
		3.0	20,200	4.4	1295	68,700
	170	1.5	11,860	7.0	569	46,100
		2.0	15,120	5.2	892	53,500
		2.5	17,720	4.2	1205	57,800
		3.0	20,200	3.5	1548	61,900
Tetrapods	150	1.5	11,860	14.5	368	70,700
		2.0	15,120	10.9	559	81,100
		2.5	17,720	8.7	780	89,700
		3.0	20,200	7.2	1010	97,000
	160	1.5	11,860	11.1	463	64,400
		2.0	15,120	8.3	711	73,900
		2.5	17,720	6.7	957	80,400
		3.0	20,200	5.6	1232	86,200
	170	1.5	11,860	8.8	557	57,400
		2.0	15,120	6.6	862	66,400
		2.5	17,720	5.3	1170	72,500
		3.0	20,200	4.4	1515	78,800

*   Area = $(30 + crest\ elev.)(100)/\sin θ$ where crest elevation is from runup analysis on page 8-66.

**   Number of units and concrete volumes determined from figures on next two pages. These figures were derived from Figures 7-91 and 7-89.
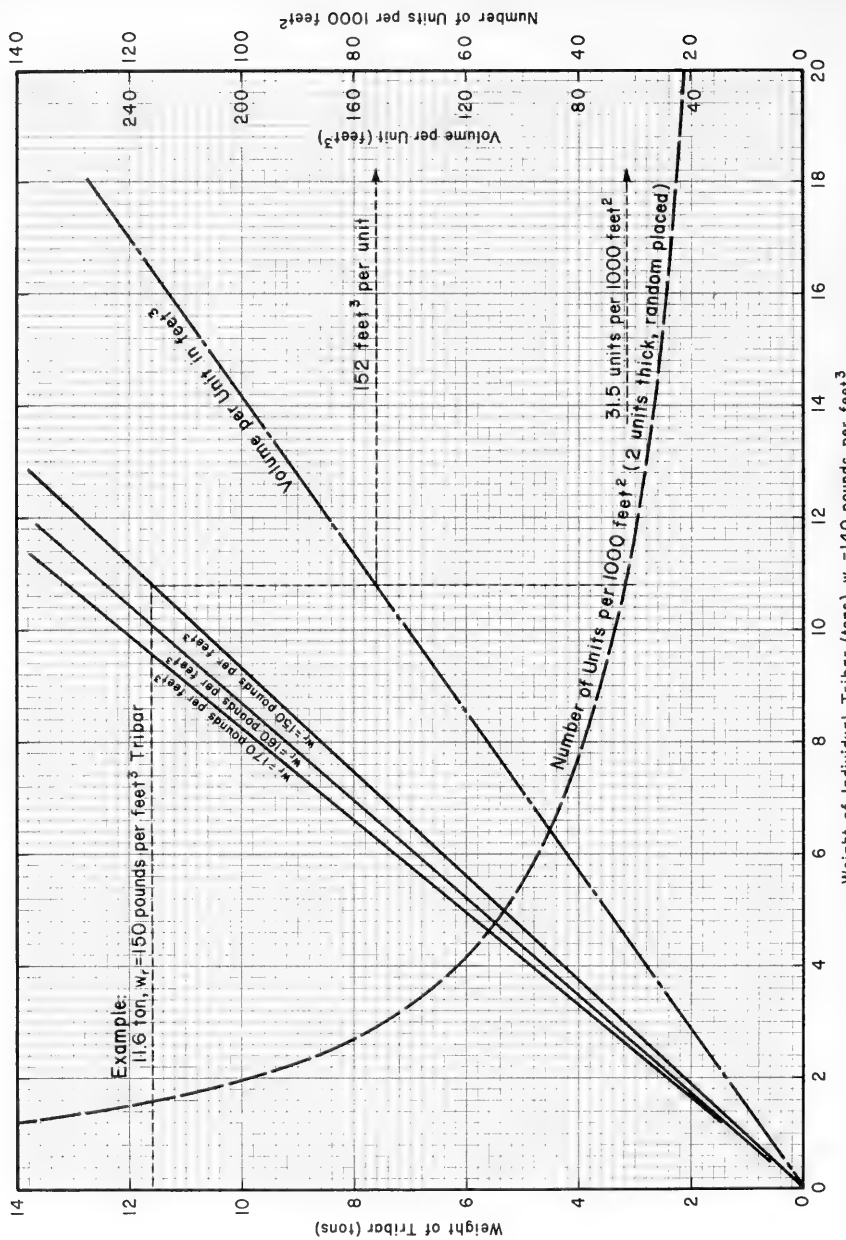
Figure 8-23. Engineering Data — Tribars

8-70
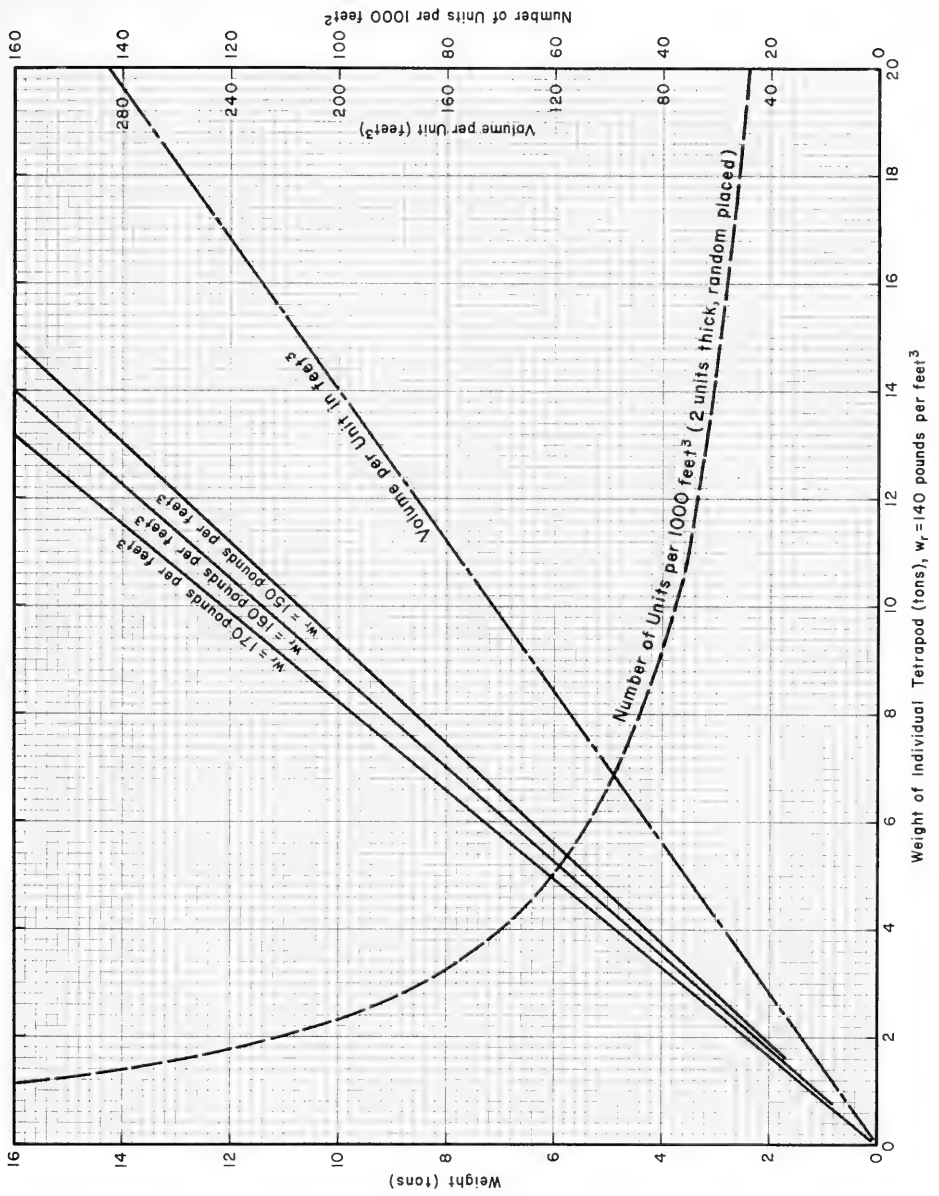
Figure 8-24. Engineering Data — Tetrapods

8-71
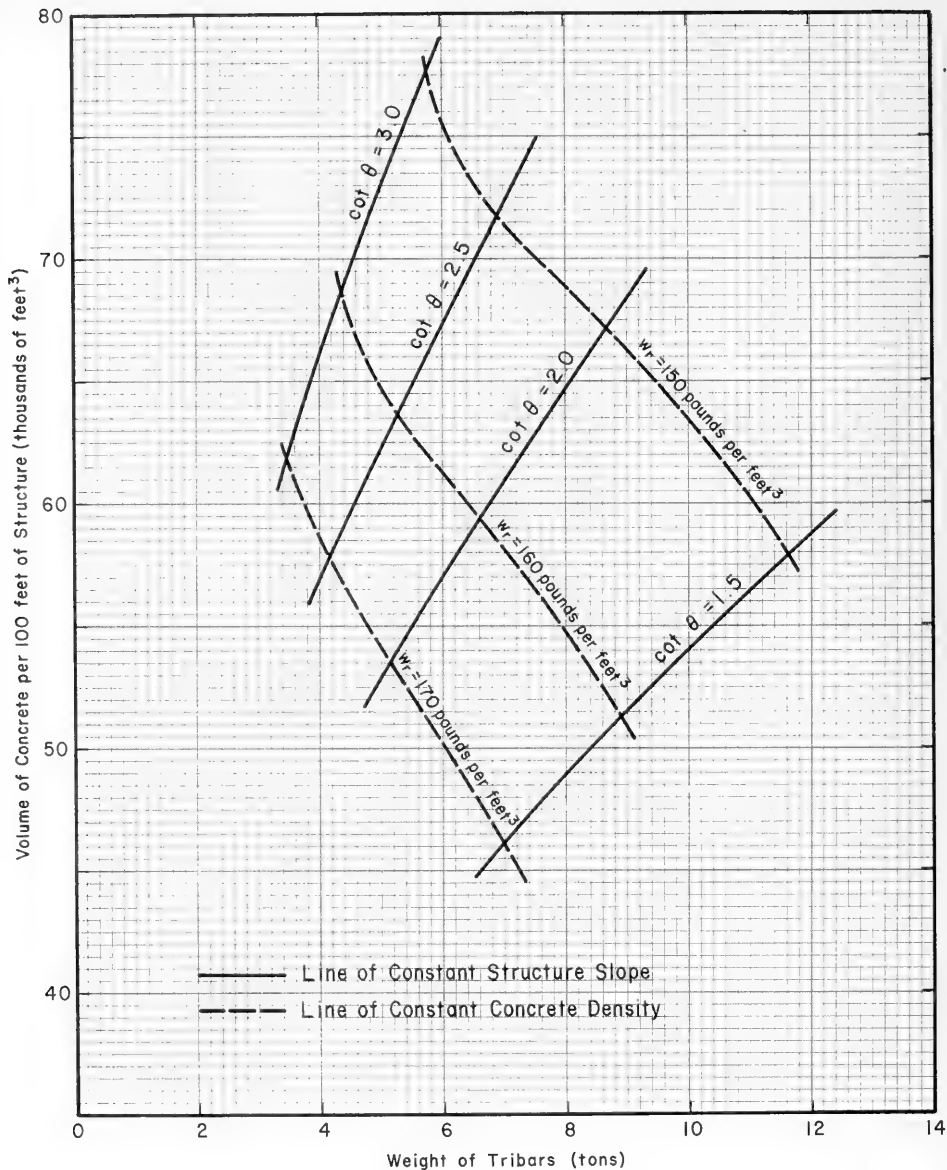
Figure 8-25. Volume of Concrete Required per 100 feet of Structure as a Function of Tribar Weight, Concrete Unit Weight and Structure Slope

8-72
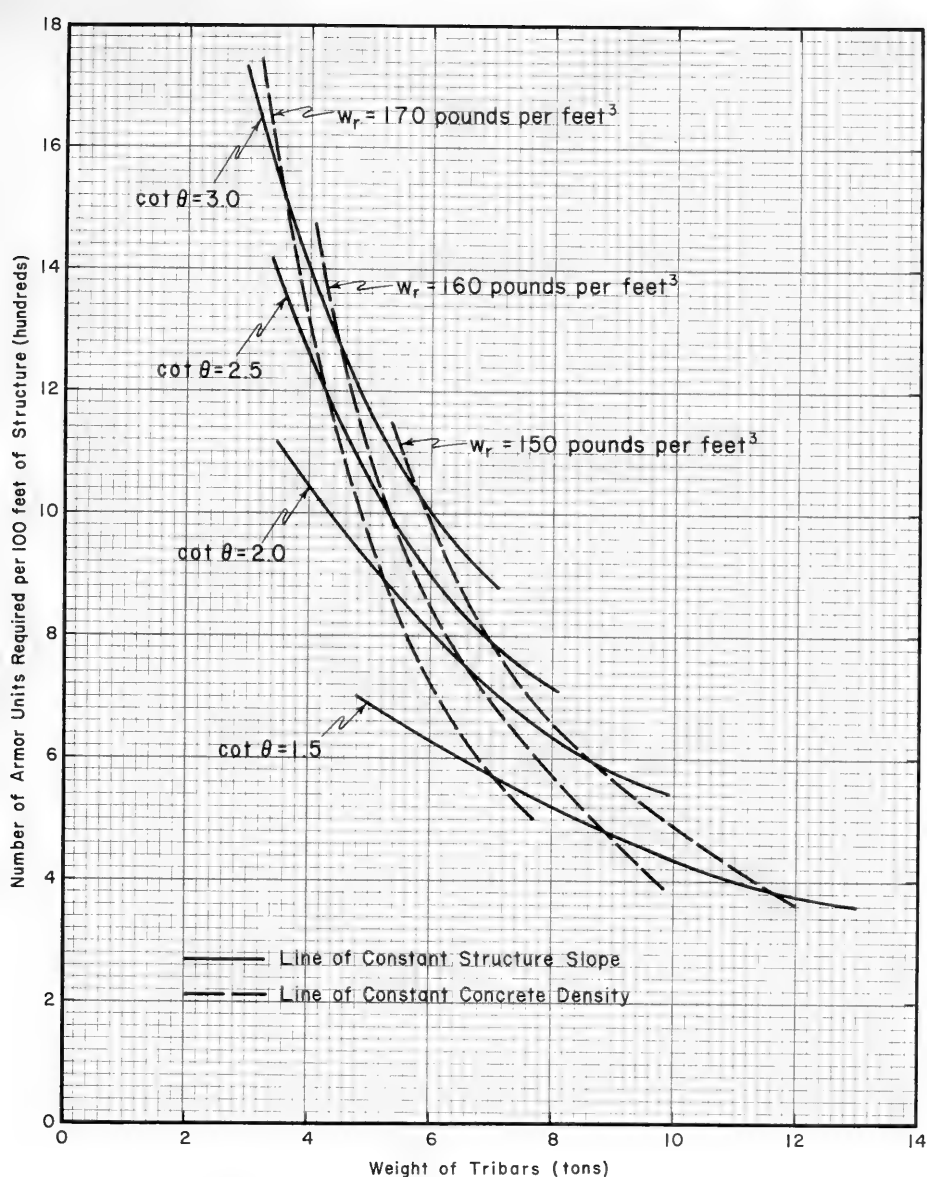
Figure 8-26. Number of Tribars Required per 100 feet of Structure as a Function of Tribar Weight, Concrete Unit Weight and Structure Slope
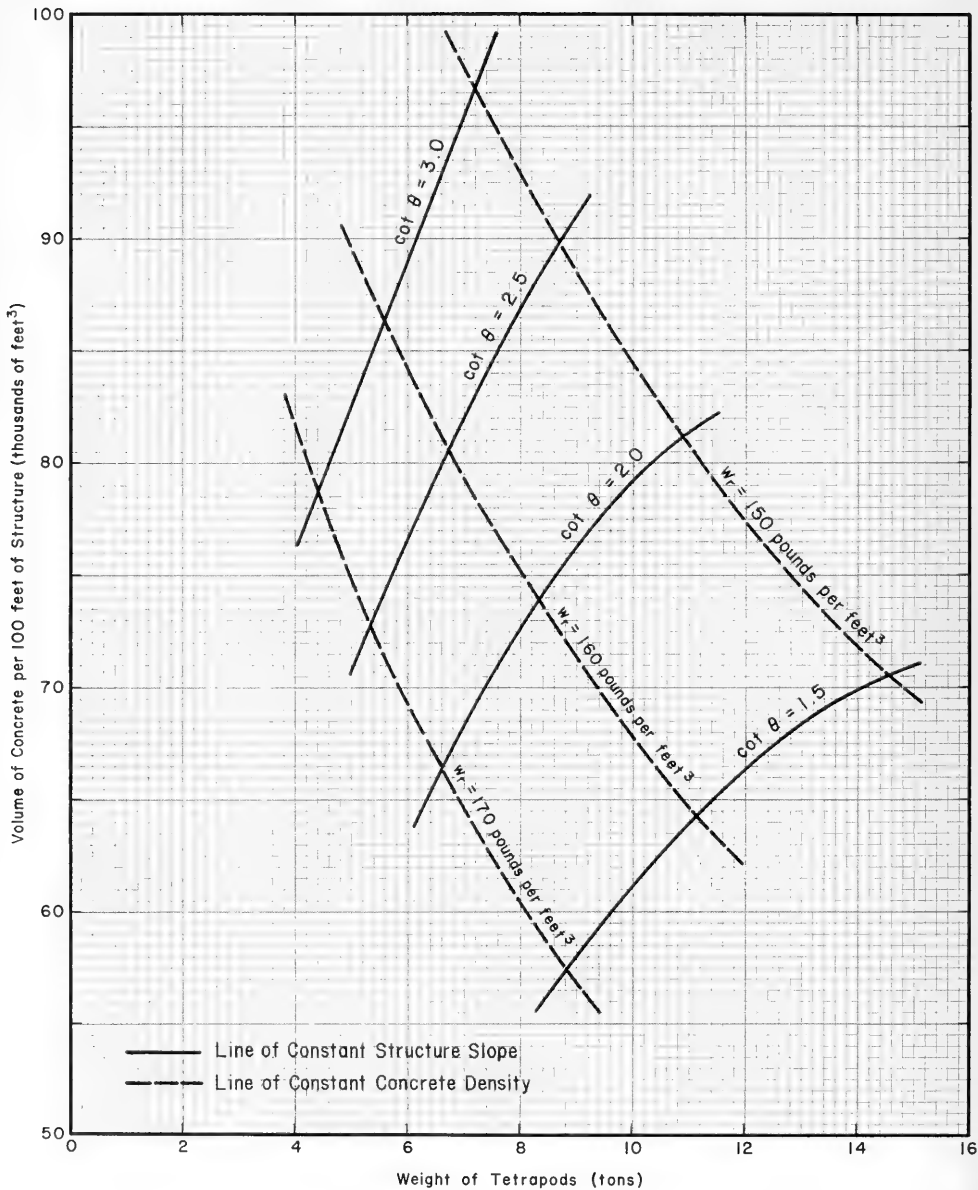
Figure 8-27. Volume of Concrete Required per 100 feet of Structure as a Function of Tetrapod Weight, Concrete Unit Weight and Structure Slope

Figure 8-28. Number of Tetrapods Required per 100 feet of Structure as a Function of Tetrapod Weight, Concrete Unit Weight and Structure Slope

Revetment Design (cont.)

Thickness of Armor Layer & First Underlayer

$$r = n k_\Delta \left(\frac{W}{w_r}\right)^{\frac{1}{3}}$$

Eq. 7-108

r = layer thickness in ft.

n = number of stones or armor units comprising the layer (either armor layer or first underlayer)

W = weight of individual stones making up the layer in pounds.

w_r = unit weight of stone material (concrete or quarrystone)

Number of Stones Required

$$N_r = A n k_\Delta \left(1 - \frac{P}{100}\right)\left(\frac{w_r}{W}\right)^{\frac{2}{3}}$$

Eq. 7-109

N_r = number of armor units or stones.

A = area in ft^2

P = porosity in percent

Thickness of Armor Layer (n=2)

Type of Armor Unit	W (tons)	$w_r = 150\ lbs/ft^3$	$w_r = 160\ lbs/ft^3$	$w_r = 170\ lbs/ft^3$
Tribars	12	r_A = 11.07 ft.	r_A = 10.84 ft.	r_A = 10.62 ft.
*k_Δ = 1.02	10	10.42	10.20	10.00
P = 54%	8	9.67	9.47	9.28
	6	8.79	8.60	8.43
	4	7.68	7.52	7.37
	2	6.09	5.96	5.85

Table continued on next page

* k_Δ & P from Table 7-10

8-76

Revetment Design (cont.)

Thickness of Armor Layer (n=2) (cont.)

Type of Armor Unit	W (tons)	$w_r =$ 150 lbs/ft³	$w_r =$ 160 lbs/ft³	$w_r =$ 170 lbs/ft³
Tetrapods	16	r_A= 12.43 ft.	r_A= 12.16 ft.	r_A= 11.92 ft.
*k_Δ = 1.04	14	11.89	11.63	11.40
	12	11.29	11.05	10.83
P= 50%	10	10.63	10.40	10.19
	8	9.86	9.65	9.46
	6	8.96	8.77	8.60
	4	7.83	7.66	7.51

Thickness of First Underlayer

Quarrystone

$k_\Delta = 1.15$ (rough quarrystone)

$P = 37\%$

$w_r = 165$ lbs/ft.³

$n = 2$

Weight of Armor Unit W (tons)	Weight of underlayer stone W/10 (tons)	Thickness of underlayer r_1 (ft) **	Number of stones/1000 ft² of underlayer ***	Weight of rock/1000 ft² of underlayer
16	1.6	6.18	201	322
14	1.4	5.91	219	307
12	1.2	5.61	243	292
10	1.0	5.28	275	275
8	0.8	4.90	319	255
6	0.6	4.46	386	232
4	0.4	3.89	506	202
2	0.2	3.09	803	161

* k_Δ & P from Table 7-10

** From Equation 7-108

*** From Equation 7-109 with A = 1000 ft²

	Page no :	**78** of **133**
	Calculated by :	*J. R. W.*
	Checked by :	*R. F. J*
	Date :	*16 Mar. 73*

Design Problem   Preliminary Design

Revetment Design (cont.)

Equation for Volume of First Underlayer

$$V_1 = \left\{ \frac{E+30}{2 \sin\theta} + \frac{E+30 - r_1/\cos\theta}{2 \sin\theta} \right\} r_1 + 10 \left\{ \frac{r_1 + r_A}{\sin\theta} \right\}$$

Equation derived from preliminary geometry of cross-section on page 8-66.

E = crest elevation (ft. above MLW)

r_A = thickness of armor layer (ft.)

r_1 = thickness of first underlayer (ft.)

V_1 = volume of first underlayer per ft. of structure (ft^3)

Equation for Volume of Core

$$V_c = \frac{1}{2} \left\{ 40 + E - \frac{r_1}{\cos\theta} \right\}^2 (1.5 + \cot\theta)$$

Equation derived from preliminary geometry of cross-section on page 8-66.

Design Problem _Preliminary Design_

Revetment Design (cont.)

Volume of First Underlayer - Tribars

Volume per 100 ft. of structure
(thousands of ft^3)

Tribar size (tons)	w_r (lbs/ft^3)	$\cot \theta$			
		1.5	2.0	2.5	3.0
12	150	93.2	118.2	139.7	161.0
10		87.9	111.4	131.8	151.9
8		81.8	103.6	122.6	141.2
6		74.6	94.6	111.8	128.8
4		65.4	82.8	97.9	112.8
2		52.2	66.0	78.1	90.0
12	160	92.8	117.6	139.1	160.3
10		87.5	110.9	131.2	151.2
8		81.4	103.2	122.0	140.6
6		74.3	94.1	111.3	128.2
4		65.1	82.4	97.4	112.3
2		51.9	65.8	77.7	89.6
12	170	92.4	117.2	138.5	159.6
10		87.2	110.5	130.6	150.5
8		81.1	102.8	121.5	140.0
6		74.0	93.8	110.8	127.7
4		64.8	82.1	97.0	111.8
2		51.7	65.5	77.4	89.2
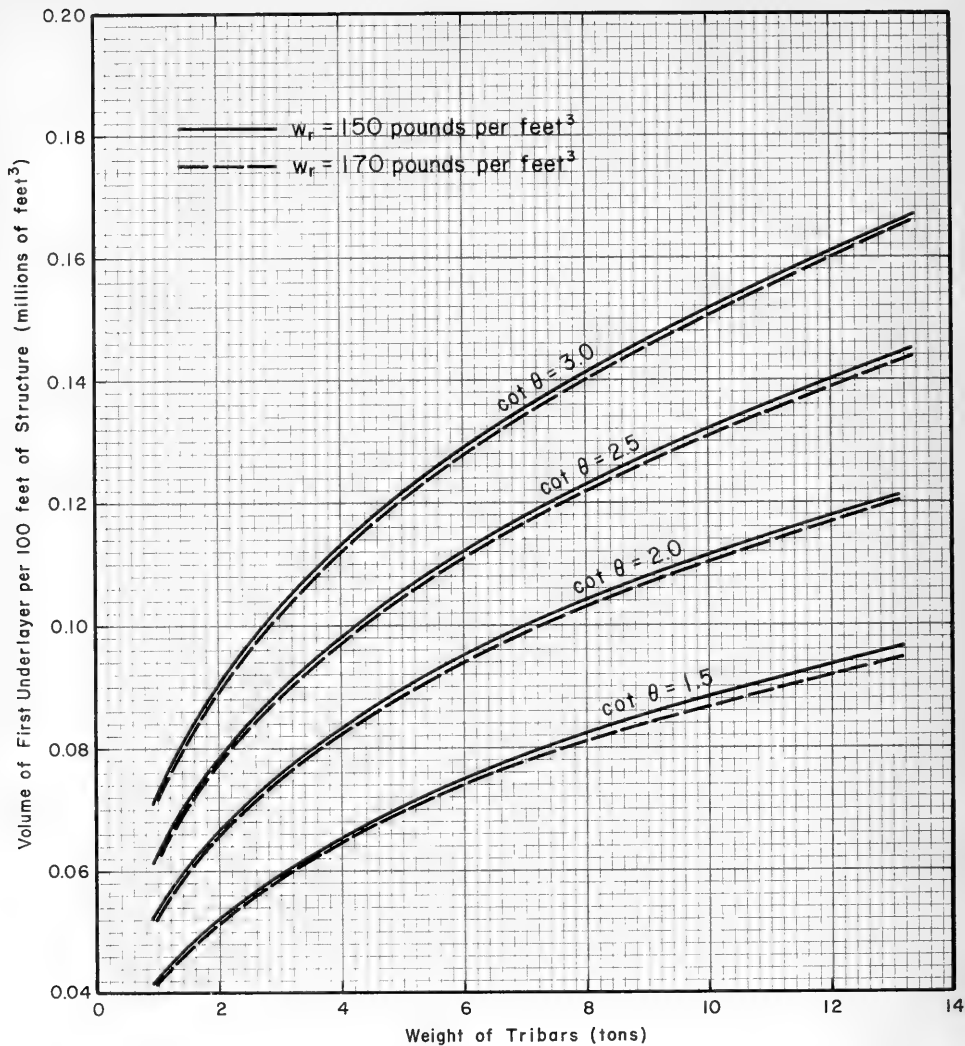
Figure 8-29. Volume of First Underlayer per 100 feet of Structure as a Function of Tribar Weight, Concrete Unit Weight and Structure Slope
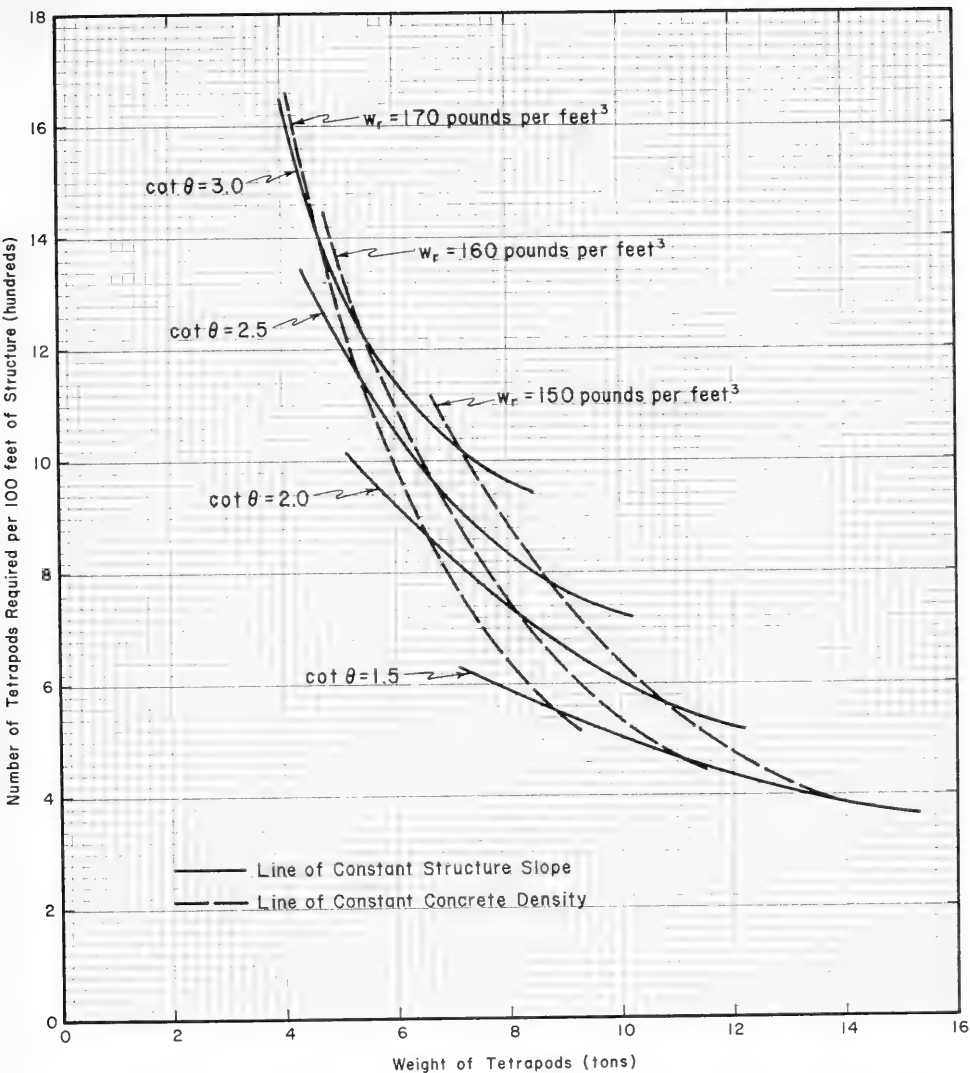
Revetment Design (cont.)

Volume of First Underlayer - Tetrapods

Volume per 100 ft. of structure
(thousands of ft³)

Tetrapod size (tons)	Wr (lbs/ft³)	cot θ			
		1.5	2.0	2.5	3.0
16	150	102.7	130.3	154.1	181.1
14		98.4	124.8	147.6	173.4
12		93.6	118.7	140.3	164.9
10		88.3	111.9	132.3	155.5
8		82.1	104.1	123.1	144.6
6		74.9	94.9	112.3	131.9
4		65.6	83.1	98.3	115.5
16	160	102.2	129.7	153.3	180.2
14		97.9	124.2	146.9	172.6
12		93.2	118.1	139.7	164.2
10		87.9	111.4	131.7	154.8
8		81.8	103.6	122.5	144.0
6		74.6	94.5	111.8	131.3
4		65.3	82.7	97.8	114.9
16	170	101.8	129.1	152.7	179.5
14		97.5	123.7	146.3	171.8
12		92.8	117.6	139.1	163.5
10		87.5	110.9	131.2	154.1
8		81.4	103.2	122.0	143.4
6		74.3	94.1	111.3	130.8
4		65.1	82.4	97.4	114.5
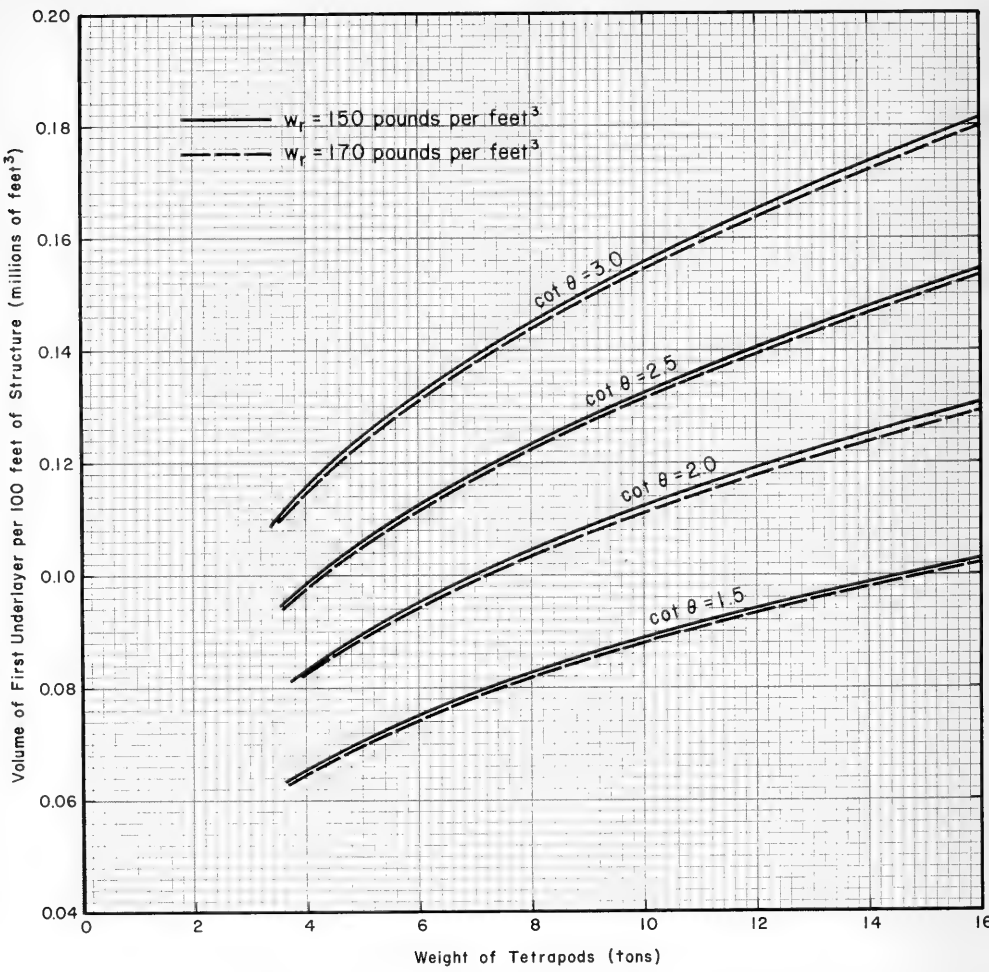
Figure 8-30. Volume of First Underlayer per 100 feet of Structure as a Function of Tetrapod Weight, Concrete Unit Weight and Structure Slope

Design Problem   Preliminary Design

Revetment Design (cont.)

Volume of Core - Tribars & Tetrapods

Volume per 100 ft. of structure
(thousands of ft^3)

Weight of Tribar or Tetrapod	$\cot \theta$			
	1.5	2.0	2.5	3.0
16	701.2	874.5	956.2	1024.7
14	707.9	882.0	964.2	1033.4
12	715.3	890.3	973.2	1043.1
10	723.4	899.6	983.2	1053.7
8	733.1	910.3	994.7	1066.1
6	744.3	922.7	1008.1	1080.5
4	758.8	939.0	1025.6	1099.3
2	779.5	962.1	1050.4	1126.0

Cost Analysis

The following cost data will be assumed for the illustrative purposes of this problem. Actual costs for a particular project would have to be based on the prevailing costs in the project area. Costs will vary with location, time and the availability of suitable materials.

Unit Costs of Concrete

W_r (lbs/ft³)	Cost per yd³ $	Cost per ft³ $
150	$ 40 00	1 48
160	42 00	1 56
170	55 00	2 04
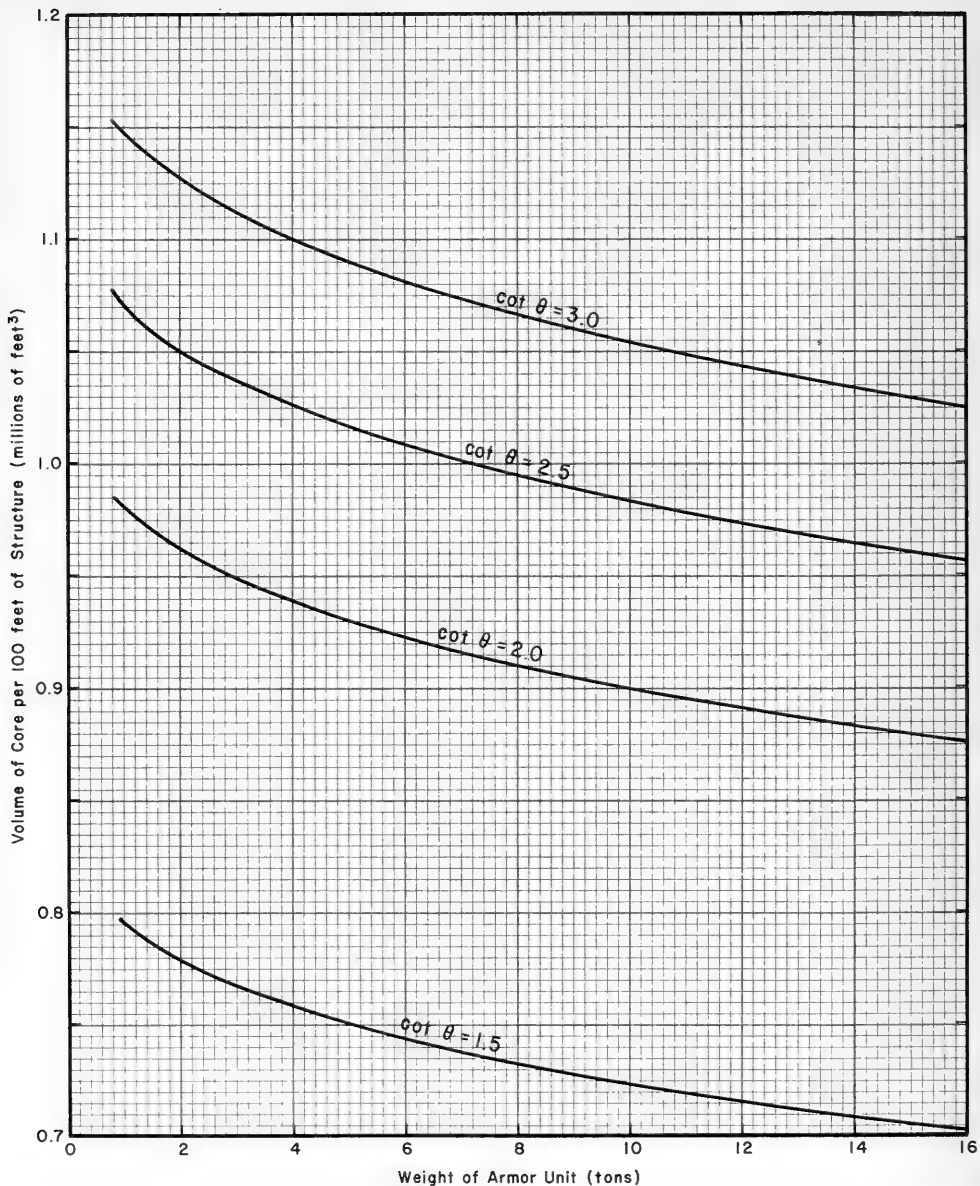
Figure 8-31. Volume of Core per 100 feet of Structure as a Function of Armor Unit Weight and Structure Slope

8-84

<u>Revetment Design (cont.)</u>

<u>Cost Analysis (cont.)</u>

<u>Cost of Forming, Handling and Placing</u>
<u>Tribars and Tetrapods</u>
(cost per unit)

Weight of Armor Unit (tons)	Cost/ton $\cot\theta = 1.5$ & 2.0	Cost/unit $\cot\theta = 1.5$ & 2.0	Cost/ton $\cot\theta = 2.5$ & 3.0	Cost/unit $\cot\theta = 2.5$ & 3.0
16	$ 19 $\frac{38}{}$	$ 310 $\frac{00}{}$	$ 21 $\frac{88}{}$	$ 350 $\frac{00}{}$
14	20 $\frac{50}{}$	287 $\frac{00}{}$	23 $\frac{21}{}$	325 $\frac{00}{}$
12	22 $\frac{08}{}$	265 $\frac{00}{}$	24 $\frac{67}{}$	296 $\frac{00}{}$
10	23 $\frac{00}{}$	230 $\frac{00}{}$	26 $\frac{00}{}$	260 $\frac{00}{}$
8	23 $\frac{12}{}$	185 $\frac{00}{}$	26 $\frac{88}{}$	215 $\frac{00}{}$
6	22 $\frac{50}{}$	135 $\frac{00}{}$	26 $\frac{67}{}$	160 $\frac{00}{}$
4	25 $\frac{00}{}$	100 $\frac{00}{}$	27 $\frac{50}{}$	110 $\frac{00}{}$
2	39 $\frac{00}{}$	78 $\frac{00}{}$	42 $\frac{50}{}$	85 $\frac{00}{}$

<u>Rock Costs</u>   In place, $w_r = 165 \, lbs/ft^3$

Weight (tons)	Cost ($/ton)
1.0 to 1.5	$ 12 $\frac{50}{}$ /ton
0.5 to 1.0	10 $\frac{50}{}$
up to 0.5	10 $\frac{00}{}$
quarry * run	9 $\frac{00}{}$

* Core material
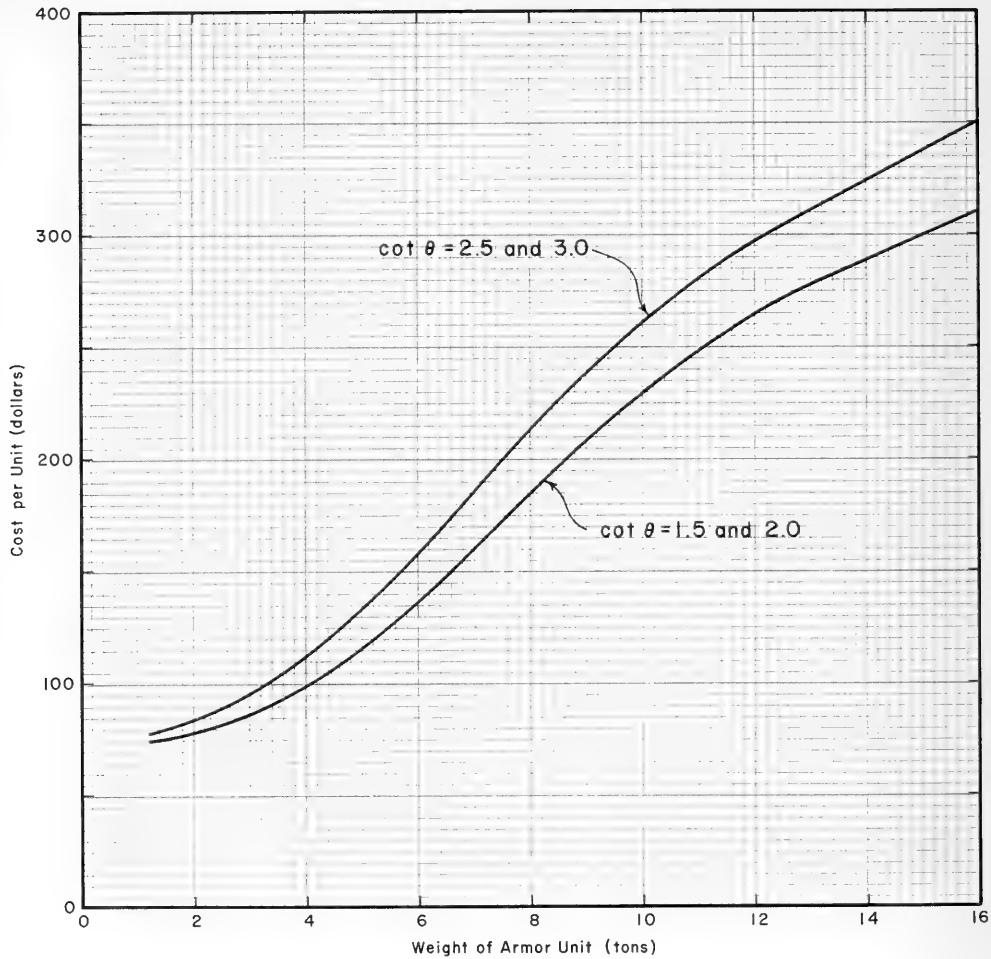
Figure 8-32. Costs of Casting, Handling and Placing Concrete Armor Units as a Function of Armor Unit Weight and Structure Slope

<u>Design Problem</u> <u>Preliminary Design</u>

<u>Revetment Design (cont.)</u>

<u>Total Cost per 100 ft. of Structure - Tribars</u>

| Weight of Armor Unit W (tons)	cot θ	Concrete cost, per 100' of structure *	Handling costs per 100' of structure *	First under-layer cost *	Core cost *	Total cost *
11.6	1.5	85.4	97.7	60.4	334.9	578.4
8.7	2.0 $W_r = 150$	99.5	118.4	58.4	423.8	700.1
6.9	2.5 lbs/ft^3	106.2	145.9	63.9	468.7	784.7
5.8	3.0	115.0	157.4	69.9	506.6	848.9
8.9	1.5	80.0	97.4	46.1	340.5	564.5
6.6	2.0 $W_r = 160$	92.4	111.2	52.7	429.4	685.7
5.3	2.5 lbs/ft^3	99.1	138.9	58.4	474.3	770.7
4.4	3.0	107.1	155.4	60.3	512.2	835.0
7.0	1.5	94.1	91.0	42.6	344.8	572.5
5.2	2.0 $W_r = 170$	109.2	107.0	48.8	434.1	699.1
4.2	2.5 lbs/ft^3	118.0	139.8	51.5	479.5	788.8
3.5	3.0	126.3	161.0	55.6	517.4	860.3

* All costs in thousands of dollars per 100 ft. of structure.
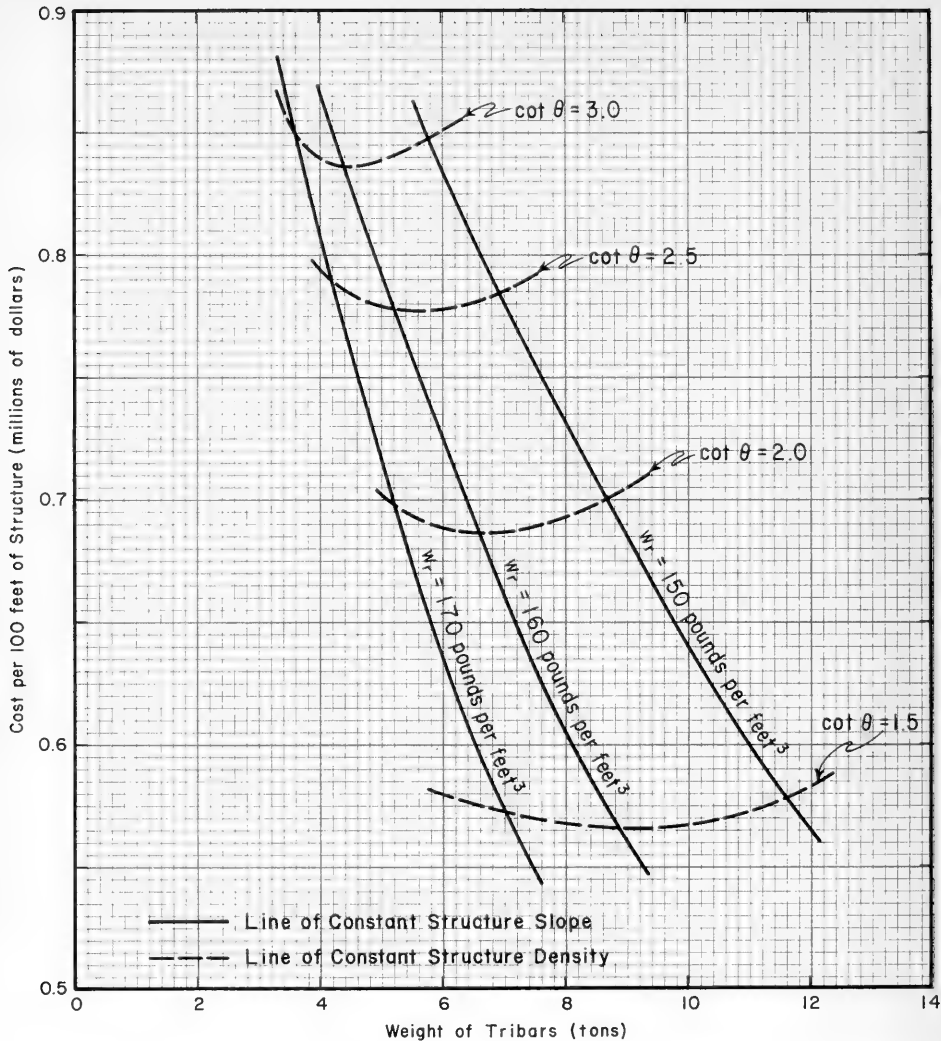
Figure 8-33. Total Cost of 100 feet of Structure as a Function of Tribar Weight, Concrete Unit Weight and Structure Slope

Design Problem   Preliminary Design

Revetment Design (cont.)

Total Cost per 100 ft. of Structure - Tetrapods

Weight of Armor Unit W (tons)	cot θ	Concrete cost per 100' of structure *	Handling costs per 100' of structure ✶	First under-layer cost ✶	Core cost ✶	Total cost ✶
14.5	1.5	104.6	107.8	64.8	330.7	607.9
10.9	2.0 $W = 150$	120.0	137.5	74.9	419.1	751.5
8.7	2.5 lbs/ft^3	132.8	180.2	69.0	463.1	845.1
7.2	3.0	143.5	193.9	76.4	478.1	891.9
11.1	1.5	100.4	115.8	59.4	335.9	611.5
8.3	2.0 $W = 160$	115.4	137.2	57.3	424.7	734.6
6.7	2.5 lbs/ft^3	126.4	170.3	63.3	469.2	828.2
5.6	3.0	134.5	182.3	70.1	507.5	894.4
8.8	1.5	117.0	113.6	45.8	340.5	616.9
6.6	2.0 $W = 170$	135.4	129.3	52.9	429.4	747.0
5.3	2.5 lbs/ft^3	148.0	165.0	58.4	474.3	845.7
4.4	3.0	160.7	181.8	61.3	512.2	916.0

* All costs in thousands of dollars per 100 ft. of structure.

Note: Total cost given here does not include royalty costs for using tetrapods.
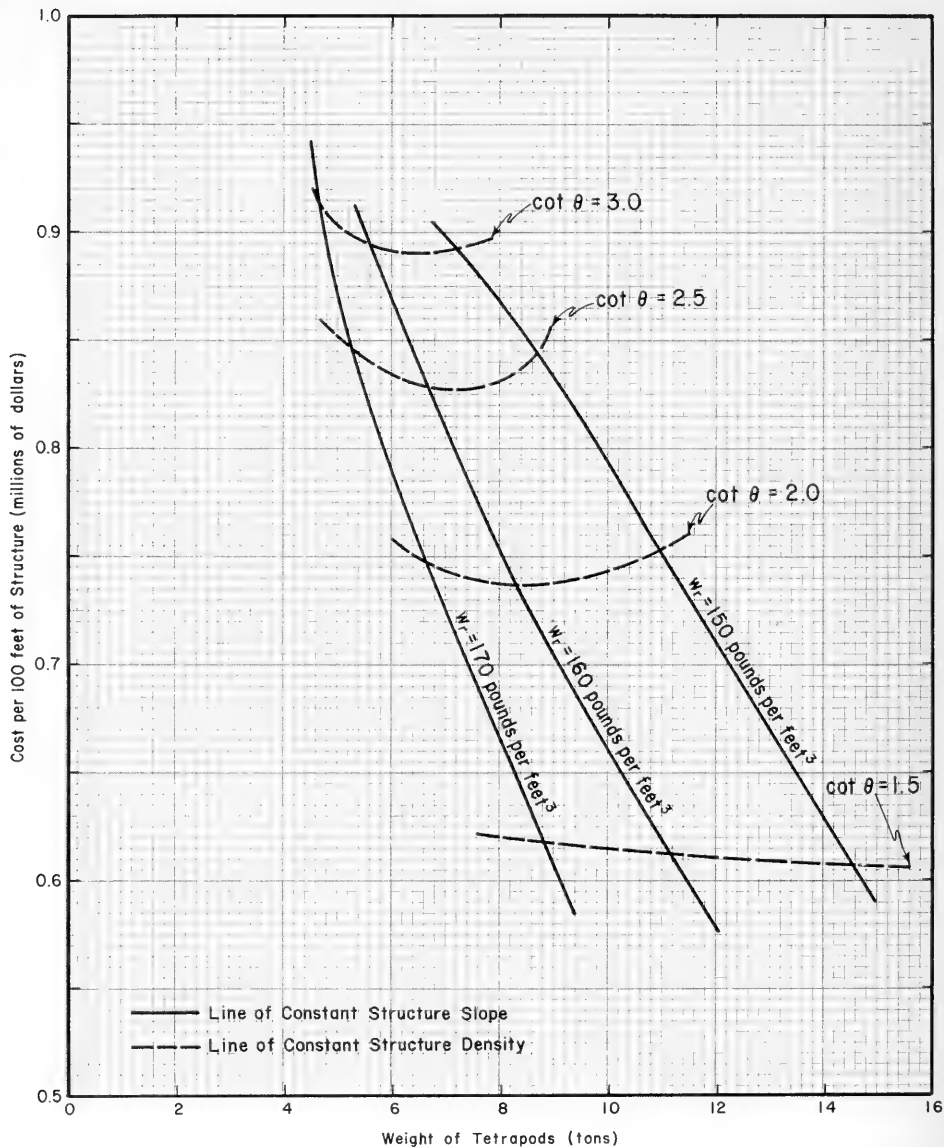
Figure 8-34. Total Cost of 100 feet of Structure as a Function of Tetrapod Weight, Concrete Unit Weight and Structure Slope

Design Problem *Preliminary Design*

Revetment Design (cont.)

### Selection of Armor Unit, Concrete Density & Structure Slope

The preceding analysis considered the *first cost* of the structure. To complete the analysis, average annual maintenance and repair costs need to be established for each alternative and for a range of design wave heights. Maintenance and repair costs may modify the conditions established here as the most economical based on first cost.

Selection Based on First Cost (Construction Cost)

1. Type of Unit: Tribars
2. Weight of Unit: 9.1 tons ±
3. Structure Slope: $\cot \theta = 1.5$
4. Unit Weight of Concrete: 158 lb/ft^3
5. Cost per 100 ft. of structure: $^\$ 566,000$

Stability Check

$$W = \frac{w_r H^3}{K_D (S_r - 1)^3 \cot \theta}$$

$K_D = 10.4$

$w_r = 158 \ lb/ft^3$

$\cot \theta = 1.5$

$S_r = \dfrac{w_r}{64 \ lbs/ft^3} = 2.47$

$H = 18 \ ft.$

$$W = \frac{(158)(18)^3}{(10.4)(1.47)^3(1.5)} = 18,600 \ lb \ (9.3 \ tons)$$

Revetment Design (cont.)

Selection Based on First Cost (cont.)

6. Volume of Concrete/100′:   51,800 ft³

7. Number of Armor Units/100′:   470

8. Thickness of Armor Layer :   9.91 ft.

9. Volume of First Underlayer/100′:   85,000 ft³

10. Thickness of First Underlayer: 4.60 ft.

11. Weight of Underlayer Stone :   0.91 to 0.61 ton

12. Volume of Core/100′:   727,000 ft³

13. Weight of Core Stone: 0.0455 to 0.00152 ton
                         91 to 3 lbs

Diffraction Around Breakwater

Sect. 2.4

For purposes of this problem, establish the required breakwater length so that the maximum wave height in the harbor is 3 ft. when the incident wave height is 14.9 ft (1% wave for $H_s = 8.9$ ft) and the period is $T = 6.6$ sec. Assume normal incidence, waves generated in Delaware Bay.
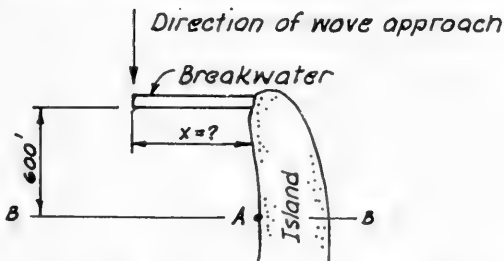
Diffracted wave height at A is to be less than 3 ft for an incident wave with

$$H_1 = 14.9 \text{ ft.}$$

$$T = 6.6 \text{ sec.}$$

$$L_0 = \frac{gT^2}{2\pi} = \frac{32.2 \,(6.6)^2}{2\,(3.1416)} = 223.2 \text{ ft.}$$

Eq. 2-8

Depth at breakwater: $d = 56$ ft.
Depth in basin: $d = 106$ ft.

$$\frac{d}{L_0} = \frac{106}{223.2} = 0.475$$

From Appendix C, Table C-1,

Appendix C Table C-1

$$\frac{d}{L} = 0.477 \qquad \therefore L \approx L_0 = 223 \text{ ft.}$$

Diffraction Analysis (cont.)

Change in wave height as wave moves into deeper water around breakwater.

Wave height $(d = 56 ft.) = H_1 = 14.9 ft.$

$$\frac{d}{L_0} = \frac{56}{223} = 0.251$$

From Appendix C, Table C-1, with $\frac{d}{L_0} = 0.251$ Appendix C
    Table C-1

$$\frac{H}{H_0'} = 0.9327$$

$$H_0' = \frac{14.9}{0.9327} = 16.0 \ ft.$$

From Appendix C, Table C-1, with $\frac{d}{L_0} = \frac{106}{223} = 0.475$ Appendix C
    Table C-1

$$\frac{H}{H_0'} = 0.9878$$

$$H_{(d = 106 ft)} = 0.9878 (16.0) = 15.8 \ ft.$$

This is the change in wave height caused only by shoaling effects as the wave moves from a depth, $d = 56$ ft. to a depth, $d = 106$ ft.

Distance of point A from breakwater axis in wave length units. $L \sim L_0 \sim 223$ ft.

$$y = \frac{600}{223} = 2.7 \ wave \ lengths$$

Required diffraction coefficient to reduce wave height to 3 ft.

$$K' = \frac{3}{15.8} = 0.190$$

This assumes no reflection of waves in harbor. If perfect reflection occurs, required $K' = 0.190/2 = 0.095$

8-94

Diffraction Analysis (cont.)

From Figure 2-33, for $y = 2.7$, the required
x to give $K' = 0.095$

$$x = 7.0 \text{ wave lengths}$$

or,

$$x = 7.0(223) = 1561 \text{ ft.}$$
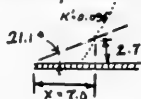
Required Breakwater Length = 1560 ft.

A similar analysis is required to deter-
mine the length of the breakwater on the
ocean side of the island.

Preliminary Design of Quay Wall Caisson

Since quay will be protected by
breakwaters after construction is complete,
caisson will experience extreme wave action
only during construction. For illustrative
purposes the following conditions will be
used to evaluate the stability of the
caisson against wave action. It should be
noted that these conditions have a low
probability of occurrence during construct-
ion.

$$H_s = 8.9 \text{ ft.}$$

$$H_1 = 14.9 \text{ ft.}$$

$$T_s = 6.6 \text{ sec.}$$

$$* \quad d = 40.0 + 6.0 \text{ ft}$$

$$d = 46 \text{ ft.}$$

* Probability of extreme surge during construct-
ion assumed negligible.

Design Problem   Preliminary Design

Quay Wall Caisson (cont.)

Stability During Construction

Sect. 7.32
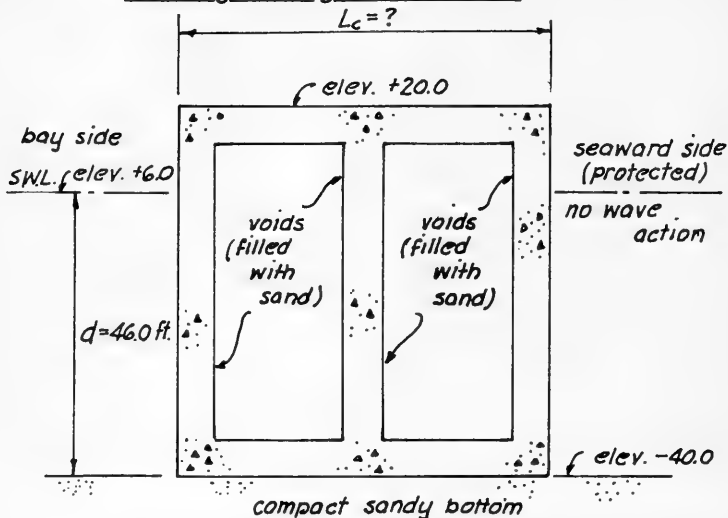
For preliminary analysis, assume 75% voids filled with _seawater_. $w_w = 64$ lbs/ft^3.

Non-breaking Wave Forces on Caisson

1. Incident Wave Height: $H_i = 14.9$ ft.

2. Wave Period: $T = 6.6$ sec.

3. Structure Reflection Coefficient: $\chi = 1.0$

4. Depth: $d_s = 46.0$ ft.

$$\frac{H_i}{T^2} = \frac{14.9}{(6.6)^2} = 0.342$$

$$\frac{H_i}{d_s} = \frac{14.9}{46} = 0.324$$

Design Problem Preliminary Design

Quay Wall Caisson (cont.)

5. Height of orbit center above S.W.L.: $\qquad$ *Fig. 7-65*

$$\frac{h_o}{H_i} = 0.31$$

$$h_o = 0.31\, H_i = 0.31\,(14.9) = 4.62 \text{ ft.}$$

6. Height of wave crest above bottom: $\qquad$ *Eq. 7-66*

$$y_c = d_s + h_o + \frac{1+\chi}{2}\, H_i$$

$$y_c = 46.0 + 4.62 + 14.9 = 65.5 \text{ ft.}$$

Wave will overtop caisson by 5.5 ft., therefore assume that structure is not 100% reflective. Use $\chi = 0.9$ and recalculate h_o

$$\frac{h_o}{H_i} = 0.28 \qquad\qquad \text{\textit{Fig. 7-68}}$$

$$h_o = 0.28\, H_i = 0.28\,(14.9) = 4.17 \text{ ft.}$$

$$y_c = 46.0 + 4.17 + \frac{1+0.9}{2}\,(14.9) = 64.3 \text{ ft.}$$

$$\text{say} \quad y_c = 64 \text{ ft.}$$

7. Dimensionless Force (wave crest at structure): $\qquad$ *Fig. 7-69*

for $\dfrac{H_i}{T^2} = 0.342;\qquad \dfrac{H_i}{d_s} = 0.324$ & $\chi = 0.9,$

$$\frac{F_c}{w d_s^2} = 0.68$$

$$F_c = 0.68\, w d_s^2 = 0.68\,(64)(46)^2 = 92{,}100$$

$$F_c = 92.1 \text{ k/ft.}$$

Quay Wall Caisson (cont.)

8. Force reduction for low height:

$$b = 40.0 + 20.0 = 60.0 \text{ ft.}$$
$$y_c = 64 \text{ ft.}$$

Fig. 7·72

$$\frac{b}{y_c} = \frac{60}{64} = 0.94$$

From Figure 7-72, $\Gamma_f = 0.996$

$$F_c' = \Gamma_f F_c = 0.996(92.1) = 91.7 \text{ k/ft.}$$

9. Hydrostatic force on leeward side:

$$F = \frac{wd^2}{2} = \frac{64(46)^2}{2} = 67.7 \text{ k/ft.}$$

10. Net horizontal force (due to presence of waves):

$$F_{net} = 91.7 - 67.7 = 24 \text{ k/ft.}$$

11. Dimensionless Moment (wave crest at structure):

Fig. 7-70

for $\frac{H_i}{T^2} = 0.342$, $\frac{H_i}{d_s} = 0.324$ & $\chi = 0.9$,

$$\frac{M_c}{wd_s^3} = 0.295$$

$$M_c = 0.295 w d_s^3 = 0.295(64)(46)^3 = 1,838,000$$

$$M_c = 1,838 \text{ ft·k/ft.}$$

12. Moment reduction for low height:

Fig. 7-72

From Figure 7·72, with $\frac{b}{y_c} = 0.94$

$$\Gamma_m = 0.990$$

$$M_c' = \Gamma_m M = 0.990(1,838) = 1,820 \text{ ft·k/ft.}$$

Quay Wall Caisson (cont.)

13. Hydrostatic moment on leeward side :

$$M = \frac{w d_s^3}{6} = \frac{64(46)^3}{6} = 1,038 \ ft \cdot k/ft.$$

14. Net overturning moment about bottom (due to presence of waves) :

$$M_{net} = 1,820 - 1,038 = 782 \ ft \cdot k/ft.$$

Stability Computations

Overturning :
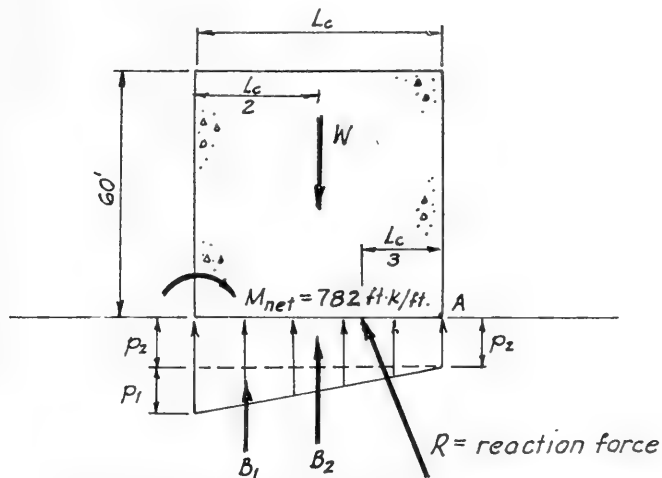
1. Weight per unit width per unit length of structure.

Concrete, $w_r = 150 \ lbs/ft^3$ (25% of area)

Water in voids, $w_w = 64 \ lbs/ft^3$ (75% of area)

Height = 60.0 ft.

Quay Wall Caisson (cont.)

Equation for Weight/unit length

$$W = 60 L_c \left\{ (0.25)(150) + (0.75)(64) \right\}$$

$$W = 5130 L_c \; lb/ft = 5.13 L_c \; k/ft.$$

2. Uplift per unit length of structure

$$p_1 = \frac{1+\chi}{2} \frac{w_w H_i}{\cosh(2\pi d/L)}$$ Eq. 7-68
Fig. 7-64

$$L_0 = \frac{gT^2}{2\pi} = \frac{32.2 (6.6)^2}{2(3.1416)} = 223.2 ft.$$

$$\frac{d}{L_0} = \frac{46}{223.2} = 0.206$$

$$\frac{d}{L} = 0.230 ; \quad L = \frac{d}{0.230} = \frac{46}{0.230} = 200 \; ft.$$ Appendix C
Table C-1

$$\cosh(2\pi d/L) = 2.242$$

$$p_1 = \frac{1+0.9}{2} \frac{(64)(14.9)}{2.242} = 404.1 \; lbs/ft.^2$$

$$p_1 = 0.4041 \; k/ft.^2$$

$$p_2 = w_w d \quad (hydrostatic \; uplift)$$

$$p_2 = 64(46) = 2,944 \; lbs/ft^2$$

$$p_2 = 2.944 \; k/ft^2$$

Equation for Uplift Forces/unit length

$$B_1 = \frac{p_1 L_c}{2} = 0.202 L_c \; k/ft.$$

$$B_2 = p_2 L_c = 2.944 L_c \; k/ft.$$

Design Problem _Preliminary Design_

Quay Wall Caisson (cont.)

Summation of Vertical Forces

$$B_1 + B_2 - W + R_v^* = 0$$

$$0.202 \, L_c + 2.944 \, L_c - 5.13 \, L_c + R_v = 0$$

$$R_v = 1.984 \, L_c \quad k/ft.$$

Summation of Moments about A.

$$B_1 \frac{2}{3} L_c + B_2 \frac{1}{2} L_c - W \frac{1}{2} L_c + R_v \frac{1}{3} L_c + M_{NET} = 0$$

$$0.202 \left(\frac{2}{3}\right) L_c^2 + 2.944 \left(\frac{1}{2}\right) L_c^2 - 5.13 \left(\frac{1}{2}\right) L_c^2 + 1.984 \left(\frac{1}{3}\right) L_c^2$$
$$+ 782 = 0$$

$$L_c^2 = \frac{782}{0.915} = 854.6$$

$$L_c = 29.2 \, ft.$$

Width required to prevent negative soil bearing pressure under caisson. (Reaction within middle third)

$$Assume \; L_c = 36 \; ft.$$

Sliding

Coefficient of friction
(concrete on sand) $\quad \mu_s = 0.40$ $\qquad$ Table 7-14

Vertical Force for $L_c = 36 \, ft.$

$$W = 5.13 \, L_c = 5.13 (36) = 184.7 \; k/ft.$$

$$B_1 = -0.202 \, L_c = -0.202 (36) = -7.3 \; k/ft.$$

----

* R_v = vertical component of R.

Page no :	*102* of *133*
Calculated by:	*J. R. W.*
Checked by:	*R. H. J*
Date :	*20 Mar. 73*

Design Problem   *Preliminary Design*

Quay Wall Caisson (cont.)

Sliding (cont.)

$$B_2 = -2.944 \, L_c = -2.944 \, (36) = -106.0 \, k/ft.$$

$$\Sigma F_v = 184.7 - 7.3 - 106.0 = 71.4 \; k/ft.$$

Horizontal Force to Initiate Sliding

$$F_H = \mu \, F_v = 0.40 \, (71.4) = 21.4 \; k/ft.$$

Since the actual net horizontal force is only 10 k/ft., caisson will not slide.

Caisson Stability after Backfilling

Assumptions:
1. No wave action. (Protected by breakwater)
2. Voids filled with dry sand.
3. Minimum water level at −3.0 MLW.
4. Surcharge of 2 ft. on fill. (dry sand)

Overturning Seaward

Design Problem Preliminary Design
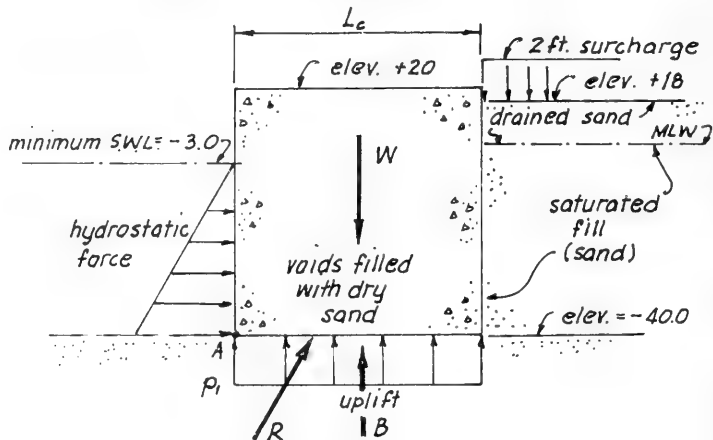
Quay Wall Caisson (cont.)

Earth Pressure Diagrams

Note: $\phi = 25°$

$\tan^2\left(\dfrac{90-\phi}{2}\right) = 0.406$

① surcharge
$2(120)\ lb/ft^3 =$
$240\ lb/ft^2$

② submerged sand
$65\ lb/ft^3$

③ hydrostatic
$64\ lb/ft^3$

④ drained sand
$120\ lb/ft^3$
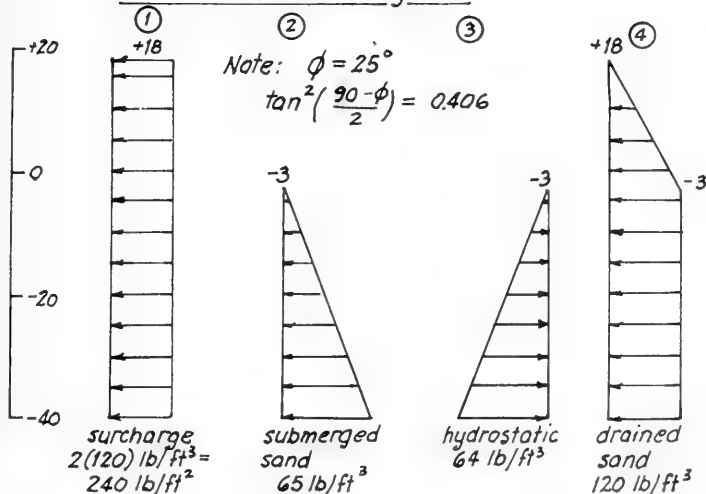
Diagram number	Force	Moment arm	Moment
①	$0.406(2)(120)(58)$ $= 5650\ lbs$	$\dfrac{58}{2} = 29\ ft.$	$163.9\ ft\cdot k$
②	$\dfrac{0.406(65)(37)^2}{2} =$ $18100\ lbs$	$\dfrac{37}{3} = 12.3\ ft.$	$222.6\ ft\cdot k$
③	$\dfrac{64(37)^2}{2} =$ $43800\ lbs$	$\dfrac{37}{3} = 12.3\ ft.$	$538.7\ ft\cdot k$
④	$0.406\left\{\dfrac{120(21)^2}{2} + 21(120)(37)\right\} =$ $48,600\ lbs$	$24.1\ ft.$	$1171.3\ ft\cdot k$

Quay Wall Caisson (cont.)

Summation of Vertical Forces

$$B + R_v^* - W = 0$$

$$2.37 L_c + R_v - 7.65 L_c = 0$$

Summation of Moments about A.

$$W \frac{L_c}{2} + F_h (12.3) - B \frac{L_c}{2} - M_E - R_v \frac{L_c}{3} = 0$$

$$\frac{7.65}{2} L_c^2 + 43.8 (12.3) - \frac{2.37}{2} L_c^2 - 2096.5 - R_v \frac{L_c}{3} = 0$$

but $R_v = 5.28 L_c$

Therefore,

$$3.825 L_c^2 - 1.185 L_c^2 - 1.760 L_c^2 - 1557.8 = 0$$

$$0.88 L_c^2 = 1557.8$$

$$L_c^2 = 1770$$

$$L_c = 42.1 \ ft.$$

$$R_v = 5.28 L_c = 5.28 (42.1) = 222.3 k$$

Required width of caisson, $L_c = 42.1 \ ft.$

Soil Bearing Pressure

Triangular pressure distribution,
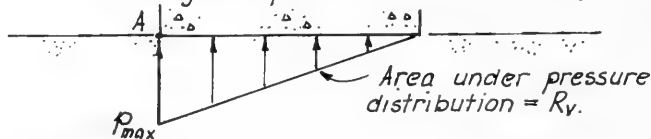
P_{max}

Area under pressure distribution = R_v.

* R_v = vertical component of reaction, R.

Quay Wall Caisson (cont.)

Total Horizontal Earth Force

$$F_E = 116.2 \ k/ft$$

Total Overturning Moment (Earth Pressure)

$$M_E = 2096.5 \ ft \cdot k/ft.$$

Moment Arm

$$r = \frac{M_E}{F_E} = \frac{2096.5}{116.2} = 18.0 \ ft$$

Weight / Unit Length
Voids filled with dry sand

$$W = L_c (60)\left\{150(0.25) + 120(0.75)\right\} = 7650 \ L_c$$

$$W = 7.65 L_c \ k/ft.$$

Uplift Force

$$p_1 = wd = 64(37) = 2368 \ lbs/ft^2$$

$$B = 2.37 L_c \ k/ft.$$

Hydrostatic Force (Seaward side)

$$F_h = \frac{wd^2}{2} = \frac{64(37)^2}{2} = 43810 \ lbs/ft$$

$$F_h = 43.8 \ k/ft$$

(moment arm $= \frac{37}{3} ft = 12.3 \ ft$ above bottom)

<u>Design Problem</u> <u>Preliminary Design</u>

Quay Wall Caisson (cont.)

Soil Bearing Pressure (cont.)

$$R_v = \frac{p_{max} L_c}{2}$$

$$p_{max} = \frac{2 R_v}{L_c} = \frac{2 (222.3)}{42.1} = 10.6 \ k/ft.^2$$

Sliding

Summation of Horizontal Forces

$$F_E - F_h - R_H^* = 0$$

$$R_H = 116.2 - 43.8 = 72.4 \ k/ft.$$

Vertical Force

$$R_v = 222.3 \ k/ft.$$

Coefficient of Friction, $\mu = 0.40$

Horizontal Force to Initiate Sliding

$$F_H = \mu R_v$$

$$F_H = 0.40 (222.3) = 88.9 \ k/ft.$$

$$F_H > R_H^{**} \ \text{Caisson will not slide.}$$

<u>Summary</u> - The preceding calculations illustrate the type of calculations required to determine the stability of the proposed quay wall. Many additional loading conditions also require investigation as do the foundation & soil conditions. Field investigations to determine soil conditions are required in addition to hydraulic model studies to determine wave effects on the proposed island.

---

* R_H = horizontal component of reaction, R.

** Factor of safety against sliding should be 2; hence $F_H \geq 2 R_H$ for safe design. Caisson should be widened.

8-106

Design Problem _Longshore Transport_

Chapt. 4
Sect. 4.

Computation of Longshore Component of Wave Energy & Potential Transport Rates

Using the hindcast deepwater wave data from page 8-38, the net and gross potential sand transport rates will be estimated for the beaches south of Ocean City, Maryland. (See map on next page) Assume refraction is by straight, parallel bottom contours.

Table of Deepwater Wave Steepnesses, H_0/gT^2

Corresponds to mid-interval values on Table, page 8-38 of calculations.

H_s (ft.)	T (sec)									
	5	7	9	11	13	15	17	19	21	23
1.25	.00155 (*.016)	.0008 (.023)	.0005 (.029)	.0003 (.035)	.0002 (.042)	.0002 (.048)				
3.0	.00373 (.093)	.0019 (.130)	.0012 (.167)	.0008 (.204)	.0006 (.241)	.0004 (.278)	.0003 (.315)	.0003 (.352)		
5.0	.00621 (.257)	.0032 (.360)	.0019 (.463)	.0013 (.566)	.0009 (.669)	.0007 (.772)	.0005 (.875)	.0004 (.978)		
7.0	.00870 (.504)	.0044 (.706)	.0027 (.908)	.0018 (1.11)	.0013 (1.31)	.0010 (1.51)	.0008 (1.72)	.0006 (1.92)		
9.0	.0112 (.834)	.0057 (1.17)	.0035 (1.50)	.0023 (1.83)	.0017 (2.17)	.0012 (2.50)	.0010 (2.84)	.0008 (3.17)		
11.0		.0070 (1.74)	.0042 (2.24)	.0028 (2.74)	.0020 (3.24)	.0015 (3.74)	.0012 (4.24)	.0009 (4.73)	.0008 (5.23)	
13.0		.0082 (2.44)	.0050 (3.13)	.0033 (3.83)	.0024 (4.52)	.0018 (5.22)	.0014 (5.92)	.0011 (6.61)	.0009 (7.30)	
15.0		.0095 (3.24)	.0058 (4.17)	.0038 (5.10)	.0028 (6.02)	.0021 (6.95)	.0016 (7.88)	.0013 (8.80)	.0010 (9.73)	
17.0			.0065 (5.36)	.0044 (6.55)	.0031 (7.74)	.0023 (8.93)	.0018 (10.1)	.0015 (11.3)	.0012 (12.5)	
19.0			.0073 (6.69)	.0049 (8.18)	.0035 (9.66)	.0026 (11.1)	.0020 (12.6)	.0016 (14.1)	.0013 (15.6)	
22.5			.0086 (9.38)	.0058 (11.5)	.0041 (13.6)	.0031 (15.6)	.0024 (17.7)	.0019 (19.8)	.0016 (21.9)	.0013 (24.0)
27.5				.0071 (17.1)	.0051 (20.2)	.0038 (23.4)	.0030 (26.5)	.0024 (29.6)	.0019 (32.7)	.0016 (35.8)

*Numbers in parentheses are $wg H_0^2 T \times 10^{-6}$

Figure 8-35. Local Shoreline Alignment in Vicinity of
Ocean City, Maryland

<u>Design Problem</u> <u>Longshore Transport</u>

<u>Longshore Wave Energy (cont.)</u>

Azimuth of shoreline $= 20°$

<u>Deepwater Wave Angle (α_o)</u>

Angle wave crest makes with shoreline (equal to angle wave ray makes with normal to shoreline)

Compass direction of Wave Approach	Deepwater angle α_o	
N	—	southward
NNE	* 87.5°	
NE	65.0°	
ENE	42.5°	
E	20.0°	
ESE	2.5°	
SE	25.0°	northward
SSE	47.5°	
S	70.0°	
SSW	—	

* Disregard as contributing little to longshore energy.

Longshore Wave Energy (cont.)

Typical Calculations for Waves from NE.

Use Figure 4-35 to determine longshore wave energy.

Fig. 4-35

$\dfrac{H_0}{gT^2}$ * (1)	wgH_0^2T * (2)	$\dfrac{P_\ell}{wgH_0^2T}$ ** (3)	P_ℓ (ft·lb/ft·sec) *** (4)	t (hrs/3yr) † (5)	$P_\ell \cdot t$ (ft·lb/ft·3yr) †† (6)
0.5 < H_0 < 2.0					
.00155	.016×10⁶	1.00×10⁻³	0.016×10³	22	1.3×10⁶
.0008	.023	0.77	0.018	88	5.6
.0005	.029	0.62	0.018	514	33.3
.0003	.035	0.50	0.018	430	27.1
.0002	.042	0.43	0.018	16	1.0
2.0 < H_0 < 4.0					
.00373	.093×10⁶	1.42×10⁻³	0.13 ×10³	56	26.6×10⁶
.0019	.130	1.08	0.14	24	12.1
.0012	.167	0.90	0.15	126	68.2
.0008	.204	0.77	0.16	346	195.7
.0006	.241	0.68	0.16	294	173.5
.0004	.278	0.57	0.16	38	21.7
.0003	.315	0.50	0.16	4	2.3
.0003	.352	0.50	0.18	2	1.3
4.0 < H_0 < 6.0					
.00621	.257×10⁶	1.75×10⁻³	0.45×10³	46	74.5×10⁶
.0032	.360	1.34	0.48	38	66.0
.0019	.463	1.08	0.50	54	97.2
.0013	.566	0.94	0.53	96	183.9
.0009	.669	0.81	0.54	122	238.0
.0007	.772	0.73	0.56	100	202.9
.0005	.875	0.62	0.54	30	58.6
.0004	.978	0.57	0.56	4	8.0
			Subtotal		1,498.8×10⁶

* From page 8-107 of calculations

** From Figure 4-35 (See curve on next page derived from Figure 4-35)

*** Column 2 × Column 3

† From Table, page 8-38 (for 3 yrs. of hindcast data)

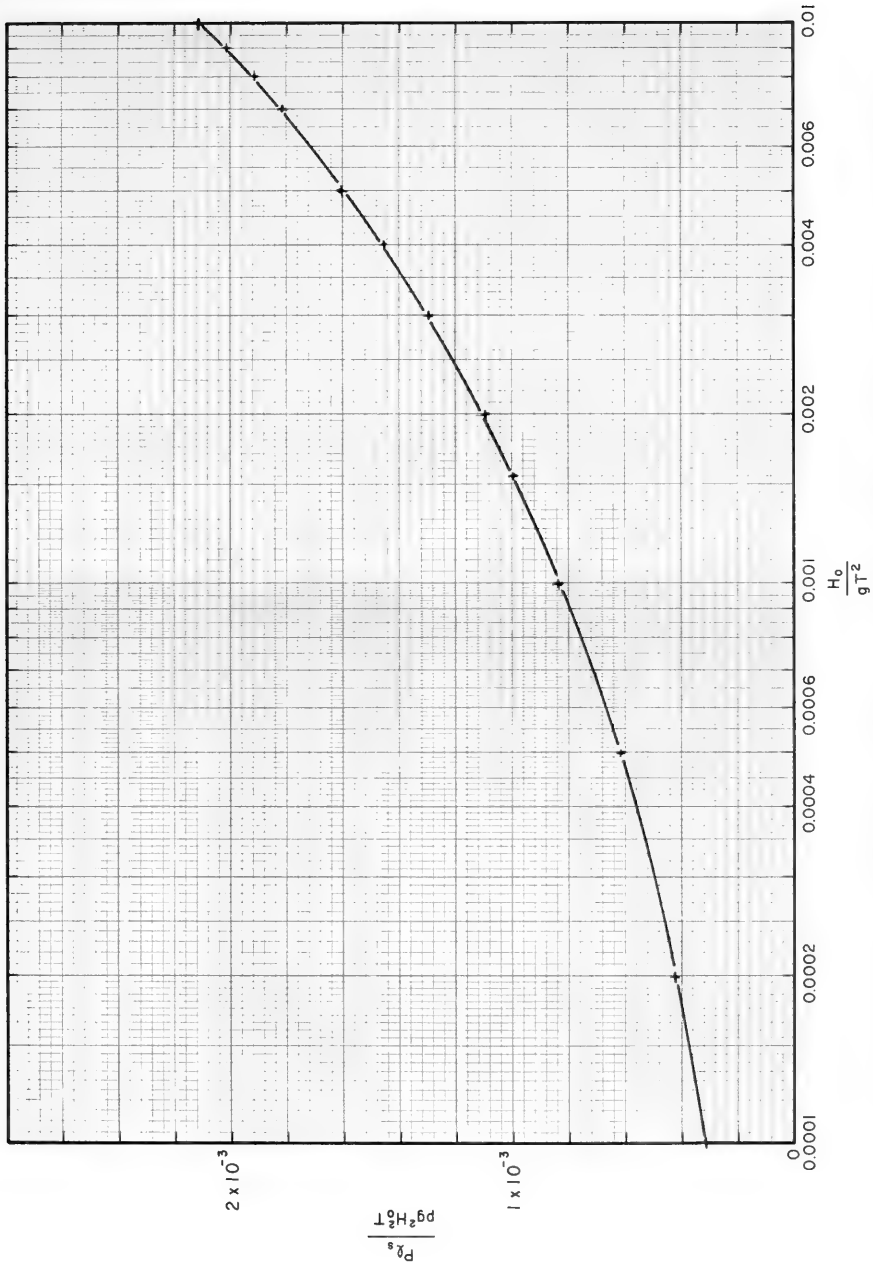†† Column 4 × column 5 ×3600 (ft-lb/ft-3yr.)

Fig. 4-35

Figure 8-36. Dimensionless Longshore Component of Wave Energy as a Function of Deepwater Wave Steepness — Waves from Northeast at Ocean City, Maryland

Design Problem   Longshore Transport

Longshore Wave Energy (cont.)

Typical Calculations for Waves from NE (cont.)

	$\dfrac{H_0}{gT^2}$	$wg\,H_0^2\,T$	$\dfrac{P_\ell}{wg\,H_0^2\,T}$	P_ℓ (ft·lb/ft·sec)	t (hrs/3yr)	$P_\ell \cdot t$ (ft·lb/ft·3yr)
	(1)	(2)	(3)	(4)	(5)	(6)
	.0087	$.504 \times 10^6$	2.00×10^{-3}	1.01×10^3	6	21.9×10^6
	.0044	.706	1.52	1.07	56	216.3
	.0027	.908	1.25	1.14	32	130.8
$6.0 < H_0 < 8.0$	.0018	1.11	1.06	1.18	44	186.4
	.0013	1.31	0.94	1.23	48	212.8
	.0010	1.51	0.84	1.27	38	173.5
	.0008	1.72	0.77	1.32	26	124.0
	.0006	1.92	0.68	1.31	4	18.8
	.0057	1.17×10^6	1.68×10^{-3}	1.97×10^3	26	184.0×10^6
	.0035	1.50	1.38	2.07	30	223.6
	.0023	1.83	1.16	2.12	12	91.7
$8.0 < H_0 < 10.0$	.0017	2.17	1.04	2.26	16	130.0
	.0012	2.50	0.90	2.25	32	259.2
	.0010	2.84	0.84	2.39	24	206.1
	.0008	3.17	0.77	2.44	12	105.4
	.0070	1.74×10^6	1.82×10^{-3}	3.17×10^3	16	182.4×10^6
	.0042	2.24	1.49	3.34	12	144.2
	.0028	2.74	1.27	3.48	16	200.4
$10.0 < H_0 < 12.0$	.0020	3.24	1.10	3.56	14	179.6
	.0015	3.74	0.99	3.70	6	80.0
	.0012	4.24	0.90	3.82	20	274.8
	.0009	4.73	0.81	3.83	6	82.8
	.0050	3.13×10^6	1.61×10^{-3}	5.04×10^3	24	435.4×10^6
	.0033	3.83	1.36	5.21	4	75.0
	.0024	4.52	1.19	5.38	6	116.2
$12.0 < H_0 < 14.0$	.0018	5.22	1.06	5.53	6	119.5
	.0014	5.92	0.96	5.68	14	286.4
	.0011	6.61	0.87	5.75	4	82.8
	.0009	7.30	0.81	5.91	8	170.3

Subtotal $6,213.1 \times 10^6$

8-112

Longshore Wave Energy (cont.)

Typical Calculations for Waves from NE (cont.)

	$\dfrac{H_o}{gT^2}$ (1)	$wgH_o^2 T$ (2)	$\dfrac{P_\ell}{wgH_o^2 T}$ (3)	P_ℓ (ft·lb/ft·sec) (4)	t (hrs/3yr) (5)	$P_\ell \cdot t$ (ft·lb/ft·3yr) (6)
$14 < H_o < 16$	.0058	4.17×10^6	1.71×10^{-3}	7.13×10^3	4	102.7×10^6
	.0038	5.10	1.43	7.29	8	210.0
	.0028	6.02	1.27	7.65	2	55.0
	.0021	6.95	1.12	7.78	4	112.1
	.0016	7.88	1.02	8.04	12	347.2
	.0010	9.73	0.84	8.17	18	529.6
$16 < H_o < 18$	.0065	5.36×10^6	1.78×10^{-3}	9.54×10^3	8	274.8×10^6
	.0044	6.55	1.52	9.96	6	215.0
	.0031	7.74	1.32	10.2	2	73.6
	.0023	8.93	1.16	10.4	2	74.6
	.0018	10.1	1.06	10.7	4	154.2
	.0012	12.5	0.90	11.3	4	162.0
$18 < H_o < 20$	.0073	6.69×10^6	1.88×10^{-3}	12.6×10^3	2	90.6×10^6
	.0049	8.18	1.59	13.0	12	561.9
	.0035	9.66	1.38	13.3	10	479.9
	.0026	11.1	1.23	13.7	2	98.3
	.0020	12.6	1.10	13.9	4	199.6
$20 < H_o < 25$	.0058	11.5×10^6	1.70×10^{-3}	19.6×10^3	16	1126.1×10^6
	.0041	13.6	1.47	20.0	10	719.7
	.0031	15.6	1.32	20.6	4	296.5
	.0024	17.7	1.19	21.1	4	303.3
	.0016	21.9	1.02	22.3	2	160.8
	.0013	24.0	0.94	22.6	4	324.9
$25 < H_o < 30$	.0051	20.2×10^6	1.62×10^{-3}	32.7×10^3	12	1413.7×10^6

Three Year Total $14{,}299 \times 10^6 \dfrac{\text{ft-lb}}{\text{ft·3yr.}}$
(waves from NE only)

Average Annual Wave Energy = 4.77×10^9 ft·lb/ft·yr.
(waves from NE only)

Longshore Wave Energy (cont.)

The preceding computations are required for the remaining wave directions (ENE, E, ESE, SE, SSE & S). Details of the computations are omitted here for brevity. The northward, southward, gross and net longshore energy are found by:

$$\text{Southward longshore energy flux} = \sum_{\substack{NNE, NE \\ ENE, E}} P_\ell = P_{south}$$

$$\text{Northward longshore energy flux} = \sum_{\substack{ESE, SE \\ SSE, S}} P_\ell = P_{north}$$

$$P_{net} = P_{south} - P_{north}$$

$$P_{gross} = P_{south} + P_{north}$$

For the example: Shoreline azimuth = 20°

$$P_{south} = 24.25 \times 10^9 \quad ft\cdot lb/ft\cdot yr$$

$$P_{north} = 3.58 \times 10^9 \quad ft\cdot lb/ft\cdot yr$$

$$P_{net} = 20.67 \times 10^9 \quad ft\cdot lb/ft\cdot yr$$

$$P_{gross} = 27.83 \times 10^9 \quad ft\cdot lb/ft\cdot yr$$

From similar calculations for other shore alignments

Shoreline azimuth = 15°

$$P_{south} = 23.98 \times 10^9 \quad ft\cdot lb/ft\cdot yr.$$

$$P_{north} = 3.99 \times 10^9 \quad ft\cdot lb/ft\cdot yr.$$

$$P_{net} = 19.99 \times 10^9 \quad ft\cdot lb/ft\cdot yr.$$

$$P_{gross} = 27.97 \times 10^9 \quad ft\cdot lb/ft\cdot yr.$$

Longshore Wave Energy (cont.)

Shoreline azimuth = 25°

$$P_{south} = 24.04 \times 10^9 \quad ft \cdot lb/ft \cdot yr$$

$$P_{north} = 3.30 \times 10^9 \quad ft \cdot lb/ft \cdot yr$$

$$P_{net} = 20.74 \times 10^9 \quad ft \cdot lb/ft \cdot yr$$

$$P_{gross} = 27.34 \times 10^9 \quad ft \cdot lb/ft \cdot yr$$

Note: The energy given is "significant wave energy" since it is computed as if the sea surface were made up of trains of periodic waves having the characteristics of the significant wave. The actual energy will be approximately one half (0.50) of the given values.

Longshore Sand Transport Estimate

Ref. 17

$$I_\ell = k P_\ell$$

where　I_ℓ = submerged weight sand transport

P_ℓ = longshore component of wave energy flux.

k = dimensionless constant

$$0.25 < k < 0.77$$

(An average value of k when no other evidence is available: $k = 0.35$)

Conversion of I_ℓ to Q_ℓ

Q_ℓ = volume transport

Design Problem Longshore Transport

Longshore Sand Transport (cont.)

$$Q_\ell = \frac{I_\ell}{(1-\frac{P}{100})(\rho_s-\rho_w)\,g}$$

Ref. 17

where, g = acceleration due to gravity
P = porosity of sand in place (%)
ρ_s = sediment density
ρ_w = water density

Assume, $P = 40\%$ and the specific gravity of sand, $S_s = 2.65$.

$$\rho_s = 2.65 \, \rho_{fw}$$

where
ρ_{fw} = density of fresh water
$\rho_{fw} = 1.94 \; slugs/ft^3$

Therefore,
$$\rho_s = 2.65\,(1.94) = 5.14 \; slugs/ft^3$$

also, $\quad \rho_w = 2.0 \; slugs/ft^3 \; (salt \; water)$

$$Q_\ell \left(\frac{ft^3}{yr}\right) = \frac{I_\ell \left(\frac{lb}{yr}\right)}{(1-\frac{40}{100})(5.14-2.0)(32.2)}$$

$$Q_\ell \left(\frac{ft^3}{yr}\right) = \left(0.0165 \, \frac{ft^3}{lb}\right) I_\ell \left(\frac{lb}{yr}\right)$$

or, $\quad I_\ell \left(\frac{lb}{yr}\right) = \left(60.6 \, \frac{lb}{ft^3}\right) Q_\ell \left(\frac{ft^3}{yr}\right)$

Therefore,

$$I_\ell \left(\frac{lb}{yr}\right) = \left(60.6 \, \frac{lb}{ft^3}\right) Q_\ell \left(\frac{ft^3}{yr}\right) = k \, P_\ell \left(\frac{ft \cdot lb}{ft \cdot yr}\right)$$

or,
$$Q_\ell \left(\frac{ft^3}{yr}\right) = \frac{k}{60.6 \; lb/ft^3} \; P_\ell \left(\frac{ft \cdot lb}{ft \cdot yr}\right)$$

Longshore Sand Transport (cont.)

Shoreline azimuth = 20° with k = 0.35

$$\{Q_\ell\}_{south} = \frac{0.35}{60.6} \, 24.25 \times 10^9 = 140 \times 10^6 \; ft^3/yr$$

$$\{Q_\ell\}_{south} = 5.00 \times 10^6 \; yd^3/yr.$$

Similarly,

$$\{Q_\ell\}_{north} = 0.766 \times 10^6 \; yd^3/yr$$

$$\{Q_\ell\}_{net} = \{Q_\ell\}_{south} - \{Q_\ell\}_{north} = 4.23 \times 10^6 \; yd^3/yr$$

$$\{Q_\ell\}_{gross} = \{Q_\ell\}_{south} + \{Q_\ell\}_{north} = 5.77 \times 10^6 \; yd^3/yr.$$

Note: The computed values are suspect since they are much larger than values measured at various east coast locations. The discrepancy could be due to several factors:

1   Energy was computed using the significant wave which is a relatively high wave in the spectrum. Actual wave energy is approximately 1/2 of the significant wave's energy. Note, however, the constant k is based partly on data arrived at by using significant wave energy.

2.   The hindcast wave data were for deep water. Energy dissipation due to bottom friction and percolation were not considered; consequently, the wave energy reaching shore will be lower than that computed.

3.   Refraction was assumed to be by straight, parallel bottom contours. This assumption may not be valid.

4.   Waves approaching shore with their crests nearly perpendicular to the

Design Problem   _Longshore Transport_

Longshore Sand Transport (cont.)

4. (cont.)   shoreline may not contribute
significantly, if at all, to the
longshore component of wave
energy and perhaps should not
have been considered in the
computations.

The preceding procedure can be
adapted to compute longshore transport
rates by calibrating it to establish k
based on known transport rates.

Site 1   Chincoteague Inlet, Virginia   Ref. 15

Based on a report entitled, "Atlantic
Coast of Maryland and Assateague Island
Virginia -Draft Survey Report on Beach
Erosion Control & Hurricane Protection,"
(Reference 15), 400,000 yd³/yr of sand are
deposited at Fishing Point at the south end
of Assateague Island. The shore alignment
at Fishing Point is approximately 20° east of
north. It will be assumed that the 400,000
yd³/yr is the southward transport.

For a shoreline azimuth of 20,°

$$P_{south} = 24.3 \times 10^9 \text{ ft·lb/ft·yr.}$$

$$Q_{south} = 4.0 \times 10^5 \text{ yd}^3/\text{yr.}$$

let k' be the ratio of Q_{ℓ}/P_{ℓ}, hence
$$k' = \frac{4.0 \times 10^5}{24.3 \times 10^9} = 16.46 \times 10^{-6} \text{ yd}^3/\text{lb}$$

Site 2   Cold Spring Inlet, New Jersey   Ref. 6

Based on a paper entitled, "Coastal
Processes and Beach Erosion," C.E.R.C. Reprint
R.1-67, Jan.1967 by J.M.Caldwell (Reference 6),
the net northward movement of sand at Cold
Spring Inlet is 500,000 yd³/yr; the net
southward movement is 700,000 yd³/yr. On
the north side of the inlet the shoreline

Page no :	119 of 133
Calculated by :	J. R. W.
Checked by :	R. H. J.
Date :	21 Mar. 73

Design Problem   Longshore Transport

Longshore Sand Transport (cont.)

azimuth is 43°; on the south side of the inlet the shoreline azimuth is 65°.

For a shoreline azimuth of 43°, a longshore wave energy analysis gives,

$$P_{south} = 18.5 \times 10^9 \text{ ft-lb/ft-yr.}$$

$$k' = Q_\ell / P_\ell = \frac{7.0 \times 10^5}{18.5 \times 10^9} = 37.8 \times 10^{-6} \text{ yd}^3/\text{lb}$$

For a shoreline azimuth of 65°,

$$P_{north} = 1.5 \times 10^9 \text{ ft-lb/ft-yr.}$$

$$k' = Q_\ell / P_\ell = \frac{5.0 \times 10^5}{1.5 \times 10^9} = 333 \times 10^{-6} \text{ yd}^3/\text{lb}$$

Based on net transport and a shoreline azimuth of 43° (general trend of shoreline at Cold Spring Inlet)

$$Q_{net} = Q_{south} - Q_{north} = 2.0 \times 10^5 \text{ yd}^3/\text{yr.}$$
$$\text{(southward)}$$

$$P_{net} = P_{south} - P_{north} = 17.0 \times 10^9 \text{ ft-lb/ft-yr.}$$

$$k' = Q_\ell / P_\ell = \frac{2.0 \times 10^5}{17.0 \times 10^9} = 11.8 \times 10^{-6} \text{ yd}^3/\text{lb}$$

Based on gross transport and shoreline azimuth of 43°.

$$Q_{gross} = Q_{south} + Q_{north} = 12.0 \times 10^5 \text{ yd}^3/\text{yr}$$

$$P_{gross} = P_{south} + P_{north} = 20.0 \times 10^9 \text{ ft-lb/ft-yr}$$

$$k' = Q_\ell / P_\ell = \frac{12.0 \times 10^5}{20.0 \times 10^9} = 60.0 \times 10^{-6} \text{ yd}^3/\text{lb.}$$

Longshore Sand Transport (cont.)

Site 3 Sea Isle, New Jersey

From Reference 6,

$$Q_{north} = 5.0 \times 10^5 \ yd^3/yr$$

$$Q_{south} = 6.5 \times 10^5 \ yd^3/yr$$

$$Q_{net} = 1.5 \times 10^5 \ yd^3/yr$$

$$Q_{gross} = 11.5 \times 10^5 \ yd^3/yr$$

For a shoreline azimuth = $33°$

$$P_{north} = 3.0 \times 10^9 \ ft\text{-}lb/ft\cdot yr$$

$$k' = Q_\ell/P_\ell = \frac{5.0 \times 10^5}{3.0 \times 10^9} = 167.0 \times 10^{-6} \ yd^3/lb$$

$$P_{south} = 22.5 \times 10^9 \ ft\text{-}lb/ft\cdot yr$$

$$k' = Q_\ell/P_\ell = \frac{6.5 \times 10^5}{22.5 \times 10^9} = 28.9 \times 10^{-6} \ yd^3/lb$$

$$P_{net} = 19.5 \times 10^9 \ ft\text{-}lb/ft\cdot yr$$

$$k' = Q_\ell/P_\ell = \frac{1.5 \times 10^5}{19.5 \times 10^9} = 7.7 \times 10^{-6} \ yd^3/lb.$$

$$P_{gross} = 25.5 \times 10^9 \ ft\text{-}lb/ft\cdot yr.$$

$$k' = Q_\ell/P_\ell = \frac{11.5 \times 10^5}{25.5 \times 10^9} = 45.1 \times 10^{-6} \ yd^3/lb.$$

Design Problem _Longshore Transport_

Longshore Sand Transport (cont.)

Table of k' Values

Site	$k' = \dfrac{Q_{north}}{P_{north}}$	$k' = \dfrac{Q_{south}}{P_{south}}$	$k' = \dfrac{Q_{net}}{P_{net}}$	$k' = \dfrac{Q_{gross}}{P_{gross}}$
Chincoteague Inlet, Va.	—	16.5×10^{-6}	—	—
Cold Spring Inlet, NJ	*333.0×10^{-6}	37.8×10^{-6}	11.8×10^{-6}	60.0×10^{-6}
Sea Isle, N.J.	16.7×10^{-6}	28.9×10^{-6}	7.7×10^{-6}	45.1×10^{-6}

* The northward transport rate at Cold Spring
Inlet is probably significantly influenced by
the proximity of Delaware Bay and local
shoals making this value of k questionable.

$$\text{Average } k' = 28.0 \times 10^{-6} \text{ ** (disregarding highest value)}$$

Potential Sand Transport, Ocean City, Md.***

$$Q_{south} = k' P_{south} = 28.0 \times 10^{-6}(24.25 \times 10^{9}) = 679,000 \text{ yd}^3/\text{yr}$$

$$Q_{north} = k' P_{north} = 28.0 \times 10^{-6}(3.58 \times 10^{9}) = 100,000 \text{ yd}^3/\text{yr}$$

$$Q_{net} = k' P_{net} = 28.0 \times 10^{-6}(20.67 \times 10^{9}) = 579,000 \text{ yd}^3/\text{yr}$$

$$Q_{gross} = k' P_{gross} = 28.0 \times 10^{-6}(27.83 \times 10^{9}) = 779,000 \text{ yd}^3/\text{yr}$$

** Note: This value of k' should be used only with
wave data as developed here and only
for this geographical area.

*** Note: Shoreline azimuth = 20°

8-121

Visual Wave Observations - Longshore Energy

During summer months, visual observations of surf conditions were made on Assateague Island. Data are available only for July & August and indicate conditions for these months only. Monthly hindcast data will be used to supplement the visual data and extrapolate to annual longshore energy values.

Visual observations produce data on breaker height, period and wave direction. The longshore component of wave energy can be computed from Figure 4-34 or from equation.[**]

Visual Observations - July, 1972

Date	Period (sec)	Height (ft)	Angle [*] (degrees)	P_ℓ [**] (ft·lb/ft·day)	
8 July	8.8	2.0	110°	-8.09 × 10⁶	
9	11.0	2.0	93	-1.32	
10	7.7	2.0	110	-8.09	
11	12.1	3.0	110	-22.29	
12	9.9	2.0	110	-8.09	
13	13.2	2.0	107	-7.05	
14	9.9	2.0	110	-8.09	
15	9.9	1.5	90	0	minus sign (-) indicates northward transport
16	12.1	1.0	93	-0.23	
17	12.1	2.0	100	-4.31	
18	11.0	2.0	110	-8.09	
19	13.1	1.0	94	-0.31	
20	8.8	1.0	100	-0.76	
21	8.8	1.0	90	0	
23	12.1	1.0	110	-1.43	
24	7.7	1.0	110	-1.43	
25	6.6	2.0	110	-8.09	
27	12.1	2.0	96	-2.62	
28	7.7	2.0	96	-2.62	
29	6.6	1.0	96	-0.46	
30	9.9	1.0	93	-0.23	
31	11.0	2.0	100	-8.09	

Average = -4.62 × 10⁶

[*] Measured clockwise from shoreline by observer looking seaward perpendicular to shoreline.

[**] $P_\ell = 0.141 \rho g^{3/2} H_b^{5/2} \cos\theta_b \sin\theta_b$ (assumed duration of wave conditions is 24 hours = 86400 sec.)

Visual Wave Observations (cont.)

Visual Observations - August, 1972

Date	Period (sec)	Height (ft)	Angle (degrees)	P_ℓ (ft·lb/ft·day)
1 Aug	8.8	2.0	110	-8.09×10^6
2	8.8	2.0	110	-8.09
3	8.8	2.0	100	-4.31
4	6.6	2.0	110	-8.09
5	5.5	3.0	110	-22.29
6	8.8	5.0	110	-79.91
7	12.1	2.0	90	0
8	7.7	2.0	110	-8.09
10	9.9	2.0	80	$+4.31$
11	6.6	2.0	93	-1.32
12	6.6	2.0	110	-8.09
13	8.8	2.0	110	-8.09
14	6.6	2.0	110	-8.09
15	4.4	3.9	75	$+33.45$
16	5.5	2.5	86	$+3.06$
17	9.9	3.0	85	$+6.03$
18	9.9	2.0	80	$+4.31$
19	7.7	2.5	87	$+2.30$
20	9.9	1.0	110	-1.43
21	7.7	2.0	90	0
22	7.7	2.0	110	-8.09
23	8.8	2.0	110	-8.09
24	9.9	1.0	91	-0.08
25	9.9	2.5	94	-3.06
26	8.8	2.0	110	-8.09
27	7.7	2.0	110	-8.09
28	9.9	2.5	105	-11.0

Average (net) = -5.89×10^6

Average (gross) = 9.85×10^6

Design Problem Longshore Transport

Visual Wave Observations (cont.)

Average Daily Longshore Component of Wave Energy.

July, 1972

$$P_{net} = -4.62 \times 10^6 \ ft\text{-}lb/ft\text{-}day$$
$$(northward)$$

$$P_{gross} = P_{net} = 4.62 \times 10^6 \ ft\text{-}lb/ft\text{-}day$$
$$(no \ reversals)$$

August, 1972

$$P_{net} = -5.89 \times 10^6 \ ft\text{-}lb/ft\text{-}day$$
$$(northward)$$

$$P_{gross} = 9.85 \times 10^6 \ ft\text{-}lb/ft\text{-}day$$

$$P_{north} = 7.87 \times 10^6 \ ft\text{-}lb/ft\text{-}day$$

$$P_{south} = 1.98 \times 10^6 \ ft\text{-}lb/ft\text{-}day$$

Hindcast Data for July & August

Ref. 7

July Data Only   shoreline azimuth = 20°

$$P_{net} = +1.69 \times 10^6 \ ft\text{-}lb/ft\text{-}day$$
$$(southward)$$

$$P_{gross} = 2.38 \times 10^6 \ ft\text{-}lb/ft\text{-}day$$

$$P_{north} = 0.345 \times 10^6 \ ft\text{-}lb/ft\text{-}day$$

$$P_{south} = 2.04 \times 10^6 \ ft\text{-}lb/ft\text{-}day$$

Visual Wave Observations (cont.)

Hindcast Data for July & August (cont.)

August Data Only   shoreline azimuth = 20°

$$P_{net} = -8.06 \times 10^6 \text{ ft-lb/ft-day}$$
$$\text{(northward)}$$

$$P_{gross} = 56.84 \times 10^6 \text{ ft-lb/ft-day}$$

$$P_{north} = 32.45 \times 10^6 \text{ ft-lb/ft-day}$$

$$P_{south} = 24.39 \times 10^6 \text{ ft-lb/ft-day}$$

Correction Factors for Visual Observations

Based on hindcast data and used to extrapolate limited visual data to annual values.

July Hindcast Data   shoreline azimuth = 20°

$$\frac{\{P_{north}\}_{July}}{\{P_{north}\}_{Annual}} = \frac{0.345 \times 10^6 (31)}{3.58 \times 10^9} = 0.0030 \quad (0.3\%) \; *$$

$$\frac{\{P_{south}\}_{July}}{\{P_{south}\}_{Annual}} = \frac{2.04 \times 10^6 (31)}{24.25 \times 10^9} = 0.0026 \quad (0.26\%) \; *$$

$$\frac{\{P_{net}\}_{July}}{\{P_{net}\}_{Annual}} = \frac{-1.69 \times 10^6 (31)}{20.67 \times 10^9} = -0.0025 \quad (0.25\%) \; *$$

$$\frac{\{P_{gross}\}_{July}}{\{P_{gross}\}_{Annual}} = \frac{2.38 \times 10^6 (31)}{27.83 \times 10^9} = 0.0027 \quad (0.27\%) \; *$$

* Wave energy obtained visually for July divided by these numbers will give annual values for P_{north}, P_{south}, P_{net} and P_{gross}.

Visual Wave Observations (cont.)

Correction Factors (cont.)

August Hindcast Data   shoreline azimuth = 20°

$$\frac{\{P_{north}\}_{Aug.}}{\{P_{north}\}_{Annual}} = \frac{32.45 \times 10^6 (31)}{3.58 \times 10^9} = 0.281 \quad (28.1\%)$$

$$\frac{\{P_{south}\}_{Aug.}}{\{P_{south}\}_{Annual}} = \frac{24.39 \times 10^6 (31)}{24.25 \times 10^9} = 0.0312 \quad (3.12\%)$$

$$\frac{\{P_{net}\}_{Aug.}}{\{P_{net}\}_{Annual}} = \frac{-8.06 \times 10^6 (31)}{20.67 \times 10^9} = -0.0121 \quad (1.21\%)$$

$$\frac{\{P_{gross}\}_{Aug.}}{\{P_{gross}\}_{Annual}} = \frac{56.84 \times 10^6 (31)}{27.83 \times 10^9} = 0.0633 \quad (6.33\%)$$

Corrected Visual Data - July

$$\{P_{north}\}_{Annual} = \{P_{north}\}^*_{July} \cdot \frac{31}{0.003} **$$

$$\{P_{north}\}_{Annual} = \frac{4.62 \times 10^6 (31)}{0.0030} = 47.7 \times 10^9 \ ft \cdot lb/ft \cdot yr$$

$$\{P_{south}\}_{Annual} = \frac{(0)(31)}{0.0026} = 0 \ ft \cdot lb/ft \cdot yr.$$

$$\{P_{net}\}_{Annual} = \frac{-4.62 \times 10^6 (31)}{-0.0025} = 57.3 \times 10^9 \ ft \cdot lb/ft \cdot yr$$
$$(southward)$$

$$\{P_{gross}\}_{Annual} = \frac{4.62 \times 10^6 (31)}{0.0027} = 53.0 \times 10^9 \ ft \cdot lb/ft \cdot yr$$

---

* From page 8-124 of calculations.

** Correction factor from page 8-125 of calculations.

Visual Wave Observations (cont.)

Corrected Visual Data - August

$$\{P_{north}\}_{Annual} = \{P_{north}\}^*_{Aug} \cdot \frac{31}{0.281} \ast\ast$$

$$\{P_{north}\}_{Annual} = \frac{7.87 \times 10^6 \,(31)}{0.281} = 0.868 \times 10^9 \, ft\cdot lb/ft\cdot yr$$

$$\{P_{south}\}_{Annual} = \frac{1.98 \times 10^6 \,(31)}{0.0312} = 1.97 \times 10^9 \, ft\cdot lb/ft\cdot yr$$

$$\{P_{net}\}_{Annual} = \frac{-5.89 \times 10^6 \,(31)}{-0.0121} = 15.1 \times 10^9 \, ft\cdot lb/ft\cdot yr. \atop (southward)$$

$$\{P_{gross}\}_{Annual} = \frac{9.85 \times 10^6 \,(31)}{0.0633} = 4.82 \times 10^9 \, ft\cdot lb/ft\cdot yr.$$

Note: Extrapolating a few months of visual
wave data to annual values is not
satisfactory in the present case. Data
for the two months is not consistent
with the hind cast data. For the
calculated energies, the following
relationships do not check :

$$P_{net} = P_{south} - P_{north}$$

$$P_{gross} = P_{south} + P_{north}$$

---

* From page 8-124 of calculations.

** Correction factor from page 8-126 of calculations.

Design Problem **Longshore Transport**

Longshore Transport Summary.

Based on Hindcast Data

$$Q_{south} = 679,000 \ yd^3/yr.$$

$$Q_{north} = 100,000 \ yd^3/yr.$$

$$Q_{net} = 579,000 \ yd^3/yr.$$

$$Q_{gross} = 779,000 \ yd^3/yr.$$

Based on Visual Observations

Because of the paucity of data for the site, satisfactory estimates of transport rates could not be obtained.

Beach Fill Requirements

Sect. 5.332

A beach fill is proposed for the beach south of Ocean City, Maryland. Determine the volume of borrow material required to widen the beach 50 ft over a distance of one mile. Borrow material is available from two sources.

Characteristics of Native Sand

Appendix C
Table C-7

$$\phi_{84} = 2.51 \phi \quad (0.1756 \text{ mm})$$

$$\phi_{16} = 1.37 \phi \quad (0.3869 \text{ mm})$$

Characteristics of Borrow – Source A

$$\phi_{84} = 2.61 \phi \quad (0.1638 \text{ mm})$$

$$\phi_{16} = 1.00 \phi \quad (0.500 \text{ mm})$$

Characteristics of Borrow – Source B

$$\phi_{84} = 3.47 \phi \quad (0.0902 \text{ mm})$$

$$\phi_{16} = 0.90 \phi \quad (0.5359 \text{ mm})$$

Native Sand

$$M_{\phi_n} = \frac{\phi_{84} + \phi_{16}}{2}$$

Eq. 5-3

$$M_{\phi_n} = \frac{2.51 + 1.37}{2} = 1.94 \phi \quad (0.2606 \text{ mm})$$

$$\sigma_{\phi_n} = \frac{\phi_{84} - \phi_{16}}{2}$$

Eq. 5-2

$$\sigma_{\phi_n} = \frac{2.51 - 1.37}{2} = 0.570$$

Beach Fill Requirements (cont.)

Source A

$$M_{\phi_A} = \frac{2.61 + 1.00}{2} = 1.81\phi \quad (0.285\,mm)$$

$$\sigma_{\phi_A} = \frac{2.61 - 1.00}{2} = 0.805$$

Source B

$$M_{\phi_B} = \frac{3.47 + 0.90}{2} = 2.19\phi \quad (0.219\,mm)$$

$$\sigma_{\phi_B} = \frac{3.47 - 0.90}{2} = 1.29$$

Evaluation of Borrow Materials

$$\frac{M_{\phi_A} - M_{\phi_n}}{\sigma_{\phi_n}} = \frac{1.81 - 1.94}{0.57} = -0.228$$

$$\frac{\sigma_{\phi_A}}{\sigma_{\phi_n}} = \frac{0.805}{0.57} = 1.412$$

Fig. 5-3

From Figure 5-3, quadrant 2,

(Source A) $R_{\phi_{critical}} = 1.45$ (upper limit for overfill ratio)

$$\frac{M_{\phi_B} - M_{\phi_n}}{\sigma_{\phi_n}} = \frac{2.19 - 1.94}{0.57} = 0.439$$

$$\frac{\sigma_{\phi_B}}{\sigma_{\phi_n}} = \frac{1.29}{0.57} = 2.26$$

Beach Fill Requirements (cont.)

From Figure 5-3, quadrant 1,

(Source B) $R_{\phi_{critical}} = 2.35$ (overfill ratio)

Use material from Source A

Required Volume of Fill

Rule of thumb: 1 yd^3 of native material
per foot of beach width.

$\begin{aligned} \text{Volume} \\ \text{of Native Sand} \end{aligned} = 50\,ft. \times 27\,\frac{ft^3}{ft^2} \times 1\,mile \times \frac{5280\,ft}{mi}$

$\begin{aligned} \text{Volume} \\ \text{of Native Sand} \end{aligned} = 7.128 \times 10^6 \ ft^3$

$\begin{aligned} \text{Volume} \\ \text{from Source A} \end{aligned} = 1.45\,(7.128 \times 10^6) = 10.34 \times 10^6 \ ft^3$
(upper limit)

Required Volume from Source A will be
less than or equal to,

$$10.34 \times 10^6 \ ft^3$$

$$(\ 383,000 \ yd^3)$$

Design Problem   *References*

Nautical Charts

1. National Ocean Survey (formerly U.S.C.&G.S.) Chart No. 1000, Atlantic Coast, Cape Sable to Cape Hatteras, Scale: 1: 1,200,000

2. National Ocean Survey (U.S.C.& G.S.) Chart No. 1218, Delaware Bay, Scale: 1: 80,000

3. National Ocean Survey (U.S.C.& G.S.) Chart No. 1219, Cape May to Fenwick Island Light, Scale: 1: 80,000

4. National Ocean Survey (U.S.C & G.S.) Chart No. 1109, Cape May to Cape Hatteras, Scale: 1: 416,944

Publications and Reports

5. Bretschneider, C.L. (1959), "Hurricane Surge Predictions for Delaware Bay and River" Beach Erosion Board, Misc. Paper No. 4-59.

6. Caldwell, J. M. (1967) "Coastal Processes and Beach Erosion," Coastal Engineering Research Center, Reprint R.1-67

7. Saville, T., Jr. (1954), "North Atlantic Coast Wave Statistics Hindcast by Bretschneider Revised Sverdrup-Munk Method," Beach Erosion Board, Tech. Memo. 55.

8. Thom, H.C.S. (1960) "Distributions of Extreme Winds in the United States," Proceedings of the Structural Division, ASCE, ST4, #2433.

9. National Ocean Survey (U.S.C.& G.S.)(1948&1960) "Tidal Current Charts-Delaware Bay and River."

10. National Ocean Survey (U.S.C.&G.S.), "Tide Tables" (available for each year)

Design Problem   *References*

Publications and Reports (cont.)

11. National Ocean Survey (U.S.C. & G.S.) "Tidal Current Tables" (available for each year)

12. U.S. Army Corps of Engineers, Philadelphia District (1956), "Beach Erosion Control Report on Cooperative Study of Delaware Coast, Kitts Hummock to Fenwick Island"

13. U.S. Army Corps of Engineers, Philadelphia District (1966), "Beach Erosion Control and Hurricane Protection Along the Delaware Coast."

14. U.S. Army Corps of Engineers, Philadelphia District (1970), "Detailed Project Report, Small Beach Erosion Control Project, Lewes, Delaware."

15. U.S. Army Corps of Engineers, Baltimore District (1970), "Atlantic Coast of Maryland and Assateague Island Virginia – Draft Survey Report on Beach Erosion Control and Hurricane Protection."

16. U.S. Weather Bureau (1957), "Winds Over Chesapeake Bay for Hurricane of September 14, 1944, Transposed and Adjusted for Filling," Weather Bureau Memorandum HUR 7-26.

17. Komar, P.D. (1969), "The Longshore Transport of Sand on Beaches," Unpublished Ph.D. Thesis, University of California, San Diego.